Nanobiomaterials in Clinical Dentistry

Every good and perfect gift is from above, coming down from The Almighty.

Thanks be to God for his blessings and this wonderful life!

I would like to dedicate this book to my parents for making me who I am today. This is a special moment to remember and thank all my teachers, research mentors, and professors who have been the guiding light throughout my career. A very special thanks to Prof. G. Thomas Kluemper, Prof. Sarandeep Huja, and Prof. James K. Hartsfield Jr. for being a source of immense motivation and moral support.

Karthikeyan Subramani

I would like to dedicate this book to my father, Muhammed Mukhtar, and mother, Shamim Anwar, for their unconditional love and guidance, and to my family—Rihana, Aisha, Imran, Omar, Usman, and Adam—who have provided an environment of fun and happiness for my work to flourish. Thank you to the most beautiful little girl in the whole wide world, my granddaughter Zoya, for coming into my life and lighting it up with joy and happiness.

Waqar Ahmed

I would like to dedicate this book to my parents Jim and Shirley, to my loving wife Karen, our son Kennedy of whom we are very proud, and our grandson Clayton. Special thanks to all my teachers, faculty, students, and patients, from whom I continue to learn.

James K. Hartsfield Jr.

Nanobiomaterials in Clinical Dentistry

Edited by
Karthikeyan Subramani
Waqar Ahmed
James K. Hartsfield, Jr.

ELSEVIER

AMSTERDAM • BOSTON • HEIDELBERG • LONDON
NEW YORK • OXFORD • PARIS • SAN DIEGO
SAN FRANCISCO • SINGAPORE • SYDNEY • TOKYO
William Andrew is an imprint of Elsevier

Every good and perfect gift is from above, coming down from The Almighty.

Thanks be to God for his blessings and this wonderful life!

I would like to dedicate this book to my parents for making me who I am today. This is a special moment to remember and thank all my teachers, research mentors, and professors who have been the guiding light throughout my career. A very special thanks to Prof. G. Thomas Kluemper, Prof. Sarandeep Huja, and Prof. James K. Hartsfield Jr. for being a source of immense motivation and moral support.

Karthikeyan Subramani

I would like to dedicate this book to my father, Muhammed Mukhtar, and mother, Shamim Anwar, for their unconditional love and guidance, and to my family—Rihana, Aisha, Imran, Omar, Usman, and Adam—who have provided an environment of fun and happiness for my work to flourish. Thank you to the most beautiful little girl in the whole wide world, my granddaughter Zoya, for coming into my life and lighting it up with joy and happiness.

Waqar Ahmed

I would like to dedicate this book to my parents Jim and Shirley, to my loving wife Karen, our son Kennedy of whom we are very proud, and our grandson Clayton. Special thanks to all my teachers, faculty, students, and patients, from whom I continue to learn.

James K. Hartsfield Jr.

William Andrew is an imprint of Elsevier
225 Wyman Street, Waltham, 02451, USA
The Boulevard, Langford Lane, Kidlington, Oxford OX5 1GB, UK

First edition 2013

Notice

Knowledge and best practice in this field are constantly changing. As new research and experience broaden our understanding, changes in research methods, professional practices, or medical treatment may become necessary.

Practitioners and researchers must always rely on their own experience and knowledge in evaluating and using any information, methods, compounds, or experiments described herein. In using such information or methods they should be mindful of their own safety and the safety of others, including parties for whom they have a professional responsibility.

To the fullest extent of the law, neither the Publisher nor the authors, contributors, or editors, assume any liability for any injury and/or damage to persons or property as a matter of products liability, negligence or otherwise, or from any use operation of any methods, products, instructions, or ideas contained in the material herein.

Library of Congress Cataloging-in-Publication Data
A catalog record for this book is available from the Library of Congress

British Library Cataloguing-in-Publication Data
A catalogue record for this book is available from the British Library

ISBN: 978-1-4557-3127-5

Typeset by MPS Limited, Chennai, India
www.adi-mps.com

Printed and bound in United States of America

13 14 15 11 10 9 8 7 6 5 4 3 2 1

Foreword by Professor C.N.R. Rao

I am glad to write a foreword for this book which, for the first time, focuses on clinical applications of nanotechnology and nanobiomaterials in dentistry.

At a fundamental level, nanotechnology helps to manipulate individual atoms and molecules to produce novel structures with unique properties or improved properties. It involves the production and applications of physical, chemical, and biological systems and materials at a size scale ranging 1−100 nm. Even though nanotechnology was first introduced over half a century ago, its progress has been slow, but in the last decade, nanotechnology has caught the imagination of scientists and the general public. Nanotechnology offers us the ability to design materials with totally new desirable characteristics. Nanotechnology can be approached in two ways: "top-down" and "bottom-up" approaches. The "top-down" approach has resulted in remarkable breakthroughs. This approach has been responsible for the rapid development of the semiconductor industry. Future impact of this approach will depend on how quickly we reach the limits in lithographic technologies. Much progress has been made in integrating nanostructured materials into larger systems. The "bottom-up" approach refers to the construction of macromolecular structures from atoms or molecules that self-assemble to form macroscopic structures. The "bottom-up" approach represents "molecular nanotechnology." The field of nanotechnology is diverse, involving the need for a good understanding of biology, chemistry, physics, and mathematics. Extensive research is being carried out worldwide to understand the advantages and scientific limitations of nanotechnology and its applications to a wide range of disciplines from materials science and biomedical research to space research.

Much has been written on the fundamental aspects of nanotechnology. This book is refreshing because it deals with recent studies and techniques used in nanotechnology to produce newer biomaterials for practical applications in clinical dentistry. Even though progress in the application of nanotechnology in biological systems and medicine has been much slower, it is evident that the "bottom-up" approach is potentially far more as we develop the ability to control and manipulate atoms and molecules more precisely. Nature uses the bottom-up approach and builds diverse structures in biological systems. The complexity and functionality of these structures is truly amazing. If we can control in fine detail the way in which these structures can be produced in the same way as nature does, remarkable and rapid advances can be made in the field of medicine and dentistry.

In recent years, there has been an explosive growth in the application of nanotechnology in medicine and dentistry. New drug delivery systems based on nanocarriers are being developed for treating diseases such as cancer, asthma, and diabetes. These developments are likely to accelerate in the future. The development of numerous new products may have a considerable economic impact.

There is intense research activity in the nanotechnology in dentistry with numerous publications appearing. Last year Subramani and Ahmed put together the first comprehensive text, *Emerging Nanotechnologies in Dentistry*. This was useful and timely for both experts and novices. However, developments in the applications of dentistry have been so rapid that they decided to work on this text along with Professor Hartsfield.

This book brings together recognized experts from across the globe to focus on clinical applications of nanobiomaterials in a comprehensive way with 24 chapters. The authors come from a number of countries including the United States, United Kingdom, Australia, Canada, Israel, Mexico, Germany, Brazil, Jordan, China, Taiwan, Korea, Japan, Oman, Hong Kong, Czech Republic, and Iran and represent many laboratories in both academia and industry which are in the forefront of the subject. Since no single person can be an expert in this vast field of nanotechnology, this book provides information that enables everyone to learn something valuable and interesting. It is written in a way that both experts and novices can benefit.

This comprehensive book will be a valuable addition as a textbook in university libraries and laboratories and as a reference source for members of the scientific, industrial, and clinical community.

The editors, Subramani, Ahmed, and Hartsfield, should be congratulated for bringing the experts together to produce a timely, useful, and comprehensive text on nanobiomaterials in clinical dentistry. I hope that readers will enjoy the book and find it useful.

Professor C.N.R. Rao
Jawaharlal Nehru Centre for Advanced Scientific Research,
Bangalore, Karnataka, India

Foreword by Professor Peixuan Guo

I am pleased to be writing a foreword for this book as nanotechnology is one of the most exciting and dynamic fields to emerge over the last century. Considerable investment, effort, and time have been spent on fundamental research and new applications of nanotechnology. New insights have emerged from scientists from multiple disciplines working together. Newer applications have been developed that have had a major impact in several industries such as semiconductors, aerospace, automotive, biomedical field, and cosmetics. Recently research and development has intensified in the field of medical nanotechnology where it is being used for drug delivery systems, medical implants, and dental and pharmaceutical products. Major diseases such as cancer, diabetes, and asthma are already being treated using nanotechnology for targeted controlled drug delivery systems. The "bottom-up" approach used by nature is being exploited and once we can precisely control the behavior of atoms and molecules, we will be able to make a staggering array of new products for a far wider range of applications.

Nanotechnology has been commonly defined as the manipulation and control of materials at the atomic and molecular level at a scale between 10 and 100 nm. This is an interesting scale because at this level the properties of materials are being defined and interesting phenomena occur. Japanese researchers are looking at it from a commercial perspective much more than the West. They define nanotechnology as a technology that will produce quantum leaps in producing new products and generating a great deal of wealth and contributing to a global economy. China is investing huge resources and efforts into nanotechnology, and it is widely agreed that this field is expected to have a massive impact on commercial applications in the near future.

It appears that Nobel laureate Richard P. Feynman's vision of nanotechnology outlined in his classic science lecture "There is Plenty of Room at the Bottom" in 1959 is finally being realized. He envisioned nanorobots and nanomachines that can do amazing things inside the body being built atom by atom. He predicted new materials having properties never seen before being created. This was years before the revolutionary "microchip" was developed. You can see how this has impacted our society by walking into any electronics store anywhere in the world or by almost everyone carrying mobile phones, computers and laptops, and the whole range of electronic equipment in homes and in cars. Nanoelectronics is huge commercially.

The academic importance of nanotechnology has been realised and acknowledged by several scientists winning Nobel prizes after Feynman for their work on nanotechnology notably Robert F. Curl Jr., Sir Harold W. Kroto, and Richard E. Smalley for the discovery of C_{60} in 1996 and much more recently in Physics 2010 to Andre Geim and Konstantin Novoselov for groundbreaking experiments regarding the two-dimensional material graphene.

Even though nanotechnology is already having a huge impact commercially, I feel that we have only scratched the surface and there is a vast array of new applications and products that will be exploiting this dynamic field. In the near future almost every product on the market will be making use of nanotechnology in one form or another. For example, research into nanotechnology in medicine and dentistry has exploded with a large number of research papers appearing from all over the

world. In 2012, Karthikeyan and Ahmed published the first comprehensive book on "Emerging nanotechnologies in dentistry." The pace of activity in nanotechnology in dentistry is so rapid that this new book became necessary. It focuses on "Nanobiomaterials in clinical dentistry." Karthikeyan, Ahmed, and Hartsfield have brought together a group of international experts from multiple backgrounds to explore a range of topics. This book contains 24 comprehensive chapters written in the unique style of the authors. This book will be useful to dental surgeons, specialists, engineers, scientists, physicists, chemists, biologists, materials scientists, and decision and policy makers at undergraduate, post graduate, and specialist levels. Since no one individual can be an expert in all aspects of nanotechnology and its applications, this book will be useful for anyone with an interest in the field. I hope that you find this book stimulating, enjoyable, and useful, and that it ignites further interest in this field.

Professor Peixuan Guo

William Farish Endowed Chair in Nanobiotechnology, Director of Nanobiotechnology Center, College of Pharmacy, University of Kentucky, Lexington, KY, USA

Acknowledgments

There has been an explosion of activity in the last few years in the research and development of nanobiomaterials for clinical applications in dentistry. Once again, as with our first book, we have had the pleasure and privilege of working with world-class experts who wrote the high-quality chapters included in this book. We are grateful for their dedication and hard work in writing the chapters in a timely manner. We would like to extend our thanks and appreciation to the following authors for their valuable time and hard work: Abdelbary Elhissi, Seyed Shahabeddin Mirsasaani, Mehran Hemati, Ehsan Sadeghian Dehkord, Golnaz Talebian Yazdi, Danesh Arshadi Poshtiri, Mrinal Bhattacharya, Wook-Jin Seong, Shin-Woo Ha, M. Neale Weitzmann, George R. Beck Jr., Abdul Samad Khan, Maria Khan, Ihtesham Ur Rehman, Hockin H. K. Xu, Lei Cheng, Ke Zhang, Mary Anne S. Melo, Michael D. Weir, Joseph M. Antonucci, Nancy J. Lin, Sheng Lin-Gibson, Laurence C. Chow, Xuedong Zhou, M. Nassif, F. El Askary, M. Hannig, C. Hannig, D.B. Barbosa, D.R. Monteiro, A.S. Takamyia, E.R. Camargo, A.M. Agostinho, A.C.B. Delbem, J.P. Pessan, R.P. Allaker, Sarandeep Huja, G. Thomas Kluemper, Lorri Morford, Tarek El-Bialy, Meir Redlich, Reshef Tenne, Ki Young Nam, Chul Jae Lee, Sandhra M. Carvalho, Agda A. R. Oliveira, Elke M. F. Lemos, Marivalda M. Pereira, Sandrine Lavenus, Julie Rozé, Guy Louarn, Pierre Layrolle, Kaifu Huo, Lingzhou Zhao, Paul K. Chu, Qing Cai, Reji T. Mathew, Xiaoping Yang, R. Dziak, K. Mohan, B. Almaghrabi, Y. Park, Shengbin Huang, Tingting Wu, Haiyang Yu, Sami Chogle, Bassam Kinaia, Harold Goodis, Chamindie Punyadeera, Paul D. Slowey, Elizabeth Piñón-Segundo, Néstor Mendoza-Muñoz, David Quintanar-Guerrero, Yashwant Pathak, and Charles Preuss.

We were fortunate to get Forewords for this book written by Prof. C. N. R. Rao and Prof. Peixuan Guo.

We are thankful to the entire team of Elsevier for bringing this book in its finest form and quality.

We hope that this book inspires our readers to explore more into the science of nanobiomaterials and their clinical application in dentistry and that they find this work useful.

Karthikeyan Subramani, Waqar Ahmed and James K. Hartsfield, Jr.

CHAPTER

Introduction to Nanotechnology

1

Waqar Ahmed[a], **Abdelbary Elhissi**[a] **and Karthikeyan Subramani**[b]

[a]*Institute of Nanotechnology and Bioengineering, School of Computing, Engineering and Physical Sciences, University of Central Lancashire, Preston, UK*

[b]*Department of Orthodontics, University of Kentucky, Lexington, KY, USA*

CHAPTER OUTLINE

1.1 Introduction

Nanotechnology has been around since the beginning of time. Nature routinely has always used nanotechnology to synthesize molecular structures in the body such as enzymes, proteins, carbohydrates, and lipids which form components of cellular structures. However, the discovery of nanotechnology has been widely attributed to the American Physicist and Nobel Laureate Dr. Richard Phillips Feynman [1] who presented a paper called

"There is plenty of room at the bottom"

in December 29, 1959, at the annual meeting of the American Physical Society at California Institute of Technology. Feynman talked about the storage of information on a very small scale, writing and reading in atoms, about miniaturization of the computer, building tiny machines, tiny factories, and electronic circuits with atoms. He stated that "In the year 2000, when they look back at this age, they will wonder why it was not until the year 1960 that anybody began seriously to move in this direction." However, he did not specifically use the term nanotechnology. The first use of the word

"nanotechnology" has been attributed to Tanaguchi [2] in a paper published in 1974 "On the basic concept of nanotechnology." Dr. K. Eric Drexler an MIT graduate later took Feynman's concept of a billion tiny factories and added the idea that they could make more copies of themselves, via computer control instead of control by a human operator, in his 1986 book *Engines of Creation: The Coming Era of Nanotechnology*, to popularize the potential of nanotechnology.

Several definitions of nanotechnology have since then evolved. For example, the dictionary [3] definition states that nanotechnology is "the art of manipulating materials on an atomic or molecular scale especially to build microscopic devices." Other definitions include the US government [4] which state that "Nanotechnology is research and technology development at the atomic, molecular or macromolecular level in the length scale of approximately 1−100 nm range, to provide a fundamental understanding of phenomena and materials at the nanoscale and to create and use structures, devices and systems that have novel properties and functions because of their small and/or intermediate size." The Japanese [5] have come up with a more focused and succinct definition. "True Nano": as nanotechnology which is expected to cause scientific or technological quantum jumps, or to provide great industrial applications by using phenomena and characteristics peculiar in nanolevel.

It is evident regardless of the definition used that the properties of matter are controlled at a scale between 1 and 100 nm. For example, chemical properties take advantage of large surface to volume ratio for catalysis, interfacial and surface chemistry is important in many applications. Mechanical properties involve improved strength hardness in lightweight nanocomposites and nanomaterials, altered bending, compression properties, and nanomechanics of molecular structures. Optical properties involve absorption and fluorescence of nanocrystals, single photon phenomena, and photonic band gap engineering. Fluidic properties give rise to enhanced flow using nanoparticles and nanoscale adsorbed films are also important. Thermal properties give increased thermoelectric performance of nanoscale materials, and interfacial thermal resistance is important.

1.2 Approaches to nanotechnology

Numerous approaches have been utilized successfully in nanotechnology and as the technology develops further, approaches may emerge. The approaches employed thus far have generally been dictated by the technology available and the background experience of the researchers involved. Nanotechnology is a truly multidisciplinary field involving chemistry, physics, biology, engineering, electronics, and social sciences, which need to be integrated together in order to generate the next level of development in nanotechnology. Fuel cells, mechanically stronger materials, nanobiological devices, molecular electronics, quantum devices, carbon nanotubes (CNTs), etc. have been made using nanotechnology. Even social scientists are debating ethical use of nanotechnology.

The "top-down" approach involves fabrication of device structures via monolithic processing on the nanoscale and has been used with spectacular success in the semiconductor devices used in consumer electronics. The "bottom-up" approach involves the fabrication of device structures via systematic assembly of atoms, molecules, or other basic units of matter. This is the approach nature uses to repair cells, tissues, and organ systems in living things and indeed for life processes such as protein synthesis. Tools are evolving which will give scientists more control over the synthesis and characterization of novel nanostructures yielding a range of new products in the near future.

1.3 Nanotechnology on a large scale and volume

Nanotechnology is being researched extensively internationally, and governments and research organizations are spending large amounts of money and human resources on nanotechnology. This has generated interesting scientific output and potential commercial applications, some of which have been translated into products produced on a large scale. However, in order to realize commercial benefits far more from lab-scale applications need to be commercialized, and for that to happen nanotechnology needs to enter the realm of nanomanufacturing. This involves using the technologies available to produce products on a large scale, which is economically viable. A nanomanufacturing technology should be:

- capable of producing components with nanometer precision,
- able to create systems from these components,
- able to produce many systems simultaneously,
- able to structure in three dimensions,
- cost-effective.

1.3.1 Top-down approach

The most successful industry utilizing the top-down approach is the electronics industry. This industry is utilizing techniques involving a range of technologies such as chemical vapor deposition (CVD), physical vapor deposition (PVD), lithography (photolithography, electron beam, and X-ray lithography), wet and plasma etching to generate functional structures at the micro- and nanoscale (Figure 1.1). Evolution and development of these technologies have allowed the emergence of numerous electronic products and devices that have enhanced the quality of life throughout the world. The feature sizes have shrunk continuously from about 75 μm to below 100 nm. This has been achieved by improvements in deposition technology and more importantly due to the development of lithographic techniques and equipment such as X-ray lithography and electron beam lithography.

Techniques such as electron beam lithography, X-ray lithography, and ion beam lithography, all have advantages in terms of resolution achieved; however, there are disadvantages associated with cost, "optics," and detrimental effects on the substrate. These methods are currently under investigation to improve upon current lithographic processes used in the integrated circuits (IC) industry. With continuous developments in these technologies, it is highly likely that the transition from microtechnology to nanotechnology will generate a whole new generation of exciting products and features.

A demonstration of how several techniques can be combined together to form a "nano" wine glass (Figure 1.2). In this example, a focused ion beam and CVD have been employed to produce this striking nanostructure.

The top-down approach is being used to coat various coatings to give improved functionality. For example, vascular stents are being coated using CVD technology with ultrathin diamond-like carbon coatings in order to improve biocompatibility and blood flow (Figure 1.3). Graded a-SixCy:H interfacial layers results in greatly reduced cracking and enhanced adhesion.

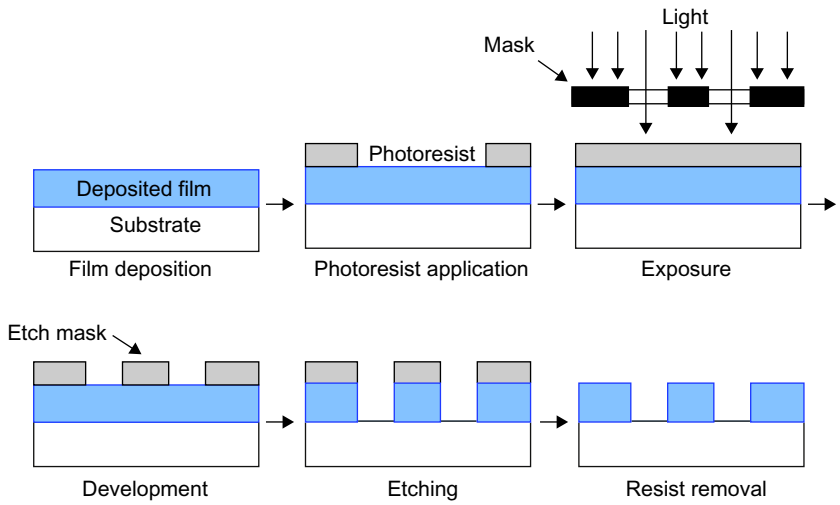

FIGURE 1.1

A typical process sequence employed in the electronics industry to generate functional devices at the micro- and nanoscale [6].

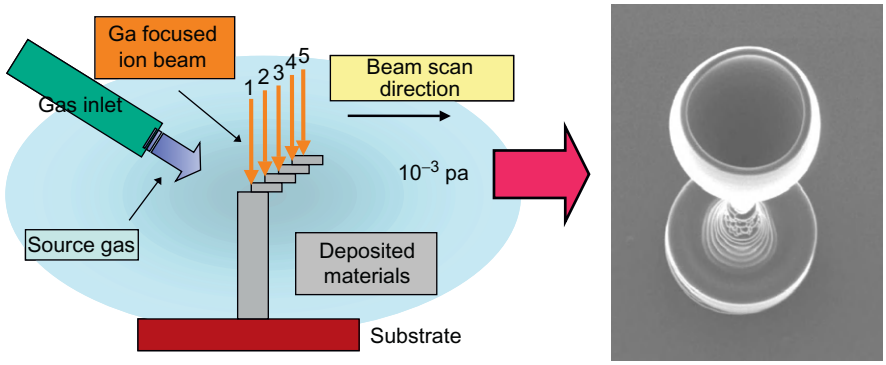

FIGURE 1.2

Demonstration of three-dimensional nanostructure fabrication [7].

1.3.2 Bottom-up approach

The bottom-up approach involves making nanostructures and devices by arranging atom by atom. The scanning tunneling microscope (STM) has been used to build nanosized atomic features such as the letters IBM written using xenon atoms on nickel [8] (Figure 1.4). While this is beautiful and exciting, it remains that the experiment was carried out under carefully controlled conditions (i.e., liquid helium cooling, high vacuum), and it took something like 24 h to get the letters right. Also

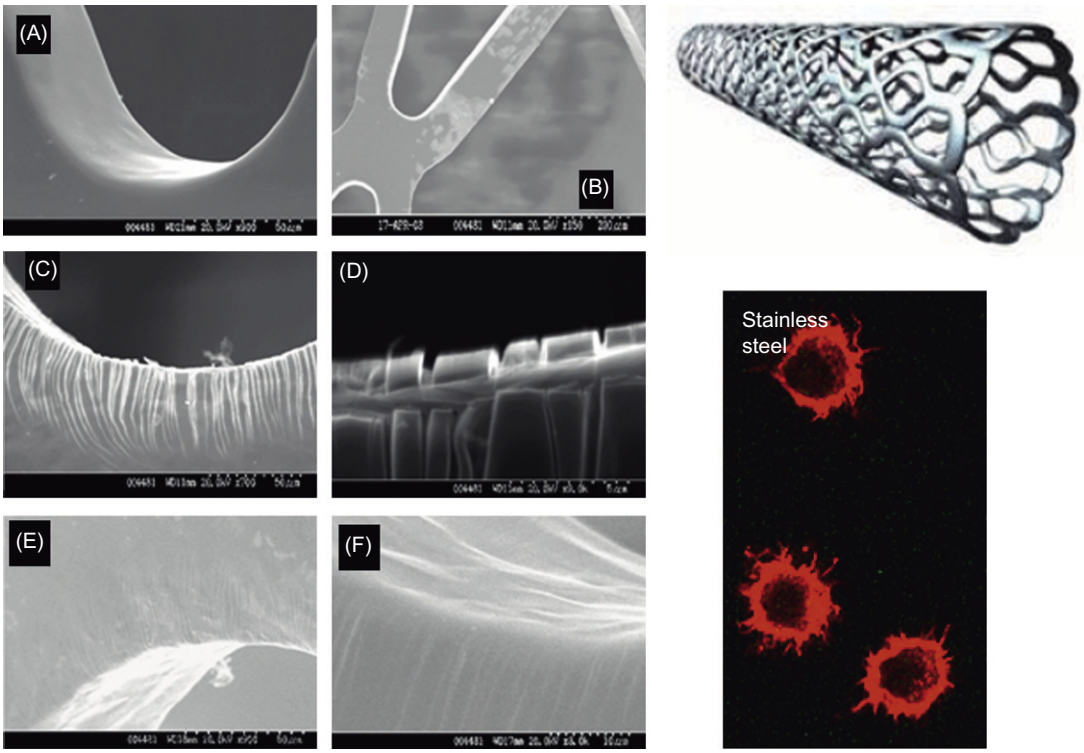

FIGURE 1.3

Examples of stents coated with diamond-like carbon using plasma enhanced CVD (Okpalugo, private communication, 2007).

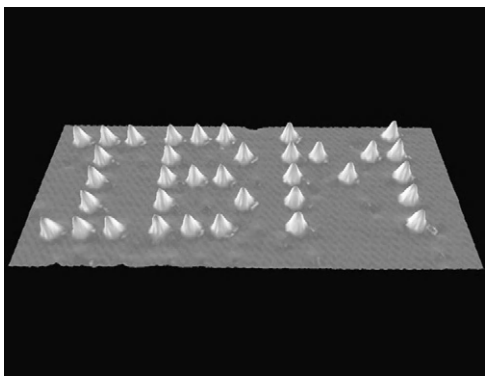

FIGURE 1.4

Positioning single atoms with an STM [8].

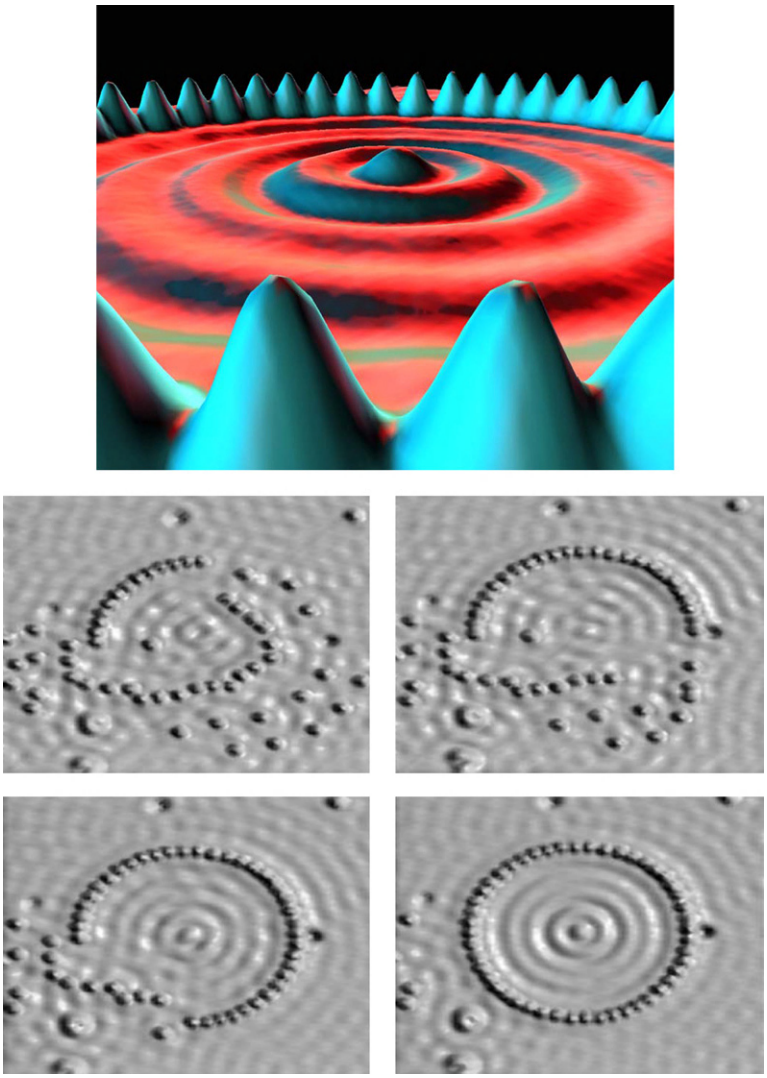

FIGURE 1.5

Confinement of electrons to quantum corrals on a metal surface [8].

the atoms are not bonded to the surface just adsorbed and a small change in temperature or pressure will dislodge them. Since this demonstration, significant advances have been made in nanomanufacturing.

The discovery of the STM's ability to image variations in the density distribution of surface state electrons created in the artists a compulsion to have complete control of not only the atomic

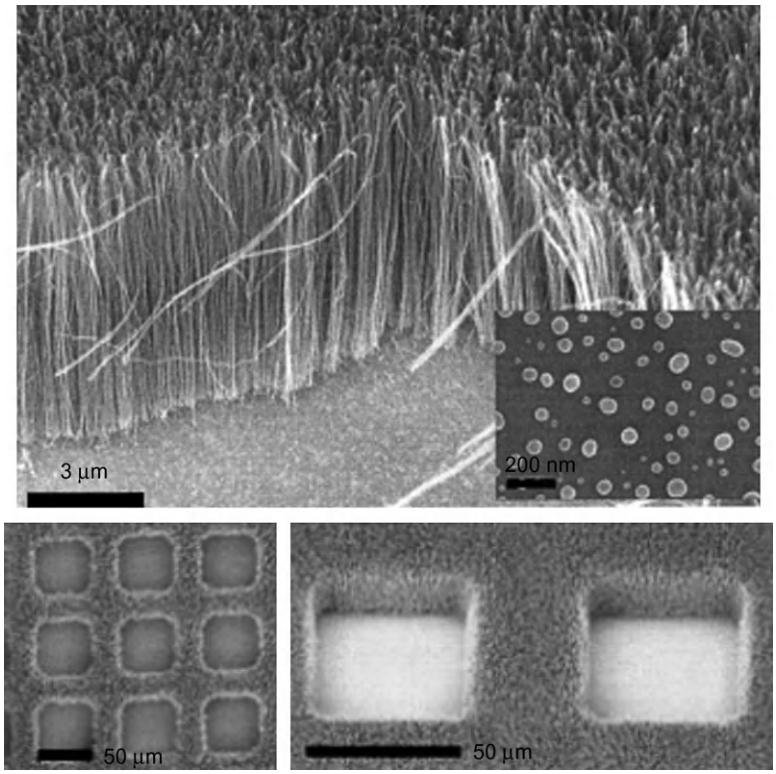

FIGURE 1.6

MWNTs with a diameter of 30 nm and length of 12 μm have been formed within 2 min [10].

landscape, but also the electronic landscape [9]. Here they have positioned 48 iron atoms into a circular ring in order to "corral" some surface state electrons and force them into "quantum" states of the circular structure (Figure 1.5). The ripples in the ring of atoms are the density distribution of a particular set of quantum states of the corral. The artists were delighted to discover that they could predict what goes on in the corral by solving the classic eigenvalue problem in quantum mechanics—a particle in a hard-wall box.

Probably the most publicized material in recent years has been CNTs. CNTs, long, thin cylinders of carbon, were discovered in 1991 by S. Iijima. These are large macromolecules that are unique for their size, shape, and remarkable physical properties. They can be thought of as a sheet of graphite (a hexagonal lattice of carbon) rolled into a cylinder. These intriguing structures have sparked much excitement in recent years and a large amount of research has been dedicated to their understanding. Currently, the physical properties are still being discovered and disputed. What makes it so difficult is that nanotubes have a very broad range of electronic, thermal, and structural properties that change depending on the different kinds of nanotube (defined by its diameter, length, and chirality, or twist). To make things more interesting, besides having a single

cylindrical wall (SWNTs), nanotubes can have multiple walls (MWNTs) cylinders inside the other cylinders.

Bower et al. [10] have grown vertically aligned CNTs using microwave plasma enhanced CVD system using a thin film cobalt catalyst at 825°C (Figure 1.6). The chamber pressure used was 20 Torr. The plasma was generated using hydrogen which was replaced completely with ammonia and acetylene at a total flow rate of 200 sccm.

Lithographic methods are important for micro- and nanofabrication. Lithography: drawing or writing on kind of yellow salty limestone so that impressions in ink can be taken and in the Oxford Dictionary the word Lithos comes from Greek for stone. In micro- and nanofabrication we mean pattern transfer. Due to limitations in current (and future) photolithographic processes, there is a challenge to develop novel lithographic processes with better resolution for smaller features. One such development is that of *Dip-pen nanolithography* (DPN). Dip-pen technology in which ink on a pointed object is transported to a surface via capillary forces is approximately 4000 years old. The difference with DPN is that the pointed object has a tip which has been sharpened to a few atoms across in some cases. DPN is a scanning probe nanopatterning technique in which an AFM tip is used to deliver molecules to a surface via a solvent meniscus, which naturally forms in the ambient atmosphere. It is a direct-write technique and is reported to give high-resolution patterning capabilities for a number of molecular and biomolecular "inks" on a variety of substrates, such as metals, semiconductors, and monolayer functionalized surfaces.

DPN allows one to precisely pattern multiple patterns with good registration. It is both a fabrication and imaging tool, as the patterned areas can be imaged with clean or ink-coated tips. The ability to achieve precise alignment of multiple patterns is an additional advantage earned by using an AFM tip to write as well as read nanoscopic features on a surface. These attributes make DPN a valuable tool for studying fundamental issues in colloid chemistry, surface science, and nanotechnology. For instance, diffusion and capillarity on a surface at the nanometer level, organization and crystallization of particles onto chemical or biomolecular templates, monolayer etching resists for semiconductors, and nanometer-sized tethered polymer structures can be investigated using this technique. In order to create stable nanostructures, it is beneficial to use molecules that can anchor themselves to the substrate via chemisorption or electrostatic interactions. When alkane thiols are patterned on a gold substrate, a monolayer is formed in which the thiol head groups form relatively strong bonds to the gold and the alkane chains extend roughly perpendicular to surface. Creating nanostructures using DPN is a single step process which does not require the use of resists. Using a conventional atomic force microscope (AFM), DPN has been reported to achieve ultrahigh-resolution features with line widths as small as 10−15 nm with approximately 5 nm spatial resolution. For nanotechnological applications, it is important not only to pattern molecules in high resolution, but also to functionalize surfaces with patterns of two or more components (Figure 1.7).

Figure 1.8 shows the basic concept of nanomanufacturing. Individual atoms, which are given in the periodic table, form the basis of nanomanufacturing. These can be assembled into molecules and various structures using various methods including directed self-assembly and templating, and may be positioned appropriately depending on the final requirements. Further along the devices architecture, integration, in situ processing may be employed culminating in nanosystems, molecular devices, etc.

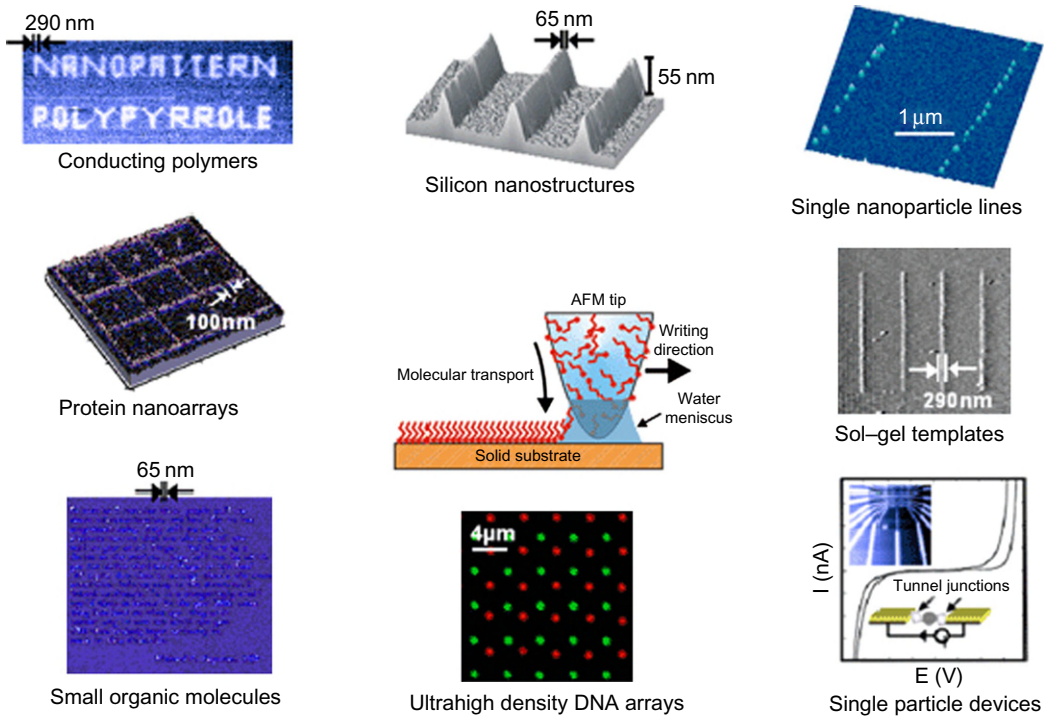

FIGURE 1.7

Some of the potential applications of DPN (Byrne, private communication, 2006).

1.4 Applications

Over the years, developments in dentistry have made many dental treatment procedures fast, reliable, safe, and much less painful. New technologies such as nanotechnology, dental implantology, cosmetic surgery, use of lasers, and digital dentistry have had great impact on dental treatment methodologies and recovery time. Even though the concept of nanotechnology has always existed, its discovery is attributed to Richard Feynman who won the Nobel Prize in 1959 for his theories regarding nanosized devices. In the field of medicine, nanotechnology has been applied in diagnosis, prevention, and treatment of diseases. Nanotechnology offers considerable scope in dentistry to improve dental treatment, care and prevention of oral diseases. The following chapters in this book discuss about the recent developments in this interdisciplinary field bridging nanotechnology and dentistry.

Nanotechnology has been in dentistry for tooth sealants and fillers that use nanosized particles to improve their strength, luster, and resist wear. The application of nanoparticles in dental materials and their synthesis has been discussed in the next chapter. Antimicrobial nanoparticles in restorative composite materials are being used to prevent dental caries. For example, silver particles as antibacterial agents when used in fillers and toothpastes can retard bacterial growth and reduce

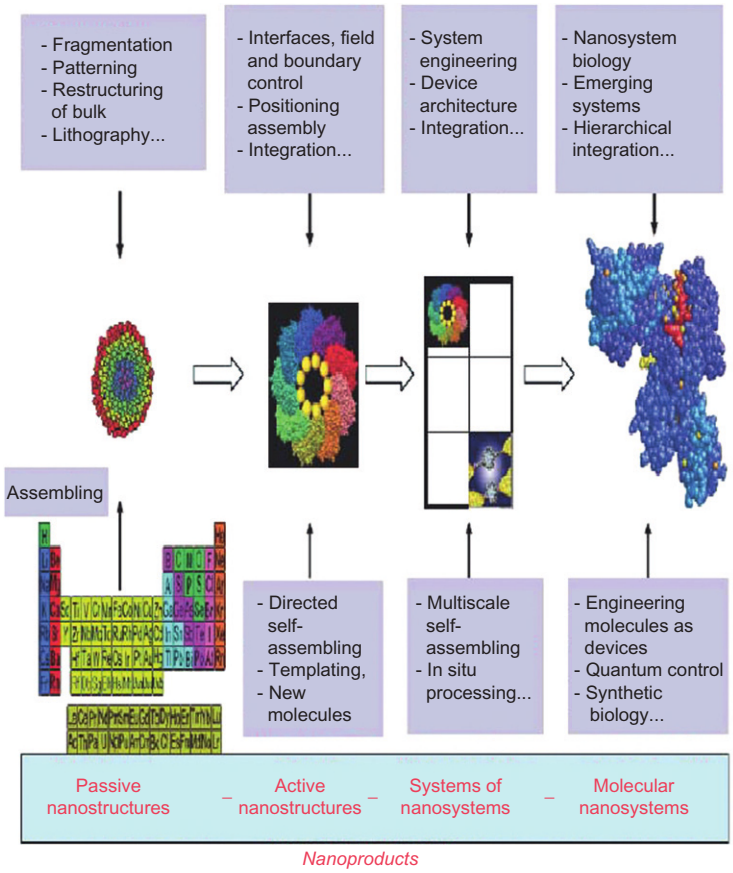

FIGURE 1.8

Summary of nanotechnology [11].

tooth decay. It is envisaged that in the longer term, biomimetic approaches and nanotechnology will be used to repair and rebuild damaged enamel. Composite materials are becoming popular due to their esthetic appearance and superior wear properties designed to replicate the properties of enamel. The properties of these materials such as compressive strength, material flow, tensile strength, and flexural strength have been improved using nanotechnology. Microfill composites are made using the top-down approach to nanotechnology where materials such as ceramics, quartz, and glasses start off as bulk materials and then they are ground into particle sizes below 100 nm. However, nanocomposites are made using a bottom-up approach where atoms and molecules combine to produce nanoparticles much smaller than those produced by the first approach.

Nanoparticle-based drug delivery systems have been widely used in targeted treatment of various forms of cancer. For example, liposomes can be used for drug delivery in oral cancer and asthma applications. The basic structures of liposomes are shown in Figure 1.9.

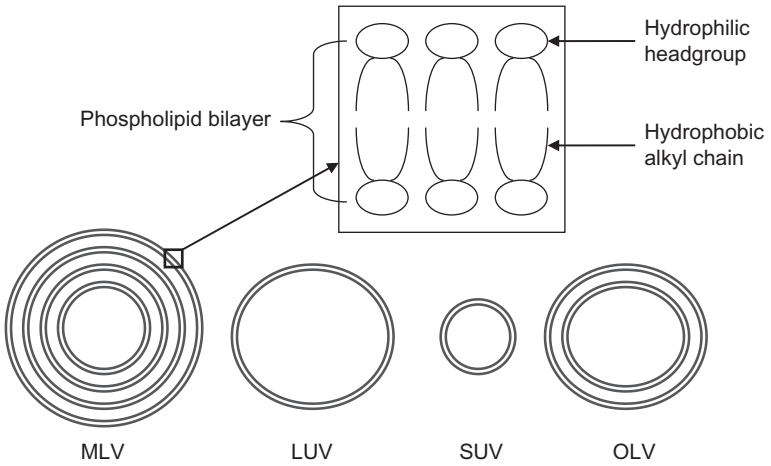

FIGURE 1.9

Types of liposomes based on microscopic morphology. Liposomes bilayers (lamella) are made of phospholipid molecules each having a cylindrical geometry. MLV = multilamellar liposome/vesicle; LUV = large unilamellar liposome/vesicle; SUV = small unilamellar liposome/vesicle; OLV = oligolamellar liposome/vesicle.

Liposomes are promising drug delivery carriers owing to their safety, biocompatibility, and biodegradability. However, liposomes are unstable in aqueous dispersions and most of the methods used to prepare liposomes are unsuitable for large-scale production. This review has come across a range of technologies which may be applied to scale up the production of stable liposomes. These include freeze drying (lyophilization) to produce powdered liposome formulations or proliposome technologies to produce liposome precursor formulations. Various types of liposomes have been manufactured with biological functionality. These are summarized below.

The biological functionality of liposomes is determined by liposome size and bilayer composition. Accordingly, liposomes are classified into conventional liposomes, cationic liposomes, thermosensitive liposomes, pH-sensitive liposomes, long-circulating (sterically stabilized) liposomes, and ultradeformable liposomes. Some liposome formulations may however fall under more than one category. For instance, inclusion of certain copolymers within pH-sensitive liposomes may enhance their escaping tendency from the blood phagocytes and hence such liposomes can be classified as both pH sensitive and long circulating.

Conventional liposomes are multilamellar vesicles (MLVs) made of lipids having neutral or negative charge. These liposomes are large, and because of their surface characteristics they are readily cleared from blood circulation by reticuloendothelial system (RES) cells and hence they have short biological half-life. Conventional liposomes are most commonly used in research to investigate the entrapment of compounds and their release profiles. They are commonly studied as model biological membranes.

Delivery of gene to diseased cells may repair the cause of the disease. This approach of delivery is commonly called gene therapy. Because DNA molecules are very large, their ability to penetrate the target cell and be expressed may be poor. This necessitates the presence of safe carriers, such

as liposomes to facilitate the internalization of the genetic material into the cell. Cationic liposomes contain positively charged lipids such as *N*-[1-(2,3-dioleoyloxy)propyl] *N*,*N*,*N*-trimethylammonium chloride (DOTAP) which may complex with negatively charged macromolecules (e.g. DNA and siRNA) to be used in gene therapy. The presence of fusogenic phospholipids such as 1,2-didecanoyl-*sn*-glycero-3-phosphocholine (DOPE) within formulation may facilitate the fusion of liposomes with the target cells to enhance the internalization of the genetic material.

Thermosensitive liposomes are made from phospholipids whose membrane undergoes the gel-to-liquid crystalline phase transition a few degrees above physiological temperature. Increasing the temperature of tumor cells using an external source may induce drug release from thermosensitive liposomes at the tumor site. It has been recently shown that when certain copolymers incorporated in liposome bilayers, the vesicles become thermosensitive and the tumor targeting is enhanced upon induction of hyperthermia.

Liposomes can be made by incorporating a phospholipid which becomes destabilized or fusogenic under the slightly acidic conditions of inflamed tissues or tumors, to release the encapsulated therapeutic material intracellularly. This approach has been suggested by including phospholipids such as palmitoyl homocysteine or a mixture of oleic acid and phosphatidylethanolamine (3:7 mole ratio), which causes the resultant liposomes to fuse with endosomal membrane (pH 5−6.5) and release the entrapped contents. Formation of the inverted hexagonal phase is believed to be responsible for the fusogenic propensity of some lipids at mild acidic environments. An approach to preparation of pH-sensitive liposomes is to include materials within the liposomes that maintain the bilayers stable at the physiological pH of the blood (pH 7.4) while undergo instability at the mildly acidic environment inside the target cell, most specifically in the late endosomes. This can result in fusion of the liposome vesicles with the membranes of the late endosomes and subsequent release of the liposome-encapsulated contents in the cytosol, avoiding degradation in the lysosomes.

Conventional liposomes are rapidly cleared by the RES of the blood circulation. The rapid clearance may be overcome by the inclusion of certain amphiphiles within liposome formulation such as monosialoganglioside (GM_1), hydrogenated phosphatidylinositol (HPI), or more recently the hydrophilic polymers polyethylene glycol. Incorporation of polyethylene glycol is nowadays considered a novel strategy in manufacturing biologically stable liposomes. This technology of liposome manufacture is termed the Stealth™ technology, and liposomes made by using this method are termed PEGylated, sterically stabilized or long-circulating liposomes. Steric stabilization has resulted in the marketing of PEGylated doxorubicin HCl liposomes as Doxil® in The United States and Caelyx® in Europe, for the treatment of Kaposi's sarcoma.

Liposomes can be made elastic or ultradeformable by inclusion of certain surfactants or cosolvents within liposome formulation in certain concentrations to make the vesicles able to pass through the narrow pores of the skin and deliver associated small or large molecules. Ultradeformable liposomes have been reported to be more efficient in transdermal delivery of therapeutic agents compared to conventional liposomes such as in the delivery of protein vaccine, anticancer immunotherapeutic agent's gene, and dexamethasone. Cationic liposomes have been prepared by inclusion of sodium cholate to be ultradeformable. The resultant vesicles have been reported to enhance gene transportation through the skin.

1.5 Future considerations

Biomedical scientists and clinicians all over the world are working toward prevention and early delivery of care to maintain human health. It is envisaged that nanotechnology will have a great impact in dental research and improvement in current treatment methodologies leading to superior oral health care in the near future.

Nanomaterials will be used far more widely and will yield superior properties and when combined with biotechnology, laser and digital guided surgery will thus provide excellent dental care. Smarter preventive measures and earlier interventions to avert craniofacial disorders using nanodiagnostics seem a reality. Nanotechnology research will definitely pave the way for development of tools, which would allow clinicians to diagnose and treat oral malignancies at their earliest stage.

Biomimetics and nanotechnology have given us the knowledge to bioengineer lost tooth and remineralization of carious lesions. This is one field which has stimulated immense interest among the dental and nanotechnology researchers. Salivary glands can be a gateway to the body for the delivery of precise molecular therapies using nanoparticle-based drug delivery systems with fewer side effects. Nanofillers have improved the esthetic, physical, and mechanical properties of dental composite materials.

Futuristic applications have been proposed on utilizing nanobots (nanoscale robots) to treat carious lesions, dentin hypersensitivity, induce dental anesthesia, teeth repositioning (using orthodontic nanobots that could directly manipulate periodontal tissues allowing rapid, painless movement). Dentifrobots (nanorobots in dentifrices) delivered through mouthwash or toothpaste could patrol supra- and subgingival surfaces of tooth performing continuous plaque/calculus removal and metabolize trapped organic matter into harmless and odorless vapor. These proposals may seemingly look outrageous, but inventions have always been the brainchildren of outrageous ideas of the scientific community. Predictive tools like “lab-on-a-chip” can utilize saliva as a media to diagnose dental and other physical anomalies of the human body.

1.6 Nanobiomaterials in clinical dentistry

There has been a huge surge in the number of studies over the recent few years focusing on the clinical applications of nanobiomaterials in dentistry. This book aims to address these recent developments and is an effort to bring concepts and research studies in this interdisciplinary field under one roof. The book has been divided into various sections to give the readers an idea about the specific applications and uses of nanobiomaterials in various dental specialties like preventive dentistry, orthodontics, prosthodontics, periodontics, implant dentistry, dental tissue engineering, and endodontics. The last section discusses the use of saliva for diagnostic purposes and the potential use of nanoparticles as dental drug delivery systems and their biocompatibility/toxicity. While this chapter discusses the basic concepts of nanotechnology, the second chapter gives a general overview of the applications of nanobiomaterials in dentistry. CNTs have been gaining increased interest among the scientific community for their excellent physical and mechanical properties.

Different techniques of CNT manufacturing and its potential applications in dental restorative materials, bone regeneration, and gene delivery have been discussed briefly in Chapter 3. Another interesting group of nanomaterials is silica-based nanomaterials. Their manufacturing techniques, properties, and potential use for skeletal and dental applications are addressed in Chapter 4. The applications of nanoparticles in glass ionomer cements (GICs), dental composite resin, and adhesives used in dentistry are presented in Chapter 5, 6 and 7, respectively. The uses of antimicrobial nanomaterials to prevent biofilm and caries formation are discussed in Chapters 8–10. Chapters 11–13 focus on the applications of nanobiomaterials and nanoscale imaging systems like AFM in orthodontic materials. Potential applications of such nanobiomaterials and how they can improve the current orthodontic armamentarium are also outlined in these chapters. The application of silver nanoparticles incorporated into acrylic-based tissue conditioner to prevent denture stomatitis has been discussed briefly in Chapter 14. Bioactive glass nanoparticles and their application for periodontal regeneration have been presented in Chapter 15.

Chapter 16 discusses the impact of nanotechnology/nanofabrication techniques for dental implants. Chapter 17 addresses the potential applications of titania nanotube coatings for dental implants to enhance osseointegration. Chapter 18 discusses carbon nanotube coatings/scaffolds and their potential applications in dental implants and bone regeneration. In Chapter 19, various nanostructured ceramics evaluated for bone regeneration in oral and maxillofacial complex have been reviewed briefly. Chapter 20 addresses the applications of biomimetics for periodontal and dental tissue regeneration. The potential applications and research studies done on the utilization of nanobiomaterials for endodontics is described in Chapter 21. Chapter 22 covers the applications of saliva as a diagnostic material and the potential use of microelectro mechanical systems/nanoelectro mechanical systems (MEMS/NEMS) as salivary diagnostic tool. Chapter 23 outlines the recent advances in nanoparticles as drug delivery systems in dentistry and Chapter 24 discusses the cytotoxicity of orally delivered nanoparticle on systemic organs.

References

[1] R.P. Feynman, There is plenty of room at the bottom, Eng. Sci. 23 (1960) 22–36 and <www.zyvex.com/nanotech/feynman.html/> (1959).
[2] N. Tanaguchi, On the basic concept of nanotechnology, in: 1974 Proc. ICPE.
[3] Merriam Webster dictionary 2010.
[4] US government, <http://www.nano.gov/>.
[5] K. Shimizu, INC 2, USA, 2006.
[6] B. Bushan, Springer Handbook of Nanotechnology, 2003, 147–180.
[7] T. Fujii, J. Micromech. Microeng. 15 (2005) S286–S291.
[8] D.M. Eigler, E.K. Schweizer, Positioning single atoms with a scanning tunnelling microscope, Nature 344 (1990) 524–526.
[9] M.F. Crommie, C.P. Lutz, D.M. Eigler, Confinement of electrons to quantum corrals on a metal surface, Science 262 (1993) 218–220.
[10] C. Bower, et al., Appl. Phys. Lett. 77 (2000) 6.
[11] M.C. Roco, NSF Nanoscale Science and Engineering Grantees Conference, December 12–15, 2005.

CHAPTER

Nanotechnology and Nanobiomaterials in Dentistry

2

Seyed Shahabeddin Mirsasaani[a,b], Mehran Hemati[a,c], Tina Tavasoli[d], Ehsan Sadeghian Dehkord[a], Golnaz Talebian Yazdi[a] and Danesh Arshadi Poshtiri[b]

[a]*Biomaterials Group, Faculty of Biomedical Engineering (Center of Excellence), Amirkabir University of Technology, Tehran, Iran*

[b]*Faculty of Dentistry, Tehran University of Medical Sciences, Tehran, Iran*

[c]*Dental School, Shiraz University of Medical Sciences, Shiraz, Iran*

[d]*Biotechnology Engineering Department, Faculty of Engineering, University of Isfahan, Isfahan, Iran*

CHAPTER OUTLINE

2.1 Introduction

Humans have been using nanotechnology for a long time without realizing it. The processes of making steel, vulcanizing rubber, and sharpening a razor all rely on manipulations of nanoparticles. The term "nanotechnology" was coined by Prof. Eric Drexler, a lecturer and researcher of nanotechnology. "Nano" is derived from the Greek word for "dwarf." Nanotechnology is an umbrella term that encompasses all fields of science that operate on the nanoscale. A nanometer is one

Nanobiomaterials in Clinical Dentistry.

billionth of a meter, or three to five atoms in width. It would take approximately 40,000 nanometers lined up in a row to equal the width of a human hair. The basic idea of nanotechnology, used in the narrow sense of the world, is to employ individual atoms and molecules to construct functional structures [1].

In 1959, Nobel award winner Richard Feynman first proposed the seminal idea of nanotechnology by suggesting the development of molecular machines. In his historic lecture in 1959, he concluded saying, "this is a development which I think cannot be avoided" [2]. Ever since, the scientific community has investigated the role that nanotechnology can play in every aspect of science. The intrigue of nanotechnology comes from the ability to control material properties by assembling such materials at the nanoscale. The tunable material properties that nanotechnology can provide were stated in Norio Taniguchi's paper in 1974 where the term "nanotechnology" was first used in a scientific publication [3]. The reason for the omnipresence of the word "nano" as one of the most attractive prefixes in the contemporary materials science is simpler than it seems [4]. Namely, the progress of humanity is underlaid by a continual increase in sensitivity of human interactions with their physical surrounding. As the human societies evolved, the critical length of cutting-edge functional devices has shifted from millimeter to micrometer to nanometer scale. With the scientific ability to control physical processes at nanometer scale, we have entered the era of research and application of nanoscale phenomena. Finally, as material properties often significantly alter following the micro-to-nano shift in the scale at which critical boundaries are found, a new field was born to explain these rather strange phenomena, named nanoscience; the application of its discoveries is known as nanotechnology [5].

Nanotechnologies are on the verge of initiating extraordinary advances in biological and biomedical sciences. These would be associated with both providing the tools for improved understanding of fundamental building blocks of materials and tissues at the nanoscale and designing technologies for probing, analyzing, and reconstructing them. It is not surprising that the development of novel technologies provides the foundations for creation and application of newer and more advanced ones. Expansion of novel technologies, particularly those involved in enriching methods of research, have already changed the way we view and define the standards of high-quality dental materials, tools, and practices. As we see, nanotechnology has favored our understanding of dental materials at the nanoscale and enabled the design of materials with ultrafine architecture [6].

Nanoengineering is one field of nanotechnology. Nanoengineering concerns itself with manipulating processes that occur on the scale of 1–100 nm. Nanoengineering is an interdisciplinary science that builds biochemical structures smaller than bacterium, which function like microscopic factories. This is possible by utilizing basic biochemical processes at the atomic or molecular level. In simple terms, molecules interact through natural processes, and nanoengineering takes advantage of those processes by direct manipulation. Current developments are limited to the creation of nanoscale objects for use as materials in different technologies. Material engineered using nanotechnology is often more precise and durable because of certain properties of matter at extremely small scales [4].

2.2 Nanoscale materials

The nanomaterial field takes a science-based approach to study materials with morphological features on the nanoscale, and especially those that have special properties stemming from their

nanoscale dimensions. Nanoscale is usually defined as smaller than one-tenth of a micrometer in at least one dimension, though this term is sometimes also used for materials smaller than 1 μm. A natural, incidental, or manufactured material containing particles, in an unbound state or as an aggregate or as an agglomerate and where, for 50% or more of the particles in the number size distribution, one or more external dimensions is in the size range 1−100 nm. In specific cases and where warranted by concerns for the environment, health, safety, or competitiveness, the number size distribution threshold of 50% may be replaced by a threshold between 1% and 50% [7].

An important aspect of nanotechnology is the vastly increased ratio of surface area to volume present in many nanoscale materials, which makes possible new quantum mechanical effects. One example is the "quantum size effect" where the electronic properties of solids are altered with great reductions in particle size. This effect does not come into play by going from macro- to microdimensions. However, it becomes pronounced when the nanometer size range is reached. A certain number of physical properties also alter with the change from macroscopic systems. Novel mechanical properties of nanobiomaterials are the subject of nanomechanics research. Catalytic activities also reveal new behavior in the interaction with biomaterials [8]. The chemical processing and synthesis of high-performance technological components for the private, industrial, and military sectors require the use of high-purity ceramics, polymers, glass-ceramics, and material composites. In condensed bodies formed from fine powders, the irregular sizes and shapes of nanoparticles in a typical powder often lead to nonuniform packing morphologies that result in packing density variations in the powder compact [9].

Uncontrolled agglomeration of powders due to attractive Vander Waals forces can also give rise to microstructural inhomogeneity. Differential stresses that develop as a result of nonuniform drying shrinkage are directly related to the rate at which the solvent can be removed and thus highly dependent upon the distribution of porosity. Such stresses have been associated with a plastic-to-brittle transition in consolidated bodies and can yield to crack propagation in the unfired body if not relieved [10,11]. In addition, any fluctuations in packing density in the compact as it is prepared for the kiln are often amplified during the sintering process, yielding inhomogeneous densification. Some pores and other structural defects associated with density variations have been shown to play a detrimental role in the sintering process by growing and thus limiting end-point densities. Differential stresses arising from inhomogeneous densification have also been shown to result in the propagation of internal cracks, thus becoming the strength-controlling flaws [12,13]. It would therefore appear desirable to process a material in such a way that it is physically uniform with regard to the distribution of components and porosity, rather than using particle size distributions which will maximize density. The containment of a uniformly dispersed assembly of strongly interacting particles in suspension requires total control over particle−particle interactions. It should be noted here that a number of dispersants such as ammonium citrate (aqueous) and imidazoline or oleyl alcohol (nonaqueous) are promising solutions as possible additives for enhanced dispersion and deagglomeration. Monodisperse nanoparticles and colloids provide this potential [14]. Monodisperse powders of colloidal silica, for example, may therefore be stabilized sufficiently to ensure a high degree of order in the colloidal crystal or polycrystalline colloidal solid which results from aggregation. The degree of order appears to be limited by the time and space allowed for longer-range correlations to be established. Such defective polycrystalline colloidal structures would appear to be the basic elements of submicrometer colloidal materials science, and, therefore, provide the first step in developing a more rigorous understanding of the mechanisms involved in microstructural evolution in high-performance materials and components [15].

2.2.1 Nanoparticles

Nanoparticles are nanometer-sized particles that are nanoscale in three dimensions. They include nanopores, nanotubes, quantum dots, nanoshells, dendrimers, liposomes, nanorods, fullerenes, nanospheres, nanowires, nanobelts, nanorings, and nanocapsules. The applications of nanoparticles include drug delivery systems, cancer targeting, and dentistry [2]. Nanoparticles are of great scientific interest as they are effectively a bridge between bulk materials and atomic or molecular structures. A bulk material should have constant physical properties regardless of its size, but for the nanoscale this is often not the case. Size-dependent properties are observed such as quantum confinement in semiconductor particles, surface plasmon resonance in some metal particles, and super paramagnetism in magnetic materials [16]. Nanoparticles exhibit a number of special properties relative to bulk material. Nanoparticles often have unexpected visual properties because they are small enough to confine their electrons and produce quantum effects. For example, gold nanoparticles appear deep red to black in solution. The often very high surface-area-to-volume ratio of nanoparticles provides a tremendous driving force for diffusion, especially at elevated temperatures. Sintering is possible at lower temperatures and over shorter durations than for larger particles. This theoretically does not affect the density of the final product, though flow difficulties and the tendency of nanoparticles to agglomerate do complicate matters. The surface effects of nanoparticles also reduce the incipient melting temperature. Nanoparticles are being applied in various industries, including medicine, due to various properties such as increased resistance to wear and the killing of bacteria, but there are worries due to the unknown consequences to the environment and human health [17].

2.2.2 Characterization

The first observations and size measurements of nanoparticles were made during the first decade of the twentieth century. They are mostly associated with the name of Zsigmondy who made detailed studies of gold sols and other nanobiomaterials with sizes down to 10 nm and less. Zsigmondy published a book in 1914. He used an ultramicroscope that employs a dark field method for seeing particles with sizes much less than light wavelength. Applications began in the 1980s with the invention of the scanning tunneling microscope and the discovery of carbon nanotubes and fullerenes. In 2000, the US government founded the National Nanotechnology Initiative to direct nanotechnological development. There are traditional techniques developed during twentieth century in Interface and Colloid Science for characterizing nanobiomaterials. These are widely used for first generation passive nanobiomaterials [18]. These methods include several different techniques for characterizing particle size distribution. This characterization is imperative because many materials that are expected to be nanosized are actually aggregated in solutions. Some of the methods are based on light scattering. Others apply ultrasound, such as ultrasound attenuation spectroscopy for testing concentrated nanodispersions and microemulsions. There is also a group of traditional techniques for characterizing surface charge or zeta potential of nanoparticles in solutions. This information is required for proper system stabilization, preventing its aggregation or flocculation. These methods include microelectrophoresis, electrophoretic light scattering, and electroacoustics. Nanobiomaterials behave differently than other similarly sized particles. It is therefore necessary to develop specialized approaches to testing and monitoring their effects on human health and on the environment [19].

2.2.3 Nanofibers

Nanotechnology has improved the properties of various kinds of fibers. Polymer nanofibers with diameters in the nanometer range possess a larger surface area per unit mass and permit an easier addition of surface functionalities compared to polymer microfibers. Polymer nanofiber materials have been studied as drug delivery systems, scaffolds for tissue engineering, and filters. Carbon fibers with nanometer dimensions showed a selective increase in osteoblast adhesion necessary for successful orthopedic/dental implant applications due to a high degree of nanometer surface roughness [20–23].

2.3 Nanodentistry

Nanodentistry is an emerging field with significant potential to yield new generation of technologically advanced clinical tools and devices for oral health care. There is a hope that nanotechnology will likewise bring tangible benefits to dentistry, from the bench to the clinical level. As described by Saunders [24], the subject of comparing anticipated versus realized in the transition of an emerging technology to the actual practice is not new; however, the pace of application of nanotechnology in dentistry has been less than revolutionary. Nanotechnology has been applied in dentistry in the early 1970s with the beginning of the era of microfills. Nanodentistry is an emerging field with significant potential to yield new generation of technologically advanced materials in prosthodontics. Nanodentistry will make possible the maintenance of comprehensive oral health by employing nanobiomaterials [2,25]. It is noticeable that increases in the versatility of scientific knowledge and the ability to control physical processes at a finer resolution naturally led to more information and, henceforth, to more questions. The broader our knowledge, the more amazement arises in face of the natural wonders [26]. The same could certainly be said for the field of dentistry. The historic progress in this area naturally goes hand-in-hand with many new questions and challenges that provide opportunities for improvement. The comparatively moderate progressiveness of dentistry throughout the history, admittedly, has been slower than might be considered desirable for those who would wish to put a cutting-edge technology to clinical use. For example, early descriptions of the extraction of teeth with the use of forceps by Hippocrates and Aristotle date back to 300–500 BC, a technique that has remained essentially unchanged up to this date. Likewise, restorations with gold and amalgam date back to years 700 and 1746, respectively, and are still a part of our clinical setting without much change [27].

2.4 Nanobiomaterials in dentistry

Tissue engineering and regeneration improve damaged tissue and organ functionality. While tissue engineering has hinted at much promise in the last several decades, significant research is still required to provide exciting alternative materials to finally solve the numerous problems associated with traditional materials. Nanotechnology may have the answers since only nanobiomaterials can mimic surface properties (including topography and energy) of natural tissues. For these reasons, over the last decade, nanobiomaterials have been highlighted as promising candidates for improving traditional tissue

engineering materials. Importantly, these efforts have highlighted that nanobiomaterials exhibit superior cytocompatible, mechanical, electrical, optical, catalytic, and magnetic properties compared to conventional (or micron structured) materials. These unique properties of nanobiomaterials have helped to improve various tissue growths over what is achievable today [28]. Recently, nanobiomaterials, which are materials with basic structural units, grains, particles, fibers, or other constituent components smaller than 100 nm in at least one dimension, have evoked a great amount of attention for improving disease prevention, diagnosis, and treatment. The intrigue in nanomaterial research for regenerative medicine is easy to see and is widespread. For example, from a material property point of view, nanobiomaterials can be made of metals, ceramics, polymers, organic materials, and composites thereof, just like conventional or micron structured materials. Nanobiomaterials include nanoparticles, nanoclusters, nanocrystals, nanofibers, nanowires, and nanofilms [29].

Two types of methods exist for working with nanotechnology, each approaching the problem from a different direction. Bottom-up methods use various processes to induce structures to self-assemble at the scale desired. Top-down methods build a structure at a scale easily worked at to, in turn build another structure at a smaller, unreachable scale. To date, numerous top-down and bottom-up nanofabrication technologies (such as electrospinning, phase separation, self-assembly processes, thin film deposition, chemical vapor deposition, chemical etching, nanoimprinting, photolithography, and electron beam or nanosphere lithography) are available to synthesize nanobiomaterials with ordered or random nanotopographies. After decreasing material size into the nanoscale, dramatically increased surface area, surface roughness, and surface-area-to-volume ratios can be created to lead to superior physiochemical properties (i.e., mechanical, electrical, optical, catalytic, and magnetic properties). Therefore, nanobiomaterials with such excellent properties have been extensively investigated in a wide range of biomedical applications, in particular prosthodontics [30].

2.5 Nanobiomaterials in preventive dentistry

The purpose of modern dentistry is the early prevention of tooth decay rather than invasive restorative therapy. However, despite tremendous efforts in promoting oral hygiene and fluoridation, the prevention and biomimetic treatment of early caries lesions are still challenges for dental research and public health, particularly for individuals with a high risk for developing caries, which is the most widespread oral disease. Recent studies indicate that nanotechnology might provide novel strategies in preventive dentistry, specifically in the control and management of bacterial biofilms or remineralization of submicrometer-sized tooth decay [31–33]. Dental caries is caused by bacterial biofilms on the tooth surface, and the process of caries formation is modulated by complex interactions between acid-producing bacteria and host factors including teeth and saliva (Figures 2.1A and B, and 2.2). On exposure to oral fluids, a proteinaceous surface coating—termed pellicle—is formed immediately on all solid substrates [4]. This conditioning layer, which defines the surface charge and the nature of chemical groups exposed at the surface, changes the properties of the substrate [34]. Bacteria colonize the surface by adhering to the pellicle through adhesion–receptor interactions and form a biofilm, known as dental plaque. Maturation of the plaque is characterized by bacterial interactions (such as coaggregation and quorum sensing) and increasingly diverse bacterial populations. Each human host harbors different bacterial populations,

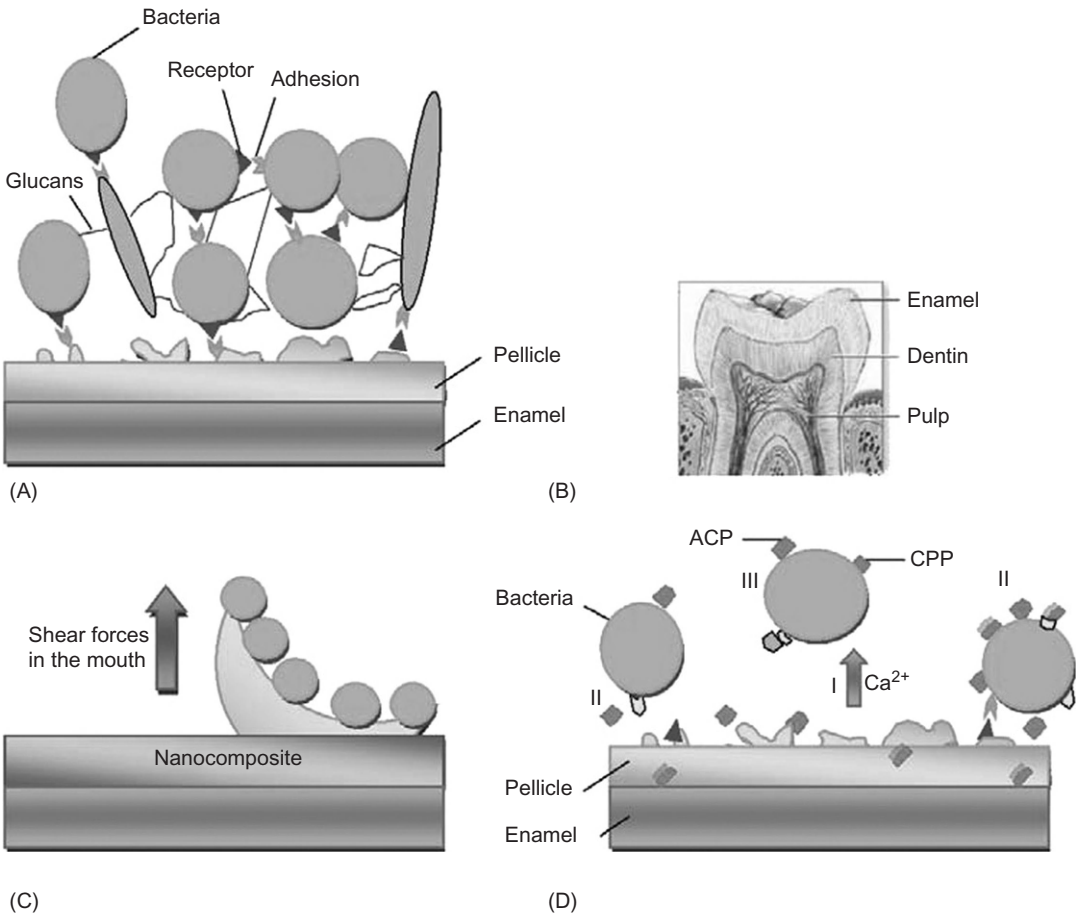

FIGURE 2.1

Bioadhesion and biofilm management in the oral cavity. (A) Bioadhesion in the oral cavity. Proteins interact with the enamel surface to form a proteinaceous pellicle layer. Bacteria adhere to this conditioning film through calcium bridges and specific adhesion–receptor interactions. Bacteria are surrounded by an extracellular matrix of water insoluble glucans, and they communicate through quorum sensing (arrows). (B) Cross section of a human molar tooth showing the enamel, dentin, and pulp chamber. (C) Easy-to-clean nanocomposite surface coating. The low-surface-free-energy coating (circles) causes poor protein–protein binding. Shear forces in the mouth can easily detach the outer layer of the pellicle and bacterial biofilm from the surface. (D) CPP–ACP inhibits bacterial adhesion and oral biofilm formation. CPP attaches to the pellicle and limits bacterial adhesion. It competes with calcium for plaque–calcium binding sites (I), and decreases the amount of calcium bridging the pellicle and bacteria, and between the bacterial cells. Specific receptor molecules in the pellicle layer and on the bacterial surfaces are blocked; further reducing adhesion and coadhesion (II). This affects the viability of the bacteria (III) [36].

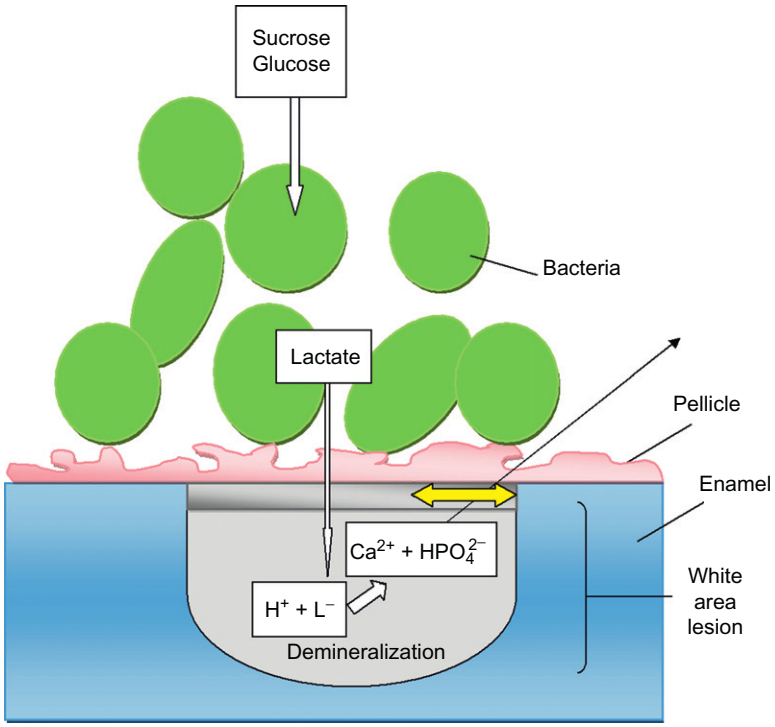

FIGURE 2.2

Early stages of tooth decay caused by bacterial biofilm. Bacteria metabolize sugar and other carbohydrates to produce lactate (HL) and other acids that, in turn, dissociate to form H^+ ions that demineralize the enamel beneath the surface of the tooth; calcium and phosphate are dissolved in the process. This is known as a white-spot lesion. Owing to reprecipitation, a pseudointact surface layer is observed on top of the body of the carious lesion in this early stage of tooth decay. This pseudointact layer is permeable to ions [36].

and it is thought that the metabolic interactions between different bacterial species play a key role in the maturation process of the biofilm [35]. Therefore, the number of streptococci and lactobacilli bacteria that cause caries can increase, especially in the presence of dietary sugars [31]. These bacterial species produce acids as by-products from the metabolism of fermentable carbohydrates and cause demineralization below the surface of the tooth [32,33] (Figure 2.2).

Further to conventional oral hygiene, antiadhesive surface coatings can be used to control the formation of dental biofilms because nanostructured surface topography and surface chemistry can both determine initial bioadhesion [37]. The classic lotus effect in ultrahydrophobic surfaces is an example of a self-cleaning surface [38,39]. However, such nanostructured surfaces are not suitable for application in the oral cavity because of surface wear and equilibration of the surface nanotopography by the ubiquitous pellicle layer [34]. To prevent the pathogenic consequences of tenacious intraoral biofilm formation over a longer interval, wear-resistant nanocomposite surface

coatings have been developed for the modification of the tooth surface in vivo. Easy-to-clean surface properties are achieved by integrating nanometer-sized inorganic particles into a fluoro-polymer matrix [40]. These biocompatible surface coatings have a surface free energy of 20−25 mJ/m^2—known as theta surfaces [41]—and therefore can facilitate the detachment of adsorbed salivary proteins and adherent bacteria under the influence of physiological shearing forces in the mouth (Figure 2.1C) [40]. Easy-to-clean coatings are conceivable for patients with high caries risk, such as those suffering from mouth dryness owing to dysfunctional salivary glands—termed xerostomia—or for individuals who do not practice proper oral hygiene. Possible applications could be tooth sealants as well as coatings of restorations, dentures, or transmucosal parts of implants. Even tooth fissures sealed with this material could be cleaned more easily by the shear forces from tooth brushing.

Other nano-enabled approaches for biofilm management are oral health-care products that contain bioinspired apatite nanoparticles, either alone or in combination with proteinaceous additives such as casein phosphopeptides (CPP) [42,43]. CPP-stabilized amorphous calcium phosphate (ACP) nanocomplexes with a diameter of 2.12 nm [44,45] seem to play a pronounced role in biomimetic strategies for biofilm management. There is in vivo evidence indicating that CPP−ACP complexes reduce bacterial adherence by binding to the surfaces of bacterial cells, the components of the intercellular plaque matrix, and to adsorbed macromolecules on the tooth surface (Figure 2.1D) [46,47]. CPP−ACP-treated germanium surfaces that are applied in the oral cavity for up to 1 week have been shown to significantly delay the formation of biofilms. However, it should be emphasized that because germanium is not a biomineral, the clinical relevance of the study remains limited. Other in vivo experiments have shown that nonaggregated and clustered hydroxyapatite (HAP) nanocrystallite particles (average size $100 \times 10 \times 5$ nm^3) can adsorb onto the bacterial surface and interact with bacterial adhesions to interfere with the binding of microorganisms to the tooth surface [42].

These bioinspired strategies for biofilm management are based on size-specific effects of the apatite nanoparticles and are thought to be more effective than traditional approaches that use micrometer-sized HAP in toothpastes. HAP has been adopted for years in preventive dentistry; however, effective interaction of the biomineral with the bacteria is only possible if nanosized particles that are used are smaller than the microorganisms (Figure 2.1D). Finally, oral health-care products based on bioinspired nanobiomaterials have moved from the laboratory to daily application—as a supplement to conventional approaches—for biofilm control and remineralization of submicrometer-sized enamel lesions. Easy-to-clean, wear-resistant, and biocompatible nanocomposite surface coatings for biofilm management are close to being used in dental practice. However, biomimetic restoration and filling of small clinically visible cavities with nanobiomaterials is not conceivable at the moment and requires further extensive research with respect to clinical applicability. It should also be kept in mind that biomimetic enamel surfaces are still susceptible to caries if patients neglect conventional oral health care such as tooth brushing or fluoride application [48].

2.6 Nanobiomaterials in restorative dentistry

2.6.1 Dental nanocomposites

The demand by patients for tooth-colored restorations, concerns regarding environmental impact, and the adverse clinical reactions to amalgam-filling materials have accelerated research into the development of alternative restoratives. However, despite the development of resin-based

composite (RBC) materials, clinical longevity of dental amalgam remains superior [49]. Dental composite resins have been used as popular materials to restore teeth since their introduction about 50 years ago [50]. Compared to dental amalgams, they have less safety concern and possess better esthetic property. Based on the report in 2005, the composites were used in more than 95% of all anterior tooth direct restorations and about 50% of all posterior tooth direct restorations [51]. Dental composites are increasingly popular due to their esthetics, direct-filling ability, and enhanced performance. Dental composites are typically composed of four major components: organic polymer matrix (2,2-bis[*p*-(2′-hydroxy-3′methacryloxypropoxy)phenylene]propane (BisGMA), bisphenol A ethoxylated dimethacrylate (BisEMA), triethylene glycol dimethacrylate (TEGDMA), urethane dimethacrylate (UDMA), etc.) (Figure 2.3), inorganic filler particles,

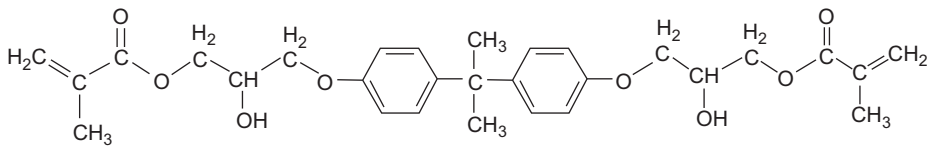

BisGMA

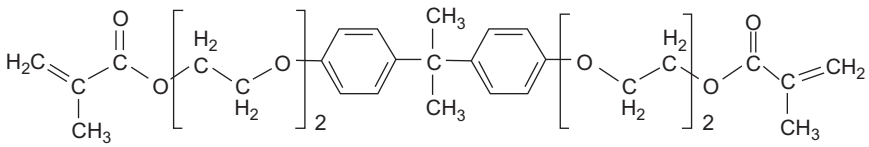

BisEMA

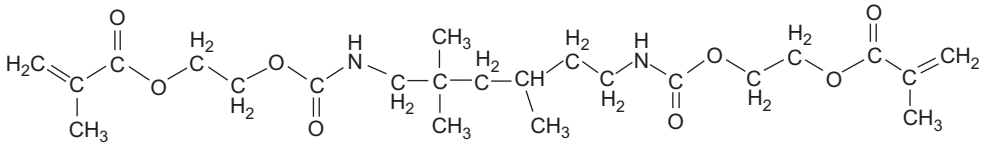

UDMA

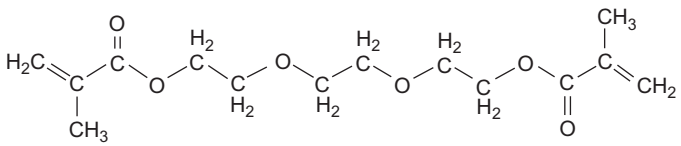

TEGDMA

FIGURE 2.3

Chemical structures of monomers used in dental nanocomposites.

coupling agents, and the initiator−accelerator system. Despite the significant improvement of RBC, restorative composites still suffer from several key shortcomings: deficiencies of mechanical strength and high polymerization shrinkage, which are responsible for the shorter median survival life span of RBCs (5−7 years) in comparison with amalgam (13 years) [52], and secondary caries and bulk fracture. Caries at the restoration margins is a frequent reason for replacement of existing restorations, which accounts for 50−70% of all restorations.

During the past decade, more efforts have been focused on dental nanocomposite, with a hope that contemporary nanocomposites with ceramic nanofillers should offer increased esthetics, strength, and durability. However, research to date shows that most nanofillers provide only incremental improvements in the mechanical properties with a few exceptions [53]. Variety of calcium phosphates (CaPs), such as HAP, ACP, tetracalcium phosphate (TTCP), and dicalcium phosphate anhydrous (DCPA) have been studied as fillers to make mineral releasing dental composites. Skrtic et al. [54] conducted pioneering research to investigate the physicochemical properties of dental composites containing unhybridized and hybridized ACP. Their research demonstrated that hybridization of ACP fillers using agents, such as tetraethoxysilane (TEOS) or $ZrOCl_2$ solution, improved the mechanical properties, e.g., biaxial flexural strength, of the composites containing ACP fillers. However, the addition of both hybridized and unhybridized ACP fillers generally degraded the biaxial flexural strength of the resin materials [55]. It was hypothesized that the strength degradation compared to unfilled resin is attributed to poor dispersion and insufficient interaction between ACP and resin. Such hypothesis has been supported by mechanical testing of dental composites containing particles with different sizes [55]. Both nanosized and microsized HAP particles were also studied as dental fillers and the mechanical tests indicated that microsized instead of nanosized HAP was favored in terms of mechanical properties [56].

From the point of view of composite mechanics, fibers are the preferred reinforced materials compared to particles since fibers can provide larger load transfer and they can also facilitate some well-known toughening mechanisms, such as fiber bridging and fiber pullout. Reinforcement with high-strength inorganic fibers indeed demonstrates significant improvement on the mechanical properties of dental composite. Beyond the benefits of strengthening effects, it has been reported that fibers can reduce the polymerization shrinkage as well [57]. The development of RBCs as an alternative to dental amalgam has resulted in optimization of the particle size distributions and filler loading, resulting in an improvement in the mechanical properties [58]. In order to achieve superior esthetics, submicron fillers were introduced to the development of RBC materials. However, filler loading of the early "homogeneous microfill" RBC types was reduced due to a high surface-area-to-volume ratio, thereby limiting mechanical properties. The introduction of "heterogeneous microfills" increased the filler loading (~50 vol%), as prepolymers containing a high-volume fraction of silanated nanofillers (~50 nm) were incorporated into a resin matrix containing discrete submicron particles. Although the approach improved the flexural strength of "heterogeneous" RBCs (80−160 MPa) compared with "homogeneous" microfills (60−80 MPa), the mechanical properties remained inferior to hybrid RBC systems, which are loaded to approximately 55−65 vol% and possess flexure strengths in the region of 120−145 MPa [59].

Microfilled composites comprise silicon dioxide filler particles with less than 100 nm in diameter in conjunction with prepolymerized organic fillers, aggregated by crushing them into larger filler particles. Nowadays, the most commonly used resin composites, i.e., microhybrids

and nanofilled composites, comprise filler particles ranging from approximately 20 to 600 nm. In composite resin technology, particle size and the amount of particles represent crucial information in determining how best to use the composite materials. Alteration of the filler component remains the most significant development in the evolution of composite resins [60] because filler particle size, distribution, and the quantity incorporated dramatically affect the mechanical properties and the clinical success of composite resins. In general, mechanical and physical properties of composites improve in relationship to the amount of filler added [61]. Many of the mechanical properties depend upon this filler phase, including compression strength and/or hardness, flexural strength, the elastic modulus, coefficient of thermal expansion, water absorption, and wear resistance.

Nanotechnology or molecular manufacturing may provide resin with filler particle size that is dramatically smaller in size, can be dissolved in higher concentrations and polymerized into the resin system with molecules that can be designed to be compatible when coupled with a polymer, and provide unique characteristics (physical, mechanical, and optical) [62]. In addition, optimizing the adhesion of restorative biomaterials to the mineralized hard tissues of the tooth is a decisive factor in enhancing the mechanical strength and marginal adaptation and seal, while improving the reliability and longevity of the adhesive restoration. Currently, the particle sizes of conventional composites are dissimilar to the structural sizes of the HAP crystal, dental tubule, and enamel rod, and there is a potential for compromises in adhesion between the macroscopic (40 nm to 0.7 μm) restorative material and the nanoscopic (1 to 10 nm in size) tooth structure. However, nanotechnology has the potential to improve this continuity between the tooth structure and the nanosized filler particle and provide a more stable and natural interface between the mineralized hard tissues of the tooth and these advanced restorative biomaterials [63].

The surface quality of the composite is influenced not only by the polishing instruments and polishing pastes but also by the composition and filler characteristics of the composite. The newer formulations of nanocomposites with smaller particle size, shape and orientation, and increased filler concentration provide improved physical, mechanical, and optical characteristics. Although clinical evidence of polishability with these new nanoparticle hybrids appears promising, the long-term durability of the polish will need to be evaluated in future clinical trials [64]. Research in modern dentistry has discovered the uses for nanoparticles for fillings and sealant, and could lead to the creation of artificial bone and teeth. The mechano-physical properties and resultant clinical longevity of dental composites are insufficient. To improve these properties, the ongoing development of RBCs has sought to modify the filler size and morphology and to improve the loading and distribution of constituent filler particles. This has resulted in the introduction of the so-called nanofills which possess a combination of nano- and microsized filler to produce a hybrid material. A variation to this approach was the introduction of "nanocluster" particles, which are essentially an agglomeration of nanosized silica and zirconia particles. Although these materials have demonstrated a degree of clinical and experimental success, debate remains as to their specific benefit compared with existing conventionally filled systems. The "nanoclusters" provided a distinct reinforcing mechanism compared with the microhybrid, microfill, or nanohybrid RBC systems resulting in significant improvements to the strength and reliability, irrespective of the environmental storage and testing conditions. Silane infiltration within interstices of the nanoclusters may modify the response to preloading induced stress, thereby enhancing damage tolerance and providing the potential for improved clinical performance [16].

2.6.2 Silver nanoparticles in restorative dental materials

Silver has a long and intriguing history as an antibiotic in human health care [65]. It has been used in water purification, wound care, bone prostheses, reconstructive orthopedic surgery, cardiac devices, catheters, and surgical appliances. Advancing biotechnology has enabled the incorporation of ionizable silver into fabrics, for clinical use to reduce the risk of nosocomial infections and for personal hygiene [66]. The antimicrobial, antifungal, and antiviral action of silver or silver compounds is proportional to the amount of released bioactive silver ions (Ag^+) and its availability to interact with bacterial or fungal cell membranes [67]. Silver and inorganic silver compounds can ionize in the presence of water, body fluids, or tissue exudates. The silver ion is biologically active and can readily interact with proteins, especially those with thiol groups, amino acid residues, free anions, and receptors on mammalian and eukaryotic cell membranes [68]. Bacterial sensitivity to silver is genetically determined and relates to the levels of intracellular silver uptake and its ability to interact and irreversibly denature key enzyme systems [66]. Bacterial biofilms are responsible for dental diseases, such as caries and periodontitis. Due to the high frequency of recurrent caries after restorative treatment, much attention has been paid to the therapeutic effects revealed by direct-filling materials. Resin composites containing silver ion implanted fillers that release silver ions have been found to have antibacterial effects on oral bacteria, e.g., *Streptococcus mutans* [69]. Most studies available on the antimicrobial effect of silver containing composites describe the effect of the silver particles on different species of cariogenic bacteria or deal with modified material properties related to the addition of silver particles. Some of these studies tested the mechanical properties of the silver containing composite [70].

2.7 Nanocomposites in bone regeneration

Replacement of tooth and bone with metal implants and plates is one of the most frequently used and successful surgical procedures. The introduction of modern implants started with the work of Branemark, who in 1969 observed that a piece of titanium embedded in rabbit bone became firmly attached and difficult to remove [71]. Due to their strength and toughness, metal implants have been used in orthopedic and dental surgeries for many years. Titanium (Ti) and its alloys have had considerable advantages over other metals because of their inertness, which yields excellent biocompatibility and nonsensitization of tissues. However, issues concerning the release of Ti and alloying elements from implants and the formation of Ti debris due to wear during implantation still remain. Metal and metal alloys (i.e., Ti, Al, V, and Ni) in implants and dental bridges have the potential for allergic reactions. Ceramic materials are known to have excellent esthetics, corrosion resistance, and biocompatibility; several ceramic implants have been already commercialized. The continuing interest in the use of modern ceramics for the fabrication of dental implants is underscored by several presentations during recent meetings of the International Association of Dental Research and by recent research efforts by several European and Japanese companies (Kyocera, Dentsply, Metoxit, etc). Unfortunately, in contrast to metallic materials, most ceramics suffer from almost a complete lack of plastic deformation; this is due to the absence of mobile dislocation activity, although other modes of inelastic deformation, such as microcracking and in situ phase transformation, can provide limited alternative deformation mechanisms [72]. Alumina/zirconia

nanocomposites offer an example of how nanotechnology offers an attractive path to the development of new implant materials, but ceramics, even nanocomposite ceramics, will not replicate the unique combinations of mechanical properties of tooth tissues as they are, for example, much stiffer and wear resistant. A possibility is to develop new hybrid organic/inorganic materials whose properties will closely match those of the tissue for which they substitute. However, the use of synthetic composite materials as permanent replacements for bone, which generated much excitement 30–40 years ago [73], remains largely unmet due to significant challenges related to fabrication, performance, and cost. Current hybrid organic/inorganic composites have significant problems related mostly to their mechanical performance and their degradation in vivo. As a result, the use of synthetic composite materials as permanent replacements for bone is nearly nonexistent. To achieve dramatic improvements in in vivo performance of composites for dental implants and skeletal tissue repair, new ways of approaching composite design and fabrication are needed. Ideally, these materials would be capable of self-healing, as is the case in many biological materials. In addition, teeth have a complex structure in which several tissues (enamel, dentin, cementum, and pulp) with very different properties and structure are arranged. An ideal artificial tooth requires the combination of several synthetic materials with prescribed properties [74].

2.8 Conclusions

Nanotechnology has achieved tremendous progress in the past several decades. It is expected that nanotechnology will change dentistry, health care, and human life more profoundly than many developments of the past. As with all technologies, nanotechnology carries a significant potential for misuse and abuse on a scale and scope never seen before. However, they also have potential to bring about significant benefits, such as improved health, better use of natural resources, and reduced environmental pollution. Nanotechnology has been used for dental applications in several forms, including the field of prosthodontics with the development of nanobiomaterials as a useful tool. To date, there has been an exponential increase in studies using nanotechnology for other dental applications. It is not too early to consider, evaluate, and attempt to shape potential effects of nanodentistry. Nanodentistry will lead to efficient and highly effective personalized dental treatments. Nanotechnology seems to be where the world is headed if technology keeps advancing and competition practically guarantees that advance will continue. It will open a huge range of opportunities of benefit for both the dentist and the patient.

References

[1] T. Kaehler, Nanotechnology: basic concepts and definitions, Clin. Chem. 40 (9) (1994) 1797–1799.
[2] R.A. Freitas, Nanomedicine/Basic Capabilities, vol. 1, Landes Bioscience, Georgetown, TX, 1999, pp. 345–347.
[3] N. Taniguchi, Proc. International Conference on Precision Engineering (ICPE), Tokyo, Japan, 1974, pp. 18–23.
[4] T.J. Webster, Int. J. Nanomed. 2 (2007) 1.

[5] V. Uskoković, Nanotechnologies: what we do not know, Technol. Soc. 29 (2007) 43–61.
[6] V. Uskoković, Nanomaterials and nanotechnologies: approaching the crest of this big wave, Curr. Nanosci. 4 (2008) 119–129.
[7] C. Buzea, I. Pacheco, K. Robbie, Nanomaterials and nanoparticles: sources and toxicity, Biointerphases 2 (4) (2007) 17–71, doi:10.1116/1.2815690.
[8] Study sizes up nanomaterial toxicity, Chem. Eng. News 86 (35) (2008) 44.
[9] Y. George, J.R. Onoda, L. Larry, L.L. Hench, Ceramic Processing Before Firing, Wiley & Sons, New York, NY, 1979, 0471654108.
[10] I.A. Aksay, F.F. Lange, B.I. Davis, Uniformity of Al_2O_3–ZrO_2 composites by colloidal filtration, J. Am. Ceram. Soc. 66 (10) (1983) 190.
[11] G.V. Franks, F.F. Lange, Plastic-to-brittle transition of saturated, alumina powder compacts, J. Am. Ceram. Soc. 79 (12) (1996) 3161.
[12] A.G. Evans, R.W. Davidge, The strength and fracture of fully dense polycrystalline magnesium oxide, Phil. Mag. 20 (164) (1969) 373.
[13] F.F. Lange, M. Metcalf, Processing-related fracture origins: II, agglomerate motion and cracklike internal surfaces caused by differential sintering, J. Am. Ceram. Soc. 66 (6) (1983) 398.
[14] A.G. Evans, Considerations of inhomogeneity effects in sintering, J. Am. Ceram. Soc. 65 (10) (1987) 497.
[15] G.M. Whitesides, et al., Molecular self-assembly and nanochemistry: a chemical strategy for the synthesis of nanostructures, Science 254 (5036) (1991) 1312–1319.
[16] D.M. Dubbs, I.A. Aksay, Self-assembled ceramics, Ann. Rev. Phys. Chem. 51 (2000) 601–622.
[17] S. Iijima, C. Brabec, A. Maiti, Structural flexibility of carbon nanotubes, J. Chem. Physiol. 104 (5) (1996) 2089–2092.
[18] R. Zsigmondy, Colloids and the ultramicroscope, Wiley & Sons, New York, NY, 1914.
[19] A.S. Dukhin, P.J. Goetz, Ultrasound for Characterizing Colloids, Elsevier, 2002.
[20] K. Jayraman, M. Kotaki, Y. Zhang, et al., Recent advances in polymer nanofibers, J. Nanosci. Nanotechnol. 4 (52) (2004) 65–67.
[21] R.L. Price, K. Ellison, K.M. Haberstroh, et al., Nanometer surface roughness increases select osteoblasts adhesion on carbon nanofiber compacts, J. Biomed. Mater. 70 (129) (2004) 38–40.
[22] D.S. Katti, K.W. Robinson, C.T. Laurenci, Bioresorbable nanofiber based systems for wound healing and drug delivery: optimization of fabrication parameters, J. Biomed. Mater. 70 (282) (2004) 96–97.
[23] E.M. Reifman, Diamond teeth, in: B.C. Crandall (Ed.), Nanotechnology: Molecular Speculations on Global Abundance, MIT Press, Cambridge, MA, 1996, p. 81.
[24] S.A. Saunders, Current practicality of nanotechnology in dentistry. Part 1: Focus on nanocomposite restoratives and biomimetics, Clin. Cosmet. Invest. Dent. 1 (2009) 47–61.
[25] J.H. Kinney, S. Habelitz, S.J. Marshall, G.W. Marshall, The importance of intrafibrillar mineralization of collagen on the mechanical properties of dentin, J. Dent. Res. 82 (2003) 957–961.
[26] V. Uskoković, On the light doves and learning on mistakes, Axiomathes 19 (2009) 17–50.
[27] V. Uskoković, On science of metaphors and the nature of systemic reasoning, World Futures 65 (2009) 241–269.
[28] R.W. Siegel, G.E. Fougere, Nanostruct. Mater. 6 (1995) 205.
[29] J.W. Freeman, L.D. Wright, C.T. Laurencin, S. Bhattacharyya, in: K.E. Gonsalves, C.R. Halberstadt, C.T. Laurencin, L.S. Nair (Eds.), Biomedical Nanostructures, Wiley & Sons, NJ, 2008, pp. 3–24.
[30] B.D. Fahlman, Materials Chemistry, Springer, Dordrecht, The Netherlands, 2007.
[31] R.H. Selwitz, A.I. Ismail, N.B. Pitts, Dental caries, Lancet 369 (2007) 51–59.
[32] N. Takahashi, B. Nyvad, Caries ecology revisited: microbial dynamics and the caries process, Caries Res. 42 (2008) 409–418.

[33] S. Filoche, L Wong, C.H. Sissons, Oral biofilms: emerging concepts in microbial ecology, J. Dent. Res. 89 (2010) 8−18.
[34] C. Hannig, M. Hannig, The oral cavity—a key system to understand substratum-dependent bioadhesion on solid surfaces in man, Clin. Oral Investig. 13 (2009) 123−139.
[35] P.E. Kolenbrander, et al., Bacterial interactions and successions during plaque development, Periodontology 42 (2006) 47−79.
[36] M. Hannig, C. Hannig, Nanomaterials in preventive dentistry, Nature Nanotechnol 5 (8) (2010) 565−569.
[37] D. Khang, J. Carpenter, Y.W. Chun, R. Pareta, T.J. Webster, Nanotechnology for regenerative medicine, Biomed. Microdevices (2008) doi:10.1007/s10544-008-9264−6.
[38] R. Blossey, Self-cleaning surfaces—virtual realities, Nat. Mater. 2 (2003) 301−306.
[39] A. Solga, Z. Cerman, B.F. Striffler, M. Spaeth, W. Barthlott, The dream of staying clean: lotus and biomimetic surfaces, Bioinspir. Biomim. 2 (2007) 126−134.
[40] M. Hannig, L. Kriener, W. Hoth-Hannig, C. Becker-Willinger, H. Schmidt, Influence of nanocomposite surface coating on biofilm formation in situ, J. Nanosci. Nanotechnol. 7 (2007) 4642−4648.
[41] R.E. Baier, Surface behaviour of biomaterials: the theta surface for biocompatibility, J. Mater. Sci. Mater. Med. 17 (2006) 1057−1062.
[42] C. Rahiotis, G. Vougiouklakis, G. Eliades, Characterization of oral films formed in the presence of a CPP−ACP agent: an in situ study, J. Dent. 36 (2008) 272−280.
[43] E.C. Reynolds, F. Cai, P. Shen, G.D. Walker, Retention in plaque and remineralization of enamel lesions by various forms of calcium in a mouthrinse or sugar-free chewing gum, J. Dent. Res. 82 (2003) 206−211.
[44] E.C. Reynolds, Calcium phosphate-based remineralization systems: scientific evidence? Aust. Dent. J. 53 (2008) 268−273.
[45] E.C. Reynolds, Remineralization of enamel subsurface lesions by casein phosphopeptide-stabilized calcium phosphate solutions, J. Dent. Res. 76 (1997) 1587−1595.
[46] K.J. Cross, N.L. Huq, E.C. Reynolds, Casein phosphopeptides in oral health—chemistry and clinical applications, Curr. Pharm. Des. 13 (2007) 793−800.
[47] R.K. Rose, Binding characteristics of *Streptococcus mutans* for calcium and casein phosphopeptide, Caries. Res. 34 (2000) 427−431.
[48] S.C. Venegas, J.M. Palacios, M.C. Apella, P.J. Morando, M.A. Blesa, Calcium modulates interactions between bacteria and hydroxyapatite, J. Dent. Res. 85 (2006) 1124−1128.
[49] P.S.K. Lucarotti, R.L. Holder, F.J.T. Burke, Outcome of direct restorations placed within the general dental services in England and Wales. Part 1: Variation by type of restoration and re-intervention, J. Dent. 33 (2005) 805−815.
[50] R.L. Bowen, Properties of a silica-reinforced polymer for dental restorations, J. Am. Dental. Assoc. 66 (1963) 57−64.
[51] S. Pamela, J.S. Stein, J.E. Haubenreicb, P.B. Osborne, Composite resin in medicine and dentistry, J. Long-Term Eff. Med. Implants 15 (2005) 641−654.
[52] S.S.H. Mirsasaani, M. Hajipour Manjili, N. Baheiraei, Dental nanomaterials, in: B. Reddy (Ed.), Advances in Diverse Industrial Applications of Nanocomposites, INTECH, Vienna, Austria, 2011, pp. 441−474.
[53] D.A. Terry, Direct applications of a nanocomposite resin system. Part 2: Procedures for anterior restorations, Pract. Proced. Aesthet. Dent. 16 (2004) 677−684.
[54] D. Skrtic, A.W. Aailer, S. Takagi, J.M. Antonucci, E.D. Eanes, Quantitative assessment of the efficacy of amorphous calcium phosphate/methacrylate composites in remineralizing caries-like lesions artificially produced in bovine enamel, J. Dent. Res. 75 (1996) 1679−1686.

[55] S.Y. Lee, W.F. Regnault, J.M. Antonucci, D. Skrtic, Effect of particle size of an amorphous calcium phosphate filler on the mechanical strength and ion release of polymeric composites, J. Biomed. Mater. Res. B Appl. Biomater. 80 (2007) 11–17.
[56] C. Santos, R.L. Clarke, M. Braden, F. Guitian, K.W. Davy, Water absorption characteristics of dental composites incorporating hydroxyapatite filler, Biomaterials 23 (2002) 1897–1904.
[57] H.K. Hockin, J.B.Q. Xu, D.T. Smith, A.A. Giuseppetti, F.C. Eichmiller, Effects of different whiskers on the reinforcement of dental resin composites, Dent. Mater. 19 (2003) 359–367.
[58] J.L. Ferracane, Current trends in dental composites, Crit. Rev. Oral. Biol. Med. 6 (1995) 302–318.
[59] D.S. Cobb, B.S. McGreggor, M.A. Vargas, G.E. Denehy, The physical properties of package and conventional posterior resin-based composites: a comparison, J. Am. Dent. Assoc. 131 (2000) 1610.
[60] J.F. Roulet, Degradation of Dental Polymers, first ed., S. Karger AG, Basel, Switzerland, 1987.
[61] S.S.H. Mirsasaani, M. Atai, M.M. Hasani-Sadrabadi, Photopolymerization of a dental nanocomposite as restorative material using the argon laser, Lasers Med. Sci. 26 (5) (2011) 553–561.
[62] S.S.H. Mirsasaani, M. Sarmast Shoushtari, Dental nanocomposites, in: F.C. Calhoun (Ed.), Dental Composites, Nova Publisher, New York, NY, 2011, p. 195.
[63] M. Muselmann, Composites make large difference in “small” medical, dental applications, Comp. Tech. December 24–27 (2003).
[64] S.R. Jefferies, R.L. Smith, W.W. Barkmeier, et al., Comparison of surface smoothness of restorative resin materials, J. Esthet. Dent. 1 (5) (1989) 169–175.
[65] J.W. Alexander, History of the medical use of silver, Surg. Infect. (Larchmt) 10 (2009) 289–292.
[66] A.B. Lansdown, Silver in health care: antimicrobial effects and safety in use, Curr. Probl. Dermatol. 33 (2006) 17–34.
[67] A.B. Lansdown, Silver I: Its antibacterial properties and mechanism of action, J. Wound Care 11 (2002) 125–130.
[68] A.B. Lansdown, Silver 2: Toxicity in mammals and how its products aid wound repair, J. Wound Care 11 (2002) 173–177.
[69] K. Yamamoto, S. Ohashi, M. Aono, T. Kokubo, I. Yamada, J. Yamauchi, Antibacterial activity of silver ions implanted in SiO_2 filler on oral streptococci, Dent. Mater. 12 (1996) 227–229.
[70] S.J. Ahn, S.J. Lee, J.K. Kook, B.S. Lim, Experimental antimicrobial orthodontic adhesives using nanofillers and silver nanoparticles, Dent. Mater. 25 (2009) 206–213.
[71] P. Worthington, Introduction: history of implants, in: WPLBR, RJE (Ed.), Osseointegration in Dentistry: An Overview, Quintessence Publishing, IL, (2003) 2.
[72] Y. Li, C. Wong, J. Xiong, P. Hodgson, C. Wen, Cytotoxicity of titanium and titanium alloying elements, J. Dent. Res. 89 (5) (2010) 493–497.
[73] M. Schehl, L.A. Diaz, R. Torrecillas, Alumina nanocomposites from powder–alkoxide mixtures, Acta Mater. 50 (5) (2002) 1125–1139.
[74] J.M. Karp, R. Langer, Development and therapeutic applications of advanced biomaterials, Curr. Opin. Biotechnol. 18 (5) (2007) 454–459.

CHAPTER

Carbon Nanotube-Based Materials—Preparation, Biocompatibility, and Applications in Dentistry

3

Mrinal Bhattacharya[a] **and Wook-Jin Seong**[b]

[a]*Department of Bioproducts and Biosystems Engineering, University of Minnesota, St. Paul, MN, USA*

[b]*Division of Prosthodontics, Department of Restorative Sciences, School of Dentistry, University of Minnesota, Minneapolis, MN, USA*

CHAPTER OUTLINE

3.1 Introduction

Carbon has the unique ability to assume a wide variety of different structures and forms. At the atomic scale, carbon nanotubes (CNTs) are hexagonal sheets of graphite wrapped into single or multiple sheets. They have unique mechanical, thermal, and electronic properties that derive from the special property of carbon bond, their cylindrical symmetry, and their unique one-dimensional (1D) nature. Nanotubes can also be metallic or semiconducting depending on their chirality. They

Nanobiomaterials in Clinical Dentistry.

are stable up to 2800°C in vacuum, possess a thermal conductivity whose value is twice that of diamond, and have an electric-current carrying capacity that is 1000 times that of copper [1].

Studies [2,3] have shown that nanotubes display extraordinary mechanical properties—tensile modulus of 1 TPa, tensile strength in the range of 50−150 GPa, and a failure strain in excess of 5%. The elastic modulus and strengths are one to two orders of magnitude higher than that of the strongest steel. They also display outstanding electrical and thermal properties. These extraordinary properties of nanotubes have sparked an interest in using them as reinforcing materials in composites or as additives to impart novel functionalities. Given their unique properties, CNT-based materials have attracted attention in the field of biomaterials with potential applications in load-bearing application, radiotracers, Magnetic Resonance Imaging (MRI) contrast agents, drug delivery, tissue engineering, and sensors. In addition, CNT-based scaffolds that are electrically conducting is also an attractive potential. However, before its wide spread usage, the safety of CNT-based materials must be established.

3.2 Preparation of CNT composites

There have been different techniques used to prepare composites using CNTs [4]. These include melt blending [5], solution blending [6], in situ polymerization [7], electrospinning [8,9], and layer-by-layer (LbL) assembly [10,11]. In melt blending, the polymer in a molten state and the nanotubes are mixed in a shear environment in a mixing device (typically in a screw extruder). The objective is to uniformly disperse the nanotubes in the polymer matrix for reinforcement. In solution blending, the polymer is dissolved in solution and the nanotubes are added. Since the tubes are held together by van der Waals forces, they are separated and dispersed in solution using sonication. Once adequate dispersion and homogeneity are obtained, the solvent is evaporated to yield the nanotube-filled polymer. This process is mainly used where the polymer is soluble in common organic solvents. CNT composites using in situ polymerization involve polymerizing vinyl monomers and CNT. This process is very attractive for polymers that are thermally unstable or are insoluble in solvents. It is possible to have a high nanotube loading [12], including grafting the polymer to nanotube surface which promotes interfacial adhesion between the polymer and the nanotube increasing its bulk properties. Electrospinning is a technique for the production of fibers with diameters ranging from microns to few nanometers. It was originally applied to polymers, but more recently the process has been applied to the production of glass, metal, and ceramic [13]. In the electrospinning process, static electric charges are induced on the polymeric solution which is extruded through a syringe. Initially, the polymer solution is held by its surface tension in the form of a droplet at the end of a capillary. If the charge density is high enough, the repulsive force overcomes the surface tension. Within a few centimeters of travel from the tip, the discharged jet undergoes bending instability and begins to whip and split into bundles of smaller fibers. In addition to bending instability, the jet undergoes elongation that causes it to become thinner. The solvent evaporates leading to the solidification of the fluid jet. The fibers are collected on a collector, usually in the form of nonwoven fabric. The LbL technique exploits the electrostatic attraction between oppositely charged species to induce the growth of one-dimensional (1D) structure. An important characteristic of the LbL assembly is to precisely control the thickness of individual layers. It is also possible to incorporate a number of different materials, particularly biomolecules,

into the multilayer composite, as long as alternating charge is maintained. The technique is cheap and easy to assemble. Functionalized CNTs (f-CNT) can be incorporated into the multilayer and by varying the number of layers, the properties of the films can be controlled.

It is widely recognized that the excellent properties of nanotubes have yet to be realized. Little of the data reported achieve the reinforcement predicted by the rule of mixtures especially at concentrations of 10 vol% of CNT [14]. This is because efficient load transfer depends on the interfacial bonding between the polymer matrix and the CNT. Because of the strong van der Waals forces and electrostatic interactions, CNTs tend to aggregate in solvents. Although van der Waals forces are considered to be weak intermolecular forces, they become significant at the nanoscale due to the large surface area per unit mass of the material. This diminishes the interfacial bonding (probably because of the smooth grapheme-like surface of nanotubes) leading to lower than predicted properties. Agglomerated nanotubes form ropes that slip when stressed due to their poor adhesion to the polymer matrix, affecting their elastic properties [15]. Nanotube bundles act as stress concentration points within the polymer matrix and can, in some cases, reduce the mechanical properties of the original polymer. The reduced aspect ratio due to agglomeration of nanotubes also leads to a reduction in reinforcement. Thus, nanotube dispersion is critical to efficient reinforcement.

Reinforcement of materials using fillers are affected by four parameters—aspect ratio, extent of dispersion in the matrix, alignment, and interfacial stress transfer [4]. Large aspect ratio maximizes load transfer to the nanotubes. Nanotubes must be well dispersed in the matrix to the point of individual tubes coated by the polymer. Good dispersion helps achieve good load transfer to the nanotube network resulting in more uniform stress distribution. Alignment while important is not critical. While alignment maximizes modulus and strength, it makes the composite anisotropic. Bonding between the nanotube and the polymer is essential to allow the external stress applied to the composite to be transferred to the nanotubes, enabling them to bear most of the applied load. Hence, CNTs are functionalized to improve their dispersibility and enable their interactions with polymers.

There are several reviews available on the functionalization of CNTs [16,17]. Chemical functionalization of nanotubes was discovered in an attempt to purify single-walled carbon nanotubes (SWNT) with acids. Depending on the method of nanotube production, CNTs are often mixed with impurities such as metal catalysts, amorphous carbon, and soot. Strong acids are utilized to eat away the impurities leaving behind pure CNTs. The acid reacts with the nanotube caps, which are reactive because of their high degree of curvature. This method of functionalization creates bonds that are progressively oxidized, depending on the intensity of treatment to hydroxyl (−OH), carbonyl ($>C{=}O$) and carboxyl (−COOH) groups [18]. The carboxylic acid groups are employed as anchoring sites for functional groups that make the nanotubes soluble in organic solvents [19−21]. Other oxygenated functionalities include anhydrides, quinines, and esters [17]. Such functionalities can also be introduced by treatment with ozone [22]. The formation of carboxylic acid sites has the potential for the attachment of various moieties through amidization and esterification reactions. Various materials have been electrostatically [23], hydrophobically [24], or covalently [25,26] attached to the surface of CNTs. There are examples in the literature of DNA and protein functionalized CNTs [27] which can be exploited in biological application.

In order to ensure a strong bond at the interface, a molecular level entanglement between the polymer and nanotube is essential [28]. This is one of the reasons behind the use of functionalized nanotubes in composites. Even with improved adhesion and dispersion in the polymer matrix, the

nanotubes remain randomly dispersed. Attempts have been made to align nanotubes to increase reinforcement. Alignments techniques include melt drawing [29], polymer stretching [30–33], alternating-current electric field [34–36], surface acoustic waves [37], direct-current electric field [35,36,38,39] and magnetic fields [40–42]. Several studies [29,33,43–46] have shown that in composites where the nanotubes were aligned, a significant increase in the modulus was obtained over nonaligned composites. Alignment of nanotubes in the composite also caused anisotropy with improvement in the perpendicular direction being significantly less [43]. The use of magnetic field as a technique to align nanotubes gave conflicting results on modulus enhancement [40]. However, magnetic field was found to disrupt van der Waals interactions, improving dispersion and electrical conductivity [41].

3.2.1 Melt processing of CNT composites

There has been extensive work published in the melt processing of CNT with polymers. This process involves heat processing the polymer and the CNT in a mixing equipment (screw extruder or batch mixer). The mixer imparts shear and elongational stress to the process helping to break apart the CNT agglomerates and dispersing them uniformly in the polymer matrix. The extruder is much more versatile where by simply changing the screw configuration (in a twin-screw system) better control of shear and mixing is obtained. Production rates and material throughputs in a continuous extrusion process can be high. Another advantage of melt processing is that it does not require the use of organic solvents during processing. The compounded CNT–polymer composite can be further processed using other polymer-processing techniques such as injection molding, profile extrusion, blow molding, and so on. Because of the large number of variables involved (temperature, screw speed, residence time, shear stress) the mixing process needs to be fine-tuned for optimal properties.

Most of the work reported in the literature has involved polymers such as low-density polyethylene [47], high-density polyethylene [48,49], polypropylene (PP) [50], polystyrene (PS) [50], poly (methyl methylacrylate) (PMMA) [32,51], polyamide [52], polyesters [53,54], and polycarbonate (PC) [47]. In most instances, the mechanical, electrical, and morphological properties were evaluated. There are several reviews that detail the important findings [4,12,55,56]. Melt processing has shown modest improvement in mechanical properties. Jin et al. [57] reported a 132% increase in Young's modulus when 17 wt% multiwalled carbon nanotubes (MWNT) were mixed with PMMA. MWNT (1% by weight) added to PS increased the modulus by 36–42% and strength by 25% [58]. Significant increases (15–60%) in modulus was obtained in MWNT-polyamide 6 blends [59] with increasing nanotube concentration. Addition of amine-functionalized MWNT made nylon 6 tougher [60]. SWNT increased the modulus of PC [61] and PP [62] by 50% and 28% for nanotube loading of 7.5 and 0.75 wt%, respectively. Results for composites made from different type of tubes show that the reinforcement scales linearly with the total nanotube surface area in the films, indicating that low-diameter multiwall nanotubes are the best tube type for reinforcement [63]. The properties of several CNT–polymer composites produced by various techniques are summarized in Table 3.1.

The dispersion of nanotubes in polymer matrix is affected by material and processing parameters [53,54]. Varying methods of synthesis used by different manufacturers of nanotubes lead to differing characteristics such as agglomerate structure, packing density, length to diameter ratio, and purity. These variations affect dispersibility of the MWNT in polymeric matrix. In addition,

Table 3.1 Summary of Mechanical Properties of Various Carbon Nanotubes Composites Processed Using Different Techniques

Polymer	Type of NT	Concentration (%)	Processing Method	Nanotube Functionality	Modulus (GPa)	Tensile Strength (MPa)	Reference
HDPE (High density polyethylene)	MWNT	1	Melt	Acid	1.2	28	[48]
PS	MWNT	1	Melt	None	2.0	35	[50]
PP	MWNT	1	Melt	None	1.5	26	[50]
PA-12	SWNT	0–15	Melt	None	2.4–13.2	–	[51]
PA-6	SWNT	2–12	Melt	None	3.0–4.18	–	[58]
PA-6	MWNT	0–2	Melt	Acid	2.0–3.0	35–54	[59]
PMMA	MWNT	1–10	In situ polymerization	None	–	47.2–71.5	[50]
PVA (Poly Vinyl Alcohol)	SWNT	0–0.8	Solution casting	Hydroxyl	2.4–4.3	74–107	[64]
PVA	MWNT	1.5	Solution casting	Ferritin protein	7.2	–	[65]
PS	MWNT	1	Solution casting	Chlorinated polypropylene	2.63		[66]
PU	MWNT	0–20	Solution casting	Acid	0.05–0.42	7.6–21.3	[67]
Nylon 610	MWNT	0–1.2	In situ polymerization	Acid	0.9–1.4	36–54	[7]
Nylon 610	MWNT	0–1.5	In situ polymerization	Acid	0.9–2.4	36–52	[68]
Epoxy	SWNT	0–4	In situ polymerization	Acid	2.62–3.40	83–102	[69]

the polymer matrix (specifically the melt viscosity) also affects the degree of dispersion. Unfortunately, the shear forces generated in most mixing equipment are not large enough to break and disperse the CNT in the polymer matrix efficiently. Special mixers where shear rates are an order of magnitude higher than obtained in a typical screw extruder are often used leading to better dispersion and improved properties. However, it also has the potential for degrading the polymer (particularly aliphatic polyesters used in tissue engineering) and the CNT.

3.2.2 Solution processing of CNT composites

Processing of composites using solution casting remains the most popular method of producing composites, particularly on a laboratory scale. As the name suggests, solvent casting involves the agitation of CNTs in a polymer dissolved in a solvent before casting in a mold and evaporating the solvent. The lower viscosity of the polymer in solution (as opposed to a melt) coupled with agitation by mechanical stirrer or ultrasonication aids in the dispersion of the CNTs. The choice of solvent is determined by the solubility of the polymer. Since it is difficult to disperse pristine nanotubes, a surfactant is added to aid in the dispersion before adding to the polymer solution. In general, this leads to good wetting of the CNT surface by the polymer. Also, studies with high CNT loading (>50 wt%) have been reported [56]. An important issue in the solution casting system is the speed at which solvent is removed as nanotubes often reaggregate particularly at high concentrations [70] in a low-viscosity liquid.

3.2.3 In situ polymerization technique

A variety of CNT−polymer composite has been prepared using in situ polymerization. This technique can be used to produce both thermoset and thermoplastic materials. Free radical initiator AIBN (2,2′-azobisisobutyronitrile) led to the formation of strong interface between CNT and PMMA matrices [51]. The tensile strength increased up to 7% by weight addition of CNT after which it decreased. This decrease in properties at higher fractions due to nanotube agglomeration is evidence that dispersion affects mechanical properties. Majority of the thermoset-CNT studies have focused on CNT−epoxy [69,71] and CNT−thermosetting polyimide composites [68,72,73]. The mechanical properties of epoxy/CNT composites with and without CNT functionalization have been the focus of several studies [12]. Here, the nanotubes are dispersed in the monomer which is then polymerized. Dispersants may be added to assist in the deagglomeration of the nanotubes [74]. Alternately, functionalization [75,76] or polymer adsorption [77] techniques have been used to aid in dispersion. Polymerization is initiated by increasing the temperature, adding chemical that initiates the reaction or by mixing two monomers. Since nanotubes are microwave absorbing causing an increase in temperature, microwaves have been used to induce polymerization [78,79]. One of the advantages of this technique is that it allows the grafting of polymer molecules on to the walls of the tube. The technique is useful in making CNT composites with polymers that are insoluble in most common solvents or are thermally unstable (thereby making melt processing difficult). Some of the composites developed include polyethylene [80], PP [81], PMMA [82], polyurethane [83,84], polycaprolactone (PCL) [85,86], and polylactide [87]. One potential problem in making CNT−aliphatic polyester composites using this method is the ability to obtain

sufficiently high molecular weight polyester. Few of the studies associated with aliphatic polyester conducted the molecular weight studies.

3.2.4 Electrospinning

An alternate technique to fabricate polymer/CNT composite fibers is electrospinning. This technique allows the alignment of the CNTs along the fiber axis. The diameter of electrospun polymeric fibers ranges from tens of nanometers to several microns. Many biologically functional molecules and cells often interact at the nanoscale level making these electrospun matrix attractive for tissue engineering. A number of CNT/polymer composites (mostly consisting of MWNT) have been successfully electrospun making it a versatile fiber processing technique. The alignment of the CNT in the polymer enhances the aspect ratio for reinforcing and increases the area for interfacial bonding [88].

The elements of a basic electrospinning unit include an electrode connected to a high voltage power supply that is inserted into a syringe-like container containing the polymeric solution. Connected to the syringe is a capillary. The syringe−capillary setup can be mounted vertically [89], horizontally [90], or tilted at a defined angle [91]. A grounded collector plate, which is connected to the other end of the electrode, is placed at a distance of 10−30 cm from the tip of the capillary (Figure 3.1).

The polymer solution at the end of the capillary upon the application of high voltage becomes charged. As the voltage is increased, a charge is induced on the surface of the liquid. Mutual charge repulsion leads to the development of force directly opposite to the surface tension. A jet is ejected

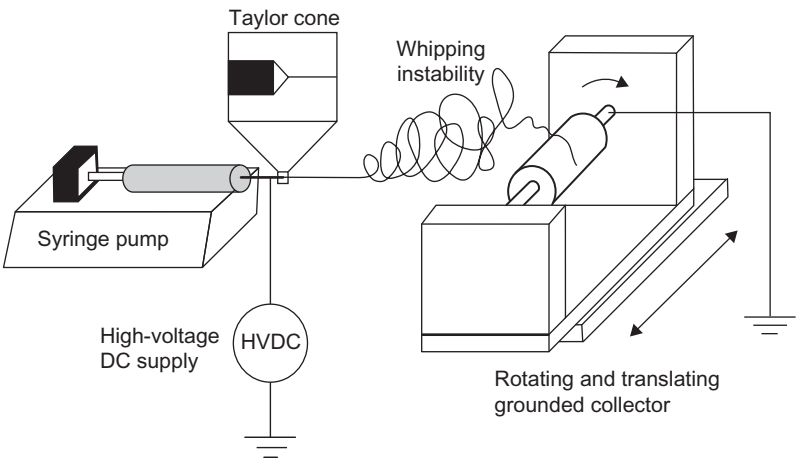

FIGURE 3.1

Schematic of a typical electrospinning system. If the electrostatic charge is able to overcome the surface tension, the Taylor cone is formed and the solution is ejected from the apex of the needle. Whipping instability depicted here further thins the fiber. It is collected on the drum which can be rotated to further align the fiber.

From Ref. [92].

from the suspended liquid meniscus at the end of the capillary when the applied electric field overcomes the surface tension of the liquid. Further increase in the electric field causes the hemispherical surface of the droplet at the tip of the capillary tube to elongate and form a conical shape known as the Taylor cone. When the repulsive electrostatic force overcomes the surface tension of the fluid, the charged jet is ejected from the tip of the Taylor cone. Within a few centimeters of travel from the tip, the discharged jet undergoes bending instability (Raleigh instability) and begins to whip and splits into bundles of smaller fibers. In addition to bending instability, the jet undergoes elongation (strain $\sim 10^5$ and rate of strain $\sim 10^3\ s^{-1}$) which causes it to become very long and thin (diameter in the range of nanometers to micrometers). The solvent evaporates, leading to the formation of skin and solidification of the fluid jet followed by the collection of solid charged polymer fibers on the collector, usually in the form of nonwoven fabric.

Parameters that affect the formation of nanofibers during the electrospinning process include (i) solution properties—viscosity, elasticity, conductivity, and surface tension, (ii) system properties—hydrostatic pressure in the capillary, applied voltage, distance between tip and collecting screen, and (iii) ambient parameters—solution temperature, humidity, and air velocity [93]. Comprehensive reviews on this topic can be found in several monologues [8,9,13,94]. Parameters that control fiber diameter are concentration of the spinning solution, electrical conductivity of the solution, and the feeding rate of the solution through the nozzle.

The 1D electrospun fibers can be allowed to stack on the electrode to produce a three-dimensional (3D) fiber mesh. These 3D structures have been used in cell cultures to test for tissue engineering applications [95–97]. The orientation induced during the bending instability experienced by electrospun fibers have shown to aid in cell growth and differentiation [98]. It is also possible to produce core/shell fiber composite consisting of polymeric core and a low molar mass materials as core. Two dies arranged in a concentric configuration and are connected to two reservoirs containing different spinning solutions. The low molar mass of the core (such as water) makes it possible to serve as carriers for biological materials.

A number of biological molecules can be incorporated into electrospun fibers. Immobilization of bacteria in electrospun nanofibers has been reported [99]. This opens up the possibility of electrospun fibers to serve as carriers for drug and as controlled release agent. Drugs ranging from antibiotics to anticancer agents and proteins [92] have been incorporated into electrospun scaffolds. Electrospinning of core-shell fibers containing fluorescent proteins or the enzyme bovine serum albumin has shown [100] that many of the functions of these proteins were retained.

While many natural fibers such as chitosan [101], collagen [102], silk [103], hyaluronic acid [104,105], gelatin [106], and fibrinogen [107,108] have been electrospun into fibers, there have been few reports of CNT and natural polymer electrospun composite. Electrospinning silk with CNT resulted in a sevenfold increase in strength, 35-fold increase in modulus, and a fourfold increase in electrical conductivity with the addition of 1% CNT [109]. At concentrations below percolation threshold (see discussion on conductivity), addition of CNTs increased the mechanical properties of PS/CNT electrospun fibers, while at threshold concentrations and above, the properties decline to level below that of pure PS [110]. Significant increase in both modulus and tensile strength was reported upon the addition of small amounts of MWNT to cellulose-MWNT fibers [111].

Electrospun fibers have been reported to show promise in engineering a number of tissues [92,98,112,113]. The micro- and nanoscale features of fabricated fibers are similar to the hierarchical structure of extracellular matrix. The high surface area–volume ratio of electrospun meshes

ensures significant area for cellular attachment. This enables higher density of cells to be cultured when compared to 2D flat surface. In addition, synthetic electrospun polymer scaffolds are amenable to surface modification with different functional groups that provide integrin-binding specificity [114]. Hence, electrospun nanofibers combine topographical and biochemical cues within a single scaffold to provide synergistic impact [113]. The material selection (biodegradable or nondegradable) can be used to control over drug release kinetics—via diffusion for nondegradable polymers or diffusion and scaffold degradation for biodegradable polymers.

Electrospinning also offers the opportunity to align the nanotubes along the axis of the fibers. Mechanical (modulus and strength), electrical, magnetic, and optical properties of CNT composites are affected by alignment of nanotubes in the matrix. Because of the sink-like flow in the wedge of the syringe, the nanotubes become oriented in the direction of flow. The aligned CNT in the fiber increases the surface area for contact with the polymer matrix and enhances the aspect ratio for reinforcement. Cells cultured on electrospun scaffolds have been shown to adhere and elongate along the fiber axis [115–117]. Alignment can also be achieved by depositing the fibers onto a rotating collector or to the edge of a spinning disk which orients the fiber along the axis of rotation (Figure 3.1). Fiber orientation is relevant since many tissues such as skeletal muscle tissue, ligaments, articular cartilage, and blood vessel walls intrinsically possess anisotropic cell organization. The orientation of the fiber induces anisotropy. This is critical to mimic in vivo the function of skeletal muscle cells, whose alignments permit the fusion of myoblasts into myotubes which forms the structural building blocks of densely packed muscle fibers that generate longitudinal muscle contraction [118]. Electrospun PCL–MWNT scaffolds seeded with primary rat muscle cells displayed multinucleated cells with interacting actin filaments [117]. Smooth muscle cells attached and migrated along the axis of electrospun poly(L-lactate-*co*-ε-caprolactone) copolymer [119]. In addition, it was reported [116] that electrically stimulated Poly (Lactic Acid) (PLA/MWNT) enhanced osteoblast growth along the axis of aligned nanofibers. This is an example of synergistic effect of electrical stimulation and topological cue on osteoblast growth that an electrospun nanofiber can induce (Figure 3.2).

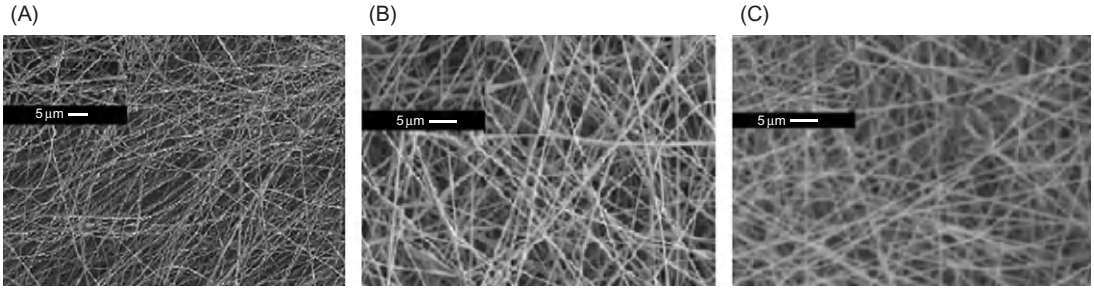

FIGURE 3.2

Scanning electron micrographs of polystyrene solution with different MWCNT concentration: (A) 0.5%, (B) 5%, and (C) 7%.

From Ref. [110].

3.2.5 Layer-by-layer assembly

The LbL technique is a powerful tool to assemble multilayer and multimaterial thin films. The alternate deposition of oppositely charged particles to form multiple-layer thin films was initially reported by Iller in 1966 [120] but picked up popularity after the work of Decher and coworkers [121,122] in the mid-1990s. The technique involves immersing a negatively (or positively) charged substrate in an oppositely charged polyelectrolyte which is adsorbed onto the substrate. After equilibrium is reached, the substrate is removed, rinsed, dried, and immersed in a negatively charged polyelectrolyte solution. This process is repeated until the desired thickness is achieved. The absorption of the polyelectrolyte is irreversible and charge overcompensation leads to charge reversal at the surface [123]. Different materials can be inserted between layers as long as they have the opposite charge. LbL assembly can also be performed on a colloidal substrate [11,124]. It enables the coating of various different shapes and sizes by uniformly layered materials with controllable thickness.

Initial results from multilayered film assembly [125] showed linear growth of mass and film thickness. Examples of linearly growing systems include poly (styrene sulfonate) and poly (allyamine hydrochloride) [126,127]. In these films, each polyelectrolyte interpenetrates only its neighboring layers. However, films that experience exponential growth have also been reported [128–130]. This exponential growth pattern was attributed to the vertical diffusion of polyelectrolyte into the film. Diffusion is controlled by the molecular weight (MW) of the polyelectrolyte, with higher MW diffusing much more slowly. Other factors that affect diffusion include polymer charge density and nature of chemical groups present on the polymer.

LbL assembly initially focused on construction films based on electrostatic interaction; subsequent works have focused on developing LbL composites based on hydrogen bonding [10,11], charge–transfer interactions [131,132], coordination bonding, and covalent bonding [133,134]. Through hydrogen bonding, a number of additional materials can be incorporated into multilayered composites in a water solution or organic phase. A number of polymers can act as donors and acceptors for hydrogen bonding. Hydrogen-bonding multilayer film assembly is based on the alternate deposition of polymers containing a hydrogen bond acceptor and a hydrogen bond donor, respectively. This enables the incorporation of biodegradable and biocompatible natural and synthetic polymers to be incorporated as they cannot be assembled via the electrostatic LbL approach. The double stranded DNA is a combination of hydrogen bonds between the bases and the $\pi-\pi$ stacking of the aromatic rings contained in the bases. While DNA multilayer systems have been produced using electrostatic attractions [135,136], it does not utilize the interactions between the base pairs which can be used to manipulate the structure of the multilayer film [137,138]. Compared to films assembled using electrostatic attractions, the pH range where hydrogen bonded multilayer form stable films is limited. Hence, the ability of these materials to disassemble within a narrow range of pH offers new possibilities for drug delivery applications. Disassembly can be achieved through fine tuning the pH by varying the hydrogen-bonding pairs or the conditions under which the layers are assembled. However, the films can also be made stable by cross-linking using chemical, thermal, and photochemical techniques.

Covalently bonded multilayered films have also been assembled using the LbL techniques. The presence of covalent bonds imparts stability to the films. The strength of the composites depends on the strong adhesion between the two polymers. The films can be assembled in organic solvents.

LbL composites containing CNTs have been assembled using electrostatic interactions [139,140] or hydrogen bonding [141–143]. Covalent cross-linking can increase the modulus of the films [144,145] and is achieved by using polymers that have functional groups that are capable of reacting with one another or can react with a bifunctional agent (using diamines, diimides, or dialdehydes). It is generally believed that cell processes are affected by their surrounding microenvironment which include their mechanical and biochemical stimuli [146–148].

In summary, the mechanical properties of CNT–polymer composites depend on the fabrication and processing technique used. A number of materials have served as a matrix for CNT-based composite including synthetic polymer, natural polymer, and ceramics. Irrespective of the processing technique used, two important criteria must be satisfied to effectively improve the material properties—interfacial adhesion between the CNT and the polymeric matrix, and a homogeneous dispersion of CNT in the matrix. CNTs have been chemically modified to incorporate functional groups in the end or sidewalls to enhance interactions with the matrix. Several dispersion techniques (e.g., screw extrusion, agitation, and ultrasonication) have been used to achieve efficient dispersion. One of the potential drawbacks of CNT composites made using traditional polymer-processing techniques is its inherent inability to include functional components. Biomolecules such as proteins are unable to withstand the harsh processing conditions encountered in traditional polymer techniques. In both the LbL assembly and electrospinning, it is possible to include biomolecules into the composite. Hence, the latter two techniques are more appealing for use in the field of tissue engineering.

3.3 Conductivity

Composites based on conductive polymer and conductive filler are of interest as biomaterials [12,149]. Polyaniline, polypyrrole, and polythiopene are conductive polymers that are available. However, conductive polymers have limited thermal and electrical stability, poor solubility in solvents, and poor mechanical properties. CNTs, in addition to improving the mechanical properties of composite, also make the composite more conductive. CNT–polymer composites become electrically conductive when a critical CNT concentration, referred to as percolation threshold, is attained. At percolation concentration, CNTs form an interconnected network of conductive pathways. The critical concentration is affected by various factors and includes polymer, nanotube type, processing technique, and processing conditions. For a given nanotube concentration, processing parameters during molding such as holding pressure and melt and mold temperature have a significant effect (~5–10 orders of magnitude) on the resistivity [54,150]. Type of nanotube (single wall versus multiple wall) affects percolation threshold [151] with SWNT requiring significantly lower amount to reach percolation threshold than MWNT [152]. While functionalization aids in dispersion and enhance matrix interaction, it decreased the electrical conductivity [153]. The mechanism for charge transport and modulus reinforcement of CNT-based composite materials are different [154]. For increased electrical conductivity, nanotube agglomeration is preferred. Pristine CNTs exhibited lower electrical percolation threshold than amino-functionalized ones, probably due to the lower aspect ratio of functionalized nanotubes [55]. In addition to electrical conductivity, the thermal conductivity of polymers can also be enhanced by the addition of CNTs [155].

The conductivity of CNT can be advantageous in many biological applications. For example, small current can stimulate osteogenesis of fractures [156]. Electrically induced osteogenesis has been extensively studied in vitro [157–159] and in vivo [160–164]. Blends of CNT and polylactic acid were used as conductive composite and exposed osteoblast cells to electrical stimulation [165]. Results indicate that alternating-current electrical stimulation promotes cell proliferation, gene expressions for collagenous and noncollagenous proteins, and enhanced calcium deposition in the extracellular matrix.

The conductive properties of CNT composites can be exploited to offer neural stimulation by prosthesis used to heal a damaged or diseased portion of the nervous system by delivering electrical pulses. Electrical conductivity can affect neural signal transmission [166]. Traditional neural electrodes are made from stable metals such as platinum, gold, titanium, and stainless steel. These metals suffer from poor contact with tissue or scar formation. Several coating materials such as iridium oxide [167] and conducting polymers such as polypyrrole [168] and polythiopene [169] have emerged as materials for neural interfacing. However, they suffer from long-term instability [170]. Recently poly (3,4-ethylenedioxythipene) doped with CNT and deposited on platinum microelectrodes gave promising results in terms of stability, toxicity, and in supporting the growth of neurons [171,172]. It has been shown [173–177] that CNT microelectrodes have superior electrochemical properties, which are further enhanced by surface coating [178–180]. The CNT-based microelectrodes allow the growth and differentiation of neurons.

3.4 CNT cytotoxicity

Given the remarkable properties of CNTs, there is considerable interest in its applications in the fields of biomaterials, biosensors, drug delivery, and tissue engineering. Hence, it is paramount that the safety of CNTs to human health and the environment be assessed. It is known that sub-micron size particles (such as asbestos fibers) influence cell behavior [181]. The higher surface area for small particles makes them more reactive than larger particles [182,183].

Most of the as-produced CNTs contain substantial amounts of impurities such as metal catalyst (Co, Fe, Ni, Mo, and Pt). Some of the metals (Co, Ni, Co^{2+}) cause cytotoxic or genotoxic effects as well as lung diseases including fibrosis and asthma [184]. Nickel is known to be cytotoxic and carcinogenic to the human body [185]. Hence, the toxic effects of unpurified CNT were evoked by the heavy metal residues rather than the nanotubes themselves [186]. Other factors that induce cytotoxicity include length and size distribution, surface area, dispersion and aggregation status, coating or functionalization, immobilization, internalization, or cellular uptake and cell type [149]. Furthermore, these factors could interact with each other. This has led to contradictory results in the literature. While some studies have reported that CNTs are toxic to mammalian cells [187–191], other reports have suggested that CNTs are biocompatible [192–195]. In general, the negative results have come from research groups concerned with environmental aspects [187,190,196]. The discrepancy lies in the source from where the nanotubes were obtained, dose, and time of exposure.

Several techniques have been used to purify the as-processed nanotubes. These include acid treatment [197,198], thermal oxidation [199], acid treatment with thermal oxidation [200], and a

combination of ultrasonication and centrifugation using organic solvents [201]. During the purification by strong acids, chemical oxidation occurs at the end cap of CNTs and at the wall-defect sites resulting in the introduction of functional oxygenated groups [193]. Purified SWNTs have the most adverse effect on cellular behavior because of its larger surface area when compared to MWNT, carbon graphite, active carbon, and carbon black [188]. Purified SWNTs are more cytotoxic than unmodified SWNTs, due to the functional group (carboxyl and hydroxyl) density on SWNT surface generated by acid treatment [191,202,203]. Other studies have indicated that higher degree of sidewall functionalization leads to reduced cytotoxicity [204]. Functionalized CNTs can cross the cell membrane and accumulate in the cytoplasm without being toxic to cells [205]. Furthermore, these functional groups also allow CNTs to conjugate with other biomolecules such as nucleic acids and proteins enhancing biocompatibility [206]. Surface chemistry also affects aggregation of nanotubes resulting from van der Waals interactions between the tubes. Unmodified CNTs cannot disperse in water due to their hydrophobic nature and accumulate into cells, tissues, and organs leading to toxicity [207]. Cytotoxic effects of well-dispersed SWNT were compared with the toxicity of agglomerated SWNTs with asbestos as a reference. Rope-like agglomerated nanotubes were reported to be the most toxic.

MWNTs with diameter of 20−40 nm and average lengths of 220 and 825 nm induce similar activities and slight toxicities [208]. SWNTs with length shorter than ∼189 nm are more easily consumed and induce greater toxicity [209]. Larger lengths of CNT (in micron range) are unable to cross the cell membranes. Methods used to disperse CNTs affect cytotoxicity [210,211]. The type of CNT (single wall versus multiple walls) could also affect toxicity since the surface area per unit mass of SWNT is greater than that of MWNT. It is difficult to compare the results between toxicity induced by SWNT versus MWNT as it is unclear whether results should be compared to same mass concentration of CNT or the same total surface area.

In vivo toxicity studies have been conducted using CNTs. Pulmonary toxicity was attributed to mechanical blockage of the airways in both rat [182,212] and mice [213−215] models. Warheit et al. [182] suggested that granuloma formation within the lungs of rats occurred due to the presence of SWNT aggregates. Other studies have reported that intravenously administered low doses of functionalized CNTs showed no toxicity even after persisting in the body for 4 months [216]. Even at high concentrations, modified MWNT showed only low acute toxicity [211]. In vivo studies for applications in bone−tissue engineering have also yielded promising results. Usui et al. [217] reported that MWNT implanted into mouse skull induced minimal local inflammation and showed high bone−tissue compatibility by permitting bone repair. In one study [218], a threefold increase in bone−tissue growth was observed in defects repaired with scaffolds containing nanotube composite over polymer scaffolds. CNT composites also permitted bone formation and bone repair without signs of rejection and inflammation when implanted in critical-sized rat calvaria [219]. Composites of MWNT/polycarbosilane implanted in the subcutaneous tissue and femur of rats showed little inflammatory response and supported newly formed bone [220]. Nanotube-filled nanocomposite-derived microcatheters exhibited highly reduced thrombus formation compared to pure nylon-derived microcatheters when implanted in adult beagle dogs [221].

It is more relevant to evaluate the toxicity of scaffolds that are assembled for tissue engineering. Here substrates are developed with the aim of directing and controlling cellular behavior on these scaffolds capable of replacing or regenerating tissues [222−225]. The scaffolds are 3D structures that act as substrates for cell adhesion and proliferation. Recently scaffolds based on CNTs have

been explored as templates for bone and neural tissue engineering. In these circumstances, the surrounding tissues come in contact with CNT-based composites. Unrestricted growth and proliferation of human osteoblast hFOB 1.19 cells were observed around CNT regions indicating biocompatibility [226]. Studies of bone cells interaction with polyurethane−CNT foams indicated no osteoblast cytotoxicity or hindrance on osteoblast differentiation or mineralization [227]. SWNTs with negative charge allow the nucleation and crystallization of hydroxyapatite (HA), a component of bone [228,229]. Polyurethane−CNT composites also displayed improved anticoagulant functions [230].

Several studies have been conducted that evaluated CNTs as templates for neuronal growth [173,174,231−233]. Neurons were observed to grow on unmodified MWNT [177], while more branched neuritis were observed when grown on 4-hydroxynonenal-coated MWNT. Positively charged MWNTs yielded more numerous growth cones, longer average neurite length, and elaborate neurite branching than neutrally or negatively charged MWNTs. In a subsequent study [232], positively charged poly(ethylenimine) (PEI)-grafted SWNT had reduced neuronal growth characteristic than a pure PEI. CNT-based composites improve the neural signal transfer probably due to the high electrical conductivity [174].

3.5 CNT applications in dentistry

The use of CNT in the dentistry field has been explored modestly since its introduction in the early 1990s. The applications of CNT in the dental field can be categorized into three areas: (i) application to dental restoration materials, (ii) application to bony defect replacement therapy, and (iii) application to protein, gene, and drug delivery and cancer treatment.

3.5.1 Dental restorative materials

Dental composite resin is a tooth-colored restorative material used to replace a decayed portion of tooth structure. Its esthetic appearance is the main advantage over the conventional dental amalgam. Typical composite resin is composed of a resin-based matrix, such as bisphenol A-glycidyl methacrylate and inorganic filler like silica. The filler gives the composite improved mechanical property, wear resistance, and translucency. Functionalized SWNT has been applied to the dental composite to increase its tensile strength and Young's modulus to help improve the longevity of composite restoration in oral cavity. Addition of functionalized SWNT increased its flexural strength significantly by absorbing more stress [234]. However, further effort in development of CNT-reinforced composite resin has been hampered because of its dark color primarily from CNT, which is a major drawback for esthetic composite resin.

CNT has been applied to the interface of dentin and composite resin to compensate for microleakage development in long-term use, which is a major cause of restoration failure. Once microleakage develops between tooth and composite resin interface, it works as a nidus for bacterial colonization; thus, secondary decay can develop. CNT has shown the potential to provide protection against bacteria and initiates the nucleation of HA on its surface [235]. Studies have reported that hydrophobic interaction between CNTs and exposed collagen fibers from dentin as a mechanism for CNT's attachment to the dentin surface [236] and that the bond strength between CNT-coated dentin and composite resin restoration material was not affected by the presence of the

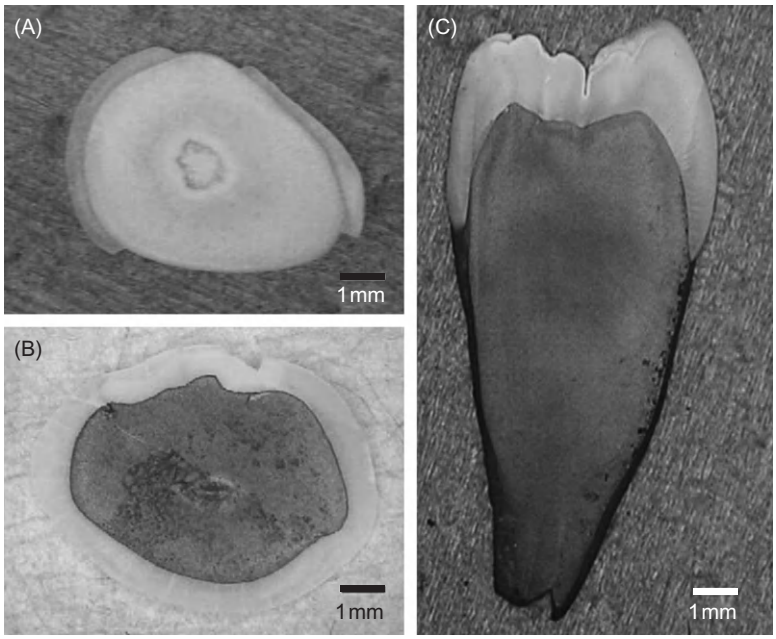

FIGURE 3.3

Photographs of tooth slices coated with CNTs. (A) Nontreated tooth slice (control), (B) transverse view of CNT-coated tooth slice, and (C) sagittal view of CNT-coated tooth slice.

From Ref. [235].

CNT [235]. The presence of CNT at the interface of dentin and composite resin can reduce the chance of secondary decay development in the long term by providing protection against decay inducing bacteria and initiating HA nucleation on its surface. However, the gray discoloration (Figure 3.3) at the dentin−composite resin interface due to CNT needs to be overcome to make this application a reality.

One of the most common complications of denture prostheses is the cracking of denture base from either accidental dropping or long-term fatigue failure. Denture base is usually made of PMMA because of its excellent esthetics, low density, low cost, and ability to be repaired. However, it has relatively low fracture strength which makes a denture base vulnerable to crack by either impact or flexural fatigue under chewing [237]. Recently, MWNT (0.1−1.0 wt%) has been incorporated into PMMA to increase flexural strength and fracture toughness of denture base materials [238]. A similar application of MWNT (0−10 wt%) to PMMA-based bone cement used in the orthopedic area has shown to improve the fatigue performance of bone cement [239]. Authors of both studies found that loading of MWNT in PMMA improved flexural strength and fatigue performances of polymers in a dose-dependent manner. It was speculated that well-dispersed MWNT was able to reinforce PMMA matrix prior to crack initiation and to arrest/retard early phase of crack propagation. Even with the significant improvement in mechanical properties, resultant black color of the denture base remains as a disadvantage of CNT application.

3.5.2 Bony defect replacement therapy

As dental implant treatment of replacing missing teeth becomes highly predictable, supplemental bone augmentation therapy using synthetic and cadaveric bone biomaterials also attains increased popularity. Insufficient volume or bony defects of alveolar bone can be caused by the periodontal disease, tooth loss, and/or trauma. Wide range of biomaterials from bone fillers to tissue engineered composite materials, such as calcium sulfate, calcium phosphate, HA, polymers, and CNTs have been explored as candidates to achieve predictable bony defect replacement. It was reported that nanoscale HA was formed on the surface of MWNT when immersed in calcium phosphate solution of 37°C for 2 weeks, indicating CNTs potential use for bone−tissue engineering.

Guided bone regeneration is a dental surgical procedure that utilizes barrier membrane to guide the new bone formation at sites having insufficient volumes of bone while inhibiting the epithelial cell growth into the bony defect sites. Researchers have developed a biomembrane by electron-spinning a suspension of poly (L-lactic acid) (PLLA), MWNT and HA to promote guided bone regeneration. Authors found that the membrane was able to promote desirable periodontal ligament cell (PDLC) adhesion and proliferation by 30% while inhibiting less desirable epithelial cell proliferation (Figure 3.4) [240]. Furthermore, a new chitosan−MWNT composite has been developed which can promote osteoblast proliferation and apatite crystal formation on the surface of MWNT while discouraging adhesion of fibroblast [241]. However, whether and how these engineered membranes used for guided bone regeneration can be removed or will be resorbed completely in a pattern similar to that of currently available Teflon-based and collagen-based membranes are the questions that need to be answered before they are introduced to the clinic.

The key factors for the successful bony defect replacement therapy are whether sufficient blood supply can be maintained to the grafted sites and whether the grafted materials can be immobilized and protected to achieve a desired dimension after healing. A small bony defect which is well surrounded by the adjacent native bone can be replaced predictably using patient's own bone or cadaveric/animal particulated bone graft materials. However, larger bony defects which do not have surrounding native bone supports face challenges of achieving immobilization of the grafted materials as well as sufficient blood supply. Engineered bone scaffolds which mimic the anatomy of bone structure and can provide structures for new bone formation have been studied widely. Highly porous interconnected scaffolds were fabricated using thermal-cross-linking particulate-leaching technique for bone defect replacement therapy [242]. The porogen content was found to dictate the porosity of scaffold and the higher porosity improved the interconnectivity of the pores. However, compressive mechanical properties declined as porosity increased. Authors found that nanocomposites with ultrashort SWNT showed higher compressive strength compared to poly(propylene fumarate) scaffold, indicating that highly porous polymer scaffold which mimicks natural trabecular bone structure can be strengthened by the incorporation of CNT. Composite scaffolds of electrospun poly(lactic-*co*-glycolic acid) nanofibers onto the knitted scaffold made from MWNT yarn [243] resulted in uniform cell distribution and spanning of cells on the knotted scaffold surface. This indicates the potential of knitted composite to be used as a scaffold for bone replacement.

Mineral formation on CNT−PCL composite fabricated using LbL self-assembly technique by human fetal osteoblast was better than mineral formation on the titanium surface (Figure 3.5) [219]. Increasing the number of layers of SWNT on PCL polymer increased the mechanical properties.

Researchers have continued to work on 3D scaffold using compression molding and salt leaching technique to mimic trabecular pattern of bone. Multiple layers of SWNT and gelatin were coated using LbL self-assembly technique on 3D porous PCL scaffold. This technique might increase the mechanical properties of the 3D scaffold while maintaining high levels of porosity and interconnectivity, mimicking highly porous trabecular bone and possibly facilitate osteogenic cell proliferation by utilizing CNTs electrical properties.

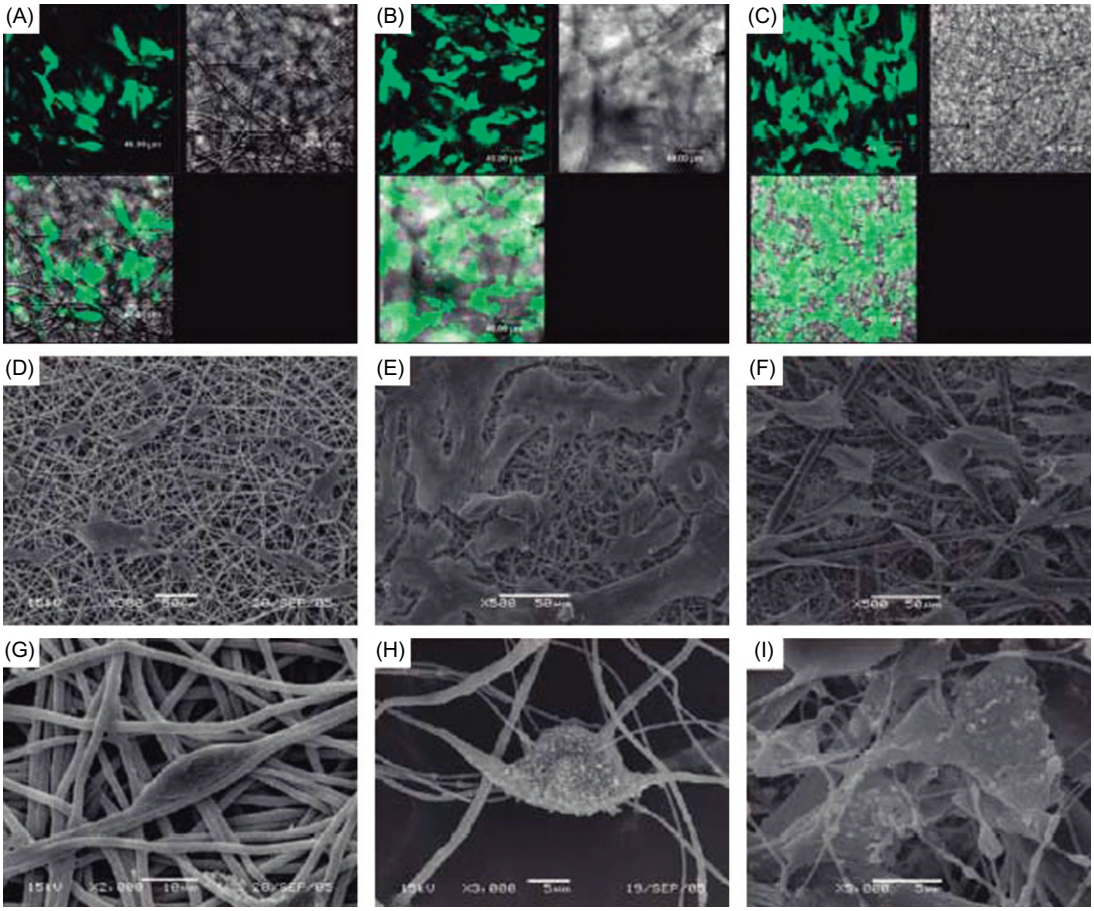

FIGURE 3.4

Morphology observation of PDLCs cultured on three kinds of membranes: (A), (B), and (C) represent confocal laser microscope images of PDLCs on PLLA, PLLA/HA, and PLLA/MWNTs/HA membranes, respectively. (D), (E), and (F) represent SEM images of PDLCs on PLLA, PLLA/HA, and PLLA/MWNTs/HA membranes, respectively, at low magnification. (G), (H), and (I) represent them at high magnification.

From Ref. [240].

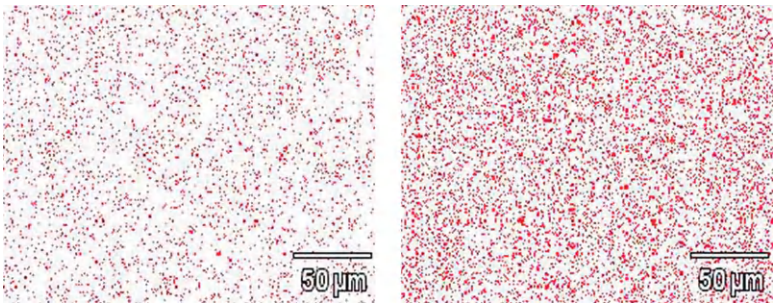

FIGURE 3.5

Surface calcium mapping using EDS (Energy Dispersive Spectroscopy) on substrates with cells 4 weeks after cell plating. The red dots indicate locations of calcium. All the three substrates showed uniform distribution of calcium, while CNT-comp had higher amount of calcium compared to cpTi (commercially pure titanium) ($P < 0.05$). (For interpretation of the references to color in this figure legend, the reader is referred to the web version of this book.)

From Ref. [219].

3.5.3 Protein, gene, and drug delivery

The findings that biomolecules such as proteins and DNA can be immobilized with CNTs hollow cavity or on its surface have embarked significant research efforts on bioconjugated CNTs potential role in gene therapy and drug delivery [244,245]. MWNT has higher ability to adsorb proteins than graphite when the maturation of the osteoblast by MWNT was examined [246,247]. This finding of CNTs ability to adsorb proteins on its surface has indicated its potential role as a carrier for protein or gene delivery. Also, the adsorption of the recombinant human bone morphogenetic protein-2 (rhBMP-2) on the surface of MWNT−chitosan scaffolds was shown to be satisfactory, and researchers were able to induce ectopic bone formation by implanting MWNT−chitosan scaffold adsorbed with the rhBMP-2 in mouse muscle (Figure 3.6) [248].

Various functional groups can be attached to the tips or sidewalls of nanotubes to make functionalized CNT which can be used for the delivery of drugs, proteins, and genes because functionalization can improve CNTs solubility and biocompatibility [249]. During gene therapy, due to the potential undesired immune and oncogenic side effects toward the viral vector, nonviral vectors such as nucleic acid conjugate with cationic lipids and polymers, and nanoparticles have been explored as an alternative to guarantee a high degree of safety [250]. Functionalized CNT was used as a gene delivery medium because the macromolecular and cationic nature of the functionalized CNT can help to form supramolecular complexes with plasmid DNA [251]. Authors showed that supramolecular complexes with plasmid DNA were successfully formed on f-SWNT, indicating the potential of functionalized CNTs in gene therapy and genetic vaccination. Furthermore, it was reported that gene expression offered by the supramolecular complexes of functionalized CNT and plasmid DNA was five to ten times higher than that of DNA alone [252].

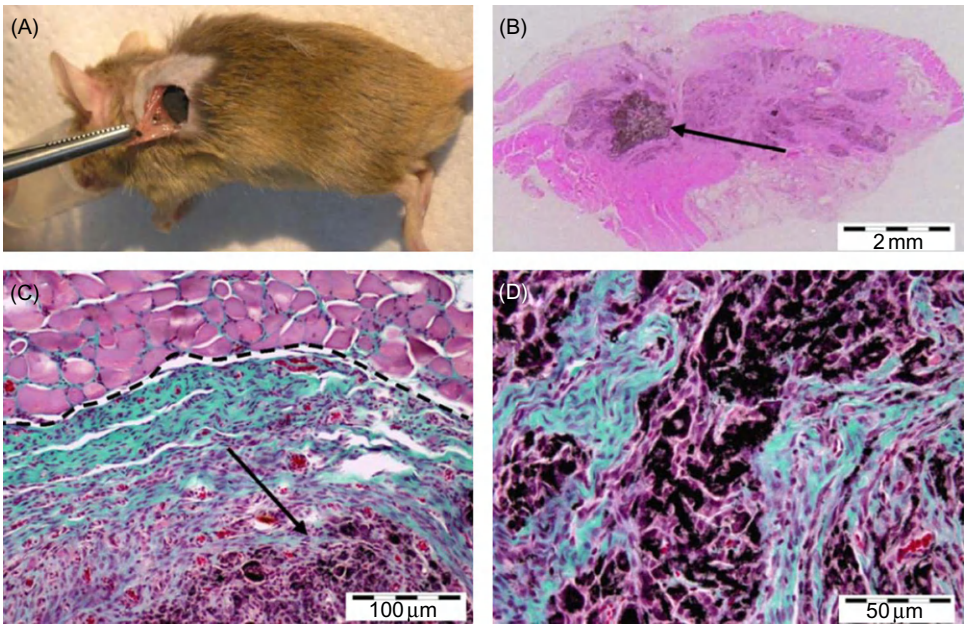

FIGURE 3.6

Picture (A) shows the surgery implantation of rhBMP-2 adsorbed MWNT/CHI (chitosan) scaffolds into mouse subcutaneous muscular pocket. Optical microscope micrograph (B) shows regenerated bone tissue and a minor fraction of remaining MWNT/CHI scaffold. Optical micrograph (C) shows a detail of regenerated bone tissue (collagen expressing cells, blue–green colored) after major disassembly of the MWNT/CHI scaffold, surrounded by muscle tissue (pink colored). The well-limited interface between adjacent tissues is remarkable (see black dash line). The remaining MWNT/CHI scaffold (black colored) is pointed by black arrow. Optical micrograph (D) shows a detail of remaining scaffold plenty of fibroblasts (purple colored), prior to its disassembly and colonization by collagen expressing cells (blue–green colored). (For interpretation of the references to color in this figure legend, the reader is referred to the web version of this book.)

From Ref. [248].

Due to its nanoscale size, solubility, reduced cellular toxicity, and cationic surface of functionalized CNT, its potential use as a novel drug delivery vehicle has been studied extensively. Functionalized CNT conjugated with peptides was able to penetrate into the cells such as HeLa immortal cells, fibroblasts, and keratocytes, indicating the potential of functionalized CNT as a carrier for drug delivery [253].

A group of researchers conjugated SWNT with the anticancer drug cisplatin and a receptor ligand, epidermal growth factor (EGF) to treat squamous cell carcinoma, which is one of the most common oral cancers [254]. By having EGF, which has a strong affinity to the cell-surface receptor which is overexpressed in squamous cell carcinoma, the compound was able to target cancer cells with high specificity. Authors found that functionalized and bioconjugated CNT caused endocytosis by drawing CNT into the cell.

3.6 Summary and conclusions

Polymer-based composites reinforced by carbon fibers have been used for reinforcing structures. CNTs have significantly better properties than carbon fibers making them superior fillers in composites. However, nanotubes easily agglomerate, bundle together, and entangle, thus limiting the reinforcing efficiency on polymer matrix. The poor dispersion along with the rope-like entanglement leads to reduced properties of the composites. Hence, to maximize the potential of CNTs as effective reinforcements in composites, the nanotubes must be well dispersed and interact with the matrix to prevent slippage. Dispersing nanofillers in a polymeric matrix is significantly more difficult due to their strong tendency to agglomerate. The problem is compounded if high volume fraction composites are to be realized. Methods such as high-speed shearing and ultrasonication have been attempted with limited success. To achieve strong interfacial adhesion with the surrounding polymer matrix, the surface of the nanotubes needs to be chemically functionalized.

In addition to the traditional polymer-processing techniques (melt blending, solution casting, and in situ polymerization) electrospinning and LbL assembly methods of compounding composites deserve special attention. Both techniques are versatile and offer the potential to incorporate biological entities in the composite. Electrospinning offers the potential of combining material properties with morphological characteristics (3D) that are attractive for tissue engineering application. Multilayered films assembled using the LbL technique appears promising for drug delivery application.

An added advantage of using CNTs in composites is that it makes the composite conductive which aids in bone healing and in neural stimulation. Given the importance of orientation with respect to electrical conduction, it is important to be able to align CNTs in composites. Since higher conductivities are desirable, it is also imperative that methods to incorporate well-dispersed nanotubes at higher concentration be developed.

Mixed and conflicting results have been obtained for the toxicity of CNTs. The reason lies in the presence of impurities, degree of functionalization, types of cells used, and even the techniques used to assess cytotoxicity. It has been suggested [255] that at least two or more independent tests be used to test for toxicity of nanotubes. Results from studies conducted in vivo and in vitro are difficult to compare. Before nanotubes can be widely accepted in medical applications, its long-term toxicity needs to be evaluated.

References

[1] P.G. Collins, P. Avouris, Nanotubes for electronics, Sci. Am. 283 (2000) 62–69.

[2] E.W. Wong, P.E. Sheehan, C.M. Lieber, Nanobeam mechanics: elasticity, strength, and toughness of nanorods and nanotubes, Science 277 (1997) 1971–1975.

[3] M. Yu, et al., Strength and breaking mechanism of multiwalled carbon nanotubes under tensile load, Science 287 (2000) 637–640.

[4] J.N. Coleman, U. Khan, Y.K. Gun'ko, Mechanical reinforcement of polymers using carbon nanotubes, Adv. Mater. 18 (2006) 689–706.

[5] W. Kaminsky, Polyolefin−carbon nanotube composites by in situ polymerization, in: T.M.a.P. Potschke (Ed.), Polymer Carbon Nanotube Composites—Preparation Properties and Applications, Woodhead, Cambridge, UK, 2011, p. 3.
[6] A.R. Bhattacharyya, et al., Crystallization and orientation studies in polypropylene/single wall carbon nanotube composite, Polymer 44 (2003) 2373−2377.
[7] J. Jeong, et al., Nylon 610 functionalized multiwalled carbon nanotube composite prepared from in situ interfacial polymerization, J. Polym. Sci. 108 (2008) 1506−1513.
[8] S. Agarwal, A. Greiner, J. Wendorff, Electrospinning of manmade and biopolymer nanofibers—progress in techniques, materials, and applications, Adv. Funct. Mater. 19 (2009) 2863−2879.
[9] W. Teo, R. Inai, S. Ramakrishna, Technological advances in electrospinning of nanofibers, Sci. Technol. Adv. Mater. 12 (2011) p013002 (19 pp).
[10] T. Boudou, et al., Multiple functionalities of polyelectrolyte multilayer films: new biomedical applications, Adv. Mater. 21 (2009) 1−27.
[11] G.K. Such, A.P.R. Johnston, F. Caruso, Engineered hydrogen-bonded polymer multilayers: from assembly to biomedical applications, Chem. Soc. Rev. 40 (2011) 19−29.
[12] C. McClory, S.J. Chin, T. McNally, Polymer/carbon nanotube composites, Aust. J. Chem. 62 (2009) 762−785.
[13] A. Greiner, J.H. Wendorff, Functional self-assembled nanofibers by electrospinning, Adv. Polym. Sci. 219 (2008) 107−171.
[14] R. Andrews, M.C. Weisenberger, Carbon nanotube polymer composites, Curr. Opin. Solid State Mater. Sci. 8 (2004) 31−37.
[15] J.P. Salvetat, et al., Elastic and shear moduli of single-walled carbon nanotubes ropes, Phys. Rev. Lett. 82 (1999) 944−947.
[16] S.B. Sinnott, Chemical functionalization of carbon nanotubes, J. Nanosci. Nanotechnol. 2 (2002) 113−123.
[17] J.L. Bahr, J.M. Tour, Covalent chemistry of single-walled carbon nanotubes, J. Mater. Chem. 12 (2002) 1952−1958.
[18] V. Lordi, N. Yao, J. Wei, Method for supporting platinum on single-walled carbon nanotubes for selective hydrogenation catalyst, Chem. Mater. 13 (2001) 733−737.
[19] J. Chen, et al., Solution properties of single-walled carbon nanotubes, Science 282 (1998) 95−98.
[20] J. Chen, et al., Dissolution of full-length single-walled carbon nanotubes, J. Phys. Chem. B 105 (2001) 2525−2528.
[21] M.A. Hamon, et al., Dissolution of single-walled nanotubes, Adv. Mater. 11 (1999) 834−840.
[22] D.B. Mawhinney, et al., Infrared spectral evidence for the etching of carbon nanotubes: ozone oxidation at 298K, J. Am. Chem. Soc. 122 (2000) 2383−2384.
[23] K. Jiang, et al., Selective attachment of gold nanoparticles to nitrogen-doped carbon nanotubes, Nano Lett. 3 (2003) 275−277.
[24] A.V. Ellis, et al., Hydrophobic anchoring of monolayer-protected gold-nanoclusters to carbon nanotubes, Nano Lett. 3 (2003) 279−282.
[25] R. Saini, et al., Covalent sidewall functionalization of single wall carbon nanotubes, J. Am. Chem. Soc. 125 (2003) 3617−3621.
[26] V. Georgakilas, et al., Organic functionalization of carbon nanotubes, J. Am. Chem. Soc. 124 (2002) 760−761.
[27] W. Huang, et al., Attaching proteins to carbon nanotubes via diimide-activated amidation, Nano Lett. 2 (2002) 311−314.
[28] V. Lordi, N. Yao, Molecular mechanics of binding in carbon nanotube-polymer composites, J. Mater. Res. 15 (2000) 1049−1052.

[29] E.K. Thostenson, T.W. Chou, Aligned multi-walled carbon nanotube-reinforced composites: processing and mechanical characterization, J. Phys. D Appl. Phys. 35 (2002) L77–L80.
[30] C. Bower, et al., Deformation of carbon nanotubes in nanotube polymer composites, Appl. Phys. Lett. 74 (1999) 3317–3319.
[31] L. Jin, C. Bower, O. Zhou, Alignment of carbon nanotubes in polymer matrix by mechanical stretching, Appl. Phys. Lett. 73 (1998) 1197–1199.
[32] R. Haggenmueller, et al., Aligned single-wall carbon nanotubes in composites by melt processing methods, Chem. Phys. Lett. 330 (2000) 219–225.
[33] R. Haggenmueller, et al., Production and characterization of polymer nanocomposites with highly aligned single-walled carbon nanotubes, J. Nanosci. Nanotechnol. 3 (2003) 105–110.
[34] X.Q. Chen, et al., Aligning single-wall carbon nanotubes with an alternating-current electric field, Appl. Phys. Lett. 78 (2001) 3714–3716.
[35] M.S. Kumar, et al., Influence of electric field type on the assembly of single walled carbon nanotubes, Chem. Phys. Lett. 383 (2004) 235–239.
[36] C.A. Martin, et al., Electric field-induced aligned multi-wall carbon nanotube networks in epoxy composites, Polymer 46 (2005) 866–877.
[37] C.J. Strobl, et al., Carbon nanotube alignment by surface acoustic waves, Appl. Phys. Lett. 85 (2004) 1427–1429.
[38] M.S. Kumar, et al., DC electric field assisted alignment of carbon nanotubes on metal electrodes, Solid-State Electron. 47 (2003) 2075–2080.
[39] P.V. Kamat, et al., Self-assembled linear bundles of single wall carbon nanotubes and their alignment and deposition as a film in a dc field, J. Am. Chem. Soc. 126 (2004) 10757–10762.
[40] E. Camponeschi, et al., Properties of carbon nanotube-polymer composites in a magnetic field, Carbon 45 (2007) 2037–2046.
[41] B.W. Steinart, D.R. Dean, Magnetic field alignment and electrical properties of solution cast PET-carbon nanotube composite films, Polymer 50 (2009) 898–904.
[42] H. Garmestani, et al., Polymer-mediated alignment of carbon nanotubes under high magnetic fields, Adv. Mater. 15 (2003) 1918–1921.
[43] Q. Wang, et al., The effects of CNT alignment on electrical conductivity and mechanical properties of SWNT/epoxy nanocomposites, Compo. Sci. Technol. 68 (2008) 1644–1648.
[44] J.H. Yang, et al., Direct formation of nanohybrid shish-kebab in the injection molded bar of polyethylene/multiwalled carbon nanotubes composites, Macromolecules 42 (2009) 7016–7023.
[45] Y. Bin, et al., Development of highly oriented polyethylene filled with aligned carbon nanotubes by gelation/crystallization from solutions, Macromolecules 36 (2003) 6213–6219.
[46] W. Chen, X. Tao, Production and characterization of polymer nanocomposite with aligned single wall carbon nanotubes, Appl. Surf. Sci. 252 (2006) 3547–3552.
[47] P. Potschke, A.R. Bhattacharya, A. Janke, Morphology and electrical resistivity of melt mixed blends of polyethylene and carbon nanotube filled polycarbonate, Polymer 44 (2003) 8061–8069.
[48] Y. Zuo, et al., Processing and properties of MWNT/HDPE composites, Carbon 42 (2004) 271–277.
[49] W. Tang, M.H. Santare, S.G. Advani, Melt processing and mechanical property characterization of multi-walled carbon nanotube/high density polyethylene (MWNT/HDPE) composite films, Carbon 41 (2003) 2779–2785.
[50] R. Andrews, et al., Fabrication of carbon multiwall nanotube/polymer composites by shear mixing, Macromol. Mater. Eng. 287 (2002) 395–403.
[51] Z. Jia, et al., Study on poly(methyl methacrylate): carbon nanotube composites, Mater. Sci. Eng, A 271 (1999) 395–400.

[52] J.K.W. Sandler, et al., A comparative study of melt spun polyamide-12 fibres reinforced with carbon nanotubes and nanofibres, Polymer 45 (2004) 2001−2015.
[53] T. Villmow, B. Kretzschmar, P. Potschke, Influence of screw configuration, residence time, and specific mechanical energy in twin-screw extrusion of polycaprolactone/multi-walled carbon nanotube composites, Compos. Sci. Technol. 70 (2010) 2045−2055.
[54] T. Villmow, et al., Influence of twin-screw extrusion conditions on the dispersion of multi-walled carbon nanotubes in poly(lactic acid) matrix, Polymer 49 (2008) 3500−3509.
[55] M.T. Byrne, Y.K. Gun'ko, Recent advances in research on carbon nanotube-polymer composites, Adv. Mater. 22 (2010) 1672−1688.
[56] J.N. Coleman, et al., Small but strong: a review of the mechanical properties of carbon nanotube-polymer composites, Carbon 44 (2006) 1624−1652.
[57] Z. Jin, et al., Dynamic mechanical behavior of melt-processed multi-walled carbon nanotube/poly (methyl methacrylate) composites, Chem. Phys. Lett. 337 (2001) 43−47.
[58] D. Qian, et al., Load transfer and deformation mechanism in carbon nanotube−polystyrene composites, Appl. Phys. Lett. 76 (2000) 2868−2870.
[59] O. Meincke, et al., Mechanical properties and electrical conductivity of carbon-nanotube filled polyamide-6 and its blends with acrylonitrile/butadiene/styrene, Polymer 45 (2004) 739−748.
[60] G.X. Chen, et al., Multi-walled carbon nanotubes reinforced nylon 6 composites, Polymer 47 (2006) 4760−4767.
[61] P. Potschke, et al., Dispersion of carbon nanotubes into thermoplastic polymers using melt mixing, Am. Inst. Phys. Conf. Proc. 723 (2004) 478−484.
[62] M.A. Lopez-Manchado, et al., Thermal and mechanical properties of single-walled carbon nanotubes−polypropylene composites prepared by melt processing, Carbon 43 (2005) 1499−1505.
[63] M. Cadek, et al., Reinforcement of polymers with carbon nanotubes: the role of nanotube surface area, Nano Lett. 4 (2004) 353−356.
[64] L. Liu, et al., Mechanical properties of functionalized single-walled carbon-nanotube/poly(vinyl alcohol) nanocomposites, Adv. Funct. Mater. 15 (2005) 975−980.
[65] S. Bhattacharyya, et al., Protein-functionalized carbon nanotube-polymer composites, Appl. Phys. Lett. 86 (2005) 113104.
[66] R. Blake, et al., Reinforcement of poly(vinyl chloride) and polystyrene using chlorinated polypropylene grafted carbon nanotubes, J.. Mater. Chem. 16 (2006) 4206−4213.
[67] N.G. Sahoo, et al., Effect of functionalized carbon nanotubes on molecular interaction and properties of polyurethane composites, Macromol. Chem. Phys. 207 (2006) 1773−1780.
[68] M. Kang, S.J. Myung, H.J. Jin, Nylon 610 and carbon nanotube composite by in situ interfacial polymerization, Polymer 47 (2006) 3961−3966.
[69] J. Zhu, et al., Reinforcing epoxy polymer composites through covalent integration of functionalized nanotubes, Adv. Funct. Mater. 14 (2004) 643−648.
[70] S.D. Bergin, et al., Towards solution of single-walled carbon nanotubes in common solvents, Adv. Mater. 20 (2008) 1876−1881.
[71] Y.J. Kim, et al., Electrical conductivity of chemically modified multiwalled carbon nanotube/epoxy composites, Carbon 43 (2005) 23−30.
[72] R. Haggenmueller, et al., Interfacial in situ polymerization of single wall carbon nanotube/nylon 6,6 composites, Polymer 47 (2006) 2381−2388.
[73] J.Y. Jeong, et al., Nylon 610/functionalized multiwalled carbon nanotube composite prepared from in situ interfacial polymerization, J. Polym. Sci. A 46 (2008) 6041−6050.
[74] Y. Geng, et al., Effects of surfactant treatment on the mechanical and electrical properties of CNT/epoxy nanocomposites, Compos. Appl. Sci. Manuf 39 (2008) 1876−1883.

[75] P.C. Ma, J.K. Kim, B.Z. Tang, Effects of silane functionalization on the properties of carbon nanotube/epoxy nanocomposites, Compos. Sci. Technol. 67 (2007) 2965−2972.
[76] F.H. Gojny, K. Schulte, Functionalization effect on the thermo-mechanical behavior of multi-wall carbon nanotube/epoxy composites, Compos. Sci. Technol. 64 (2004) 2303−2308.
[77] X.Q. Liu, M.B. Chan-Park, Facile way to disperse single-walled carbon nanotubes using a noncovalent method and their reinforcing effect in poly(methyl methyacrylate) composites, J. Appl. Polym. Sci. 114 (2009) 3414−3419.
[78] S.R. Chowdhury, et al., Microwave-induced rapid nanocomposite using dispersed single-wall carbon nanotubes as the nuclei, J. Mater. Sci. 44 (2009) 1245−1250.
[79] J.M. Yuan, et al., Preparation of polystyrene−multiwalled carbon nanotube composites with individual-dispersed nanotubes and strong interfacial adhesion, Polymer 50 (2009) 3285−3291.
[80] M. Trujillo, et al., Thermal and morphological characterization of nanocomposites prepared by in situ polymerization of high-density polyethylene on carbon nanotubes, Macromolecules 40 (2007) 6268−6276.
[81] W. Kaminsky, A. Funck, In situ polymerization of olefins with nanoparticles by metallocene-catalysis, Macromol. Symp. 260 (2007) 1−8.
[82] S.M. Kwon, et al., Poly(methyl methacrylate)/multiwalled carbon nanotube microspheres fabricated via in situ polymerization, J. Polym. Sci. Polym. Phys. 46 (2008) 182−189.
[83] W.H. Songa, et al., The preparation of biodegradable polyurethane/carbon nanotube composite based on in situ cross-linking, Polym. Adv. Technol. 20 (2009) 327−331.
[84] J. Kwon, H. Kim, Comparison of the properties of waterborne polyurethane/multiwalled carbon nanotube and acid-treated multiwalled carbon nanotube composites prepared by in situ polymerization, J. Polym. Sci. Polym. Chem. 43 (2005) 3973−3985.
[85] M. Castro, et al., Carbon nanotube/poly(e-caprolcatone) composite vapor sensors, Carbon 47 (2009) 1930−1942.
[86] D. Priftis, et al., Surface modification of multiwalled carbon nanotubes with biocompatible polymers via ring opening and living anionic surface initiated polymerization. Kinetics and crystallization hehavior, J. Polym. Sci. Polym. Chem. 47 (2009) 4379−4390.
[87] T. Biedron, L. Pietrzak, P. Kubisa, Ionic liquid functionalized polylactide by cationic polymerization: synthesis and stabilization of carbon nanotube suspensions, J. Polym. Sci. Polym. Chem. 49 (2011) 5239−5244.
[88] G.M. Kim, G.H. Michler, P. Potschke, Deformation processes of ultrahigh porous multiwalled carbon nanotubes/polycarbonate composite fibers prepared by electrospinning, Polymer 46 (2005) 7346−7351.
[89] W. Teo, et al., A dynamic liquid support system for continuous electrospun yarn fabrication, Polymer 48 (2007) 3400−3405.
[90] F. Ko, et al., Electrospinning of continuous carbon nanotuble-filled nanofiber yarns, Adv. Mater. 15 (2003) 1161−1165.
[91] J. Yu, et al., Production of aligned helical polymer nanofibers by electrospinning, Eur. Polym. J. 44 (2008) 2838−2844.
[92] T.J. Sill, H.A.v. Recum, Electrospinning: applications in drug delivery and tissue engineering, Biomaterials 29 (2008) 1989−2006.
[93] J. Doshi, D.H. Reneker, Electrospinning process and applications of electrospun fibers, J. Electrostat. 35 (1995) 151−160.
[94] L.Y. Yeo, J.R. Friend, Electrospinning carbon nanotube polymer composite nanofibers, J. Exp. Nanosci. 1 (2006) 177−209.
[95] U. Boudriot, et al., Electrospinning approaches towards scaffold engineering—a brief overview, Artif. Organs. 30 (2006) 785−792.

[96] L. Moroni, et al., 3D fiber-deposited electrospun integrated scaffolds enhance cartilage tissue formation, Adv. Funct. Mater. 18 (2008) 53–60.
[97] J.H. Kim, et al., Hybrid process for fabricating 3D hierarchical scaffolds combining rapid prototyping and electrospinning, Macromol. Rapid Commun. 29 (2008) 1577–1581.
[98] R. Murugan, S. Ramakrishna, Design strategies of tissue engineering scaffolds with controlled fiber orientation, Tissue Eng. 13 (2007) 1845–1866.
[99] M. Gensheimer, et al., Novel biohybrid materials by electrospinning: nanofibers of poly(ethylene oxide) and living bacteria, Adv. Mater. 19 (2007) 2480–2482.
[100] Y.Z. Zhang, et al., Coaxial electrospinning of (fluorescein isothiocyanate-conjugated bovine serum albumin)-encapsulated poly(ε-caprolactone) nanofibers for sustained release, Biomacromolecules 7 (2006) 1049–1057.
[101] K. Okhawa, et al., Electrospinning of chitosan, Macromol. Rapid. Commun. 25 (2004) 1600–1605.
[102] J.A. Matthews, et al., Electrospinning of collagen nanofibers, Biomacromolecules 3 (2002) 232–238.
[103] J.S. Stephens, et al., Effects of electrospinning and solution casting protocols on the secondary structure of a genetically engineered dragline spider silk analogue investigated via Fourier transform Raman spectroscopy, Biomacromolecules 6 (2005) 1405–1413.
[104] J. Li, et al., Electro-spinning and electro-blowing of hyaluronic acid, Biomacromolecules 5 (2004) 1428–1436.
[105] E.K. Brenner, et al., Electrospinning of hyaluronic acid nanofibers from aqueous ammonium solutions, Carbohydr. Polym. 87 (2012) 926–929.
[106] M. Stotak, et al., Electrospun cross-linked gelatin fibers with controlled diameter: the effect of matrix stiffness on proliferative and biosynthetic activity of chondrocytes cultured in vitro, J. Biomed. Res. 95A (2010) 826–828.
[107] M.C. McManus, et al., Electrospun fibrinogen: feasibility as a tissue engineering scaffold in a rat cell culture model, J. Biomed. Res. 81A (2007) 299–309.
[108] G.E. Wnek, et al., Electrospinning of nanofiber fibrogen structures, Nano Lett. 3 (2003) 213–216.
[109] M. Gandhi, et al., Post-spinning modification of electrospun nanofiber nanocomposite from Bombyx mori silk and carbon nanotubes, Polymer 50 (2009) 1918–1924.
[110] S. Mazinani, A. Ajji, C. Dubois, Morphology, structure and properties of conductive PS/CNT nanocomposite electrospun mat, Polymer 50 (2009) 3329–3342.
[111] P. Lu, Y.L. Hsieh, Multiwalled carbon nanotube (MWCNT) reinforced cellulose fibers by electrospinning, Appl. Mater. Interfaces 2 (2010) 2413–2420.
[112] W. Ji, et al., Bioactive electrospun scaffolds delivering growth factors and genes for tissue engineering applications, Pharm. Res. 28 (2011) 1259–1272.
[113] S.H. Lim, H.Q. Mao, Electrospun scaffolds for stem cell engineering, Adv. Drug. Deliv. Rev. 61 (2009) 1084–1096.
[114] B.G. Keselowsky, D.M. Collard, A.J. Garcia, Surface chemistry modulates focal adhesion composition and signaling through changes in integrin binding, Biomaterials 25 (2004) 5947–5954.
[115] H. Zhang, Z. Chen, Fabrication and characterization of electrospun PLGA/MWNTs/hydroxyapatite biocomposite scaffolds for bone tissue engineering, J. Bioact. Compat. Polym. 25 (2010) 241–259.
[116] S. Shao, et al., Osteoblast function on electrically conductive electrospun PLA/MWCNTs nanofibers, Biomaterials 32 (2011) 2821–2833.
[117] K.D. McKeon-Fischer, D.H. Flagg, J.W. Freeman, Coaxial electrospun poly(e-caprolactone), multiwalled carbon nanotubes, and polyacrylic acid/polyvinyl alcohol for skeletal muscle tissue engineering, J. Biomed. Res. A 99 (2011) 493–499.
[118] J.C. Chen, D.J. Goldhamer, Skeletal muscle stem cells, Reprod. Biol. Endocrinol. 1 (2003) 101.

[119] C.Y. Xu, et al., Aligned biodegradable nanofibrous structure: a potential scaffold for blood vessel engineering, Biomaterials 24 (2004) 866–877.
[120] R.K. Iller, Multilayers of colloidal layers, J. Colloid. Interface Sci. 21 (1966) 569–594.
[121] G. Decher, Fuzzy nanoassemblies: toward layered polymeric multicomposites, Science 277 (1997) 1232–1237.
[122] G. Decher, et al., Highly ordered ultrathin LC multilayer films on solid substrates, Adv. Mater. 3 (1991) 617–619.
[123] F. Caruso, R.A. Caruso, H. Mohwald, Nanoengineering of inorganic and hybrid hollow spheres by colloidal templating, Science 282 (1998) 1111–1114.
[124] A.L. Becker, A.P.R. Johnston, F. Caruso, Layer-by-layer-assembled capsules and films for therapeutic delivery, Small 6 (2010) 1836–1852.
[125] G. Decher, J.D. Hong, J. Schmitt, Buildup of ultrathin multilayer films by a self-assembly process: III. Consecutively alternating adsorption of anionic and cationic polyelectrolytes on charged surfaces, Thin Solid Films 210 (1992) 831–835.
[126] F. Caruso, et al., Ultrathin multilayer polyelectrolyte films on gold: construction and thickness determination, Langmuir 13 (1997) 3422–3426.
[127] C. Picart, et al., Determination of structural parameters characterizing thin films by optical methods: a comparison between scanning angle reflectometry and optical waveguide lightmode spectroscopy, J. Chem. Phys. 115 (2001) 1086–1095.
[128] C. Picart, et al., Buildup mechanism for poly(L-lysine)/hyaluronic acid films onto a solid surface, Langmuir 17 (2001) 7414–7424.
[129] D.L. Elbert, C.B. Herbert, J.A. Hubbell, Thin polymer layers formed by polyelectrolyte multilayer techniques on biological surfaces, Langmuir 15 (1999) 5355–5362.
[130] L. Richert, et al., Layer by layer buildup of polysaccharide films: physical chemistry and cellular adhesion aspects, Langmuir 20 (2004) 448–458.
[131] F. Wang, et al., Halogen bonding as a new driving force for layer-by-layer assembly, Langmuir 23 (2007) 9540–9542.
[132] Y. Shimazaki, et al., Preparation of layer-by-layer deposited ultrathin film based on charge-transfer interactions, Langmuir 13 (1997) 1385–1387.
[133] C.R. Kinnane, et al., Peptide-functionalized, low-biofouling click multilayers for promoting cell adhesion and growth, Small 5 (2005) 444–448.
[134] P. Kohli, G.J. Blanchard, Applying polymer chemistry to interfaces: layer-by-layer and spontaneous growth of covalently bound multilayers, Langmuir 16 (2000) 4655–4661.
[135] D. Philip, J.F. Stoddart, Self-assembly in natural and unnatural systems, Angew. Chem. Int. Ed. 35 (1996) 1154–1196.
[136] C.S. Peyratout, L. Daehne, Tailor-made polyelectrolyte microcapsules: from multilayers to smart containers, Angew. Chem. Int. Ed. 43 (2004) 3762–3783.
[137] A.P.R. Johnston, et al., Composition and structural engineering of DNA multilayer films, Langmuir 22 (2006) 3251–3258.
[138] A.P.R. Johnston, E.S. Read, F. Caruso, DNA multilayer films on planar and colloidal supports: sequential assembly of like-charged polyelectrolytes, Nano Lett. 5 (2005) 953–956.
[139] J.H. Rouse, P.T. Lillehei, Electrostatic assembly of polymer/single walled carbon nanotube multilayer films, Nano Lett. 3 (2003) 59–62.
[140] A.B. Artukhin, et al., Layer-by-layer electrostatic self-assembly of polyelectrolyte nanoshells on individual carbon nanotube templates, Langmuir 20 (2004) 1442–1448.
[141] J.S. Jan, P.J. Chen, Y.H. Ho, Bioassisted synthesis of catalytic gold/silica nanotubes using layer-by-layer assembled polypeptide templates, J. Colloid Interface Sci. 358 (2011) 409–415.

[142] V. Kozlovskaya, et al., Hydrogen-bonded LbL shells for living cell surface engineering, Soft Matter 7 (2011) 2364−2372.
[143] D. Chen, et al., Electrically conductive poly(vinyl alcohol) hybrid films containing graphene and layered double hydroxide fabricated via layer-by-layer self-assembly, Appl. Mater. Interfaces 2 (2010) 2005−2011.
[144] A.A. Mamedov, et al., Molecular design of strong single-wall carbon nanotube/polyelectrolyte multilayer composites, Nat. Mater. 1 (2002) 190−194.
[145] G. Francius, et al., Effect of crosslinking on the elasticity of polyelectrolyte multilayer films measured by colloidal probe AFM, Microsc. Res. Tech. 69 (2006) 84−92.
[146] M.M. Stevens, J.H. George, Exploring and engineering the cell surface interface, Science 310 (2005) 1135−1139.
[147] A.A. Chen, et al., Modulation of hepatocyte phenotype in vitro via chemomechanical tuning of polyelectrolyte multilayers, Biomaterials 30 (2009) 1113−1120.
[148] D.E. Discher, P. Jamaney, Y.L. Wang, Tissue cells feel and respond to the stiffness of the substrate, Science 310 (2005) 1139−1143.
[149] H.F. Cui, et al., Interfacing carbon nanotubes with living mammalian cells and cytotoxicity issues, Chem. Res. Toxicity 23 (2010) 1131−1147.
[150] G. Kasaliwal, A. Godel, P. Potschke, Influence of processing conditions in small-scale melt mixing and compression molding on the resistivity and morphology of polycarbonate−MWNT composites, J. Appl. Polym. Sci. 112 (2009) 3494−3509.
[151] A. Celzard, et al., Critical concentration in percolating systems containing a high-aspect-ratio filler, Phys. Rev. B 53 (1996) 6209−6214.
[152] P. Potschke, et al., Melt mixing as method to disperse carbon nanotubes into thermoplastic polymers, Fullerenes, Nanotubes, Carbon Nanostruct. 13 (2005) 211−214.
[153] F.H. Gojny, et al., Evaluation and identification of electrical and thermal conduction mechanisms in carbon nanotube/epoxy composites, Polymer 47 (2006) 2036−2045.
[154] I. Alig, D. Lellinger, T. Skipa, Influence of thermo-rheological history on electrical and rheological properties of polymer−carbon nanotube composite, in: T.M.a.P. Potschke (Ed.), Polymer−Carbon Nanotube Composites, Woodhead, Cambridge, UK, 2011, pp. 295−328.
[155] P. Bonnet, et al., Thermal properties and percolation in carbon nanotube-polymer composites, Appl. Phys. Lett. 91 (2007) 210910.
[156] J. Black, T.J. Baranowski, C.T. Brighton, Electrochemical aspects of d.c. stimulation of osteogenesis, Bioeletrochem. Bioenerg. 12 (1984) 323−327.
[157] R. Korenstein, et al., Capacitative pulsed electric simulation of bone cells. Induction of cyclic-AMP and DNA synthesis, Biochem. Biophys. Acta 803 (1984) 302−307.
[158] R.A. Luben, et al., Effects of electromagnetic stimuli on bone and bone cells in vitro: inhibition of responses to parathyroid hormone by low-frequency fields, Proc. Nat. Acad. Sci. U.S.A. 79 (1982) 4180−4184.
[159] G.A. Rodan, L.A. Bourret, L.A. Norton, DNA synthesis in cartilage cells in stimulated by oscillating electric fields, Science 199 (1978) 690−692.
[160] Z.B. Friedenberg, et al., Stimulation of fracture healing by direct current in rabbit fibula, J. Bone Joint Surg. 53A (1971) 1400−1408.
[161] Z.B. Friedenberg, et al., The response of non-traumatized bone to direct current, J. Bone Joint Surg. 56A (1974) 1023−1030.
[162] D.D. Levy, B. Rubin, Inducing bone growth in vivo by pulse stimulation, Clin. Orthop. 88 (1972) 218−222.
[163] B.T. O'Connor, et al., Effect of electric current in bone in vivo, Nature 222 (1969) 162−163.

[164] J.A. Spadaro, S.A. Albanese, S.E. Chase, Electromagnetic effects on bone formation at implants in the medullary canal in rabbits, J. Orthop. Res. 8 (1990) 685–693.
[165] P.R. Supronowicz, et al., Novel current-conducting composite substrates for exposing osteoblasts to alternating current stimulation, J. Biomed. Res. 59 (2002) 499–506.
[166] V. Lovatt, et al., Carbon nanotube substrates boost neuronal electronic signalling, Nano Lett. 5 (2005) 1107–1110.
[167] J.D. Weiland, D.J. Anderson, Chronic neural stimulation with thin-film, iridium oxide electrodes, IEEE Trans. Biomed. Eng. 47 (2000) 911–918.
[168] X.Y. Cui, et al., Electrochemical deposition and characterization of conducting polymer polypyrrole/PSS on multichannel neural probes, Sens. Actuators A Phys. 93 (2001) 8–18.
[169] A.S. Widge, et al., Self-assembled monolayers of polythiophene conductive polymers improve biocompatibility and electrical impedance of neural electrodes, Biosens. Bioelectron. 22 (2007) 1723–1732.
[170] S.F. Cogan, et al., Over-pulsing degrades activated iridium oxide films used for intracortical neural stimulation, J. Neurosci. Methods 137 (2004) 141–150.
[171] B.L. Groenendaal, et al., Poly(3,4-ethylenedioxythiophene) and its derivaties: past, present, and future, Adv. Mater. 12 (2000) 481–494.
[172] X.T. Cui, D.D. Zhou, Poly (3,4-ethylenedioxythiophene) for chronic neural stimulation, IEEE Trans. Neural Syst. Rehabil. Eng. 15 (2007) 502–508.
[173] E. Jan, et al., Layered carbon nanotube-polyelectrolyte electrodes outperform traditional neural interface materials, Nano Lett. 9 (2009) 4012–4018.
[174] V. Lovat, et al., Carbon nanotube substrates boost neuronal electrical signaling, Nano Lett. 5 (2005) 1107–1110.
[175] E.W. Keefer, et al., Carbon nanotube coatings improves neuronal recordings, Nat. Nanotechnol. 21 (2008) 139–152.
[176] K. Matsumoto, et al., Stimulation of neuronal neurite outgrowth using functionalized carbon nanotubes, Nanotechnology 21 (2010) 115101.
[177] M.P. Mattson, R.C. Haddon, A.M. Rao, Molecular functionalization of carbon nanotubes and use as substrates for neuronal growth, J. Mol. Neurosci. 14 (2000) 175–182.
[178] X. Luo, et al., Highly stable carbon nanotube doped poly(3,4-ethylenedioxythiopene) for chronic neural stimulation, Biomaterials 32 (2011) 5551–5557.
[179] J.H. Zou, et al., Transparent carbon nanotube/poly (3,4-ethylenedioxythiopene) composite electrical conductors, Soft Mater. 7 (2009) 355–365.
[180] X.Y. Cui, D.C. Martin, Electrochemical deposition and characterization of poly (3,4-ethylenedioxythiophene) on neural microelectrode arrays, Sens. Actuators B Chem. 89 (2003) 92–102.
[181] J. Niklinski, et al., The epidemiology of asbestos-related diseases, Lung Cancer 45 (Suppl. 1) (2004) S7–S15.
[182] D.B. Warheit, et al., Comparitive pulmonary toxicity assessment of single-wall carbon nanotubes in rats, Toxicol. Sci. 77 (2004) 117–125.
[183] D.B. Warheit, et al., Pulmonary toxicity study in rats with three forms of ultrafine–TiO_2 particles: different responses related to surface properties, Toxicology 230 (2007) 90–104.
[184] R. Colognato, et al., Comparative genotoxicity of cobalt nanoparticles and ions on human peripheral leukocytes in vitro, Mutagenesis 23 (2008) 377–382.
[185] M. Taira, et al., Studies on cytotoxicity of nickel ions using C3H10T1/2 fibroblast cells, J. Oral Rehabil. 27 (2000) 1068–1072.
[186] V.E. Kagan, et al., Direct and indirect effects of single walled carbon nanotubes on RAW264.7 macrophages: role of iron, Toxicol. Lett. 165 (2006) 88–100.

[187] D. Cui, et al., Effect of single wall carbon nanotubes on human HEK293 cells, Toxicol. Lett. 155 (2005) 73–85.
[188] F. Tian, et al., Cytotoxicity of single-walled carbon nanotubes on human fibroblasts, Toxicol. In Vitro 20 (2006) 1202–1212.
[189] A.A. Shvedova, et al., Exposure to carbon nanotube material, assessment of nanotube cytoxicity using human keratinocyte cells, J. Toxicol. Environ. Health A 66 (2003) 1909–1926.
[190] N.A. Monteiro-Riviere, et al., Multi-walled carbon nanotubes interactions with human epidermal keratinocytes, Toxicol. Lett. 155 (2005) 377–384.
[191] M. Bottini, et al., Multi-walled carbon nanotubes induce T lymphocyte apoptosis, Toxicol. Lett. 160 (2006) 121–126.
[192] S. Garibaldi, et al., Carbon nanotube biocompatibility with cardiac muscle cells, Nanotechnology 17 (2006) 391–397.
[193] X. Chen, et al., Interfacing carbon nanotubes with living cells, J. Am. Chem. Soc. 128 (2006) 6292–6293.
[194] H. Dumortier, et al., Functionalized carbon nanotubes are non-cytotoxic and preserve the functionality of primary immune cells, Nano Lett. 6 (2006) 1522–1528.
[195] E. Flahaut, et al., Investigation of the cytotoxicity of CCVD carbon nanotubes towards human umbilical vein endothelial cells, Carbon 44 (2006) 1093–1099.
[196] G. Jia, et al., Cytotoxicity of carbon nanomaterials: single-wall nanotube, multi-wall nanotube, and fullerene, Environ. Sci. Technol. 39 (2005) 1378–1383.
[197] J. Liu, et al., Fullerene pipes, Science 280 (1998) 1253–1256.
[198] A.G. Rinzler, et al., Large-scale purification of single-wall carbon nanotubes: process, product, and characterization, Appl. Phys. A: Mater. Sci. Proc. 67 (1998) 29–37.
[199] Y.S. Park, et al., High yield purification of multiwalled carbon nanotubes by selective oxidation during thermal annealing, Carbon 39 (2001) 655–661.
[200] S.H. Tana, et al., Purification of single-walled carbon nanotubes using a fixed bed reactor packed with zirconia beads, Carbon 46 (2008) 245–254.
[201] B. Fei, et al., Solubilization, purification and functionalization of carbon nanotubes using polyoxometalate, Nanotechnology 17 (2006) 1589–1593.
[202] A. Magrez, et al., Cellular toxicity of carbon-based nanomaterials, Nano Lett. 6 (2006) 1121–1125.
[203] A. Jos, et al., Cytotoxicity of carboxylic acid functionalized single wall carbon nanotubes on the human intestinal cell line Caco-2, Toxicol. In Vitro 23 (2009) 1491–1496.
[204] C.M. Sayes, et al., Functionalization density dependence of single-walled carbon nanotubes cytotoxicity in vitro, Toxicol. Lett. 161 (2006) 135–142.
[205] D. Pantarotto, et al., Translocation of bioactive peptides across cell membranes by carbon nanotubes, Chem. Commun. 1 (2004) 16–17.
[206] K. Kostarelos, et al., Cellular uptake of functionalized carbon nanotubes is independent of functional group and cell type, Nat. Nanotechnol. 2 (2007) 108–113.
[207] V.L. Colvin, The potential environmental impact of engineered nanomaterials, Nat. Biotechnol. 21 (2003) 1166–1170.
[208] Y. Sato, et al., Influence of length on cytotoxicity of multiwalled carbon nanotubes against human acute monocytic luekemia cell line THP-1 in vitro and subcutaneous tissue of rats in vivo, Mol. Biosyst. 1 (2005) 176–182.
[209] M.L. Becker, et al., Length-dependent uptake of DNA-wrapped single-walled carbon nanotubes, Adv. Mater. 19 (2007) 939–945.
[210] L.W. Zhang, et al., Biological interactions of functionalized single-wall carbon nanotubes in human epidermal keratibocytes, Int. J. Toxicol. 26 (2007) 103–113.

[211] H. Li, et al., In vivo evaluation of acute toxicity of water-soluble carbon nanotubes, Toxicol. Environ. Chem. 93 (2011) 603−615.
[212] J. Muller, et al., Respiratory toxicity of multi-wall carbon nanotubes, Toxicol. Appl. Pharmacol. 207 (2005) 221−231.
[213] C.W. Lam, et al., Pulmonary toxicity of single-wall carbon nanotubes in mice 7 and 90 days after intratracheal instillation, Toxicol. Sci. 77 (2004) 126−134.
[214] A.A. Shvedova, et al., Inhalation vs. aspiration of single-walled carbon nanotubes in C57BL/6 mice: inflammation, fibrosis, oxidative stress, and mutagenesis, Am. J. Physiol. Lung Cell. Mol. Physiol. 295 (2008) L552−L565.
[215] A.A. Shvedova, et al., Unusual inflammatory and fibrogenic pulmonary responses to single-walled carbon nanotubes in mice, Am. J. Physiol. Lung Cell. Mol. Physiol. 289 (2005) L698−L708.
[216] M.L. Schipper, et al., A pilot toxicology study of single-walled carbon nanotubes in a small sample of mice, Nat. Nanotechnol. 3 (2008) 216−221.
[217] Y. Usui, et al., Carbon nanotube with high bone tissue compatibility and bone-formation acceleration effects, Small 4 (2008) 240−246.
[218] B. Sitharaman, et al., In vivo biocompatibility of ultra-short single-walled carbon nanotube/biodegradable polymer nanocomposite for bone tissue engineering, Bone 43 (2008) 362−370.
[219] M. Bhattacharya, et al., Bone formation on carbon nanotube composite, J. Biomed. Res. 96A (2011) 75−82.
[220] W. Wang, et al., Mechanical properties and biological behavior of carbon nanotube/polycarbosilane composites for implant materials, J. Biomed. Res. B Appl. Biomater. 82B (2007) 223−230.
[221] S. Koyama, et al., Medical application of carbon nanotube-filled nanocomposites: the microcatheter, Small 2 (2006) 1406−1411.
[222] R. Langer, J.P. Vacanti, Tissue engineering, Science 260 (1993) 920−926.
[223] J. Meng, et al., Using single-walled carbon nanotubes nonwoven films as scaffolds to enhance long-term cell proliferation in vitro, J. Biomed. Res. 79A (2006) 298−306.
[224] M.A. Correa-Duarte, et al., Fabrication and biocompatibility of carbon nanotube-based 3D networks as scaffolds for cell seeding and growth, Nano Lett. 4 (2004) 2233−2236.
[225] R.A. MacDonald, et al., Collagen-carbon nanotube composite materials as scaffolds in tissue engineering, J. Biomed. Res. 74A (2005) 489−496.
[226] K. Balani, et al., Plasma-sprayed carbon nanotube reinforced hydroxyapatite coatings and their interaction with human osteoblasts in vitro, Biomaterials 28 (2007) 618−624.
[227] R. Verdejo, et al., Reactive polyurethane carbon nanotube foams and their interactions with osteoblasts, J. Biomed. Res. 88 (2009) 65−73.
[228] L.P. Zanello, et al., Bone cell proliferation on carbon nanotubes, Nano Lett. 6 (2006) 562−567.
[229] B. Zhao, et al., A bone mimic based on self-assembly of hydroxyapatite on chemically functionalized single-walled carbon nanotubes, Chem. Mater. 17 (2005) 3235−3241.
[230] J. Meng, et al., Improving the blood compatibility of polyurethane using carbon nanotubes as fillers and its implications to cardiovascular surgery, J. Biomed. Res. 74A (2005) 208−214.
[231] J.N. Xie, et al., Somatosensory neurons grown on functionalized carbon nanotube mats, Smart Mater. Struct. 15 (2006) N85−N88.
[232] H. Hu, et al., Polyethyleneimine functionalized single walled carbon nanotubes as substrate for neuronal growth, J. Phys. Chem. B 109 (2005) 4285−4289.
[233] H. Hu, et al., Chemically functionalized carbon nanotubes as substrates for neuronal growth, Nano Lett. 4 (2004) 507−511.
[234] E. Zhang, et al., Surface modification and microstructure of single-walled carbon nanotubes for dental resin-based composites, J. Biomed. Res. B Appl. Biomater. 86 (2008) 90−97.

[235] T. Akasaka, et al., Modification of the dentin surface by using carbon nanotubes, Biomed. Mater. Eng. 19 (2009) 179–185.
[236] S. Karajanagi, et al., Protein-assisted solubilization of single-walled carbon nanotubes, Langmuir 22 (2006) 1392–1395.
[237] T. Meng, M. Latta, Physical properties of four acrylic denture base resins, J. Contemp. Dent. Practise 16 (2005) 93–100.
[238] Z. Zhou, *Augmentation of PMMA denture base materials with multi-walled nanotubes, MS thesis*, Queen's University, Belfast, Ireland, 2009.
[239] B. Marr, Carbon Nanotube Augmentation of a Bone Cement Polymer, University of Kentucky, Lexington, KY, 2007.
[240] F. Mei, et al., Improved biological characteristics of poly(L-lactic acid) electrospun membrane by incorporation of multiwalled carbon nanotubes/hydroxyapatite nanoprticles, Biomacromolecules 8 (2007) 3729–3735.
[241] J. Yang, et al., Growth of apatite on chitosan-multiwall carbon nanotube composite membranes, Appl. Surf. Sci. 255 (2009) 8551–8555.
[242] X. Shi, et al., Fabrication of porous ultra-short single-walled carbon nanotube nanocomposite scaffolds for bone tissue engineering, Biomaterials 28 (2007) 4078–4090.
[243] S. Edwards, et al., Tubular micro-scale multiwalled carbon nanotube-based scaffolds for tissue engineering, Biomaterials 30 (2009) 1725–1731.
[244] J. Davis, et al., The immobilization of proteins in carbon nanotubes, Inorg. Chim. Acta 272 (1998) 261–266.
[245] D. Cui, Advances and prospects on biomolecules functionalized carbon nanotubes, J. Nanosci. Nanotechnol. 7 (2007) 1298–1314.
[246] X. Li, et al., Maturation of osteoblast-like SaoS2 induced by carbon nanotubes, Biomed. Mater. 4 (2009) 015005.
[247] X. Li, et al., Effect of carbon nanotubes on cellular functions in vitro, J. Biomed. Res. 91 (2009) 132–139.
[248] A. Abarrategi, et al., Multiwall carbon nanotube scaffolds for tissue engineering purposes, Biomaterials 29 (2008) 94–102.
[249] X. Li, Y. Fan, F. Watari, Current investigations into carbon nanotubes for biomedical application, Biomed. Mater. 5 (2010) 022001.
[250] C. Thomas, A. Ehrhardt, M. Kay, Progress and problems with the use of viral vectors for gene therapy, Nat. Rev. Genet. 4 (2003) 346–358.
[251] A. Bianco, et al., Biomedical applications of functionalized carbon nanotubes, Chem. Commun. 5 (2005) 571–577.
[252] D. Pantarotto, et al., Functionalized carbon nanotubes for plasmid DNA gene delivery, Angew. Chem. Int. Ed. 43 (2004) 5242–5246.
[253] K. Park, et al., Single-walled carbon nanotubes are a new class of ion channel blockers, J. Biol. Chem. 278 (2003) 50212–50216.
[254] A. Bhirde, et al., Targeted killing of cancer cells in vivo and in vitro with EGF-directed carbon nanotube-based drug delivery, ACS Nano 3 (2009) 307–316.
[255] J.M. Worle-Knirsch, K. Pulskamp, H.F. Krug, Oops they did it again! Carbon nanotubes hoax scientists in viability assays, Nano Lett. 6 (2006) 1261–1268.

CHAPTER

Dental and Skeletal Applications of Silica-Based Nanomaterials

4

Shin-Woo Ha[a], M. Neale Weitzmann[a,b,c] and George R. Beck, Jr.[a,b]

[a]*Emory University School of Medicine, Department of Medicine, Division of Endocrinology, Metabolism, and Lipids, Atlanta, GA, USA*

[b]*The Winship Cancer Institute, Emory University School of Medicine, Atlanta, GA, USA*

[c]*The Atlanta Department of Veterans Affairs Medical Center, Decatur, GA, USA*

CHAPTER OUTLINE

Nanobiomaterials in Clinical Dentistry.

4.1 Introduction

Nanoparticles, engineered or naturally occurring, are broadly defined as compounds that exist on a scale of ~1−100 nm. Advances in nanotechnology over the last decade have raised exciting possibilities for the application of nanomaterials in medicine. Nanoparticles can be grouped into three general categories: (i) environmental, such as those generated from forest fires and volcanoes, (ii) nonengineered, which often represent by-products of human activity including those produced by power plants and incinerators, and (iii) engineered, such as those being developed for diagnostic imaging and as vehicles for drug delivery. Engineered materials can be synthesized as pure particles or composites and in various shapes and sizes as well as surface features which can additionally be conjugated to different bioactive molecules, creating an almost infinite number of variations with an unlimited potential for biological applications [1].

Engineered nanomaterials can be organized into five general types: (i) *metal-based* metal oxides (e.g., TiO_2) with biocompatibility often increased by the use of incorporating a silica coating or shell, (ii) semiconductor nanocrystal-*quantum dots* which are also metal based and have silica shells to provide some degree of biocompatibility, (iii) *silica-based*, which are composed entirely of silica and are considered highly biologically compatible materials, (iv) *carbon-based*, which are composed entirely of carbon and come in various shapes such as hollow spheres and tubes, and (v) *dendrimers*, which are three-dimensional polymer structures that can be used for drug and gene delivery [2] (Table 4.1). Within each category, size, shape, and surface alterations such as charge and biologically compatible/active coatings play key roles in determining the physicochemical properties of nanoparticles [3]. Nanosized materials can have very different biological effects from the bulk forms based on an increased surface-to-mass ratio. Although the application of nanomaterials to medicine (nanomedicine) holds great promise, current biomedical applications are still in their infancy. The unique combination of semistructured extracellular matrix, biomechanical properties, and active remodeling makes dentin and bone unique tissues particularly suited to nanomedicine [4].

4.2 Silica nanoparticles

Silica represents a well-suited material for biomedical applications and in particular to dentistry. Chemically, silica is an oxide of silicon (silicon dioxide, SiO_2). Silica in the form of orthosilicic acid is the form predominantly absorbed by humans and is found in numerous tissues including bone, tendons, aorta, liver, and kidney. Dietary silica is generally presumed safe in humans and no adverse effects are observed in rodents at doses as high as 50,000 ppm [5]. Silica is used extensively as a food additive, used as an anticaking agent, as a means to clarify beverages, to control viscosity, as an antifoaming agent, dough modifier, and as an inactive filler in drugs and vitamins [6]. Furthermore, the FDA classifies silica as a "generally regarded as safe" (GRAS) agent, making it an ideal candidate for biomedical applications. Being the second most prevalent element after oxygen [5], silica is abundant and cheap. Silica has long been used for dental applications, mainly as a component of fillers because of its physical and optical properties as well as compatibility in composites [7]. The emergence of nanotechnology has provided new opportunities to package and deliver certain elements at the nanoscale, with the intent of enhancing biological effects or properties.

Table 4.1 General Types and Properties of Nanoparticles

Type	Shells	Cores	Surfaces	Shape	Sizes (nm)
Carbon based	None	Solid, hollow	OH/COOH	Sphere—(C_{60},C_{70}), Tube—SWNT, DWNT, MWNT	~1, 10–20, 30–50, >50
Metal based	None, metal oxide, silica	Ag, Al, Au, C, Co, Cu, Fe, In, Mo, Nb, Ni, Pt, Sn, Ta, Ti, W, Zn + binary (mainly oxides) + complex compounds (above) + Cs, Cd, Co, Mg, Sr + SiO_2	PEG, antibody, positive or negative charged, heparin, biotin	Sphere, rod	1 ~ 100
Quantum dots (metal chalcogenide)	None, other metal sulfide	CdSe, CdS, CdSe/ZnS, CdTe	Alkyl phosphine oxide, organic acid, COOH, phospholipids, PEG	Sphere, rod	1 ~ 10
Dendrimers	Generation: 0–7	Thousands of potential cores	Amines, COOH, PEG AA, CDs, sugars, biotin	Sphere	2–100 kDa
Silica based	None	Solid or mesoporous		Sphere, rod, fiber, sheet	>10

Note: *CNTs (carbon nanotubes) come in single-walled (SWNTs), double-walled (DWNTs), and multiwalled (MWNTs) varieties. AA, amino acid; CDs, cyclodextrins; PEG, polyethylene glycol.*

In this chapter, we will discuss the specific physicochemical properties of silica-based nanomaterials including synthesis methods, size, shape, surface properties, and biocompatibility in the context of both mechanical properties and potential biological applications to living cells.

4.3 Synthesis of silica-based nanomaterials

The excitement surrounding the potential applications of nanotechnology to medicine in part revolves around the almost unlimited possibilities for varying the physicochemical properties. A key aspect of controlling these properties is the method of synthesis. Silica-based nanomaterials can be synthesized in a number of different ways and the method is critical to the potential dental or biomedical application. Different synthesis methods have relative advantages and disadvantages in the control of shape, size, charge, and postsynthesis surface modifications as well as the practical issues of scale and cost associated with manufacturing (Figure 4.1).

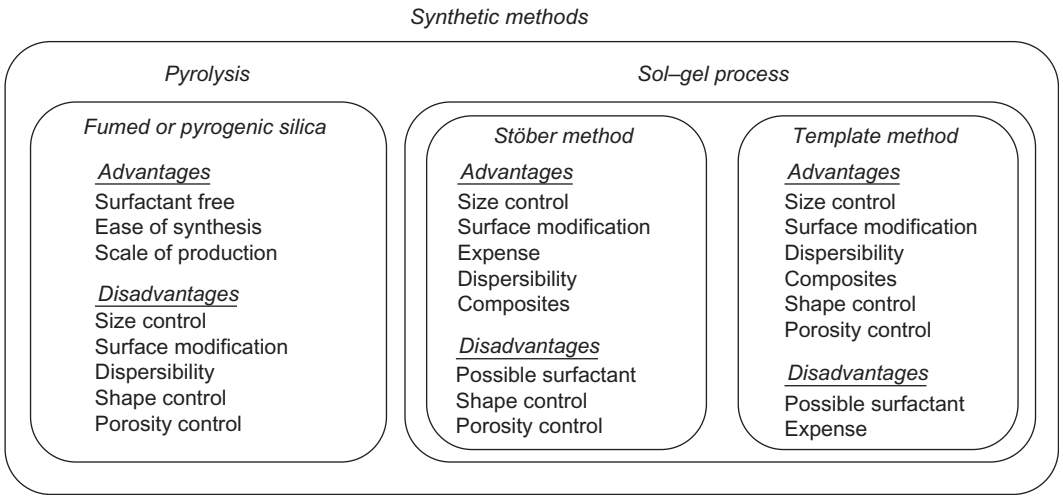

FIGURE 4.1

Schematic of various synthesis methods for silica-based nanoparticles. The most commonly used silica nanoparticles are synthesized by either pyrolysis (fumed silica) or the sol–gel process (engineered nanoparticles). Each method has advantages and disadvantages for biomedical applications including size control, scale of synthesis, surface modification, and incorporation of other compounds.

4.3.1 Methods

Fumed silica is synthesized by the pyrolysis method in which silicon tetrachloride reacts with oxygen in a flame, and the SiO_2 seed grows in size or aggregates [8]. The sol–gel process [9,10] is performed in a liquid phase and silica nanoparticles are synthesized with an acidic or basic catalyst and alcoholic solvent in the presence of silicon alkoxide. When the reaction occurs under alkaline conditions, this is referred to as the Stöber method [11] (Figure 4.2). In this method, the concentration of precursor and catalyst can be used to control the size and results in a sphere, the most stable shape in nature. Using the template method, nanomaterials can be synthesized similar to a confined nanosized cavity that can be generated by surfactants including polymers. The surfactant, which has a hydrophilic head (or part) and hydrophobic tail (or part) in a single molecule (or polymer), forms a micelle in water or an inverse micelle (or reverse micelle) in organic solvent as shown in Figure 4.3. This micelle size is dependent on the water-to-surfactant molar ratio ($W_0 = [H_2O]/[\text{surfactant}]$). In this case, both basic and acidic catalyst can be used [12,13].

Mesoporous silica nanoparticles (MSNs) are essentially silica particles with pores of varying sizes. The pores allow the resulting particles to be used as carriers for therapeutics or biological active compounds [14]. Pore width, which can be measured and analyzed by N_2 adsorption/desorption [15], is classified by the International Union of Pure and Applied Chemistry (IUPAC) as macropores—exceeding 50 nm, mesopores—2–50 nm, and micropores—not exceeding 2 nm [16]. MSNs can also be synthesized by the sol–gel process although this process tends to aggregate MSNs that are large in size (typically greater than a micrometer). More recently MSNs in the range of 20–100 nm have been achieved using a double surfactant system [17].

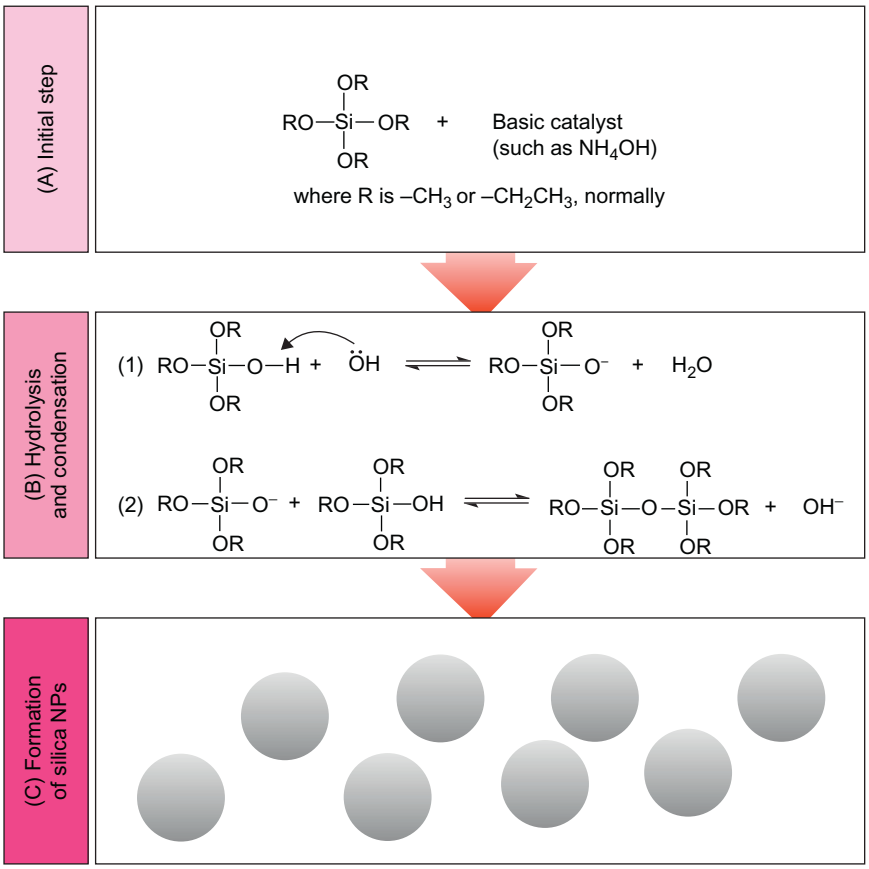

FIGURE 4.2

General synthesis of silica nanoparticles under basic conditions: (A) silica precursor and catalyst are added in an alcoholic solution, if R is a methyl group, the precursor is TMOS and if R is an ethyl group, the precursor is TEOS. (B) The precursor is then hydrolyzed by a hydroxyl ion (hydrolysis, B1) and the activated precursor is condensed with another activated precursor or precursor (condensation, B2). (C) As a result of hydrolysis and condensation, silica nanoparticles are generated.

4.3.2 Dispersibility and purification

Dispersibility, generally defined as a uniform distribution in solution, not to be confused with solubility, is an important factor for both biomaterials and biomedical applications, with monodispersed often being the most desirable. The sol–gel process can generate highly dispersible products, whereas fumed products do not generate a good polydispersion index, a measure of dispersibility. Silica's characteristics such as size distribution, surface charge, and porosity will vary depending on their synthetic method and it is therefore important to select the synthesis method based on application, irrespective of whether fabricated in the laboratory or purchased commercially.

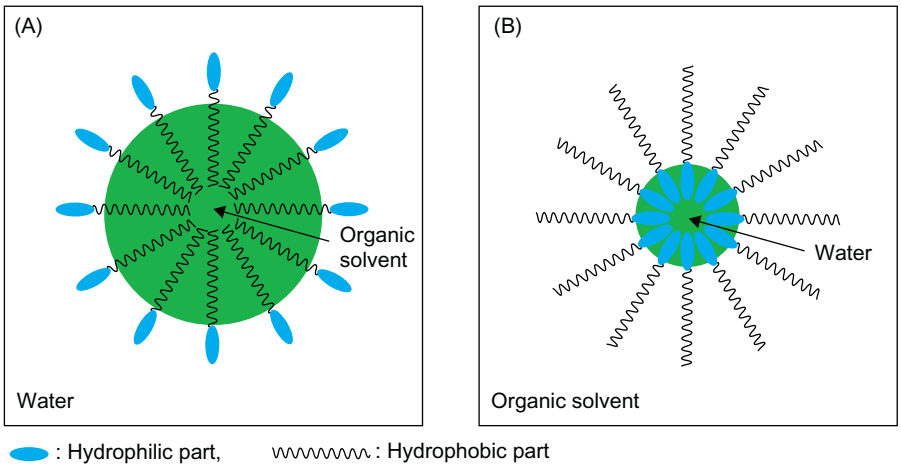

FIGURE 4.3

Synthesis of template-assisted silica nanoparticles by formation of micelles and inverse micelles. (A) A micelle in aqueous solution and (B) inverse micelle in organic solvents such as CTAB, AOT, phospholipids, and block copolymers (PS-b-PVP, where PS is polystyrene and PVP is polyvinylpyridine) are normally used for their formation. By adjusting the proportions of water, organic solvent, and surfactant, the size and shape of the micelles can be tightly and reproducibly controlled.

A second important consideration regarding the method of synthesis is the potential need to remove residual surfactant before application. Fumed silica is essentially surfactant free following synthesis; however, both the sol–gel and template methods will require purification, the removal of excess surfactants or reactants. For example, the template-assisted method results in surfactants such as CTAB (cetyl trimethylammonium bromide) and AOT (aero OT, dioctyl sulfosuccinate sodium salt). CTAB will have to be completely removed before biological application as free CTAB results in acute toxicity at the cellular level [18]. Purification can be as simple as centrifugation, acid extraction, or osmosis. Repeated purification steps such as washing and redispersion after centrifugation may be important to achieve a neutral pH and/or completely remove the surfactants/contaminants necessary to avoid unintended secondary effects on biological systems.

4.3.3 Composites and functionalization

In addition to pure silica-based materials, silica is also used in combination with other materials to increase biocompatibility. A common scenario is to coat a metal core (e.g., gold, silver, iron oxide, or cobalt ferrite (see Table 4.1)), with a silica shell. The shell may function to decrease acute toxicity of certain metals such as cadmium and lead (e.g., quantum dots) or allow for easy surface modification (such as antibody conjugation). In addition, the selective removal of the core can be used to synthesize hollow typed nanoparticles [9] suitable for delivery of compounds such as therapeutics. Despite masking the potentially toxic core with an inert silica shell, the potential long-term negative effects of a metal core may preclude their general use in humans. However, these types of

particles can be very useful for more acute animal and cell studies providing a number of advantages for preclinical investigations. For example, the electron dense, magnetic metal core can be useful as a contrast agent to identify and track particles in vitro by electron microscopy and in vivo by magnetic resonance imaging (MRI). Additionally, magnetic cores have been found to be useful agents in both immunomagnetic isolation systems when combined with antibody conjugates as demonstrated with microspheres [19] and even for cell targeting using magnetic fields [20].

Another key advantage of the sol−gel and template methods for biomedical applications is the ability to incorporate dyes into the silica during synthesis [21] providing visualization and tracking capabilities. Fluorescent dyes have been used extensively for tracking nanoparticles in biological assays [22−26] and for in vivo pharmacokinetic studies [27]. When combined with a metal core, the resulting core-shell nanoparticles may be multifunctional containing magnetic (metal core) and fluorescent of luminescent (doped shell) properties. Another potential application is the incorporation of biologically active compounds, such as antimicrobials or fluoride. MSNs are candidate silica-based particles that are being investigated for such a purpose. Although few actual therapeutic successes have been reported in dentistry to date, some in vitro studies have reported success in delivering antibacterial compounds such as nitric oxide (discussed in 4.5.2.2).

4.4 Physicochemical properties of silica-based nanomaterials

Three important physical attributes of silica nanomaterials are size, shape, and surface functionalization. The ability to control these three properties results in a wide variety of potential silica-based nanomaterials and almost infinite number of physicochemical responses.

4.4.1 Size

Relevant to biomedical applications, the most attractive size range of silica materials appears to be in the range of 10−1000 nm. Although applications vary, one goal is to reproducibly synthesize particles within a narrow size range and the synthesis method has a strong influence on size distribution. The size of silica-based nanomaterials can be relatively easily controlled over a wide range spanning nanometer to micrometer. Both the sol−gel and template-assisted methods have good size controllability and reproducibility, whereas the pyrolysis (fumed silica) is less controllable. Factors that will influence size during synthesis include silica sources such as tetramethyl orthosilicate (TMOS), tetraethyl orthosilicate (TEOS), and sodium silicate, acidic or basic catalysts, temperature, solvents, and surfactant. Using the template method, size can be controlled by adjusting the amounts of surfactants, including polymers, or the ratio of water-to-surfactant or organic solvent. The surfactant forms a micelle (or inverse micelle) similar to a nanosized cavity (Figure 4.3). The silica deposition occurs based on the micelles' size and keeps the spherical shape. When using the sol−gel process, increasing the concentration of the silica source and catalyst will increase the silica's size in a linear manner (Figure 4.4).

Nanoparticle size is extremely important for a number of reasons. Specific materials when synthesized at the nanosize often possess different properties to those of the bulk or macroform because of increased surface area. In regard to dental application, the size of the particle may influence the density that can be achieved in composite resins ultimately influencing mechanical and

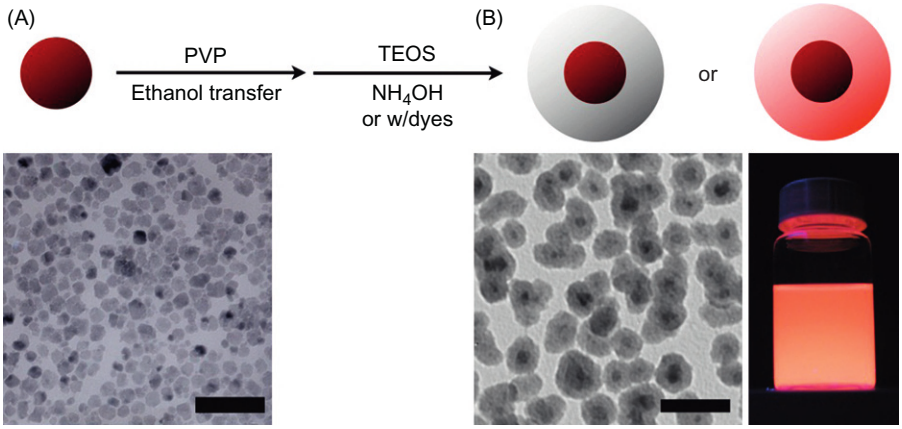

FIGURE 4.4

Synthesis of fluorescent metal core-shell nanoparticles [20]. The core, in this case a 20-nm-sized cobalt ferrite ($CoFe_2O_4$) magnetic particle, is synthesized first (A). To increase biocompatibility the core can be coated with silica via polyvinyl pyrrolidone (PVP) to form a silica shell on the core surface (middle panel). A fluorescent property can be added by a chemical bonding group such as an alkoxysilane that is incorporated into the silica shell (B). All scale bars are 100 nm in TEM images.

physical properties. Particle size might also influence the topography of a surface in the case of either adhesion or polishing, and biocompatibility as discussed below. Related to more general biomedical applications, different sized particles may have different capacities to enter cells and cellular organelles. The mechanisms by which particles are endocytosed are size dependent and likely influence the manner in which the internalized particles are processed by the cell [28]. Once in the cell, the ability to enter or be excluded from certain organelles is likely highly size dependent. In vivo, size also influences half-life with 6 nm particles rapidly removed by the kidneys [29] and particles larger than 200 accumulating in the spleen and liver [30].

4.4.2 Shape

Shape can be controlled by a number of methods; however, varying the concentration of the primary or secondary surfactant or addition of a secondary silica source, such as aminopropyltrimethoxysilane (APS), is common. Semiconductor, metal oxide, and metal nanoparticles can be controlled by changing the ratio of surfactants and precursors, growing under harsh and mild conditions, adding polymers, and so on [31,32]. These nanomaterials have crystallinity and because surfactants are often more interactive with a certain crystalline facet, the less interactive facets will result in relative faster growth. The nonuniform growth can be manipulated to synthesize nanomaterials with different shapes. Silica also has various crystalline forms, such as quartz. Because these crystalline silicas are formed under high temperature or pressure, referred to as calcination, they cannot be synthesized by the sol–gel process. Silica amorphously and entropically favors a spherical shape and therefore silica-based nanomaterials made by the sol–gel process in the absence of

surfactant will be spherical. However, shape may be controlled by using templates such as anodic aluminum oxide (AAO). AAO has been employed in the manufacturing of nanoparticles as a template due to the fact that the pore size and length can be easily controlled and can be used to synthesize various shapes. Metal and polymer nanorods, wires, and tubes can be created by generating an AAO template followed by selectively removing the template [33,34]. Recently, Huang and coworkers [35] demonstrated that the shape of MSNs could be controlled by changing the surfactant and ammonia concentration, which was proportional to increased length and thickness, respectively.

Nonmesoporous silica-based nanomaterials can also be manufactured in various shapes in addition to size including rods, fibers, and even cubes [36–38]. Shape can influence the cellular response to the nanoparticle such as uptake efficiency and potential toxicity [39,40]. A study investigating cellular uptake efficiency among various size and shape nanomaterials demonstrated that 50 nm spherical gold nanoparticles have the highest uptake efficiency and that short rods were more effectively internalized relative to long [41]. At present the spherical particles have been demonstrated to be mostly biocompatible regardless of composition and are usually taken up by cells through an organized and energy-dependent endocytosis [42]. Shape also effects biodistribution and clearance in vivo. MSNs as short rods (aspect ratio $\sim$1.5, length 185 ± 22 nm) were mainly detected in the liver; however, long rods (aspect ratio $\sim$5, length 720 ± 65 nm) were detected preferentially in the spleen. The clearance of the short rods was faster than the long rods [35]. The above studies have been performed in biological systems; however, the somewhat unique applications of nanotechnology to dentistry may allow for the use of shapes not compatible with biological systems. For example, the rod shape may be more useful in dental applications as an antibacterial although, to date, the effect of shape on various dental applications has not been completely explored.

4.4.3 Surface properties and modifications

One of the most important features of a nanoparticle in terms of mechanical and biological properties is surface charge. Changes in surface charge lead to differences in dispersibility in aqueous and organic solutions, the ability to interact with and translocate cell membranes, and the potential reactivity with numerous proteins, enzymes, and surfaces. The sol–gel process results in a terminal OH group (Si–OH or silanol group) on the surface which is relatively easily coupled with silane containing compounds by condensation. The silanol group gives a hydrophilic character to the nanoparticles as shown in Figure 4.5.

The ability to modify the surface of nanoparticles is an important advantage in selective targeting of specific cell populations and organs. Modifications involve surface decoration of nanoparticles using targeting proteins such as antibodies or ligands recognized by specific cell surface receptors. Examples of modifications include the addition of avidin, avidin antibody conjugates, and direct immunoglobulin conjugation. In order to link biomolecules for specific targeting, avidin–biotin couple or antigen–antibody coupling reactions can be employed through the surface modification with APS to generate amine groups. There are potentially infinite numbers of different molecules that could be coupled to the surface of nanoparticles in order to target them to specific cell populations, as would be important in the rational design of novel nanoparticles for therapeutic applications (Figure 4.6). Changes to the surface of nanoparticles are likely to also change important properties such as the ability to enter cells and location to specific organelles ultimately

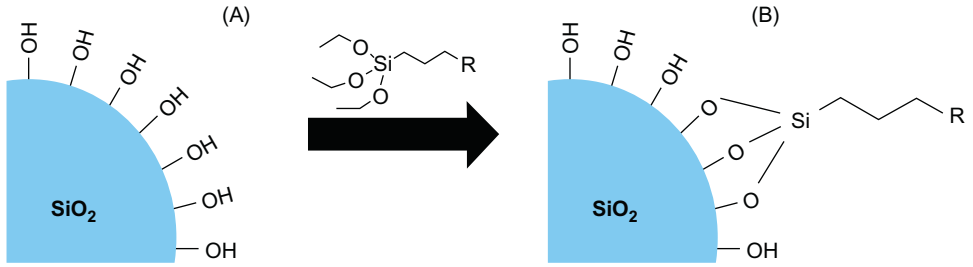

FIGURE 4.5

The silica surface (A) has silanol groups. To modify the surface, the modified ligand, organosilane, will have a silane group necessary for chemical bonding and a functional group (R), which can alter the surface charge or be used for an additional coupling reaction (B).

altering their biological effects. Surface modification might also increase adherence to external surfaces as well as within composite resins (Figure 4.7).

Once again, the rather unique mechanical intent of dental applications suggests that the fundamentals which are often applied to biomedical purposes may be different. For example, a common modification used in dentistry is addition of γ-methacryloxypropyltrimethoxysilane (γ-MPS) to silica-based nanomaterials used to improve adhesion of the nanoparticles within the resin matrix, as well as to reduce agglomeration, discussed in more detail below. This adhesive property may be beneficial in dentistry; however, these types of particles would not be very useful for systemic applications required in the development of a therapeutic for cancer, for example. For such systemic applications, particles are often surface modified with polyethylene glycol (PEG or PEGylation) which decreases phagocyte system uptake and increases in vivo half-life [46,47]. To date, attempts to use biological active modifications of silica-based nanomaterials in dentistry have not been reported.

4.5 Dental applications of silica-based nanomaterials

The structured matrix and physical properties of dentition and the skeleton are very well suited for the application of silica-based nanomaterials. Studies investigating the use of controlling the physicochemical properties of silica nanomaterials for dental applications have only begun to be realized (summarized in Table 4.2).

4.5.1 Composite resins

Composite resins generally consist of a resin polymer matrix, inorganic filler, coupling reagent, coloring agent, and initiator [59]. Three key properties of composite resins used in dental applications are mechanical, physical, and esthetic qualities all of which can be enhanced by silica. Although silica has long been used as the reinforcing filler, the potential novel properties introduced by the

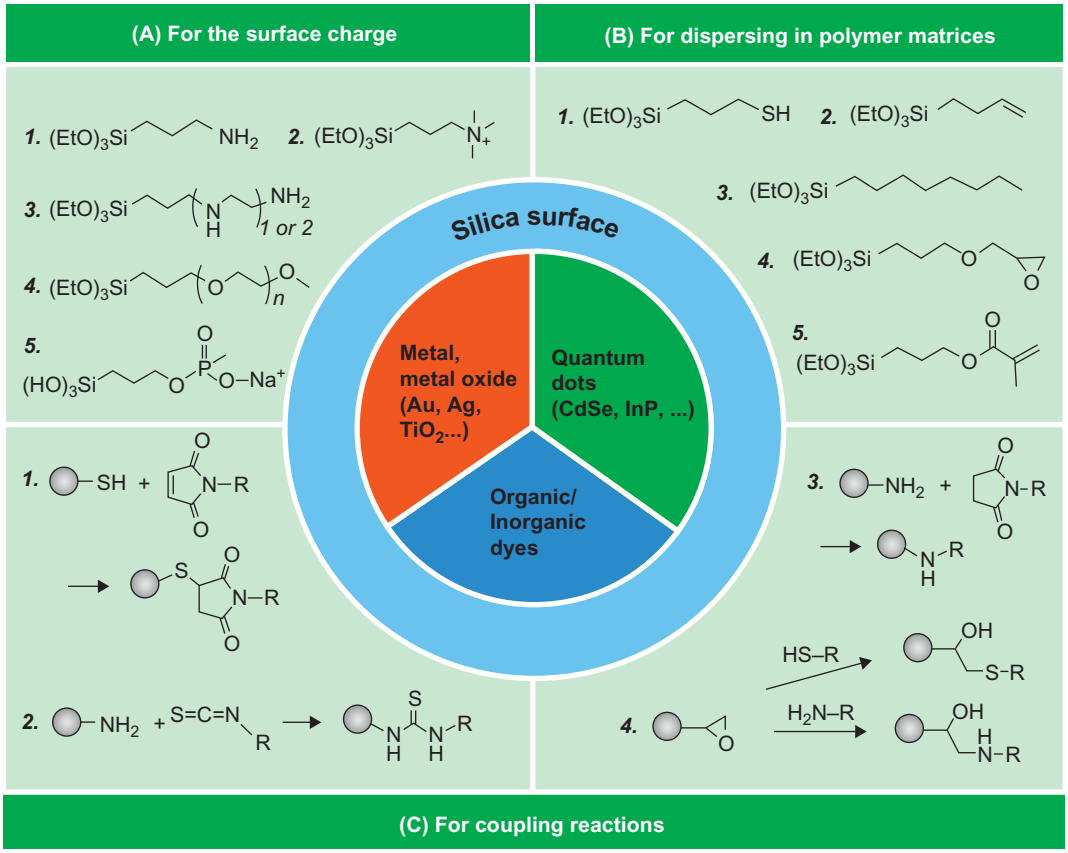

FIGURE 4.6

Metal and metal oxide nanoparticles and quantum dots (central circles) can be incorporated to make core-shell structure or homogeneously embedded in silica matrices. Since both have silanol (Si—OH) groups on the surface, modifications are possible [43–45]. (A) Ligands for modifying surface charge: A1 and A3 induce to positive charge under acidic condition, and its amine is very important in the coupling reaction. A2 also results in a positive charge independent of pH due to quaternary ammonium salt. A4 "PEGylation" is a good ligand for bioapplications and it helps to increase circulation time in vivo and to enhance the dispersibility of nanoparticles in biological buffer and medium reducing the interaction between nanoparticles and proteins. A5 provides a negative charge and introduces a phosphonate. (B) Ligands for modifying dispersion in polymer matrices: B1 is widely used in dentistry to mix bis-GMA/TEGDMA resin. Nanoparticles having terminal double bonds via condensation of B2 can be polymerized with monomers such as styrene. Because most polymers such as polystyrene and polyethylene are hydrophobic, B3-modifed nanoparticles can be readily blended into common polymers. The B4-modifed materials can make epoxy resin composites, and the B5-modified structures can form PMMA, poly(methyl methacrylate) composites, a major component of contact lenses. (C) Ligands for coupling reactions: the surface reaction of nanoparticles is different from a general reaction due to possible hindrance of spatial configuration and therefore a highly effective coupling reaction might be required. C1 is the formation of thioether. Nanoparticles condensed with B1 are reacted with maleimide-linked protein or antibody. The amine terminated can be synthesized with A1 and A3. As most biomolecules including proteins have an amine group, C2 reaction is very useful for tagging proteins or used on the surface of MSNs with isothiocyanated dyes such as RITC (rhodamine B isothiocyanate) and FITC (fluorescein isothiocyanate). C3 is frequently used in biotinylation reacted with a primary amine and the activated biotin by *N*-hydroxysuccinimide (NHS) with a linker. The epoxide-terminated B4 can be used not only for mixing polymer matrices, but also for coupling reactions with primary amine and thiol groups.

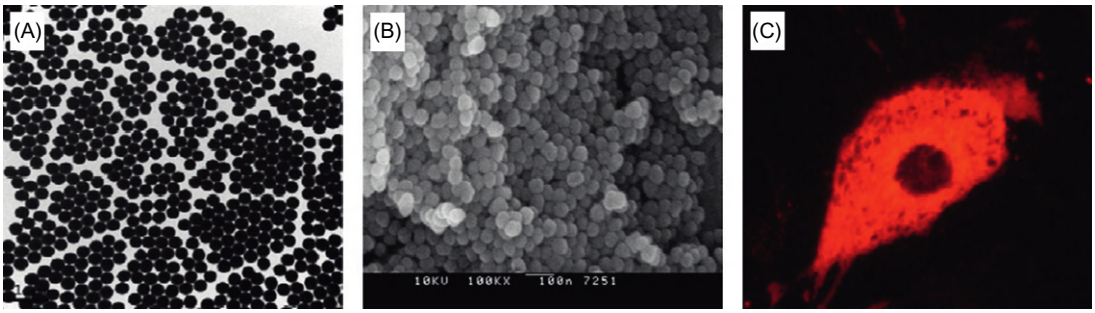

FIGURE 4.7

Fluorescent silica nanoparticles. (A) Transmission electron microscopy (TEM) and (B) scanning electron microscopy (SEM) of 50 nm silica nanoparticles. The particles were incorporated with rhodamine B to allow cellular tracking. (C) MC3T3 preosteoblasts efficiently take up the particles and the cytoplasm becomes saturated. Note that the particles are excluded from the nucleus (dark circle).

nanoscale and various synthesis and surface modifications have only begun to be explored in dentistry. Recent studies have begun testing the effects of altering size and surface properties on the functional properties of silica-based nanomaterials in composite resins.

Using the sol−gel process, Kim et al. [54] synthesized spherical silica nanoparticles having different sizes (from 5 to 450 nm) that were tested for dispersion in, and adhesion to, a resin matrix of 70 wt% bisphenol-α-glycidyl methacrylate (bis-GMA) and 30 wt% triethyleneglycol dimethacrylate (TEGDMA). This study determined that particles with γ-MPS-modified surface were more adhesive and had better dispersion than nontreated particles regardless of size. A similar study used silica nanoparticles with a size range of 20−50 nm and filler mass fractions of 20%, 30%, 40%, and 50% [53]. These composites were compared to a conventional composite containing 10−40 μm silica particles. The use of nanosized silica resulted in increased mechanical properties with mass fractions up to 40% producing an increase in fracture toughness, flexural strength, and hardness in comparison to control. A third study recently tested similar spherical nanosilica fillers with a size range of 10−20 nm for dispersion, surface roughness, and flexural strength [60]. Two filler ratios were tested, 30 and 35 wt%. The surface modification of γ-MPS was determined important for use in the resin matrix and the higher filler ratio decreased surface roughness but decreased flexural strength relative to the lower filler ratio.

Spherical particle may not be the only shape that can be used to enhance composite resins, as other silica-based nanomaterials are now being tested. Tian et al. [56] used fibrillar silicate (diameter in tens of nm and length in μm) in small mass fractions (1% and 2.5%) and determined that uniform impregnation of fibrillar silicate into dental resins significantly improved mechanical properties such as flexural strength, elastic modulus, and work to fracture. MSNs have also recently been explored for enhanced properties in dental composites. The particles were synthesized using the nonsurfactant templating method in the 500 nm range and the composites prepared using combinations of MSNs and nonporous fillers [61]. The authors concluded that including porous fillers increased mechanical properties potentially due to the interconnecting pores. These studies

Table 4.2 Dental Applications of Silica-Based Nanoparticles

Function	Specification	Purpose	Result	Reference
Polishing	60 nm silica nanoparticles	A component of slurry to make dentinal surface smoother	*Streptococcus mutans* bacteria could be easily removed on the smooth silica particle coated surface	[48]
Antimicrobial	4–21 nm silica nanoparticles	The effect of silica nanoparticles by themselves	Silica nanoparticles reduced the attachment and growth of *C. albicans*	[49]
	220 and 510 nm silica–polymer core-shell nanoparticles	A chlorine-ion source	Increased bacteria killing by releasing *N*-halamine-functionalized particles	[50]
	30 nm flame-derived bioactive glass 45S5	Comparison of antimicrobial effect between nano- and micron-sized bioactive glasses	Micron-sized glass did not show any antibacterial effect, but the nanosize was decreased in *Enterococcus faecalis* cells after direct exposure	[51]
	90 and 136 nm NO-release silica nanoparticles	Antimicrobial effect of NO-release silica nanoparticles	The NO-release nanoparticles killed over 99% of cells from each type of biofilm, *Pseudomonas aeruginosa*, *Escherichia coli*, *Streptococcus aureus*, *Staphylococcus epidermidis*, and *C. albicans*	[52]
Filler	26 nm silica and bis-GMA/TEGDMA polymer	A filler to enhance mechanical properties	One of restorative resins in dentistry could be used by mechanical enhancement	[53]
	45 nm MPS-modified silica and bis-GMA/TEGDMA polymer	A filler to enhance mechanical properties	Improved dispersion in resins as well as mechanical properties	[54]
	Nanosheet-shaped montmorillonite and PMMA polymer	A filler to enhance thermal stability and mechanical strength	This could be used as a denture base material due to good biocompatibility	[55]
	Crystalline fibrillar silicate (FS, 100–3000 nm × 10–25 nm) and bis-GMA/TEGDMA polymer	A filler to enhance mechanical properties	Flexural strength, elastic modulus, and work of fracture of 1% and 2.5% of composites are reinforced	[56]

(*Continued*)

Table 4.2 (Continued)

Function	Specification	Purpose	Result	Reference
	10–20 nm silica nanoparticles and bis-GMA/TEGDMA polymer	A filler to enhance mechanical properties	35% filler composite showed better properties in modulus and roughness, but 35% is better in flexural strength	[57]
	20 nm, 20–50 nm, and 20–80 nm silica nanoparticles and bis-GMA/TEGDMA polymers	Mechanical properties of the composites with three commercial silica nanoparticles	20 nm silica nanoparticles showed the smoothest surface roughness	[58]

identify the potential benefit of using nanosilica in composite resins and highlight the potential of manipulating size, shape, and surface modifications for increased performance.

4.5.2 Surface topography: roughness, polishing, and antimicrobial properties

Tooth enamel is gradually but constantly damaged throughout life. The rate of damage can be limited or exaggerated based on personal habits. The damaged enamel creates an environment for caries through the production of lactic acid by bacteria [62]. Reducing roughness by polishing the surface reduces the opportunities for bacteria and plaque to establish [63]. Topographical properties are known to alter bacteria and mammalian cell attachment as well as generate changes in function [64–68].

4.5.2.1 Polishing

The ability of silica-based particles to alter topography not only as a component of resins but also as a polishing agent represents yet another potential use of nanoparticles in dentistry. Larger silica particles, in the micron range, have previously been used as a polishing tool. A recent study was performed investigating the use of nanosized silica particles for polishing [48]. This study used atomic force microscopy to measure roughness. The results of the study suggested that in fact silica nanoparticles (60 ± 4 nm) decreased roughness by an order of magnitude relative to regular toothpaste or professional prophylactic toothpaste (1–180 μm size). This study also determined that the nanoparticle polished surface reduced bacterial adhesion.

4.5.2.2 Antimicrobial properties

Silica-based nanoparticles might reduce bacterial damage by altering the enamel surface or releasing antimicrobial agents. A study by Cousins et al. [49] examined the effect of spherical silica nanoparticles with diameters of 4, 7, 14, or 21 nm on the attachment and/or growth of *Candida albicans*. All four sized particles reduced cell attachment and growth of *C. albicans* on tissue culture polystyrene substrates although the 7 and 14 nm particles were the most efficacious.

Waltimo et al. [51] synthesized nanometric bioactive glass 45S5 and compared the antimicrobial activity to micron-sized bioactive glass against enterococci from root canal infections and found higher increased killing efficacy with the nanometric glass. This was possibly due to a tenfold increase in silica release corresponding to a tenfold increase in surface area of the nanosized glass. Delivery of bioactive compounds is yet another mechanism by which silica nanoparticles could be used as an antimicrobial. A recent study investigated a novel nitric oxide releasing silica nanoparticle as an antimicrobial on biofilm-based microbial cells [52]. Nitric oxide (NO) has been reported to have antimicrobial properties and in fact these NO containing particles resulted in ≥99% killing of five common bacteria. Another study used *N*-halamine-functionalized silica core-shell nanoparticles (∼200−500 nm) and demonstrated increased antibacterial activity against both gram-positive and -negative bacteria relative to bulk powder *N*-halamine [50].

4.6 Skeletal applications of silica-based nanomaterials

Although the skeleton and dentition have obvious differences, they also share some common features such as similarities in the cells that create the mineralized matrix, osteoblasts, odontoblasts, and cementoblasts [69]. Osteoblasts are bone forming cells of the skeleton, cementoblasts form the mineralized tissue of the tooth root [70,71], and odontoblasts function to create dentin [72] all of which are thought to derive from cranial neural crest mesenchymal cells [73], at least for osteoblasts of craniofacial bones [74]. All three cell types are active throughout life and mature cells can be differentiated from precursors when required. Several genetic disorders also effect the skeleton and dentin including hypophosphatemic rickets and osteogenesis imperfecta among others [75]. Genetic studies in mice have identified a number of genes that are important for both dentin and bone formation, two examples are the alkaline phosphatase knockout mouse which presents with malformed incisors and defective enamel [76] as well as skeletal mineralization defects [77] and the dentin matrix protein (DMP1) knockout mouse which also presents with defects in dentin and skeleton [78−80].

4.6.1 Skeletal modeling and remodeling, osteoblast, and osteoclasts

The skeleton is a dynamic organ that undergoes continuous regeneration. During development and growth, the skeleton is sculpted to achieve its shape and size by the removal of bone from one site and deposition at a different one (modeling) [81]. In contrast to modeling, bone remodeling serves to maintain mechanical integrity of the adult skeleton and provides a mechanism by which calcium and phosphate ions may be released from or conserved within the skeleton, a process central to metabolic and cellular functions. In healthy young adult bone, remodeling is homeostatic, i.e., the amount of bone resorbed is equivalent to the amount of new bone formed, with no net change in bone mass [81].

The two main cell types involved in homeostasis of the adult skeleton are osteoblasts and osteoclasts. Osteoblasts are the bone building cells of the body and derive from pluripotent mesenchymal stem cells [82]. Runt-related transcription factor-2 (Runx2) is a critical transcription factor that drives the initial differentiation of precursors toward an osteoblast phenotype, while an additional transcriptional regulator, osterix, is critical for continued osteoblast development [83−85].

Differentiation is marked by increasing alkaline phosphatase activity and expression of osteoblast-specific genes such as osteocalcin [86]. Opposing bone formation by osteoblasts is bone resorption by osteoclasts. Osteoclast precursors circulate within the monocyte population and express on their membranes receptor activator of nuclear factor kappa B (RANK), the receptor for the key osteoclastogenic cytokine RANK ligand (RANKL) [87]. In the presence of RANKL, the upregulation of key transcription factors including nuclear factor kappa B (NF-κB), c-Fos, and nuclear factor of activated T cells (NFAT) induce early osteoclast precursors to differentiate into mononucleated preosteoclasts, characterized by expression of the enzyme tartrate-resistant acid phosphatase (TRAP). These multinucleated preosteoclasts fuse together to form giant multinucleated mature bone-resorbing osteoclasts.

4.6.2 Silica and osteoblasts

Silicon has been suggested to play a physiological role in bone formation [88,89] and silica deficiency leads to detrimental effects on the skeleton including skull and peripheral bone deformities, poorly formed joints, defects in cartilage and collagen, and disruption of mineral balance in the femur and vertebrae [5]. Osteoblasts grown on silica-coated disks demonstrated increased hydroxyapatite formation although alkaline phosphatase and cell number was not changed [90]. Orthosilicate (10−1000 μM) was demonstrated to increase proliferation, mineralization, and osteoprotegerin (OPG) RNA of human osteoblast like SaOS-2 cells [91]. OPG acts as a decoy receptor for RANKL, inhibiting RANKL-induced RANK-mediated activation of important signal transduction pathways, including NF-κB, that are necessary for osteoclast formation. Silica has also been incorporated into hydroxyapatite/bioceramic artificial bone scaffolds, where it is reported to enhance osteoconductivity and proliferation [92−95]. A recent study synthesized mesoporous silica xerogels by the sol−gel process with different surface area (401, 647 and 810 m^2/g, respectively) and found an increase in proliferation and osteoblast synthesis of attachment proteins [96]. MSNs were not found to affect viability, proliferation, immunophenotype, or differentiation of mesenchymal stem cells (osteoblast precursors) in vitro [27].

4.6.3 Silica nanoparticles and bone metabolism

We recently reported that engineered silica nanoparticles (50 nm) possess intrinsic properties that endow them with therapeutic properties for the skeleton. The nanoparticles were demonstrated to have a direct promoting effect on osteoblasts in culture, not only increasing mineralization but also increasing gene expression associated with osteoblast differentiation such as osterix and osteocalcin [97]. These data suggested that the particles are capable of altering cell behavior and not simply altering the matrix. We also examined the effect on bone-resorbing osteoclasts and found a strong inhibition of osteoclast formation by the silica nanoparticles as measured by the number of TRAP-positive multinucleated cells [97]. This study also identified NF-κB signaling as target of the particles, resulting in decreased signaling activity in both preosteoblasts and preosteoclasts. These in vitro studies predicted a positive effect on bone mass accrual. Intraperitoneal injection of mice with the 50 nm fluorescent PEGylated silica nanoparticles (Figure 4.7) twice a week for 6 weeks increased bone mineral density relative to vehicle injection. The results suggested that silica nanoparticles, absent of significant surface functionalization or deliverable cargo, are capable of

intrinsically altering cell behavior both in vitro and in vivo. This is significant for bone and dentition in that it represents an additional mechanism, beyond mechanical properties, by which silica-based nanoparticles might be used for therapeutic applications.

4.6.4 Osseointegration

Osseointegration is generally defined as the direct, functional interaction between bone and an implant [98]. This process is particularly important to the fields of dentistry and bone biology [98,99]. The response of the bone to the implant can be influenced by a number of factors including the quality of the bone, surface properties of the implant, as well as topography of the implant [100]. Furthermore, deformities caused by injury, disease, or wear in the alveolar process, the ridge of bone that contains the tooth sockets, present problems associated with implants. In this case, bone grafts or substitutes are often used to correct the deformities. Although titanium has been the focus of much of the work-related implants, the physical properties of nanosilica, as discussed above, suggest that this material could have significant beneficial effects on surface and topography modification both altering the interface of the implant with bone and cell recruitment as well as incorporation of bioactive molecules [100]. The studies described throughout this chapter suggest that the use of silica-based nanomaterials on skeletal regulation may also be applicable to the formation and healing/repair of the jaw in preparation of dental implants.

4.6.5 Biocompatibility/toxicology

Although dietary silica is considered generally safe and even beneficial, the nanoscale has the potential to alter physicochemical properties from the bulk form of any substance. Somewhat surprisingly, 50 nm silica nanoparticles have been detected to cross the blood–brain barrier in mice although without apparent negative effects or toxicity [101]. The topical nature of many potential dental applications reduces the potential significance of both the biocompatibility and toxicology profile of novel silica nanomaterials. Long-term inhalation of silica which can occur by those involved with various dental procedures such as milling and grinding can cause inflammation and even silicosis. These silica particles are however generally thought to be larger crystalline forms (0.5–10 μm). As human applications of nanomaterials move toward bioactively altering or targeting cells or the implant–bone interface, a more concerted effort to understand the biocompatibility and/or toxicology of silica-based nanomaterials will be required. The same properties that make nanoparticles so exciting; size, shape, and surface properties might also alter the biocompatibility of the resulting novel material.

4.7 Conclusions

Nanotechnology presents many opportunities in dental medicine. Because of the nature of dental applications, mostly topical with limited systemic exposure, nanotechnology has the potential to have a much more immediate impact than other fields of medicine. Silica-based nanomaterials are particularly well suited to dental applications because of the mechanical and esthetic properties. Additionally, the ease of surface modification, size control, and biocompatibility make silica an

ideal compound for a number of dental purposes. Potential applications include filler as a key constituent of composites, an abrasive to polish and reduce bacterial attachment, as well as a delivery vehicle for antimicrobials. Recent studies also suggest that silica nanoparticles hold the potential to influence cell types in the tooth and possibly gum. If silica-based nanomaterials will be used in the context of an active biological agent to influence cells, a toxicology profile will need to be established and the environmental impact of nanoparticles, which is still not fully understood, will need to be carefully assessed.

Acknowledgments

The authors are supported by grants from the NIH/NIAMS (AR056090), Georgia Research Alliance (GRA.VL12.C2), and the Emory Center for Pediatric Nanomedicine. MNW is also supported in part by funding from the Biomedical Laboratory Research and Development Service of the VA Office of Research and Development (5I01BX000105) and by grants AR059364 and AR053607 from NIAMS, and AG040013 from NIA. GRB is also supported in part by grants from the NCI (CA136059 and CA136716).

References

[1] R. Hao, R. Xing, Z. Xu, Y. Hou, S. Gao, S. Sun, Synthesis, functionalization, and biomedical applications of multifunctional magnetic nanoparticles, Adv. Mater. 22 (25) (2010) 2729–2742.
[2] N.W.G. U.S. Environmental Protection Agency (U.S. EPA), Nanotechnology Whitepaper, External Draft for Review, 2005, <www.gov.epa/osa/nanotech.htm/>.
[3] G. Oberdorster, E. Oberdorster, J. Oberdorster, Nanotoxicology: an emerging discipline evolving from studies of ultrafine particles, Environ. Health Perspect. 113 (7) (2005) 823–839.
[4] D.A. Terry, Applications of nanotechnology, Pract. Proced. Aesthet. Dent. 16 (3) (2004) 220–222.
[5] K.R. Martin, The chemistry of silica and its potential health benefits, J. Nutr. Health Aging 11 (2) (2007) 94–97.
[6] Q. Chaudhry, M. Scotter, J. Blackburn, B. Ross, A. Boxall, L. Castle, et al., Applications and implications of nanotechnologies for the food sector, Food Addit. Contam. Part A Chem. Anal. Control. Expo. Risk Assess. 25 (3) (2008) 241–258.
[7] A.K. Luhrs, W. Geurtsen, The application of silicon and silicates in dentistry: a review, Prog. Mol. Subcell. Biol. 47 (2009) 359–380.
[8] B. Buesser, S.E. Pratsinis, Design of nanomaterial synthesis by aerosol processes, Annu. Rev. Chem. Biomol. Eng. 3 (2012) 103–127.
[9] Y. Piao, A. Burns, J. Kim, U. Wiesner, T. Hyeon, Designed fabrication of silica-based nanostructured particle systems for nanomedicine applications, Adv. Funct. Mater. 18 (23) (2008) 3745–3758.
[10] B.L. Cushing, V.L. Kolesnichenko, C.J. O'Connor, Recent advances in the liquid-phase syntheses of inorganic nanoparticles, Chem. Rev. 104 (9) (2004) 3893–3946.
[11] W. Stober, A. Fink, E. Bohn, Controlled growth of monodisperse silica spheres in the micron size range, J. Colloid Interface Sci. 26 (1968) 62–69.
[12] T. Andl, K. Ahn, A. Kairo, E.Y. Chu, L. Wine-Lee, S.T. Reddy, et al., Epithelial Bmpr1a regulates differentiation and proliferation in postnatal hair follicles and is essential for tooth development, Development 131 (10) (2004) 2257–2268.

[13] N. Pinna, M. Niederberger, Surfactant-free nonaqueous synthesis of metal oxide nanostructures, Angew. Chem. Int. Ed Engl. 47 (29) (2008) 5292−5304.
[14] Z. Li, J.C. Barnes, A. Bosoy, J.F. Stoddart, J.I. Zink, Mesoporous silica nanoparticles in biomedical applications, Chem. Soc. Rev. 41 (7) (2012) 2590−2605.
[15] K.S.W. Sing, D.H. Everett, R.A.W. Haul, L. Moscou, R.A. Pierotti, J. Rouquerol, et al., Reporting physisorption data for gas solid systems with special reference to the determination of surface-area and porosity (recommendations 1984), Pure Appl. Chem. 57 (4) (1985) 603−619.
[16] L.O. Ohrnell, J.M. Hirsch, I. Ericsson, P.I. Branemark, Single-tooth rehabilitation using osseointegration. A modified surgical and prosthodontic approach, Quintessence Int. 19 (12) (1988) 871−876.
[17] K. Suzuki, K. Ikari, H. Imai, Synthesis of silica nanoparticles having a well-ordered mesostructure using a double surfactant system, J. Am. Chem. Soc. 126 (2) (2004) 462−463.
[18] E.E. Connor, J. Mwamuka, A. Gole, C.J. Murphy, M.D. Wyatt, Gold nanoparticles are taken up by human cells but do not cause acute cytotoxicity, Small 1 (3) (2005) 325−327.
[19] F. Vartdal, G. Gaudernack, S. Funderud, A. Bratlie, T. Lea, J. Ugelstad, et al., HLA class I and II typing using cells positively selected from blood by immunomagnetic isolation—a fast and reliable technique, Tissue Antigens 28 (5) (1986) 301−312.
[20] T.J. Yoon, J.S. Kim, B.G. Kim, K.N. Yu, M.H. Cho, J.K. Lee, Multifunctional nanoparticles possessing a "magnetic motor effect" for drug or gene delivery, Angew. Chem. Int. Ed Engl. 44 (7) (2005) 1068−1071.
[21] S.W. Ha, C.E. Camalier, G.R. Beck Jr., J.K. Lee, New method to prepare very stable and biocompatible fluorescent silica nanoparticles, Chem. Commun. (Camb.) 20 (2009) 2881−2883.
[22] A. Vanblaaderen, A. Vrij, Synthesis and characterization of colloidal dispersions of fluorescent, monodisperse silica spheres, Langmuir 8 (12) (1992) 2921−2931.
[23] H. Ow, D.R. Larson, M. Srivastava, B.A. Baird, W.W. Webb, U. Wiesner, Bright and stable core-shell fluorescent silica nanoparticles, Nano Lett. 5 (1) (2005) 113−117.
[24] L. Wang, W.H. Tan, Multicolor FRET silica nanoparticles by single wavelength excitation, Nano Lett. 6 (1) (2006) 84−88.
[25] R. Kumar, I. Roy, T.Y. Hulchanskyy, L.N. Goswami, A.C. Bonoiu, E.J. Bergey, et al., Covalently dye-linked, surface-controlled, and bioconjugated organically modified silica nanoparticles as targeted probes for optical imaging, Acs. Nano. 2 (3) (2008) 449−456.
[26] S.W. Bae, W.H. Tan, J.I. Hong, Fluorescent dye-doped silica nanoparticles: new tools for bioapplications, Chem. Commun. 48 (17) (2012) 2270−2282.
[27] D.M. Huang, Y. Hung, B.S. Ko, S.C. Hsu, W.H. Chen, C.L. Chien, et al., Highly efficient cellular labeling of mesoporous nanoparticles in human mesenchymal stem cells: implication for stem cell tracking, FASEB J. 19 (14) (2005) 2014−2016.
[28] R.A. Petros, J.M. DeSimone, Strategies in the design of nanoparticles for therapeutic applications, Nat. Rev. Drug. Discov. 9 (8) (2010) 615−627.
[29] H.S. Choi, W. Liu, P. Misra, E. Tanaka, J.P. Zimmer, B. Itty Ipe, et al., Renal clearance of quantum dots, Nat. Biotechnol. 25 (10) (2007) 1165−1170.
[30] A. Albanese, P.S. Tang, W.C. Chan, The effect of nanoparticle size, shape, and surface chemistry on biological systems, Annu. Rev. Biomed. Eng., (2012.
[31] Y.W. Jun, J.S. Choi, J. Cheon, Shape control of semiconductor and metal oxide nanocrystals through nonhydrolytic colloidal routes, Angew. Chem. Int. Ed. 45 (21) (2006) 3414−3439.
[32] Y.G. Sun, Y.N. Xia, Shape-controlled synthesis of gold and silver nanoparticles, Science 298 (5601) (2002) 2176−2179.
[33] G.E.J. Poinern, N. Ali, D. Fawcett, Progress in nano-engineered anodic aluminum oxide membrane development, Materials 4 (3) (2011) 487−526.

[34] A.J. Nan, X. Bai, S.J. Son, S.B. Lee, H. Ghandehari, Cellular uptake and cytotoxicity of silica nanotubes, Nano. Lett. 8 (8) (2008) 2150−2154.
[35] X.L. Huang, L.L. Li, T.L. Liu, N.J. Hao, H.Y. Liu, D. Chen, et al., The shape effect of mesoporous silica nanoparticles on biodistribution, clearance, and biocompatibility in vivo, Acs. Nano. 5 (7) (2011) 5390−5399.
[36] S. Huh, J.W. Wiench, J.C. Yoo, M. Pruski, V.S.Y. Lin, Organic functionalization and morphology control of mesoporous silicas via a co-condensation synthesis method, Chem. Mater. 15 (22) (2003) 4247−4256.
[37] M.W. Zhao, W.P. Kang, L.Q. Zheng, Y.A. Gao, Synthesis of silica nanoboxes via a simple hard-template method and their application in controlled release, Mater. Lett. 64 (8) (2010) 990−992.
[38] L.R. Kong, X.C. Liu, X.J. Bian, C Wang, Silica nanocubes with a hierarchically porous structure, Rsc. Adv. 2 (7) (2012) 2887−2894.
[39] X.L. Huang, X. Teng, D. Chen, F.Q. Tang, J.Q. He, The effect of the shape of mesoporous silica nanoparticles on cellular uptake and cell function, Biomaterials 31 (3) (2010) 438−448.
[40] H.L. Herd, A. Malugin, H. Ghandehari, Silica nanoconstruct cellular toleration threshold in vitro, J. Control. Release 153 (1) (2011) 40−48.
[41] B.D. Chithrani, A.A. Ghazani, W.C. Chan, Determining the size and shape dependence of gold nanoparticle uptake into mammalian cells, Nano Lett. 6 (4) (2006) 662−668.
[42] J.S. Kim, T.J. Yoon, K.N. Yu, M.S. Noh, M. Woo, B.G. Kim, et al., Cellular uptake of magnetic nanoparticle is mediated through energy-dependent endocytosis in A549 cells, J. Vet. Sci. 7 (4) (2006) 321−326.
[43] G.T. Hermanson, Bioconjugate Techniques, second ed., Academic Press, Amsterdam, 2008.
[44] S. Chen, Y.J. Wei, M.M. Chen, Z.T. Zhang, Bilateral treatment: a strategy for enhancing the mechanical strength of machinable veneers, Dent. Mater. 26 (10) (2010) 961−967.
[45] H. Zou, S. Wu, J. Shen, Polymer/silica nanocomposites: preparation, characterization, properties, and applications, Chem. Rev. 108 (2008) 3893−3957.
[46] A.S. Karakoti, S. Das, S. Thevuthasan, S. Seal, PEGylated inorganic nanoparticles, Angew. Chem. Int. Ed. 50 (9) (2011) 1980−1994.
[47] J.V. Jokerst, T. Lobovkina, R.N. Zare, S.S. Gambhir, Nanoparticle PEGylation for imaging and therapy, Nanomedicine 6 (4) (2011) 715−728.
[48] R.M. Gaikwad, I. Sokolov, Silica nanoparticles to polish tooth surfaces for caries prevention, J. Dent. Res. 87 (10) (2008) 980−983.
[49] B.G. Cousins, H.E. Allison, P.J. Doherty, C. Edwards, M.J. Garvey, D.S. Martin, et al., Effects of a nanoparticulate silica substrate on cell attachment of *Candida albicans*, J. Appl. Microbiol. 102 (3) (2007) 757−765.
[50] A. Dong, J. Huang, S. Lan, T. Wang, L. Xiao, W. Wang, et al., Synthesis of *N*-halamine-functionalized silica-polymer core-shell nanoparticles and their enhanced antibacterial activity, Nanotechnology 22 (29) (2011) 295602.
[51] T. Waltimo, T.J. Brunner, M. Vollenweider, W.J. Stark, M. Zehnder, Antimicrobial effect of nanometric bioactive glass 45S5, J. Dent. Res. 86 (8) (2007) 754−757.
[52] E.M. Hetrick, J.H. Shin, H.S. Paul, M.H. Schoenfisch, Anti-biofilm efficacy of nitric oxide-releasing silica nanoparticles, Biomaterials 30 (14) (2009) 2782−2789.
[53] M. Hosseinalipour, J. Javadpour, H. Rezaie, T. Dadras, A.N. Hayati, Investigation of mechanical properties of experimental Bis-GMA/TEGDMA dental composite resins containing various mass fractions of silica nanoparticles, J. Prosthodont. 19 (2) (2010) 112−117.
[54] J.W. Kim, L.U. Kim, C.K. Kim, Size control of silica nanoparticles and their surface treatment for fabrication of dental nanocomposites, Biomacromolecules 8 (1) (2007) 215−222.

[55] J. Zheng, Q. Su, C. Wang, G. Cheng, R. Zhu, J. Shi, et al., Synthesis and biological evaluation of PMMA/MMT nanocomposite as denture base material, J. Mater. Sci. Mater. Med. 22 (4) (2011) 1063−1071.
[56] M. Tian, Y. Gao, Y. Liu, Y. Liao, N.E. Hedin, H. Fong, Fabrication and evaluation of Bis-GMA/TEGDMA dental resins/composites containing nano fibrillar silicate, Dent. Mater. 24 (2) (2008) 235−243.
[57] T.N.A.T. Rahim, D. Mohamad, A.R. Ismaila, H.M. Akil, Synthesis of nanosilica fillers for experimental dental nanocomposites and their characterisations, J. Phys. Sci. 22 (1) (2011) 93−105.
[58] J. Janus, G. Fauxpoint, Y. Arntz, H. Pelletier, O. Etienne, Surface roughness and morphology of three nanocomposites after two different polishing treatments by a multitechnique approach, Dent. Mater. 26 (5) (2010) 416−425.
[59] M.H. Chen, Update on dental nanocomposites, J. Dent. Res. 89 (6) (2010) 549−560.
[60] T.N.A.T. Rahim, D. Mohamad, A.R. Ismail, H.M. Akil, Synthesis of nanosilica fillers for experimental dental nanocomposites and their characterization, J. Phys. Sci. 22 (2) (2011) 93−105.
[61] S.P. Samuel, S. Li, I. Mukherjee, Y. Guo, A.C. Patel, G. Baran, et al., Mechanical properties of experimental dental composites containing a combination of mesoporous and nonporous spherical silica as fillers, Dent. Mater. 25 (3) (2009) 296−301.
[62] W.J. Loesche, Role of *Streptococcus mutans* in human dental decay, Microbiol. Rev. 50 (4) (1986) 353−380.
[63] C.M. Bollen, P. Lambrechts, M. Quirynen, Comparison of surface roughness of oral hard materials to the threshold surface roughness for bacterial plaque retention: a review of the literature, Dent. Mater. 13 (4) (1997) 258−269.
[64] B.C. Lee, G.Y. Jung, D.J. Kim, J.S. Han, Initial bacterial adhesion on resin, titanium and zirconia in vitro, J. Adv. Prosthodont. 3 (2) (2011) 81−84.
[65] N. Mitik-Dineva, J. Wang, R.C. Mocanasu, P.R. Stoddart, R.J. Crawford, E.P. Ivanova, Impact of nano-topography on bacterial attachment, Biotechnol. J. 3 (4) (2008) 536−544.
[66] W. Teughels, N. Van Assche, I. Sliepen, M. Quirynen, Effect of material characteristics and/or surface topography on biofilm development, Clin. Oral. Implants Res. 17 (Suppl. 2) (2006) 68−81.
[67] K. Subramani, R.E. Jung, A. Molenberg, C.H. Hammerle, Biofilm on dental implants: a review of the literature, Int. J. Oral. Maxillofac. Implants 24 (4) (2009) 616−626.
[68] L.D. Renner, D.B. Weibel, Physicochemical regulation of biofilm formation, MRS Bull. 36 (5) (2011) 347−355.
[69] A. Linde, Dentin matrix proteins: composition and possible functions in calcification, Anat. Rec. 224 (2) (1989) 154−166.
[70] M. Kitagawa, H. Tahara, S. Kitagawa, H. Oka, Y. Kudo, S. Sato, et al., Characterization of established cementoblast-like cell lines from human cementum-lining cells in vitro and in vivo, Bone 39 (5) (2006) 1035−1042.
[71] S.M. Carvalho, A.A. Oliveira, C.A. Jardim, C.B. Melo, D.A. Gomes, M.D. Leite, et al., Characterization and induction of cementoblast cell proliferation by bioactive glass nanoparticles, J. Tissue Eng. Regen. Med. (2011).
[72] V.E. Arana-Chavez, L.F. Massa, Odontoblasts: the cells forming and maintaining dentin, Int. J. Biochem. Cell Biol. 36 (8) (2004) 1367−1373.
[73] S.W. Cho, H.J. Hwang, J.Y. Kim, W.C. Song, S.J. Song, H. Yamamoto, et al., Lineage of non-cranial neural crest cell in the dental mesenchyme: using a lacZ reporter gene during early tooth development, J. Electron. Microsc. (Tokyo) 52 (6) (2003) 567−571.
[74] F. Long, Building strong bones: molecular regulation of the osteoblast lineage, Nat. Rev. Mol. Cell. Biol. 13 (1) (2012) 27−38.

[75] S. Opsahl Vital, C. Gaucher, C. Bardet, P.S. Rowe, A. George, A. Linglart, et al., Tooth dentin defects reflect genetic disorders affecting bone mineralization, Bone 50 (4) (2012) 989–997.
[76] K.G. Waymire, J.D. Mahuren, J.M. Jaje, T.R. Guilarte, S.P. Coburn, G.R. MacGregor, Mice lacking tissue non-specific alkaline phosphatase die from seizures due to defective metabolism of vitamin B-6, Nat. Genet. 11 (1) (1995) 45–51.
[77] K.N. Fedde, L. Blair, J. Silverstein, S.P. Coburn, L.M. Ryan, R.S. Weinstein, et al., Alkaline phosphatase knock-out mice recapitulate the metabolic and skeletal defects of infantile hypophosphatasia, J. Bone Miner. Res. 14 (12) (1999) 2015–2026.
[78] L. Ye, M. MacDougall, S. Zhang, Y. Xie, J. Zhang, Z. Li, et al., Deletion of dentin matrix protein-1 leads to a partial failure of maturation of predentin into dentin, hypomineralization, and expanded cavities of pulp and root canal during postnatal tooth development, J. Biol. Chem. 279 (18) (2004) 19141–19148.
[79] L. Ye, Y. Mishina, D. Chen, H. Huang, S.L. Dallas, M.R. Dallas, et al., Dmp1-deficient mice display severe defects in cartilage formation responsible for a chondrodysplasia-like phenotype, J. Biol. Chem. 280 (7) (2005) 6197–6203.
[80] J.Q. Feng, L.M. Ward, S. Liu, Y. Lu, Y. Xie, B. Yuan, et al., Loss of DMP1 causes rickets and osteomalacia and identifies a role for osteocytes in mineral metabolism, Nat. Genet. 38 (11) (2006) 1310–1315.
[81] S.C. Manolagas, Birth and death of bone cells: basic regulatory mechanisms and implications for the pathogenesis and treatment of osteoporosis, Endocr. Rev. 21 (2) (2000) 115–137.
[82] J.E. Aubin, J.T. Triffitt, Mesenchymal stem cells and osteoblast differentiation, in: J.P. Bilezikian, L.G. Raisz, G.A. Rodan (Eds.), Principles of Bone Biology, second ed. Vol. 1, Academic Press, San Diego, CA, 2002, pp. 59–81.
[83] K. Nakashima, X. Zhou, G. Kunkel, Z. Zhang, J.M. Deng, R.R. Behringer, et al., The novel zinc finger-containing transcription factor osterix is required for osteoblast differentiation and bone formation, Cell 108 (1) (2002) 17–29.
[84] P. Ducy, R. Zhang, V. Geoffroy, A.L. Ridall, G. Karsenty, Osf2/Cbfa1: a transcriptional activator of osteoblast differentiation, Cell 89 (5) (1997) 747–754.
[85] C. Banerjee, L.R. McCabe, J.Y. Choi, S.W. Hiebert, J.L. Stein, G.S. Stein, et al., Runt homology domain proteins in osteoblast differentiation: AML3/CBFA1 is a major component of a bone-specific complex, J. Cell Biochem. 66 (1) (1997) 1–8.
[86] J.E. Aubin, Advances in the osteoblast lineage, Biochem. Cell Biol. 76 (6) (1998) 899–910.
[87] S.L. Teitelbaum, Bone resorption by osteoclasts, Science 289 (5484) (2000) 1504–1508.
[88] C.D. Seaborn, F.H. Nielsen, Silicon deprivation decreases collagen formation in wounds and bone, and ornithine transaminase enzyme activity in liver, Biol. Trace Elem. Res. 89 (3) (2002) 251–261.
[89] C.D. Seaborn, F.H. Nielsen, Dietary silicon and arginine affect mineral element composition of rat femur and vertebra, Biol. Trace Elem. Res. 89 (3) (2002) 239–250.
[90] S.I. Anderson, S. Downes, C.C. Perry, A.M. Caballero, Evaluation of the osteoblast response to a silica gel in vitro, J. Mater. Sci. Mater. Med. 9 (12) (1998) 731–735.
[91] M. Wiens, X. Wang, U. Schlossmacher, I. Lieberwirth, G. Glasser, H. Ushijima, et al., Osteogenic potential of biosilica on human osteoblast-like (SaOS-2) cells, Calcif. Tissue Int. 87 (6) (2010) 513–524.
[92] I.R. Gibson, S.M. Best, W. Bonfield, Chemical characterization of silicon-substituted hydroxyapatite, J. Biomed. Mater. Res. 44 (4) (1999) 422–428.
[93] P.E. Keeting, M.J. Oursler, K.E. Wiegand, S.K. Bonde, T.C. Spelsberg, B.L. Riggs, Zeolite A increases proliferation, differentiation, and transforming growth factor beta production in normal adult human osteoblast-like cells in vitro, J. Bone Miner. Res. 7 (11) (1992) 1281–1289.

[94] S. Zou, D. Ireland, R.A. Brooks, N. Rushton, S. Best, The effects of silicate ions on human osteoblast adhesion, proliferation, and differentiation, J. Biomed. Mater. Res. B Appl. Biomater. 90 (1) (2009) 123–130.
[95] C.Q. Ning, J. Mehta, A. El-Ghannam, Effects of silica on the bioactivity of calcium phosphate composites in vitro, J. Mater. Sci. Mater. Med. 16 (4) (2005) 355–360.
[96] H. Zhou, X. Wu, J. Wei, X. Lu, S. Zhang, J. Shi, et al., Stimulated osteoblastic proliferation by mesoporous silica xerogel with high specific surface area, J. Mater. Sci. Mater. Med. 22 (3) (2011) 731–739.
[97] G.R. Beck, Jr., S.W. Ha, C.E. Camalier, M. Yamaguchi, Y. Li, J.K. Lee, et al., Bioactive silica-based nanoparticles stimulate bone-forming osteoblasts, suppress bone-resorbing osteoclasts, and enhance bone mineral density in vivo, Nanomedicine, 8 (6) (2012) 793–803.
[98] P.I. Branemark, Osseointegration and its experimental background, J. Prosthet. Dent. 50 (3) (1983) 399–410.
[99] R. Branemark, P.I. Branemark, B. Rydevik, R.R. Myers, Osseointegration in skeletal reconstruction and rehabilitation: a review, J. Rehabil. Res. Dev. 38 (2) (2001) 175–181.
[100] A.B. Novaes Jr., S.L. de Souza, R.R. de Barros, K.K. Pereira, G. Iezzi, A. Piattelli, Influence of implant surfaces on osseointegration, Braz. Dent. J. 21 (6) (2010) 471–481.
[101] J.S. Kim, T.J. Yoon, K.N. Yu, B.G. Kim, S.J. Park, H.W. Kim, et al., Toxicity and tissue distribution of magnetic nanoparticles in mice, Toxicol. Sci. 89 (1) (2006) 338–347.

CHAPTER

Nanoparticles, Properties, and Applications in Glass Ionomer Cements

5

Abdul Samad Khan[a], Maria Khan[b] and Ihtesham Ur Rehman[c]

[a]*Interdisciplinary Research Centre in Biomedical Materials, COMSATS Institute of Information Technology, Lahore, Pakistan*

[b]*Department of Dentistry, Pakistan Institute of Medical Sciences, Islamabad, Pakistan*

[c]*Department of Materials Science and Engineering, The Kroto Research Institute, University of Sheffield, Sheffield, UK*

CHAPTER OUTLINE

5.1 Introduction

Dentistry is a much developed field in the last few decades. New techniques have changed the conventional treatment methods as applications of new dental materials give better outcomes. The current century has suddenly forced on dentistry a new paradigm regarding expected standards for state-of-the-art patient care. Traditional methods and procedures that have served the profession well are being questioned within the context of evidence-based rationales and emerging information/technologies. Dental materials science for restorative dentistry is derived from material science. Material science is classified into four categories: metals, ceramics, polymers, and composites. Each of these materials has characteristic microstructures and resulting properties [1]. A large number of materials have been used in dentistry for a wide spectrum of applications [2].

Nanobiomaterials in Clinical Dentistry.

Restorative dental materials include synthetic components, acid−base cements, amalgam, resin-based composites, noble and base metals, ceramics, and denture polymers [3,4]. The ideal restorative material should be biocompatible, bond permanently to tooth structure or bone, match the natural appearance of tooth structure and other visible tissues, and be capable of initiating tissue repair or regeneration of missing or damaged tissues [4]. The moisture environment of oral cavity poses many challenges to restorative materials; in addition, they should withstand the effect of masticatory forces, enzymatic attacks, variation of pH, and temperature. Bite forces can vary from 100 to 500 N depending on the position in the mouth and of the individual [5]. Microleakage between the tooth and restoration can lead to colonization by bacteria and development of secondary caries, and subsequently, failure of restoration [6].

5.2 Smart dental materials

Within the field of restorative dentistry, the incredible advances in dental materials research have led to the current availability of esthetic adhesive restorations, conducting the profession into the "post-amalgam era" [7]. It has been clearly established that this new biomimetic approach to restorative dentistry is possible through the use of composite resins/porcelains and the generation of a hard tissue bond. The development of nanomaterials has moved nanotechnology from its theoretical foundations into mainstream practice [8]. Clinicians have been using certain criteria to select dental materials, e.g., (i) analysis of the problem, (ii) consideration of requirement, and (iii) available materials and their properties [9].

Materials demonstrating an optimum combination of smart interactions and longevity are likely to have some combination of stable resin matrix combined with a coexistent salt matrix or discreet phase. The rapid developments in nanotechnology propose that such features can be manufactured into compounds using building blocks at an atomic or molecular level. Friend [10] reported that *The development of true smart materials at the atomic scale is still some way off, although the enabling technologies are under development. These require novel aspects of nanotechnology (technologies associated with materials and processes at the nano-meter scale, 10^{-9}m) and the newly developing science of shape chemistry.*

5.3 Nanotechnology and dentistry

Nanotechnology has revolutionized the field of science and technology. It is the production of functional materials and structures in the range of 0.1−100 nm by various physical and chemical methods and also known as molecular nanotechnology or molecular engineering. It has led to the development of new restorative materials containing nanoparticles. The interest in using nanomaterials stems from the idea that they can be used to manipulate the structure and properties of the materials [11]. Nanotechnology is of great interest in biomaterials engineering and in the development of dental materials [2]. The particle size of dental restorative materials is so dissimilar to the tooth structure such as hydroxyapatite (HA) crystal, dentinal tubules and enamel rod that there is a potential for compromises in adhesion between the macroscopic (40−0.7 nm) restorative material

and the nanoscopic (1−10 nm in size) tooth structure [12]. Nanoscale particles have more similarities to natural tooth as far as crystal size is concerned. Additionally, the high surface area of the nanoscopic particles would offer a good mechanical interlocking with the polymer matrix [13]. This is true for purpose-designed nanostructures, which can be used to produce low shrinkage, high wear resistance, and biocompatibility of the dental materials. The fundamental application is the resistance of nanoparticles-filled materials to the loss of substance during the propagation of microfracture through cyclic fatigue loading [14]. Inorganic nanoparticles are hard and dense and these characteristics make them interesting for improving a material's mechanical properties. Due to large surface area, the particles show thixotropic thickening effect and low viscosity and improve the handling properties. Nanofillers also show smooth surface effects and volume effects as well as high optical properties. In addition, they have higher contact surface with the organic phase when compared to minifilled composites, consequently improving the material hardness [15].

The hybrid system of nanoparticles dispersed in polymer matrix has received extensive attention recently [16]. The major difference between nanometric (< 100 nm) and micrometric (> 100 nm) particles is that nanoparticle facilitates the transfer of load from polymer matrix to nanoparticles [17]. Therefore, nanoparticle-reinforced hybrid system exhibits higher stiffness and better resistance to wear [18]. In contrast, large specific surface area can easily lead to particle agglomeration, which makes nanoparticles more difficult to be evenly dispersed into polymer matrix, thus resulting in a strength reduction. In restorative dentistry, there has also been a growing interest in using nanoparticles to improve the properties of dental restoratives [11]. However, little work has been reported so far regarding use of any nanoparticles to improve dental glass ionomer cement (GIC) [19].

5.4 Glass ionomer cement

GIC was invented by Wilson and Kent in 1969 at the English Laboratory of the Government Chemist [20]. GIC commonly known as polyalkenoate cement is water-based cement and formed by the reaction of an acidic polymer and a basic glass in the presence of water [21,22]. The generic name of glass ionomers is based on the original components fluorosilicate glass and polyacrylic acid. The resulting cement is an inorganic and organic network with a highly cross-linked structure that adheres to tooth structure and is translucent [23,24]. The first GIC introduced had the acronym "ASPA," and comprised alumina-silicate glass as the powder and polyacrylic acid as the liquid. This product was first sold in Europe (De Trey Company and Amalgamated Dental Company) and later in the United States [25]. For glass ionomers the mixing process and working time combined should last about 2−3 min and the setting reaction should be complete several minutes after placement. GIC have exceptional properties that make them useful as restorative and adhesive materials, which include chemical bonding to tooth structure, adhesion to base metals, anticariogenic properties due to fluoride release, thermal compatibility with tooth structure, biocompatibility, and low cytotoxicity. This material has tendency to be used as luting cements, filling materials, and lining cements [26]; hereas, limitations of GIC include brittleness, poor fracture toughness material, and sensitivity to moisture in the early stages of the placement. Although stronger and more esthetic glass ionomers with improved handling characteristics are now available, low fracture toughness

and lack of strength are still major problems for GICs. Despite major improvements since their invention, significant advances are still needed, e.g., chemistries that increase the degree of the cross-linking and polysalt bridge formation improve mechanical properties, making the material a suitable choice for both posterior tooth restorations and bone grafting material in stress-bearing areas.

GICs contain ion leachable calcium fluoroaluminosilicate (FAS) glass to which other components, such as lanthanum, strontium, barium, and zinc oxide, have been added that can react with water-soluble acids such as polyacrylic acid and tartaric acid. The setting reaction is based on acid−base reaction between the FAS glass and homo- and copolymers of polyacrylic acid [4]. The glass ionomer powder comprises silica (SiO_2), alumina (Al_2O_3), and calcium fluoride (CaF_2) as flux and typically sodium fluoride (NaF), cryolite (Na_3AlF_6) and aluminum phosphate ($AlPO_4$), which are soluble in acids. Phosphate and fluoride ions are used in the basic glass to modify the setting characteristics of the material ([25]); however, still alumina and silica, which form the skeletal backbone of the glass, are the main structural components [27]. These components are melted at high temperature (fusion of oxides at temperatures between 1100 and 1500°C). The use of high temperatures, particularly on an industrial scale, consumes a huge quantity of energy since the oxide links need to be ruptured and then formed again for the synthesis of glass. This makes production cost higher. Alternatively, soft chemistry has been used for synthesis of glasses because this route yields more homogeneous materials using lower processing temperatures than the conventional fusion method. The other methods are flame spraying and inductively coupled radiofrequency plasma spraying techniques [28,29], spray drying method [30], and sol−gel technique [31].

The three-dimensional structure of the glass particle is based on an aluminosilicate network. The Si^{4+} ions reside at the interstices formed by four oxygen anions, where Al^{3+} plays a dual role in the glass matrix. It can be substituted for a Si^{4+}, therefore, consider as a network-forming ion. The negative charge is offset by other network-dwelling ions such as sodium (Na^+) or calcium (Ca^{2+}). Network-dwelling ions do not take part in the three-dimensional network but reside within the glass. If sufficient sodium or calcium ions are not present to maintain charge neutrality, then the aluminum ions will be network dwelling, presumably as an oxide, fluoride, or phosphate also considered network dwelling [32,33]. The proper glass network should be formed before the glass is reactive to an acidic polymer. This occurs when counter ions are present and the Al/Si ratio is close. The glass has loosely bound negative charges that attack by the carboxylic acid from polymers and disrupt the three-dimensional matrix. Al^{3+} ions, along with other ions, are released and form ionic bonds with polymers. The Al/Si ratio is the main factor controlling the rate of setting reaction in GIC. The ratio of Al_2O_3 to SiO_2 is critical for accurate reactivity and must be 1:2 or more by mass for cement formation. Furthermore, the hydrolytic stability of GIC also depends on Al/Si ratio; higher ratios of Al/Si increase the stability of the cement [25,34]. The entrance of Al^{3+} ions in the network-forming sites increases the susceptibility of the glass structure to acid attack because the negative charge on the network is increased. Other ion concentrations also play a role in the setting and properties of GIC. The presence of Na^+ ions in the glasses has adverse effects on the hydrolytic stability. Currently, in GIC the amount of CaF_2 has been decreased, and the Al_2O_3/SiO_2 ratio has been changed to enhance the esthetics and the degree of transparency. CaF_2 has been added as a flux to decrease the melting point (the structure can be melted at a more economical temperature below 1350°C). The addition of ions of lanthanum (La), strontium (Sr), barium (Ba), or zinc (Zn) provides radiopacity for the cement.

The polyelectrolytes used in GIC can be described as polyalkenoic acids. Originally, the liquid was based on 40–50% aqueous solution of polyacrylic acid, but the solution was very viscous for optimal mixing with the powdered glass, unstable and tended to gel over time, and subsequently lowered the setting rate. Currently manufactured polyacids include the homopolymers or copolymers of unsaturated mono-, di-, or tricarboxylic acids such as maleic acid and itaconic acid to overcome the problems associated with polyacrylic acid.

During the setting reaction, the surface of glass particles release ions that cross-link the polymer, and inorganic matrixes form as a result of this reaction. The resultant cement is a highly complex composite including gel of calcium and aluminum polyacrylates that contains fluoride. The unreacted portion of the glass powders act as filler for the cement. The glass powder is partly etched by the polyacid and the outer surface is degraded to siliceous hydrogel that contains fluorite crystallites. Silicic acid is also released which polymerizes into a silica gel. The set cement contains many components, a hydrogel matrix, a silica gel matrix, and glass particles containing polysalt bridges between metallic ions and carboxylate groups [35].

In addition to the chemistry of the basic glass and the polyacid, other factors such as molecular weight of acids, powder/liquid (P/L) ratio, and particle size and their distribution [36] control the setting and mechanical properties of GICs. Higher molecular weight and P/L ratios increase the setting rate and mechanical strength [37]. Particle size and their uniform distribution substantially affect the microstructure of the cement and therefore their mechanical properties. It is reported that small particles corresponded to higher strengths, and an increased proportion of larger particles corresponded with a decrease in viscosity of the unset cement. The optimization of particle sizing and distribution can lead to enhanced physical properties and life of restoration [38]. The nature of the filler, its qualitative and quantitative analysis largely decide the mechanical properties of the restoration material. The shape of the particles is another important aspect influencing the mechanical locking of filler particles to the polymeric matrix; an irregular shape of the filler particle favors a better physical retention in the polymeric matrix. However, irregular particles possess smaller packing ability and therefore they cause a heterogeneous stress distribution.

5.5 Modified GIC

The conventional GICs have some clinical limitations such as prolonged setting reaction time, moisture sensitivity during initial setting, dehydration, and rough surface texture, which can affect mechanical resistance [38]. To overcome these problems, resin-modified GICs (RMGICs) were developed which contain monomers and photo initiators [39]. Setting reactions is based on an acid–base reaction; in addition, light exposure causes the creation of cross-linking between polymeric chains and polymerization of methacrylate. Metal-reinforced GICs were introduced in 1977, and the addition of silver-amalgam alloy powder to conventional materials increases the physical strength of the cement and provides radiopacity. They can be used to restore Class II cavities by tunnel preparation, deciduous teeth (especially Class I), core buildups, and retrograde root filling [40]. Several faster-setting, high-viscosity conventional GICs have been developed with fine glass particles, anhydrous polyacrylic acids of high molecular weight, and a high powder-to-liquid mixing ratio [41]. The setting reaction is the same as the acid–base reaction of a typical conventional GIC.

However, the advent of nanotechnology in recent years has made it possible to structurally change many dental materials including impression materials, composites, and glass ionomers. This in some cases has resulted in the overcoming of physical limitations previously thought to be insurmountable. Not only have the limited hardness and resistance to stress of GIC been overcome but it has also been possible to give GICs an appearance of translucency and coloration that are a good solution in many areas of the oral cavity. Although composite materials are now the reference material for reconstructions, a glass ionomer system based on nanotechnology can represent a good, or in certain conditions even better, alternative if the chemical properties, the protection of the ablation of caries, and the constant release of fluoride are taken into consideration case by case.

5.6 Resin-modified nano-glass ionomer composites

In addition to conventional and resin-modified GIC, a nanofilled resin-modified GIC or "nanoionomer" was developed recently by 3M ESPE—Ketac™ N100 (KN). KN light curing nanoionomer restorative is the first paste/paste, resin-modified glass ionomer material developed with nanotechnology. Because it adds benefits not usually associated with glass ionomers, it has resulted in a new category of glass ionomer restorative: the nanoionomer. The technology of KN restorative represents a blend of FAS technology and nanotechnology. Nanoparticle-filled RMGIC is developed by the addition of nanoparticles (100 nm compared to 30 μm in traditional GIC, which is equivalent to 30,000 nm) to RMGIC materials. This combination offers unique characteristics of wear and polish, and filler particle size can influence strength, optical properties, and abrasion resistance. The addition of nanoparticles to KN would be expected to provide an improved finish and a smoother, more esthetic restoration without adversely affecting other advantageous properties, including fluoride release, adhesion to enamel and dentin, high early bond strength, and less susceptibility to moisture and dehydration [42]. In vitro study demonstrates that the addition of nanofillers provides enhanced surface wear and polish relative to some other commercially available dental materials [43].

According to 3M ESPE, by using nanosized fillers and nanoclusters, along with FAS glass, KN restorative provides enhanced esthetics as well as the benefits of glass ionomer chemistry, such as fluoride release. The nanoionomer is based on the acrylic and itaconic acid copolymers necessary for the glass ionomer reaction with alumino-silicate glass and water. The nanoionomer also contains a blend of resin monomers, bisphenol A-glycidyl methacrylate (BisGMA), triethylene glycol dimethacrylate (TEGDMA), and hydroxy ethylmethacrylate (HEMA), which polymerize via the free radical addition upon curing primary curing mechanism is by light activation. The originality of this GIC is the inclusion of nanofillers which constitute up to two-thirds of the filler content (circa 69 wt%). In a study, the fluoride release pattern of KN was investigated and it was found that KN presented a similar cumulative F^- release pattern compared to resin-modified glass ionomer; however, the fluoride release was lesser than conventional GIC. Based on this, it might be speculated that the nanoparticles presented in the tested GIC (KN) do not have influence on the cumulative F release profile. This phenomenon could be due to low solubility of nanoparticles, and the material does not exhibit any voids, cracks, and microporosities after immersion in saline, as found with all other GICs tested [44]. However, it is claimed by the manufacturer that KN has the tendency for high fluoride release that is rechargeable after being exposed to a topical fluoride source. Additionally, *in vitro* tests showed that KN has the ability to create a caries inhibition zone after acid exposure [45].

It is speculated that the nanofiller components also enhance some physical properties of the hardened restorative. However, in a study it is reported that the KN showed low hardness value (39 KHN) when compared with other resin-modified glass ionomer, Vitremer (69.9 KHN). It is suggested that this nanofilled GIC could be indicated to anterior teeth or cervical restorations and does not seem to be appropriate to use in stress-bearing areas. However, according to the manufacturer (3M ESPE), KN is indicated for small Class I restorations, Class II and V, sandwich technique, primary teeth restorations, and provisional restorations. It is wise to observe that the material does not comply with the specifications of ADA (American Dental Association), which regulates the number of Knoop hardness of ionomer material indicated for restoration in 48 KHN [46]. Whereas, recently in another study, El Halim [47] found higher values of microhardness (62 KHN) of KN, which are in agreement of ADA specifications.

Bond strength of nanoionomer was analyzed and it was observed that the material interacted with dentin and enamel in a very superficial way, without evidence of demineralization and/or hybridization. They exhibited adequate bond strength to enamel (14.4 ± 5.8 MPa) and dentin (12.6 ± 6.5 MPa), at the same extent as other GICs (enamel: 12.9 ± 3.3 MPa; dentin: 12.3 ± 2.9 MPa), on the condition that the surface was beforehand treated with the proprietary primer that contains the acrylic/itaconic acid copolymer dissolved in HEMA and water. It bonded less effectively than conventional RMGIC (Fuji II LC) (enamel (38.8 ± 7.4 MPa) and dentin (31.4 ± 4.3 MPa)). Its superficial interaction provides micromechanical interlocking that is most likely supported by chemical interaction of the acrylic/itaconic acid copolymer with surface HA [48]. The transmission electron microscope (TEM) images shown in Figure 5.1 exhibited the nonhomogeneous filler distribution and there are some nanoclusters.

Another study using the shear bond strength (SBS) as an adhesion parameter showed that Er:YAG laser dentin pretreatment results in lower bond strength values compared to acid-etching or a combined acid-etching and laser pretreatment [49]. A study [50] on bonding orthodontic brackets showed

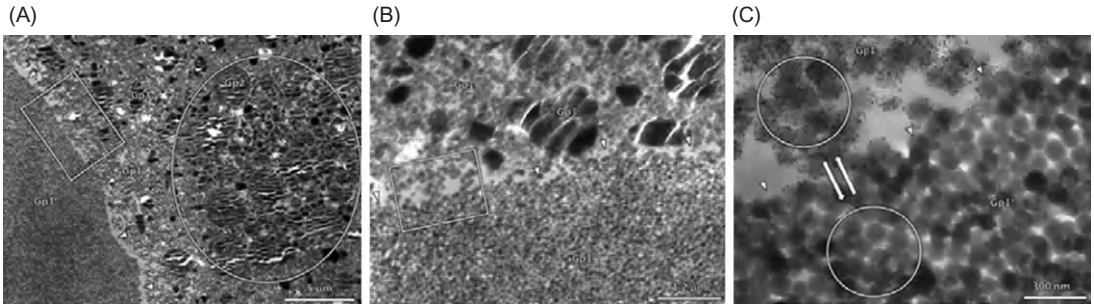

FIGURE 5.1

TEM images of the nano-RMGIC, disclosing areas of nonhomogeneous filler distribution at certain locations (A). An area of highly packed mixed glass particles is shown (round frame), as well as a cluster of nanofillers clearly apart (arrowheads) from the remaining microstructure. The rectangular frame delimits an area examined in higher magnification (B), which shows the interface between a highly packed cluster of nanofiller and the remaining microstructure (arrowheads). The rectangular frame delimits an area examined at higher magnification (C), which displays a detail of the interface (arrowheads) between the nanofiller cluster and the nanofillers in the typical microstructure [48].

significantly lower SBS for KN compared to a conventional light-cure orthodontic bonding adhesive (Transbond XT). However, it has been suggested that this nanoionomer may be used for bonding orthodontic brackets since the obtained SBS is within clinically acceptable range. The results in that study demonstrated that Transbond XT (12.60 ± 4.48 MPa) had higher SBS values than nanocomposite (8.33 ± 5.16 MPa) and nanoionomer (6.14 ± 2.12 MPa). No statistically significant differences were found between nanocomposite and nanoionomer ($P > 0.05$). The nanoionomer did not have the disadvantage of the nanocomposite wherein the consistency of the adhesive paste is thick, and the nanoionomer easily flowed into the retention pad of the bracket base. The flowability of the nanoionomer may make it superior to composite resins for penetrating the bracket retention features and possibly coating the enamel during the bonding procedure. Such an attribute might reduce the possibility of caries forming under brackets during treatment. Fluoride release and recharge might also reduce the possibility of caries formation near the bonding material excess interface between the bonding material/enamel/oral environment lines. From this perspective, KN nanoionomer should be considered a potentially useful adhesive for bonding orthodontic brackets. Reynolds [51] suggested that minimum bond strength of 5.9−7.8 MPa is adequate for most orthodontic needs during routine clinical use. A microleakage around Class V cavities was analyzed and results showed that Er:YAG preparation exhibited greater microleakage than a conventional cavity preparation with a bur when a nanoionomer (KN) and a nanocomposite (Filtek Supreme XT) were used as restorative materials [52].

Recently, another nanofilled resin-modified glass ionomer composite (Equia system) has been developed which contains inorganic nanofiller (represents 15% by weight and 80% by volume), adhesive monomer, functional methacrylate, methyl methacrylate, and photochemical initiator. The fillers are composed of silica powder with an average size of 40 nm and, being uniformly dispersed within the solution, give the restoration a high degree of wear resistance. The nanofiller particles tend to agglutinate in the resin matrix, which is used to form a layer with an average thickness of 35−40 μm that seals and protects both the surfaces of the restoration and the adhesive interface between the restoration and the dental structure. The estimated setting time is only 3 min of which 1 min and 15 s is for mixing and manipulation and 2 min for the hardening of the cement. It has a decisive advantage over traditional GIC, whose hardening requires more than 5 min. The infiltration and dispersion of the nanofilled particles protect the restoration and margins, and increase the hardness and resistance to both flexion and wear. Furthermore, the nanofilled resin also maintains the polished surface of the restoration for a long time because it hinders the dissolution and disintegration of the outermost layer of the material. In contrast, traditional finishing using abrasive polishing pastes is always accompanied by a certain amount of wear on the restoration, which becomes clinically evident after a while because of the loss of translucency. The esthetic appearance has also been improved with nanofilled resins that give the filling the same brilliance as that of a natural tooth [53]. The clinical trials showed (Figure 5.2) that after the removal of the metallic reconstructions, teeth were reconstructed, first using Vita shade A3 Equia. Then its surface was modeled and the G-Coat coating resin positioned. It was therefore possible to create effective contact points. The GIC of the Equia system called Fuji IX GP has a maturation period of 7−10 days from placement of the reconstruction.

Rehman and group [54] synthesized N-vinyl-pyrrolidone (NVP) containing polymers and altered monomeric sequences (AA-NVP-IA) and incorporated into glass ionomer liquid formulations. It was envisaged that NVP molecules interspersed between the itaconic and acrylic acid and would act as a spacer to decrease the degree of steric hindrance of carboxylic acid groups. Subsequently, the probability of ionic bond formation and polysalt bridge formation within the final set cement would be

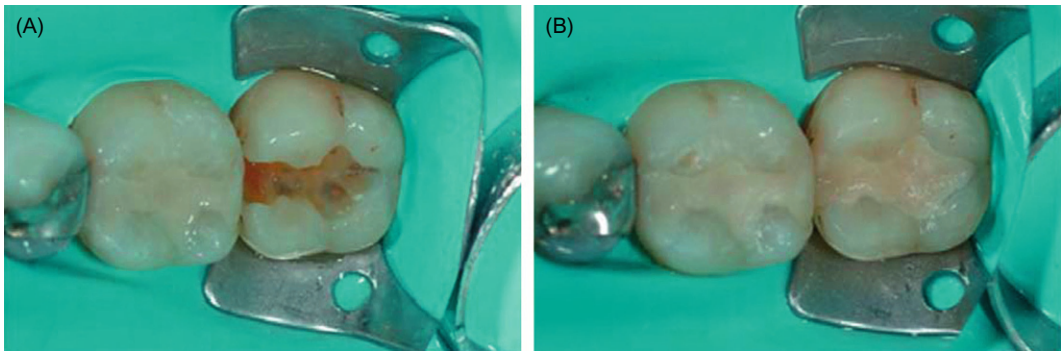

FIGURE 5.2

Teeth were restored with Equia system (Fuji IX GP) [53].

increased significantly. In this study, nanoparticles (50−100 nm) of both HA and fluoroapatite (FA) were added to glass ionomer powder (5 wt%) and the mechanical test results showed that both of the glass powders had higher strength compared to the Fuji II commercial GIC. Nano-FA/ionomers had higher values for compressive strength (CS), diametral tensile strength (DTS) and biaxial flexural strength (BFS) (179, 23, and 35 MPa, respectively) compared to HA/ionomer (178, 19, and 32 MPa, respectively), which can be related to the stability of FA and lower dissolution rate of FA in distilled water compared to the dissolution rate of nano-HA. Both nano-HA and FA take part in the acid/base reaction of the GIC and react with inorganic component of GIC network via their phosphate and calcium ions. The highest values for mechanical properties were obtained when both powder and liquid were modified, although the difference was not remarkable when it compared to the glass ionomer samples in which only their powder (by incorporation of nanoceramic particles) or liquid (by incorporation of NVP segments) were modified. By incorporation of both NVP and nanoparticles into the liquid and powder of GIC, the highest increase in strength was observed. More than 14% increase in CS was observed and the values for DTS doubled while the BFS tripled. This suggested that these additives have an effect on the setting reaction, mechanism, and degree of polysalt bridge formation of the glass ionomer, which cause higher mechanical properties of final set cement. There should be some physiochemical interactions between the carbonyl group of NVP in the polymer structure and phosphate and hydroxyl and fluoride ions of apatite. This kind of physical bonding is weak, but since there are a large number of these types of bonds, they might be partly responsible for increase in the mechanical properties of the resulting experimental glasses. Moreover, the possibility of formation of hydrogen bonds is much more because of the presence of hydroxyl, phosphate, fluoride, and carbonyl groups in the matrix. It is expected that stronger bonds between the organic and inorganic networks of the set cement lead to higher mechanical strength of final set cement. Another role for incorporated apatite nanoparticles is their ability to react with poly acrylic acid (PAA). Due to their small size, the incorporation of nanoparticles into glass powder of glass ionomers leads to wider particle size distribution (the average particle size of glass ionomer particles were around 10−20 μm) which resulted in higher mechanical values. Consequently, they can occupy the empty spaces between the glass ionomer particles and act as a reinforcing material in the composition of the GIC.

Lee et al. [55] added micro-HA (5−10 μm) and nano-HA (100−150 nm) in resin-modified glass ionomer and observed the bond strength with tooth structure, and it was found that lowest bonding strength was observed in the resin-modified glass ionomer (0.75 MPa), followed by micro-HA-added GIC group (1.02 MPa), and nano-HA-added GIC group presented highest bonding strength (1.91 MPa). The reason for the increased bonding strength of GIC with the addition of HA is that calcium ions from HA may participate in chemical ionic bonding between the tooth and the material as shown in Figure 5.3. Bonding strength was greater in the nano-HA-added GIC group compared to micro-HA added GIC group, which can be attributed to smaller particle size of nano-HA; smaller particles have increased surface area, which contributes to enhanced solubility and infiltration capacity to enamel surface, thereby reinforcing the bonding strength. The demineralized enamel surface study showed that the resin-modified GIC exhibited increased irregularities, and microporosities arise from the loss of inorganic materials from the inter-rod space in enamel. Whereas, samples with nano-HA showed smoother enamel surface with increased regularity compared to the micro-HA. Increased resistance to demineralization with nano-HA samples can be explained by smaller particle size of nano-HA compared to micro-HA; the smaller particle size enhanced its deposition into micropores in demineralized enamel. The high solubility of nano-HA leads to effective release of calcium and phosphate ions, which fills the demineralized micropores. HA particles and inorganic ions infiltrate into the demineralized

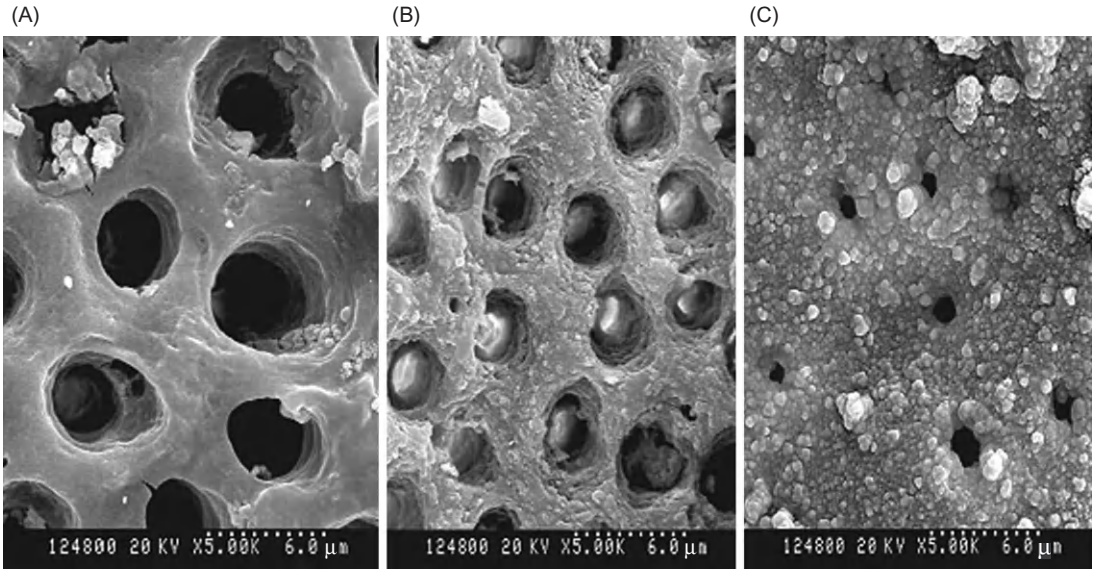

FIGURE 5.3

Fractured surface observed under SEM after bonding strength test (SEM × 5000). (A) GIC only, (B) GIC + micro-HA, (C) GIC + nano-HA. Spherical apatite particle was not observed in the control group (A). Decreased diameter of dentinal tubules and deposition of spherical apatite particle were observed in experimental groups (B and C). Increased spherical apatite particle deposition was observed in nano-HA-added GIC group (C) compared to micro-HA-added GIC group (B) [55].

surface, they obstruct the movement of calcium released from enamel surface, and therefore, resistance to demineralization is increased.

Gu et al. [28] incorporated nano-HA/ZrO2 and developed GIC composites with improved biocompatibility and bioactivity. The morphology of HA/ZrO_2 powder was a mixture of spherical ZrO_2 particles embedded within agglomerated HA needles. The nano-HA/ZrO_2−GICs prepared by the HA/ZrO_2 powders with high crystallinity showed better mechanical properties than those prepared by lower crystalline HA/ZrO_2 powders, due to the slow resorption rate for high crystallinity powders. The mechanical properties of nano-HA/ZrO_2−GICs were found to be much better than those of nano-HA−GICs because ZrO_2 was harder than the glass and nano-HA particles. The mechanical properties were increased due to the continuous formation of aluminum salt bridges, which provided the final strength of the cements. However, a decrease in the mechanical properties was found for higher volume (28 and 40 vol%) HA/ZrO_2−GICs because of the insufficient ionomer to effectively hold the relatively large amount of HA/ZrO_2 powders. It was concluded that with an increase in the HA/ZrO_2 content in the cements beyond 12 vol%, the mechanical properties were found to deteriorate.

5.7 Nanoparticles-based GIC

HA has been incorporated in GIC powder to improve its biological and mechanical properties. Rehman and group [56] synthesized nano-HA and FA using an ethanol based sol−gel technique and incorporated the synthesized nanoparticles into commercial glass ionomer powder (Fuji II GC). The Scanning Electron Microscope (SEM) images of nano-HA and nano-FA are given in Figure 5.4.

CS, DTS, and BFS of the modified GIC were analyzed, and it was found that after 24 h and 1 week of setting, the nano-HA/FA added cements exhibited higher CS (177−179 MPa), higher DTS (19−20 MPa), and higher BFS (26−28 MPa) compared to control group (160 MPa in CS, 14 MPa in

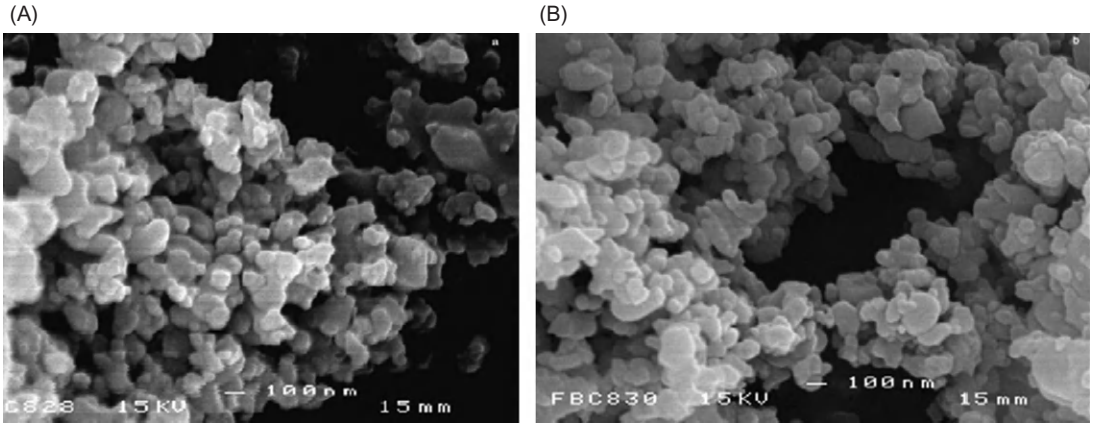

FIGURE 5.4

SEM images of (A) nano-HA and (B) nano-FA incorporated in GIC [56].

DTS, and 18 MPa in BFS). This cement also showed higher bond strength to dentin after 7 and 30 days of storage in distilled water. Gu et al. [28] mixed nanosized (5−15 nm) spherical Yttria-stabilized ZrO_2 (YSZ) powders and microsized Y_2O_3 stabilized ZrO_2 powders (5−80 μm) with glass ionomer. The SEM images are given in Figure 5.5. The experimental materials were characterized to analyzed microhardness, CS and DTS. It was found that the microhardness values were in comparison for both materials; however, the CS and DTS of microsized particles were higher than nanosized particles. It was due to high packing density of GIC with finely distributed large particles that can ensure high mechanical strength. However, due to the extremely small particle size and large surface area of the nanosized YSZ−GIC composites, there might be insufficient ionomer to hold the large amount of nanosized YSZ powders effectively. The nanosized YSZ−GIC composites can be

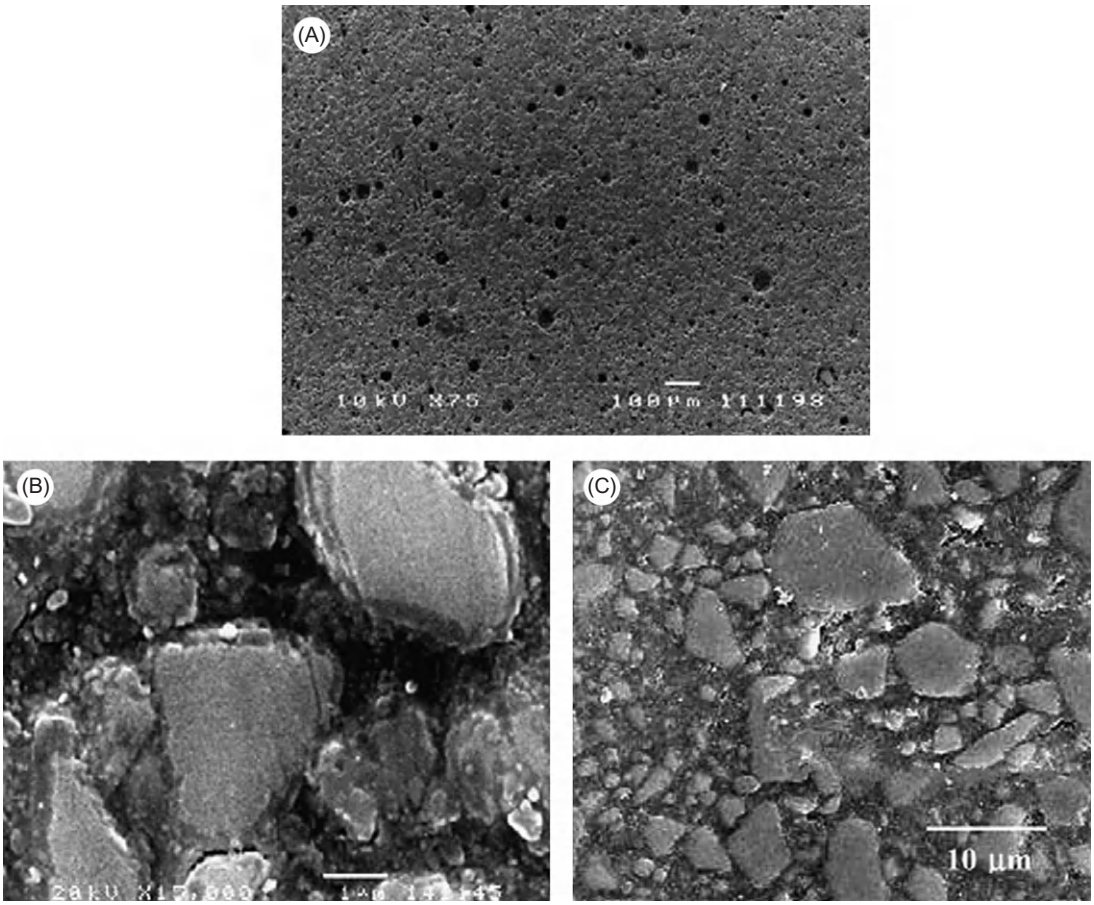

FIGURE 5.5

SEM micrographs of polished cross-sectional view of YSZ−GIC: (A) nanosized YSZ−GIC at low magnification; (B) nanosized YSZσGIC at high magnification; and (C) microsized YSZ−GIC [28].

manufactured only at low powder/liquid ratios, and higher powder/liquid ratio is unattainable because of the low packing density of the nanosized powders. Therefore, low strength values were obtained for the nanosized YSZ−GIC composites because of the low powder/liquid ratio.

A study in which preparation of niobium FAS glass powder by the sol−gel process for use as cement formers was conducted. The resulting powder was in a nanoscale range with surface area of 19 m^2/g, which affected its manipulative properties. The microhardness (Knoop Hardness: KHN) values were higher (19) compared to conventional GIC (16.4) [57].

A commercial glass ionomer powder (Riva SC) was blended in various proportions (1, 2, 5, 10, 15, and 25% (w/w)) with YbF_3/$BaSO_4$ nanoparticles. It was found that with incorporation of these nanoparticles, there was significant decrease in working and setting time of cements, which indicates a significant interaction of the nanoparticles with the glass ionomer matrix. The longer working times at 10% and 15% incorporation of nanoparticles are most likely a result of the inhibition by YbF_3 of the initial, divalent-mediated, gelation stage of the glass ionomer reaction. The decrease in working and initial setting time caused by the addition of $BaSO_4$ (significant at 2% $BaSO_4$) was due to its contribution to the initial gelation reaction of the GIC. Because of the nanostructure of the $BaSO_4$ particles, the barium ions are more easily available than the calcium or strontium ions, which are in the glass. Up to 5% BaSO4 nanoparticles addition the working time decreased and a minimum working time was achieved at 15% nanoparticles. The low solubility and reactivity of the $BaSO_4$ resulted in dilution or rate-reducing effect on the glass ionomer reaction. The CS was also decreased with these nanoparticles. The decrease in CS of the GIC was only significant at concentrations of 5% or higher, indicating that 1−2% YbF_3 addition had no significant deleterious effect. However, the investigators expected the addition of YbF_3 to improve the CS of the GIC significantly for at least three reasons. First, YbF_3 can be expected to act similarly to AlF_3 in glass ionomer systems because of its similar chemical and physical structure. Second, the release of a trivalent ion into the glass ionomer matrix may speed the cross-linking, improve its insolubility, and further its reaction extent and strength. Third, the reactivity of the YbF_3 with the glass ionomer matrix indicated that the ytterbium ions were being incorporated into the matrix and accelerating the setting reaction [58].

5.8 Conclusions

More research is needed to investigate other mechanical properties of the nanoionomer, its biochemical stability in the oral environment, fluoride release, and so on. Ultimately, well-designed randomized clinical trials will reveal the longevity and anticariogenic effect of this material in clinical conditions. However, nanofilled glass ionomers have acquired a prominent place among the restorative materials employed in direct techniques. Their considerable chemical linkage, smooth surface, and esthetic possibilities give rise to a variety of clinical applications, which continue to grow as a result of the great versatility of the presentations offered; also, these materials conserve the tooth structure better because they are retained by adhesive methods rather than depending on cavity design. However, they are technique sensitive, and hence there is a need to control certain aspects such as correct indication, good isolation, and choice of the right material for each situation. Further research in the area related to the biochemical stability of glass ionomer materials, supported by both industry and clinicians, is required.

References

[1] T.M. Roberson, H. Heymann, E.J. Swift, Sturdevant's Art and Science of Operative Dentistry, fourth ed., Mosby, NY, USA, 2002.

[2] N. Moszner, S. Klapdohr, Nanotechnology for dental composites, Int. J. Nanotechnol. 1 (2004) 130−156.

[3] R.G. Craig, J.M. Power, Restorative Dental Materials, eleventh ed., Mosby, NY, USA, 2002.

[4] J.K. Anusavice, Phillip's Science of Dental Materials, eleventh ed., Elsevier Science, NY, USA, 2003.

[5] M.C. Raadsheer, T.M. van Eijden, F.C. van Ginkel, B. Prahl-Andersen, Contribution of jaw muscle size and craniofacial morphology to human bite force magnitude, J. Dent. Res. 78 (1999) 31−42.

[6] M. Bernardo, H. Luis, M.D. Martin, B.G. Leroux, T. Rue, J. Leitao, et al., J. Am. Dent. Assoc. 138 (2007) 775−783.

[7] G.L. Adabo, C.A. dos Santos Cruz, R.G. Fonseca, L.G. Vaz, The volumetric fraction of inorganic particles and the flexural strength of composites for posterior teeth, J. Dent. 31 (2003) 353−359.

[8] N.D. Alberola, G. Merle, K. Benzarti, Unidirectional fibre-reinforced polymers: analytical morphology approach and mechanical modelling based on the percolation concept, Polymer 40 (1999) 315−328.

[9] K.S. Anseth, Photopolymerization of multifunctional monomers: reaction mechanisms and polymer structural evolution, Dissertation, University of Colorado at Boulder, Boulder, CO, 1994.

[10] C. Friend, Smart materials: the emerging technology, Mater. World 4 (1996) 16−18.

[11] S.B. Mitra, D. Wu, B.N. Holmes, An application of nanotechnology in advanced dental materials, J. Am. Dent. Assoc. 134 (2003) 1382.

[12] M. Muselmann, Direct applications of a nanocomposite resin system: Part 1—The evolution of contemporary composite materials, Compos. Technol. 1 (2003) 24.

[13] R.W. Arcis, A.M. Macipe, M. Toledano, E. Osorio, R.R. Clemente, J. Murtra, et al., Mechanical properties of visible light-cured resins reinforced with hydroxyapatite for dental restoration, Dent. Mater. 18 (2002) 49.

[14] C.P. Turssi, J.L. Ferracane, K. Vogel, Filler feature and their effects on wear and degree of conversion of particulate dental resin composite, Biomaterials 26 (2005) 4932.

[15] E.G. Mota, H.M.S. Oshima, L.H. Burnett Jr., L.A.G. Pires, R.S. Rosa, Evaluation of diametral tensile strength and Knoop microhardness of five nanofilled composites in dentin and enamel shades, Stomatol. Balt. Dent. Maxillofac. J. 8 (2006) 67−69.

[16] Y.M. Lai, J.C. Kuo, M.C. Huang, M. Chen, On the PEEK composites reinforced by surface modified nano-silica, Mater. Sci. Eng. A 458 (2007) 158−169.

[17] M. Sumita, T. Shizuma, K. Miyasaka, K. Ishikawa, Effect of reducible properties of temperature, rate of strain, and filler content on the tensile yield stress of nylon 6 composites filled with ultrafine particles, J. Macromol. Sci. B Phys. 22 (1985) 601−618.

[18] M.C. Kuo, C.M. Tsai, J.C. Huang, M. Chen, PEEK composites reinforced by nano-sized SiO_2 and Al_2O_3 particulates, Mater. Chem. Phys. 90 (2005) 185−195.

[19] J. Zhao, D. Xie, Effect of nanoparticles on wear resistance and surface hardness of a dental glass-ionomer cement, J. Compos. Mater. 43 (2009) 2739−2752.

[20] A.D. Wilson, B.E. Kent, Formation of glass-ionomer cement based on an ion-leachable glass and poly acrylic acid, J. Appl. Chem. Biotechnol. 21 (1971) 313.

[21] J.W. McLean, O. Gasser, Glass-cermet cements, Quint. Int. 16 (1985) 333−343.

[22] A.D. Wilson, J.W. McLean, Glass-Ionomer Cement, second ed., Quintessence Publishing Company, Chicago, 1988.

[23] C.L. Davidson, Advances in Glass-Ionomer Cements, Quintessence Publishing Company, Chicago, 1993.

[24] A.D. Wilson, J.W. Nicholson, Acid−Base Cements: Their Biomedical and Industrial Applications, Cambridge University Press, New York, NY, 1993.
[25] A.D. Wilson, B.E. Kent, D. Clinton, R.P. Miller, The formation and microstructure of dental silicate cements, J. Mater. Sci. 7 (1972) 220−238.
[26] A. Moshaverinia, N. Roohpour, W.W.L. Chee, S.R. Schricker, A review of powder modifications in conventional glass-ionomer dental cements, J. Mater. Chem. 21 (2011) 1319−1328.
[27] D.C. Smith, Development of glass-ionomer cements systems, Biomaterials 19 (1998) 467−478.
[28] Y.W. Gu, A.U.J. Yap, P. Cheang, Y.L. Koh, K.A. Khor, Development of zirconia-glass ionomer cement composites, J. Non-Crys. Sol. 351 (2005) 508−514.
[29] N. Monmaturapoj, W. Soodsawang, S. Tanodekaew, Enhancement effect of pre-reacted glass on strength of glass-ionomer cement, Dent. Mater. J. 31 (2012) 125−130.
[30] R. Vehrin, W.R. Foss, D. Lechuga-Ballesteros, Particle formation in spray drying, Aerosol. Sci. 38 (2007) 728−746.
[31] L.F.R. Garcia, F.C.P. Pires-De-Souza, J.M. Teofilo, A. Cestari, P.S. Calefi, K.J. Ciuffi, et al., Synthesis and biocompatibility of an experimental glass ionomer cement prepared by a non-hydrolytic sol−gel method, Braz. Dent. J. 21 (2010) 499−507.
[32] B.M. Culbertson, New polymeric materials for use in glass-ionomer cement, J. Dent. 34 (2006) 556−565.
[33] B.E. Kent, B.G. Lewis, A.D. Wilson, Glass ionomer cement formulation, J. Dent. Res. 58 (1979) 1607−1619.
[34] J.W. McLean, The clinical use of glass ionomer cement—future and current development, Biomaterials 7 (1991) 283−288.
[35] R. Guggenberger, R. May, K.P. Stefan, New trends in glass-ionomer chemistry, Biomaterials 19 (1998) 479−483.
[36] D. Xie, W.A. Brantley, B.M. Culbertson, G. Wang, D. Mater, Mechanical properties and microstructure of glass-ionomer cement, J. Biomater. 16 (2000) 129−138.
[37] R.G. Hill, A.D. Wilson, C.P. Warrens, The influence of polyacrylic acid molecular weight on the fracture of toughness of glass-ionomer cements, J. Mater. Sci 24 (1989) 363−371.
[38] L.C. Pereira, M.C. Nunes, R.G. Dibb, J.M. Powers, J.F. Roulet, M.F. Navarro, Mechanical properties and bond strength of glass-ionomer cements, J Adhes. Dent. 4 (2002) 73−80.
[39] R.A. Hickel, M. Folwaczny, Various forms of glass ionomers and compomers, Oper. Dent. (Suppl. 6) (2001) 177−190.
[40] J.A. Williams, R.W. Billington, G.J. Pearso, The comparative strengths of commercial glass-ionomer cements with and without metal additions, Br. Dent. J. 172 (1992) 279−282.
[41] J.H. Berg, The continuum of restorative materials in pediatric dentistry—a review for the clinician, Pediat. Dent. 20 (1998) 93−100.
[42] R. Wadenya, J. Smith, F. Mante, Microleakage of nano-particle-filled resin-modified glass ionomer using atraumatic restorative technique in primary molars, N. Y. State Dent. J. (2010) 36−39.
[43] O. Bala, H.D. Arisu, I. Yikilgan, S. Arslan, A. Gullu, Evaluation of surface roughness and hardness of different glass ionomer cements, Eur. J. Dent. 6 (2012) 79−86.
[44] M.A.B. Paschoal, C.V. Gurgel, D. Rios, A.C. Magalhaes, M.A.R. Buzalaf, M.A.A.M. Machado, Fluoride release profile of a nanofilled resin-modified glass ionomer cement, Braz. Dent. J. 22 (2011) 275−279.
[45] H.H.K. Xu, M.D. Weir, L. Sun, J.L. Moreau, S. Takagi, L.C. Chow, et al., Strong nanocomposites with Ca, PO4, and F release for caries inhibition, J. Dent. Res. 89 (2010) 19−28.
[46] D.P. Raggio, E.C. Branco, A.F.B. Calvo, C.C. Bonifacio, J.C.P. Imparato, L.B. Camargo, Knoop hardness of resin-modified glass-ionomer cements, Int. J. Dent. 8 (2009) 119−123.

[47] S.A.M. Abd El Halim, Effects of light curing and remineralization on micro hardness of nano esthetic restorative materials, J. Am. Sci. 8 (2012) 147−151.
[48] E. Coutinho, M.V. Cardoso, J. De Munck, A.A. Neves, K.L. Van Landuyt, A. Poitevin, et al., Bonding effectiveness and interfacial characterization of a nano-filled resin-modified glass-ionomer, Dent. Mater. 2 (5) (2009) 1347−1357.
[49] Y. Korkmaz, E. Ozel, N. Attar, C.O. Bicer, Influence of different conditioning methods on the shear bond strength of novel light-curing nano-ionomer restorative to enamel and dentin, Lasers Med. Sci. 25 (2010) 861−866.
[50] T. Uysal, A. Yagci, B. Uysal, G. Akdogan, Are nano-composites and nano-ionomers suitable for orthodontic bracket bonding?, Eur. J. Orthod. 32 (2010) 78−82.
[51] I.R. Reynolds, A review of direct orthodontic bonding, Br. J. Orthod. 2 (1975) 171−178.
[52] E. Ozel, Y. Korkmaz, N. Attar, C.O. Bicer, E. Firatli, Leakage pathway of different nano-restorative materials in class V cavities prepared by Er:YAG laser and bur preparation, Photomed. Laser Surg. 27 (2009) 783−789.
[53] M. Basso, Teeth restoration using a high viscosity glass ionomer cement: the Equia® system, J. Minim. Interv. Dent. 4 (2011) 74−76.
[54] A. Moshaverinia, S. Ansari, Z. Movasaghi, R.W. Billington, J.A. Darr, I.U. Rehman, Modification of conventional glass-ionomer cements with *N*-vinylpyrrolidone containing polyacids, nano-hydroxy and fluoroapatite to improve mechanical properties, Dent. Mater. 2 (4) (2008) 1381−1390.
[55] J.-J. Lee, Y.-K. Lee, B.-J. Choi, J.-H. Lee, H.-J. Choi, H.-K. Son, et al., Physical properties of resin-reinforced glass ionomer cement modified with micro and nano hydroxyapatite, J. Nanosci. Nanotechnol. 10 (2010) 5270−5276.
[56] A. Moshaverinia, S. Ansari, M. Moshaverinia, N. Roohpour, J.A. Darr, I. Rehman, Effects of incorporation of hydroxyapatite and fluoroapatite nanobioceramics into conventional ionomer cements (GIC), Acta Biomater. 4 (2008) 432−440.
[57] M.J. Bertolini, M.A. Zaghete, R. Gimenes, G.C. Padovani, Determination of the properties of an experimental glass polyalkenoate cement prepared from niobium silicate powder containing fluoride, Dent. Mater. 2 (4) (2008) 124−128.
[58] L.H. Prentice, M.J. Tyas, M.F. Burrow, The effect of ytterbium fluoride and barium sulphate nanoparticles on the reactivity and strength of a glass-ionomer cement, Dent. Mater. 22 (2006) 746−751.

CHAPTER

6 Nanostructured Dental Composites and Adhesives with Antibacterial and Remineralizing Capabilities for Caries Inhibition

Hockin H.K. Xu[a], Lei Cheng[b], Ke Zhang[c], Mary Anne S. Melo[d], Michael D. Weir[a], Joseph M. Antonucci[e], Nancy J. Lin[e], Sheng Lin-Gibson[e], Laurence C. Chow[f] and Xuedong Zhou[b]

[a]*Department of Endodontics, Prosthodontics and Operative Dentistry, University of Maryland Dental School, Baltimore, MD, USA,*

[b]*State Key Laboratory of Oral Diseases, West China School of Stomatology, Sichuan University, Chengdu, China,*

[c]*Department of Orthodontics, School of Stomatology, Capital Medical University, Beijing, China,*

[d]*Faculty of Pharmacy, Dentistry and Nursing, Federal University of Ceara, Fortaleza, CE, Brazil,*

[e]*Polymers Division, National Institute of Standards and Technology, Gaithersburg, MD, USA,*

[f]*Paffenbarger Research Center, American Dental Association Foundation, Gaithersburg, MD, USA.*

CHAPTER OUTLINE

6.1 Introduction

Dental composites are increasingly popular due to their esthetics and direct-filling capabilities [1,2]. Extensive studies have been performed to improve the fillers, resins, and polymerization properties [3–11]. Nonetheless, composites accumulated more biofilms/plaques than

Nanobiomaterials in Clinical Dentistry.

other restoratives in vivo [12,13]. Plaques contribute to secondary caries, which is the main reason for restoration failure [14]. Replacing the failed restorations consumes 50−70% of the dentist's time. Replacement dentistry costs $5 billion annually in the United States [15]. To combat caries, antibacterial resins and composites containing quaternary ammonium salts (QAS) were developed [16−21]. Resins containing 12-methacryloyloxydodecylpyridinium bromide (MDPB) significantly reduced the bacterial growth [22,23]. Other novel antibacterial resins were synthesized by employing antibacterial agents such as methacryloxylethyl cetyl dimethylammonium chloride (DMAE-CB) and cetylpyridinium chloride, among other compositions [18−21,24−27].

Besides antibacterial restoratives, calcium phosphate (CaP) composites represent another promising approach in inhibiting caries. CaP composites can release supersaturating levels of calcium (Ca) and phosphate (P) ions to remineralize tooth lesions [28−30]. Recently, novel CaP and calcium fluoride nanoparticles were incorporated into composites [31,32]. Nanoparticles of amorphous calcium phosphate (NACP) were synthesized via a spray-drying technique [33]. The NACP nanocomposite released Ca and P ions similar to those of traditional CaP composites, while possessing much higher mechanical properties [32]. The NACP nanocomposite was "smart" and greatly increased the Ca and P ion release at acidic pH, when these ions were most needed to combat caries [33]. When immersed in a lactic acid solution at pH 4, the NACP nanocomposite quickly neutralized the acid and increased the pH to a safe level of 6, while the pH remained at 4 for commercial control restoratives [34]. However, little has been reported on combining the best of both worlds: CaP ion release and remineralization, and antibacterial activity of QAS-containing resins.

Besides composites, it is also important to develop novel antibacterial and remineralizing adhesives because composite restorations are bonded to tooth structure via adhesives [35−39]. Extensive studies have been performed to improve, characterize, and understand enamel and dentin bonding [40−44]. It is desirable for the adhesive to be antibacterial to inhibit recurrent caries at the tooth−composite margins [16,25,26]. Residual bacteria could exist in the prepared tooth cavity, and microleakage could allow bacteria to invade the tooth-restoration interface. Adhesives that are antibacterial in the cured state could help inhibit the growth of residual and invading bacteria [23,45]. Indeed, MDPB-containing adhesives markedly inhibited the growth of *Streptococcus mutans* (*S. mutans*) [16,45]. Another study developed an antibacterial adhesive containing DMAE-CB [25]. Besides the adhesive resin, it is also beneficial for the primer to be antibacterial because it directly contacts the tooth structure [46−48]. A primer containing MDPB achieved significant antibacterial effects [46,47]. Another primer containing chlorhexidine showed an effective antimicrobial activity [48]. There have been only a few reports on antibacterial adhesives and primers. To date, there has been no report on antibacterial and remineralizing adhesives containing CaP nanoparticles, except recent studies in our group which are described in this chapter.

This chapter describes recent studies on dental nanocomposites containing novel antibacterial agents as well as CaP nanoparticles for ion release and remineralization. Dental bonding agents with a combination of antibacterial and remineralizing capabilities are also presented, and the results are promising for caries-inhibition restorations.

6.2 Development of antibacterial nanocomposite with CaP nanoparticles

A spray-drying technique described previously [49] was used to make nanoparticles of ACP (referred to as NACP). Calcium carbonate ($CaCO_3$; Fisher, Fair Lawn, NJ) and dicalcium phosphate anhydrous ($CaHPO_4$; Baker, Phillipsburg, NJ) were dissolved into an acetic acid solution to obtain final Ca and P ionic concentrations of 8 and 5.333 mmol/L, respectively [33]. This resulted in a Ca/P molar ratio of 1.5, the same as that for ACP ($Ca_3[PO_4]_2$). This solution was sprayed into a heated chamber, and an electrostatic precipitator (AirQuality, Minneapolis, MN) was used to collect the dried particles. Figure 6.1A and 6.1B shows transmission electron microscopy (TEM)

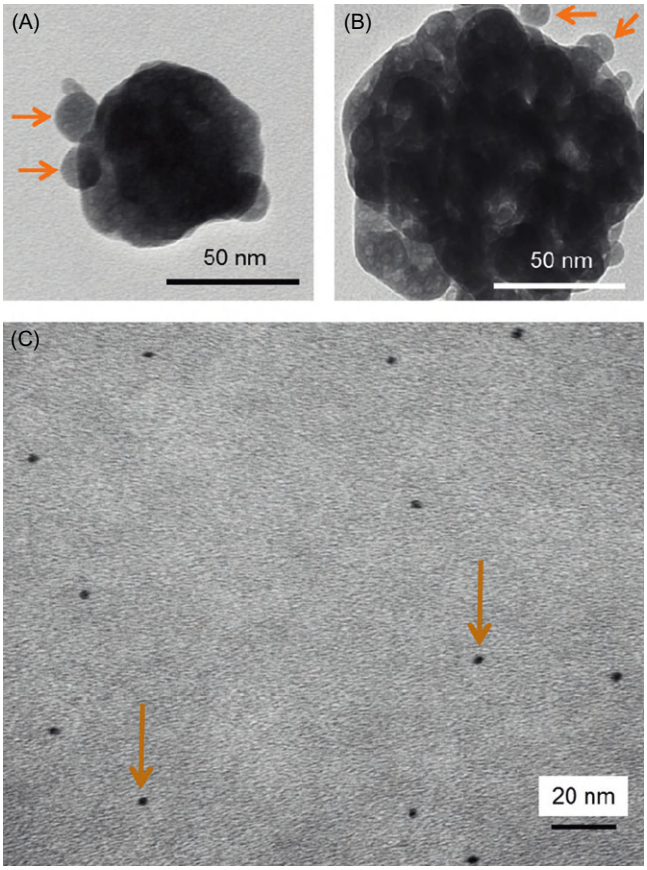

FIGURE 6.1

TEM micrograph of the spray-dried NACP: (A) small NACP and (B) NACP cluster. (C) TEM micrographs of NAg in the resin matrix. The particle size was measured (mean ± sd; $n = 100$) to be 2.7 ± 0.6 nm. Arrows indicate the silver nanoparticles, which were well dispersed in the resin with minimal appearance of nanoparticle aggregates.

Adapted from Ref. [21] and [50] with permission.

images of NACP: (A) Example of small NACP, (B) example of NACP clusters. In (A), arrows indicate individual ACP particles that overlapped a larger ACP particle. In (B), arrows indicate individual ACP particles and a cluster. The cluster appeared to contain numerous small particles, which likely had stuck to form the cluster in the spray-drying chamber before they were completely dried. Measurement of 100 random particles yielded an average size of 37 nm for individual NACP, and an average size of 225 nm for NACP clusters [50].

Two types of co-fillers were used for reinforcement: barium boroaluminosilicate glass particles of a mean diameter of 1.4 μm (Caulk/Dentsply, Milford, DE) and nanosized silica glass (Aerosil-OX50, Degussa, Ridgefield, NJ) with a mean diameter of 40 nm. Each glass was silanized with 4% 3-methacryloxypropyltrimethoxysilane and 2% *n*-propylamine (all by mass, unless otherwise noted). A resin of bisphenol glycerolate dimethacrylate (BisGMA) and triethylene glycol dimethacrylate (TEGDMA) at 1:1 mass ratio was rendered light-curable with 0.2% camphorquinone and 0.8% ethyl 4-*N*,*N*-dimethylaminobenzoate (referred to as BisGMA−TEGDMA resin). The NACP mass fraction in the resin was 30%, and the glass mass fraction was 35%, following a previous study [33]. The resin filled with 30% NACP without any glass fillers is referred to as "resin with 30% NACP without glass." The composite filled with 30% NACP + 35% nanosilica is referred to as "NACP + nano silica composite." The composite filled with 30% NACP + 35% barium boroaluminosilicate glass is referred to as "NACP composite."

The synthesis of bis(2-methacryloyloxyethyl) dimethylammonium bromide, termed ionic dimethacrylate-1 (IDMA-1), was described recently [20]. IDMA-1 was selected as the quaternary ammonium dimethacrylate (QADM) to incorporate into the nanocomposites in the present study. Its synthesis was carried out using a modified Menschutkin reaction, where a tertiary amine group was reacted with an organo-halide. A benefit of this reaction is that the reaction products are generated at virtually quantitative amounts and require minimal purification [20,21]. Briefly, 10 mmol of 2-(*N*,*N*-dimethylamino)ethyl methacrylate (DMAEMA; Sigma-Aldrich, St. Louis, MO) and 10 mmol of 2-bromoethyl methacrylate (BEMA; Monomer-Polymer and Dajec Labs, Trevose, PA) were combined with 3 g of ethanol in a 20 mL scintillation vial. A magnetic stir bar was added, and the vial was stirred at 60°C for 24 h. The solvent was removed via evaporation, forming a clear, colorless, and viscous liquid. The QADM thus obtained was then mixed with the photo-activated BisGMA−TEGDMA resin at a QADM mass fraction of 20%. This resin is referred to as the BisGMA−TEGDMA−QADM resin. A previous study showed that 20% QADM greatly reduced bacterial growth on the polymer surfaces [20]. The BisGMA−TEGDMA−QADM resin was then filled with 30% NACP and 35% barium boroaluminosilicate glass, and this composite is referred to as "NACP + QADM." Hence, the QADM mass fraction in the final composite was $20\% \times 35\% = 7\%$.

Silver 2-ethylhexanoate powder (Strem Chemicals, New Buryport, MA) at 0.08 g was dissolved into 1 g of 2-(tert-butylamino)ethyl methacrylate (TBAEMA; Sigma) by stirring, and then 1% of this solution was added to the resin. The mass fraction of Ag salt in the resin was 0.08%, according to a recent study [51]. TBAEMA improves the solubility by forming Ag−N coordination bonds with Ag ions, thereby facilitating the Ag salt to dissolve in the resin solution. TBAEMA was selected since it contains reactive methacrylate groups and can be chemically incorporated into the polymer network upon photopolymerization [51]. The nanoparticles of silver (NAg) had particle sizes of 2.7 ± 0.6 nm, as shown in Figure 6.1C. The particles appeared to be well dispersed in the resin, without noticeable clustered particles or agglomerates [21].

To fabricate the "NACP + NAg" composite, the Ag−TBAEMA was mixed with BisGMA−TEGDMA, and then 30% NACP and 35% barium boroaluminosilicate glass were added to the resin. Since the resin mass fraction was 35% in the composite, the 0.08% of Ag in the resin yielded 0.028% of Ag mass fraction in the composite. To fabricate the "NACP + QADM + NAg" composite, the Ag−TBAEMA was mixed with the BisGMA−TEGDMA−QADM resin. NACP and glass filler levels were selected to yield a cohesive paste that was readily mixed and not dry. Each paste was placed into rectangular molds of $2 \times 2 \times 25$ mm for mechanical testing, and disk molds of 9 mm in diameter and 2 mm in thickness for biofilm experiments. The specimens were photo-polymerized (Triad 2000, Dentsply, York, PA) for 1 min on each side.

In addition, a commercial composite with glass nanoparticles of 40−200 nm and a low level of fluoride (F) release was tested (Heliomolar, Ivoclar, ON, Canada) (referred to as CompositeF). The fillers were silica and ytterbium-trifluoride with a filler level of 66.7%. Heliomolar is indicated for Class I and Class II restorations in the posterior region, Class III and V restorations, and pit and fissure sealing. Another commercial composite, Renamel (Cosmedent, Chicago, IL), served as a non-releasing control (referred to as CompositeNoF). It consisted of nanofillers of 20−40 nm with 60% (by mass) fillers in a multifunctional methacrylate ester resin. Renamel is indicated for Class III, IV, and V restorations. The control specimens were also photocured in the same manner as described above.

Figure 6.2 shows the composite mechanical properties: (A) flexural strength and (B) elastic modulus (mean ± sd; $n = 6$). In (A), the resin with 30% NACP without glass had a slightly lower flexural strength. Bars with dissimilar letters indicate values that are significantly different ($P < 0.05$). The NACP composite had a strength of 62 ± 8 MPa, not significantly different from the 57 ± 12 MPa of CompositeF, and 56 ± 9 MPa of CompositeNoF ($P > 0.1$). Adding QADM, NAg, or QADM + NAg yielded strengths of 53 ± 7, 67 ± 6, and 54 ± 12 MPa, respectively ($P > 0.1$) [21].

S. mutans bacteria were obtained commercially (ATCC 700610, UA159, American Type Culture, Manassas, VA), and the use was approved by University of Maryland Baltimore IRB. The growth medium consisted of brain heart infusion (BHI) broth (BD, Franklin Lakes, NJ) supplemented with 0.2% sucrose. Fifteen microliter of stock bacteria was added to 15 mL of growth medium and incubated at 37°C with 5% CO_2 for 16 h, during which the *S. mutans* were suspended in the growth medium. The inoculation medium was formed by diluting this *S. mutans* culture 10-fold in growth medium [21].

Colony-forming unit (CFU) counts were measured. Disks with biofilms were transferred into tubes with 2 mL cysteine peptone water. The biofilms were harvested by sonicating (3510 R-MTH, Branson, Danbury, CT) for 3 min and then vortexing at maximum speed for 20 s using a vortex mixer (Fisher, Pittsburgh, PA). The bacterial suspensions were serially diluted, spread onto BHI agar plates, and incubated for 3 days at 5% CO_2 and 37°C. At 1 day and 3 days, the numbers of colonies were counted to calculate total CFU on each disk. The results are shown in Figure 6.3. At 1 day, CFU counts were 27 million per disk for CompositeNoF and 21 million for NACP composite. The CFU counts were greatly reduced to 12.5 million on NACP + QADM composite, 3.2 million on NACP + NAg composite, and 1.4 million on NACP + QADM + NAg composite ($P < 0.05$). The ranking of CFU at 1 day is maintained at 3 days, with the NACP + QADM + NAg composite having the least CFU counts, which were an order of magnitude less than that of CompositeNoF.

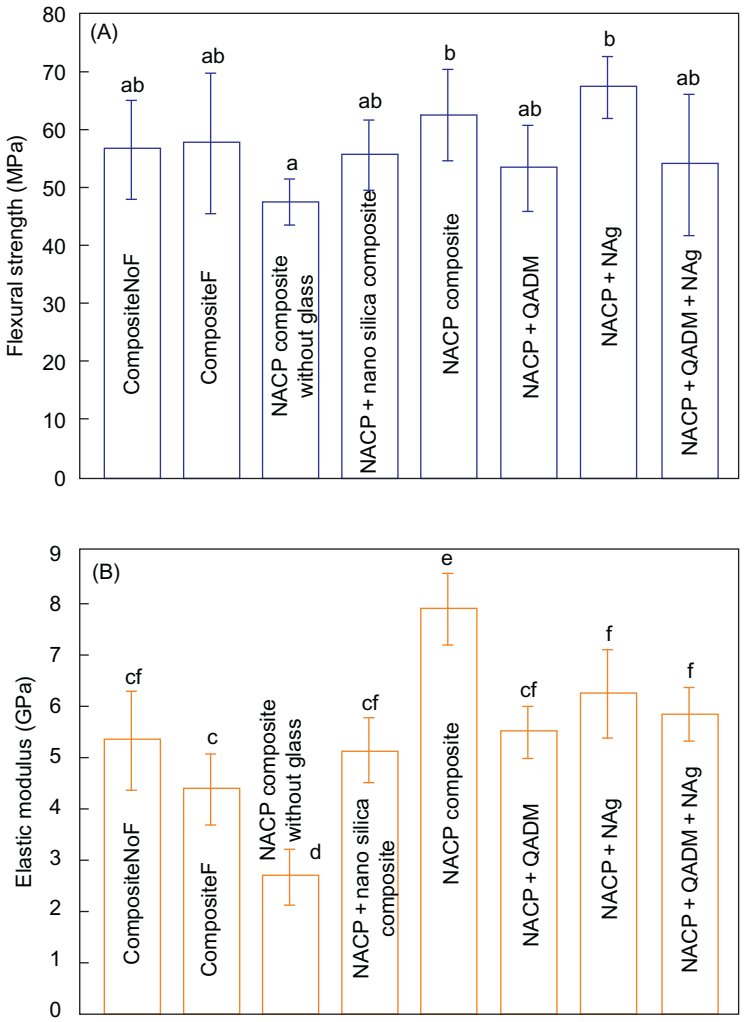

FIGURE 6.2

Mechanical properties. (A) Flexural strength and (B) elastic modulus for CompositeNoF, CompositeF, NACP composite, NACP + QADM composite, NACP + NAg composite, and NACP + QADM + NAg composite. Each value is the mean of six measurements with the error bar indicating one standard deviation (mean ± sd; $n = 6$). Values with dissimilar letters are significantly different from each other ($p < 0.05$).

Adapted from Ref. [21] with permission.

6.3 Durability of antibacterial nanocomposite in water-aging

Composite specimens were immersed in distilled water at 37°C for 1, 30, 90, and 180 days. The water-aged specimens were then inoculated with *S. mutans* (ATCC 700610). Representative live/dead staining images (Figure 6.4) showed that CompositeNoF was completely covered by dense live biofilms. Live bacteria were stained green, and dead bacteria were stained red. In some areas, the live

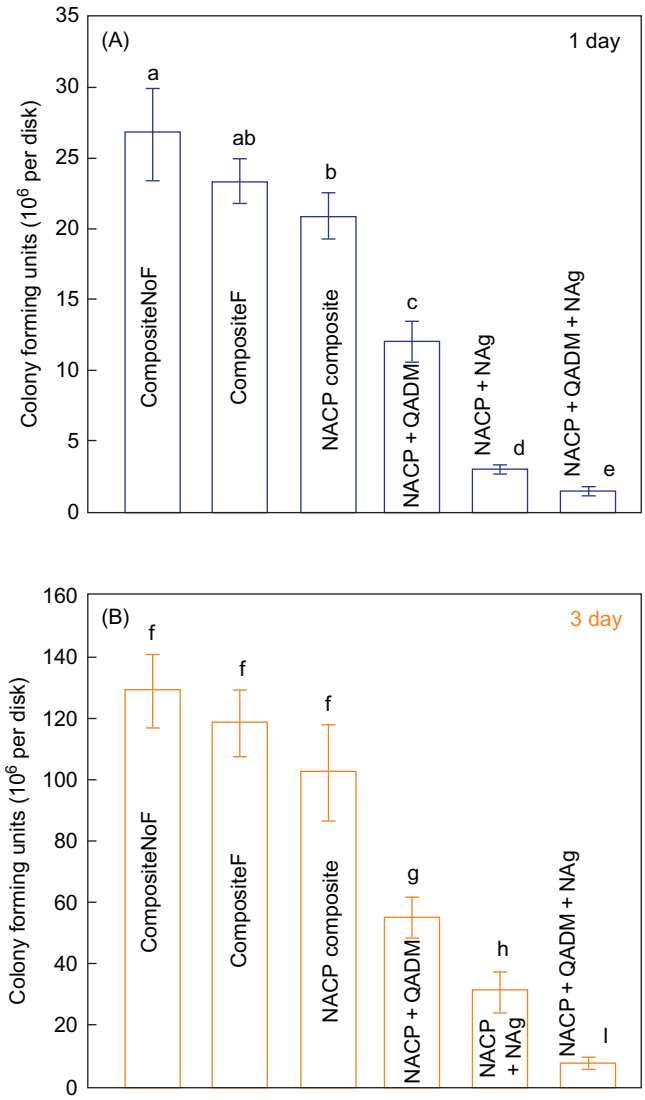

FIGURE 6.3

CFU counts of *S. mutans* biofilms adherent on the composites at (A) 1 day and (B) 3 days, with the *y*-axis units being 10^6 bacteria per composite disk. In each plot, the values (mean ± sd; $n = 6$) indicated with dissimilar letters are significantly different from each other ($P < 0.05$). The NACP + QADM + NAg composite had the least CFU which was an order of magnitude less than that of CompositeNoF.

Adapted from Ref. [21] with permission.

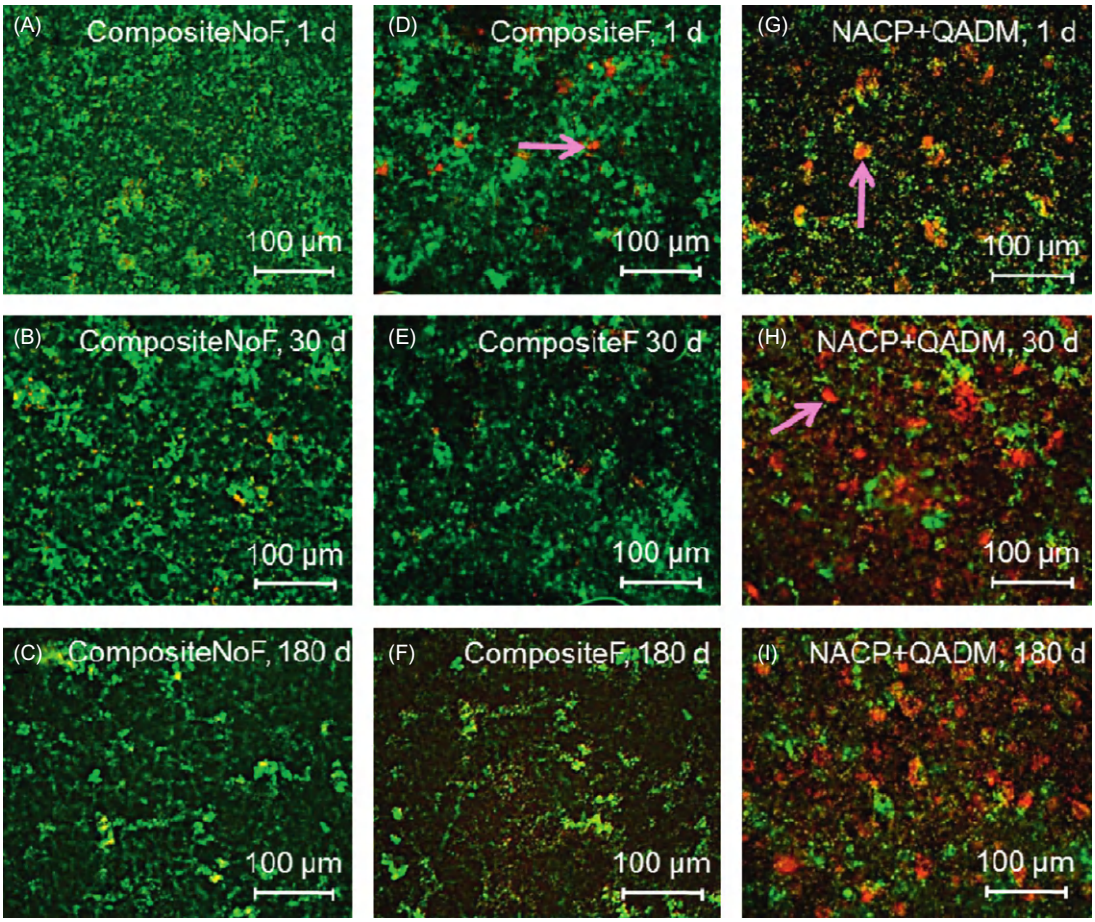

FIGURE 6.4

Live/dead staining of 3-days biofilms on composites. Live bacteria were stained green and dead bacteria were stained red. Live and dead bacteria in close proximity showed yellow/orange colors. The images shown in (A–I) are representative of each group. CompositeNoF was covered by a dense biofilm with green staining. CompositeF had some compromised bacteria. NACP + QADM had much more dead bacteria staining than the controls. The area fraction of live bacteria staining is plotted (mean ± sd; $n = 6$). There was little difference in biofilm viability versus aging time, indicating that the antibacterial activity of NACP–QADM nanocomposite was not lost in water immersion. (For interpretation of the references to color in this figure legend, the reader is referred to the web version of this book.)

Adapted from Ref. [52] with permission.

and compromised bacteria were closely associated, and the red color was mingled with green to yield yellow/orange colors. Examples of these staining colors are indicated by the arrows. Compared to CompositeNoF and CompositeF, NACP + QADM had much more red/yellow/orange staining.

Representative scanning electron microscopy (SEM) images of the biofilm structures on composites surfaces are shown in Figure 6.5. In (A) and (B), the CompositeNoF and CompositeF had

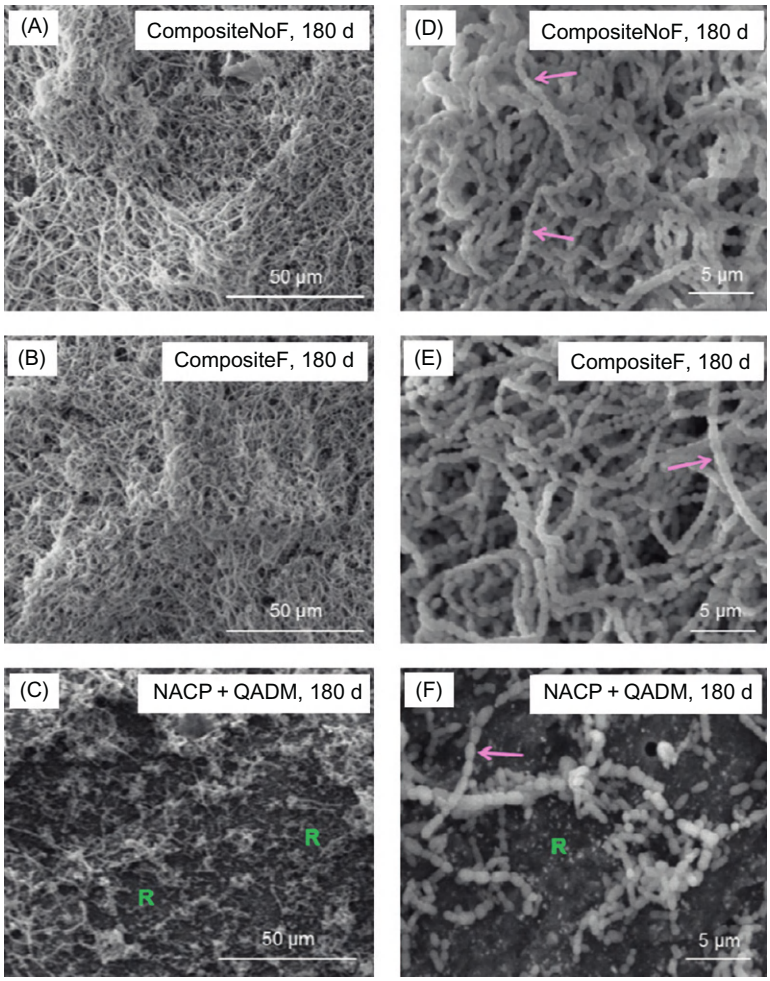

FIGURE 6.5

SEM micrographs of biofilms. (A–C) Lower and (D–F) higher magnification. Each type of composite, aged for 1–180 days, had a similar biofilm appearance. The images shown here are for composites aged for 180 days, to demonstrate the long-term antibacterial activity of NACP–QADM nanocomposite. CompositeNoF and CompositeF had dense biofilms. NACP–QADM had much less biofilm coverage. In (C) and (F), "R" indicates the resin composite surface not covered by biofilms. Arrows indicate the chain structure of *S. mutans* biofilms. The chains are much shorter on NACP–QADM in (F), along with individual cells that did not form a chain. Each bacterial cell had the shape of a short rod with a length of about 1 μm (arrow in F).

Adapted from Ref. [52] with permission.

dense biofilms. In (C), NACP−QADM had less biofilms, where "R" indicates resin composite not covered by biofilms. Higher magnification (D, E) revealed that the *S. mutans* grew in chains (arrows). The chains twisted in three-dimensions and were long or continuous in the biofilm architecture. The chains were much shorter on NACP−QADM in (F), with each chain containing 3−10 cells.

For MTT assay, disks were placed in 24-well plates, inoculated with 1.5 mL inoculation medium, and cultured for 3 days. Each disk was transferred to new 24-well plates for the MTT (3-(4,5-dimethylthiazol-2-yl)-2,5-diphenyltetrazolium bromide) assay [20,21]. MTT is a colorimetric assay that measures the enzymatic reduction of MTT, a yellow tetrazole, to formazan. One milliliter of MTT was added to each well and incubated for 1 h. Disks were transferred to new 24-well plates, and 1 mL of dimethyl sulfoxide (DMSO) was added to solubilize the formazan crystals. The DMSO solution from each well was used and the absorbance at 540 nm was measured via a microplate reader (SpectraMax M5, Molecular Devices, Sunnyvale, CA).

For lactic acid measurement, disks with 3-days biofilms were placed in new 24-well plates, and 1.5 mL of buffered-peptone water (BPW) supplemented with 0.2% sucrose was added. They were incubated for 3 h to allow the biofilms to produce acid. Then the BPW solutions were stored for lactate analysis. The microplate reader was used to measure the absorbance at 340 nm, and standard curves were prepared using a lactic acid standard (Supelco, Bellefonte, PA) [21].

Figure 6.6 plots the results for MTT metabolic activity, CFU, and lactic acid production of biofilms. For each property, the values did not vary significantly over aging time ($P > 0.1$). In (A), NACP−QADM yielded much lower MTT than commercial composites ($P < 0.05$). NACP−QADM greatly reduced the CFU (B) and lactic acid (C), compared to commercial composites ($P < 0.05$). Therefore, the novel NACP−QADM nanocomposite substantially decreased the biofilm growth and lactic acid production, and its antibacterial properties were maintained during long-term water-aging [52].

6.4 Antibacterial dentin primer

Scotchbond multi-purpose (referred as "SBMP") (3M, St. Paul, MN) was used as the parent bonding agent to test the effect of QDMA and NAg incorporation. The purpose was to develop a model system, and the novel method of QADM and NAg incorporation can then be applied to other bonding agents. SBMP etchant contained 35% phosphoric acid. SBMP primer contained 35−45% 2-hydroxyethylmethacrylate (HEMA), 10−20% copolymer of acrylic/itaconic acids, and 40−50% water. SBMP adhesive contained 60−70% BisGMA and 30−40% HEMA. QADM and NAg were incorporated into SBMP primer. SBMP etchant and adhesive were not modified.

Bis(2-methacryloyloxyethyl) dimethylammonium bromide (QADM) was recently synthesized [20,21]. Briefly, 10 mmol of 2-(*N,N*-dimethylamino)ethyl methacrylate (Sigma-Aldrich) and 10 mmol of 2-BEMA (Monomer-Polymer Labs, Trevose, PA) were combined in ethanol and stirred at 60°C for 24 h. The solvent was then evaporated, yielding the QADM. QADM was mixed with the SBMP primer at QADM/(primer + QADM) = 10 wt%. This was selected because preliminary study showed that 10% of QADM in the primer provided antibacterial activity without compromising the dentin bond strength, while 20% QADM in primer decreased the bond strength.

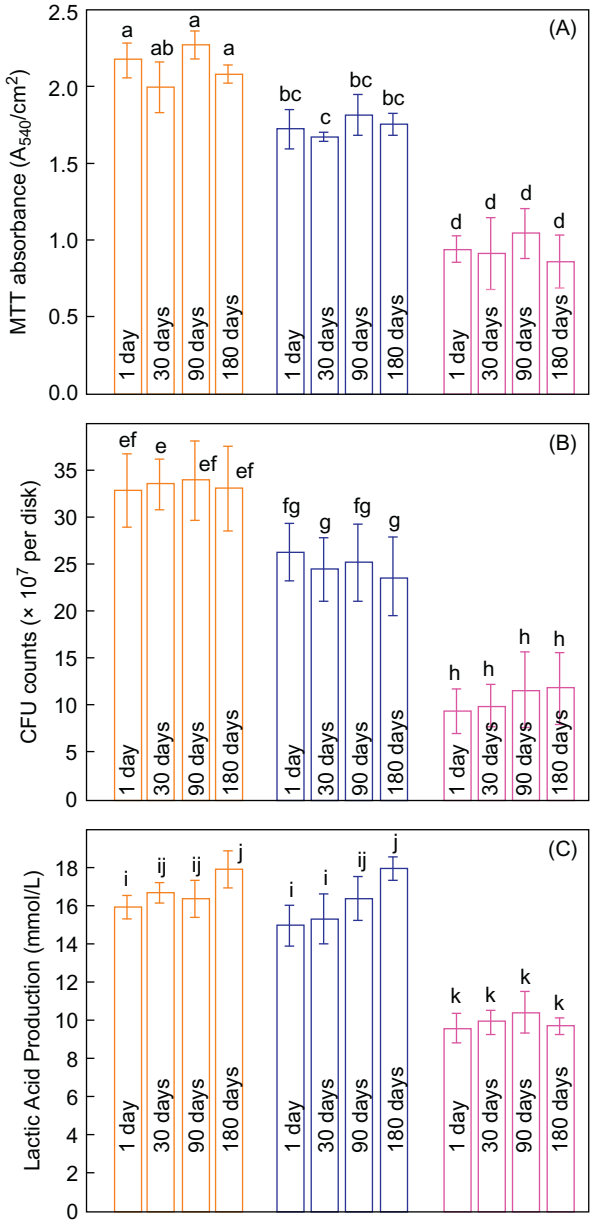

FIGURE 6.6

Biofilm viability, growth, and acid production. (A) MTT metabolic activity, (B) CFU counts, and (C) lactic acid production of 3-days biofilms on the composites water-aged for 1−180 days. Each value is mean ± sd ($n = 6$). In each plot, values with dissimilar letters are significantly different ($P < 0.05$). For the MTT assay, a higher absorbance indicates a higher formazan concentration, which in turn indicates a higher metabolic activity in the biofilm. NACP−QADM had biofilm metabolic activity and lactic acid that were about half of those on commercial composites, and CFU about one-third of those on commercial composites ($P < 0.05$). Aging for 1−180 days did not reduce the antibacterial potency of the NACP−QADM nanocomposite ($P > 0.1$).

Adapted from Ref. [52] with permission.

Silver 2-ethylhexanoate (Strem, New Buryport, MA) of 0.08 g was dissolved into 1 g of TBAEMA (Sigma). TBAEMA could facilitate Ag-salt dissolution in resin [21,51]. This Ag solution was mixed into SBMP primer at 0.05 wt% of silver 2-ethylhexanoate because preliminary study indicated that this concentration had no adverse effect on dentin bond strength and color of the primer. Hence, four primers were fabricated: (1) SBMP primer (control), (2) control primer + 10% QADM (termed "10QADM"), (3) control primer + 0.05% NAg (termed "0.05NAg"), and (4) control primer + 10% QADM + 0.05% NAg (termed "10QADM + 0.05NAg").

A dental plaque microcosm biofilm model was used [53]. Saliva was collected from a healthy donor having natural dentition without active caries or using antibiotics within 3 months. The donor did not brush teeth for 24 h and abstained from food/drink intake for 2 h prior to donating saliva [53]. Uncured primers were tested by agar disk diffusion test (ADT). Saliva was added to growth medium containing mucin at a concentration of 2.5 g/L, bacteriological peptone at 2.0 g/L, tryptone at 2.0 g/L, yeast extract at 1.0 g/L, NaCl at 0.35 g/L, KCl at 0.2 g/L, $CaCl_2$ at 0.2 g/L, and cysteine hydrochloride at 0.1 g/L (at pH 7) [54]. The inoculum was incubated (37°C, 5% CO_2) for 24 h. Three types of culture media were used. First, tryptic soy blood agar plates were used to determine total microorganisms. Second, mitis salivarius agar (MSA) plates, containing 15% sucrose, were used to determine total streptococci. Third, MSA plus 0.2 units of bacitracin per milliliter was used to determine mutans streptococci [53].

For ADT, a 0.4 mL bacterial suspension was poured onto each agar plate. Then, 30 μL of each primer was impregnated into a sterile paper disk with a diameter of 9 mm and a thickness of 1.5 mm [47]. The primer-impregnated paper disk was placed on a plate with bacteria and incubated for 48 h. The bacterial inhibition zone size was calculated as: (outer diameter of inhibition zone − paper disk diameter)/2.

The uncured QADM−NAg primers had a strong antibacterial activity, as shown in Figure 6.7. As shown in (A), the control primer had minimal inhibition zones. In (B−D), the primers 10QADM, 0.05NAg, and 10QADM + 0.05NAg had much larger inhibition zones. The inhibition zone sizes are plotted in (E−G) for total microorganisms, total streptococci, and mutans streptococci, respectively. The inhibition zone sizes for 10QADM + 0.05NAg were ninefold those of the control ($P < 0.05$) [53].

6.5 Antibacterial adhesive

As shown in Figure 6.8, six groups were used for dentin shear bond strength testing. The purpose of groups 1−3 was to investigate the effects of QADM or NAg individually. The purpose of 3 and 4 was to examine the effect of NAg mass fraction. The purpose of comparing 2, 3, and 5 was to examine the effect of combining QADM and NAg together in the same adhesive. The purpose of comparing 5 with 6 was to investigate the effects of adding QADM and NAg into both the adhesive and the primer on dentin bond strength and biofilm response.

To measure dentin shear bond strength, extracted caries-free human third molars were cleaned and stored in 0.01% thymol solution. Flat mid-coronal dentin surfaces were prepared by cutting off the tips of molar crowns with a diamond saw (Isomet, Buehler, Lake Bluff, IL) [55]. Each tooth was embedded in a polycarbonate holder (Bosworth, Skokie, IL) and ground perpendicular to the

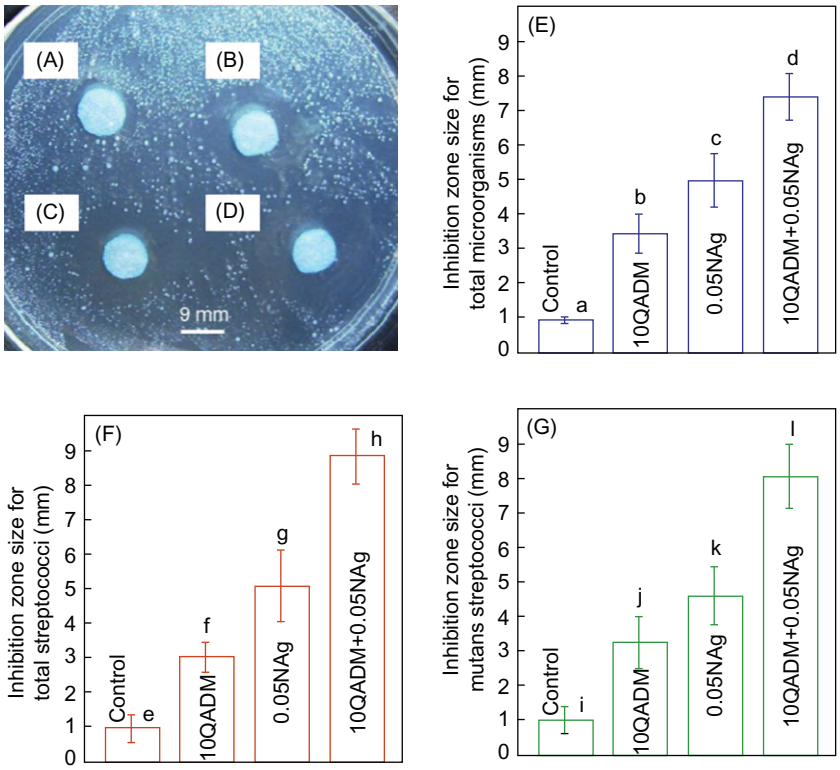

FIGURE 6.7

Antibacterial activity of uncured primers in ADT. (A–D) Control primer, 10QADM, 0.05NAg, and 10QADM + 0.05NAg, respectively. Note a small inhibition zone for control, and much wider inhibition zones for primers with QADM and NAg. This example is for mutans streptococci. Total microorganisms and total streptococci had similar results. (E–G) Inhibition zone data for total microorganisms, total streptococci, and mutans streptococci, respectively. Each value is mean ± sd ($n = 6$). Bars with dissimilar letters indicate values that are significantly different ($P < 0.05$).

Adapted from Ref. [53] with permission.

longitudinal axis on 320-grit silicon carbide paper until the occlusal enamel was completely removed. As shown in Figure 6.8A, the dentin surface was etched with 37% phosphoric acid gel for 15 s and rinsed with distilled water for 15 s, following a previous study [56]. The primer was applied with a brush-tipped applicator and rubbed in for 15 s. The solvent was removed with a stream of air for 5 s. Then the adhesive was applied and light-cured for 10 s (Optilux VCL 401, Demetron Kerr, Danbury, CT). A stainless-steel iris, having a central opening with a diameter of 4 mm and a thickness of 1.5 mm, was held against the adhesive-treated dentin surface. The central opening was filled with a composite (TPH, Caulk/Dentsply, Milford, DE), and light-cured for 60 s. The bonded specimens were stored in distilled water at 37°C for 24 h. A chisel was connected with

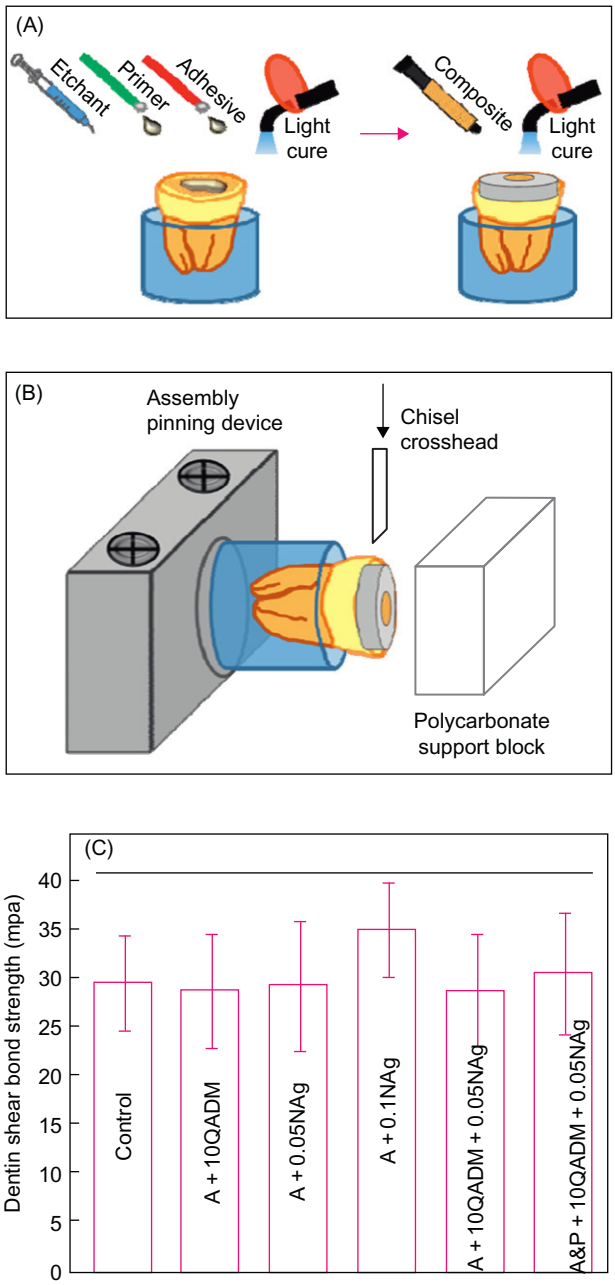

FIGURE 6.8

Human dentin shear bond testing. (A) Schematic of specimen preparation, (B) schematic of shear bond strength testing, and (C) shear bond strength data. Ten teeth were used for each group. Each value is mean ± sd ($n = 10$). Horizontal line indicates that all six groups had similar shear bond strengths ($P > 0.1$).

Adapted from Ref. [55] with permission.

a computer-controlled Universal Testing Machine (MTS, Eden Prairie, MN) and held parallel to the composite−dentin interface. Load was applied at a rate of 0.5 mm/min until the bond failed. Dentin shear bond strength, S_D, was calculated as: $S_D = 4P/(\pi d^2)$, where P is the load at failure and d is the diameter of the composite. Ten teeth were tested for each group ($n = 10$). The results are plotted in Figure 6.8C. The six groups had shear bond strengths that were not significantly different ($P > 0.1$), indicating that adding QADM and NAg to adhesive and primer did not compromise the dentin shear bond strength [55].

For biofilm experiments, layered disk specimens for biofilm experiments were fabricated following previous studies [25,46]. Six groups were tested in biofilm experiments (Figure 6.9). Groups 1−5 had specimens with adhesives covering the top surface of the composite disk, without primer, in order to test the antibacterial properties of the adhesives, as shown in Figure 6.9A. Group 6 had the QADM−NAg primer covering the adhesive on the composite disk in order to test the antibacterial properties of the primer/adhesive combination (Figure 6.9B).

Figure 6.9C plots the MTT metabolic activity of microcosm biofilms. Microcosm biofilms on the commercial adhesive had a high metabolic activity. Incorporation of QADM and NAg each markedly reduced the metabolic activity ($P < 0.05$). Adding QADM and NAg together in the adhesive resulted in a much lower metabolic activity than using QADM or NAg alone ($P < 0.05$). Adding QADM and NAg both in the primer and in the adhesive yielded the lowest biofilm metabolic activity ($P < 0.05$). The metabolic activity of biofilms on A&P + 10QADM + 0.05NAg was nearly an order of magnitude less than that on the commercial adhesive control [55].

6.6 Antibacterial and remineralizing adhesive containing NACP

NACPs were incorporated into the adhesive. The purpose was for the NACP to flow with the adhesive into the hybrid layer as well as the dentinal tubules to form resin tags, with Ca and P ions to remineralize remnants of lesions in the prepared tooth cavity. The NACP mass fraction in the adhesive varied from 10% to 40% [57]. Typical SEM images of the dentin−adhesive interfaces are shown in Figure 6.10: (A) SBMP adhesive control, (B) SBMP primer P + NAg, SBMP adhesive A + NAg + 20NACP (with 20% NACP), and (C) P + NAg, A + NAg + 40NACP (with 40% NACP). Numerous resin tags "T" from well-filled dentinal tubules were visible in all the samples. "HL" refers to the hybrid layer between the adhesive and the underlying mineralized dentin. At a higher magnification, the NACP nanoparticles were visible in (D) with 20% NACP as an example. Arrows in (D) indicate examples of NACP nanoparticles which successfully infiltrated into the dentinal tubules. This feature became more visible at higher magnifications in (E) and (F), where arrows indicate NACP, which successfully infiltrated into not only the straight and smooth tubules (E) but also the bent and irregularly-shaped tubules (F) [57].

These results show the high promise of novel bonding agents and composites containing antibacterial agents and remineralizing nanoparticles to combat biofilms and secondary caries. Further studies are needed to investigate caries inhibition in extracted human teeth at the nanostructured restoration−tooth margins cultured under biofilms.

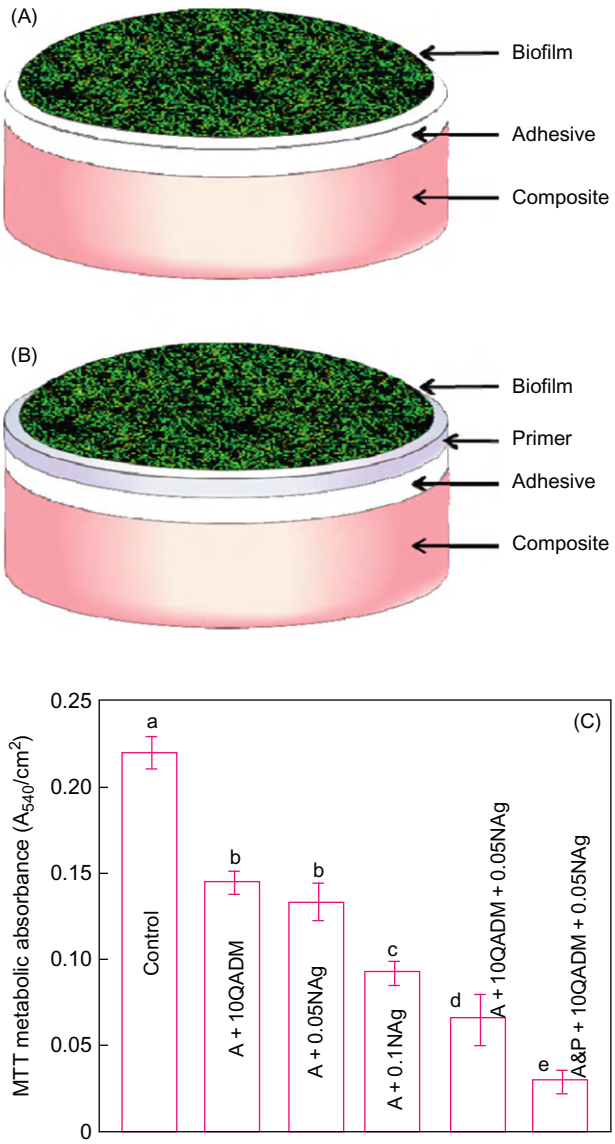

FIGURE 6.9

Biofilm experiments. (A) Schematic of biofilm on adhesive covering composite, (B) biofilm on primer covering adhesive and composite, and (C) MTT metabolic activity. Microcosm biofilms were grown for 2 days. In (C), five adhesives were tested following (A): control (unmodified SBMP adhesive), A + 10QADM ("A" refers to SBMP adhesive), A + 0.05NAg, A + 0.1NAg, A + 10QADM + 0.05NAg. The sixth group in (C) was tested following (B) with a primer layer: A&P + 10QADM + 0.05NAg (A = SBMP adhesive, P = SBMP primer). Each value is mean ± sd ($n = 6$). Values with dissimilar letters are significantly different from each other ($P < 0.05$).

Adapted from [55] with permission.

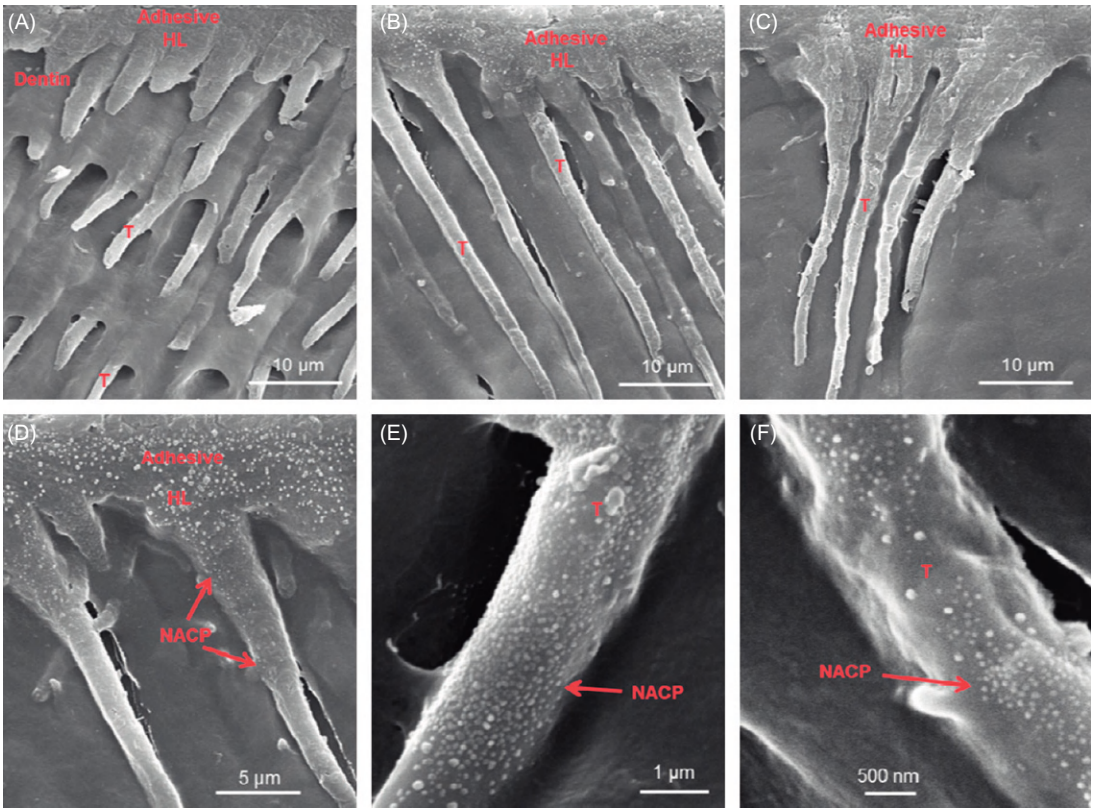

FIGURE 6.10

SEM micrographs of dentin–adhesive interfaces. (A) SBMP control (P = primer, A = adhesive), (B) P + NAg, A + NAg + 20NACP, (C) P + NAg, A + NAg + 40NACP. (D) P + NAg, A + NAg + 20NACP at a higher magnification, and (E, F) at even higher magnifications. Adhesives filled the dentinal tubules and formed resin tags "T" for all six groups. "HL" indicates the hybrid layer between the adhesive and the underlying mineralized dentin. (D–F) Numerous NACP nanoparticles were present in the adhesive layer, in the hybrid zone, and inside the dentinal tubules. Arrows in (D–F) indicate NACP in the dentinal tubules. NACP were able to infiltrate with the adhesive not only into straight tubules (E) but also into bent and irregularly-shaped tubules (F).

Adapted from Ref. [57] with permission.

6.7 Summary and conclusions

Novel calcium phosphate nanoparticles and antibacterial monomers were synthesized, and a new class of bioactive nanocomposites and nanostructured adhesives with a combination of antibacterial and remineralizing capabilities were developed for the first time. The novel NACP–QADM nanocomposite had a strong antibacterial activity that was maintained after water-aging for 6 months. Strength

and modulus of NACP−QADM nanocomposite after 6-month immersion matched those of commercial control composites without antibacterial properties. Incorporation of QADM into NACP nanocomposite greatly reduced the oral bacterial biofilm viability, metabolic activity, CFU, and lactic acid production. The antibacterial results were not significantly different after water-aging for 1, 30, 90, and 180 days. The durable antibacterial properties, plus the previously-reported CaP release and acid neutralization properties, indicate that the novel NACP−QADM nanocomposite may be useful in restorations to inhibit secondary caries. In addition, QADM and NAg were incorporated into dental adhesive and primer, which achieved potent antibacterial effects against dental plaque microcosm biofilms for the first time. The novel QADM−NAg-containing antibacterial adhesives with NACP for remineralization are promising to combat residual bacteria in the prepared tooth cavity and invading bacteria along the tooth−restoration interfaces due to bacterial leakage, thereby inhibiting recurrent caries. Furthermore, the QADM, NAg, and NACP incorporation methods may have a wide applicability to other dental resin composites and bonding systems.

Acknowledgments

We thank Dr. Gary E. Schumacher, Antony A. Giuseppetti, and Kathleen M. Hoffman of the Paffenbarger Research Center of the American Dental Association Foundation, Dr. Ashraf F. Fouad of the University of Maryland School of Dentistry, and Dr. Qianming Chen of the West China School of Stomatology for discussions and help. We are grateful to Esstech (Essington, PA) and Ivoclar Vivadent (Amherst, NY) for donating the materials. This study was supported by NIH R01 grants DE17974 and DE14190 (HX), NIDCR-NIST Interagency Agreement Y1-DE-7005-01, University of Maryland School of Dentistry, NIST, ADAF, and West China School of Stomatology.

Disclaimer

Certain commercial materials and equipment are identified to specify the experimental procedure. In no instance does such identification imply recommendation or endorsement by NIST and ADAF or that the material or equipment identified is the best available for the purpose.

References

[1] J.L. Ferracane, Resin composite—state of the art, Dent. Mater. 27 (2011) 29−38.
[2] F.F. Demarco, M.B. Correa, M.S. Cenci, R.R. Moraes, N.J.M. Opdam, Longevity of posterior composite restorations: not only a matter of materials, Dent. Mater. (2012) 87−101.
[3] S.C. Bayne, J.Y. Thompson, E.J. Swift Jr., P. Stamatiades, M. Wilkerson, A characterization of first-generation flowable composites, J. Am. Dent. Assoc. 129 (1998) 567−577.
[4] B.S. Lim, J.L. Ferracane, R.L. Sakaguchi, J.R. Condon, Reduction of polymerization contraction stress for dental composites by two-step light-activation, Dent. Mater. 18 (2002) 436−444.
[5] D.C. Watts, A.S. Marouf, A.M. Al-Hindi, Photo-polymerization shrinkage-stress kinetics in resin-composites: methods development, Dent. Mater. 19 (2003) 1−11.

[6] X. Xu, L. Ling, R. Wang, J.O. Burgess, Formation and characterization of a novel fluoride-releasing dental composite, Dent. Mater. 22 (2006) 1014–1023.
[7] J.L. Ferracane, Hygroscopic and hydrolytic effects in dental polymer networks, Dent. Mater. 22 (2006) 211–222.
[8] Q. Wan, J. Sheffield, J. McCool, G.R. Baran, Light curable dental composites designed with colloidal crystal reinforcement, Dent. Mater. 24 (2008) 1694–1701.
[9] J.L. Drummond, Degradation, fatigue, and failure of resin dental composite materials, J. Dent. Res. 87 (2008) 710–719.
[10] S.P. Samuel, S. Li, I. Mukherjee, Y. Guo, A.C. Patel, G.R. Baran, et al., Mechanical properties of experimental dental composites containing a combination of mesoporous and nonporous spherical silica as fillers, Dent. Mater. 25 (2009) 296–301.
[11] R.M. Carvalho, A.P. Manso, S. Geraldeli, F.R. Tay, D.H. Pashley, Durability of bonds and clinical success of adhesive restorations, Dent. Mater. 28 (2012) 72–86.
[12] M.M. Zalkind, O. Keisar, P. Ever-Hadani, R. Grinberg, M.N. Sela, Accumulation of *Streptococcus mutans* on light-cured composites and amalgam: an in vitro study, J. Esthet. Dent. 10 (1998) 187–190.
[13] N. Beyth, A.J. Domb, E.I. Weiss, An in vitro quantitative antibacterial analysis of amalgam and composite resins, J. Dent. 35 (2007) 201–206.
[14] V. Deligeorgi, I.A. Mjor, N.H. Wilson, An overview of reasons for the placement and replacement of restorations, Prim. Dent. Care 8 (2001) 5–11.
[15] A. Jokstad, S. Bayne, U. Blunck, M. Tyas, N. Wilson, Quality of dental restorations. FDI Commission Projects 2–95, Int. Dent. J. 51 (2001) 117–158.
[16] S. Imazato, Review: antibacterial properties of resin composites and dentin bonding systems, Dent. Mater. 19 (2003) 449–457.
[17] S. Imazato, Bioactive restorative materials with antibacterial effects: new dimension of innovation in restorative dentistry, Dent. Mater. J. 28 (2009) 11–19.
[18] X. Xu, Y. Wang, S. Liao, Z.T. Wen, Y. Fan, Synthesis and characterization of antibacterial dental monomers and composites, J. Biomed. Mater. Res. B 100 (2012) 1162–1511.
[19] Y. Weng, L. Howard, X. Guo, V.J. Chong, R.L. Gregory, D. Xie, A novel antibacterial resin composite for improved dental restoratives, J. Mater. Sci. Mater. Med. 23 (2012) 1553–1561.
[20] J.M. Antonucci, D.N. Zeiger, K. Tang, S. Lin-Gibson, B.O. Fowler, N.J. Lin, Synthesis and characterization of dimethacrylates containing quaternary ammonium functionalities for dental applications, Dent. Mater. 28 (2012) 219–228.
[21] L. Cheng, M.D. Weir, H.H.K. Xu, J.M. Antonucci, A.M. Kraigsley, N.J. Lin, et al., Antibacterial amorphous calcium phosphate nanocomposite with quaternary ammonium salt and silver nanoparticles, Dent. Mater. 28 (2012) 561–572.
[22] S. Imazato, M. Torii, Y. Tsuchitani, J.F. McCabe, R.R.B. Russell, Incorporation of bacterial inhibitor into resin composite, J. Dent. Res. 73 (1994) 1437–1443.
[23] S. Imazato, F.R. Tay, A.V. Kaneshiro, Y. Takahashi, S. Ebisu, An in vivo evaluation of bonding ability of comprehensive antibacterial adhesive system incorporating MDPB, Dent. Mater. 23 (2007) 170–176.
[24] N. Beyth, I. Yudovin-Farber, R. Bahir, A.J. Domb, E.I. Weiss, Antibacterial activity of dental composites containing quaternary ammonium polyethylenimine nanoparticles against *Streptococcus mutans*, Biomaterials 27 (2006) 3995–4002.
[25] F. Li, Z.G. Chai, M.N. Sun, F. Wang, S. Ma, L. Zhang, et al., Anti-biofilm effect of dental adhesive with cationic monomer, J. Dent. 88 (2009) 372–376.
[26] N. Namba, Y. Yoshida, N. Nagaoka, S. Takashima, K. Matsuura-Yoshimoto, H. Maeda, et al., Antibacterial effect of bactericide immobilized in resin matrix, Dent. Mater. 25 (2009) 424–430.

[27] D. Xie, Y. Weng, X. Guo, J. Zhao, R.L. Gregory, C. Zheng, Preparation and evaluation of a novel glass-ionomer cement with antibacterial functions, Dent. Mater. 27 (2011) 487–496.
[28] D. Skrtic, J.M. Antonucci, E.D. Eanes, F.C. Eichmiller, G.E. Schumacher, Physiological evaluation of bioactive polymeric composites based on hybrid amorphous calcium phosphates, J. Biomed. Mater. Res. B 53 (2000) 381–391.
[29] S.H. Dickens, G.M. Flaim, S. Takagi, Mechanical properties and biochemical activity of remineralizing resin-based Ca-PO_4 cements, Dent. Mater. 19 (2003) 558–566.
[30] S.E. Langhorst, J.N. O'Donnell, D. Skrtic, In vitro remineralization of enamel by polymeric amorphous calcium phosphate composite: Quantitative microradiographic study, Dent. Mater. 25 (2009) 884–891.
[31] H.H.K. Xu, L. Sun, M.D. Weir, J.M. Antonucci, S. Takagi, L.C. Chow, Nano dicalcium phosphate anhydrous-whisker composites with high strength and Ca and PO_4 release, J. Dent. Res. 85 (2006) 722–727.
[32] H.H.K. Xu, M.D. Weir, L. Sun, J.L. Moreau, S. Takagi, L.C. Chow, et al., Strong nanocomposites with Ca, PO_4 and F release for caries inhibition, J. Dent. Res. 89 (2010) 19–28.
[33] H.H.K. Xu, J.L. Moreau, L. Sun, L.C. Chow, Nanocomposite containing amorphous calcium phosphate nanoparticles for caries inhibition, Dent. Mater. 27 (2011) 762–769.
[34] J.L. Moreau, L. Sun, L.C. Chow, H.H.K. Xu, Mechanical and acid neutralizing properties and inhibition of bacterial growth of amorphous calcium phosphate dental nanocomposite, J. Biomed. Mater. Res. B 98 (2011) 80–88.
[35] P. Spencer, Y. Wang, Adhesive phase separation at the dentin interface under wet bonding conditions, J. Biomed. Mater. Res. 62 (2002) 447–456.
[36] K. Ikemura, F.R. Tay, T. Endo, D.H. Pashley, A review of chemical-approach and ultramorphological studies on the development of fluoride-releasing dental adhesives comprising new pre-reacted glass ionomer (PRG) fillers, Dent. Mater. J. 27 (2008) 315–329.
[37] J. Park, Q. Ye, E. Topp, A. Misra, S.L. Kieweg, P. Spencer, Water sorption and dynamic mechanical properties of dentin adhesives with a urethane-based multifunctional methacrylate monomer, Dent. Mater. 25 (2009) 1569–1575.
[38] A.V. Ritter, E.J. Swift Jr., H.O. Heymann, J.R. Sturdevant, A.D. Wilder Jr., An eight-year clinical evaluation of filled and unfilled one-bottle dental adhesives, J. Am. Dent. Assoc. 140 (2009) 28–37.
[39] F. Garcia-Godoy, N. Kramer, A.J. Feilzer, R. Frankenberger, Long-term degradation of enamel and dentin bonds: 6-year results in vitro vs. in vivo, Dent. Mater. 26 (2010) 1113–1118.
[40] M.S. Shinohara, M.F. De Goes, L.F. Schneider, J.L. Ferracane, P.N. Pereira, V.D. Hipolito, et al., Fluoride-containing adhesive: durability on dentin bonding, Dent. Mater. 25 (2009) 1383–1391.
[41] J. Park, J. Eslick, Q. Ye, A. Misra, P. Spencer, The influence of chemical structure on the properties in methacrylate-based dentin adhesives, Dent. Mater. 27 (2011) 1086–1093.
[42] D.H. Pashley, F.R. Tay, L. Breschi, L. Tjaderhane, R.M. Carvalho, M. Carrilho, et al., State of the art etch-and-rinse adhesives, Dent. Mater. 27 (2011) 1–16.
[43] L. Roeder, R.N.R. Pereira, T. Yamamoto, N. Ilie, S. Armstrong, J. Ferracane, Spotlight on bond strength testing—unraveling the complexities, Dent. Mater. 27 (2011) 1197–1203.
[44] B. Van Meerbeek, K. Yoshihara, Y. Yoshida, A. Mine, J. De Munck, State of the art of self-etch adhesives, Dent. Mater. 27 (2011) 17–28.
[45] S. Imazato, Y. Kinomoto, H. Tarumi, S. Ebisu, F.R. Tay, Antibacterial activity and bonding characteristics of an adhesive resin containing antibacterial monomer MDPB, Dent. Mater. 19 (2003) 313–319.
[46] S. Imazato, A. Ehara, M. Torii, S. Ebisu, Antibacterial activity of dentin primer containing MDPB after curing, J. Dent. 26 (1998) 267–271.
[47] S. Imazato, A. Kuramoto, Y. Takahashi, S. Ebisu, M.C. Peters, In vitro antibacterial effects of the dentin primer of clearfil protect bond, Dent. Mater. 22 (2006) 527–532.

[48] N. Hiraishi, C.K. Yiu, N.M. King, F.R. Tay, Effect of chlorhexidine incorporation into a self-etching primer on dentin bond strength of a luting cement, J. Dent. 38 (2010) 496–502.
[49] L.C. Chow, L. Sun, B. Hockey, Properties of nanostructured hydroxyapatite prepared by a spray drying technique, J. Res. Natl. Inst. Stand. Technol. 109 (2004) 543–551.
[50] L. Cheng, M.D. Weir, H.H.K. Xu, A.M. Kraigsley, N.J. Lin, S. Lin-Gibson, et al., Antibacterial and physical properties of calcium-phosphate and calcium-fluoride nanocomposites with chlorhexidine, Dent. Mater. 28 (2012) 573–583.
[51] Y.J. Cheng, D.N. Zeiger, J.A. Howarter, X. Zhang, N.J. Lin, J.M. Antonucci, et al., In situ formation of silver nanoparticles in photocrosslinking polymers, J. Biomed. Mater. Res. B 97 (2011) 124–131.
[52] L. Cheng, M.D. Weir, K. Zhang, S.M. Xu, Q. Chen, X.D. Zhou, et al., Antibacterial nanocomposite with calcium phosphate and quaternary ammonium, J. Dent. Res. 91 (2012) 460–466.
[53] L. Cheng, K. Zhang, M.A.S. Melo, M.D. Weir, X.D. Zhou, H.H.K. Xu, Anti-biofilm dentin primer with quaternary ammonium and silver nanoparticles, J. Dent. Res. 91 (2012) 598–604.
[54] A.J. McBain, In vitro biofilm models: an overview, Adv. Appl. Microbiol. 69 (2009) 99–132.
[55] K. Zhang, M.A.S. Melo, L. Cheng, M.D. Weir, Y.X. Bai, H.H.K. Xu, Effect of quaternary ammonium and silver nanoparticle-containing adhesives on dentin bond strength and dental plaque microcosm biofilms, Dent. Mater. 28 (2012) 842–852.
[56] J.M. Antonucci, J.N. O'Donnell, G.E. Schumacher, D. Skrtic, Amorphous calcium phosphate composites and their effect on composite-adhesive-dentin bonding, J. Adhes. Sci. Technol. 23 (2009) 1133–1147.
[57] M.A.S. Melo, L. Cheng, K. Zhang, M.D. Weir, L.K.A. Rodrigues, H.H.K. Xu, Antibacterial dental adhesive containing silver and amorphous calcium phosphate nanoparticles, Dent. Mater. (2012) http://dx.doi.org/10.1016/j.dental.2012.10.005.

CHAPTER

Nanotechnology and Nanoparticles in Contemporary Dental Adhesives

7

Mohammad Nassif[a] **and Farid El Askary**[b]

[a]*Biomaterials Department, Faculty of Dentistry, Ain Shams University, Cairo, Egypt*

[b]*Operative Dentistry Department, Faculty of Dentistry, Ain Shams University, Cairo, Egypt*

CHAPTER OUTLINE

Nanobiomaterials in Clinical Dentistry.

7.1 Introduction

The field of adhesion to dental substrates has gained a lot of interest with massive research work aiming at improving bond strength and increasing bond durability. Nanoscience and nanotechnology are expected to play a major role in understanding and improving the outcome of adhesion and dental restorative procedures. These improvements are expected to yield adhesives with antibacterial capacities through the incorporation of antimicrobial nanoparticles. Self-healing adhesives will be available for the dental profession through nanoencapsulation of monomers and incorporation of these nanocapsules in the adhesives. Adhesives incorporating nanoparticles or nanorods will show improved physicomechanical properties and catalytic activity with better polymerization and conversion of adhesive monomers.

7.2 Brief history of dental adhesives

In the dental research area, Kramer and McLean in 1952 [1] were the first to make an experimental study in the field of adhesion to tooth substrate, but this was poorly unnoticeable until the Buonocore's attempt in 1955 [2]. Nowadays, the concept of "minimum interventions" or "minimally invasive cavity preparations" has been widely accepted [3] which means that the diseased dental tissues is only removed and replaced with adhesive restorations.

Previously, van Meerbeek et al. [4] classified the dental adhesives according to their actions on the smear layer. One-step or two-step adhesives that modify the smear layer were the first category in this classification. Another approach was the total removal of the smear layer, which involved two-step or three-step adhesives. The last approach was the adhesive that dissolved the smear layer rather than remove it. These adhesives utilize acidic "self-etching primers" that dissolve the smear layer making it a part of the hybrid layer (Figure 7.1).

With the introduction of one-step self-etching adhesives, several brands were being available in the market, which made wide varieties of such adhesives [5]. Dental adhesives were categorized into (i) etch-and-rinse, either three-step or two-step, (ii) self-etching adhesives, either two-step or one-step, and (iii) the glass ionomer adhesive which is considered a two-step etch-and-rinse adhesive based on resin-modified glass ionomer (RMGI) formulation. Among all adhesive categories, three-step etch-and-rinse adhesive is considered the "gold standard" regarding its clinical durability (Figure 7.2).

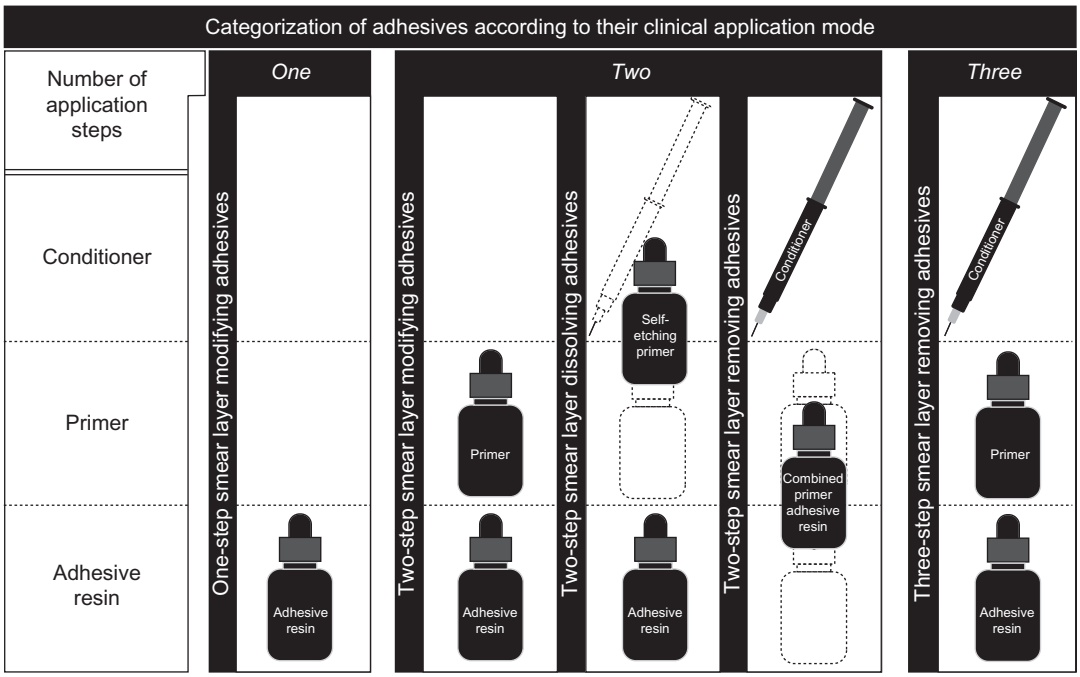

FIGURE 7.1

Schematic presentation of categorization of dental adhesives classified according to their clinical application mode.

The one-step self-etching adhesives are available as mixed/two-bottles, or no-mix/one-bottle adhesives, 2-hydroxyethyl methacrylate (HEMA)-free or HEMA-containing adhesives, water-free or water-containing adhesives, and recently solvent-free or solvent-containing adhesives.

7.3 Contemporary adhesive systems

When the acid etchant is applied to enamel and dentin, superficial decalcification with the loss of minerals occurs. Application of adhesive resin will replace the lost minerals of tooth structure and when cured in situ becomes micromechanically retained within the porosities that are being created during the acid-etching process [5]. John Gwinnett [6] was the first to evaluate the adhesive/enamel interface and described an acid-resistance layer. This layer was the first true "hybrid layer" discovered. Unfortunately, the term "hybrid layer" was not applied until the study by Nakabayashi et al. in 1982 [7]. They pointed to the existence of such intermediate layer between the adhesive layer and dentin and gave it the name "hybrid layer" (Figure 7.3).

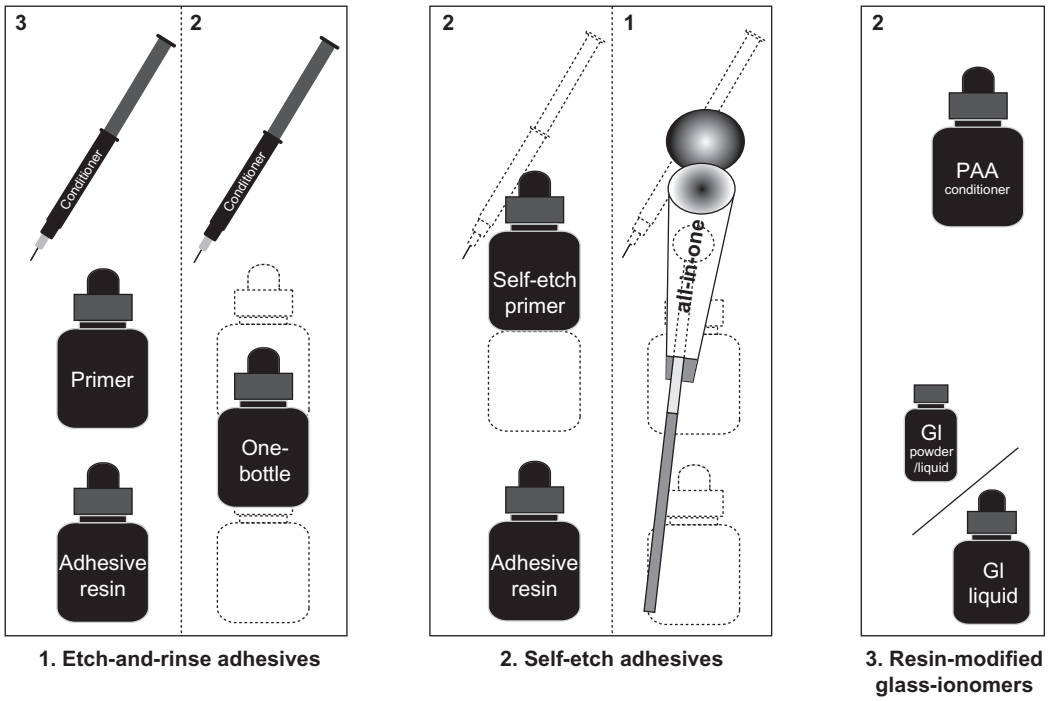

FIGURE 7.2

Classification of contemporary adhesives following adhesion strategy and the number of clinical application steps according to De Munck et al. [5]. GI, glass ionomer; PAA, polyalkenoic acid.

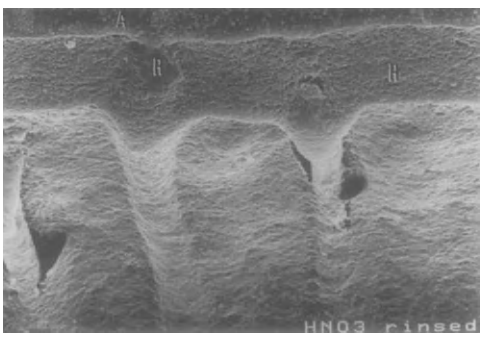

FIGURE 7.3

Field-Emission SEM photomicrograph when nitric acid conditioner was rinsed off before the application of the primer and adhesive with the formation of hybrid layer (H), which is clearly shown.

7.3.1 Etch-and-rinse adhesives

These adhesives utilize the use of acid etching of both enamel and dentin and the application of both primer and adhesive in separate steps or the application of the primer/adhesive mixture in a single bonding step. Phosphoric acid with a concentration of 30−40% is the acid of choice for such adhesive systems. Although enamel etching was established since Buonocore's study, acid etching of dentin was not recognized until Fusayama [8] introduced the total-etch concept. One of the causes for previously reported failures of such concept was the dry bonding technique, until Kanca [9] described the so-called "wet bonding" (Figure 7.4). In this regard, the complete demineralization of dentin with phosphoric acid etching gel is limited to the superficial 5−8 μm (Figure 7.5) of intertubular dentin [10], which is followed by the application of solvated primer or solvated primer/adhesive mixture to gain retention through the formation of microresin tags.

Ideally, the resin monomer should completely replace the lost minerals (Figure 7.5). This could never be ideally performed [9], which is due to the presence of residual solvent or due to the fluid infiltration through the movement of dentinal fluid from inside the dentinal tubules [11,12]. This will cause incomplete infiltration of monomer inside the created porosities (Figures 7.6 and 7.7). Incomplete infiltration of resin monomer is one of the causes that make the etch-and-rinse adhesives technique sensitive.

7.3.2 Self-etching adhesives

Self-etching adhesives can be classified into four categories according to the pH of the functional monomer: the strong self-etching adhesives (pH < 1), intermediate adhesives (pH ≈ 1.5), mild adhesives (pH ≈ 2) [13], and extra-mild adhesives (pH > 2.5) [14].

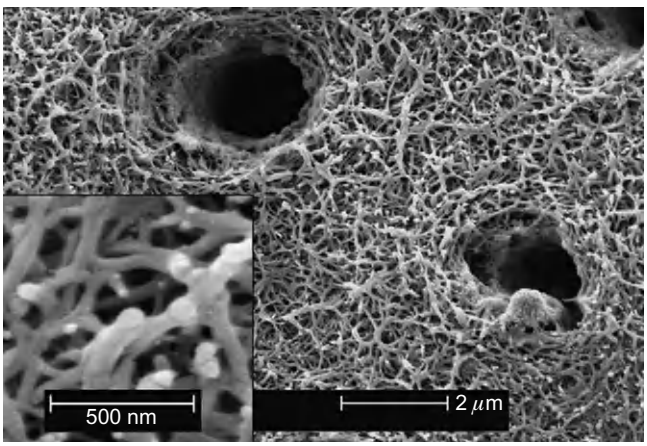

FIGURE 7.4

Scanning electron micrograph of acid-etched dentin showing two dentinal tubules containing remnants of peritubular dentin matrix. Inset: High magnification of branching collagen fibrils (ca. 75 nm in diameter) separated by interfibrillar spaces that serve as channels for resin infiltrations during bonding.

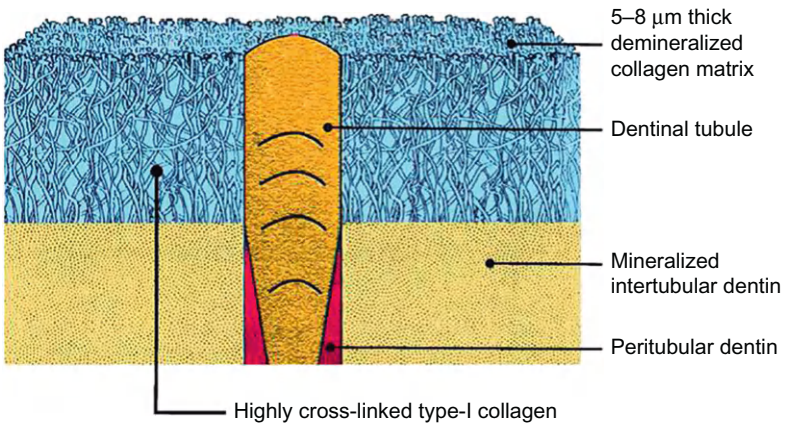

FIGURE 7.5

Schematic of a hybrid layer (HL) created by an etch-and-rinse adhesive. Note that the depth of the hybrid layer (green) is about four acid-etched tubule diameters (i.e. ca. 8 μm). The collagen fibrils in the HL are continuous with the underlying mineralized matrix. A single dentinal tubule is shown devoid of a resin tag to illustrate its presence. (For interpretation of the references to color in this figure legend, the reader is referred to the web version of this book.)

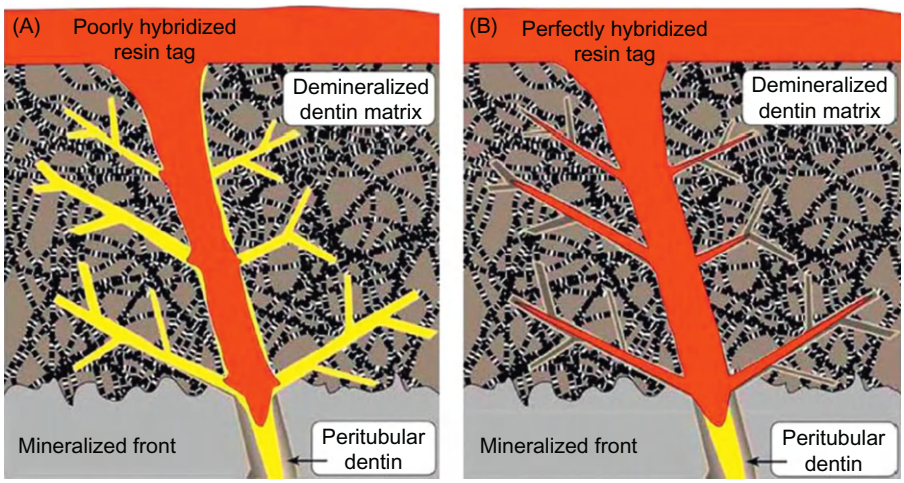

FIGURE 7.6

Schematic of micropermeability of (A) poorly hybridized resin tags in etched dentin saturated with water prior to resin infiltration versus (B) perfectly hybridized resin tags in etched dentin saturated with ethanol prior to resin infiltration. Yellow fluorescent tracer was forced from the pulp chamber, out the tubules toward the hybrid layer. In (A) the resin could not displace water-filled lateral branches of tubules in the hybrid layer. This allowed yellow tracer to diffuse throughout the hybrid layer. In (B) the resin easily dissolved in the ethanol-filled lateral branches sealing the hybrid layer from dentinal fluid.

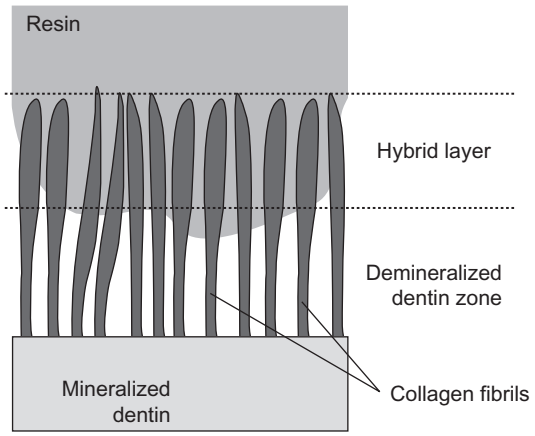

FIGURE 7.7

Schematic illustration of demineralized dentin zone of total-etch adhesives. Inadequate resin infiltration into collagen fibrils leaves nano- or microspaces within the adhesive interface. This zone is not common for self-etching adhesive systems. Collagen hydrolysis of the demineralized dentin zone is one of the degradation patterns for total-etch adhesives. In the absence of a demineralized dentin zone within the bonds, this collagen hydrolysis does not occur because the encapsulation of cured adhesive resins or protection of the mineral matrix of dentin prevents chemical degradation of the collagen fibrils even after long-term function.

The self-etching (etch-and-dry) [14] adhesives utilize simultaneous etch and prime of the dental substrates. These adhesives do not require a separate acid-etching step. They are less technique sensitive, compared to the etch-and-rinse ones, due to the lack of wet bonding approach. However, water-free self-etching adhesives require the wet dentin surface, which raise the same question again: how wet is wet? [14] They are also user friendly, due to the decrease in clinical bonding steps and shortening application time.

Self-etching adhesives were introduced as two-step adhesives, where the self-etching primer and adhesive are presented in two separate bottles or as one-step adhesives, where all components are presented in single solution. The one-step self-etching adhesives can be provided either as mixed/two-bottles adhesives or no-mix/single-bottle adhesives.

Self-etching adhesives simultaneously etch and infiltrate the tooth substrate, which ensure a complete infiltration of the demineralized zone. On the other hand, they are not free from shortcomings (Figure 7.8). The decrease in 24-h bond strength as well as a limited durability of such adhesive compared to multistep adhesives was reported. HEMA-containing adhesives suffer from water sorption and HEMA-free adhesives are prone to phase separation. Decrease in the shelf-life of such adhesives that combine all components in a single bottle is another shortcoming for such adhesives [14].

7.3.3 Glass ionomer adhesive

Glass ionomer adhesive is considered a two-step etch-and-rinse adhesive, its chemical composition being based on the glass ionomer cement. It is the diluted version of the RMGI cement, Fuji II LC.

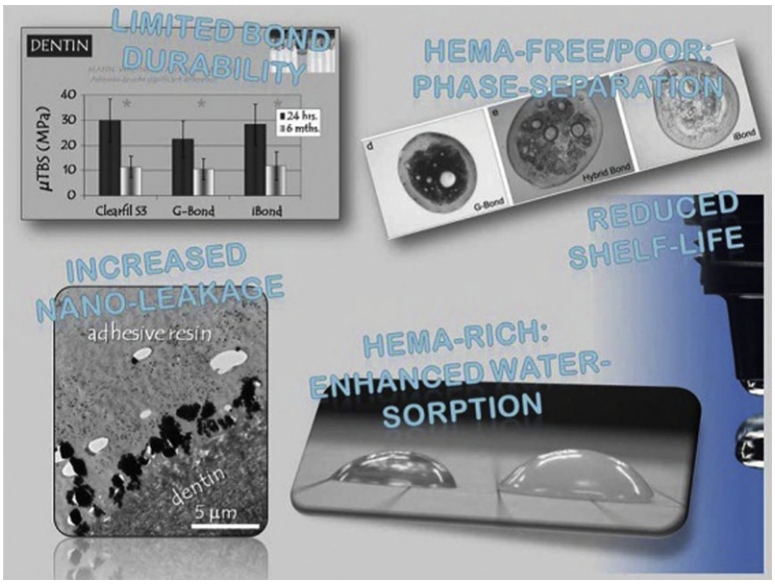

FIGURE 7.8

The major shortcomings of current one-step adhesives.

Glass ionomer is the only material that has the self-adhering property. The pretreatment of dentin surface with 10% or 20% polyacrylic acid (PAA) cleans the surface, removes the smear layer, and decalcifies the dentin surface to a depth ranging from 0.5 to 1 μm. The glass ionomer adhesive then infiltrates and mechanically interlocks through the process of hybridization. In addition, a chemical bond is formed through the ionic exchange between the carboxylic group of the PAA and the calcium ions, which remain attached to the collagen fibrils [5].

7.4 Chemical compositions of contemporary adhesives

Retention of restoration and providing a perfect seal to cavity wall and margin are the prime aims for the use of adhesives. Micromechanical bond to enamel and dentin is the primary mechanism of adhesion to tooth structure, which is achieved by the infiltration of the resin monomer into the acid-etching-created porosities and become interlocked upon its curing [5]. Another mechanism of bonding is the ion exchange between the acidic monomers and calcium through adding specific monomers, which are able to react with the hydroxyapatite (HAP) [15]. The adhesion of adhesives is not only limited to tooth substrates but also it should provide excellent bond to the overlying resin composite. The chemical compositions of the adhesive systems should provide components that are able to achieve such goals (Figure 7.9). Resin monomers, solvents, initiators, inhibitors, and sometimes fillers are the main constituents of adhesive systems [16].

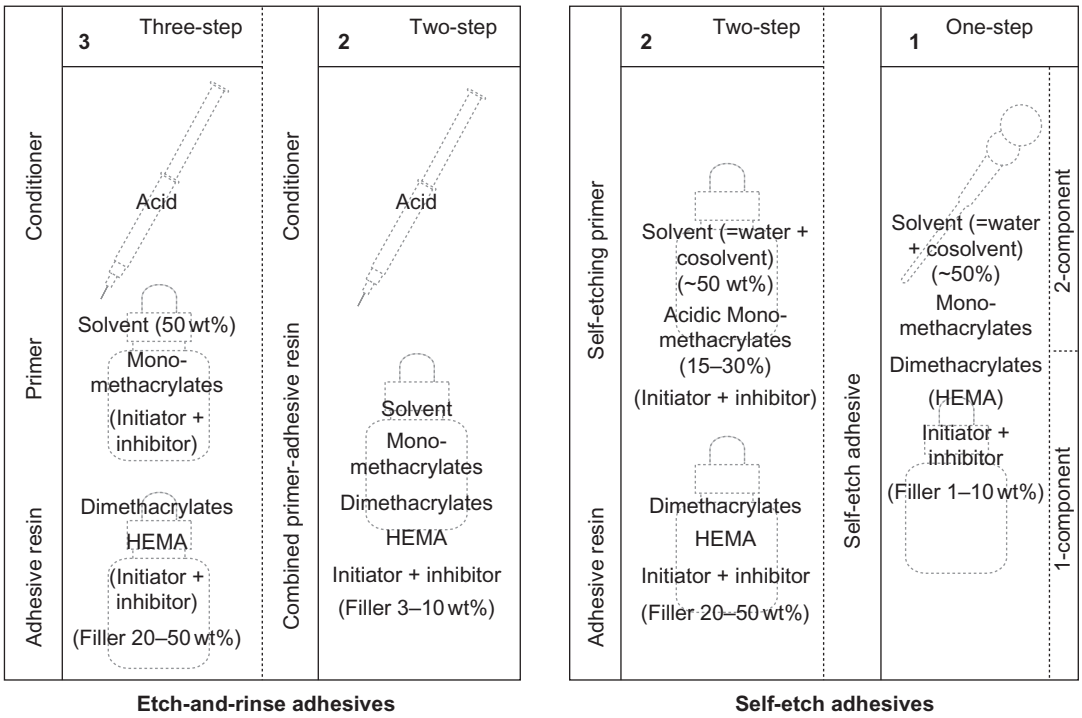

FIGURE 7.9

Classification of contemporary adhesives according to Van Landuyt et al. [16]. Even though most adhesives contain the same components, they may differ significantly considering the proportional amount of ingredients. As indicated, most adhesives contain methacrylate-based monomers. The mentioned percentages of ingredients are approximations; nevertheless a lot of variation considering the proportional composition of adhesives exists between different products. Two-step etch-and-rinse adhesives often referred to as "one-bottle" systems. Irrespective of the classification, each component, either primer or bonding or self-etching adhesive can come in two bottles that need to be mixed prior to application. As such, one-step self-etch adhesives are often subdivided in one- and two-component systems.

7.4.1 Resin monomers

Monomers are the most important components of the adhesive, which are considered the key constituents of adhesives. To provide excellent bond with resin composite, monomers in the adhesive should be similar to those of the resin composite. Two types of monomers are presented, either the cross-linked monomers or the functional monomers. The latter are presented mainly in the self-etching adhesives. The most cross-linking monomers, which are used in dental adhesives, are bisphenol A-glycidyl methacrylate, urethane dimethacrylate, and triethylene glycol dimethacrylate (TEGDMA), while 4-methacryloxy-ethyl trimellitate anhydride, 4-methacryloyloxy-ethyl trimellitic acid, dipentaerythritol penta acrylate monophosphate, 2-(methacryloyloxyethyl) phenyl hydrogen phosphate, and 10-methacryloyloxydecyl dihydrogen phosphate are the most used

functional monomers [16]. On the other hand, 2-hydroxyethyl methacrylate (HEMA) is a low molecular weight monomer, which is characterized by its hydrophilic properties and is an important constituent of most adhesive systems.

The cross-linking monomers provide strength to the adhesive and have hydrophobic properties which prevent water sorption of the cured adhesive, while functional monomers are responsible for the demineralization of tooth substrates and provide chemical bond to calcium in the HAP; nevertheless, their ability to decalcify and adhere to the HAP differs from one functional monomer to another [16].

7.4.2 Solvents

Bonding to dentin requires the addition of solvent to the adhesive composition. The presence of solvent is responsible for the improvement of wetting of the hydrophilic monomer and decrease in the viscosity of the adhesive for enhancement of the diffusivity of primer or primer/adhesive mixture into the acid-etching-created microporosities. Three main solvents used in the adhesives irrespective of their adhesion strategy are acetone, ethanol, and water.

Adhesives that contain acetone or ethanol are recommended in the wet bonding technique. Although acetone has a higher vapor pressure than ethanol, both have better evaporation during the air-drying step [16], but both the solvents lack the rewetting capacity of collagen fibers, especially when etch-and-rinse adhesives are used. On the other hand, water is an excellent rewetting agent [9] but hardly gets evaporated during the air-drying step. A water/ethanol mixture is presented in some etch-and-rinse adhesive systems to improve the evaporation of water [16]. Acetone is only found as a mixture with water in the self-etching adhesives, as water is an essential component in the self-etching adhesives.

7.4.3 Fillers

Adhesive can be found with fillers (filled adhesive) or without filler contents (unfilled resin). Unlike resin composite materials, fillers in the adhesive are presented in small amounts compared to resin composite and the filler size should be small enough to enable the fillers to penetrate into dentinal tubules or between the collagen fibril spaces.

7.4.3.1 Role of fillers in dental adhesives

Fillers are added to resin adhesives to improve the strength of the adhesive layer. Increasing the strength of adhesive layer will improve the bond strength of the adhesive [17] to either enamel or dentin, but such improvement was dependent on filler loading [18,19]. Increase in microfiller loading up to 40% had not only negatively affected the shear bond strength but also adversely affected the polymerization rate (PR) of the adhesive layer [19]. On the other hand, adding 10% silica nanofillers did not affect the degree of conversion (DC), but it significantly improved the cohesive strength of the adhesive [20].

Increasing the viscosity of the adhesive to a level that does not affect its wetting to tooth substrate is another issue for adding fillers to the adhesives. During the air-drying step, excessive air drying could result in excessive thinning of the adhesive. Very thin adhesive layer suffers from incomplete PR due to oxygen inhibited layer [16]. Adding filler prevents the excessive thinning of

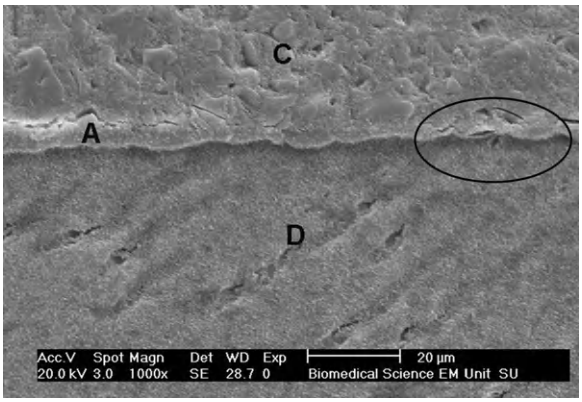

FIGURE 7.10

SEM micrograph of resin–dentin interface when the adhesive was air dried at short distance using high air-drying pressure. C, composite; A, adhesive, and D, dentin. Black oval represents area without the adhesive layer.

From Ref. [21].

the adhesive layer. A recent study [21] demonstrated that even with adding nanofillers to the adhesive, excessive air-drying procedure through the use of high air-drying pressure did not only excessively thin the adhesive layer but also it completely washed away the adhesive to the level that resin composite was directly bonded to dentin (Figure 7.10). Unfortunately, this result did not confirm whether this problem was related to the tested self-etching adhesive used in this study or it could be a general problem related to all self-etching adhesives.

Fillers are also added for therapeutic purpose. The presence of prereacted glass ionomer microfillers offers the advantage of fluoride releasing from some adhesive systems [22]. Fillers are also added to improve the radiopacity of the adhesives [23]. Improving the radiopacity of the adhesives helps in the evaluation of recurrence of decay under resin restorations.

7.4.3.2 Effect of filler composition and particle size

Different fillers are used, which are incorporated for two purposes: (i) to reinforce the adhesive layer and (ii) to perform a specific function. As mentioned before, there is a wide range of role for the fillers in the adhesives. Based on the "adhesion/decalcification concept" [24], Zhang and Wang [25,26] incorporated HAP microfillers into two commercially self-etching adhesives. The aim of their study was to evaluate the reaction/interaction of monomer and HAP fillers on the DC and PR of the two adhesives. They found that HAP fillers significantly increased the DC and PR of the aggressive self-etching adhesive; on the contrary, they had no significant effect on the DC and PR of the mild one. A 7 nm silica filler size of 10 wt% concentration had a significant effect on the cohesive strength of the adhesive with no effect on DC [20].

When 0.2–0.5 wt% of HAP nanorods (Figures 7.11 and 7.12) were incorporated into an experimental adhesive, the study results showed a significant positive effect on both the diametral tensile strength (DT) and flexure strength (FS) of the adhesive. A 5 wt% of the nanorods dramatically

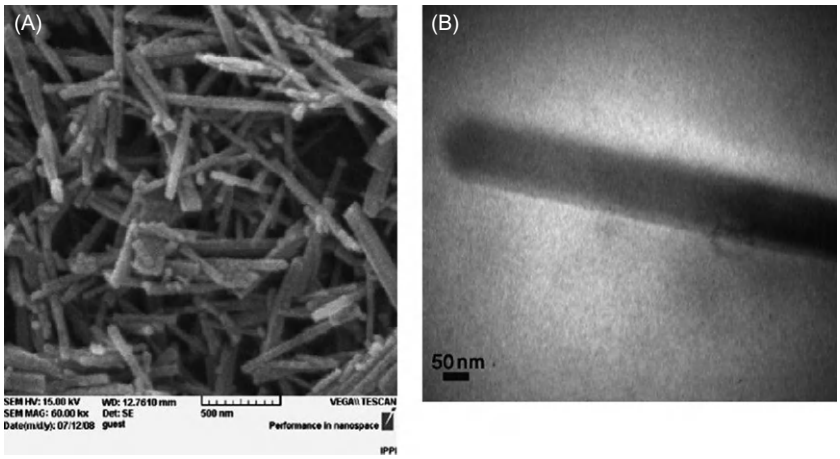

FIGURE 7.11

(A) SEM and (B) TEM photomicrographs of synthesized HAP nanorods.

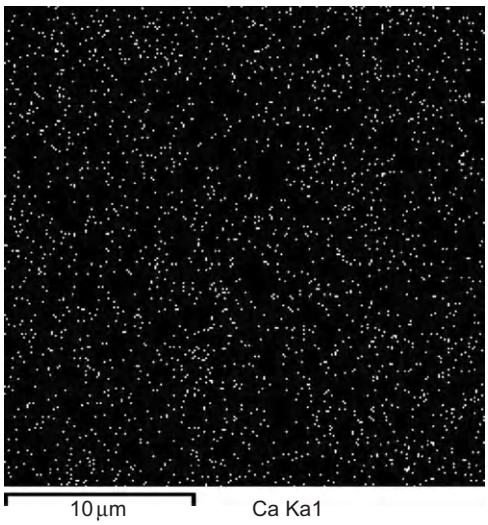

FIGURE 7.12

EDX—calcium mapping image of the adhesive system containing 0.5 wt% HAP nanorods. The bright spots show the distribution of the HAP nanorods in the adhesive.

decreased both DT and FS, which was due to the decrease in curing depth of such adhesive. A significant higher microshear bond strength was recorded with 0.2 wt% nanorods filler. Since high dispersion stability of nanorods in the experimental adhesive was demonstrated, the HAP nanorods could be used as an alternative to other nanofillers in the adhesives and that the advantage of these fillers might influence the remineralization at the resin/dentin interface [27].

Another filler type is the titanium dioxide nanofillers (TiO_2), which was added in small amount to improve the mechanical properties of the adhesive. By mixing the TiO_2 nanoparticles with acrylic acid, agglomerated fillers were produced. By adding these agglomerated fillers at a concentration of 0.08% mass fraction, the DC was significantly higher with approximately 5% more than the unfilled one. The flexure modulus was increased by about 48% when 0.06% mass fraction of nanofillers was added and the hardness was almost double with this amount of mass fraction. The shear bond strength was significantly improved (about 30% higher compared to the unfilled one) when the filler mass fraction was 0.1%. Nevertheless, the durability and stability of such filler type in dental adhesive should be given much attention in the future research [28].

Recently, poly-methyl methacrylate (PMMA)-grafted nanoclay fillers were evaluated (Figure 7.13). The authors dispersed the nanoclay fillers as a part of the chemical composition of an experimental adhesive. The 1 wt% PMMA-grafted nanoclay dispersion showed dispersion stability over 12 h and the DC was not affected with different percentage of the PMMA-grafted nanoclay. On the other hand, the microshear bond strength was significantly improved with adding PMMA-grafted nanoclay as filler [29].

With the improvement of the nanotechnology in the dental field, newly developed fillers are being incorporated within the adhesives. Solhi et al. [30] synthesized PAA nanoclay as reinforced fillers within an experimental adhesive (Figures 7.14 and 7.15). Adding of PAA-grafted nanoclay fillers did not affect the DC of the experimental adhesive at any percent filler loading (0.2−5 wt%). The microshear bond strength was significantly improved by adding only 0.2 wt% of the PAA-grafted fillers (Figure 7.16). It could be suggested that the incorporation of PAA-grafted nanoclay fillers could enhance chemical bonding through ion exchange between the carboxylic group in the PAA and the calcium ion in dentin. However, this suggestion needs further research investigation.

As the filler type could also affect adhesives' properties, certain fillers were added to enhance specific properties of the adhesive. Flame-made tantalum butoxide/silicon oxide (Ta_2O_5/SiO_2) nanofillers were added to increase the radiopacity of the adhesive (Figure 7.17). During routine radiograph examination, the difference between the recognition of the adhesive layer and the

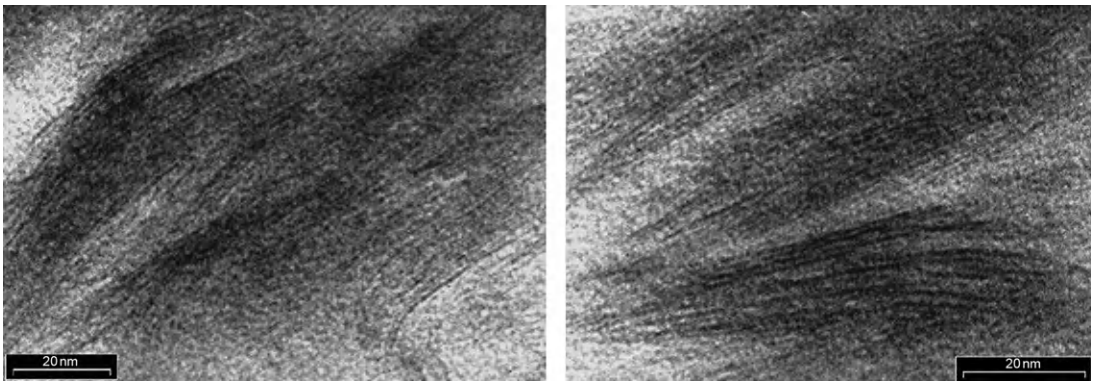

FIGURE 7.13

TEM micrographs of the adhesive containing 1 wt% PMMA-grafted nanoclay showing partially delaminated clay platelets.

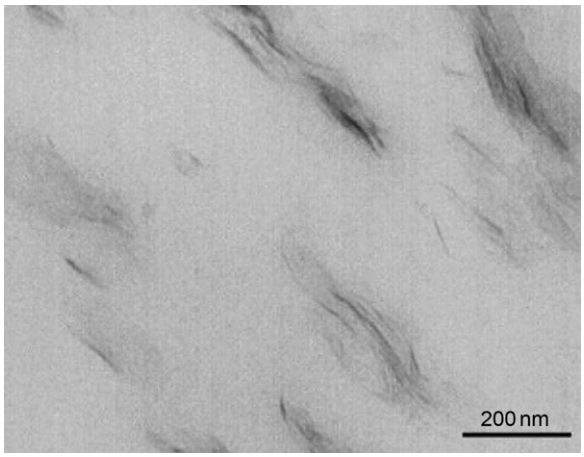

FIGURE 7.14

TEM micrographs of the adhesive containing 1 wt% PAA-grafted nanoclay showing partially delaminated clay platelets.

FIGURE 7.15

Silicone map of the cured adhesive containing 0.5% PAA-grafted-nanoclay showing a good dispersion of the modified fillers.

recurrence of decay could be mistaken. Radiopacity of the adhesive could be of importance to avoid such misinterpretation. Adding 20 wt% of Ti_2O_5/SiO_2 nanoparticles (primary filler size of 10 nm) made an adhesive more radiopaque than enamel and dentin. Although the viscosity was slightly higher than the unfilled one, shear bond strength was not affected [23].

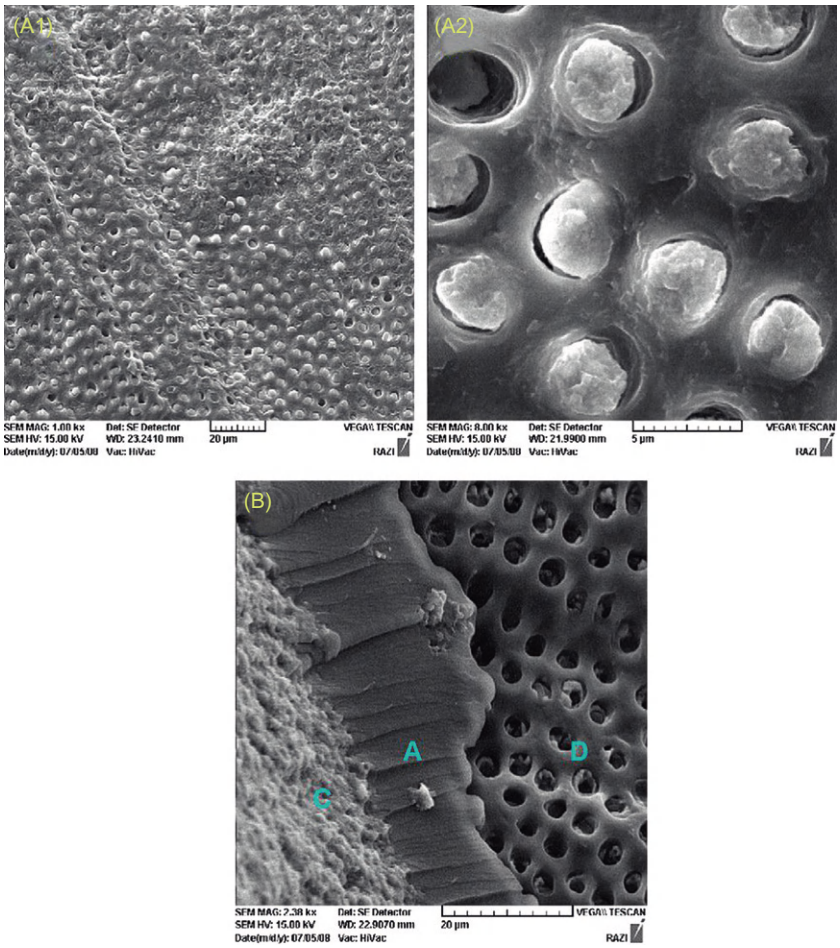

FIGURE 7.16

SEM micrographs of the fracture area in microshear bond strength test. (A1) The area for adhesive containing 0.2 wt% PAA-grafted nanoclay representing good penetration of adhesive into dentin tubules. (A2) shows the tubules in higher magnification. (B) The area for adhesive containing 5 wt% PAA grafted nanoclay. Lack of complete penetration is clear (C, composite; A, adhesive; D, dentin).

7.5 Ketac nanoprimer

Recently, 3M ESPE introduced a new product, a nanofilled RMGI cement utilizing a Ketac nanoprimer for optimum bonding to enamel and dentin. Ketac nanoprimer is one-component water-based acidic primer with a pH $\approx$ 3. Due to its high pH, removal of smear layer was not performed leading to lower bond strength, and the remnant of the smear layer was observed on scanning

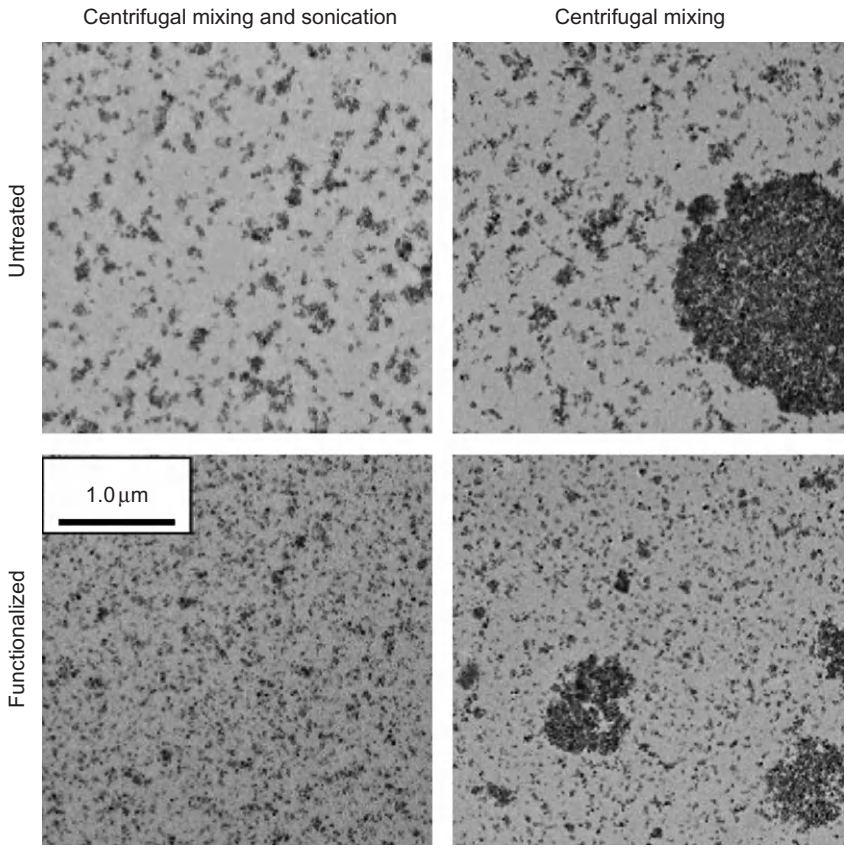

FIGURE 7.17

Images of composites containing 20 wt% untreated (top) and functionalized (bottom) fillers. Particles have been dispersed by ultrasonication and centrifugal mixing (left) and by just centrifugal mixing (right). Two-step dispersion resulted in smaller and lump-free agglomerates than by sole centrifugal mixing regardless of particle functionalization. The latter, however, contributed to smaller agglomerates.

electron microscopy (SEM) photomicrograph (Figure 7.18A) [31]. However, it was reported that the exact mechanism of smear layer treatment is not clear with the nano-RMGI primer [32]. The use of Ketac nanoprimer does not require the preconditioning step; nevertheless the use of either 37% phosphoric acid or Ethylene Diamine Tetra Acetic acid (EDTA) solution prior to the application of the Ketac nanoprimer to dentin significantly improved the bond strength. In SEM photomicrographs (Figure 7.18B), the nanofillers were distributed within the hybrid layer and around the orifices of the funnel-shaped dentinal tubules [31]. Unfortunately, the studies on the adhesion of Ketac-nano primer was evaluated after 24 h storage period. However, long-term water storage or long-term clinical evaluation is required to evaluate its bonding durability.

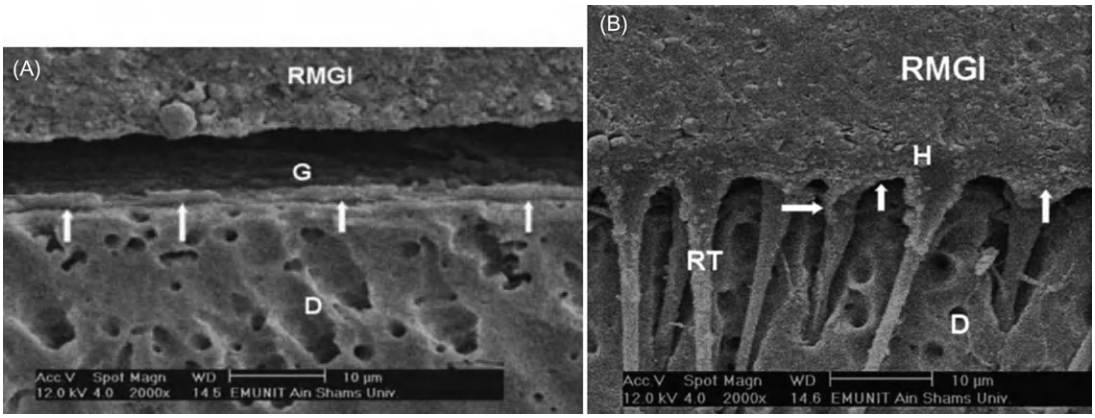

FIGURE 7.18

(A) SEM photomicrograph of nanofilled RMGI/dentin interface treated with Ketac nanoprimer. No evidence of hybrid layer or resin tag extensions, with a gap (G) between the restoration and underlying dentin. Smear layer remnants (arrows) are noticed over the dentin surface. RMGI, nanofilled resin-modified glass ionomer; D, dentin. (B) SEM photomicrograph of nanofilled RMGI/dentin interface treated with 35% phosphoric acid before the application of Ketac nanoprimer. Numerous long, funnel-shaped resin tag extensions (RT) with a thick hybrid layer (H). Fillers distributed at the bottom of and within the hybrid layer as well as around the orifices of the dentinal tubules (arrows).

From Ref. 31.

7.6 Nanoleakage

Nanometer-sized porosities within the hybrid layer were first described by Sano et al. [33–35]. By observing the penetration of silver nitrate along gap-free margins with several dentin bonding systems under SEM or transmission electron microscopy (TEM), they described a leakage pattern occurring within the nanometer-sized spaces around the collagen fibrils within the hybrid layer. They termed this phenomenon as "nanoleakage." This represents permeation laterally through the hybrid layer and may be the result of incomplete infiltration of adhesive resin into the demineralized dentin. This kind of leakage may allow the penetration of bacterial products and dentinal or oral fluid along the interface, which may result in hydrolytic breakdown of either the adhesive resin or collagen within the hybrid layer, thereby compromising the stability of the resin–dentin bond [36].

Recently, a 50 wt% ammoniacal silver nitrate solution has been used to detect nanometer-sized defects in bonds analyzed by SEM [37] or TEM [38]. Several recent TEM studies (Figure 7.19) [39] have revealed several types of nanoleakage (i.e., spotted, reticular patterns, and water tree). Recently developed resin adhesives contain more acidic hydrophilic monomers and higher amounts of water to improve monomer impregnation into wet dentin substrate, resulting in lower degrees of polymerization of adhesive resin. This results in increased silver uptake into the hybrid and adhesive layers (i.e., increased nanoleakage). In addition, it has been reported that there is often a discrepancy between the depth of acid etching and the degree of resin infiltration and exposed collagen network [40]. This

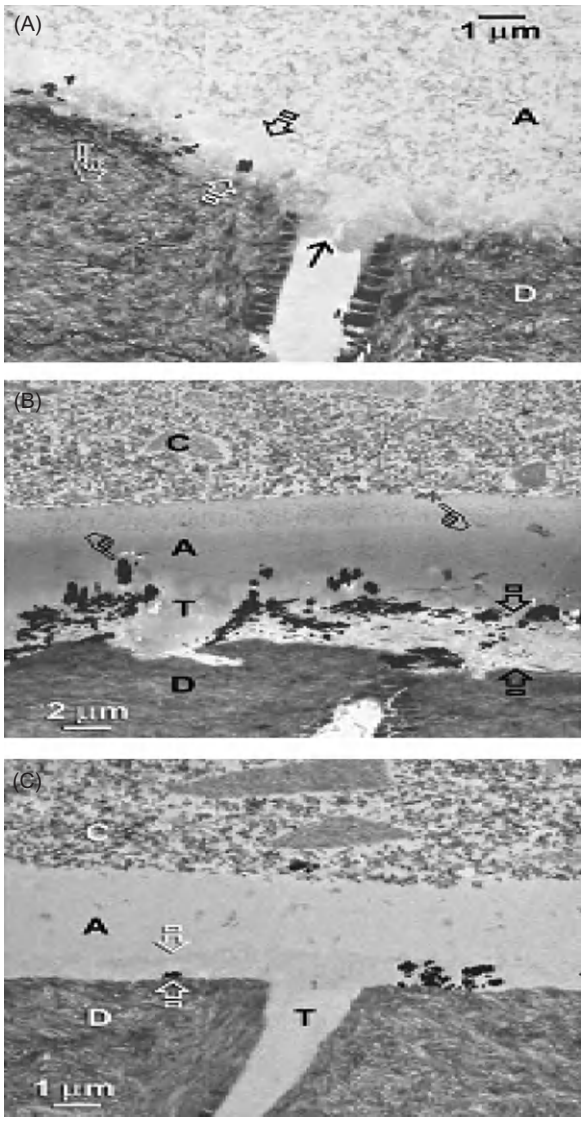

FIGURE 7.19

Different nanoleakage patterns as shown by TEM images. (A) An example of two-step self-etch adhesives (Clearfil SE Bond) in which a thin basal zone of fine, reticular silver deposits (pointer) was occasionally observed beneath the hybrid layer (between open arrows). C, composite; A, filled adhesive; arrow, smear plug; D, mineralized dentin. (B) Adper Prompt and (C) AdheSE. Examples of one-step and two-step self-etch adhesives in which a basal zone of fine, reticular silver deposits was not observed beneath the hybrid layer, despite the presence of nanoleakage within the completely demineralized hybrid layer (between open arrows). In Adper Prompt, silver impregnation (pointers) was also observed to extend within the adhesive layer beneath the composite (C).

region may be another site for silver uptake. Although the amount of nanoleakage may be very small (nanometer size) in the bonded assembly, it has the potential to serve as a pathway for water movement within the adhesive–dentin interface over time. The water movement within the adhesive–dentin interface may extract unconverted monomers from resin adhesive or hybrid layer which contributes to reductions of bond strength [41]. Therefore, the effect of nanoleakage on the bond strength, and on the integrity of resin–dentin bonds has gained importance not only for short-term, but especially for long-term adhesion. Evaluation of silver uptake (i.e. nanoleakage evaluation) provides good spatial resolution of submicron defects in resin infiltration or inadequate polymerization. Nanometer-sized spaces within resin–dentin interfaces, evidenced by the nanoleakage technique, might be large enough for enzymes to enter [42]. It is currently believed that exposed collagen fibrils in resin–dentin interfaces might be digested by host-derived matrix metalloproteinases (MMPs) [43].

MMPs were identified in either nonmineralized or mineralized compartments of human dentin matrices. MMPs belong to a group of zinc- and calcium-dependent enzymes that have been shown to be able to cleave native collagenous tissues at neutral pH in the metabolism of all connective tissues. Dentin matrix has shown to contain at least four MMPs: the stromelysin-1 (MMP-3), the true collagenase (MMP-8), and the gelatinases A and B (MMP-2 and MMP-9, respectively). These host-derived proteases are thought to play an important role in numerous physiological and pathological processes occurring in dentin, including the degradation of collagen fibrils that are exposed by suboptimally infiltrated dental adhesive systems after acid etching [44].

7.7 Atomic force microscopy in the field of dental adhesion

Atomic force microscopy (AFM) is one of the most important tools in the field of nanoscience and nanotechnology. AFM could be used for the study of microstructure of dental substrates and can supply valuable data in this field. It could also be used in the field of characterization of resin tooth bonds by studying nanoscale mechanical properties of the dental adhesive junctions so that the quality of hybrid layers could be assessed in terms of its elastic modulus and hardness by nanoindentation. Many research tools were used to investigate microstructure of hard dental substrates. These tools included SEM and TEM. Extensive sample preparation and coating for SEM or TEM technique arises the problem of viewing and imaging samples in their natural conditions. On the contrary to SEM and TEM, scanning probe microscopes and, in particular, AFM has facilitated the imaging and analysis of biological surfaces with little or no sample preparation. AFM can operate in air or in liquid, and the imaging of macromolecules like proteins or DNA has been reported by several authors [45]. AFM could be used to investigate the effect of conditioner on dentin morphology and structure, giving clinicians more knowledge and better understanding of the adhesion procedure and problems associated with it.

Dentin collagen fibrils were studied in situ by AFM (Figure 7.20). New data on size distribution and the axial repeat distance of hydrated and dehydrated collagen type-I fibrils are presented [46]. This method provides additional insight into the structure and organization of dentin collagen and may contribute to a better understanding of alterations in collagen structure induced by chemical or biochemical treatments, age, or diseases. Modeling of the fibril structure using these data is encouraged to better understand the effect of dehydration on the molecular level [46].

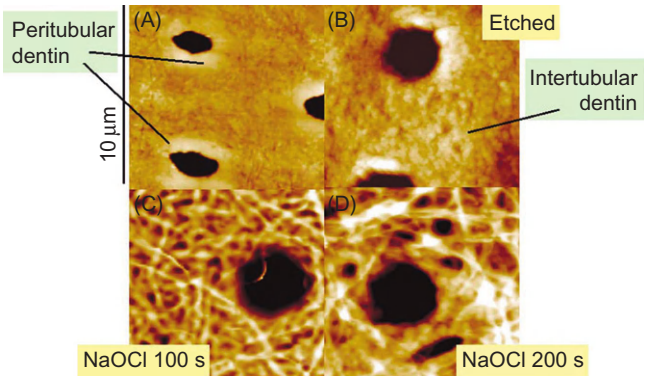

FIGURE 7.20

AFM images showing open dentinal collagen network after acid etching followed by NaOCl treatment.

From Ref. [46]—needs permission.

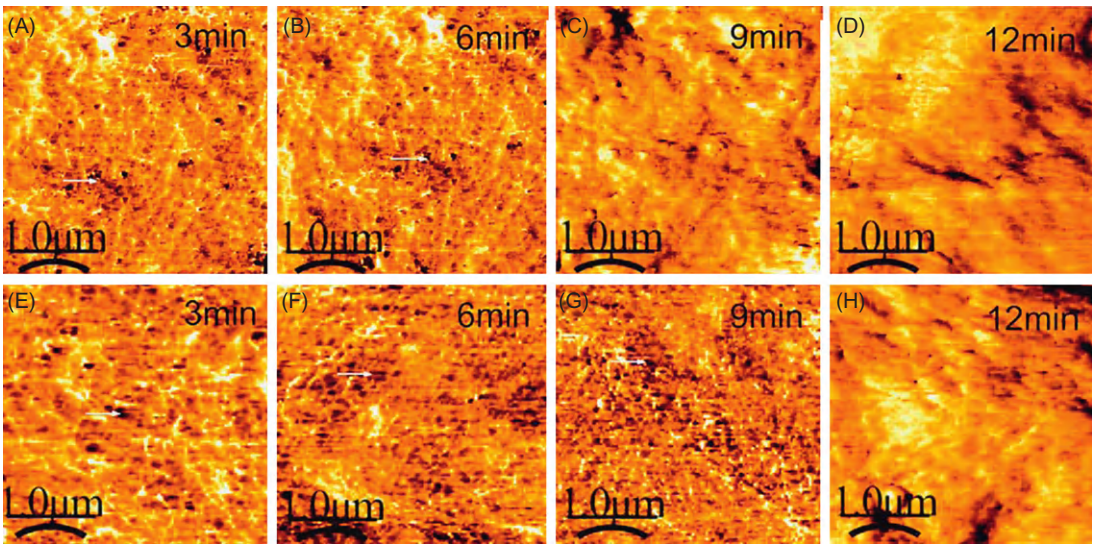

FIGURE 7.21

AFM images of acid-etched dentinal collagen showing dehydration collapse of collagen network by time for superficial dentin (A–D) and deep dentin (E–H).

El Feninat et al. [47] used AFM to study the air drying of etched dentin. Air drying resulted in the collapse of the collagen network but not in the denaturation of collagen fibrils. This study indicated that collapse and denaturation are separate phenomena. It further showed that water loss occurred rapidly and disrupted the native conformation of the collagen network. This could have adverse effects on adhesion. It was shown that it is possible to obtain images of demineralized

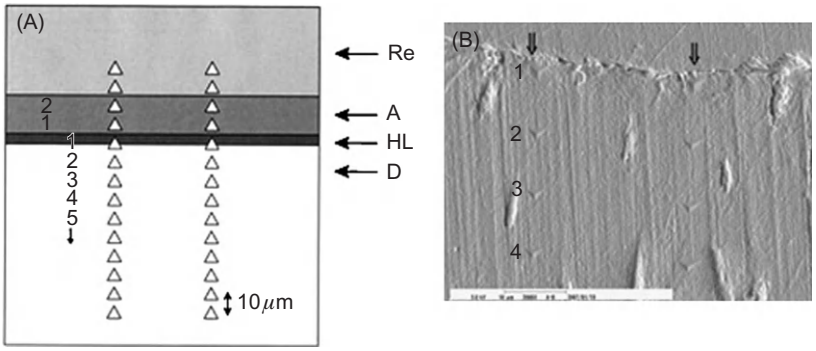

FIGURE 7.22

Nanoindentation along composite, adhesive layer, hybrid layer, and dentin for nanoscale mechanical evaluation of the adhesive junction.

dentin having the same morphology as those shown by field-emission SEM, but without the need for coating or sample preparation. Another important AFM study on collagen collapse due to dehydration was conducted by Fawzy [48] where he showed that the ability of the demineralized dentin collagen network to resist air dehydration and to preserve the integrity of open network structure with the increase in air exposure time is increased with dentin depth (Figure 7.21).

Another important aspect of AFM as a research tool in the field of adhesion is nanoindentation (Figure 7.22) to evaluate mechanical properties of adhesive junctions and hybrid layers [49].

Sauro et al. [50] studied the quality of resin dentin interfaces using AFM nanoindentation and they found that a HEMA-containing adhesive applied onto phosphoric acid etched ethanol or water-wet dentin created hybrid layers with the lowest biomechanical nanoproperties. Nanoindentation allows the investigation of selected material properties on small amounts of materials, based on the load-displacement data of indentations on a submicron scale. Measurement of mechanical properties by nanoindentation has been suggested as advantageous over the conventional methods for its high resolution of force and accurate indent positioning [51–53]. This method has been used to measure the elastic modulus and hardness of the dental adhesives by some researchers [51,52,54].

7.8 How can nanoscience and nanotechnology improve the outcome of clinical adhesive dentistry?

Based on nanoleakage data and extensive research on the degradation of the adhesive bonds, the following approaches seem to be promising in the field of clinical adhesive dentistry.

7.8.1 Use of hydrophobic coating

Since the incorporation of hydrophilic monomer blends in simplified adhesives (two-step etch-and-rinse and one-step self-etch adhesives) dramatically reduced bond longevity, the need of a hydrophobic coating with a not-solvated bonding layer seems to be pivotal to reduce water sorption and

stabilize the hybrid layer over time, i.e., etch-and-rinse three steps and self-etch two-step adhesives should be preferred to simplified ones. Also applying a hydrophobic layer on one-step self-etching adhesives could improve bond strength and durability [55].

7.8.2 Extended polymerization time

Extending the curing times of simplified adhesives beyond those recommended by the manufacturers resulted in improved polymerization and reduced permeability and appears to be a possible means for improving the performance of these adhesives [56].

7.8.3 Use of MMPs inhibitors

The use of MMPs inhibitors as additional primer has been claimed to reduce interfacial aging over time by inhibiting the activation of endogenous dentin enzymes which are responsible for the degradation of collagen fibrils in the absence of bacterial contamination [57]. The recent finding that chlorhexidine (CHX) also has potent anti-MMP-2, -8, and -9 activity encouraged some researchers to determine whether CHX could stabilize the organic matrix of resin–dentin bonds. This led to numerous in vitro [58] and in vivo studies [59] that demonstrated that CHX has beneficial effects on the preservation of resin–dentin bonds, thereby offering a valuable alternative to clinicians who seek to delay the degradation process of adhesive restorations. The effectiveness of CHX, as an antimicrobial or an antiproteolytic agent, has been reported to be related with its substantivity to oral/dental structures [60]. Substantivity is the prolonged association between a material (e.g.,

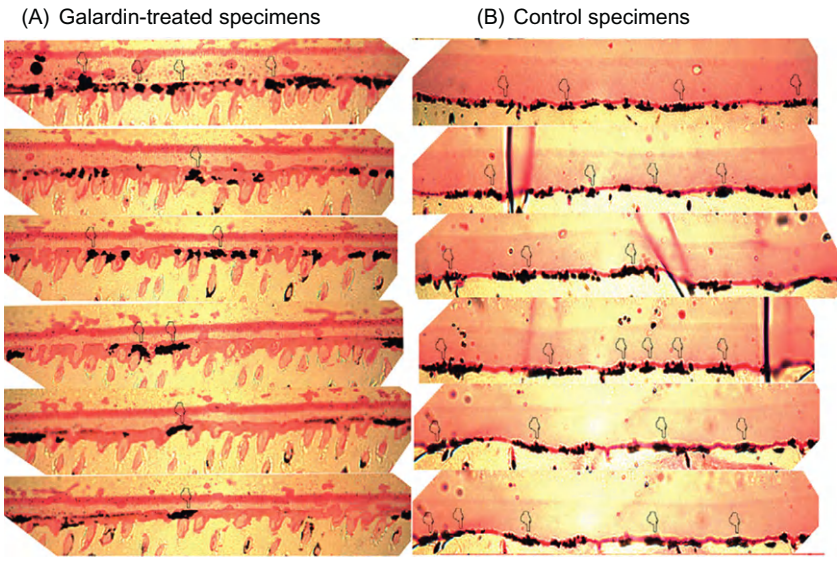

FIGURE 7.23

Much less nanoleakage as demonstrated by silver depositions with galardin-treated specimens (A). Compared with non treated specimens (B).

CHX) and a substrate (e.g., oral mucosa, oral proteins, dental plaque, or dental surface), an association that can be greater and more extended than would be expected from a simple deposition mechanism. It is considered that the delivery of an agent to its site of action in a biologically active form and in effective doses increases the effects for prolonged periods of time. Substantivity of CHX or its ability to be retained in dentin matrices could be the reason why CHX-treated acid-etched dentin may form hybrid layers that are more stable over time. Recently Breshi et al. [61] investigated the pretreatment of dentin with a specific MMP inhibitor galardin (Figure 7.23). The inhibitory effect of galardin on dentinal MMPs was confirmed by zymographic analysis as complete inhibition of both MMP-2 and -9 was observed. The use of galardin had no effect on immediate bond strength while it significantly decreased bond degradation after 1 year. Interfacial nanoleakage expression after aging revealed reduced silver deposits in galardin-treated dentin compared to untreated dentin.

7.8.4 Improved impregnation

Various methods have been recently proposed to enhance dentin impregnation, i.e., prolonged application time, vigorous brushing technique, and electric impulse assisted adhesive application [62]. The latter technique recently revealed increased bond strength and reduced nanoleakage expression if adhesives are applied under the effects of an electric signal. Junior et al. [63] improved impregnation of dentinal collagen by adhesives via the evaporation of adhesive solvent by a stream of warm air (Figure 7.24). The use of a warm air-dry stream to evaporate the solvent of adhesives seems to be a clinical tool to improve the bond strength and the quality of the hybrid layer (less nanoleakage infiltration).

Another approach to improve impregnation of collagen by the adhesive after acid etching was the simultaneous acid etching and deproteinization suggested by Nassif and El Korashy [64]. The simultaneous etching and deproteinization by NaOCl/phosphoric acid for 15 s showed a hybrid layer with improved bond strength. This was attributed to removal of shredded collagen found in the smear layer that could not be removed by acid etching only. Removal of this disorganized collagen would give more open structure to the collagen network and improve its impregnation by the adhesive.

7.8.5 Wet ethanol bonding approach

Tay et al. [65] proposed the ethanol-wet bonding technique. Ethanol is used to replace water just prior to bonding, thus avoiding the collapse of the collagen matrix. Ethanol-wet dentin may permit the infiltration of hydrophobic monomers to disperse into the demineralized dentin, creating a hydrophobic hybrid layer. Since the concept of ‘‘ethanol-wet bonding’’ was proposed, various ethanol-wet protocols have been developed to optimize this technique [66,67]. The ethanol-wet bonding is a time-consuming technique since it needs consecutive application of ascending concentrations of ethanol. A simplified protocol for wet ethanol bonding to dentin was suggested by Sadek et al. [68]. They suggested a protocol of reduced time for each ascending ethanol concentration application to dentin prior to bonding. This technique achieved high bond strengths, minimal nanoleakage infiltration, and maintained bond stability after 6 months of artificial aging. A shorter dehydration period (135 s) may render the bonding of hydrophobic monomers to dentin easily.

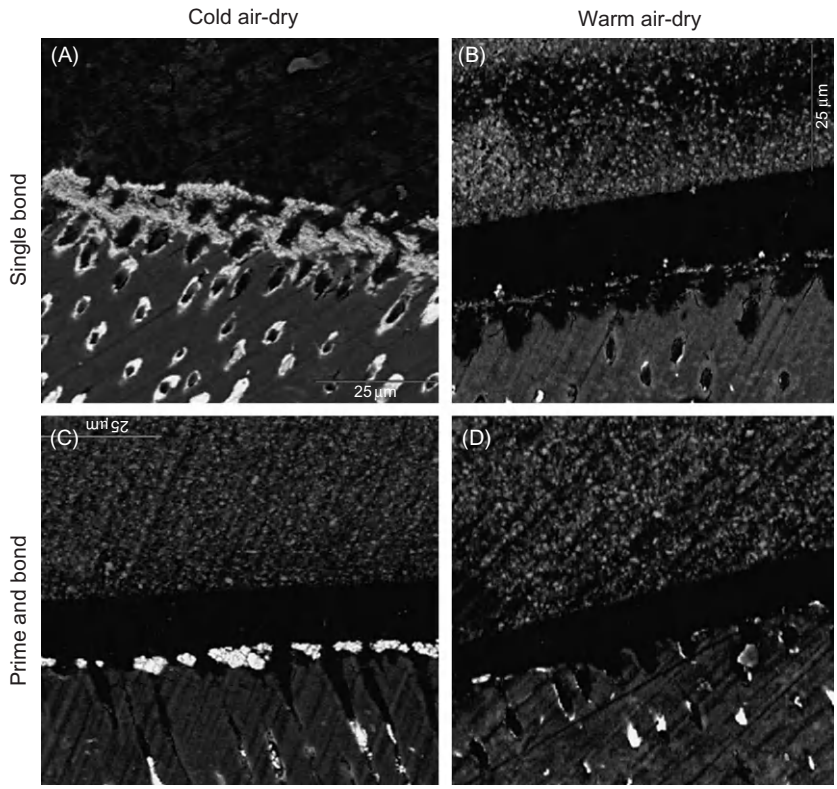

FIGURE 7.24

SEM photomicrographs showing less nanoleakage (Ag deposition) after warm air drying of the adhesive.

However, biocompatibility issues and bond stability over longer storage periods should be addressed before such a technique may be recommended for clinical use.

7.8.6 Improving dental collagen network mechanical properties prior to bonding

Priming acid-etched dentin with glutaraldehyde before application of the adhesive is one of the suggested methods to improve bond strength and durability [69]. Glutaraldehyde, a substance that has been used in the adhesive dentistry field, appears to be a potential element to improve demineralized dentin properties. Its capacity to fix proteins irreversibly [70] and to increase the modulus of elasticity of collagen fibrils [71] is of great interest to maintain the collagen structure in position during bonding. In addition, its well-reported ability to react chemically with collagen and resin components such as HEMA [72] may also contribute to facilitating adhesive system penetration into and wettability of the dentin substrate.

7.8.7 Enhancing biomimetic remineralization

Biomimetic remineralization is a process that allows remineralization of dentinal collagen fibrils around and within collagen that still have intermolecular cross-links, like collagen fibrils in caries-affected dentin and phosphoric acid demineralized dentin. Biomimetic remineralization helps the rebuilding of dentin minerals in the same hierarchical pattern of apatite nanocrystals deposition both intrafibrillar and interfibrillar.

Tay and Pashly [73] suggested a guided remineralization of partially demineralized human dentin where they used set white Portland cement as a source of Ca ions in a phosphate-containing fluid to precipitate apatite nanocrystals around demineralized collagen. When polyvinyl phosphonic acid and PAA were included, these nanoprecursors were attracted to the acid-demineralized collagen matrix and transformed into polyelectrolyte-stabilized apatite nanocrystals that assembled along the microfibrils (intrafibrillar remineralization) and surface of the collagen fibrils (interfibrillar remineralization). Transition from nanocrystals to larger apatite platelets probably occurred via the formation of mesocrystal intermediates. Guided tissue remineralization is potentially useful in the remineralization of acid-etched dentin that is incompletely infiltrated by dentin adhesives as well as partially demineralized caries-affected dentin. Gandolfi et al. [74] suggested the use of bioactive "smart" composites containing reactive calcium-silicate Portland-derived mineral powder as tailored filler. This innovative method for the biomimetic remineralization of apatite-depleted dentin surfaces and for preventing the demineralization of hypomineralized/carious dentin could be potentially great advantage in clinical applications.

7.9 Future prospective of nanotechnology in the field of adhesive dentistry

7.9.1 On-demand antibacterial adhesives

Welch et al. [75] incorporated TiO_2 nanoparticles in dental adhesives aiming at achieving the combined features of bioactivity and on-demand bactericidal effect. The photocatalytic activity of adhesives containing TiO_2 nanoparticles, initiated by UV irradiation, proved to interfere with bacterial activity. Also TiO_2 nanoparticles-containing adhesives were found to have the potential of tooth remineralization in simulated body fluids. This could open up the potential to create dental adhesives that reduce the incidence of secondary caries and promote closure of gaps forming at the interface toward the tooth via remineralization of adjacent tooth substance as well as prevention of bacterial infections via on-demand UV irradiation.

7.9.2 Improving adhesive polymerization through catalytic activity of nanoparticles

Nanoparticles could improve DC of adhesive polymers yielding an adhesive layer with improved mechanical properties and resistance to degradation. Yasumoto et al. [76] used colloidal platinum nanoparticles as a pretreatment to dentin after acid etching and before adhesive application to improve the resin polymerization resulting in enhanced bond strength. Based on the same principle,

Sun et al. [28] showed that TiO_2 nanoparticles in adhesives could improve DC and mechanical properties expecting better bond strength and durability.

7.9.3 Antibacterial orthodontic adhesives containing nanosilver

Enamel demineralization is a commonly recognized complication of orthodontic treatment with fixed appliance. Preventing these lesions is an important concern for orthodontists because the lesions are unesthetic, unhealthy, and potentially irreversible. The introduction of antibacterial adhesives would improve the outcome of orthodontic treatment due to less bacterial adhesion to the orthodontic appliance. Ahn et al. [77] suggested an orthodontic adhesive containing nanosilver particles as antimicrobial agent. The adhesive showed less bacterial adhesion and less bacterial growth without affecting bond strength.

7.9.4 Radiopaque dental adhesives

Secondary caries may be detected visually by the discolorations at the tooth/restoration interface, though X-ray photographs are often required to safely discriminate such lesions from stained margins. Radiographs rely on the difference in radiopacity between healthy dental tissue, cariogenic hard tissue, and restorative material. Modern composite-filling materials commonly contain radiopaque components, such as Sr- or Ba-glass fillers, making them easily distinguishable by X-ray from the tooth. Dental adhesives, however, do not contain such radiopaque materials today making them hard to distinguish from caries. Schulz et al. [23] focused on the development of radiopaque adhesives by incorporating flame-made Ta_2O_5/SiO_2 nanoparticles in methacrylic matrices. The nanofilled adhesive had radiopacity better than enamel and dentin without adverse effect on bonding to hard dental tissues.

7.9.5 Self-adhesive composites

The introduction of self-adhesive composites will offer clinicians the simple approach toward the restorative procedure by eliminating the number of steps associated with bonding procedure. The latest trend has been toward the development of flowable composites containing adhesive monomers such as Vertise Flow (Kerr) and Fusio Liquid Dentin (Pentron Clinical). These formulations are based on traditional methacrylate systems, but incorporating acidic monomers typically found in dentin bonding agents such as glycerol phosphate dimethacrylate in Vertise Flow may be capable of generating adhesion through mechanical and possibly chemical interactions with tooth structure. These materials are currently recommended for liners and small restorations and are serving as the entry point for universal self-adhesive composites [78].

7.9.6 Self-healing adhesives

The concept of self-healing polymers relies on encapsulation of monomers and catalyst and incorporating these encapsulated healing precursors into the polymer. When cracks are initiated in the polymer, the capsules rupture and healing monomers fill the crack and polymerize there allowing healing of the crack. In the field of dental adhesion, self-healing bonding resins may provide a new

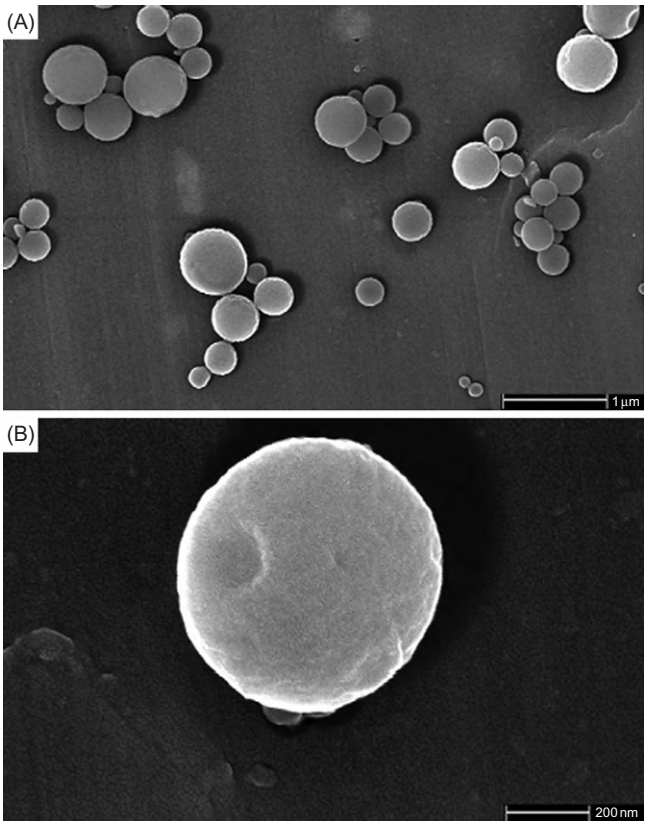

FIGURE 7.25

Field Emission Scanning Electron Microscope (FESEM) micrographs of nanocapsules (A and B). FESEM micrographs indicate that the TEGDMA nanocapsules are spherical with smooth and condense surface.

direction for the improvement of the bonding durability. To allow the healing precursors in dental adhesives to reach the submicron spaces created by acid etching within dentin, the need for nanoencapsulation is needed. Ouyang et al. [79] prepared, characterized, and incorporated polyurethane nanocapsules encapsulated with the core material TEGDMA for use as a major component in a self-healing bonding resin (Figure 7.25). The incorporation of nanoencapsulated monomers in dental adhesives showed enhancement of bond strength and expected to improve durability of resin tooth bonding (Figure 7.26).

7.9.7 High-speed AFM

The future advancement in research tools will improve our understanding of adhesion and will further clarify the associated obstacles. One of the most promising tools is the high-speed AFM (HS-AFM), which is becoming a reference tool for the study of dynamic biological processes.

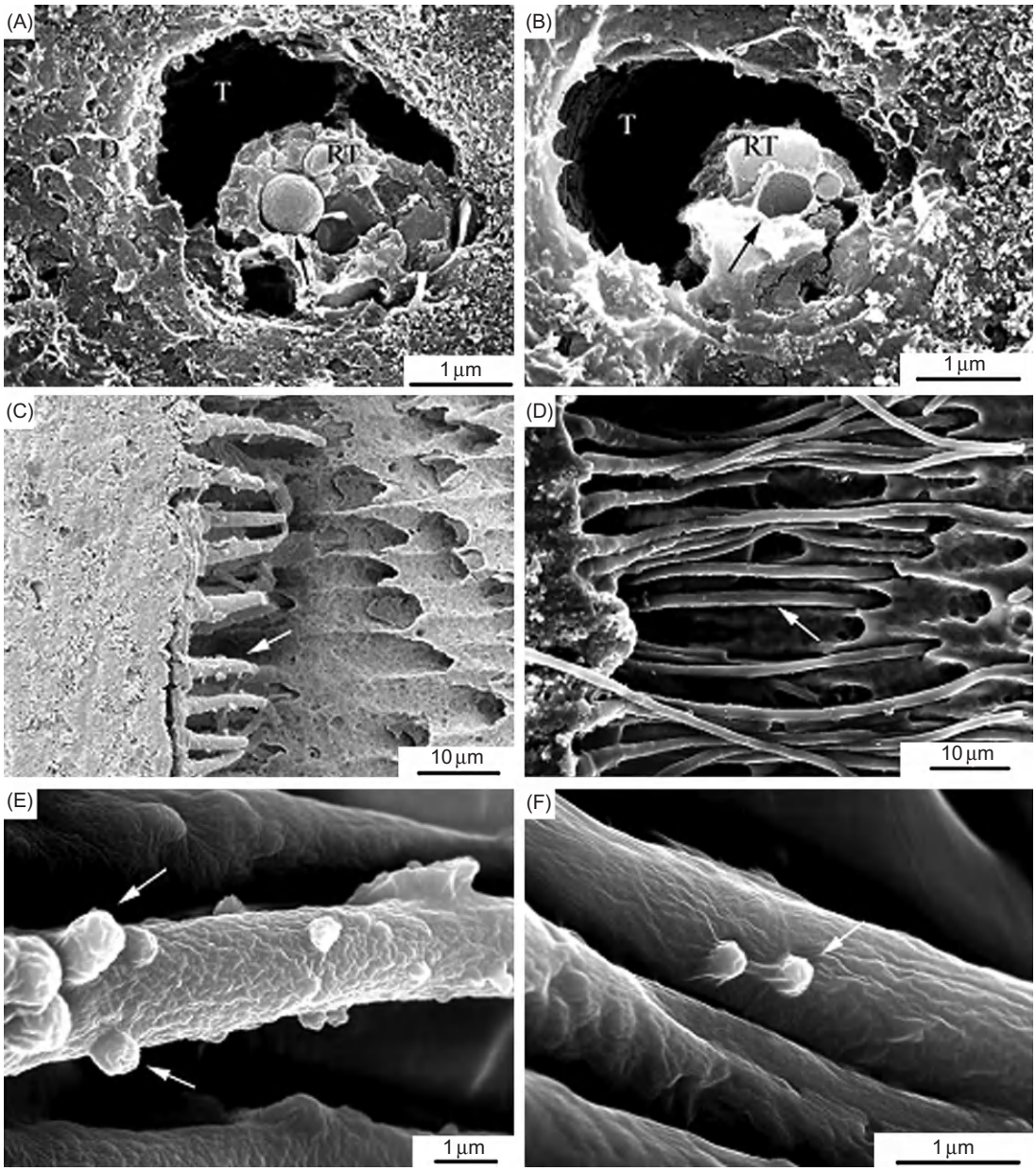

FIGURE 7.26

FESEM observations of the adhesive/dentin interfaces. (A, B) FESEM images of dentin (D) surface show that TEGDMA nanocapsule (black arrow) surrounded by adhesive are infiltrated into dentinal tubule (T) with resin tag (RT). (C, D) FESEM micrograph of the adhesive/dentin interface bonded with Prime & Bond NT or Prime & Bond NT incorporated with TEGDMA nanocapsules. The resin tags (white arrow) were longer and more regular as compared with the control. (E, F) Local magnification from (D) shows that TEGDMA nanocapsules (white arrows) could be notified on the surface of resin tag (RT).

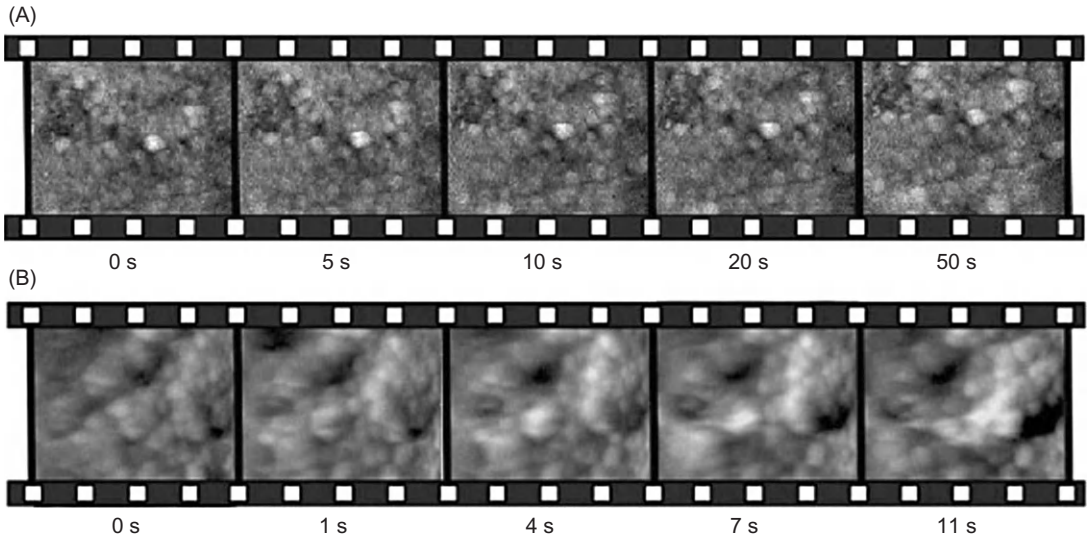

FIGURE 7.27

Sequences of HS-AFM images of an HAP surface taken (A) in water (3 μm × 3 μm) and (B) in citric acid at pH 3 (1.5 μm × 1.5 μm). Time is indicated in seconds under each image.

From Ref. [81].

The spatial and time resolutions of HS-AFM are on the order of nanometers and milliseconds, respectively, and allow structural and functional characterization of biological processes at the single-molecule level [80]. Pyne et al. [81] used HS-AFM to study the demineralizing effect of citric acid on enamel. They imaged the dissolution of enamel in a real time or movie mode and concluded that the HS-AFM is able to follow the large changes in height (on the micrometer scale) that occur during the dissolution process (Figure 7.27). Such real-time imaging can provide dental profession with valuable data on how surface conditioner interacts with dental substrates and how we can make use of these data to improve the outcome of the restorative procedures.

7.10 Conclusions and future directions

Nanoscience and nanotechnology will have strong impact on adhesion to dental substrates through the development of nanofilled dental adhesives with improved mechanical properties. Stronger adhesive junctions with much less defects and more durability will be achieved through improved penetration of the adhesives, antibacterial potential, and self-healing capacity.

Adhesion to oral mucosa will be an efficient route of nanodrug delivery where oral adhesive patch, tablets, or stripes could be loaded with nanocarriers with controlled drug release and other benefits could be obtained through administering the drugs via buccal mucosa. Among the various

transmucosal routes, buccal mucosa has excellent accessibility, an expanse of smooth muscle, and relatively immobile mucosa, and hence suitable for administration of retentive dosage forms. Direct access to the systemic circulation through the internal jugular vein bypasses drugs from the hepatic first-pass metabolism leading to high bioavailability. Other advantages such as low enzymatic activity, suitability for drugs or excipients that mildly and reversibly damages or irritates the mucosa, painless administration, easy drug withdrawal, facility to include permeation enhancer/enzyme inhibitor or pH modifier in the formulation, and versatility in designing as multidirectional or unidirectional release systems for local or systemic actions opt buccal adhesive drug delivery systems as a promising option [82].

References

[1] I. Kramer, J. McLean, Alterations in the staining reactions of dentin resulting from a constituent of a new self-polymerizing resin, Br. Dent. J. 93 (1952) 150−153.
[2] M. Buonocore, A simple method of increasing the adhesion of acrylic filling materials to enamel surfaces, J. Dent. Res. 34 (1955) 849−853.
[3] M. Peters, M. McLean, Minimally invasive operative care. I. Minimal intervention and concepts for minimally invasive cavity preparations, J. Adhes. Dent. 3 (2001) 7−16.
[4] B. Meerbeek, J. Perdiggo, P. Lambrecht, G. Vanherle, The clinical performance of adhesives, J. Dent. 26 (1998) l−20.
[5] J. De Munck, K. Van Landuyt, M. Peumans, A. Poitevin, P. Lambrechts, M. Braem, et al., A critical review of the durability of adhesion to tooth tissue: methods and results, J. Dent. Res. 84 (2005) 118−132.
[6] A. Gwinnett, A.J. Matsui, A study of enamel adhesives. The physical relationship between enamel and adhesives, Arch. Oral. Biol. 12 (1967) 1615−1620.
[7] N. Nakabayashi, K. Kojima, E. Masuhara, The promotion of adhesion by the infiltration of monomers into tooth substrates, J. Biomed. Mater. Res. 16 (1982) 1240−1243.
[8] T. Fusayama, New Concepts in Operative Dentistry, Quitessence Publishing Co., Inc, Tokyo, 1980, pp. 61−156.
[9] J. Kanca, Improved bond strength through acid-etching of dentin and bonding to wet dentin surfaces, J. Am. Dent. Assoc. 123 (1992) 35−43.
[10] D. Pashley, F. Tay, L. Breschi, L. Tjaderhane, R. Carvalho, M. Carrilho, et al., State of the art etch-and-rinse adhesives, Dent. Mater. 27 (2011) 1−16.
[11] D. Pashley, J. Horner, P. Brewer, Interactions of conditioners on the dentin surfaces, Oper. Dent. 17 (Suppl. 5) (1992) 127−150.
[12] M. Cadenaro, L. Breschi, F. Rueggeberg, M. Suchko, E. Grodin, K. Agee, et al., Effects of residual ethanol on the rate and degree of conversion of five experimental resins, Dent. Mater. 25 (2009) 621−628.
[13] B. Van Meerbeek, J. De Munck, Y. Yoshida, S. Inoue, M. Vargas, P. Vijay, Buonocore memorial lecture. Adhesion to enamel and dentin: current status and future challenges, Oper. Dent. 28 (2003) 215−235.
[14] B. Van Meerbeek, K. Yoshihara, Y. Yoshida, A. Mine, J. De Munck, K. Van Landuyt, State of the art of self-etch adhesives, Dent. Mater. 27 (2011) 17−28.
[15] Y. Yoshida, K. Nagakane, R. Fukuda, Y. Nakayama, M. Okazaki, H. Shintani, et al., Comparative study on adhesive performance of functional monomers, J. Dent. Res. 83 (2004) 454−458.

[16] K. Van Landuyt, J. Snauwaert, J. De Munck, M. Peumans, Y. Yoshida, A. Poitevin, et al., Systematic review of the chemical composition of contemporary dental adhesives, Biomaterials 28 (2007) 3757–3785.
[17] A. Takahashi, Y. Sato, S. Uno, P. Pereira, H. Sano, Effect of mechanical properties of adhesive resin on bond strength to dentin, Dent. Mater. 18 (2002) 263–268.
[18] H. Honmoto, Study on light cured composite resins—effect of filler contents in the bonding agent on the tensile bond strength to enamel, Nihon. Univ. Dent. J. 65 (1991) 246–257.
[19] M. Miyazak, S. Ando, K. Hinoura, H. Onose, B. Moore, Influence of filler addition to bonding agents on shear bond strength to bovine dentin, Dent. Mater. 11 (1995) 234–238.
[20] M. Conde, C. Zanchi, S. Junior, N. Carreno, F. Ogliari, E. Piva, Nanofiller loading level: influence on selected properties of an adhesive resin, J. Dent. 37 (2009) 331–335.
[21] F. El-Askary, R. van Noort, The effect of airy-drying pressure and distance on the microtensile bond strength of a self-etching adhesive, J. Adhes. Dent. 11 (2011) 135–147.
[22] K. Ikemora, F. Tay, Y. Kouro, T. Endo, M. Yoshiyama, K. Miyai, et al., Optimizing filler content of an adhesive containing pre-reacted glass ionomer fillers, Dent. Mater. 19 (2003) 137–146.
[23] H. Schulz, B. Schimmoeller, S. Pratsinis, U. Salz, T. Bock, Radiopaque dental adhesives: dispersion of flame-made Ta2O5/SiO2 nanoparticles in methacrylic matrices, J. Dent. 36 (2008) 579–587.
[24] Y. Yoshida, B. Van Meerbeek, Y. Nakayama, J. Snauwaert, L. Hellemans, P. Lambrechts, et al., Evidence of chemical bonding at biomaterial-hard tissue interfaces, J. Dent. Res. 79 (2000) 709–714.
[25] Y. Zhang, Y. Wang, Hydroxyapatite effect on photopolymerization of self-etching adhesives with different aggressiveness, J. Dent. 40 (2012) 564–570.
[26] Y. Zhang, Y. Wang, The effect of hydroxyapatite presence on the degree of conversion and polymerization rate in a model self-etching adhesive, Dent. Mater. 28 (2010) 237–244.
[27] M. Shojai, M. Atai, A. Nodehi, L. Khanlarb, Hydroxyapatite nanorods as novel fillers for improving the properties of dental adhesives: synthesis and application, Dent. Mater. 26 (2010) 471–482.
[28] J. Sun, A. Forster, P. Johnson, N. Eidelman, G. Quinn, G. Schumacher, et al., Improving performance of dental resins by adding titaniumdioxide nanoparticles, Dent. Mater. 27 (2011) 972–982.
[29] M. Atai, L. Solhi, A. Nodehi, S. Mirabedini, S. Kasraei, K. Akbari, et al., PMMA-grafted nanoclay as novel filler for dental adhesives, Dent. Mater. 25 (2009) 339–347.
[30] L. Solhi, M. Atai, A. Nodehi, M. Imani, A. Ghaemi, K. Khosravi, Poly(acrylic acid) grafted montmorillonite as novel fillers for dental adhesives: synthesis, characterization and properties of the adhesive, Dent. Mater. 28 (2012) 369–377.
[31] F. El-Askary, M. Nassif, Bonding nano-filled resin modified glass ionomer to dentin using different self etch adhesives, Oper. Dent. 36 (2011) 413–421.
[32] E. Coutinho, M. Cardoso, J. De Munck, A. Neves, K. Van Landuyt, A. Poitevin, et al., Bonding effectiveness and interfacial characterization of a nano-filled resin-modified glass-ionomer, Dent. Mater. 25 (2009) 1347–1357.
[33] H. Sano, T. Shono, T. Takatsu, H. Hosoda, Microporous dentin zone beneath resin-impregnated layer, Oper. Dent. 19 (1994) 59–64.
[34] H. Sano, T. Takatsu, B. Ciucchi, A. Herner, W. Mattews, D. Pashley, Nanoleakage: leakage within the hybrid layer, Oper. Dent. 20 (1995) 18–25.
[35] H. Sano, M. Yoshiyama, S. Ebisu, M. Burrow, T. Takatsu, B. Ciucchi, et al., Comparative SEM and TEM observations of nanoleakage within the hybrid layer, Oper. Dent. 20 (1995) 160–167.
[36] H. Li, M. Burrow, M. Tyas, Nanoleakage patterns of four dentin bonding systems, Dent. Mater. 16 (2000) 48–56.
[37] T. Pioch, H. Staehle, H. Duschner, F. Godoy, Nanoleakage at the composite–dentin interface: a review, Am. J. Dent. 14 (2001) 252–258.

[38] F. Tay, D. Pashley, M. Yoshiyama, Two modes of nanoleakage expression in single-step adhesives, J. Dent. Res. 81 (2002) 472–476.
[39] A. Gwinnet, F. Tay, M. Pang, S. Wei, Quantitative contribution of the collagen network in dentin hybridization, Am. J. Dent. 9 (1996) 140–144.
[40] A. Gwinnet, S. Yu, Effect of long-term water storage on dentin bonding, Am. J. Dent. 7 (1994) 109–111.
[41] M. Hashimoto, J. De Munck, S. Ito, H. Sano, M. Kaga, H. Oguchi, et al., In vitro effect of nanoleakage expression on resin-dentin bond strengths analyzed by microtensile bond test, SEM/EDX and TEM, Biomaterials 25 (2004) 5565–5574.
[42] R. Carvalho, S. Chersoni, R. Frankenberger, D. Pashley, C. Prati, F. Tay, A challenge to the conventional wisdom that simultaneous etching and resin infiltration always occurs in self-etch adhesives, Biomaterials 26 (2005) 1035–1042.
[43] A. Reisa, M. Giannini, P. Pereira, Long-term TEM analysis of the nanoleakage patterns in resin–dentin interfaces produced by different bonding strategies, Dent. Mater. 2 (3) (2007) 1164–1172.
[44] L. Breschi, P. Martin, A. Mazzoni, F. Nato, M. Carrilhoe, L. Tjäderhane, et al., Use of a specific MMP-inhibitor (galardin) for preservation of hybrid layer, Dent. Mater. 26 (2010) 571–578.
[45] C. Chen, H. Hansma, Basement membrane macromolecules: insights from atomic force microscopy, J. Struct. Biol. 131 (2000) 44–55.
[46] S. Habelitz, M. Balooch, S. Marshall, G. Balooch, G. Marshall, In situ atomic force microscopy of partially demineralized human dentin collagen fibrils, J. Struct. Biol. 138 (2002) 227–236.
[47] F. El Feninat, T. Ellis, E. Sacher, I. Stangel, A tapping mode AFM study of collapse and denaturation in dentinal collagen, Dent. Mater. 17 (2001) 284–288.
[48] A. Fawzy, Variations in collagen fibrils network structure and surface dehydration of acid demineralized intertubular dentin: effect of dentin depth and air-exposure time, Dent. Mater. 26 (2010) 35–43.
[49] Y. Hosoya, F. Tay, O. Miyazaki, Hardness, elasticity and ultrastructure of primary tooth dentin bonded with a self-reinforcing one-step self-etch adhesive, J. Dent. 38 (2010) 214–221.
[50] S. Sauro, R. Osorio, T. Watson, M. Toledano, Assessment of the quality of resin–dentin bonded interfaces: an AFM nano-indentation, μTBS and confocal ultramorphology study, Dent. Mater. 28 (2012) 622–631.
[51] A. Takahashi, Y. Sato, S. Uno, P. Pereira, H. Sano, Effects of mechanical properties of adhesive resins on bond strength to dentin, Dent. Mater. 18 (2002) 263–268.
[52] B. Van Meerbeek, G. Willems, J. Celis, J. Roos, M. Braem, P. Lambrechts, et al., Assessment by nano-indentation of the hardness and elasticity of the resin–dentin bonding area, J. Dent. Res. 72 (1993) 1434–1442.
[53] W. Oliver, G. Pharr, An improved technique for determining hardness and elastic-modulus using load and displacement sensing indentation experiments, J. Mater. Res. 7 (1992) 1564–1583.
[54] Y. Hosoya, Hardness and elasticity of bonded carious and sound primary tooth dentin, J. Dent. 34 (2006) 164–171.
[55] A. Reis, M. Albuquerque, M. Pegoraro, G. Mattei, J. Bauer, R. Grande, et al., Can the durability of one-step self-etch adhesives be improved by double application or by an extra layer of hydrophobic resin? J. Dent. 36 (2008) 309–315.
[56] M. Cadenaro, F. Antoniolli, S. Sauro, F. Tay, R. Di Lenarda, C. Prati, et al., Degree of conversion and permeability of dental adhesives, Eur. J. Oral. Sci. 113 (2005) 525–530.
[57] M. Carrilhoa, R. Carvalho, E. Sousa, J. Nicolau, L. Breschi, A. Mazzoni, et al., Substantivity of chlorhexidine to human dentin, Dent Mater. 26 (2010) 779–785.
[58] R. Stanislawczuk, R. Amaral, C. Grande, D. Gagler, A. Reis, A. Loguercio, Chlorhexidine-containing acid conditioner preserves the longevity of resin dentin bonds, Oper. Dent. 34 (2009) 481–490.

[59] W. Brackett, F. Tay, M. Brackett, A. Dib, R. Sword, D. Pashley, The effect of chlorhexidine on dentin hybrid layers in vivo, Oper. Dent. 32 (2007) 107–111.
[60] M. Carrilho, F. Tay, A. Donnelly, K. Agee, L. Tjäderhane, A. Mazzoni, et al., Host-derived loss of dentin matrix stiffness associated with solubilization of collagen, J. Biomed. Mater. Res. B Appl. Biomater. 90 (2009) 373–380.
[61] L. Breschi, P. Martin, A. Mazzoni, F. Nato, M. Carrilhoe, L. Tjäderhane, et al., Use of a specific MMP-inhibitor (galardin) for preservation of hybrid layer, Dent. Mater. 26 (2010) 571–578.
[62] G. Pasquantonio, F. Tay, A. Mazzoni, P. Suppa, A. Ruggeri, M. Falconi, et al., Electric device improves bonds of simplified etch-and-rinse adhesives, Dent. Mater. 23 (2007) 513–518.
[63] C. Júnior, C. Grande, R. Amaral, R. Stanislawczuk, E. Garcia, R. Neto, et al., Evaporating solvents with a warm air-stream: effects on adhesive layer properties and resin–dentin bond strengths, J. Dent. 36 (2008) 618–625.
[64] M. Nassif, D. El Korashy, Phosphoric acid/sodium hypochlorite mixture as dentin conditioner: a new approach, J. Adhes. Dent. 11 (2009) 455–460.
[65] F. Tay, D. Pashley, R. Kapur, M. Carrilho, Y. Hur, L. Garrett, et al., Bonding BisGMA to dentin—a proof of concept for hydrophobic dentin bonding, J. Dent. Res. 86 (2007) 1034–1039.
[66] S. Sauro, M. Toledano, F. Aguilera, F. Mannocci, D. Pashley, F. Tay, et al., Resin–dentin bonds to EDTA-treated vs. acid-etched dentin using ethanol wet bonding, Dent. Mater. 26 (2010) 368–379.
[67] F. Tay, F. Sadek, D. Pashley, Y. Nishitani, M. Carrilho, A. Donnelly, et al., Application of hydrophobic resin adhesives to acid-etched dentin with an alternative wet bonding technique, J. Biomed. Mater. Res. A 84A (2008) 19–29.
[68] F. Sadek, A. Mazzoni, L. Breschi, F. Tay, R. Braga, Six-month evaluation of adhesives interface created by a hydrophobic adhesive to acid-etched ethanol-wet bonded dentin with simplified dehydration protocols, J. Dent. 38 (2010) 276–283.
[69] R. Cilli, A. Prakki, P. Jose, J. Pereira, Influence of glutaraldehyde priming on bond strength of an experimental adhesive system applied to wet and dry dentin, J. Dent. 37 (2009) 212–218.
[70] J. Kiernan, Formaldehyde, formalin, paraformaldehyde and glutaraldehyde. What they are and what they do, Microsc. Today 1 (2000) 8–12.
[71] D. Pashley, Y. Zhang, R. Carvalho, F. Rueggeberg, C. Russel, Induced tension development in demineralized dentin matrix, J. Dent. Res. 79 (2000) 1579–1583.
[72] E. Asmussen, E. Munksgaard, Bonding of restorative resins to dentin promoted by aqueous mixtures of aldehydes and active monomers, Int. Dent. J. 35 (1985) 160–165.
[73] F. Tay, D. Pashley, Guided tissue remineralisation of partially demineralized human dentin, Biomaterials 29 (2008) 1127–1137.
[74] M. Gandolfi, P. Taddei, F. Siboni, E. Modenab, E. De Stefano, C. Prati, Biomimetic remineralization of human dentin using promising innovative calcium-silicate hybrid “smart” materials, Dent. Mater. 27 (2011) 1055–1069.
[75] K. Welch, Y. Cai, H. Engqvist, M. Stromme, Dental adhesives with bioactive and on-demand bactericidal properties, Dent. Mater. 26 (2010) 491–499.
[76] K. Yasumoto, S. Hoshika, F. Nagano, T. Tanaka, D. Selimovic, Y. Miyamoto, et al., Application of wet bonding for one-step bonding systems, Dent. Mater. 26 (2010) e125–e157.
[77] S. Ahn, S. Lee, J. Kook, B. Lim, Experimental antimicrobial orthodontic adhesives using nanofillers and silver nanoparticles, Dent. Mater. 25 (2009) 206–213.
[78] J. Ferracane, Resin composite—state of the art, Dent. Mater. 27 (2011) 29–38.
[79] X. Ouyang, X. Huang, Q. Pan, C. Zuo, C. Huang, X. Yang, et al., Synthesis and characterization of triethylene glycol dimethacrylate nanocapsules used in a self-healing bonding resin, J. Dent. 39 (2011) 825–833.

[80] T. Ando, T. Uchihashi, N. Kodera, D. Yamamoto, M. Taniguchi, A. Miyagi, et al., High-speed atomic force microscopy for observing dynamic biomolecular processes, J. Mol. Recognit. 20 (2007) 448−458.
[81] A. Pyne, W. Marks, L. Picco, P. Dunton, A. Ulcinas, M. Barbour, et al., High-speed atomic force microscopy of dental enamel dissolution in citric acid, Arch. Histol. Cytol. 72 (2009) 209−215.
[82] Y. Sudhakar, K. Kuotsu, A. Bandyopadhyay, Buccal bioadhesive drug delivery—a promising option for orally less efficient drugs, J. Control. Release 114 (2006) 15−40.

CHAPTER

Nanobiomaterials in Preventive Dentistry

8

Matthias Hannig[a] **and Christian Hannig**[b]

[a]*Clinic of Operative Dentistry, Periodontology and Preventive Dentistry, University Hospital, Saarland University Homburg/Saar, Germany*

[b]*Clinic of Operative Dentistry, Faculty of Medicine 'Carl Gustav Carus', Technical University of Dresden, Dresden, Germany*

CHAPTER OUTLINE

8.1 Introduction—current challenges in preventive dentistry

Dental prophylaxis based on mechanical biofilm management and fluoride application has resulted in considerable improvement of oral health; however, caries is still a great challenge worldwide. The caries prevalence in newly industrializing countries is still increasing, in industrialized countries it is stagnating or decreases in some sections of the population [1,2]. Noteworthy, the distribution of caries in the population has shifted. On the one hand, many seniors of today have their own teeth but are faced with caries especially at the neck region of the teeth due to exposed dentin surfaces [3]. On the other hand, many children are nearly free of caries, but a significant percentage is faced with extensive early childhood caries [2,4]. If thorough mechanical biofilm management is performed daily on every site of the teeth, there will be no new caries lesion formation or

Nanobiomaterials in Clinical Dentistry.

progression, respectively. Despite these considerations and regular use of tooth brushes, most patients do not clean their teeth as properly as necessary for caries prevention. Accordingly, additional strategies and new preparations for optimized biofilm management as well as remineralization of incipient dental lesions are necessary. In general, a vast number of artificial materials and related products are available for oral health care and preventive dentistry. However, they are not as effective as desirable. Furthermore, the conventional oral health-care products represent no biomimetic or at least biological approaches for biofilm management in the oral cavity. Furthermore, since the physiological remineralization is frequently inadequate to maintain the integrity of enamel and dentin exposed to modern diet and nutrition behaviors, the natural remineralization process after an acidic challenge needs to be augmented. This applies not only for carious attacks but also for dental erosion. The prevalence of erosions is increasing due to the extensive consumption of acidic beverages in the industrialized countries [5]. In particular, eating disorders combined with often high resistance to psychological therapy cause extensive erosive defects [6]. Accordingly, also for dental erosion, additional strategies are required to prevent demineralization and to improve remineralization. Thereby, the specific mode of demineralization which is different from dental caries has to be considered as well as the interactions of proteolytic enzymes with the demineralized dentin matrix [7,8]. Due to the interaction of acidic agents with the hierarchically nanostructured dental hard substances, especially nanomaterials are of interest for treatment of initial erosive lesions [9].

Loss of periodontal attachment as well as gingival recession leads to the exposure of the root surface. Wrong or excessive tooth brushing can induce abrasion and accelerated loss of the exposed dental hard substance. This often results in tooth hypersensitivities, which are characterized by opened dentinal tubules. Nanoscaled particles might help to obturate the open dentin tubules, which are responsible for the hydrodynamic and osmotic effects inducing the hypersensitivities [9,10]. Nanomaterials might also be of interest for preventive, therapeutic, and regenerative strategies in periodontal disease itself, but this is not the topic of the present review.

The relevance of nanotechnology and nanobiomaterials to overcome these challenges in oral medicine is clearly mirrored by the increasing number of papers that had been published over the last few years describing nanotechnological approaches and nanosized materials with proposed applications in preventive dentistry [9,11–14]. In principle, the effects of such nanobiomaterials are governed by surface interactions and the process of bioadhesion at the tooth surface [15]. This applies for physiological as well as pathophysiological mechanisms and processes taking place at the tooth–biofilm–saliva interface. Thereby, strategies mimicking nature at the nanolevel seem to be the most promising approaches as they try to avoid successfully unpredictable adverse effects potentially caused by artificial agents [16]. For the development and understanding of these strategies, it is necessary to have a closer look on the process of bioadhesion, surface interactions, as well as de- and remineralization occurring at the tooth to saliva interface.

8.2 The ubiquitous phenomenon of bioadhesion on dental hard tissues

The teeth are characterized by nonshedding surfaces which are the essential fundament for the incidence of caries, periodontal diseases, and dental erosion [15]. In this context, the bioadhesion of

acellular and cellular organic structures is a matter of special importance. Thereby, the first step is represented by the formation of the acquired pellicle which occurs almost instantaneously on all solid substrates exposed to the oral fluids [17]. The adsorption process is driven by physicochemical interactions of the tooth surface with proteins and glycoproteins from the oral fluids; the pellicle formation means a gain in entropy. Fast area-wide pellicle formation is provided by the adsorption of micelle-like globular structures, as most salivary components are not released as single molecules but as aggregates [17]. These globularly structured aggregates have a diameter of 100−200 nm and are quite similar to milk micelles which could be a starting point for the development of new strategies in preventive dentistry based on organic nanostructures [18].

The physiological pellicle layer fulfills several functions besides lubricating the tooth surfaces. It offers protection against erosive mineral loss and modulates de- and remineralization [19−23]. However, these effects seem to be limited to short exposure duration and fluids with moderate acidic pH [20]. Longer exposure to beverages or acids at low pH inevitably leads to destruction of the pellicle and continuous mineral loss as shown in vitro and in situ. Due to the tremendous increase in the consumption of erosive beverages and the prevalence of eating disorders, there is a strong demand for preparations improving the antierosive properties of the pellicle.

Furthermore, the pellicle contains a couple of specific and unspecific antibacterial and antimicrobial proteins, glycoproteins, and peptides (such as secretory immunoglobulin A or lactoferrin) as well as, and enzymes (such as lysozyme or peroxidase) [17,24]. Despite these antibacterial properties, the pioneer bacteria have adapted to the protective properties of the pellicle layer [25]. Many pellicle components serve as receptors for specific and irreversible bacterial adhesion after the initial unspecific approach of bacteria to the tooth surface mediated by hydrophobic interactions, van der Waal's forces, and other physicochemical interactions [15,17]. Thereby, bacterial glycosyl transferases are remarkable key molecules synthesizing water insoluble and soluble glucans [25]. These enzymes are already present in the acquired pellicle in an active conformation within minutes and can be regarded as pioneer molecules for bacterial biofilm formation [25,26]. In this closer sense, biofilms have been defined as a structured community of bacterial cells enclosed in a self-produced polymeric matrix adherent to an inert or living surface [27].

The initial process of bioadhesion is an essential target of recent approaches in dental research based on nanotechnology in order to prevent bacterial adhesion, to ameliorate remineralization, and to avoid demineralization [9,14]. Furthermore, the more mature three-dimensionally organized bacterial biofilm could be prone to modification by nanomaterials. This means removal of already established biofilms as well as direct antibacterial effects on adherent bacteria which is still a drawback of many conventional antibacterial preparations. They are often of high efficacy against planktonic microorganisms, but fail to substantially affect the adherent bacteria organized in three-dimensional biofilms and embedded in an extracellular matrix [28,29]. Bacteria living organized in these biofilms are effectively shielded and protected against external attacks like treatment with detergents or antibiotics [28]. Nanoscaled particles may yield size-specific interactions with the biofilm, but they could also serve as drug-release carriers with high affinity to the bacterial surfaces or the extracellular matrix, respectively.

Besides the biofilm, the substrate of caries, and erosions, the dental hard substances themselves have moved into the focus of nanoscientists. Both enamel as well as dentin represent unique and hierarchically organized biological nanostructures [9,30−32]. The inorganic building units are hydroxyapatite (HA) nanocrystallites; in dental enamel, their length amounts up to several

100 nm and in dentin up to 50 nm. The acid-related destruction of the dental hard substance as a biocomposite is initiated on the nanolevel. Due to its nonregenerative nature, enamel is unable to heal and repair itself after surface alterations. Accordingly, modern prophylactic strategies intend to substitute mineral loss with artificial or biomimetic nanoscopic mineral components or HA particles fitting to the initial tooth surface nanosized defects. Thereby, it is has to be kept in mind that from a theoretical point of view, remineralization is the process of transferring anions and cations to nucleation sites, where the lattices leading to mineralized structures are generated.

8.3 Main strategies for implementation of nanosized materials in dental prophylaxis

Basically, there are two potential mechanisms for size-dependent effects of nanomaterials in preventive dentistry: (i) the interaction with bacterial adherence and oral biofilm formation and (ii) the impact on de- and remineralization. As the process of demineralization starts at the nanolevel caused by either caries or erosion-induced acidic challenges, it makes sense to supply small nanosized building units for optimized remineralization. This applies also for particle-size-related interactions with bacteria and the bacterial membrane, where nanoparticles are much more effective than microparticles. Many preparations considering these deliberations were developed; most of them are in the experimental state and few are already available for the consumers [11,33–36].

Pure inorganic nanomaterials applied in preventive dentistry are mostly HA or its derivatives modified with zinc, fluoride, or carbonate, respectively. Also mineral nanotubes, nanorods, or other geometric forms are tested, but represent rather a minority [9,14,37–42].

Another group is represented by organic/inorganic compound materials. Nanosized organic structures are components of several beverages and foodstuffs and contribute considerably to their characteristic properties. A typical example is milk containing casein micelles and lipid vesicles. Casein micelles are quite similar to micelle-like salivary structures involved in the formation of the pellicle layer. These natural structures may be processed to serve as tailored carriers with high affinity to the pellicle in order to accumulate minerals and protective proteins at the tooth surface. All the promising options of caseins have not been exploited in full until now, but there is already a widespread preparation based on casein phosphopeptide (CPP)–stabilized amorphous calcium phosphate (ACP) nanocomplexes with a diameter of 2.12 nm [11,34,35]. Other unexplored nanosized components of foodstuffs or animals such as chitin skeletons of diatoms could serve as carriers [36,43–45].

Besides these biomimetic or even biological approaches, silver nanoparticles or nanosized synthetic glass structures also have been described for possible application in preventive dentistry [46–49]. However, though these materials might be efficient, their side effects are not foreseeable. Thus, the present overview will focus on biological or biomimetic strategies.

8.4 Modulation of bioadhesion and biofilm management

In principle, there are two general approaches to modulate and to minimize bacterial biofilm formation on the tooth surface or on the surface of dental materials. It is either possible to establish a

permanent modification/coating of the substrate's surface providing antiadhesive or easy-to-clean characteristics, or to adopt dentifrices and mouthwashes, that will be applied frequently. For both approaches, there are examples based on nanomaterials [9,14]. If mouthwashes or dentifrices are adopted, the principal idea is that nanosized particles could interact more effectively with the structures of the bacterial membrane and the bacterial receptors than microparticles [9,14]. This might apply for microscaled HA which has been a component of oral care products without appreciable efficacy. HA does not exhibit cytotoxic effects and shows excellent biocompatibility. However, previous approaches using microsized HA in toothpastes were not successful. This is different for nanoscaled particles [9,50]. Various types of bioinspired nanosized apatites have been synthesized during the last few years in order to develop and create innovative toothpastes, mouth rinsing solutions, and remineralizing pastes (fluids) for use in preventive dentistry [9,33,40,50,51]. On the one hand, apatite nanoparticles could become integrated in the pellicle layer at the enamel surface under oral conditions, thereby changing the chemical composition and tenacity of the pellicle, and thus modifying the subsequent bacterial adherence and the pattern of biofilm formation. On the other hand, the nanosized apatite particles could also be adsorbed to the surface of planktonic bacteria as well as to the surface of bacteria adherent at the tooth surface.

Venegas et al. (2006) [52] investigated the interaction of nanosized HA with bacterial cells in aqueous solution and in human saliva under in vitro conditions. Crystallized HA nanoparticles (average size $100 \times 10 \times 5$ nm), distinctly smaller than the bacteria (diameter of 1 μm), were used in these experiments. Electron microscopic investigation of the bacteria cells and HA in saliva revealed adsorption of nonaggregated and clustered apatite particles at the bacterial surface [52]. The nanosized apatite particles adsorbed to the bacterial surface might interfere with the bacterial adhesins, which are important for irreversible binding of bacteria to the tooth surface.

Interestingly, at the same time Lu et al. [53,54] reported that needle-like or spheroidal nano-HA (with dimensions of less than 100 nm) not only has the potential to improve the remineralization of artificial caries lesions but also could modify bacterial colonization of the tooth surface in a rat animal model, thus revealing a certain anticaries potential. The capability of nano-HA (spherical HA with diameters of less than 100 nm) to reduce bacterial adherence and subsequent biofilm accumulation was confirmed by a laboratory experiment using a four-organism bacterial consortium (*Streptococci mutans, S. sanguis, Actinomyces viscosus, Lactobacillus rhamnosus*) for biofilm formation over 48 h under in vitro conditions [55]. In addition, treatment of bovine enamel slabs with an experimental dentifrice containing 15% nano-HA reduced bacterial adherence and colonization in vitro compared to a test dentifrice without nanoapatite particles [56]. Pretreatment of rough enamel surfaces with a 10% HA spherulite (particle diameter size of 0.02−1.00 μm) watery suspension significantly decreases adherence of *S. mutans* to the enamel surface under in vitro conditions, probably due to a reduction of enamel surface roughness [57]. Furthermore, in vivo application of an experimental dentifrice containing 38% nanosized HA spherulites (particle diameter size of 0.02−1.00 μm) using an individual tray one time daily over 7 days decreased the number of *S. mutans* in saliva over a 4-week post-treatment evaluation period, whereas application of a dentifrice containing 38% of dicalcium phosphate dihydrate placebo beads did not decrease *S. mutans* levels [57].

An already widespread biological nanomaterial based on derivatives of milk components is a preparation containing CPP−ACP nanocomplexes with a diameter of 2.12 nm [58]. The effect of CPP−ACP (GC Tooth-Mousse) nanocomplexes on 24-h *S. mutans* biofilm formation has been

investigated under in vitro conditions [35,59]. This investigation indicates a decrease in the total number of adherent bacteria and a reduction in the viability of *S. mutans* as compared to the controls, when HA-disks specimens had been pretreated with CPP−ACP in combination with acidulated phosphate fluoride [59]. Immunolocalization studies showed that CPP−ACP can be incorporated into supragingival dental plaque by binding to the surfaces of bacterial cells, to components of the intercellular plaque matrix, and to adsorbed proteins on the tooth surfaces, thereby influencing the process of biofilm formation [9,60]. In addition, CPP−ACP might become incorporated into the pellicle layer in exchange for the *streptococci*-related receptors, thus inhibiting or modifying the bacterial adherence [61]. The effects of CPP−ACP on intraoral biofilm have been also reported by an in situ study using germanium surfaces as substrate for the investigation of bacterial biofilm formation [61]. This study demonstrated that treatment with CPP−ACP resulted in strongly reduced biofilm formation within the 7-days observation period [62].

Since a few years, there are oral health-care products on the market containing clustered zinc carbonate−HA nanoparticles [33,63]. Actually, we could prove the applicability of a mouth rinsing solution that contains (besides other components) zinc carbonate−HA nanoparticle clusters (Biorepair Zahn- und Mundspülung, Dr. Wolff, Bielefeld, Germany) for decreasing bacterial adherence and reducing initial biofilm formation [64]. Interestingly, pure zinc carbonate−HA nanoparticle clusters in saline solution also reduced initial bacterial adherence over 12 h considerably as shown with different fluorescence microscopic techniques such as DAPI (diaminophenolindol)-staining or BacLight live-dead staining [64].

Furthermore, a new bifunctional system (either as paste or rinsing solution) containing calcium phosphate nanoparticles (with a diameter of 150−200 nm), functionalized by the antibacterial agent chlorhexidine and modified by carboxymethyl cellulose to increase the adhesion properties, has been described for dental maintenance treatment providing both mineralizing and antibacterial properties [65]. In vitro results indicate that this material sticks to tooth surfaces and closes dentin tubules and also provides efficient inhibition of bacterial growth under in vitro conditions. However, much more extensive studies are necessary to prove the activity against bacterial adherence and biofilm formation occurring in the mouth [65].

Besides the application of HA or calcium phosphate nanoparticles for biofilm management, the nanotechnological modification of microbicide/antimicrobial agents also could provide new routes in dental prophylaxis. A nanoemulsion composed of 25% soybean oil, 65% water, 10% Triton X-100, and 1% cetylpyridinium chloride has been tested recently, regarding its effects on in vitro biofilm formation and related anticariogenic effects. Antimicrobial nanoemulsions are surfactant-containing oil and water emulsions (droplet size 100−300 nm) which provide antibacterial effects [66]. Indeed, the data from Lee et al. [66] indicate that the cetylpyridinium-containing nanoemulsion causes strong inhibition of bacterial growth under in vitro conditions. Although the mechanism of antibacterial action of nanoemulsion has not been clarified in detail yet, it has been supposed that the nanodroplets could fuse with the outer bacterial membrane, thereby destabilizing the bacteria's lipid envelope and initiating its disruption [66].

Another way for biofilm management could be the use of activated carbon as an adsorbent; hence it is used in a wide range of oral care products such as toothpastes and mouth rinses. Carbon nanotubes can adsorb bacteria [67] and exhibit strong antimicrobial activity. Carbon nanotubes binding oral pathogens might be useful tools at the nanolevel for capturing oral pathogens [67]. Thereby, carbon nanotubes of different diameters provide significantly different effects on the

precipitation and capturing of *S. mutans* cells under in vitro conditions [67]. It has been shown that multiwalled carbon nanotubes with a diameter of approximately 30 nm had the highest precipitation efficiency which is attributable to both their dispersibility and adequate aggregation activity. Bundles of flexible single-walled and multiwalled carbon nanotubes (with average diameters of 30 nm) can wind around the curved surface of *S. mutans*. However, from a toxicological point of view, such artificial nanotubes could mean a considerable harm for the human organism in contrast to biomimetic apatites or other biomimetic preparations based on components of foodstuffs.

Various attempts to inhibit biofilm formation have been performed in recent years with newly developed coating materials characterized by (supposed) self-cleaning properties. Surface coatings providing self-cleaning properties could be applied to the natural tooth as well as to any artificial solid surface and restorative material used in dentistry (i.e., fissure sealants, restorations, crown and bridge work, dentures or implants) in order to topically control biofilm formation. Experimental coating materials containing fluoroalkylated acrylic acid oligomers (FAAO) have been applied to dental resin composite substrates [68]. Contact angle measurements have shown that an increase in the concentration of FAAO in the coating material enhanced surface hydrophobicity and oil repellence. However, biofilm assays clearly demonstrated that the amount of in vitro biofilm formation on these surface coatings decreased only gradually when the concentration of FAAO increased [68]. Thus, the data indicate that this type of coating material containing incorporated FAAO does not possess sufficient self-cleansing properties and will not inhibit biofilm [68]. In addition, experimental resin composites with incorporated poly-tetrafluoro-ethylene (PTFE) microparticles have been developed, which theoretically could improve the surface properties of the materials and thus inhibit bacterial adherence [69]. Although the hydrophobicity of the resin composites is significantly increased by incorporation of the PTFE microfillers, the surface resistance against biofilm formation is not improved. Resin composites with and without microsized PTFE particles harbors the same amount of bacteria under in vitro conditions [69]. In contrast, a recently developed nanocomposite surface coating composed of nanoscaled inorganic particles integrated into a fluoropolymer matrix indeed provides easy-to-clean properties due to a low surface free energy of 20−25 mJ/m^2. Coating of enamel or titanium surfaces by this nanocomposite material leads to the detachment of the outer pellicle layers and adherent biofilms, as confirmed by an in situ study [70]. Such nanocomposite coatings are conceivable for the coating of implant necks or fissure sealants, just to give some examples. It has been postulated that the bacteria are faced with different physicochemical surface characteristics alternating at the nanoscale. This could result in a low tenacity of the adherent bacteria or bacterial biofilm [70]. In contrast to the above mentioned coatings, this nanomaterial yields the physicochemical properties required for adoption in the oral cavity.

Further approaches to gain durable easy-to-clean surfaces are in advance in materials science; thereby, novel manufacturing techniques such as spraying are established. Though some of these preparations might be of interest for dentistry, their efficacy must be proved under the specific conditions of the oral cavity after ascertainment of toxicological innocuousness [71,72]. It is noteworthy that these new approaches are also based on the hierarchical arrangement of particles to achieve certain surface properties [72].

The lotus effect in its classical sense based on an ultrahydrophobic surface is not suitable for the application in the oral cavity due to the very low mechanical stability [73,74]. Even if this subtle surface texture would be of high tenacity, it will be masked by the ubiquitous pellicle layer under the conditions prevailing in the oral cavity. Thereby, it has to be pointed out that the surface

of the plant's leaves only sporadically comes in contact with water, whereas the teeth are rather in a marine environment, which means completely different requirements. However, there are other unexplored or even undetected strategies in the fauna and the flora which could also mean new stimuli for dental research. These biological phenomena of self-cleaning surfaces are usually based on certain nanoscaled surface textures as well as on a specific chemical composition [75]. These biological surface structures with a hierarchical nanostructure may serve as archetype for the establishment of new easy-to-clean surfaces in preventive dentistry. However, this requires further research in the field of bionics. Presumably, a combination of special physical surface structures and chemical surface coating is the key to biomimetic and therewith biological biofilm management on the nanoscale.

8.5 Effects on de- and remineralization

De- and remineralization are critical to the formation of dental caries and tooth erosion. Both demineralization and remineralization occur on the tooth surface, and thus can be considered as highly dynamic processes, characterized by the flow of calcium and phosphate out of and back into the tooth enamel. Fluoride promotes remineralization and this has been suggested as the main mechanism by which fluoride protects the teeth. The essence of the remineralization concept of demineralized tooth surfaces might be achieved by simultaneously supplying calcium, phosphate, and fluoride ions to the teeth in order to induce formation of various apatites that remineralize and strengthen the tooth. Therefore, intensive investigations on the remineralizing potential of new toothpastes and fluid formulations based on nanotechnology are in progress. Nanomaterials might optimize the process of remineralization. On the one hand, they could fit to the nanoscopic defects of the enamel which are to be reconstituted; on the other hand, they can serve as carriers for remineralizing ions with high affinity to the pellicle. Thereby, a supersaturation at the tooth surface or in the pellicle layer would be achieved; this means a slow-release depot.

Biomimetic HA nanocrystals have been designed and synthesized in order to facilitate remineralization of the altered enamel surface. HA nanocrystals provide excellent biological properties such as biocompatibility, lack of toxicity, as well as lack of inflammatory and immunological responses. In early in vitro studies, the effects of nano-HA on enamel remineralization were evaluated in static models [50,76–78]. These pilot studies reveal that nanosized HA possess a certain potential to remineralize incipient caries lesions. More recently, the potential of an experimental 10 wt% nano-HA aqueous slurry (HA crystals with a length of 60–80 nm and a diameter of 10–20 nm) or a toothpaste containing 20 wt% clustered zinc carbonate–nano-HA to remineralize initial caries lesions under dynamic pH-cycling conditions in vitro has been demonstrated [33,79]. Detailed investigations indicated that application of nanosized HA under these in vitro conditions promotes preferential mineral deposition in the outer layer of the initial caries lesion and had a limited capacity to reduce lesion depth or to increase the mineral content in the body of the lesion [33,79]. Interestingly, the remineralization effect strongly depends on the pH during application of the nanosized HA: under neutral conditions, full remineralization effect is not achievable, while under acidic conditions (pH of 4.0) nano-HA can significantly increase the depth of penetration and the extent of remineralization of artificial incipient caries lesions [79].

To the best knowledge of the authors, up to now only one randomized, double-blind, crossover, in situ study has been published concerning the efficacy of nano-HA dentifrices on caries remineralization and demineralization [51]. Demineralized enamel specimens were exposed to dentifrices containing 5% or 10% nano-HA, or 1100 ppm fluoride, respectively, via an intraoral appliance worn by 30 adults over a 28-day period. Treatment with all three dentifrices caused significant reduction of the lesion depth and extent of demineralization detected at baseline. In addition, no demineralization occurred in sound enamel specimens exposed intraorally over 28 days, while using the 10% nano-HA toothpaste. From these in situ data, the authors concluded that a nano-HA containing dentifrice can be an effective alternative to fluoride toothpastes [51].

Also CPP−ACP nanocomplexes have been tested with respect to remineralizing properties, and considerable effects were observed. For this preparation, not only in vitro but also clinical data are available [11,80−82]. In particular, a special chewing gum has been tested in vivo [81,82]. Remarkably a clinical 2-year-study showed that application of a chewing gum containing CPP−ACP significantly diminished the progression of carious lesions and promoted regression of initial proximal carious lesions. More than 2500 children were enrolled in this project. Furthermore, CPP−ACP has been combined with fluoride to enhance the remineralizing properties [34,83,84].

Most studies focus on the remineralization of enamel. However, the remineralization of demineralized dentin is even more challenging, as it represents a biological compound structure with inorganic and organic components. The organic matrix is mainly composed of type-I collagen fibrils forming a three-dimensional matrix that is reinforced by HA nanocrystallites. Though demineralized collagen fibrils may serve as some kind of scaffold for mineral crystallites in the reconstitution of the dentin, they are quite prone to proteolytic degradation if exposed to oral fluids. However, remineralization of carious dentin has as its ultimate goal the reestablishment of the functionality of the affected tissue [31].

Remineralization of dentin can occur either by precipitation of mineral between collagen fibrils or functionally bound to its structure [31]. Therefore, simple precipitation of mineral into the loose demineralized dentinal matrix means an increased mineral content but may not necessarily provide an optimal interaction with the organic components of the dentin matrix [31]. Partial recovery and remineralization of human carious dentin were achieved in vitro using colloidal HA and β-tricalcium phosphate over a period of 10 days [85]. Treatment with β-tricalcium phosphate yielded better reconstitution of the dentin's micromechanical properties. The β-tricalcium phosphate is assumed to be partially dissolved in the acidic carious regions recovering intermolecular collagen cross-linking by combining with corresponding intrafibrillar sites. However, intrafibrillar remineralization of dentin is difficult due to the denaturation of collagen fibrils by proteolytic enzymes of cariogenic bacteria [85].

Also nanosized bioactive glass particles for remineralization of the demineralized dentin were investigated in vitro [49]. After treatment of demineralized dentin for 10−30 days, an increase in mineral content was observed, but the mechanical properties were below native dentin. These examples and the required application time illustrate the difficulties of dentin remineralization. However, also under pure in vitro conditions, toothpastes containing HA nanoparticles revealed better remineralizing effects when compared to a conventional amine fluoride toothpaste [33].

8.6 Erosion

For treatment of eroded tooth surfaces, carbonate−HA nanocrystals were synthesized by precipitation from an aqueous suspension of $Ca(OH)_2$ by slow addition of H_3PO_4 [86,87]. The nanocrystals were allowed to form clusters of dimensions ranging from 0.5 to 3.0 μm. They are quite similar as compared to dentinal apatite crystals. Enamel surfaces etched with phosphoric acid for 1 min were treated by aqueous slurries containing these experimental carbonate−HA nanocrystals for 10 min under in vitro conditions [86] and washed. After application of the nanoparticles to the etched enamel surface, a coating of carbonate−HA is deposited on the enamel surface [86]. This coating is less crystalline than native enamel apatite and consists of apatite mineral depositions which fill the micro-rough surface pattern of the etched enamel [86]. Commercially available toothpastes containing comparable HA nanoparticles have been shown to remineralize experimental erosive enamel defects in vitro [33,63]. Despite these promising in vitro observations, the effects have to be confirmed by in situ or in vivo investigations considering the pellicle and the dynamic environment of the oral cavity.

Another approach for treatment of the demineralized enamel surface is also based on HA nanoparticles, however with a smaller particle size of only 20 nm [40]. It has been shown by in vitro experiments that adsorption of these nanoparticles onto the tooth surface strongly reduced the process of erosive demineralization of natural enamel. This observation indicated that the 20-nm HA particles themselves are comparatively resistant to dissolution in the acidic milieu which can be understood by a nanodissolution model [40]. Briefly, this model suggests that active dissolution pits cannot be produced on nanoparticles. Thus, the nanostructured materials will be kinetically protected due to their size and remain relatively stable even in case of undersaturated conditions [40]. Therefore, not only repair but also prevention of enamel erosion might be enhanced by the application of nanosized HA [40].

However, concerning the protective effect of ACP−CPP-containing agents against dental erosion, the published data are controversial [88]. On the one hand, it had been reported that application of CPP−ACP paste is effective in preventing dental erosion produced by a soft drink in vitro [88]. On the other hand, according to measurements of the surface nanohardness, tooth erosion could not be prevented or repaired by CPP−ACP pastes in an in vitro cyclic erosion model regardless of the paste's fluoride content [88].

Apatite nanoparticles or calcium phosphate nanocomplexes had been also applied to reduce the erosive potential of acidic beverages such as sport and soft drinks [88]. Addition of 0.25% or 0.5% of nano-HA to a low-pH sport drink (pH 2.96) will increase the pH (up to 4.38 or 4.63, respectively), thereby significantly reducing the erosive effect of the acidic drink [88]. A follow-up study indicated that adding 0.25% nano-HA to Powerade sport drink could prevent erosion in vitro [89]. Furthermore, addition of 0.2% w/v of CPP−ACP to commercially available soft drinks has been shown to significantly reduce the erosivity of these beverages under in vitro conditions [90].

In summary, based on the results from in vitro experiments it can be proposed that HA nanoparticles are able to fill microdefects on the enamel surface and might modify the process of erosive tooth destruction. However, up to now in vivo evidence for these effects is lacking.

8.7 Nanosized calcium fluoride

Calcium fluoride (CaF_2) preparations are of significant interest in preventive dentistry due to their role as labile fluoride reservoir in caries prophylaxis. Low concentrations of fluoride in the oral fluid in the range of 0.1 ppm F^- derived from dentifrices or mouth rinses have been shown to reveal a profound effect on the progression of dental caries. However, the low salivary calcium concentration provides a limited driving force for the formation of CaF_2 deposits. Nano-CaF_2 powder containing clusters of 10–15 nm sized crystallite particles has been prepared from $Ca(OH)_2$ and NH_4F solutions using a spray drying technique [91]. The advantage of this technique over conventional solution precipitation methods is that the nanoparticles, once formed, are not subject to further washing, and thus maintain the high surface reactivity, innate to nanosized particles [91]. Interestingly, the nano-CaF_2 powder displayed much higher solubility and reactivity than its macrosized counterpart [91]. Thus, nano-CaF_2 might be used as an effective anticaries agent in increasing the labile fluoride concentration in the oral fluid, thereby enhancing the process of remineralization. The nanosized calcium fluoride will be more effectively retained in the mouth due its high affinity to oral substances, thereby serving as a long-lasting source for ambient fluoride than that produced by currently used NaF products [91]. Results of a pilot in vivo study indicate that a 1-min application of this nano-CaF_2 rinse produces a significantly greater 1-h postrinse salivary fluoride content (158 μmol/L) than a NaF rinse (36 μmol/L) [91].

8.8 Dentin hypersensitivity

Dentin hypersensitivity is a widespread and increasing problem especially in the dentate elderly population. Due to the loss of the root cement, the dentinal tubules are exposed. Liquid movement in these tubules induced by cold and hot beverages or osmotically active substrates provokes irritation of the subodontoblastic plexus [10]. According to this hydrodynamic theory, some kind of biomimetic sealing of the dentin surface and especially of the open tubules is demandable. Carbonate–HA nanocrystals with size, morphology, chemical composition and crystallinity similar to that of dentin were synthesized and are available as preparation for clinical application [92]. TEM (transmission electron microscopic) analysis indicates that the nanocrystals present a length ranging from 20 to 100 nm and a thickness ranging from 5 to 10 nm [92]. It has been shown by in vitro experiments that patent dentinal tubules can be sufficiently closed by application of carbonate–HA nanocrystals for 10 min [92]. These in vitro effects were confirmed in a double-blind, randomized clinical trial with 70 patients [93]. A dentifrice based on zinc carbonate–HA nanocrystals was adopted at regular intervals and repeatedly applied. It reduced dentinal hypersensitivity significantly and yielded greater improvement than a conventional fluoride-based preparation, if an airblast test was conducted [93]. It might be postulated that the preparation also obturated the openings of the dentinal tubules in vivo. In contrast, singular application of CPP–ACP (Tooth-Mousse) revealed insufficient effectiveness in treating hypersensitivity in a clinical study, and the therapeutic effect was short termed [94]. Accordingly, repeated application of the material is necessary. Besides these preparations which are available on the market, other experimental preparations were tested in vitro. A composite material based on nanostructured calcium phosphate and collagen yielded successful sealing of dentin

tubules in vitro [95]. Another in vitro study showed that tenacious occlusion of the dentinal tubules could be achieved with nanosized carbonate apatite [96].

Currently, Guentsch et al. (2012) [97] could provide evidence that a biomimetic mineralization system (BIMIN, Heraeus Kulzer, Wehrheim, Germany) based on the diffusion of calcium ions from solution into a glycerine-enriched gelatine gel containing phosphate and fluoride ions is as effective as the clinically established application of a glutaraldehyde containing agent (Gluma) in treatment of patients suffering from dentin hypersensitivity [97]. SEM (scanning electron microscopic) analysis performed on replica models which had been produced from impressions of the patients' teeth demonstrates that a single BIMIN application (over 8 h) caused deposition of a mineral-like layer on the dentinal surfaces and occlusion of the dentinal tubules and that this layer (effect) was stable over the observation period of 12 months [97].

8.9 Regeneration of dental hard substances

Several recent studies have documented the formation of enamel-like structures from mineral solutions under ambient conditions. Various strategies for self-assembling one-dimensional HA crystallites or nanorods resulting in an enamel-like organized rod array suprastructure have been described [9,32,98,99]. However, only very thin layers at the micron- or even nanoscale are obtained; the process of guided mineral formation is quite time consuming. In general, there are two different approaches to achieve these mineral layers: with and without the application of organic scaffolds [100]. Especially for the formation of thicker structures, these scaffolds seem to be necessary in many models [100]. Controlled binding and assembly of proteins onto inorganics is the core of biological materials science and tissue engineering [101].

A typical scaffold protein used widely is amelogenin. It has been suggested that this predominant enamel matrix protein has self-assembling properties, thereby facilitating the organization of organic nanostructures in developing enamel crystallites [102,103]. Higher order HA nanocrystals were observed, if crystal formation emerged from aggregates of nanospheres with HA cores and amorphous calcium phosphate shells [104]. Thereby, enamel-like HA architecture was achieved in the presence of amelogenin or glycine, respectively [104].

In a follow-up study, an oriented amelogenin fluoridated HA layer could be precipitated on etched enamel indicating a synergistic interaction of fluoride and enamel [105]. This cooperating role of amelogenin and fluoride ions in formation of oriented apatite-like crystals was also proven in a cation-selective membrane system as a model for enamel formation [106]. Under in vitro conditions, amelogenin accelerates HA nucleation kinetics, thus decreasing the induction time in a concentration-dependent manner [32]. Hierarchically organized apatite microstructures are achieved by self-assembly involving nucleated nanocrystallites and amelogenin oligomers and nanospheres at low supersaturation and protein concentrations. This in vitro observation provides direct evidence that amelogenin promotes apatite crystallization and organization [32].

It has been demonstrated recently by in vitro experiments on apatite nucleation in the presence of amelogenin that hierarchical self-assembly, by a nucleation-growth pathway, gives rise to a remarkably high degree of cooperativity, mimicking the self-organized microstructure of tooth enamel [32]. However, also with the aid of organic structures only very thin layers on the

microscale can be generated, their formation often requires high pressure, or is at least very time consuming. All these experiments are still on the pure in vitro level, and the entire regeneration of micronsized defects or even of small cavities is not accomplishable at the moment.

Busch et al. [107,108] have studied fluoroapatite formation in gelatin matrices. It could be shown that the morphogenesis of hierarchically ordered spherical aggregates of fluoroapatite/gelatin nanocomposites starts from elongated hexagonal prismatic seed crystals. At later stages of mineralization, fractal branching and the development of growing dumbbell states were observed. Based on these results, a technique was developed to form dense fluorapatite layers on the human enamel surface, using the diffusion of calcium ions from solution into a glycerin-enriched gelatin gel containing phosphate and fluoride ions at 37°C [107,108]. To induce mineralization of fluorapatite on the tooth surface, samples were immersed in a neutral calcium solution [107,108]. The similarity of the biomimetically grown mineral layer with the natural enamel suggests that the experimental setup is an attractive model for resembling mineralization of enamel, but the formation rate of approximately 500 nm/day is very low. Interestingly, one time overnight application of this BIMIN in patients for at least 8 h caused—according to the authors' interpretation—deposition/precipitation of a smooth enamel-like layer on the tooth enamel under in vivo conditions [97].

Even if the formation of hierarchically structured and durable minerals would be possible, there is still the challenge of bonding this biomineral tenaciously to the surrounding dental hard tissue. It has to be pointed out that the physiological binding between dentin and enamel has not been understood in detail until now [30].

8.10 Discussion and clinical recommendations

The research on the application of nanobiomaterials in preventive dentistry is just beginning, and there are numerous open questions, though there are many promising ideas. At the moment, most of these novel approaches are at the theoretical level or at the experimental stage, and only few preparations are already available on the market [9]. However, it is not evident at the moment whether the adoption of these nanomaterials means an improvement in preventive dentistry as compared with conventional dentifrices or mouthwashes. This has to be proved in broad clinical studies. If this would be the case, biological and biomimetic nanomaterials without adverse effects could potentially substitute fluorides. This would be of special interest for young children to improve caries prophylaxis without running the risk of dental fluorosis. Dental fluorosis occurs in a dose-dependent manner, and low-dose fluoridated toothpastes suitable for children are of limited efficacy for prevention of caries [109–111].

The nanomaterials' mode of action is based on surface interactions. This applies for the effects on biomineralization as well as for the modulation of bioadhesion [9]. In this context, it has to be pointed out that many aspects of these physiological processes are not even approximately understood. Accordingly, extensive basic research is necessary in this field. One example are fluorides—their clinical efficacy has been proven but the in vivo interactions are not fully understood until now [112]. For conventional as well as for nanotechnology based preparations, it is necessary to understand their mode of action besides the evaluation of clinical efficacy. This is also of relevance for rating the toxicology of the very different materials. It is very difficult to assess potential

adverse effects. The chemistry and composition of the nanomaterials are extremely different—some might degrade fast, others have a long biological half lifetime, or they are completely inert with potential effects on cellular and subcellular structures. It is to be expected that biological or biomimetic nanomaterials mean a minor hazard than completely artificial preparations such as carbon nanotubes or silver nanoparticles.

Nanosized structures are present in milk and other foods. Due to abrasion and attrition, nanosized HA particles are assumed to be present in the oral fluids [16]. Due to these considerations, future research should focus on biological and biomimetic approaches. The fauna and the flora offer many unexplored strategies which could be helpful for dental prophylaxis and biofilm management. The famous lotus effect, though not directly applicable for the adoption in the oral cavity, is only one prominent example. Experts in dental research have to define the demands not only from a clinical point of view but also especially with respect to the surface interactions in the oral cavity; cooperating scientists are to explore possible solutions in the nature. Only interdisciplinary research will lead to really new strategies in preventive dentistry based on nanotechnology. Thereby, the patients and the society become more and more interested in biological approaches.

Despite all these promising strategies and research approaches, the application of nanosized particles or materials in the oral cavity requires a thorough examination of potential risks. Especially, artificial nanosized particles such as nanotubes mean unpredictable hazards for the human organism; because their degradation is not provided. Thus, biologic or biomimetic strategies seem to be advantageous. However, also the fate and behavior of these substances in the organism require further research since the processing and modification of the basically biological materials possibly alter the process of degradation. This also applies for slight differences of native and biomimetic HA nanoparticles. To the best knowledge of the authors, there are no publications so far on this relevant topic investigating the special characteristics of already available preparations [9,14,16]. Nanomaterials applied as components of mouth rinses or dentifrices could mean an unphysiological challenge for the organism, and several models are discussed for the oral uptake of nanoparticles [113−115]. Besides the size of the particles, their physicochemical properties determine their interaction with the physiological barriers and the cells. Organic nanoparticles not only might be digested or hydrolyzed by proteolytic enzymes or denatured by gastric juice but could also be resistant to these mechanisms. Both organic and inorganic nanoparticles can interact with organic molecules in saliva, mucous layer, or blood respectively. This nanoscaled process of bioadhesion of course modifies the possible resorption and properties of the protein-covered particles with possible impact on the function of underlying cells and structures. The interaction of nanomaterials with acellular layers of the orogastrointestinal tract has been investigated [115]. Often, but not always, smaller particles pass mucous layers much faster than bigger ones. This is modulated by the surface charge of the particles [115,116].

8.11 Conclusions

Some biomimetic nanomaterials seem to be promising amendments for dental prophylaxis, but fundamental research is necessary in this field, before any clinical recommendations are possible.

References

[1] P. Cleaton-Jones, P. Fatti, Dental caries in children in South Africa and Swaziland: a systematic review 1919–2007, Int. Dent. J. 59 (2009) 363–368.

[2] R.L. Ettinger, Epidemiology of dental caries. A broad review, Dent. Clin. North. Am. 43 (1999) 679–694.

[3] J.M. Sadowsky, R.D. Bebermeyer, G. Gibson, Root caries–a review of the etiology, diagnosis, restorative and preventive interventions, Tex. Dent. J. 125 (2008) 1070–1082; quiz 1083–1085.

[4] R. Harris, A.D. Nicoll, P.M. Adair, C.M. Pine, Risk factors for dental caries in young children: a systematic review of the literature, Community Dent. Health 21 (2004) 71–85.

[5] T. Jaeggi, A. Lussi, Prevalence, incidence and distribution of erosion, Monogr. Oral Sci. 20 (2006) 44–65.

[6] D. Bartlett, Intrinsic causes of erosion, Monogr. Oral Sci. 20 (2006) 119–139.

[7] N. Schlueter, C. Ganss, S. Potschke, J. Klimek, C. Hannig, Enzyme activities in the oral fluids of patients suffering from bulimia: a controlled clinical trial, Caries Res. 46 (2012) 130–139.

[8] J.D. Featherstone, A. Lussi, Understanding the chemistry of dental erosion, Monogr. Oral Sci. 20 (2006) 66–76.

[9] M. Hannig, C. Hannig, Nanomaterials in preventive dentistry, Nat. Nanotechnol. 5 (2010) 565–569.

[10] M. Brännström, Sensitivity of dentin, Oral Surg. Oral Med. Oral Pathol. 21 (1966) 517–526.

[11] E.C. Reynolds, Calcium phosphate-based remineralization systems: scientific evidence? Aust. Dent. J. 53 (2008) 268–273.

[12] E.C. Reynolds, Anticariogenic complexes of amorphous calcium phosphate stabilized by casein phosphopeptides: a review, Spec. Care Dent. 18 (1998) 8–16.

[13] R.P. Allaker, The use of nanoparticles to control oral biofilm formation, J. Dent. Res. 89 (2010) 1175–1186.

[14] M. Hannig, C. Hannig, Nanotechnology and its role in caries therapy, Adv. Dent. Res. 24 (2012) 53–57.

[15] C. Hannig, M. Hannig, The oral cavity—a key system to understand substratum-dependent bioadhesion on solid surfaces in man, Clin. Oral Invest. 13 (2009) 123–139.

[16] C. Hannig, M. Hannig, Natural enamel wear—a physiological source of hydroxylapatite nanoparticles for biofilm management and tooth repair? Med. Hypotheses 74 (2010) 670–672.

[17] M. Hannig, A. Joiner, The structure, function and properties of the acquired pellicle, Monogr. Oral Sci. 19 (2006) 29–64.

[18] L. Vitkov, M. Hannig, Y. Nekrashevych, W.D. Krautgartner, Supramolecular pellicle precursors, Eur. J. Oral Sci. 112 (2004) 320–325.

[19] C. Hannig, K. Becker, N. Hausler, W. Hoth-Hannig, T. Attin, M. Hannig, Protective effect of the in situ pellicle on dentin erosion—an ex vivo pilot study, Arch. Oral Biol. 52 (2007) 444–449.

[20] C. Hannig, D. Berndt, W. Hoth-Hannig, M. Hannig, The effect of acidic beverages on the ultrastructure of the acquired pellicle—an in situ study, Arch. Oral Biol. 54 (2009) 518–526.

[21] M. Hannig, M. Balz, Influence of in vivo formed salivary pellicle on enamel erosion, Caries Res. 33 (1999) 372–379.

[22] M. Hannig, M. Balz, Protective properties of salivary pellicles from two different intraoral sites on enamel erosion, Caries Res. 35 (2001) 142–148.

[23] M. Hannig, M. Fiebiger, M. Guntzer, A. Dobert, R. Zimehl, Y. Nekrashevych, Protective effect of the in situ formed short-term salivary pellicle, Arch. Oral Biol. 49 (2004) 903–910.

[24] C. Hannig, M. Hannig, T. Attin, Enzymes in the acquired enamel pellicle, Eur. J. Oral Sci. 113 (2005) 2–13.

[25] W.H. Bowen, H. Koo, Biology of *Streptococcus mutans*-derived glucosyltransferases: role in extracellular matrix formation of cariogenic biofilms, Caries Res. 45 (2011) 69−86.
[26] C. Hannig, A. Ruggeri, B. Al-Khayer, P. Schmitz, B. Spitzmuller, D. Deimling, et al., Electron microscopic detection and activity of glucosyltransferase B, C, and D in the in situ formed pellicle, Arch. Oral Biol. 53 (2008) 1003−1010.
[27] J.W. Costerton, P.S. Stewart, E.P. Greenberg, Bacterial biofilms: a common cause of persistent infections, Science 284 (1999) 1318−1322.
[28] P.D. Marsh, Controlling the oral biofilm with antimicrobials, J. Dent. 38 (Suppl. 1) (2010) S11−S15.
[29] P.D. Marsh, D.J. Bradshaw, Dental plaque as a biofilm, J. Ind. Microbiol. 15 (1995) 169−175.
[30] V. Imbeni, J.J. Kruzic, G.W. Marshall, S.J. Marshall, R.O. Ritchie, The dentin-enamel junction and the fracture of human teeth, Nat. Mater. 4 (2005) 229−232.
[31] L.E. Bertassoni, S. Habelitz, J.H. Kinney, S.J. Marshall, G.W. Marshall Jr., Biomechanical perspective on the remineralization of dentin, Caries Res. 43 (2009) 70−77.
[32] L.J. Wang, X.Y. Guan, H.Y. Yin, J. Moradian-Oldak, G.H. Nancollas, Mimicking the self-organized microstructure of tooth enamel, J. Phys. Chem. C 112 (2008) 5892−5899.
[33] P. Tschoppe, D.L. Zandim, P. Martus, A.M. Kielbassa, Enamel and dentin remineralization by nano-hydroxyapatite toothpastes, J. Dent. 39 (2011) 430−437.
[34] Y.J. Tang, Y.F. Tang, C.T. Lv, Z.H. Zhou, Preparation of uniform porous hydroxyapatite biomaterials by a new method, Appl. Surf. Sci. 254 (2008) 5359−5362.
[35] L.R. Mo, Y.B. Li, G.Y. Lv, J.D. Li, L. Zhang, Comparison of hydroxyapatite synthesized under different conditions, Mater. Sci. Forum 510−511 (2006) 814−817.
[36] M.Y. Ma, Y.J. Zhu, L. Li, S.W. Cao, Nanostructured porous hollow ellipsoidal capsules of hydroxyapatite and calcium silicate: preparation and application in drug delivery, J. Mater. Chem. 18 (2008) 2722−2727.
[37] L. Li, H.H. Pan, J.H. Tao, X.R. Xu, C.Y. Mao, X.H. Gu, et al., Repair of enamel by using hydroxyapatite nanoparticles as the building blocks, J. Mater. Chem. 18 (2008) 4079−4084.
[38] Y.M. Chen, T.F. Xi, Y.P. Lv, Y.D. Zheng, In vitro biological performance of nano-particles on the surface of hydroxyapatite coatings, Appl. Surf. Sci. 255 (2008) 375−378.
[39] S.H. Jung, E. Oh, K.H. Lee, W. Park, S.H. Jeong, A sonochemical method for fabricating aligned ZnO nanorods, Adv. Mater. 19 (2007) 749.
[40] E.C. Reynolds, F. Cai, N.J. Cochrane, P. Shen, G.D. Walker, M.V. Morgan, et al., Fluoride and casein phosphopeptide-amorphous calcium phosphate, J. Dent. Res. 87 (2008) 344−348.
[41] K.J. Cross, N.L. Huq, E.C. Reynolds, Casein phosphopeptides in oral health—chemistry and clinical applications, Curr. Pharm. Des. 13 (2007) 793−800.
[42] P. Richthammer, M. Bormel, E. Brunner, K.H. van Pee, Biomineralization in diatoms: the role of silacidins, Chembiochem 12 (2011) 1362−1366.
[43] K. Spinde, M. Kammer, K. Freyer, H. Ehrlich, J.N. Vournakis, E. Brunner, Biomimetic silicification of fibrous chitin from diatoms, Chem. Mater. 23 (2011) 2973−2978.
[44] M. Sumper, E. Brunner, Learning from diatoms: nature's tools for the production of nanostructured silica, Adv. Funct. Mater. 16 (2006) 17−26.
[45] M. Sumper, E. Brunner, G. Lehmann, Biomineralization in diatoms: characterization of novel polyamines associated with silica, FEBS Lett. 579 (2005) 3765−3769.
[46] T. Waltimo, T.J. Brunner, M. Vollenweider, W.J. Stark, M. Zehnder, Antimicrobial effect of nanometric bioactive glass 45S5, J. Dent. Res. 86 (2007) 754−757.
[47] R. Garcia-Contreras, L. Argueta-Figueroa, C. Mejia-Rubalcava, R. Jimenez-Martinez, S. Cuevas-Guajardo, P.A. Sanchez-Reyna, et al., Perspectives for the use of silver nanoparticles in dental practice, Int. Dent. J. 61 (2011) 297−301.

[48] G.Y. Lv, Y.B. Li, A.P. Yang, X. Zhang, W.H. Yang, J.D. Li, Preparation and antibacterial activity of silver ions-substituted hydroxyapatite/titania, Mater. Sci. Forum 510–511 (2006) 78–81.
[49] M. Vollenweider, T.J. Brunner, S. Knecht, R.N. Grass, M. Zehnder, T. Imfeld, et al., Remineralization of human dentin using ultrafine bioactive glass particles, Acta Biomater. 3 (2007) 936–943.
[50] S.H. Jeong, S.O. Jang, K.N. Kim, H.K. Kwon, Y.D. Park, B.I. Kim, Remineralization potential of new toothpaste containing nano-hydroxyapatite, Key Eng. Mater. 309–311 (Pts 1 and 2) (2006) 537–540.
[51] K. Najibfard, K. Ramalingam, I. Chedjieu, B.T. Amaechi, Remineralization of early caries by a nano-hydroxyapatite dentifrice, J. Clin. Dent. 22 (2011) 139–143.
[52] C. Venegas, J.M. Palacios, M.C. Apella, P.J. Morando, M.A. Blesa, Calcium modulates interactions between bacteria and hydroxyapatite, J. Dent. Res. 85 (2006) 1124–1128.
[53] K.-L. Lu, J.-X. Zhang, X.-C. Meng, G.-Z. Wie, M.-L. Zhou, Effects of nano-hydroxyapatite on the artificial caries, Mater. Sci. Technol. 14 (6) (2006) 633–636.
[54] K. Lu, X. Meng, J. Zhang, X. Li, M. Zhou, Inhibitory effect of synthetic nano-hydroxyapatite on dental caries, Key Eng. Mater. 336–338 (2007) 1538–1541.
[55] X. Meng, K. Lv, J. Zhang, D. Qu, Caries inhibitory activity of the nano-HA in vitro, Key Eng. Mater. 330–332 (2007) 251–254.
[56] Y. Park, J. Kim, K. Hwang, Research about tooth whitening and bacteria sticking capability with using dentifrice including nano-hydroxyapatite, sodium metaphosphate, Key Eng. Mater. 330–332 (2007) 283–286.
[57] T. Arakawa, T. Fujimaru, T. Ishizak, H. Takeuchi, M. Kageyama, T. Ikemi, et al., Unique functions of hydroxyapatite with mutans streptococci adherence, Quintessence Int. 41 (2010) e11–e19.
[58] E.C. Reynolds, Remineralization of enamel subsurface lesions by casein phosphopeptide-stabilized calcium phosphate solutions, J. Dent. Res. 76 (1997) 1587–1595.
[59] A.P. Erdem, E. Sepet, T. Avshalom, V. Gutkin, D. Steinberg, Effect of CPP-ACP and APF on *Streptococcus mutans* biofilm: a laboratory study, Am. J. Dent. 24 (2011) 119–123.
[60] E.C. Reynolds, F. Cai, P. Shen, G.D. Walker, Retention in plaque and remineralization of enamel lesions by various forms of calcium in a mouthrinse or sugar-free chewing gum, J. Dent. Res. 82 (2003) 206–211.
[61] C. Rahiotis, G. Vougiouklakis, G. Eliades, Characterization of oral films formed in the presence of a CPP-ACP agent: an in situ study, J. Dent. 36 (2008) 272–280.
[62] C. Rahiotis, G. Vougiouklakis, Effect of a CPP–ACP agent on the demineralization and remineralization of dentin in vitro, J. Dent. 35 (2007) 695–698.
[63] C. Poggio, M. Lombardini, M. Colombo, S. Bianchi, Impact of two toothpastes on repairing enamel erosion produced by a soft drink: an AFM in vitro study, J. Dent. 38 (2010) 868–874.
[64] C. Hannig, S. Basche, T. Burghardt, A. Al-Ahmad, M. Hannig, Influence of a mouthwash containing hydroxyapatite microclusters on bacterial adherence in situ, Clin. Oral Invest. (2012) In press.
[65] A. Kovtun, D. Kozlova, K. Ganesan, C. Biewald, N. Seipold, P. Gaengler, et al., Chlorhexidine-loaded calcium phosphate nanoparticles for dental maintenance treatment: combination of mineralising and antibacterial effects, RSC Adv. 2 (2012) 870–875.
[66] V.A. Lee, R. Karthikeyan, H.R. Rawls, B.T. Amaechi, Anti-cariogenic effect of a cetylpyridinium chloride-containing nanoemulsion, J. Dent. 38 (2010) 742–749.
[67] T. Akasaka, F. Watari, Capture of bacteria by flexible carbon nanotubes, Acta Biomater. 5 (2009) 607–612.
[68] A. Okada, T. Nikaido, M. Ikeda, K. Okada, J. Yamauchi, R.M. Foxton, et al., Inhibition of biofilm formation using newly developed coating materials with self-cleaning properties, Dent. Mater. J. 27 (2008) 565–572.

[69] M. Gyo, T. Nikaido, K. Okada, J. Yamauchi, J. Tagami, K. Matin, Surface response of fluorine polymer-incorporated resin composites to cariogenic biofilm adherence, Appl. Environ. Microbiol. 74 (2008) 1428−1435.
[70] M. Hannig, L. Kriener, W. Hoth-Hannig, C. Becker-Willinger, H. Schmidt, Influence of nanocomposite surface coating on biofilm formation in situ, J. Nanosci. Nanotechnol. 7 (2007) 4642−4648.
[71] C.H. Su, A simple and cost-effective method for fabricating lotus-effect composite coatings, J. Coating Technol. Res. 9 (2012) 135−141.
[72] D. Ebert, B. Bhushan, Durable lotus-effect surfaces with hierarchical structure using micro- and nano-sized hydrophobic silica particles, J. Colloid Interface Sci. 368 (2012) 584−591.
[73] W. Barthlott, C. Neinhuis, The lotus effect: a self-cleaning surface based on a model taken from nature, Tekstil 50 (2001) 461−465.
[74] R. Furstner, C. Neinhuis, W. Barthlott, The lotus effect: self-purification of microstructured surfaces, Nachr. Aus. Der. Chem. 48 (2000) 24−28.
[75] R. Helbig, J. Nickerl, C. Neinhuis, C. Werner, Smart skin patterns protect springtails, PLoS One 6 (2011).
[76] M.Y. Kim, H.K. Kwon, C.H. Choi, B.I. Kim, Combined effects of nano-hydroxyapatite and NaF on remineralisation of early caries lesions, Key Eng. Mater. 330−332 (2007) 1347−1350.
[77] L. Kuilong, Z. Jiuxing, M. Xiangcai, L. Xingyi, Remineralization effect of the nano-HA toothpaste on artificial caries, Key Eng. Mater. 330−332 (2007) 267−270.
[78] B. Li, J. Wang, Z. Zhao, Y. Sui, Y. Zhang, Mineralizing of nano-hydroxyapatite powders on artificial caries, Rare Metal Mater. Eng. 36 (Suppl. 2) (2007) 128−130.
[79] S. Huang, S. Gao, L. Cheng, H. Yu, Remineralization potential of nanohydroxyapatite on initial enamel lesions: an *in vitro* study, Caries Res. 45 (2011) 460−468.
[80] D.J. Manton, G.D. Walker, F. Cai, N.J. Cochrane, P.Y. Shen, E.C. Reynolds, Remineralization of enamel subsurface lesions in situ by the use of three commercially available sugar-free gums, Int. J. Paediatr. Dent. 18 (2008) 284−290.
[81] M.V. Morgan, G.G. Adams, D.L. Bailey, C.E. Tsao, S.L. Fischman, E.C. Reynolds, The anticariogenic effect of sugar-free gum containing CPP−ACP nanocomplexes on approximal caries determined using digital bitewing radiography, Caries Res. 42 (2008) 171−184.
[82] F. Cai, D.J. Manton, P. Shen, G.D. Walker, K.J. Cross, Y. Yuan, et al., Effect of addition of citric acid and casein phosphopeptide−amorphous calcium phosphate to a sugar-free chewing gum on enamel remineralization in situ, Caries Res. 41 (2007) 377−383.
[83] F. Cai, P. Shen, G.D. Walker, C. Reynolds, Y. Yuan, E.C. Reynolds, Remineralization of enamel subsurface lesions by chewing gum with added calcium, J. Dent. 37 (2009) 763−768.
[84] P. Shen, D.J. Manton, N.J. Cochrane, G.D. Walker, Y. Yuan, C. Reynolds, et al., Effect of added calcium phosphate on enamel remineralization by fluoride in a randomized controlled in situ trial, J. Dent. 39 (2011) 518−525.
[85] Y. Shibata, L.H. He, Y. Kataoka, T. Miyazaki, M.V. Swain, Micromechanical property recovery of human carious dentin achieved with colloidal nano-beta-tricalcium phosphate, J. Dent. Res. 87 (2008) 233−237.
[86] N. Roveri, B. Palazzo, M. Iafisco, The role of biomimetism in developing nanostructured inorganic matrices for drug delivery, Expert Opin. Drug Deliv. 5 (2008) 861−877.
[87] N. Roveri, E. Battistello, C.L. Bianchi, I. Foltran, E. Foresti, M. Iafisco, et al., Surface enamel remineralisation: biomimetic apatite nanocrystals and fluoride ions different effects, J. Nanomater. (2009).
[88] H.J. Lee, J.H. Min, C.H. Choi, H.G. Kwon, B.I. Kim, Remineralization potential of sports drink containing nano-sized hydroxyapatite, Key Eng. Mater. 330−332 (2007) 275−278.

[89] J.H. Min, H.K. Kwon, B.I. Kim, The addition of nano-sized hydroxyapatite to a sports drink to inhibit dental erosion—in vitro study using bovine enamel, J. Dent. 39 (2011) 629–635.
[90] D.J. Manton, F. Cai, Y. Yuan, G.D. Walker, N.J. Cochrane, C. Reynolds, et al., Effect of casein phosphopeptide–amorphous calcium phosphate added to acidic beverages on enamel erosion in vitro, Aust. Dent. J. 55 (2010) 275–279.
[91] L. Sun, L.C. Chow, Preparation and properties of nano-sized calcium fluoride for dental applications, Dent. Mater. 24 (2008) 111–116.
[92] L. Rimondini, B. Palazzo, M. Iafisco, L. Canegallo, F. Denarosi, M. Merlo, et al., The remineralizing effect of carbonate–hydroxyapatite nanocrystals on dentin, Mater. Sci. Forum (2007) 602–605.
[93] G. Orsini, M. Procaccini, L. Manzoli, F. Giuliodori, A. Lorenzini, A. Putignano, A double-blind randomized-controlled trial comparing the desensitizing efficacy of a new dentifrice containing carbonate/hydroxyapatite nanocrystals and a sodium fluoride/potassium nitrate dentifrice, J. Clin. Periodontol. 37 (2010) 510–517.
[94] A. Kowalczyk, B. Botulinski, M. Jaworska, A. Kierklo, M. Pawinska, E. Dabrowska, Evaluation of the product based on recaldent technology in the treatment of dentin hypersensitivity, Adv. Med. Sci. 51 (Suppl. 1) (2006) 40–42.
[95] C. Braunbarth, H. Franke, R. Kniep, C. Kropf, T. Poth, G. Schechner, et al., The mineralising effect of a nanoscaled calcium phosphate protein composite (Nano®active) on dentin, VDI Berichte 1803 (2003) 283–286.
[96] S.Y. Lee, H.K. Kwon, B.I. Kim, Effect of dentinal tubule occlusion by dentifrice containing nano-carbonate apatite, J. Oral Rehabil. 35 (2008) 847–853.
[97] A. Guentsch, K. Seidler, S. Nietzsche, A.F. Hefti, P.M. Preshaw, D.C. Watts, et al., Biomimetic mineralization: long-term observations in patients with dentin sensitivity, Dent. Mater. 28 (2012) 457–464.
[98] K. Yamagishi, K. Onuma, T. Suzuki, F. Okada, J. Tagami, M. Otsuki, et al., A synthetic enamel for rapid tooth repair, Nature 433 (2005) 819.
[99] H.F. Chen, Z.Y. Tang, J. Liu, K. Sun, S.R. Chang, M.C. Peters, et al., Acellular synthesis of a human enamel-like microstructure, Adv. Mater. 18 (2006) 1846–1851.
[100] F.C. Meldrum, H. Colfen, Controlling mineral morphologies and structures in biological and synthetic systems, Chem. Rev. 108 (2008) 4332–4432.
[101] M. Sarikaya, C. Tamerler, A.K. Jen, K. Schulten, F. Baneyx, Molecular biomimetics: nanotechnology through biology, Nat. Mater. 2 (2003) 577–585.
[102] A.G. Fincham, J. Moradian-Oldak, J.P. Simmer, The structural biology of the developing dental enamel matrix, J. Struct. Biol. 126 (1999) 270–299.
[103] J. Moradian-Oldak, Amelogenins: assembly, processing and control of crystal morphology, Matrix Biol. 20 (2001) 293–305.
[104] J. Tao, H. Pan, Y. Zeng, X. Xu, R. Tang, Roles of amorphous calcium phosphate and biological additives in the assembly of hydroxyapatite nanoparticles, J. Phys. Chem. B 111 (2007) 13410–13418.
[105] Y. Fan, Z. Sun, J. Moradian-Oldak, Controlled remineralization of enamel in the presence of amelogenin and fluoride, Biomaterials 30 (2009) 478–483.
[106] Y. Iijima, J. Moradian-Oldak, Control of apatite crystal growth in a fluoride containing amelogenin-rich matrix, Biomaterials 26 (2005) 1595–1603.
[107] S. Busch, U. Schwarz, R. Kniep, Chemical and structural investigations of biomimetically grown fluorapatite-gelatin composite aggregates, Adv. Funct. Mater. 13 (2003) 189–198.
[108] S. Busch, Regeneration of human tooth enamel, Angew. Chem. 43 (2004) 1428–1431.
[109] J.A. Tavener, G.M. Davies, R.M. Davies, R.P. Ellwood, The prevalence and severity of fluorosis in children who received toothpaste containing either 440 or 1,450 ppm F from the age of 12 months in deprived and less deprived communities, Caries Res. 40 (2006) 66–72.

[110] T. Walsh, H.V. Worthington, A.M. Glenny, P. Appelbe, V.C. Marinho, X. Shi, Fluoride toothpastes of different concentrations for preventing dental caries in children and adolescents, Cochrane Database Syst. Rev. (2010) CD007868.
[111] M.C. Wong, A.M. Glenny, B.W. Tsang, E.C. Lo, H.V. Worthington, V.C. Marinho, Topical fluoride as a cause of dental fluorosis in children, Cochrane Database Syst. Rev. (2010) CD007693.
[112] C. Van Loveren, Antimicrobial activity of fluoride and its in vivo importance: identification of research questions, Caries Res. 35 (Suppl. 1) (2001) 65–70.
[113] Z. Yang, Z.W. Liu, R.P. Allaker, P. Reip, J. Oxford, Z. Ahmad, et al., A review of nanoparticle functionality and toxicity on the central nervous system, J. R. Soc. Interface 7 (Suppl. 4) (2010) S411–S422.
[114] S. Sonkaria, S.H. Ahn, V. Khare, Nanotechnology and its impact on food and nutrition: a review, Recent Pat. Food Nutr. Agric. 4 (2012) 8–18.
[115] E. Frohlich, E. Roblegg, Models for oral uptake of nanoparticles in consumer products, Toxicology 291 (2012) 10–17.
[116] P.D. Dwivedi, A. Tripathi, K.M. Ansari, R. Shanker, M. Das, Impact of nanoparticles on the immune system, J. Biomed. Nanotechnol. 7 (2011) 193–194.

CHAPTER

Silver and Phosphate Nanoparticles: Antimicrobial Approach and Caries Prevention Application

9

D.B. Barbosa[a], D.R. Monteiro[a], A.S. Takamyia[a], E.R. Camargo[b], A.M. Agostinho[c], A.C.B. Delbem[a] and J.P. Pessan[a]

[a]*São Paulo State University, Araçatuba Dental School, Brazil*

[b]*LIEC-Department of Chemistry, Federal University of São Carlos, Brazil*

[c]*Center for Engineering Biofilm, Montanta State University, USA*

CHAPTER OUTLINE

9.1 Welcome to nanoworld

For centuries, chemists have been able to organize matter, atom by atom, to make molecules. Particularly, since the nineteenth century, organic chemistry has shown that nearly infinite number of different molecules could be synthesized, isolated, and purified. Therefore, what is new in this branch of science of the twenty-first century named *nanoscience*? Or, what is the difference

between an ordinary molecule and a typical nanoparticle? It is a simple question that cannot be easily answered. First, nature is the same and we are talking about galaxies, trees, and atoms. Indeed, the same laws are applied for biological systems or artificial devices invented by the human mind. It means that a computer or a sunflower obey exactly the same restrictions regarding thermodynamics, kinetics, or quantum mechanics. Second, the classification in nanometric or kilometric scale is just a human way to organize our universe. There are not intrinsic compartments in nature to define a system as "nanometric" or "macroscopic." It is just human interpretation.

From the words of Ozin and Arsenault [1], *nanoscience* is defined being the discipline concerned with making, manipulating, and imaging materials having at least one special dimension in the size range 1−1000 nm and *nanotechnology* being a device or machine, product or process, based upon individual or multiple integrated nanoscale components. However, this definition did not show the most important question: Why was it so important to us classifying matter in this way? The answer is *properties*, not length.

We are accustomed to observe nature as a continuum. All the shapes are possible and all the sizes are allowed. Although shape and size are the easiest method to classify a system, the most important property of a system is related to *energy*. Differently to our common and classical assumption of nature, energy is a discrete variable and any amount of energy (E) should be proportional to an integral multiple of a specific frequency (ν), represented by Eq. (9.1), where n is an integer and h is the proportionality constant (the Planck constant) that has the value of 6.629×10^{-24} J/s, which is an extremely small value of power.

$$E = nh\nu \tag{9.1}$$

For sake of comparison, a human being has an average power of 100 J/s, which is millions of billions of billions higher than the Planck constant. While a molecular event involves *quanta* of approximately 10^{-18} J, any energetic process occurring in our scale of time and length are infinitely higher, which makes virtually impossible to us to distinguish the existence of discrete levels [2].

A single atom is fully characterized by very precise energetic transitions that can be easily measured using spectroscopy techniques. The existence of these energetic levels results from the confinement of electrons in movement under the influence of the atomic nucleus and has been well explained by quantum mechanics [3]. When a finite number of atoms, for example one hundred of them, are put together, there is complex interaction between their electronic densities, which results in chemical bonds and new energetic transitions that were forbidden in an isolated atom. If more and more atoms are added to the system, their energetic properties reach macroscopic values that characterize a substance.

"Silver is silver," a silver miner can say. However, it is true only when the number of atoms is large enough to achieve the limit properties of a macroscopic sample. "One gram of silver has the same properties of 1 ton." But 1 g of silver has 1.6×10^{22} atoms. It is a huge number. For samples with a few atoms, the properties that depend on the energetic levels will be evidently different. Since each silver atom has a diameter of 0.165 nm, just seven atoms aligned results in a *nanometric* system of *1 nm*.

That is the point. Nanoscience is the manipulation of a sufficiently small number of atoms to form particles with energetic characteristics that are intermediate between a single atom and a macroscopic sample. It is the reason why chemists and materials scientists are always developing new techniques to control the number of atoms in their nanoparticles. If a molecule is a fixed number of atoms organized in a precise structure, a nanoparticle, on the other hand, can be prepared with

different size and shape to tune some specific property of interest. For example, some nanoparticles can present different colors in function of their sizes because of the modification in the electronic band gap of semiconductors (Figure 9.1) or in the surface plasmon band of metals (Figure 9.2). Moreover, the shape and symmetry of a nanoparticle are as important as the size on the energetic properties.

One fundamental aspect of all nanoparticles is the high surface area to volume ratio [6]. When an atom is on the surface of a nanoparticle, its coordination number presents imperfections, which causes a spontaneous contraction of the remaining bond. This bond contraction can be associated to a potential energy depression that increases the interaction between electrons and the nucleus of this atom, which enhance the local density of charge, modifying significantly the chemical properties of the surface. It means that the surface of a nanoparticle is much more reactive than any flat surface of similar composition and any reaction that occurs on the surface of the nanoparticles will be immediately accelerated.

It is not difficult to imagine the impact of the *nanoscience* in the field of human health, particularly in dentistry with treatment opportunities that may include the formulation of functional dentifrices, tooth repair, dentition renaturalization, drug delivery for local anesthesia, teeth prosthesis with superior performance, antimicrobial action and oral cancer treatment and diagnostics. The advent of the *nanotechnology* resulted in a new paradigm in several fields, and because of their interdisciplinary character, the potential of *nanodentistry* to improve the welfare of our society will be achieved only through an intensive and collaborative work of researchers and experts from different fields.

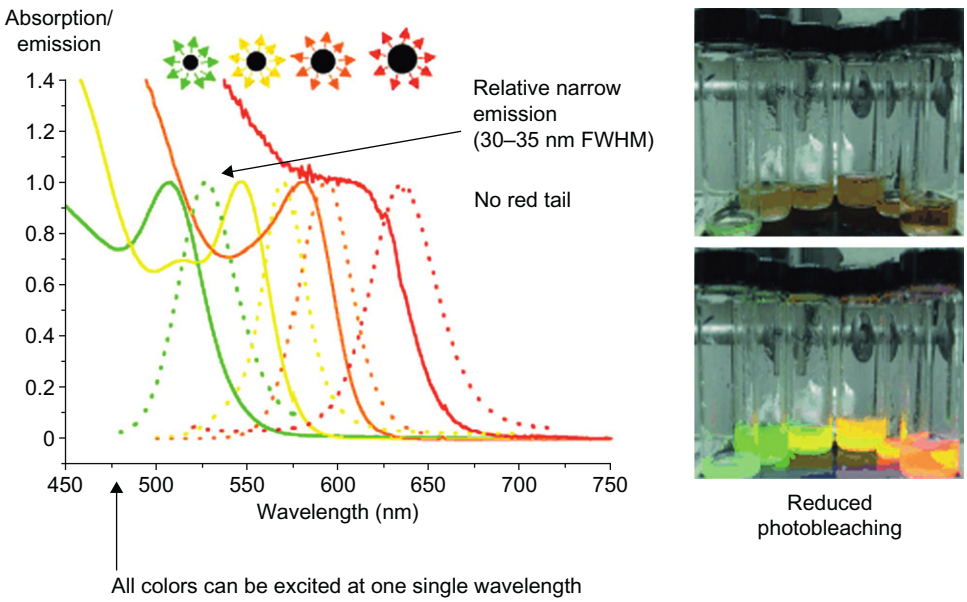

FIGURE 9.1

Influence of size on the optical properties of colloidal CdSe [4].

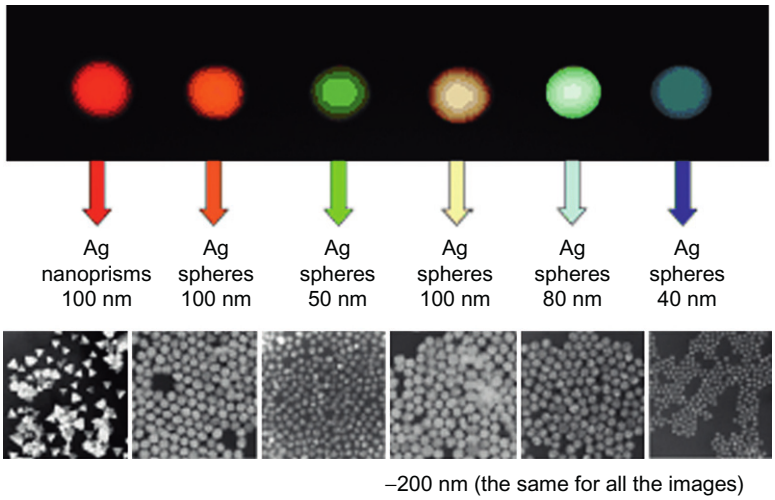

FIGURE 9.2

Influence of size on the light scattering of silver nanoparticles [5].

9.2 Nanoparticles X "BUGS"

9.2.1 Microbial biofilms and tolerance

Microbial biofilms are communities of microorganisms attached to a living or inert surface in an aqueous environment and surrounded in a matrix of extracellular polymeric substances (EPS) [7]. The EPS synthesized by microbial cells consist of polysaccharides, proteins, glycoproteins, glycolipids and, in some cases, extracellular DNA. These substances form a network that influence the porosity, density, water content, charge, sorption, hydrophobicity, and mechanical stability of biofilms. In addition, the extracellular matrix provides nutrients for biofilm cells through interaction with the environment [8].

Oral biofilms (Figure 9.3) are polymicrobial and formed by more than 700 different species of microorganisms, and their composition may vary according to different substrates (soft shedding tissues and hard nonshedding surfaces) within the oral cavity [7,9]. In healthy oral environment, there is a balance between the biofilm cells and human host [9]; however, the accumulation of oral bacteria and yeast biofilms can lead to the development of diseases such as caries, periodontitis, candidiasis (e.g., denture stomatitis), peri-implantitis, and endodontic infections [10]. Biofilm cells are different from their planktonic counterparts, given that biofilms exhibit increased tolerance/resistance to antimicrobial agents and to the host immune response. Thus, the control of oral biofilms is crucial to prevent disease and preserve the homeostasis in the oral cavity.

However, biofilms are known to be more tolerant to antimicrobials than planktonic cells. Although over the years the traditional minimal inhibitory concentration (MIC) and minimal bactericidal concentration (MBC) have been used to determine antimicrobial doses in vitro, they cannot be used to correctly predict the doses of antimicrobials needed to control biofilm infections [11].

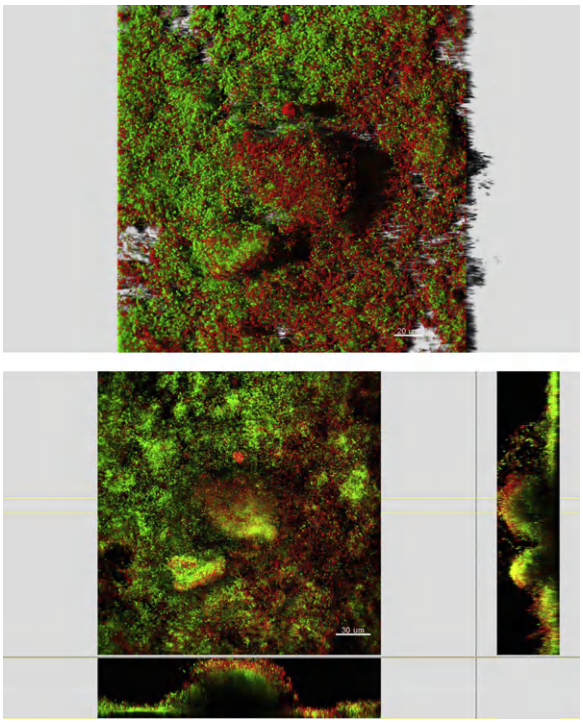

FIGURE 9.3

Dental biofilms grown on hydroxyapatite chips in situ. The biofilms were stained with LIVE/DEAD® BacLight™ Bacterial Viability Kit and imaged with a confocal microscope. Green cells represent live microorganisms while red are dead. (For interpretation of the references to color in this figure legend, the reader is referred to the web version of this book.)

Image courtesy of The Center for Biofilm Engineering at Montana State University.

Several factors influence biofilm tolerance to antimicrobials including nanoparticles. The first factor that sets biofilms apart is the presence of EPS. The slime layer that involves the microbial cells may not only limit the penetration of the agents but also react with it, reducing its effectiveness [12]. In addition, biofilms are very heterogeneous; so in a community there are not only highly active cells but also dormant cells. In fact, the presence of dormant cells has been reported as the major factor in antimicrobial tolerance [13,14].

As many antimicrobial and antibiotics target macromolecule synthesis, when the cells are not growing or dividing they are less susceptible. Other factors involved in tolerance are the phenotypic variations, the existence of a highly developed communications system between the cells (quorum sensing), and the bacterial multidrug efflux pumps [13,15]. A possible strategy to overcome biofilm tolerance may be the use of several antimicrobials combined or even the combination of physical and chemical treatments.

9.2.2 Silver nanoparticles and biofilms

9.2.2.1 Mechanisms of action and literature data

Inorganic nanoparticles represent a new era in the nanoparticle field. They exhibit unique physical and chemical properties and can be used in many physical, biological, biomedical, and pharmaceutical applications [16].

Silver nanoparticles are known for their broad-spectrum antimicrobial activity against bacteria, fungi, and viruses [17], and multifactorial mechanism of action. Nevertheless, data have shown that biofilm-forming cells are less susceptible to nanosilver (nano-Ag) than planktonic counterparts [18,19]. An in vitro study found that the MIC of nano-Ag for *Escherichia coli* biofilms was four-fold higher than the MIC for planktonic cells [18]. For *Candida albicans* and *Candida glabrata* biofilms, the MIC was 17- to 135-fold and 16.5- to 34-fold higher, respectively, than for planktonic cells [19].

However, nano-Ag may have an important role in the prevention of biofilm formation. Kalishwaralal et al. [20] verified that treating *Pseudomonas aeruginosa* and *Staphylococcus epidermidis* with nano-Ag caused 95% inhibition in biofilm formation. A similar result was observed by Monteiro et al. [21] with respect to *C. albicans* and *C. glabrata* biofilms. These authors found that nano-Ag at 3.3 μg/mL were more effective in inhibiting biofilm formation than in controlling preformed biofilms.

Although biofilms have water channels through which nanoparticles may diffuse [20], many nanoparticles may be retained in the extracellular matrix, contributing to biofilm resistance. Furthermore, several mechanisms have been proposed to explain why nanoparticles have a better effect when applied to planktonic cells than on mature biofilms.

Another important aspect that may hinder the action of nano-Ag against biofilm cultures is their predisposition to form aggregates of particles (Figure 9.4). This aggregation can occur due to changes in ionic strength and interactions of nanoparticles with several substances present in

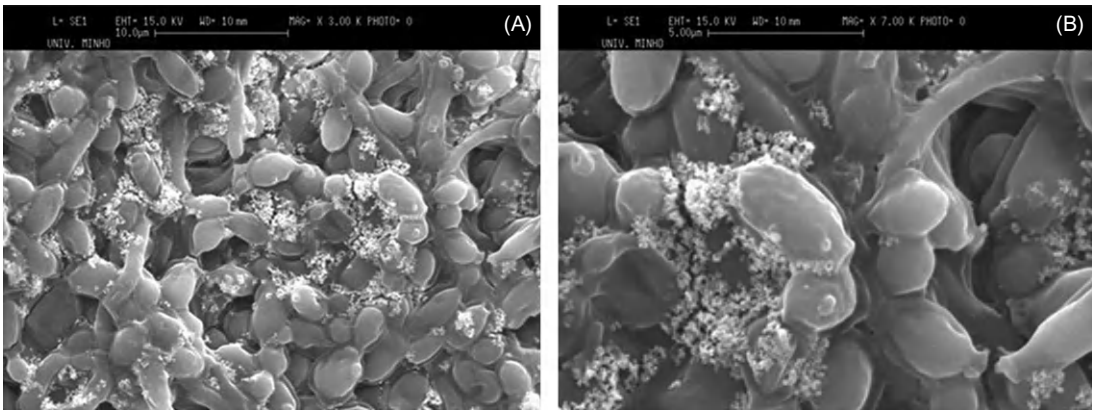

FIGURE 9.4

Scanning electron microscopy images showing clusters of silver nanoparticles in contact with mature *Candida albicans* biofilm. (B) represents an enlarged view of part of biofilm displayed in (A).

extracellular matrix produced by microorganisms [18]. Microscopic observations have indicated that the interactions of *E. coli* biofilm cells and nano-Ag resulted in an increase in final average aggregate size by a factor of 40 [18]. The increase in the particle size may reduce the silver toxicity and retard the particle diffusion within the biofilms, resulting in resistance to nano-Ag [18].

The size of nanoparticle and the type of stabilizing agent are not crucial to their efficacy against biofilms probably due to particle aggregation. Nano-Ag with different diameters (5, 10, and 60 nm) formed through the reduction of silver nitrate with sodium citrate [22] and stabilized with ammonia or polyvinyl pyrrolidone (PVP) (to control particle growth and prevent aggregation) showed no significant differences in the effect against *C. albicans* and *C. glabrata* mature biofilms [19]. Thus, the size of nano-Ag originally synthesized is not a good indication of the true nanoparticle size when in contact with biofilms.

The uptake of nano-Ag by biofilms has also been studied. Interestingly, in a study by Fabrega et al. [23], only approximately 10% of the total mass of nano-Ag to which *Pseudomonas putida* biofilms were exposed (during 24 h) remained trapped through the biofilms.

A study on the diffusion of nanoparticles in *Pseudomonas fluorescens* biofilms found that self-diffusion coefficients decreased with the square of the radius of the nanoparticles [24]. In addition, nano-Ag showed a greater tendency to accumulate in dense biofilms when compared to loose flakes. These aspects may influence the susceptibility of biofilms to nano-Ag.

In conclusion, the interaction between biofilms and nano-Ag is complex and, possibly, several factors may interfere with the efficacy of these particles against biofilms. Thus, these issues need to be more explored in order to better understand the behavior of nanoparticles on biofilms.

9.2.2.2 Processing silver nanoparticles

To obtain small metallic colloidal nanoparticles, a high density of nuclei at the beginning of the process is necessary. For this reason, the addition of a reducing agent, such as sodium citrate, into a solution of silver nitrate should be carried out as fast as possible to form a large number of nanoparticles simultaneously. However, unlike other noble metals, only a fraction of silver ions are reduced to metal, even when using an excess of sodium citrate or any different reducing reagent. Due to this inevitable presence of silver ions, new nuclei will still be formed while the nanoparticles initially formed will continue to grow, fed by Ag^+ that was not consumed during the formation of the first nuclei. This process results in a system with a broad size distribution, consisting of large particles formed initially and small particles that were formed subsequently. To overcome this problem and obtain stable aqueous colloidal suspensions of spherical silver nanoparticles with sharp size distribution, there is a way to prevent particle growth and the generation of new nuclei using ammonia to trap all free silver ions. It is well known that when an excess of ammonia is added in the presence of Ag^+, soluble diamine silver (I) complexes are formed immediately (Eq. (9.2)), removing the silver ions that have not yet been reduced. It prevents the formation of new nuclei and the growth of already formed nanoparticles, resulting in virtually monodisperse silver nanoparticles [22].

$$Ag^+ + 2NH_3 \rightarrow [Ag(NH_3)_2]^+ \tag{9.2}$$

It is not easy to propose a kinetic model for the growth of silver nanoparticles since there are many variables to consider in this case. However, the interdependence of density of nuclei and reaction time may serve to shed light on the formation of a monodisperse system of nanoparticles, and

how ammonia acts as a moderator of nanoparticle growth in the colloidal medium (Figure 9.5) [22]. This apparently simple idea effectively results in stable colloidal aqueous suspensions of spherical silver nanoparticles with narrow size distributions. The addition of ammonia, or any agent to trap the excess of silver ions, to the system immediately after the nucleation stage is an efficient way to stabilize colloidal suspensions of monodisperse silver nanoparticles with controlled size, since free silver ions, which are responsible for particle growth and the formation of new nuclei, are trapped by the formation of soluble complexes, preserving the silver nanoparticles for long storage periods without coalescing or precipitating. This procedure, which involves the use of inexpensive and nontoxic reagents, also allows the particle size to be determined by choosing the right moment at which ammonia. The earlier the ammonia is added the smaller the average particle size will be.

When silver nanoparticles are synthesized based on Turkevich [25] methods, it is fundamental to use deionized water to prepare the solution, although the chemicals used are usually of analytical grade, with no further purification. Silver nanoparticles can be prepared by the reduction of silver nitrate with sodium citrate or any reducing agent. In a typical procedure, a volume of 100 mL of an aqueous solution of silver nitrate (1.0 mmol/L) is heated and stirred gently. The silver nitrate solution should be heated to temperatures between 60°C and 90°C before the addition of 1.0 mL of a solution of sodium citrate (0.3 mol/L) to accelerate the reaction. At room temperature, this reaction is too slow that is not possible to follow it. This reaction can be monitored through the typical yellow color the characteristic plasmon absorbance band at approximately 425 nm. The intensity is proportional to the nanoparticle concentration; however concentrated colloidal dispersion is not stable for long time and in this case, an extra stabilizing agent such as PVP is necessary.

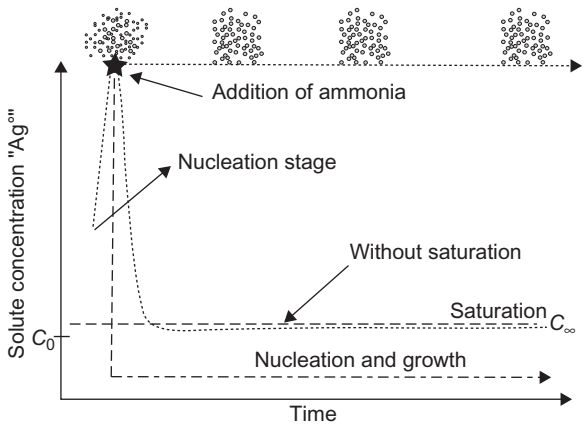

FIGURE 9.5

Reduction in the metallic silver concentration as a function of reaction time, showing the initial nucleation stage after the addition of citrate ion and the addition of ammonia immediately after the system turned yellow, reducing the amount of metallic silver to a quantity below the saturation limit [22].

9.3 Phosphates micro- and nanoparticles and caries prevention

9.3.1 De- and remineralization process

Dental caries is a dietobacterial disease resulting from the slow but progressive dissolution of the tooth surfaces by acids produced by bacteria in the dental biofilm [26]. It has a multifactorial nature, in which the concomitant interaction of dietary sugars, dental biofilm, and the host is needed [27]. In order to understand the dynamics of dental enamel demineralization (DE) and remineralization (RE) processes, a few biochemical aspects of the oral environment must be highlighted.

In general terms, tooth enamel is mostly composed by hydroxyapatite (HAP) and fluoro hydroxyapatite (FAP). The supersaturation of saliva with respect to these minerals has important clinical implications, as HAP and FAP will not dissolve unless significant changes in the oral pH occur. When the dental biofilm is exposed to fermentable sugars, the pH in the biofilm fluid rapidly decreases to values below the critical pH for HAP (5.5) and/or FAP (4.5), so that saliva becomes undersaturated with respect to these minerals. This leads to enamel DE. With time, the pH in the biofilm fluid begins to rise, due to the action of salivary buffers. When the pH in the biofilm fluid reaches values above the critical pH for HAP and FAP, enamel RE occurs [28]. The equilibrium between DE and RE processes will determine that the enamel structure will not dissolve. However, when DE episodes occur at a higher frequency and intensity, RE cycles will not be able to reverse enamel dissolution, causing dental caries lesion.

Among the strategies to shift the balance from DE to RE, fluoride therapy is the most widely used, as it reduces the enamel acid solubility (by converting HAP in FAP after acid challenges) and increases the RE process (by promoting the reprecipitation of calcium and phosphates into the dental mineral) [26,29]. However, due to the increase in dental fluorosis prevalence observed over the last few decades, the search for nonfluoride therapeutic agents have been studied, which include calcium and phosphate salts. These have been studied in association or not with fluoride in dentifrices, gels, varnishes, and rinses, and include $CaCl_2$, calcium lactate, calcium glycerophosphate, sodium trimetaphosphate (TMP), nanocomplexes of casein phosphopeptide−amorphous calcium phosphate, among others.

9.3.2 Nanophosphates and microbial adhesion

Phosphates have great affinity with HAP, preventing the release of calcium and phosphate ions and reducing the surface area available for dissolution [30,31]. In vitro studies showed that it is possible to reduce the concentration of fluoride in dentifrices and mouth rinses, yet maintaining their protective action against both dental caries and erosion by adding inorganic phosphate (sodium TMP) to the products [32−36]. Given the high adsorption of phosphates to the enamel surface, it would be interesting to investigate whether the use of phosphate would influence bacterial adhesion to tooth enamel, as well as on mineral loss. The effects of TMP on dental biofilm and its efficacy when combined to different antimicrobials effect on biofilm were analyzed by colony forming unit (CFU) counts and lactic acid production. The data presented in that study demonstrated that the biofilm model used was suitable to grow biofilm on different substrata, both in microcosm and single species biofilms. The model allows the evaluation of antimicrobial agents and TMP on

biofilm survival and metabolism [35]. It was concluded that TMP, alone or combined to antimicrobials, had no direct action on biofilm. In addition, a pilot study compared the effect of treatment (during 5 min) of bovine enamel blocks with commercial TMP and TMP with smaller particles in different concentrations (3% and 5%) on the adhesion of *C. albicans* and *C. glabrata*. It was possible to observe that, regardless of the concentration, the treatment with TMP with different particle sizes did not reduce the number of CFUs on the enamel blocks after a period of 2 h (initial adhesion) for *Candida* species tested.

9.4 Pros and cons of nanoparticles toward biological-dental application

9.4.1 Toxicity

Profile toxicity of nanomaterials can be considered different from larger particles mainly because of their small size and high reactivity [37–39]. Toxicology associated to nanostructures, in general, is affected by different physical and chemical properties of each nanomaterial [37,38]. Precisely, because of the number of variables interfering on the toxicity of nanomaterials, it is difficult to generalize their effects on the biological systems [40].

Composition is clearly a key factor in determining the toxicity of nanomaterials. Actually, taking into consideration the chemical composition, there are an enormous number of different nanomaterials [40,41]. One of the most widely studied categories of nanomaterials are metal nanoparticles; among them silver nanoparticles are those that generate more interest in nanotoxicological research, precisely because of their use as antimicrobial agent in the medical area [17,21,42].

In general, shape and size of the nanomaterials directly influence on the toxicity [39,43]. It has been stated that cubic nanoparticles induce lower level of toxicity compared to those that are cylindrical, spherical, and rod shaped [44]. Usually, smaller particles are considered more toxic since they occupy less volume in a greater surface area per unit of mass increasing the availability for the biological interactions [37,38]. Furthermore, it has been amply exposed that the internalization of nanomaterials is a size-dependent process; smaller particles are much more easily internalized into the cells and therefore more available for interaction with cellular components [43,45].

The main objectives of surface treatment or functionalization of nanoparticles are ensuring stability and promote favorable characteristics to a specific proposal [46,47]. Nanoparticles can be superficially modified with polymers, drugs, peptides, proteins, oligonucleotides, and biological molecules [46,47] and show different cytotoxic characteristics depending on the coating material [47,48]. Thus, surface treatment or functionalization can be considered one of the most relevant factors of cytotoxicity [43,49] since the process modifies chemical properties inherent to the nanomaterials and determines their toxicity profile [43,49].

Considering the agglomeration state of the nanomaterials and their related cytotoxicity, it has been suggested that the process of agglomeration makes the particles become larger or even exceed the nanoscale [50]. As discussed above, size is considered to be a relevant factor in determining the toxicity profile. Recently, it was confirmed that large agglomerates are not effectively cell internalized; therefore, agglomerated particles can be considered lower cytotoxic, once that the agglomeration state of the particles significantly reduces surface area availability and access into the cells [50].

Bearing in mind the role of silver nanoparticles on current scenario, questions can arise about the action of silver nanoparticles on human cells. Important preliminary data regarding the toxicity of nanoparticles at cellular level have been reported. In this sense, it has been accepted that the mechanisms of cytotoxicity of nanoparticles are the same for microorganisms and human cells [17,51].

Human contact with silver nanoparticles for therapeutic applications can occur mainly through inhalation and dermal absorption [52]. From the site of the contact, the particles can be biodistributed in the organism by the circulatory and lymphatic systems [53]. Thus, it has been accepted that nanoparticles can achieve different parts of the human body promoting adverse effects that are not completely understood [37,43,46,53–55].

It has been stated that silver nanoparticles penetrate the cells mainly by the process of endocytosis, and once into the cell they interact with different structures in the cytoplasm and nucleus. Silver nanoparticles are considered highly mobile and they can be sequestered in various intracellular compartments or organelles but preferentially are located in the mitochondria [51,53,56]. The deposition of the silver nanoparticles in this cellular organelle can cause suspension of electron transport chain, resulting in low ATP production and higher production of reactive oxygen species (ROS) [51,53,56]. Increased concentrations of ROS can initiate the apoptotic cascade [41,53,56]. Furthermore, it has been known that cellular oxidation–reduction homeostasis is maintained in part by the glutathione (GSH) intracellular levels [41,56]. Recently, it was found that silver nanoparticles can deplete GSH inhibiting antioxidant defense mechanisms [41].

Silver nanoparticles can also induce DNA damage, as they can be deposited in the nucleus, affect the DNA synthesis, and cause chromosomal abnormalities; however, the exact mechanisms that promote these events are not completely understood [39,53,56].

Although the biological effects of nanomaterials constitute research area of growing interest, the use of biomaterials in nanoscale range in the biomedical area requires more information. It is necessary to assess the toxicological profiles of different nanomaterials taking in account their several specific properties. Without accurate toxicity data, the use of nanomaterials can become a risk for human health.

9.4.2 Processing costs

The science and technology of nanomaterials has created great excitement and expectations in the last few years. The burgeoning of *nanoscience* creates new opportunities for advanced medical protocols and disease treatments. However, it is widely claimed that research effort to discover and develop new pharmaceuticals entails high costs and high risks, mainly when it involves *nanotechnology*. The principal justification for the high prices on patented drugs has been the high cost of research and development (R&D). Recently, the average cost of a new patented molecule was estimated at $802 million [57,58], although some authors disagree with the methodology used, proposing a median of $43.3 million per new drug [59]. These extremely expensive values imposed by multinational corporations are related to therapeutic drugs for complex diseases, such as cancer, HIV, and depression. For the particular use in dentistry, the costs are evidently smaller, which represent an opportunity for innovative university spin-off companies based on *nanotechnology* and advanced materials. Nanoparticles are expensive since they are difficult to isolate and, eventually, tedious to purify. On the other hand, a commercial *nanocomposite* shows functional nanofiller loads

typically less than 10 wt%. Obviously, taxes and marketing margins are a few of the components that impact the final price for the consumer, and the packaging represents more than one-third of the final price without any gain of economy of scale. The average cost of fabrication of functional nanoparticles is usually in the range from $100 to $1000 per gram, but its impact in the price composition of dentistry products is proportional to the parcel of others components, resulting in a product with commercial viability considering their advantages regarding the performance and patient comfort.

9.4.3 Potential use in dental field and future directions

In general, the great interest of nanoparticles is related to its highly small size. By reducing the size of a material, the surface to volume ratio increases. As a consequence, the majority of the atoms are at the margin of the particle making them much more reactive [60]. This reactivity is specially noted in inorganic nanoparticles and might conduce to instabilities and then to degradation and corrosion processes [60]. Regarding silver nanoparticles, several methods of synthesis have been developed in the last decade, although most of them are still under development [61]. They are basically focused on increasing the stability and reducing the aggregation of nanoparticles since the small size would ensure that an expressive surface area would be in contact with the microbial effluent [62,63]. However, we agree with Pal et al. [62] when they said that "smallness in itself" should not be the only purpose in the development of functional inorganic nanoparticles. The majority of our studies related to the action of silver nanoparticles against Candida species testified it, especially the study carried out by Monteiro et al. [19] where the size of the particles did not interfere with its efficacy. Surface interactions of nanoparticles with the surrounding medium (bioactivity) before they reach the aimed target are a significant aspect to be considered [64]. Bastús et al. [60] clearly explained that in functional colloidal inorganic nanoparticles, these interactions are determined not only by the size, shape, or structure of the center (core) of the nanoparticle but also by the organic or inorganic molecules that cover the core (shell) [60]. This might be the most relevant insight that those authors specially pointed out about nanostructured materials, and their applicability in biomedical/dental field relies on more understanding and comprehension about not only controlled synthesis but also particles interfacial interactions and their toxicity [65,66].

Besides the predominant role of the shell on the interactions of the nanoparticle, it may also protect the particle and, therefore, defines its selectivity against the microorganism or the molecular target [60]. We could take advantage of this particular bioactivity of functional nanoparticles and intentionally engineer them for both core and shell to provide therapeutic effects with low toxicity on the mammalian cells.

9.5 Conclusions

Concluding, the field of dentistry should be encouraged by the multiple studies in nanotechnology that have been widely published in different fields like medical, chemical, biological engineering, and at least environmental field to create "intelligent bionanomaterials" which could act multifunctionally: (i) by preventing/controlling the infection in or on oral tissues as well as (ii) by stimulating/contributing for the RE of dental and bone tissues. Very recent literature has been

driving us to this pathway [63,67,68]. Possibly bionanomaterials of silver phosphates are a promising candidate for different dental materials purposes, like in titanium implants coatings, bone fillings, dental varnish or sealants, toothpastes and even in dental floss covering, since they would combine the antimicrobial action of silver and the bioactivity of phosphates [63].

From now, the door for future perspectives is open to welcome the readers into the "nanoworld" to give their appropriate judgments in regard to the disadvantages and the real benefits of the use of nanostructured biomaterials in the dental field.

References

[1] G.A. Ozin, A.C. Arsenault, Nanochemistry. A chemical approach to nanomaterials, R. Soc. Chem. (2005).

[2] D.A. McQuarrie, J.D. Simon, Physical Chemistry. A Molecular Approach, University Science Books, 1997.

[3] I. Levine, Quantum Chemistry, sixth ed., Prentice Hall, 2008.

[4] T. Pellegrino, S. Kudera, T. Liedl, A.M. Javier, L. Manna, W.J. Parak, On the development of colloidal nanoparticles towards multifunctional structures and their possible use for biological applications, Small 1 (1) (2005) 48.

[5] C.A. Mirkin, The beginning of a small revolution, Small 1 (1) (2005) 14.

[6] A.Z. Moshfegh, Nanoparticle catalysts, J. Phys. D. Appl. Phys. 42 (23) (2009).

[7] V. Zijnge, M.B. van Leeuwen, J.E. Degener, F. Abbas, T. Thurnheer, R. Gmur, et al., Oral biofilm architecture on natural teeth, PLoS One 5 (2) (2010) e9321.

[8] H.C. Flemming, T.R. Neu, D.J. Wozniak, The EPS matrix: the "house of biofilm cells", J. Bacteriol. 189 (22) (2007) 7945.

[9] S. Filoche, L. Wong, C.H. Sissons, Oral biofilms: emerging concepts in microbial ecology, J. Dent. Res. 89 (1) (2010) 8.

[10] R.P. Allaker, The use of nanoparticles to control oral biofilm formation, J. Dent. Res. 89 (11) (2010) 1175.

[11] C.A. Fux, J.W. Costerton, P.S. Stewart, P. Stoodley, Survival strategies of infectious biofilms, Trends Microbiol. 13 (1) (2005) 34.

[12] T.R. Zuroff, H. Bernstein, J. Lloyd-Randolfi, L. Jimenez-Taracido, P.S. Stewart, R.P. Carlson, Robustness analysis of culturing perturbations on *Escherichia coli* colony biofilm beta-lactam and aminoglycoside antibiotic tolerance, BMC Microbiol. 10 (2010) 185.

[13] S.A. Rani, B. Pitts, H. Beyenal, R.A. Veluchamy, Z. Lewandowski, W.M. Davison, et al., Spatial patterns of DNA replication, protein synthesis, and oxygen concentration within bacterial biofilms reveal diverse physiological states, J. Bacteriol. 189 (11) (2007) 4223.

[14] J.P. Folsom, L. Richards, B. Pitts, F. Roe, G.D. Ehrlich, A. Parker, et al., Physiology of *Pseudomonas aeruginosa* in biofilms as revealed by transcriptome analysis, BMC Microbiol. 10 (2010) 294.

[15] J. Kim, J.S. Hahn, M.J. Franklin, P.S. Stewart, J. Yoon, Tolerance of dormant and active cells in *Pseudomonas aeruginosa* PA01 biofilm to antimicrobial agents, J. Antimicrob. Chemother. 63 (1) (2009) 129.

[16] K. Chaloupka, Y. Malam, A.M. Seifalian, Nanosilver as a new generation of nanoproduct in biomedical applications, Trends Biotechnol. 28 (11) (2010) 580.

[17] D.R. Monteiro, L.F. Gorup, A.S. Takamiya, A.C. Ruvollo-Filho, E.R. de Camargo, D.B. Barbosa, The growing importance of materials that prevent microbial adhesion: antimicrobial effect of medical devices containing silver, Int. J. Antimicrob. Agents 34 (2) (2009) 103.

[18] O. Choi, C.P. Yu, G. Esteban Fernandez, Z. Hu, Interactions of nanosilver with *Escherichia coli* cells in planktonic and biofilm cultures, Water Res. 44 (20) (2010) 6095.
[19] D.R. Monteiro, S. Silva, M. Negri, L.F. Gorup, E.R. de Camargo, R. Oliveira, et al., Silver nanoparticles: influence of stabilizing agent and diameter on antifungal activity against *Candida albicans* and *Candida glabrata* biofilms, Lett. Appl. Microbiol. 54 (5) (2012) 383.
[20] K. Kalishwaralal, S. BarathManiKanth, S.R. Pandian, V. Deepak, S. Gurunathan, Silver nanoparticles impede the biofilm formation by *Pseudomonas aeruginosa* and *Staphylococcus epidermidis*, colloids surf, Colloids Surf. B Biointerfaces 79 (2) (2010) 340.
[21] D.R. Monteiro, L.F. Gorup, S. Silva, M. Negri, E.R. de Camargo, R. Oliveira, et al., Silver colloidal nanoparticles: antifungal effect against adhered cells and biofilms of *Candida albicans* and *Candida glabrata*, Biofouling 27 (7) (2011) 711.
[22] L.F. Gorup, E. Longo, E.R. Leite, E.R. Camargo, Moderating effect of ammonia on particle growth and stability of quasi-monodisperse silver nanoparticles synthesized by the Turkevich method, J. Colloid Interface Sci. 360 (2) (2011) 355.
[23] J. Fabrega, J.C. Renshaw, J.R. Lead, Interactions of silver nanoparticles with *Pseudomonas putida* biofilms, Environ. Sci. Technol. 43 (23) (2009) 9004.
[24] T.O. Peulen, K.J. Wilkinson, Diffusion of nanoparticles in a biofilm, Environ. Sci. Technol. 45 (8) (2011) 3367.
[25] J. Turkevich, J. Hillier, A study of the nucleation and growth processes in the synthesis of colloidal gold, Discuss. Faraday Soc. 11 (1951) 55.
[26] G.M. Whitford, J.L. Wasdin, T.E. Schafer, S.M. Adair, Plaque fluoride concentrations are dependent on plaque calcium concentrations, Caries Res. 36 (4) (2002) 256.
[27] M.A. Buzalaf, J.P. Pessan, H.M. Honorio, J.M. ten Cate, Mechanisms of action of fluoride for caries control, Monogr. Oral Sci. 22 (2011) 97.
[28] J.M. ten Cate, J.M. Larsen, E.I.F. Pearce, O. Fejerskov, Chemical interactions between the tooth and the oral fluids, in: O. Fejerskov, E.A.M. Kidd (Eds.), Dental Caries: The Disease and Its Clinical Management, Blackwell Munksgaard, Oxford, 2008, pp. 209−231.
[29] R.P. Shellis, R.M. Duckworth, Studies on the cariostatic mechanisms of fluoride, Int. Dent. J. 44 (3 Suppl. 1) (1994) 263.
[30] M.E. Barbour, R.P. Shellis, D.M. Parker, G.C. Allen, M. Addy, Inhibition of hydroxyapatite dissolution by whole casein: the effects of pH, protein concentration, calcium, and ionic strength, Eur. J. Oral Sci. 116 (5) (2008) 473.
[31] M.E. Barbour, R.P. Shellis, D.M. Parker, G.C. Allen, M. Addy, An investigation of some food-approved polymers as agents to inhibit hydroxyapatite dissolution, Eur. J. Oral Sci. 113 (6) (2005) 457.
[32] M.M. Manarelli, A.E. Vieira, A.A. Matheus, K.T. Sassaki, A.C. Delbem, Effect of mouth rinses with fluoride and trimetaphosphate on enamel erosion: an in vitro study, Caries Res. 45 (6) (2011) 506.
[33] M.J. Moretto, A.C. Magalhaes, K.T. Sassaki, A.C. Delbem, C.C. Martinhon, Effect of different fluoride concentrations of experimental dentifrices on enamel erosion and abrasion, Caries Res. 44 (2) (2010) 135.
[34] E.M. Takeshita, L.P. Castro, K.T. Sassaki, A.C. Delbem, In vitro evaluation of dentifrice with low fluoride content supplemented with trimetaphosphate, Caries Res. 43 (1) (2009) 50.
[35] E.M. Takeshita, Evaluation of sodium trimetaphosphate (TMP) effect on biolfim and enamel de- and remineralization: in vitro and in situ study, Thesis, São Paulo State University, Araçatuba, 2010.
[36] E.M. Takeshita, R.A. Exterkate, A.C. Delbem, J.M. ten Cate, Evaluation of different fluoride concentrations supplemented with trimetaphosphate on enamel de- and remineralization in vitro, Caries Res. 45 (5) (2011) 494.
[37] X. Deng, Q. Luan, W. Chen, Y. Wang, M. Wu, H. Zhang, et al., Nanosized zinc oxide particles induce neural stem cell apoptosis, Nanotechnology 20 (11) (2009) 115101.

[38] M. Horie, K. Nishio, K. Fujita, S. Endoh, A. Miyauchi, Y. Saito, et al., Protein adsorption of ultrafine metal oxide and its influence on cytotoxicity toward cultured cells, Chem. Res. Toxicol. 22 (3) (2009) 543.
[39] M. Mahmood, D.A. Casciano, T. Mocan, C. Iancu, Y. Xu, L. Mocan, et al., Cytotoxicity and biological effects of functional nanomaterials delivered to various cell lines, J. Appl. Toxicol. 30 (1) (2010) 74.
[40] M. Mahmoudi, K. Azadmanesh, M.A. Shokrgozar, W.S. Journeay, S. Laurent, Effect of nanoparticles on the cell life cycle, Chem. Rev. 111 (5) (2011) 3407.
[41] S.M. Hussain, K.L. Hess, J.M. Gearhart, K.T. Geiss, J.J. Schlager, In vitro toxicity of nanoparticles in BRL 3A rat liver cells, Toxicol. In Vitro 19 (7) (2005) 975.
[42] K.J. Kim, W.S. Sung, B.K. Suh, S.K. Moon, J.S. Choi, J.G. Kim, et al., Antifungal activity and mode of action of silver nano-particles on *Candida albicans*, Biometals 22 (2) (2009) 235.
[43] Y. Teow, P.V. Asharani, M.P. Hande, S. Valiyaveettil, Health impact and safety of engineered nanomaterials, Chem. Commun. (Camb) 47 (25) (2011) 7025.
[44] A. Albanese, P.S. Tang, W.C. Chan, The effect of nanoparticle size, shape, and surface chemistry on biological systems, Annu. Rev. Biomed. Eng. (2012).
[45] C. Carlson, S.M. Hussain, A.M. Schrand, L.K. Braydich-Stolle, K.L. Hess, R.L. Jones, et al., Unique cellular interaction of silver nanoparticles: size-dependent generation of reactive oxygen species, J. Phys. Chem. B. 112 (43) (2008) 13608.
[46] R. Foldbjerg, D.A. Dang, H. Autrup, Cytotoxicity and genotoxicity of silver nanoparticles in the human lung cancer cell line, A549, Arch. Toxicol. 85 (7) (2011) 743.
[47] I. Sur, D. Cam, M. Kahraman, A. Baysal, M. Culha, Interaction of multi-functional silver nanoparticles with living cells, Nanotechnology 21 (17) (2010) 175104.
[48] L. Bohmert, B. Niemann, A.F. Thunemann, A. Lampen, Cytotoxicity of peptide-coated silver nanoparticles on the human intestinal cell line Caco-2, Arch. Toxicol. (2012).
[49] A.M. El Badawy, R.G. Silva, B. Morris, K.G. Scheckel, M.T. Suidan, T.M. Tolaymat, Surface charge-dependent toxicity of silver nanoparticles, Environ. Sci. Technol. 45 (1) (2011) 283.
[50] M. Ahamed, M. Karns, M. Goodson, J. Rowe, S.M. Hussain, J.J. Schlager, et al., DNA damage response to different surface chemistry of silver nanoparticles in mammalian cells, Toxicol. Appl. Pharmacol. 233 (3) (2008) 404.
[51] P.V. AshaRani, G. Low Kah Mun, M.P. Hande, S. Valiyaveettil, Cytotoxicity and genotoxicity of silver nanoparticles in human cells, ACS Nano 3 (2) (2009) 279.
[52] L. Braydich-Stolle, S. Hussain, J.J. Schlager, M.C. Hofmann, In vitro cytotoxicity of nanoparticles in mammalian germline stem cells, Toxicol. Sci. 88 (2) (2005) 412.
[53] P.V. Asharani, M.P. Hande, S. Valiyaveettil, Anti-proliferative activity of silver nanoparticles, BMC Cell. Biol. 10 (2009) 65.
[54] L. Wei, J. Tang, Z. Zhang, Y. Chen, G. Zhou, T. Xi, Investigation of the cytotoxicity mechanism of silver nanoparticles in vitro, Biomed. Mater. 5 (4) (2010) 044103.
[55] M.V. Park, A.M. Neigh, J.P. Vermeulen, L.J. de la Fonteyne, H.W. Verharen, J.J. Briede, et al., The effect of particle size on the cytotoxicity, inflammation, developmental toxicity and genotoxicity of silver nanoparticles, Biomaterials 32 (36) (2011) 9810.
[56] S. Arora, J. Jain, J.M. Rajwade, K.M. Paknikar, Cellular responses induced by silver nanoparticles: in vitro studies, Toxicol. Lett. 179 (2) (2008) 93.
[57] J.A. DiMasi, R.W. Hansen, H.G. Grabowski, The price of innovation: new estimates of drug development costs, J. Health Econ. 22 (2) (2003) 151.
[58] C.P. Adams, V.V. Brantner, Estimating the cost of new drug development: is it really 802 million dollars? Health Aff. (Millwood) 25 (2) (2006) 420.

[59] D.W. Light, R. Warburton, Demythologizing the high costs of pharmaceutical research, Biosocieties 6 (1) (2011) 34.
[60] N.G. Bastús, E. Casals, I. Ojea, M. Varon, V. Puntes, The reactivity of colloidal inorganic nanoparticles, The Delivery of Nanoparticles, InTech, 2012, pp. 377−400, (Chapter 18), ISBN: 978-953-51-0615-9.
[61] H. Korbekandi, S. Iravani, Silver nanoparticles, The Delivery of Nanoparticles, InTech, 2012, pp. 3−36, (Chapter 1), ISBN: 978-953-51-0615-9.
[62] S. Pal, Y.K. Tak, J.M. Song, Does the antibacterial activity of silver nanoparticles depend on the shape of the nanoparticle? A study of the Gram-negative bacterium *Escherichia coli*, Appl. Environ. Microbiol. 73 (6) (2007) 1712.
[63] M. Miranda, A. Fernandez, S. Lopez-Esteban, F. Malpartida, J.S. Moya, R. Torrecillas, Ceramic/metal biocidal nanocomposites for bone-related applications, J. Mater. Sci. Mater. Med. (2012).
[64] G. Garnweitneir, In situ versus post-synthetic stabilization of metal oxide nanoparticles, The Delivery of Nanoparticles, InTech, 2012, pp. 71−92, (Chapter 4), ISBN: 978-953-51-0615-9.
[65] P. Dallas, V.K. Sharma, R. Zboril, Silver polymeric nanocomposites as advanced antimicrobial agents: classification, synthetic paths, applications, and perspectives, Adv. Colloid Interface Sci. 166 (1−2) (2011) 119.
[66] H.-M. Liu, J.-K. Hsiao, Magnetic nanoparticles: its effect on cellular behavior and potential applications, Smart Nanoparticles Technology, InTech, 2012, pp. 358−72, (Chapter 16), ISBN: 978-953-51-0500-8.
[67] L. Cheng, M.D. Weir, H.H. Xu, J.M. Antonucci, N.J. Lin, S. Lin-Gibson, et al., Effect of amorphous calcium phosphate and silver nanocomposites on dental plaque microcosm biofilms, J. Biomed. Mater. Res. B Appl. Biomater. 100 (5) (2012) 1378.
[68] L. Cheng, M.D. Weir, H.H. Xu, J.M. Antonucci, A.M. Kraigsley, N.J. Lin, et al., Antibacterial amorphous calcium phosphate nanocomposites with a quaternary ammonium dimethacrylate and silver nanoparticles, Dent. Mater. 28 (5) (2012) 561.

CHAPTER

Nanoparticles and the Control of Oral Biofilms

10

Robert Patrick Allaker

Queen Mary University of London, Barts & The London School of Medicine and Dentistry, Institute of Dentistry, London, UK

CHAPTER OUTLINE

Nanobiomaterials in Clinical Dentistry.

10.1 Introduction

Nanoparticles can be classified as particles of a size no greater than 100 nm, and their unique attributes to combat infections have received considerable attention within a range of diverse fields, including medicine and dentistry. Nanomaterials are increasingly finding uses in products such as antimicrobial surface coatings and semiconductors. These include spherical, cubic, and needle-like nanoscaled particles (approximately 5−100 nm) and near-nanoscaled devices (up to micrometers) [1]. Properties of nanoparticles, for example, their active surface area, chemical reactivity, and biological activity, can be dramatically different from those of micrometer-sized particles [2], and indeed the biocidal effectiveness of metallic nanoparticles has been suggested to be due to both their size and their high surface-to-volume ratio. These characteristics should allow them to closely interact with microbial membranes, and thus elicit an antimicrobial effect that is not solely due to the release of metal ions [3]. Metallic and other nanoparticles are now being combined with polymers and other base materials and coated onto surfaces which may have a variety of potential antimicrobial applications within the oral cavity [4,5].

The oral cavity supports the growth of a wide diversity of microorganisms including bacteria, yeasts, and viruses—members of all groups being associated with oral infections. Bacteria are the predominant components of this resident microflora, and the diversity of species found in the oral cavity reflects the wide range of endogenously derived nutrients, the varied types of habitat for colonization including surfaces on the teeth, mucosa, and tongue, and the opportunity to survive as a biofilm. An oral biofilm can be classed as an aggregate of microorganisms in which cells adhere to each other and to a surface [6]. However, the relationship between this microflora and the host can be disrupted in a number of ways, resulting in the development of disease of the oral structures.

Potential habitats suitable for attachment within the oral cavity include the nonshedding hard tooth surfaces or soft, constantly replaced epithelial surfaces, and conditions vary with respect to oxygen levels and anaerobiosis, availability of nutrients, exposure to salivary secretions or gingival crevicular fluid (GCF), masticatory forces, and other variables such as oral hygiene procedures. The composition of the microbial flora of the mouth thus varies considerably from site to site and at different time points. Up to 1000 different species of bacteria at 10^8−10^9 bacteria per milliliter saliva or per milligram dental plaque are known to be associated with the oral cavity, and it has been suggested that only 50% of the bacteria found at these sites can be cultured [6].

Most bacterial infections within the oral cavity are polymicrobial in nature, and it is quite unusual to find any that are clearly due to a single species. The relative contribution of different bacterial components in such infections is thus difficult to determine. Oral infections may arise either from an endogenous source, i.e., one yielding microorganisms normally found in the mouth, such as plaque-related dental caries and periodontal disease, or an exogenous source yielding microorganisms not normally found as part of the oral microflora. Dental caries and periodontal disease involve the adherence of bacteria and development of biofilms on both the natural and the

restored tooth surface. The use of nanotechnology offers the possibility to control the formation of these and other oral biofilms through the use of nanoparticles with biocidal, antiadhesive, and delivery capabilities.

10.2 Biofilms and oral infections

Biofilms of oral bacteria and yeasts can cause a number of localized diseases in the oral cavity, including dental caries, gingivitis, periodontitis, candidiasis, endodontic infections, orthodontic infections, and peri-implantitis [6].

10.2.1 Formation and properties of oral biofilms

Within the oral cavity, the survival of microorganisms is dependent on their ability to adhere to surfaces and subsequently develop into a biofilm, a process influenced by the physical and chemical properties of the underlying surface [7]. On the tooth surface, the initial colonizers adhere to the acquired pellicle, a salivary/dietary-derived proteinaceous layer, which can then influence the subsequent sequence of colonization by microorganisms [8]. The acquired pellicle also contains several salivary components such as secretory immunoglobulin A (sIgA) and lysozyme, and these provide both barrier and buffering functions [9]. Both de- and remineralization processes of the teeth are also mediated by the pellicle. In terms of bacterial colonization, many of the proteins that make up the pellicle act as receptors for the specific interaction with adhesins on the surface of pioneer bacterial species [9]. The pellicle layer is therefore of particular relevance for the interactions of both bacteria and nanoparticles with the tooth surface.

The strength of the forces involved in the initial attachment of bacteria is critical to their survival and the subsequent growth of the biofilm. The major growth of dental plaque mass then occurs by bacterial cell division within the biofilm rather than by coaggregation at the surface of the developing biofilm [10]. The initial communities of bacteria found within the supragingival plaque biofilm are of a relatively low diversity in comparison to those present in the mature communities of both supra- and subgingival plaque. Initial colonizers include *Streptococcus oralis*, *Streptococcus sanguinis,* and *Streptococcus mitis*. The coaggregating partners with these bacteria would then include predominantly gram-negative species, e.g., *Veillonella atypica, Eikenella corrodens,* and *Prevotella loescheii*. Coaggregation bridges between these early colonizers and *Fusobacterium nucleatum* are common and the latter then coaggregates with numerous late colonizers. Late colonizers include *Aggregatibacter actinomycetemcomitans*, *Prevotella intermedia*, *Treponema denticola,* and *Porphyromonas gingivalis* [10]. The interactions between oral bacteria are integral to biofilm development and maturation and include physical contact, metabolic exchange, molecular communication, and genetic material exchange.

Biofilms will accumulate on both the hard and soft oral tissues, and this community of microbial species is embedded in a matrix of bacterial components, salivary proteins/peptides, and food debris [8]. Extracellular polymeric substances, produced by bacteria in a mature biofilm, contain large amounts of polysaccharides, proteins, nucleic acids, and lipids. These maintain the structural integrity of the biofilm and provide an ideal matrix for bacterial cell growth and survival [11]. The biofilm mode of growth is clearly distinguished from planktonic growth by a number of features,

which includes the resistance to antimicrobial agents at concentrations that approach 1000 times greater than that required to kill planktonic microorganisms [12,13]. This is of particular significance in the development of nanoantimicrobials and the extrapolation of in vitro findings.

10.2.2 Oral biofilms and disease

10.2.2.1 Dental caries and periodontal disease

Dental caries is a destructive condition of the dental hard tissues that can progress to inflammation and death of vital pulp tissue, and if untreated it may lead to the eventual spread of infection to the periapical area of the tooth and beyond. The disease process involves acidogenic plaque bacteria, including *Streptococcus mutans*, *Streptococcus sobrinus,* and *Lactobacillus* spp. [14], whereas the periodontal diseases can involve both the soft and hard tissues and are initiated by components of the plaque biofilm that develop on the hard root surface adjacent to the soft tissues of the supporting periodontium. Periodontal disease may be confined to the gingiva (gingivitis) or extend to the deeper supporting structures with destruction of the periodontal ligament and the alveolar bone that supports the teeth (periodontitis). This loss of attachment, with associated periodontal pocket formation, may ultimately lead to loosening and loss of the affected teeth. *P. gingivalis*, *Tannerella forsythia,* and *T. denticola* are now regarded as the major pathogens in advancing periodontitis [15].

Prevention of dental caries and periodontal diseases is traditionally targeted at mechanical or nonspecific control of the plaque biofilm because this is the precipitating factor. The use of antimicrobial agents represents a valuable complement to mechanical plaque control [16]. Such strategies should ideally control plaque biofilm formation without significantly affecting the biological equilibrium within the oral cavity. However, actual periods of exposure to antimicrobial agents during tooth brushing and mouth rinsing can be very short and may amount to about 30 s, rather than the recommended 2 min [17].

10.2.2.2 Peri-implantitis

Implant systems are increasingly being used to replace missing teeth and most integrate with bone without complications. Small amounts of plaque consisting mainly of *Streptococcus* and *Actinomyces* spp. will accumulate on successful implants. However, in peri-implantitis, anaerobic gram-negative organisms predominate [18]. This infection is a key cause of dental implant failure whereby the induced inflammatory changes in the soft tissues surrounding oral implants lead to a progressive destruction of the supporting bone (classified as peri-implantitis and seen in up to 43% of implant-treated subjects) or soft tissues (classified as peri-implant mucositis and seen in up to 50% of implant-treated subjects) [19]. Current forms of treatment are often inadequate and may result in chronic infection requiring implant removal and costly resective and regenerative procedures in an attempt to restore and reshape the implant supporting tissue [19]. The incorporation of nanoparticles into implant coatings may well offer useful osteoconductive and antimicrobial functionalities to prevent dental implant failure.

10.2.2.3 Candidiasis

The development of candidiasis, including denture stomatitis (chronic atrophic candidiasis), which can affect up to 65% of edentulous individuals [20] involves the formation of a biofilm. Despite the use of antifungal drugs to treat denture stomatitis, infection can often recur. Chandra et al. [20],

using a poly(methyl methacrylate) (PMMA) biofilm model, demonstrated that *Candida albicans* biofilms are potentially highly resistant to the currently used antifungal agents, with resistance developing with time and showing a correlation with biofilm maturation.

10.2.3 Control of oral biofilms

Agents classified as antiplaque generally function by removing or disrupting biofilms or by preventing the formation of a new biofilm. However, they do not necessarily kill the microorganisms within the biofilm. Whereas, agents classified as antimicrobial act by inhibiting the growth (bacteriostatic) or killing (bactericidal) microorganisms, as defined by minimum inhibitory concentration (MIC) and minimum bactericidal concentration (MBC), respectively. The uptake and penetration of antimicrobial agents into biofilms are key considerations in the administration of therapeutics [21]. This is of particular importance within the oral cavity when these agents have to reach less accessible stagnation sites or through plaque to the enamel. The development of plaque control measures that require a minimum of patient compliance and professional health-care intervention are therefore of particular interest [22]. Within this context, antimicrobial nanoparticles may be of particular value if retained at approximal teeth surfaces and below the gum margin. The anticaries potential of fluoride and other conventional antimicrobial/antiplaque agents, which are mostly deployed in mouthwashes and toothpastes, have been well characterized [16]. The potential of nanoparticles as constituents of topical agents to control oral biofilms through either their biocidal or antiadhesive capabilities has now emerged as an area that should be given serious consideration. The studies by Robinson et al. using the "Leeds in situ model," a device that allows dental plaque to develop in situ on a removable human enamel surface, have helped in the assessment of novel antimicrobial agents and take into account the extremely complex microbial composition and architecture of plaque biofilms [23]. The use of such intact biofilms on natural tooth surfaces would be of particular value to a study of the penetration of nanoparticles and released ions. This model has indicated that plaque contains voids and channels, sometimes extending completely through the biomass to the underlying enamel [24] and may have considerable influence on the transfer of nanoparticles through biofilms. The main considerations are the physical and chemical characteristics of the particular nanoparticles used, including the surface charge and degree of hydrophobicity, the surface area-to-mass ratio of the plaque biofilm and the ability of the particles to adsorb to/be taken up at the biofilm surface. Within this context, nanoparticles are potentially useful because it is possible to alter their surface charge, hydrophobicity, and other physical and chemical characteristics [25].

10.3 Antimicrobial nanoparticles and oral biofilm control

10.3.1 Nanoparticulate metals as antimicrobial agents

Metals have been used for centuries as antimicrobial agents. Silver, copper, gold, titanium, and zinc have attracted particular attention, each having different properties and spectra of activity. Many oral products, including toothpastes, now incorporate powdered (micron-sized) zinc citrate or acetate to control the formation of dental plaque [26]. Powdered titanium dioxide is also commonly used as a whitener in toothpastes.

With respect to nanoparticulate metals, the antimicrobial properties of silver [27] and copper [28] have received the most attention. Both of these have been coated onto or incorporated into various base materials [29], including PMMA [30] and hydrogels [31]. An inverse relationship between the size of nanoparticles and antimicrobial activity has been clearly demonstrated, where particles in the size range of 1−10 nm have been shown to possess the greatest biocidal activity against bacteria [3,32]. Indeed, it has been shown that smaller silver nanoparticles are more toxic than larger particles, more so when oxidized [33]. At the nanoscale, Ag^+ ions are known to be released (leached) from the surface [34]. Sotiriou et al. [35] proposed that the antimicrobial activity of small (< 10 nm) nanosilver particles is dominated by Ag^+ ions, while for larger particles (> 15 nm) the contributions of Ag^+ ions and particles to the antibacterial activity are comparable, the Ag^+ ion release being proportional to the exposed nanosilver surface area.

Particular nanoparticles, as a result of their small size, may be able to offer other advantages to the biomedical field through improved biocompatibility [36]. Also, it appears that bacteria are far less likely to acquire resistance to metal nanoparticles than they are to other conventional and narrow-spectrum antibiotics [37]. This is thought to occur because metals may act on a broad range of microbial targets, and many mutations would have to occur in order for the microorganisms to resist their antimicrobial activity. Shape may also affect the activity of nanoparticles. It has been demonstrated that the shape of silver nanoparticles can influence antimicrobial activity, as has been shown in the case of *Escherichia coli* [37]. Truncated triangular silver nanoplates with a {111} lattice plane as the basal plane showed the greatest biocidal activity compared with spherical and rod-shaped nanoparticles. The differences appear to be explained by the proportion of active facets present in nanoparticles of different shapes.

Exploitation of the toxic properties of nanoparticulate metals and metal oxides, such as titanium dioxide (TiO_2; Figure 10.1B) and zinc oxide (ZnO; Figure 10.1C), in particular those that produce reactive oxygen species (ROS) under UV light, are finding increased use in antimicrobial formulations, with silver metal nanoparticles (5−40 nm) having been reported to inactivate most microorganisms, including HIV-1 [38]. The high reactivity of nano-titanium dioxide and nano-silicon dioxide (SiO_2) is exploited extensively for their bactericidal properties in filters and coatings on substrates such as polymers, ceramics, glasses, and alumina [39]. Significant activity using metal and metal oxide nanoparticles and their compound clusters against fungal and bacterial pathogens such as methicillin-resistant *Staphylococcus aureus* (MRSA) and *E. coli* has recently been demonstrated. These have also shown the capability to inactivate viruses, including SARS (severe acute respiratory syndrome), H1N1 swine flu, and H5N1 bird flu. For example, new broad-spectrum materials (5−60 nm) can reduce virus levels by 80−100% through direct or indirect contact. Nanoparticle preparations, including those based upon nickel (Ni, NiO), zirconium (ZrO_2), copper (Cu, CuO, and Cu_2O), titanium (TiO_2), zinc (ZnO), aluminum (Al_2O_3), silicon (IV) nitride (Si_3N_4), silver (Ag), and tungsten carbide (WC) have been compared in regards to their antimicrobial potential. Significant activity with Ag, ZnO, TiO_2 (in the presence of UV light), SiO_2, Cu, Cu_2O, and CuO against bacterial pathogens, including MRSA and *Pseudomonas aeruginosa,* has been demonstrated [40]. MBCs were found to be in the range of 0.1−5 mg/mL. In comparison, traditional antibiotics are effective at concentrations 1000-fold lower. NiO, Ni, Al_2O_3, TiO_2 (in the absence of UV light), Si_3N_4, WC (tungsten carbide), and ZrO_2 were found to lack antimicrobial activity at the concentrations tested. The oral pathogens *P. gingivalis*, *F. nucleatum*, *Prev. intermedia,* and *A. actinomycetemcomitans* were also found to be susceptible to Ag and CuO nanoparticles under anaerobic conditions with MBC values in the range 0.025−2.5 mg/mL [41].

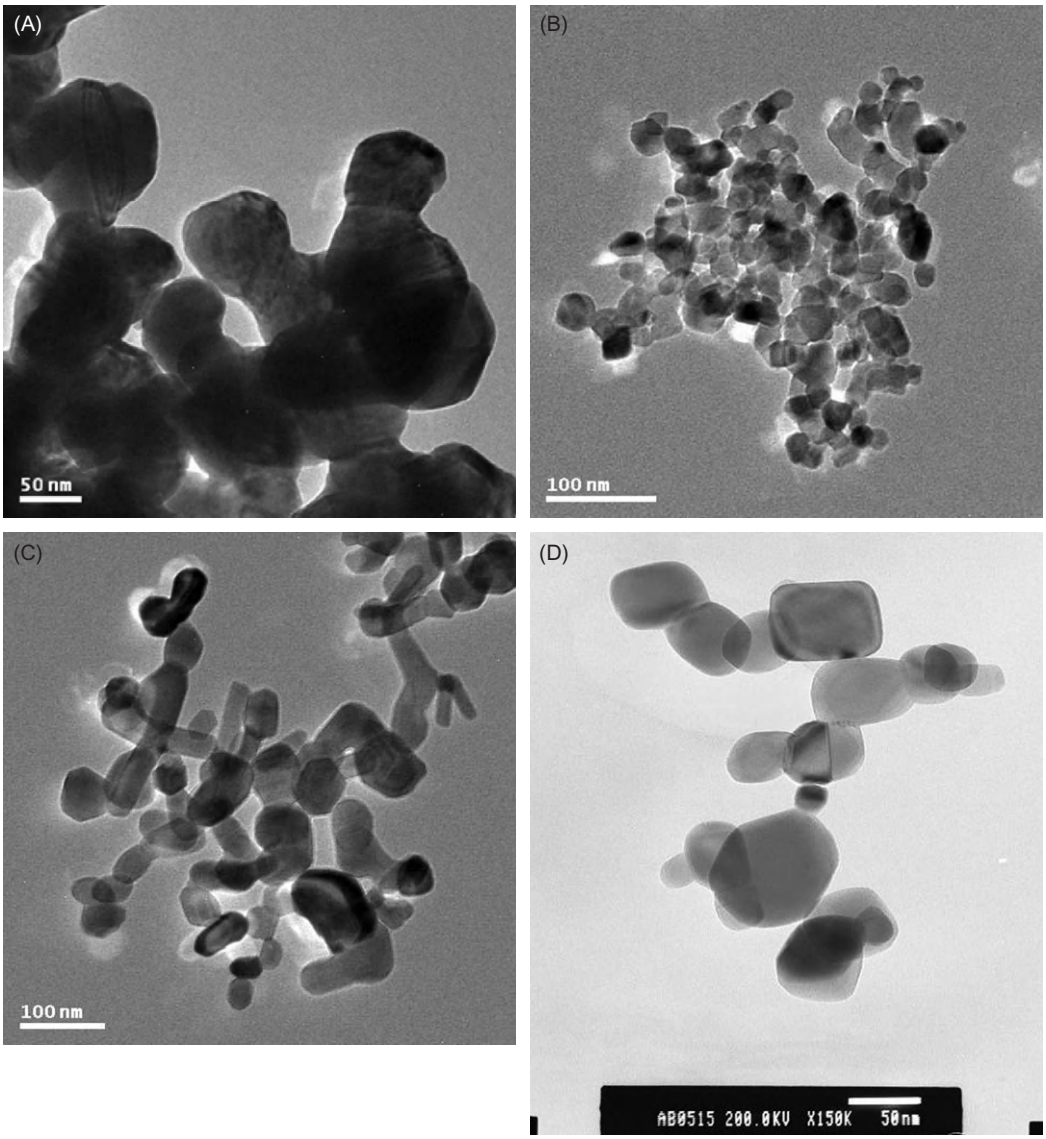

FIGURE 10.1

TEM images of agglomerated silver (A), titanium dioxide (B), zinc oxide (C), and copper oxide (D) nanoparticles.

10.3.1.1 Silver (Ag)

The antimicrobial actions of elemental silver, Ag^+ ions, and silver compounds have been extensively investigated [4]. In comparison to other metals, silver is relatively less toxic to human cells, albeit at very low concentrations. Ag^+ ions have been considered for a range of biomedical applications, including their use within the dental field as an antibacterial component in dental resin composites [42]. Silver also exhibits a strong affinity for zeolite, a porous crystalline material of hydrated aluminosilicate which can bind up to 40% Ag^+ ions within its structure. Silver zeolite has been incorporated in tissue conditioners, acrylic resins, and mouth rinses within the dental field [43–46]. Silver nanoparticles (Figure 10.1A), either alone or together with other antimicrobial agents, have shown particularly encouraging results [27,47,48]. The use of silver salt nanoparticles instead of elemental silver or complex silver compounds to prevent biofilm formation on surfaces for both biomedical and more general use has been investigated. Using silver bromide precipitation to synthesize polymer-nanocomposites, surfaces that comprised this material were shown to resist biofilm formation. It was also shown to be possible, through controlling the size of the embedded AgBr, to modify the release of biocidal Ag^+ ions [49].

Surprisingly, little is known about how nanoparticles behave in relation to microorganisms, particularly at the cellular level. The mechanism of the antimicrobial activity of silver is not completely understood but is likely to involve multiple targets in comparison to the more defined targets of antibiotics. Studies have shown that the positive charge on the Ag^+ ion is critical for antimicrobial activity, allowing the electrostatic attraction between the negative charge of the bacterial cell membrane and positively charged nanoparticles [36]. In regards to molecular mechanisms of the inhibitory action of Ag^+ ions on microorganisms, it has been shown that DNA loses its ability to replicate [50], and the expression of ribosomal subunit proteins and other cellular proteins and enzymes necessary for ATP production become inactive [51]. It has also been hypothesized that Ag^+ ions affect membrane-bound respiratory enzymes [52]. However, the precise mechanism(s) of biocidal activity of silver nanoparticles against bacteria remains to be fully elucidated. The work of Sondi and Salopek-Sondi [27] demonstrated structural changes and damage to bacterial membranes resulting in cell death. These particular studies suggest that sulfur-containing proteins in the membrane or inside the cells and phosphorus-containing elements, such as DNA, are likely to be the preferential binding sites for silver nanoparticles. The contribution of Ag^+ ion release from nanoparticles to the overall antimicrobial activity remains unclear. It is suggested that a bacterial cell in contact with silver nanoparticles will take up Ag^+ ions, which possibly in turn will inhibit respiratory enzymes and so help to generate free radicals and subsequent free-radical-induced damage to the cell membrane. In order to determine the relationship between free-radical formation and antimicrobial activity, the use of antioxidants does suggest that free radicals may be derived from the surface of silver nanoparticles [36].

10.3.1.2 Copper (Cu)

In comparison to silver, relatively few studies have reported the antimicrobial properties of copper. It is suggested that copper may well have a similar mode of action to that of silver. However, it remains unclear as to the precise mechanism by which copper nanoparticles exert activity against microorganisms. As with silver, it is thought that copper acts by combining with the −SH groups of key microbial enzymes. Yoon et al. [53] demonstrated superior antimicrobial activity with copper nanoparticles against *E. coli* and spore forming *Bacillus subtilis* when compared to silver

nanoparticles. However, other studies demonstrate silver to have superior activity to copper against a wide range of different species and strains [40].

The antimicrobial properties of both silver and copper nanoparticles were also investigated by Ruparelia et al. [54] using strains of *E. coli*, *B. subtilis,* and *S. aureus*. The bactericidal effect of the nanoparticles was compared using disc diffusion tests and MIC and MBC determinations. Bacterial sensitivity was found to differ according to the species tested and the test system employed. For all strains of *S. aureus* and *E. coli,* the action of silver nanoparticles was found to be superior. Strain-specific variation for *S. aureus* was negligible, while some strain-specific variation was observed for *E. coli*. A higher sensitivity, as shown with *B. subtilis*, may be attributed to more amine and carboxyl groups (in comparison to other species) on the cell surface; these groups having a greater affinity for copper [55]. Released copper ions within the cell may then disrupt nucleic acid and key enzymes [56]. In theory, a combination of silver and copper nanoparticles may give rise to a more complete bactericidal effect, especially against a mixed population of bacteria. Indeed, the studies of Ren et al. [40] demonstrated that populations of gram-positive and gram-negative bacteria could be reduced by 68% and 65%, respectively, in the presence of 1.0 mg/mL nanocopper oxide within 2 h. This was significantly increased to 88% and 100%, respectively, with the addition of a relatively low concentration (0.05 mg/mL) of nanosilver.

10.3.1.3 Gold (Au)

Gold shows a weak antimicrobial effect in comparison to silver and copper. However, gold nanoparticles are employed in multiple applications involving biological systems. The binding properties of gold are exceptional, and this makes it particularly suitable for attaching ligands to enhance biomolecular interactions. Gold nanoparticles also exhibit an intense color in the visible range and contrast strongly for imaging by electron microscopy [57]. Despite all the current and potential applications for gold nanoparticles, there remains little information as to how these particles affect microorganisms. Growth inhibition studies, to measure the effect of gold nanoparticles (polyethylene glycol (PEG) coated to allow dispersion) on *E. coli* at various concentrations, demonstrated no significant activity [58]. Studies with PEG-coated gold nanoparticles also showed no activity against *E. coli*. However, the growth of the gram-negative *Proteus* species and *P. aeruginosa* was inhibited at a concentration of 1.0 mg/mL (R.P. Allaker, unpublished observations).

10.3.2 Nanoparticulate metal oxides as antimicrobial agents

Nanoparticulate metal oxides have been of particular interest as antimicrobial agents as they can be prepared with extremely high surface areas and unusual crystal morphologies that have a high number of edges, corners, and other potentially reactive sites [59]. However, certain metal oxides are now coming under close scrutiny because of their potential toxic effects [60]. Oxides under consideration as antimicrobial agents include those of copper, zinc oxide, titanium dioxide (titania), and tungsten trioxide (WO_3).

10.3.2.1 Copper oxide (CuO and Cu_2O)

Copper oxide (CuO) is a semi-conducting compound with a monoclinic structure. CuO has attracted particular attention because it is the simplest member of the family of copper compounds and exhibits a range of potentially useful physical properties, such as high temperature superconductivity,

electron correlation effects, and spin dynamics [61,62]. Copper oxide is relatively cheap, easily mixed with polarized liquids (i.e., water) and polymers, and relatively stable in terms of both chemical and physical properties. Highly ionic nanoparticulate metal oxides, such as CuO, may be particularly valuable antimicrobial agents as they can be prepared with extremely high surface areas and unusual crystal morphologies [59].

Copper oxide (CuO) nanoparticles have been characterized, both physically and chemically, and investigated with respect to potential antimicrobial applications [40]. It was found that nanoscaled CuO, as generated by thermal plasma technology, demonstrated particle sizes in the range 20−95 nm with a mean surface area of 15.7 m^2/g (Figure 10.1D). CuO nanoparticles in suspension showed activity against a range of bacterial pathogens, including MRSA and *E. coli*, with MBCs ranging from 0.1 to 5.0 mg/mL. As with silver, studies of CuO nanoparticles incorporated into polymers suggest that the release of ions may be required for optimum killing [40]. Incorporation of nano-CuO into porous elastomeric polyurethane films has demonstrated potential for a number of applications. Studies have shown this approach to be effective against MRSA within 4 h of contact [63].

Cu_2O (copper (I) oxide; cuprous oxide) is a red powder and can also be produced as nanoparticles. Similar activity to CuO (copper(II) oxide; cupric oxide) has been shown against a range of species and strains [40].

10.3.2.2 Zinc oxide (ZnO)

As in the case of other nanoparticulate metals and metal oxides, the antimicrobial mechanisms of zinc are not completely understood. Nano-zinc oxide has received increasing attention, not only because it is stable under harsh processing conditions but also because it is generally regarded as safe and biocompatible [59]. Studies have shown that some nanoparticulate metal oxides, such as ZnO, have a degree of selective toxicity to bacteria with a minimal effect on human cells [64,65,66]. The proposed mechanisms of antibacterial activity include induction of ROS [67,68] and damage to the cell membrane with subsequent interaction of the nanoparticle with the intracellular contents [64].

Liu et al. [69] investigated the antimicrobial properties of ZnO nanoparticles against *E. coli* strain O157:H7 (verocytotoxin-producing). This strain was significantly inhibited as shown using scanning electron microscopy (SEM) and transmission electron microscopy (TEM) analyses to assess the morphological changes of bacterial cells. Leakage of intracellular contents and a degree of membrane disorganization were observed. Using Raman spectroscopy, the intensities of lipid and protein bands were shown to increase after exposure to ZnO nanoparticles, whereas no significant change to nucleic acid was indicated. In comparison to silver nanoparticles (0.1 mg/mL), a higher concentration of zinc oxide (particle size: approximately 15−20 nm; surface area: 47 m^2/g) is required to have growth inhibitory (0.5−2.5 mg/mL) and killing effects ($>$2.5 mg/mL) against a range of pathogens including *E. coli* and MRSA (K. Memarzadeh and R.P. Allaker, unpublished observations). While with those organisms implicated in oral infections, including *A. actinomycetemcomitans*, *P. gingivalis*, *Prev. intermedia* and *F. nucleatum*, greater sensitivity was demonstrated under anaerobic conditions, with growth inhibitory and killing concentrations of 0.25−2.5 and 0.25−2.5 mg/mL, respectively [41].

10.3.2.3 Titanium dioxide (TiO_2)

Titanium dioxide (TiO_2) is the commonest titanium compound, and its ability to act as a photocatalytic antimicrobial compound is well established [70]. TiO_2 is widely used in a number of applications, as a powder and increasingly in a nanoparticulate form, and is generally considered to be nontoxic at the concentrations normally employed. However, there are recent concerns that nano-titanium oxide may present a hazard to health through inflammation as generated by release of interleukin 1α [71]. The anatase form of nano-TiO_2 and UV light excitation are required to ensure maximum antimicrobial activity. TiO_2 photocatalysis is able to promote the peroxidation of the polyunsaturated phospholipid component of the microbial lipid membrane, induce loss of respiratory activity, and elicit cell death [72]. The study of Tsuang et al. [73] demonstrated TiO_2-mediated photocatalytic and bactericidal activities against obligate aerobes (*P. aeruginosa*), facultative anaerobes (*S. aureus, E. coli* and *Enterococcus hirae*), and obligate anaerobes (*Bacteroides fragilis*). Concentrations of titanium oxide (predominantly anatase phase; in the absence of UV light; particle size: approximately 18 nm; surface area: 87 m^2/g) required to have a growth inhibitory and killing effect against a range of pathogens including *E. coli* and MRSA have been shown to be 1.0−2.5 and >2.5 mg/mL, respectively (K. Memarzadeh and R.P. Allaker, unpublished observations). While with those organisms implicated in oral infections, including *A. actinomycetemcomitans*, *P. gingivalis*, *Prev. intermedia,* and *F. nucleatum*, growth inhibitory and killing concentrations under anaerobic conditions are in the same order at 0.25−2.5 and >2.5 mg/mL, respectively [41].

10.3.3 Oral applications of nanoparticulate metals and metal oxides

Silver nanoparticles are being investigated to reduce bacterial and fungal adhesion to oral biomaterials and devices, e.g., incorporation into denture materials (Figure 10.2) [4] and orthodontic adhesives [74]. The optimum amount of silver nanoparticles used within such polymer materials will be of critical importance to avoid an adverse effect upon their physical properties. The study of Ahn et al. [74] clearly demonstrated that experimental composite adhesives (ECAs) had rougher surfaces than conventional adhesives due to the addition of silver nanoparticles, although bacterial adhesion to ECAs was shown to be less than that to conventional adhesives and was not influenced by saliva coating. No significant difference between ECAs and conventional adhesives was shown as regards bond shear strength.

Biofilm growth is known to contribute to secondary caries and the failure of resin-based dental composites. Within this context, zinc oxide nanoparticles have undergone in vitro testing using biofilm culture test systems [75]. ZnO nanoparticles blended into a variety of composites were shown to significantly inhibit *S. sobrinus* biofilm growth at concentrations not less than 10% w/w over a 3-day test period. The structural characteristics of composites would need to be carefully assessed with a 10% ZnO loading.

With reference to dental implants, numerous companies market novel synthetic hydroxyapatite (HA) materials as the "optimal" osteoconductive implant coating available, and some companies have developed nanoscaled varieties. Some have employed coatings and application methods different from the conventional coating techniques, including a HA material available in nanophase and a nanocrystalline silver-based antimicrobial coating that should reduce the potential for bacterial

colonization. The antibacterial properties of an amorphous carbon film [76] incorporating silver nanoparticles in a 40–60 nm size range and deposited onto a standard titanium material have been evaluated. A significant reduction in mixed biofilm counts compared to the standard titanium material was observed after 7 days using the coating with silver nanoparticles.

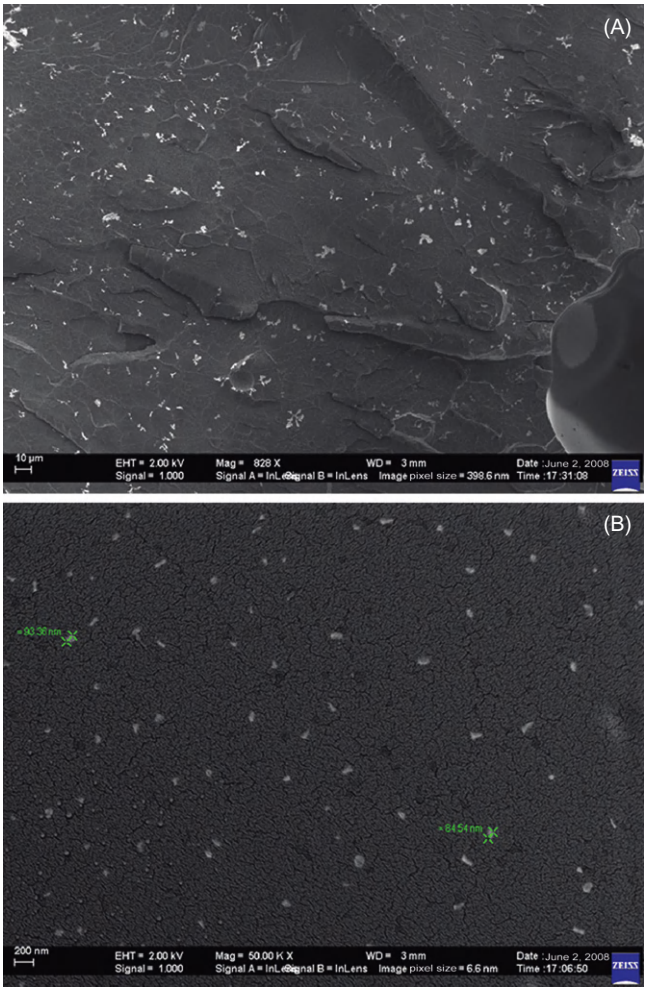

FIGURE 10.2

Scanning electron micrograph of a fractured PMMA/Ag nanocomposite containing approximately 0.04% w/w silver. Distribution of silver particles in the PMMA acrylic resin is shown. (A) White areas are agglomerated silver nanoparticles distributed in the PMMA (828 × magnification). (B) Silver nanoparticles (white dots) with approximate mean size 88 nm distributed in the PMMA matrix. (50,000 × magnification).

With permission from Ref. [4].

10.3.4 Quaternary ammonium compounds

Quaternary ammonium poly(ethylene imine) (QA-PEI) nanoparticles as an antimicrobial to incorporate into restorative composite resins have been developed [77] (Figure 10.3). This may have distinct advantages over the currently used composite resins employed to restore hard tissues, which

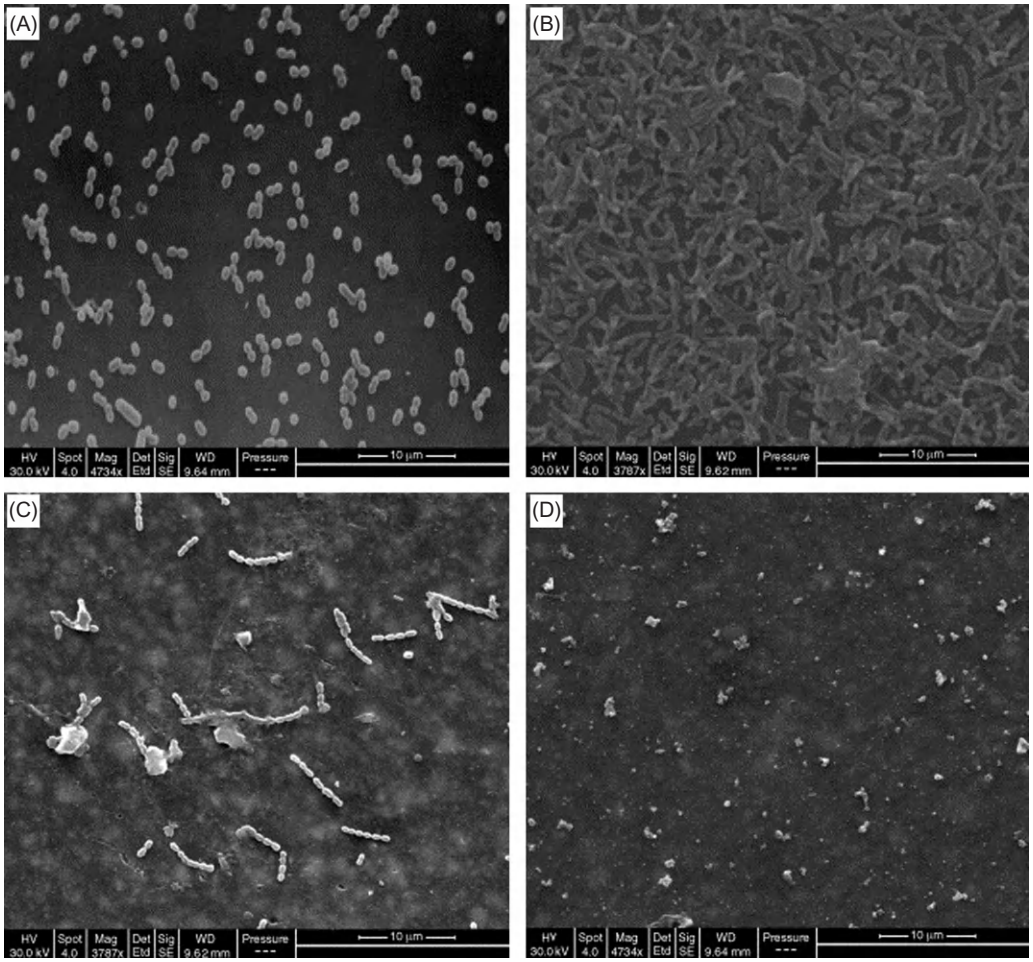

FIGURE 10.3

Scanning electron micrograph (4000 × magnification) of *S. mutans* in contact with composite resin (Z250, 3M ESPE Dental) with and without 1% w/w quaternary ammonium polyethylenimine (PEI) nanoparticles. (A) After 1 h incubation without nanoparticles. (B) After 24 h incubation without nanoparticles showing bacterial growth and typical biofilm formation. (C) After 1 h of incubation with nanoparticles. (D) After 24 h of incubation with nanoparticles. There is a decrease in the amount of *S. mutans* present illustrating the bactericidal properties of PEI nanoparticles.

With permission from Ref. [77].

are known to possess several disadvantages including development of biofilms on both teeth and the restorative material [4]. The traditional methods for preparing antibacterial composite materials have been to impregnate them with low-molecular-weight agents, such as Ag^+ ions or iodine that are then released slowly. Apart from the possible adverse effects on the mechanical properties of the composite, difficulties in controlling the release of such agents may be a potential drawback.

QA-PEI nanoparticles at a concentration of 1% w/w enabled complete in vitro growth inhibition of *S. mutans* to be achieved for at least 3 months [78]. The proposed mechanism of action of QA-PEI is suggested to be as a result of transfusion across, and damage to, the bacterial cell wall. The hydrophobic nature and positive charge of these particles are also thought to further enhance the antimicrobial activity. Surface chemical analysis of the restorative composite embedded with QA-PEI demonstrated a surface modification of higher hydrophobicity and the presence of quaternary amines when compared to the unmodified material. Further studies to optimize the release characteristics of QA-PEI and other potentially useful nanoparticulates from dental materials will be required.

10.4 Antiadhesive nanoparticles and oral biofilm control

10.4.1 Chitosan nano- and microparticles

Chitosan is a biopolymer derived by the deacetylation of chitin, a natural polymer occurring in the exoskeleton of crustaceans. Chitosan is positively charged and soluble in acidic to neutral solution, enabling it to bind to mucosal surfaces. Both chitosan nano- and microparticles have been investigated as a potential platform for local delivery of drugs [79]. Although the antimicrobial irrigants (without chitosan) are used to disinfect root canals in the treatment of endodontic infections are capable of killing *Enterococcus faecalis*, the bacterium frequently associated with this condition, endodontic restorations often fail [80]. The in vitro study of Kishen et al. [81] demonstrated that root canal surfaces treated with cationic antibacterial nanoparticulates such as zinc oxide alone and a combination of zinc oxide and chitosan nanoparticulates are able to significantly reduce *E. faecalis* adherence to dentin. In theory, such surface treatment could prevent bacterial recolonization and biofilm formation in vivo.

10.4.2 Silica and silicon nanoparticles

Particles of a nano and micro size based upon the element silicon, designed to rapidly deliver antimicrobial and antiadhesive capabilities to the desired site within the oral cavity, have received attention [82]. Companies have used silica (silicon dioxide "SiO_2" and often classed as "microfine," but with a particle size within the definition of nanoparticles) in toothpastes for many years, and some have actively sought new directions in this area through the use of porous silicon and nanocrystalline silicon technology to carry and deliver antimicrobials, e.g., triclosan. These may well offer advantages to some of the slower and more prolonged delivery systems under investigation.

The use of silica nanoparticles to polish the tooth surface may help protect against damage by cariogenic bacteria, presumably because the bacteria can more easily be removed. This has been

investigated on human teeth ex vivo [83]. Atomic force microscopy demonstrated lower nanometer-scale roughness obtained when silica nanoparticles were used to polish the surface of teeth as compared with conventional polishing pastes. It was also shown that adherent *S. mutans* could be more easily removed. However, concerns remain as to the longevity of the effect, and whether the polished surface will inhibit mineralization and plaque formation in vivo. Spherical silica nanoparticles (up to 21 nm) deposited onto polystyrene surfaces by polycationic binding have been investigated with respect to the development of *C. albicans* biofilms and invasive filament formation [84]. Modified surfaces were shown to reduce attachment and growth of *C. albicans*, with the greatest effect observed with 7 and 14 nm particles. These effects could possibly be attributed to the surface topography or slow dissolution of the bound silica. Such treatment has the advantages of being nontoxic, simple to apply and adaptable to three-dimensional surfaces.

Other novel systems based upon silica have been investigated with respect to the control of oral biofilms. The use of nitric oxide (NO)-releasing silica nanoparticles to kill biofilm-based microbial cells has been described [85]. The rapid diffusion of NO may well result in enhanced penetration into the biofilm matrix and therefore improved efficacy against biofilm-embedded bacteria. In vitro grown biofilms of *P. aeruginosa*, *E. coli*, *S. aureus*, *Staphylococcus epidermidis,* and *C. albicans* were exposed to NO-releasing silica nanoparticles. Over 99% of cells from each type of biofilm were killed via NO release. In comparison to small-molecule NO donors, the physicochemical properties, for example, hydrophobicity, charge, and size of nanoparticles, can be altered to increase antibiofilm efficacy [25].

Bioactive glasses of the $SiO_2{-}Na_2O{-}CaO{-}P_2O_5$ system have been shown to possess antimicrobial activity through the release of ionic alkaline species over time and are under consideration as dentin disinfectants to offer an alternative to calcium hydroxide [86]. Those in the form of amorphous nanoparticles with a size of 20–60 nm may show an advantage over micron-sized material as the decrease in glass particle size should increase, by more than 10-fold, the active exchange surface of glass and surrounding liquid. In turn, this would substantially increase ionic release into suspension and enhance antimicrobial efficacy. Waltimo et al. [86] monitored ionic dissolution profiles in simulated body fluid. Antimicrobial activity was assessed against *E. faecalis* as a pathogen often isolated from root canal infections. They found that a shift from a micron- to a nanosize increased the release of silica by a factor of 10 and elicited a pH elevation of at least 3 units. The killing efficacy was also significantly higher.

10.4.3 Hydroxyapatite and other calcium phosphate-based systems

The application of nanoscaled HA particles has been shown to impact on oral biofilm formation and provides a remineralization capability [87,88]. Biomimetic approaches, based upon HA nanocrystals which resemble the structure at the nanoscale of abraded dental enamel crystallites, should allow adsorbed particles to interact with bacterial adhesins, reduce bacterial adherence, and hence impact on biofilm formation [89].

A number of oral health-care products, including dentifrices and mouth rinses, have been developed containing nanosized apatite particles with and without protein-based additives [90,91]. It is suggested that the efficacy of these compounds can be attributed to the size-specific effects of the apatite nanoparticulates. Casein phosphopeptide (CPP)–amorphous calcium phosphate (ACP) nanocomplex (Recaldent™/MI Paste™) is a particular technology based upon ACP and stabilized by

CPP [92]. Use of this technology has demonstrated anticariogenic activity under both in vitro and in vivo conditions. The levels of calcium and phosphate ions in supragingival plaque have been shown to increase upon delivery of CPP−ACP in a mouth rinse form and promote remineralization of enamel subsurface lesions [91]. Analysis of plaque samples demonstrated CPP−ACP nanocomplexes to be localized in plaque on the surface of bacterial cells and essentially confirm the studies by Rose [93,94] who demonstrated tight binding to *S. mutans* and the intercellular plaque matrix to provide a calcium ion reservoir. As a result of interaction with calcium binding sites and the masking of bacterial receptors on salivary molecules, CPP−ACP is thought to reduce bacterial colonization as shown with CPP−ACP germanium treated surfaces [90].

10.5 Photodynamic therapy and the use of nanoparticles to control oral biofilms

Photodynamic therapy (PDT) is very well suited for the control of bacteria in oral plaque biofilms where there is relatively easy access for the application of the photosensitizing agent and light sources to areas requiring treatment [95]. This approach is now being utilized within the clinical setting in some countries. The killing of microorganisms with light depends upon cytotoxic singlet oxygen and free-radical generation by the excitation of a photoactivatable agent or sensitizer. The result of excitation is that the sensitizer moves from an electronic ground state to a triplet state which then interacts with microbial components to generate cytotoxic species [96]. One of the advantages of light-activated killing is that the resistance to action of singlet oxygen is unlikely to become widespread in comparison to that experienced with more traditional chemical antimicrobial agents. A sensitizer ideally should absorb light at red to near-infrared wavelengths because these wavelengths are able to penetrate more. The most commonly tested sensitizers on bacteria are tricyclic dyes (e.g., methylene blue and erythrosine), tetrapyrroles (e.g., porphyrins), and furocoumarins (e.g., psoralen). The use of nanoparticles within this area is now under investigation. For example, a complex of biodegradable and biocompatible poly(lactic-co-glycolic acid) and colloidal gold nanoparticles, loaded with methylene blue and exposed to red light at 665 nm, have been tested against planktonic *E. faecalis* and in experimentally infected root canals [97]. In theory, gold nanoparticle conjugates should have improved binding and cell wall penetration properties, and so should deliver a higher concentration of photoactive molecules. It remains to be fully established whether such conjugates will show an increased antibacterial activity when compared to more conventional treatments.

Most work on light-activated killing has been performed using suspensions of planktonic bacteria, with relatively few studies observing biofilm-grown microorganisms. In vitro biofilm-grown *S. mutans* cells demonstrated a 3-log reduction when treated with erythrosine and white light (500−650 nm) [98], while an approach using antibody- and erythrosine-labeled nanoparticles has shown the potential for targeting specific bacterial species in oral plaque biofilms (S. Wood et al., unpublished observations). These in vitro studies, employing constant-depth film fermenters with gold nanoparticles conjugated to erythrosine and antibody to either *S. mutans* or *Lactobacillus casei*, have shown specific killing of target organisms in mixed biofilm cultures.

Considerations in relation to the therapeutic use of light-activated killing of biofilms on host surfaces include (i) direct toxicity of the sensitizer, (ii) indirect toxicity of the sensitizer in terms of

"by-stander" damage to adjacent host cells, (iii) penetration into the biofilm, (iv) light exposure time required to kill bacteria within in vivo biofilms, and (v) widespread relatively nonspecific bacterial killing [95]. The photosensitizer erythrosine has an advantage over other dyes because it is currently used in dentistry to visualize dental plaque in vivo, and so its lack of toxicity in the host is well established. For use in periodontitis, the dye needs to be applied subgingivally prior to fiber-optic laser light activation. However, when disease is present, the periodontal site has a marked flow of GCF into the pocket, and most photosensitizers lose some activity in the presence of extraneous protein. Also, some have virtually no effect in the presence of saliva and other body fluids. This is because the agents complex with proteins and host cells in the GCF and effectively compete for binding to bacteria. The use of nanoparticles as applied to PDT may help to overcome some of the issues associated with serum constituents.

10.6 Biocompatibility of nanoparticles within the oral cavity

Although the development and application of nanotechnology are of major importance in both industrial and consumer areas, knowledge regarding the possible toxicity of nanotechnology products to humans is limited. Whereas it is well known that copper in a non-nanoparticulate form is actively excreted from the body, non-nanoparticulate silver can accumulate within the body. However, the threat posed by these metals in a nanoparticulate form is far from clear [99]. In order to understand the mechanism of toxicity, a thorough knowledge of the toxicokinetic properties of nanoparticles is required. This includes information on the absorption, distribution, metabolism, and excretion of nanoparticles [100]. In theory, certain nanoparticles may be retained within the body for longer than the desirable time, and thus the safety profile becomes a matter of overriding significance. Nanomaterials are able to cross biological membranes and access cells, tissues, and organs that larger-sized particles normally cannot. Nanomaterials can enter the blood stream following inhalation or ingestion, and some can even penetrate the skin. In vitro studies with lung epithelial cells, enterocytes, and skin keratinocytes indicate marked differences in susceptibility to metallic nanoparticles according to cell type tested (R.P. Allaker and M.A. Vargas-Reus, unpublished observations). However, a particle's surface chemistry, which in some cases can be modified, can govern whether it should be considered further for biomedical applications [25].

Toxicology and biodynamic studies suggest that silica, silicon, and chitosan nanoparticles are relatively safe if introduced via the oral route [99]. Testing of NO-releasing silica nanoparticles (at the highest concentration tested of 8 mg/mL) with fibroblasts demonstrated that cell proliferation was inhibited to a lesser degree than with chlorhexidine [85]. Likewise, QA-PEI nanoparticles incorporated into composite resins to restore teeth at 1% w/w demonstrate no additional toxic effects on cultured cells or experimental animal tissue in comparison to unmodified composites [78]. In comparison to other metals, silver is less toxic to human cells and is only ever used at very low concentrations in vivo [27]. For example, silver nanoparticles have been shown to inhibit *Candida* spp. at a concentration of 0.2 μg/mL, which is markedly less than the concentration (30 μg/mL) required to demonstrate a toxic effect against human fibroblasts [101].

The safe use of nanotechnology and the design of nanomaterials for biological applications, including the control of oral biofilms, involve a thorough understanding of the interface between

these materials and biological systems [25]. The interface comprises three interacting components: (i) the surface of the nanoparticle, (ii) the solid−liquid interface and the effects of the surrounding medium, and (iii) the contact zone with biological substrates. The nanoparticle characteristics of most importance as regards interaction with biological systems, whether mammalian or microbial, are chemical composition, surface function, shape and number of sides, porosity and surface crystallinity, heterogeneity, roughness, and hydrophobicity or hydrophilicity [102]. For example, it has been shown that titanium dioxide nanoparticles [103] act to resist the formation of surface biofilms through increased hydrophilicity in comparison to an unmodified surface.

The characteristics of the surface layer, such as zeta charge, nanoparticle aggregation, dispersion state, stability, and hydration as influenced by the characteristics of the surrounding medium (including ionic strength, pH, temperature, and presence of organic molecules or detergents) are critically important. The contribution of surface charge to both mammalian and microbial interactions has been illustrated using surfactant-coated nanoparticles [104]. Antiadherent and antifungal effects were shown using buccal epithelial cells treated with nondrug-loaded poly(ethylcyanoacrylate) nanoparticles. Nanoparticles were prepared using emulsion polymerization and stabilized with cationic, anionic, or nonionic surfactants. Cationic surfactants, for example, cetrimide, which are known antimicrobial agents, were the most effective in reducing *C. albicans* blastospore adhesion, and showed a growth inhibitory and biocidal effect against the yeast. Production of nanoparticles with an anionic surfactant gave lower yields and wide particle-size distributions. No evidence of killing against *C. albicans* was shown. Nonionic surfactant-coated nanoparticles produced intermediate kill rates. These studies clearly demonstrate the importance of surface charge on the nanoparticle surface. It is suggested that the buccal epithelium could possibly be treated using polymeric-type nanoparticles in a mouthwash-type formulation; in theory, this would prime the potential target cells against adhesion and infection.

The in vivo screening of around 130 nanoparticles intended for therapeutic use has allowed detailed assessments as regards biocompatibility [25]. It was shown that the main independent particle variables which determine compatibility are size, surface charge, and dispersibility (particularly the effect of hydrophobicity). Cationic particles or particles with a high surface reactivity are more likely to be toxic (to both eukaryotes and prokaryotes). Larger, more hydrophobic or poorly dispersed particles, which would be rapidly removed by the reticuloendothelial system, were shown to be less toxic. Karlsson et al. [60] have shown that metal oxide nanoparticles are more toxic than at first envisaged at concentrations down to 40 μg/mL and show a high variation as regards different nanoparticle species to cause cytotoxicity, DNA damage, and oxidative DNA lesions. Toxic effects on cultured cells were assessed using trypan blue staining, the comet assay to measure DNA damage and an oxidation-sensitive fluoroprobe to quantify the production of ROS [60]. Copper oxide was found to be the most toxic and therefore may pose the greatest health risk. Nanoparticulate ZnO and TiO_2, both ingredients in sunscreens and cosmetics, also showed significant cytotoxic and DNA-damaging effects. The potential mechanisms of toxicity for these and other selected nanoparticles are listed in Table 10.1.

In order to help prevent aggregation of nanoparticles, stabilizing (capping) agents that bind to the entire nanoparticle surface can be used; these include water-soluble polymers, oligo- and polysaccharides, sodium dodecyl sulfate, polyethylene glycol, and glycolipids. The specific impact of surface capping, size scale, and aspect ratio of ZnO particles upon antimicrobial activity and cytotoxicity have been investigated [105]. Polyethylene glycol-capped ZnO nanoparticles demonstrated

Table 10.1 Nanoparticle Cytotoxicity to Mammalian Cells

Nanoparticles	Cytotoxicity Mechanism
TiO_2	ROS production
	Glutathione depletion and toxic oxidative stress
	Cell membrane disruption
ZnO	ROS production
	Dissolution and release of toxic cations
	Lysosomal damage
	Inflammation
Ag	Dissolution and Ag^+ ion release inhibits respiratory enzymes and ATP production
ROS production	Disruption of membrane integrity and transport processes
Gold	Disruption of protein conformation
SiO_2	ROS production
	Protein unfolding
	Membrane disruption
Cu/CuO	DNA damage and oxidative stress

Adapted from Ref. [25].

an increase in antimicrobial efficacy with a reduction in particle size. Again, gram-negative bacteria were more affected than gram positive, which suggests that a membrane damage mechanism of action rather than one involving the production of ROS is of overriding significance. Polyethylene glycol-capped nanoparticles were found to be highly toxic to human cells with a very low concentration (at 100 μM) threshold for cytotoxic action, whereas the concentration for antibacterial activity was 50 times greater (at 5 mM). It is hypothesized that the toxicity to eukaryotic cells is related to nanoparticle-enhanced apoptosis by upregulation of the Fas ligand on the cell membrane [105].

An understanding of the interface between biological systems and nanomaterials should enable design features to be used to control the exposure, bioavailability, and biocatalytic activities. A number of possible approaches are now being identified [25] including changing the ability to aggregate, application of surface coatings, and altering charge density and oxidative state. However, this may well compromise the intended selective toxicity of antimicrobial nanoparticles. It remains to be determined how potential mammalian toxicity issues will fully impact on the use of nanotechnology in the control of oral biofilms.

10.7 Conclusions

The application of nanoscaled antimicrobials to control oral infections, as a function of their biocidal, antiadhesive, and delivering capabilities, is of increasing interest. Their use as constituents of prosthetic device coatings, topically applied agents, and within dental materials is currently being explored. Future developments are likely to concentrate on those nanoparticles with maximal antimicrobial activity and minimal host toxicity. Antimicrobial nanoparticulate metals have

Table 10.2 Studies Presenting Data on Effects of Nanoparticles Against Oral Microorganisms

Study	Study Design	Nanoparticles/ Materials Used	Parameters Studied	Results	Microbial Flora Studied
[41]	In vitro	Metals/metal oxides	Antimicrobial activity	Bactericidal in the range 0.025–2.5 mg/mL	*P. gingivalis, F. nucleatum, Prev. intermedia, A. actinomycetemcomitans*
[74]	In vitro	Composite adhesives with silver nanoparticles	Physical properties and antimicrobial activities	Antiadhesive properties and growth retardation	*S. mutans, S. sobrinus*
[75]	In vitro	Zinc oxide nanoparticles blended with resin-based dental composite	Antibiofilm activity	Inhibition of biofilm growth with concentration >10% w/w	*S. sobrinus*
[77]	In vitro	Composite resin with quaternary ammonium polyethylenimine nanoparticles	Antibiofilm activity	Inhibition of biofilm formation at 1 and 24 h	*S. mutans*
[81]	Ex vivo	Zinc oxide/chitosan nanoparticles	Antiadherence on treated root canal surfaces	Antiadherent	*E. faecalis*
[83]	Ex vivo	Silica nanoparticles	Antiadherence on polished teeth surfaces	Antiadherent	*S. mutans*
[84]	In vitro	Silica nanoparticles deposited onto polystyrene surfaces	Development of biofilm and invasive filament formation	Decreased attachment and growth	*C. albicans*
[85]	In vitro	Nitric oxide-releasing nanoparticles	Antibiofilm activity	>99% killing within biofilm	*C. albicans*
[86]	In vitro	Nanometric bioactive glass	Antimicrobial activity in simulated body fluid	Significant killing effects	*E. faecalis*
[92]	In vitro and in vivo	Casein phosphopeptide–amorphous calcium phosphate nanocomplex	Anticariogenic	Reduction of colonization	*S. mutans*

received particular attention as a result of their durability. Although certain nanoparticles may be toxic to oral and other tissues, the surface characteristics of a given particle will help to determine whether or not it will have potential for oral applications. Approaches to alter biocompatibility and desired function are now being identified and these include changing the ability to aggregate, application of surface coatings, and altering oxidative state and charge density.

Acknowledgments

The author is grateful to *International Journal of Antimicrobial Agents* and *Biomaterials* for the permission to use material from 34 (2009) 103–110 and 27 (2006) 3995–4002 (2006), respectively.

References

[1] B.L. Cushing, V.L. Kolesnichenko, C.J. O'Connor, Recent advances in the liquid-phase syntheses of inorganic nanoparticles, Chem. Rev. 104 (2004) 3893–3946.
[2] R.P. Allaker, G.G. Ren, Potential impact of nanotechnology on the control of infectious diseases, Trans. R. Soc. Trop. Med. Hyg. 102 (2008) 1–2.
[3] J.R. Morones, J.L. Elechiguerra, A. Camacho, K. Holt, J.B. Kouri, J.T. Ramirez, The bactericidal effect of silver nanoparticles, Nanotechnology 16 (2005) 2346–2353.
[4] D.R. Monteiro, L.F. Gorup, A.S. Takamiya, A.C. Ruvollo-Filho, E.R. de Camargo, D.B. Barbosa, The growing importance of materials that prevent microbial adhesion: antimicrobial effect of medical devices containing silver, Int. J. Antimicrob. Agents 34 (2009) 103–110.
[5] M. Hannig, L. Kriener, W. Hoth-hannig, C. Becker-Willinger, H. Schmidt, Influence of nanocomposite surface coating on biofilm formation in situ, J. Nanosci. Nanotechnol. 7 (2007) 4642–4648.
[6] P.D. Marsh, M.V. Martin, Oral Microbiology, fifth ed., Churchill Livingstone, 2009.
[7] C. Hannig, M. Hannig, The oral cavity—a key system to understand substratum-dependent bioadhesion on solid surfaces in man, Clin. Oral Invest. 13 (2009) 123–139.
[8] P.D. Marsh, D.J. Bradshaw, Dental plaque as a biofilm, J. Ind. Microbiol. 15 (1995) 169–175.
[9] M. Hannig, A. Joiner, The structure, function and properties of the acquired pellicle, Monogr. Oral Sci. 19 (2006) 29–64.
[10] P.E. Kolenbrander, R.J. Palmer, A.H. Rickard, N.S. Jakubovics, N.I. Chalmers, P.I. Diaz, Bacterial interactions and successions during plaque development, Periodontology 2000 42 (2006) 47–79.
[11] I.W. Sutherland, Biofilm exopolysaccharides: a strong and sticky framework, Microbiology 147 (2001) 3–9.
[12] H.F. Jenkinson, R.J. Lamont, Oral microbial communities in sickness and in health, Trends Microbiol. 13 (2005) 589–595.
[13] K. Lewis, Riddle of biofilm resistance, Antimicrob. Agents Chemother. 45 (2001) 999–1007.
[14] J.M. Hardie, Oral microbiology: current concepts in the microbiology of dental caries and periodontal disease, Brit. Dent. J. 172 (1992) 271–278.
[15] L.A. Ximenez-Fyvie, A.D. Haffajee, S.S. Socransky, Comparison of the microbiota of supra- and subgingival plaque in health and periodontitis, J. Clin. Periodontol. 27 (2000) 648–657.
[16] P.C. Baehni, Y. Takeuchi, Anti-plaque agents in the prevention of biofilm-associated oral diseases, Oral Dis. 9 (Suppl. 1) (2003) 23–29.
[17] F.J. van der Ouderaa, Anti-plaque agents. Rationale and prospects for prevention of gingivitis and periodontal disease, J. Clin. Periodontol. 18 (1991) 447–454.
[18] R.P. Allaker, J.M. Hardie, Oral infections, ninth ed., Topley and Wilson's Microbiology and Microbial Infections, vol. 3, Arnold, London, 1998, pp. 373–390
[19] N.U. Zitzmann, T. Berglundh, Definition and prevalence of peri-implant diseases, J. Clin. Periodontol. 35 (2008) 286–291.
[20] J. Chandra, D.M. Kuhn, P.K. Mukherjee, L.L. Hoyer, T. McCormick, M.A. Ghannoum, Biofilm formation by the fungal pathogen *Candida albicans*: development, architecture, and drug resistance, J. Bacteriol. 183 (2001) 5385–5394.

[21] P.S. Stewart, Diffusion in biofilms, J. Bacteriol. 185 (2003) 1485–1491.
[22] M. Wilson, Susceptibility of oral bacterial biofilms to antimicrobial agents, J. Med. Microbiol. 44 (1996) 79–87.
[23] P.S. Watson, H.A. Pontefract, D.A. Devine, R.C. Shore, B.R. Nattress, J. Kirkham, et al., Penetration of fluoride into natural plaque biofilms, J. Dent. Res. 84 (2005) 451–455.
[24] S.R. Wood, J. Kirham, P.D. Marsh, R.C. Shore, B. Nattress, C. Robinson, Architecture of intact natural human plaque biofilms studied by confocal laser scanning microscopy, J. Dent. Res. 79 (2000) 21–27.
[25] A.E. Nel, L. Madler, D. Velegol, T. Xia, E.M.V. Hoek, P. Somasundaran, et al., Understanding biophysicochemical interactions at the nano-bio interface, Nat. Mater. 8 (2009) 543–557.
[26] E. Giersten, Effects of mouth rinses with triclosan, zinc ions, copolymer, and sodium lauryl sulphate combined with fluoride on acid formation by dental plaque in vivo, Caries Res. 38 (2004) 430–435.
[27] I. Sondi, B. Salopek-Sondi, Silver nanoparticles as an antimicrobial agent: a case study on *E. coli* as a model for Gram-negative bacteria, J. Colloid Interface Sci. 275 (2004) 177–182.
[28] N. Cioffi, L. Torsi, N. Ditaranto, L. Sabbatini, P.G. Zambonin, G. Tantillo, et al., Copper nanoparticle/polymer composites with antifungal and bacteriostatic properties, Chem. Mater. 17 (2005) 5255–5262.
[29] Z. Li, D. Lee, X. Sheng, R.E. Cohen, M.F. Rubner, Two-level antibacterial coating with both release-killing and contact-killing capabilities, Langmuir 22 (2006) 9820–9823.
[30] H. Boldyryeva, N. Umeda, O.A. Plaskin, Y. Takeda, N. Kishimoto, High-fluence implantation of negative metal ions into polymers for surface modification and nanoparticle formation, Surf. Coat Tech. 196 (2005) 373–377.
[31] W.F. Lee, K.T. Tsao, Preparation and properties of nanocomposite hydrogels containing silver nanoparticles by *ex situ* polymerization, J. Appl. Poly. Sci. 100 (2006) 3653–3661.
[32] J. Verran, G. Sandoval, N.S. Allen, M. Edge, J. Stratton, Variables affecting the antibacterial properties of nano and pigmentary titania particles in suspension, Dyes Pigments 73 (2007) 298–304.
[33] C.N. Lok, C.M. Ho, R. Chen, Q.Y. He, W.Y. Yu, H. Sun, et al., Silver nanoparticles: partial oxidation and antibacterial activities, J. Biol. Inorg. Chem. 12 (2007) 527–534.
[34] T.M. Benn, P. Westerhoff, Nanoparticle silver released into water from commercially available sock fabrics, Environ. Sci. Technol. 42 (2008) 4133–4139.
[35] G.A. Sotiriou, S.E. Pratsinis, Antibacterial activity of nanosilver ions and particles, Environ. Sci. Technol. 44 (2010) 5649–5654.
[36] J.S. Kim, E. Kuk, K.N. Yu, J.H. Kim, S.J. Park, H.J. Lee, et al., Antimicrobial effects of silver nanoparticles, Nanomedicine 3 (2007) 95–101.
[37] S. Pal, Y.K. Tak, J.M. Song, Does the antibacterial activity of silver nanoparticles depend on the shape of the nanoparticle? A study of the Gram-negative bacterium *Escherichia coli*, Appl. Environ. Microbiol. 73 (2007) 1712–1720.
[38] J.L. Elechiguerra, J.L. Burt, J.R. Morones, A. Camacho-Bragado, X. Gao, H.H. Lara, et al., Interaction of silver nanoparticles with HIV-1, J. Nanobiotechnol. 3 (2005) 6.
[39] J. Han, L. Chen, S. Duan, Q.X. Yang, M. Yang, C. Gao, et al., Efficient and quick inactivation of SARS coronavirus and other microbes exposed to the surfaces of some metal catalysts, Biomed. Environ. Sci. 18 (2005) 176–180.
[40] G. Ren, D. Hu, E.W.C. Cheng, M.A. Vargas-Reus, P. Reip, R.P. Allaker, Characterisation of copper oxide nanoparticles for antimicrobial applications, Int. J. Antimicrob. Agents 33 (2009) 587–590.
[41] M.A. Vargas-Reus, K. Memarzadeh, J. Huang, G.G. Ren, R.P. Allaker, Antimicrobial activity of nanoparticulate metal oxides against peri-implantitis pathogens, Int. J. Antimicrob. Agents 40 (2012) 135–139.
[42] M. Herrera, P. Carrion, P. Baca, J. Liebana, A. Castillo, In vitro antibacterial activity of glass-ionomer cements, Microbios 104 (2001) 141–148.
[43] L.A. Casemiro, C.H. Gomes-Martins, C. Pires-de-Souza Fde, H. Panzeri, Antimicrobial and mechanical properties of acrylic resins with incorporated silver-zinc zeolite—Part 1, Gerodontology 25 (2008) 187–194.

[44] K. Kawahara, K. Tsuruda, M. Morishita, M. Uchida, Antibacterial effect of silver-zeolite on oral bacteria under anaerobic conditions, Dent. Mater. 16 (2000) 452–455.
[45] T. Matsuura, Y. Abe, Y. Sato, K. Okamoto, M. Ueshige, Y. Akagawa, Prolonged antimicrobial effect of tissue conditioners containing silver-zeolite, J. Dent. 25 (1997) 373–377.
[46] M. Morishita, M. Miyagi, Y. Yamasaki, K. Tsuruda, K. Kawahara, Y. Iwamoto, Pilot study on the effect of a mouthrinse containing silver zeolite on plaque formation, J. Clin. Dent. 9 (1998) 94–96.
[47] P. Li, J. Li, C. Wu, Q. Wu, J. Li, Synergistic antibacterial effects of β-lactam antibiotic combined with silver nanoparticles, Nanotechnology 16 (2005) 1912–1917.
[48] M. Rai, A. Yadav, A. Gade, Silver nanoparticles as a new generation of antimicrobials, Biotechnol. Adv. 27 (2009) 76–83.
[49] V. Sambhy, M.M. MacBride, B.R. Peterson, A. Sen, Silver bromide nanoparticle/polymer composites: dual action tuneable antimicrobial materials, J. Am. Chem. Soc. 128 (2006) 9798–9808.
[50] Q.L. Feng, J. Wu, G.Q. Chen, F.Z. Cui, T.M. Kim, J.O. Kim, A mechanistic study of the antibacterial effect of Ag^+ ions on *Escherichia coli* and *Staphylococcus aureus*, J. Biomed. Mater. Res. 52 (2000) 662–668.
[51] M. Yamanaka, K. Hara, J. Kudo, Bactericidal actions of a silver ion solution on *Escherichia coli*, studied by energy-filtering transmission electron microscopy and proteomic analysis, Appl. Environ. Microbiol. 71 (2005) 7589–7593.
[52] P.D. Bragg, D.J. Rainnie, The effect of Ag^+ ions on the respiratory chain of *E. coli*, Can. J. Microbiol. 20 (1974) 883–889.
[53] K.Y. Yoon, J.H. Byeon, J.H. Park, J. Hwang, et al., Susceptibility constants of *Escherichia coli* and *Bacillus subtilis* to silver and copper nanoparticles, Sci. Tot. Environ. 373 (2007) 572–575.
[54] J.P. Ruparelia, A.K. Chatterje, S.P. Duttagupta, S. Mukherji, Strain specificity in antimicrobial activity of silver and copper nanoparticles, Acta Biomater. 4 (2008) 707–716.
[55] T.J. Beveridge, R.G.E. Murray, Sites of metal deposition in the cell wall of *Bacillus subtilis*, J. Bacteriol. 141 (1980) 876–878.
[56] S.J. Stohs, D. Bagchi, Oxidative mechanisms in the toxicity of metal ions, Free Rad. Biol. Med. 18 (1995) 321–336.
[57] C. Lin, Y. Yeh, C. Yang, C. Chen, G. Chen, C.C. Chen, et al., Selective binding of mannose-encapsulated gold nanoparticles to type I pili in *Escherichia coli*, J. Am. Chem. Soc. 13 (2002) 155–168.
[58] D.N. Williams, S.H. Ehrman, T.R. Pulliman Holoman, Evaluation of the microbial growth response to inorganic nanoparticles, J. Nanobiotech. 4 (2006) 3.
[59] P.K. Stoimenov, R.L. Klinger, G.L. Marchin, K.J. Klabunde, Metal oxide nanoparticles as bactericidal agents, Langmuir 18 (2002) 6679–6686.
[60] H.L. Karlsson, P. Cronholm, J. Gustafsson, L. Moller, Copper oxide nanoparticles are highly toxic: a comparison between metal oxide nanoparticles and carbon nanotubes, Chem. Res. Toxicol. 21 (2008) 1726–1732.
[61] R.J. Cava, Structural chemistry and the local charge picture of copper oxide superconductors, Science 247 (1990) 656–662.
[62] J.M. Tranquada, B.J. Sternlieb, J.D. Axe, Y. Nakamura, S. Uchida, Evidence for stripe correlations of spins and holes in copper oxide superconductors, Nature 375 (1995) 561.
[63] Z. Ahmad, M.A. Vargas-Reus, R. Bakhshi, F. Ryan, G.G. Ren, F. Oktar, et al., Antimicrobial properties of electrically formed elastomeric polyurethane-copper oxide nanocomposites for medical and dental applications, Methods Enzymol. 509 (2012) 87–99.
[64] R. Brayner, R. Ferrari-Iliou, N. Brivois, S. Djediat, M.F. Benedetti, F. Fievet, Toxicological impact studies based on *Escherichia coli* bacteria in ultrafine ZnO nanoparticles colloidal medium, Nano Lett. 6 (2006) 866–870.

[65] K.M. Reddy, K. Feris, J. Bell, D.G. Wingett, C. Hanley, A. Punnoose, Selective toxicity of zinc oxide nanoparticles to prokaryotic and eukaryotic systems, Appl. Phys. Lett. 90 (2007) 213902.
[66] L.L. Zhang, Y.H. Jiang, Y.L. Ding, M. Povey, D. York, Investigation into the antibacterial behaviour of suspensions of ZnO nanoparticles (ZnO nanofluids), J. Nanopart. Res. 9 (2007) 479–489.
[67] J. Sawai, Quantitative evaluation of antibacterial activities of metallic oxide powders (ZnO, MgO and CaO) by conductometric assay, J. Microbiol. Methods 54 (2003) 177–182.
[68] N. Jones, B. Ray, K.T. Ranjit, A.C. Manna, Antibacterial activity of ZnO nanoparticle suspensions on a broad spectrum of microorganisms, FEMS Microbiol. Lett. 279 (2008) 71–76.
[69] Y. Liu, L. He, A. Mustapha, H. Li, Z.Q. Hu, M. Lin, Antibacterial activities of zinc oxide nanoparticles against *Escherichia coli* O157:H7, J. Appl. Microbiol. 107 (2009) 1193–1201.
[70] D.M. Blake, P.-C. Maness, Z. Huang, E.J. Wolfrum, W.A. Jacoby, J. Huang, Application of the photocatalytic chemistry of titanium dioxide to disinfection and the killing of cancer cells, Sep. Purif. Methods 28 (1999) 1–50.
[71] A.S. Yazdi, G. Guarda, N. Riteau, S.K. Drexler, A. Tardivel, I. Couillin, et al., Nanoparticles activate the NLR pyrin domain containing 3 (NIrp3) inflammasome and cause pulmonary inflammation through release of IL-1α and IL-1β, Proc. Natl. Acad. Sci. U. S. A. 107 (2010) 19449–19454.
[72] P.C. Maness, S. Smolinski, D.M. Blake, Z. Huang, E.J. Wolfrum, W.A. Jacoby, Bactericidal activity of photocatalytic TiO_2 reaction: toward an understanding of its killing mechanism, Appl. Envirol. Microbiol. 65 (1999) 4094–4098.
[73] Y.H. Tsuang, J.S. Sun, Y.C. Huang, C.H. Lu, W.H.S. Chang, C.C. Wang, Studies of photokilling of bacteria using titanium dioxide nanoparticles, Artif. Organs 32 (2008) 167–174.
[74] S.J. Ahn, S.J. Lee, J.K. Kook, B.S. Lim, Experimental antimicrobial orthodontic adhesives using nanofillers and silver nanoparticles, Dent. Mater. 25 (2009) 206–213.
[75] B. Aydin Sevnic, L. Hanley, Antibacterial activity of dental composites containing zinc oxide nanoparticles, J. Biomed. Mater. Res. B Appl. Biomater. 94 (2010) 22–31.
[76] A. Almaguer-Flores, L.A. Ximenez-Fyvie, S.E. Rodil, Oral bacterial adhesion on amorphous carbon and titanium films: effect of surface roughness and culture media, J. Biomed. Mater. Res. B Appl. Biomater. 92 (2010) 196–204.
[77] N. Beyth, I. Yudovin-Farber, R. Bahir, A.J. Domb, E.I. Weiss, Antibacterial activity of dental composites containing quaternary ammonium polyethylenimine nanoparticles against *Streptococcus mutans*, Biomaterials 27 (2006) 3995–4002.
[78] I. Yudovin-Farber, N. Beyth, A. Nyska, E.I. Weiss, J. Golenser, A.J. Domb, Surface characterization and biocompatibility of restorative resin containing nanoparticles, Biomacromolecules 9 (2008) 3044–3050.
[79] Y. Wu, W. Yang, C. Wang, J. Hu, S. Fu, Chitosan nanoparticles as a novel delivery system for ammonium glycyrrhizinate, Int. J. Pharm. 295 (2005) 235–245.
[80] L.M. Lin, J.E. Skribner, P. Gaengler, Factors associated with endodontic failures, J. Endod. 18 (1992) 625–627.
[81] A. Kishen, Z. Shi, A. Shrestha, K.G. Neoh, An investigation on the antibacterial and antibiofilm efficacy of cationic nanoparticulates for root canal infection, J. Endod. 34 (2008) 1515–1520.
[82] K.W. Stephen, Dentrifices: recent clinical findings and implications for use, Int. Dent. J. 43 (1993) 549–553.
[83] R.M. Gaikwaad, I. Sokolov, Silica nanoparticles to polish tooth surfaces for caries prevention, J. Dent. Res. 87 (2008) 980–983.
[84] B.G. Cousins, H.E. Allison, P.J. Doherty, C. Edwards, M.J. Garvey, D.S. Martin, et al., Effects of a nanoparticulate silica substrate on cell attachment of *Candida albicans*, J. Appl. Microbiol. 102 (2007) 757–765.
[85] E.M. Hetrick, J.H. Shin, H.S. Paul, M.H. Schoenfisch, Anti-biofilm efficacy of nitric oxide-releasing silica nanoparticles, Biomaterials 30 (2009) 2782–2789.

[86] T. Waltimo, T.J. Brunner, M. Vollenweider, W.J. Stark, M. Zehnder, Antimicrobial effect of nanometric bioactive glass 45S5, J. Dent. Res. 86 (2007) 754–757.
[87] N. Roveri, E. Battistello, I. Foltran, E. Foresti, M. Iafisco, M. Lelli, et al., Synthetic biomimetic carbonate-hydroxyapatite nanocrystals for enamel remineralization, Adv. Mater. Res. 47–50 (2008) 821–824.
[88] K.J. Cross, N.L. Huq, E.C. Reynolds, Casein phosphopeptides in oral health chemistry and clinical applications, Curr. Pharm. Des. 13 (2007) 793–800.
[89] S.C. Venegas, J.M. Palacios, M.C. Apella, P.J. Morando, M.A. Blesa, Calcium modulates interactions between bacteria and hydroxyapatite, J. Dent. Res. 85 (2006) 1124–1128.
[90] C. Rahiotis, G. Vougiouklakis, G. Eliades, Characterization of oral films formed in the presence of a CPP-ACP agent: an *in situ* study, J. Dent. 36 (2008) 272–280.
[91] E.C. Reynolds, F. Cai, P. Shen, G.D. Walker, Retention in plaque and remineralization of enamel lesions by various forms of calcium in a mouthrinse or sugar-free chewing gum, J. Dent. Res. 82 (2003) 206–211.
[92] E.C. Reynolds, Calcium phosphate-based remineralization systems: scientific evidence?, Aus. Dent. J. 53 (2008) 268–273.
[93] R.K. Rose, Binding characteristics of *Streptococcus mutans* for calcium and casein phosphopeptide, Caries Res. 34 (2000) 427–431.
[94] R.K. Rose, Effects of an anticariogenic casein phosphopeptide on calcium diffusion in streptococcal model dental plaques, Arch. Oral Biol. 45 (2000) 569–575.
[95] R.P. Allaker, C.W.I. Douglas, Novel anti-microbial therapies for dental plaque-related diseases, Int. J. Antimicrob. Agents 33 (2009) 8–13.
[96] A.J. MacRobert, S.G. Bown, D. Phillips, What are the ideal photoproperties for a sensitizer? Ciba Found. Symp. 146 (1989) 4–12.
[97] T.C. Pagonis, J. Chen, C.R. Fontana, H. Devalapally, K. Ruggiero, X. Song, et al., Nanoparticle-based endodontic antimicrobial photodynamic therapy, J. Endod. 36 (2010) 322–328.
[98] S. Wood, D. Metcalf, D. Devine, C. Robinson, Erythrosine is a potential photosensitizer for the photodynamic therapy of oral plaque biofilms, J. Antimicrob. Chemother. 57 (2006) 680–684.
[99] R.N. Seetharam, K.R. Sridhar, Nanotoxicity: threat posed by nanoparticles, Curr. Sci. 93 (2006) 769–770.
[100] W.I. Hagens, A.G. Oomen, W.H. de Jong, F.R. Cassee, A.J. Sips, What do we (need to) know about the kinetic properties of nanoparticles in the body? Reg. Toxicol. Pharmacol. 49 (2007) 217–229.
[101] A. Panacek, M. Kolar, R. Vecerova, R. Prucek, J. Soukupova, V. Krystof, et al., Antifungal activity of silver nanoparticles against *Candida* spp, Biomaterials 30 (2009) 6333–6340.
[102] A. Nel, T. Xia, I. Madler, N. Li, Toxic potential of materials at the nanolevel, Science 311 (2006) 622–627.
[103] M.L. Luo, J.Q. Zhao, W. Tang, S. Pu, Hydrophilic modification of poly (ether sulfone) ultrafiltration membrane surface by self-assembly of TiO_2 nanoparticles, Appl. Surf. Sci. 49 (2005) 76–84.
[104] P.A. McCarron, R.F. Donnelly, W. Marouf, D.E. Calvert, Anti-adherent and antifungal activities of surfactant-coated poly (ethylcyanoacrylate) nanoparticles, Int. J. Pharm. 340 (2007) 182–190.
[105] S. Nair, A. Sasidharan, V.V.D. Rani, D. Menon, S. Nair, K. Manzoor, et al., Role of size scale of ZnO nanoparticles and microparticles on toxicity toward bacteria and osteoblast cancer cells, J. Mater. Sci. Mater. Med. 20 (2009) S235–S241.

CHAPTER

11 Nanotechnology in Orthodontics—1: The Past, Present, and a Perspective of the Future

Karthikeyan Subramani, Sarandeep Huja, G. Thomas Kluemper, Lorri Morford and James K. Hartsfield, Jr.

Division of Orthodontics, College of Dentistry, University of Kentucky, Lexington, KY, USA

CHAPTER OUTLINE

11.1 Introduction

The concept and origin of nanotechnology has been attributed to the American Physicist and Nobel Laureate Richard Phillips Feynman [1] who presented a paper titled *There is Plenty of Room at the Bottom* on December 29, 1959 at the annual meeting of the American Physical Society at California Institute of Technology. Feynman proposed to employ machines to make

Nanobiomaterials in Clinical Dentistry.

smaller machine tools, which in turn could be utilized to make even smaller machine tools and so on, all the way down to the molecular and nanoscale level (1 nm = 10^{-9} m or one-billionth of a meter). He suggested that such nanomachines, nanorobots, and nanodevices could be ultimately used to develop a wide range of atomically precise micro/nanoscopic instrumentation and manufacturing tools. Feynman also discussed the storage of information on a very small scale, writing and reading in atoms, miniaturization of computers, and building tiny machines and electronic circuits with atoms. He stated that "In the year 2000, when they look back at this age, they will wonder why it was not until the year 1960 that anybody began to seriously move in this direction."

However, Feynman did not specifically use the term "nanotechnology" then. The first use of the word "nanotechnology" has been attributed to Norio Taniguchi in a paper titled *On the Basic Concept of NanoTechnology* published in 1974 [2]. Eric Drexler, an MIT graduate took Feynman's concept of a billion tiny factories and added the idea that they could replicate more copies of themselves via computer control instead of a human operator in his 1986 book *Engines of Creation: The Coming Era of Nanotechnology*, to popularize the potential of nanotechnology. Nanotechnology is described as the multidisciplinary science of the creation of materials, devices, and systems at the nanoscale level. It refers to the manipulation, precise placement, measurement, modeling, or manufacture of sub-100 nm scale matter. In other words, it has been described as the ability to work at atomic, molecular, and supramolecular levels (on a scale of $\sim 1-100$ nm) to understand, create, and use material structures, devices, and systems with fundamentally new properties and functions resulting from their small structure.

Nanotechnology has been approached in two ways: from the "top-down" or the "bottom-up" approach [3]. The "top-down" approach is the utilization of miniaturization techniques to construct micro/nanoscale structures from a macroscopic material or a group of materials by utilizing machining and etching techniques. The best example of a "top-down" approach is the photolithography technique used in the semiconductor industry to fabricate components of an integrated circuit by etching micro/nanoscale patterns on a silicon wafer. The "bottom-up" approach refers to the construction of macromolecular structures from atoms or molecules that have the ability to self-organize or self-assemble to form a macroscopic structure [4,5].

Nanotechnology has much more to offer than just simple miniaturization and building the molecular structures from the atomic scale. Over the past decade, numerous discoveries and applications of nanotechnology have revolutionized multiple disciplines of science, technology, medicine, and space exploration. In the field of medicine, nanotechnology has been applied in diagnosis, prevention, and treatment of diseases. Nanomaterials are being applied in the field of pharmacotherapeutics toward new drug synthesis, targeted drug delivery for cancer treatment, regenerative medicine, imaging, and gene therapy [6,7].

Nanotechnology offers promising scope in dentistry to improve dental treatment, care, and prevention of oral diseases. Currently, numerous nanoscale dental materials, nanocharacterization methods, and nanofabrication techniques are being employed in dentistry to improve the biomaterial properties. During the last decade, the use of nanotechnology and nanoparticles has become popular in the design and development of dental biomaterials with improved material characteristics. The purpose of this chapter is to give the reader an overview of these recent developments in nanotechnology, nanomaterials, nanoscale imaging tools, and their applications in dentistry, and more specifically in orthodontics.

11.2 Nanoindentation and atomic force microscopy studies on orthodontic brackets and archwires

Orthodontic brackets bonded to teeth provide the means to transfer force from the activated archwire to the teeth to facilitate tooth movement. Orthodontic brackets can be metallic (stainless steel, titanium, or gold) or tooth colored (plastic or ceramic). The surface characteristics (roughness and surface free energy (SFE)) of the brackets play a significant role in reducing friction and plaque (biofilm) formation. Micro- and nanoscale roughness of these brackets can facilitate early bacterial adhesion. Even though the surfaces of newly placed brackets are smoother, there can be changes in the surface roughness and SFE during the course of orthodontic treatment. A nanoindenter coupled with atomic force microscope (AFM) has been traditionally used to evaluate nanoscale surface characteristics of biomaterials. They have also been used to evaluate mechanical properties like hardness, elastic modulus, yield strength, fracture toughness, scratch hardness, and wear properties by nanoindentation studies.

AFM, also called the scanning force microscopy, was developed in 1986, subsequently to the invention of the scanning tunneling microscope (STM) [8]. Similar in operation to the STM, the AFM involves scanning a sharp cantilever tip across a sample surface while monitoring the tip-sample interaction to allow the reconstruction of the three-dimensional surface topography. A typical AFM can provide resolutions of the order of 1 nm laterally and 0.07 nm (sub-angstrom) vertically. AFM has been utilized to look at the nanoscale dimension of the orthodontic armamentarium and the changes taking place during the course of treatment. Orthodontic brackets and archwires can undergo changes in surface characteristics during treatment due to the effects of food and oral hygiene habits and/or calcification (Figure 11.1) [9].

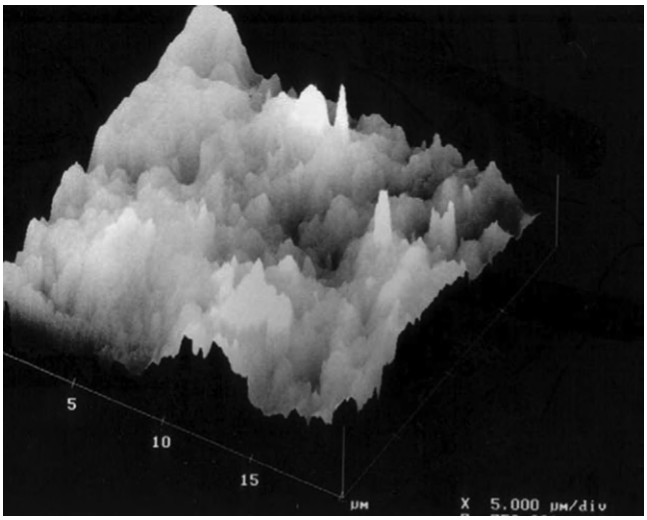

FIGURE 11.1

AFM image of retrieved Ni–Ti archwire exposed in oral cavity for 1 month, depicting rough surface produced by calcification on wire surface [9].

AFM has been utilized as a tool to evaluate the surface roughness of stainless steel, beta-titanium, and nickel—titanium (Ni—Ti) wires [10]. In this study, AFM measurement of surface roughness reiterated the fact that the roughness influences the effectiveness of sliding mechanics, corrosion behavior, and esthetics of orthodontic archwires. The effects of decontamination and clinical exposure on elastic modulus, hardness, and surface roughness of stainless steel and Ni—Ti archwires were evaluated using AFM coupled with a nanoindenter [11]. The results of AFM evaluation showed that the decontamination regimen and clinical exposure had no statistically significant effect on Ni—Ti wires but did have a statistically significant effect on stainless steel wires. The study concluded that it is difficult to predict the clinical significance of these statistically significant changes in archwire properties on orthodontic tooth movement.

Surface roughness of various orthodontic bracket slots before and after the sliding movement of an archwire in vitro and in vivo was observed quantitatively using AFM in a recent study [12]. Conventional stainless steel, ceramic, self-ligating stainless steel, and ceramic brackets were evaluated. In vitro sliding test results with beta-titanium wire in the conventional stainless steel and ceramic brackets showed that there was significant increase in surface roughness only in stainless steel brackets. The results of surface roughness with AFM measurements on the brackets after a 2-year orthodontic treatment regime showed that self-ligating ceramic brackets had undergone less significant changes in roughness parameters than self-ligating stainless steel brackets. The study concluded that the self-ligating ceramic bracket has great possibility to exhibit low friction and better biocompatibility than the other tested brackets including the conventional brackets. Such studies using AFM have shown that it can be utilized as an effective imaging tool to visualize and analyze the surface properties and understand the changes taking place at the nanoscale dimension of orthodontic wires or brackets during treatment.

11.3 Friction reducing nanocoatings on orthodontic archwires

Orthodontic archwires are used to generate mechanical forces that are transmitted through brackets to move teeth and correct malocclusion, spacing, and/or crowding. They are also used for retentive purposes, i.e., to maintain teeth in their current position. Currently orthodontic archwires are fabricated from base metal alloys. The types of wires most commonly used are stainless steel, Ni—Ti, and beta-titanium alloy wires (composed of titanium, molybdenum, zirconium, and tin). When employing sliding mechanics, friction between the wire and the bracket is one of the primary factors influencing tooth movement. When one moving object contacts another, friction is introduced at the interface, which results in resistance to tooth movement. This frictional force is proportional to the force with which the contacting surfaces are pressed together and is governed by the surface characteristics at the interface (smooth/rough, chemically reactive/passive, or modified by lubricants). Minimizing the frictional forces between the orthodontic wire and brackets has the potential to increase the velocity of desired tooth movement and therefore result in less treatment time.

In recent years, nanoparticles have been used as a component of dry lubricants. Dry lubricants are solid phase materials that are able to reduce friction between two surfaces sliding against each other without the need for a liquid media. Biocompatible nanoparticles have been coated on orthodontic stainless steel wires to reduce friction. Inorganic fullerene-like nanoparticles of tungsten

disulfide (IF-WS_2) (Figure 11.2), which are potent dry lubricants have been evaluated as self-lubricating coatings for orthodontic stainless steel wires [14]. In a recent study, orthodontic stainless steel wire was coated with a nickel–phosphorus (Ni–P) film impregnated with IF-WS_2 (Figure 11.3) [13]. Coating was done by inserting stainless steel wires into solutions of Ni–P and

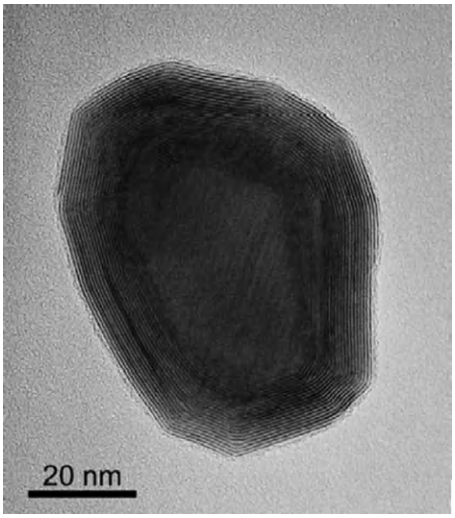

FIGURE 11.2

TEM lattice image of a typical IF-WS2 nanoparticle. Each dark line represents an atomic layer of the basal planes with a distance of 0.62 nm between the layers [13].

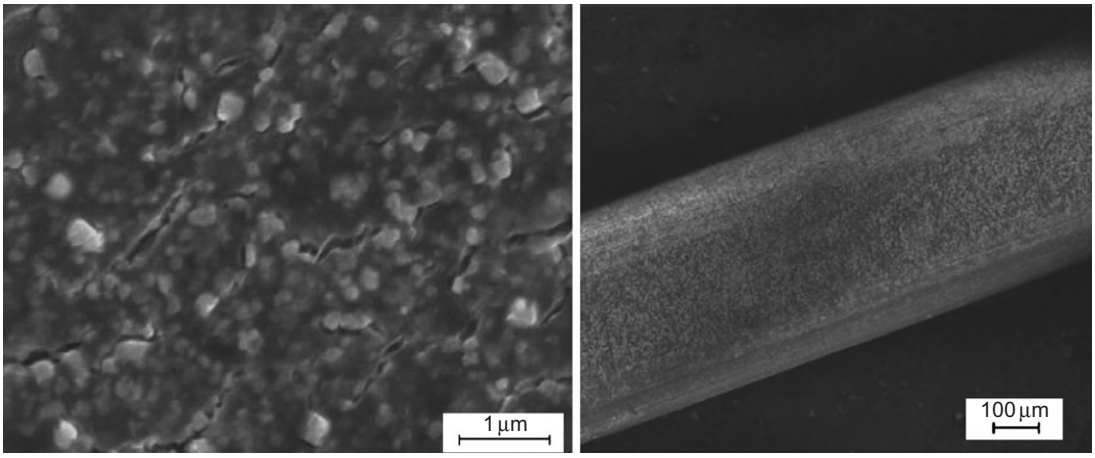

FIGURE 11.3

SEM image of a Ni–P + IF-WS2 coated stainless steel wire (right) and the same coating shown in large magnification (left). The impregnated IF nanoparticles are clearly visible in the Ni–P film [13].

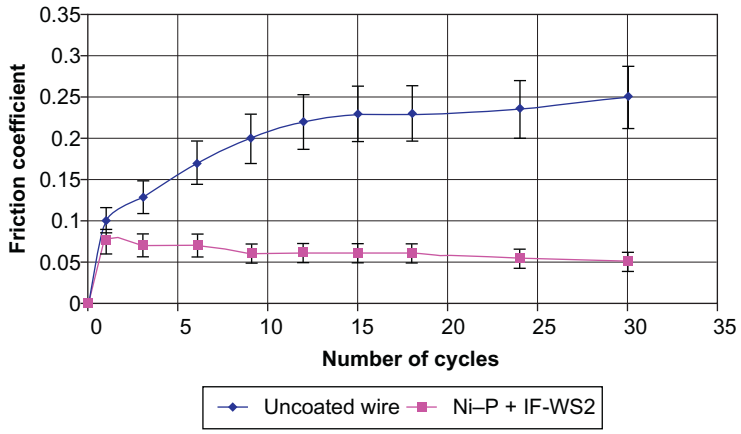

FIGURE 11.4

Friction coefficient of the orthodontic wire substrate compared to a wire coated with Ni—P and IF-WS2 [13].

IF-WS2. The coated wires were then analyzed by scanning electron microscope (SEM) and energy-dispersive X-ray spectrometer as well as by tribological tests using a ball-on-flat device. Friction tests simulating archwire functioning of coated and uncoated wires were carried out by an Instron machine. The adhesion properties of the coated wires after friction were analyzed using a Raman microscope. The frictional forces when measured on the coated wire were reduced by up to 54% when compared to uncoated stainless steel wire. The friction coefficient was also significantly reduced from 0.25 to 0.08 (Figure 11.4). These studies concluded that stainless steel wires coated with these nanoparticles might offer a novel opportunity to substantially reduce friction during orthodontic tooth movement. It has been reported in animal studies that these nanoparticles are biocompatible [14].

Tungsten disulfide nanocoating has also been evaluated for friction reduction of Ni—Ti substrates (Table 11.1). Ni—Ti substrates were coated with cobalt and IF-WS_2 nanoparticles film by electrodeposition procedure and the friction test results showed up to 66% reduction of the friction coefficient on the coated substrates when compared to uncoated substrates [15]. The results of such studies may have potential applications in reducing the friction when using orthodontic Ni—Ti wires. One drawback to the incorporation of Ni in these types of coatings is the potential for allergic reactions in patients with nickel sensitivity [20—23]. Therefore, the effect of such Ni—P coatings on stainless steel and Ni—Ti wires should be evaluated for biocompatibility in animal models and further in human trials.

11.4 Nanoparticles in orthodontic adhesives

Composite materials and glass ionomer cements (GIC) have been primarily used in orthodontics as adhesive agents for securing orthodontic brackets and bands to the surface of the teeth. The largest application of nanoparticles has been in dental composite materials, where they have been used to

Table 11.1 Summary of Studies on Nanoparticle Applications in Materials Used in Orthodontics

Material Studied	Nanoparticle/ Nanoscale Imaging Technique Used	Parameters Evaluated	Results
Orthodontic stainless steel wire [13,14]	Ni–P film impregnated with IF-WS_2 nanoparticles	(i) Frictional forces measured on coated and uncoated wires	(i) Reduced to 54% on coated wires
		(ii) Friction coefficient	(ii) Friction coefficient reduced one-third from 0.25 to 0.08
Ni–Ti substrates [15]	Cobalt and IF-WS_2 nanoparticles	Friction coefficient	66% reduction in coated substrates
Stainless steel, beta-titanium and Ni–Ti archwires [10]	AFM	Surface roughness	Surface roughness influenced the effectiveness of sliding mechanics, corrosion behavior, and esthetics
Stainless steel and Ni–Ti archwires [11]	AFM coupled with nanoindenter	Effects of decontamination and clinical exposure on elastic modulus, hardness, and surface roughness	Decontamination regimen and clinical exposure had no effect on Ni–Ti wires but did have a statistically significant effect on stainless steel wires. Decontamination of stainless steel wires significantly increased surface hardness ($P = 0.01$) and reduced the surface roughness ($P = 0.02$)
Conventional stainless steel, ceramic, self-ligating stainless steel and ceramic brackets [12]	AFM	Surface roughness	2-year orthodontic treatment regime showed that self-ligating ceramic brackets had undergone less change in roughness parameters than self-ligating stainless steel brackets. Self-ligating ceramic brackets exhibited low friction and better biocompatibility than other brackets
Fuji II GIC [16]	Nanohydroxy and fluoroapatite, *N*-vinylpyrrolidone (NVP)-containing polyacids	CS, DTS, BFS	Highest values for CS, DTS, and BFS were found for NVP-nanoceramic powder modified cements (184 MPa for CS, 22 MPa for DTS and 33 MPa for BFS)

(*Continued*)

Table 11.1 (Continued)

Material Studied	Nanoparticle/ Nanoscale Imaging Technique Used	Parameters Evaluated	Results
Nanocomposite material (Filtek Supreme Plus Universal) and the nanoionomer restorative material (Ketac™ N100 Light Curing Nano-Ionomer) and a conventional orthodontic composite material (Transbond XT) [17]	Nanofilled composite material (Filtek Supreme Plus Universal) and GIC modified with nanofillers, and nanofiller "clusters" (Ketac™ N100 Light Curing Nano-Ionomer)	Shear bond strength	Conventional orthodontic composite had higher shear bond strength than nanocomposite and nanoionomer groups
ECA material and two conventional adhesives (composite and resin-modified glass ionomer) [18]	ECA was modified by the addition of silica nanofillers and silver nanoparticles	Effect of surface characteristics, physical properties, and antibacterial activities of ECA against cariogenic *Streptococci*	ECA had rougher surfaces than conventional adhesives due to addition of silver nanoparticles and bacterial adhesion to ECA was less than to conventional adhesives. No significant difference in shear bond strength and bond failure interface between ECA and conventional adhesives were noted
BisGMA/HEMA adhesive modified with nanogel [19]	Nanogel copolymers at a 70:30 molar ratio of IBMA and either UDMA or BisEMA	Adhesive viscosity, wet mechanical properties, short-term microtensile bond strength	Parameters evaluated were enhanced by nanogel inclusion in the adhesive resin

enhance the long-term optical properties by virtue of their small size, and at the same time provide superior mechanical strength and wear resistance. Ever since the first formulation of composite resins in the 1960s, the basic compositional triad has been used: monomer, silane-treated filler, and initiators.

Filler particles improve the mechanical properties of the composite material. The filler used by Bowen in 1963 [24], consisted of milled quartz particles with average size ranging from 8 to 12 μm (8000−12,000 nm). Due to the esthetic limitations of macrofilled composites (lack of surface gloss), the minifilled composite was introduced in the 1970s. Improvement in properties such as tensile and compressive strength (CS), modulus of elasticity, abrasion resistance, radiopacity, esthetics, and handling was noted with higher filler load. The filler material used was silica particles of average diameter of 400 nm allowing a maximum filler loading of 55 wt%, with better polishability, but with a significantly lower mechanical strength [25]. It was not until the 1980s and 1990s that mixtures of filler materials were tested. These hybrid fillers (600−2000 nm) were

commercialized as hybrid, microhybrid, and condensable composites [25]. There was an improvement in mechanical strength; however, the polishability was still a limitation. A maximum filler load from 70 to 77 wt% was recorded then. Microfilled composites (10−100 nm) were not suitable for high stress bearing areas (e.g., Class I, II, and IV restorations) of the dentition. The particle sizes of these hybrid composites were not similar to the size of the hydroxyapatite crystal, dentinal tubule, and enamel rod. There was also a potential for compromise in adhesion between the macroscopic restorative material and the nanoscopic (1−10 nm in size) tooth structure. So nanofilled composite materials were introduced.

There are two distinct types of dental nanocomposites currently available: nanofills and nanohybrids [26,27]. Nanofills contain nanometer-sized particles (1−100 nm) throughout the resin matrix, with no other large primary particles included. Nanohybrids consist of larger particles (400−5000 nm) with added nanometer-sized particles. The use of nanoparticles addresses the aforementioned difficulty by combining high mechanical strength with long-term polish retention in one material.

Another adhesive material used in orthodontics is GIC. GIC is also known as polyalkenoate cement and contains components of silicate glass and polyacrylic acid [28]. GIC is translucent and adhesive to tooth structure and has unique properties such as biocompatibility, anticariogenic action (due to fluoride release), and adhesion to moist tooth structure. In addition, the coefficient of thermal expansion for GIC is low and close to the values of tooth structure. Besides its advantages, GIC has some disadvantages such as brittleness and inferior mechanical strength. The use of GIC in orthodontics became popular during the late 1980s due to its fluoride-releasing potential which made it highly attractive for orthodontic band cementation. It was shown that modifying conventional GIC with nanohydroxy and fluoroapatite (Figure 11.5) and *N*-vinylpyrrolidone containing polyacids improved its mechanical properties. When tested, it proved to have greater CS and higher diametral tensile strength (DTS) and biaxial flexural strength (BFS) than the control group consisting of conventional GIC [16].

Recently, "nanoionomer," which is resin-modified GIC (Ketac™ N100 Light Curing Nano-Ionomer), has been introduced to operative dentistry [29,30]. This light curing nanoionomer is composed of fluoroaluminosilicate glass, nanofillers, and nanofiller "clusters" combined to improve mechanical properties and high fluoride release. A recent study tested the commercially available nanocomposite material (Filtek Supreme Plus Universal) and the nanoionomer restorative material (Ketac™ N100 Light Curing Nano-Ionomer) for orthodontic bracket bonding [17]. The study evaluated their shear bond strength and failure site locations in comparison with a conventional light-cure orthodontic bonding adhesive (Transbond XT). Orthodontic brackets should withstand high shearing force in the oral cavity generated during the orthodontic teeth movement. The results of the study demonstrated that conventional orthodontic composite had higher shear bond strength than that of nanocomposite and the nanoionomer groups. The study concluded that nanocomposites and nanoionomers may be suitable for bonding but are inferior to conventional orthodontic composites.

In another study, an experimental composite adhesive material (ECA) containing silica nanofillers and silver nanoparticles was compared with two conventional adhesives (composite and resin-modified glass ionomer) to evaluate the surface characteristics, physical properties, and antibacterial activity against cariogenic *Streptococci* [18]. Bacterial adhesion was measured by incubating the adhesive discs for 6 h in saliva sample. The discs were washed with sterile phosphate buffered saline and the number of adherent cells was determined using a Beckman LS-5000TA liquid scintillation counter. The results of this study showed that ECA had rougher surfaces than conventional

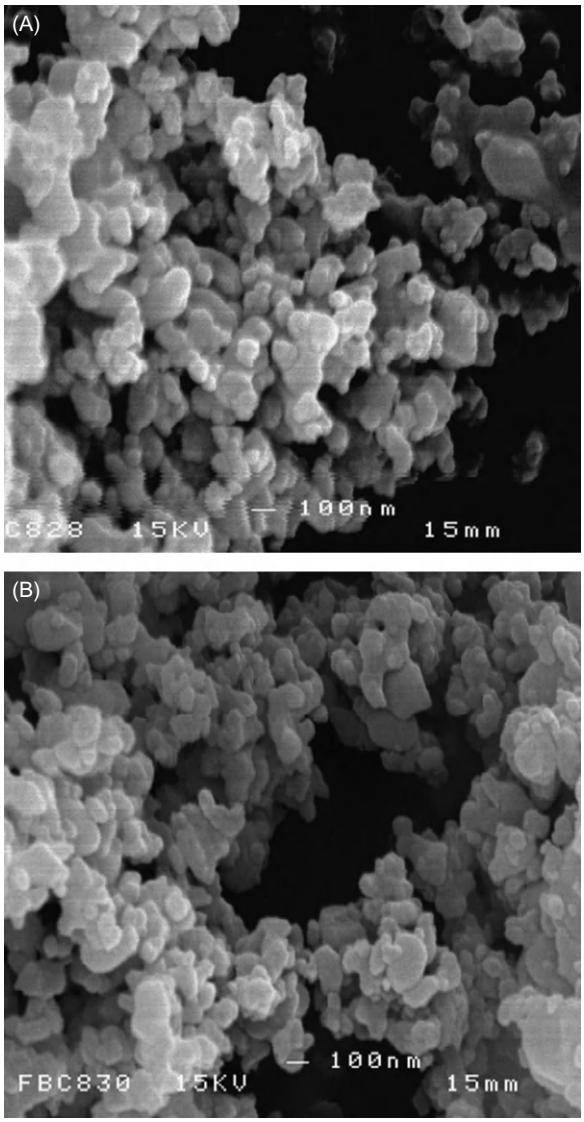

FIGURE 11.5

SEM of hydroxyapatite (A) and fluoroapatite (B) nanopowders (×40,000) [16].

adhesives due to the addition of silver nanoparticles. However, the bacterial adhesion to ECA was less than the conventional adhesives. Bacterial suspension containing ECAs showed slower bacterial growth than those containing conventional adhesives. There was no significant difference in shear bond strength and bond failure interface between ECA and conventional adhesives evaluated in this study. It can be interpreted from the study that antibacterial nanoparticles can be

incorporated into orthodontic adhesive materials to prevent bacterial adhesion and caries during orthodontic treatment.

One of the current challenges in adhesive dentistry using hybrid materials is over-hydrophilic bonding formulations, which facilitate water percolation through the hybrid layer resulting in unreliable bonded interfaces. A recent study evaluated a nanogel-modified dentin adhesive composed of BisGMA/HEMA (2,2-bis [4(2-hydroxy-3-methacryloyloxy-propyloxy)-phenyl] propane/2-hydroxyethyl methacrylate) [19]. The nanogel additives of 10- to 100-nm-sized particles with varied hydrophobicity were synthesized in solution and added to BisGMA/HEMA. Nanogel copolymers at a 70:30 molar ratio of isobornyl methacrylate (IBMA) and either urethane dimethacrylate (UDMA—less hydrophobic) or ethoxylated bis-phenol-adimethacrylate (BisEMA—more hydrophobic) was used. Adhesive viscosity, wet mechanical properties, short-term microtensile bond strength to acid-etched and primed dentin were studied. All these parameters evaluated were significantly enhanced in the nanogel-adhesive group over the control group containing just BisGMA/HEMA. These recent studies reinforce the importance of nanoscale-modified adhesive materials with improved properties for their use in orthodontics.

11.5 Nanoparticle delivery from orthodontic elastomeric ligatures

Fixed orthodontic appliance treatment significantly increases the risk of enamel decalcification and white spot lesions. These are caused due to prolonged accumulation and retention of bacterial plaque on the enamel surface adjacent to the attachments (orthodontic brackets and bands). Demineralization of enamel has been reported to occur around orthodontic brackets within 1 month of bracket placement in the absence of fluoride supplementation [31,32]. Elastomeric ligature ties have been conventionally used to hold orthodontic wires securely in the bracket during the treatment process. These elastomeric ligatures can serve as a carrier scaffold for delivery of nanoparticles that can be anticariogenic, antiinflammatory, and/or antibiotic drug molecules embedded in the elastomeric matrix. The release of anticariogenic fluoride from elastomeric ligatures has been reported in the literature previously [33–35]. The studies concluded that the fluoride release was characterized by an initial burst of fluoride during the first day and second day, followed by a logarithmic decrease. For optimum clinical benefit, the fluoride ties should be replaced monthly [33]. These ties gained weight intraorally with residual, leachable fluoride present in fluoride-impregnated and non-fluoride elastomeric ligature ties after 1 month of intraoral use, due to imbibition [34].

An in vivo study evaluating the efficacy of fluoride-releasing elastomers in the control of colony forming units (CFUs) of *Streptococcus mutans* in the oral cavity concluded that fluoride-releasing elastomeric ligature ties are not indicated for reducing the incidence of enamel decalcification in orthodontic patients. The study found no significant reduction in CFUs in saliva or plaque around the fluoride-releasing ties when compared with the conventional elastomeric ligature ties [35]. There are very few published studies evaluating the release and efficacy of nanoparticle-based anticariogenic, antiinflammatory, analgesic, or antibiotic drug delivery from orthodontic elastomeric ligatures to prevent enamel decalcification, decrease the biofilm accumulation during the orthodontic treatment, or reduce infections. Medicated wax applied to orthodontic brackets that slowly and continuously released benzocaine was shown to be significantly more effective in

reducing pain associated with mucosal irritation caused by brackets [36]. It could be highly advantageous to explore the local delivery of such therapeutic nanoparticles at the site of enamel decalcification, biofilm formation, and gingivitis. As with all new technological applications, however, it will also be important to carefully evaluate the rate of release of such nanoparticles, ingestion, biocompatibility, and systemic toxicity level for these new nanotechnology-based applications.

11.6 Developing and future applications of nanotechnology in dentistry and orthodontics

The future of nanotechnology in orthodontics has potential to develop in a number of additional applications as well including (a) the use of tooth-colored, shape-memory polymers to esthetically move teeth, (b) tooth movement using orthodontic nanobots that could directly manipulate periodontal tissues allowing rapid and perhaps painless movement, dentifrobots (nanobots in dentifrices) delivered through mouthwash or toothpaste to patrol supragingival and subgingival surfaces performing continuous plaque/calculus removal and metabolizing trapped organic matter, and (c) nanochanges on the surfaces of temporary anchorage devices (TADs) to increase their retention but still allow them to be removed when no longer needed.

11.6.1 The use of shape-memory polymer in orthodontics

Over the past decade, there has been an increased interest in producing esthetic orthodontic wires to complement tooth colored brackets. Shape-memory esthetic polymer is an area of potential research. These are a class of stimuli-responsive materials, which have the capacity to remember a preprogrammed shape imprinted during the synthesis; can be reformed at a higher temperature to impart a desired temporary shape; and recover their original shape when influenced by a stimulus, such as heat, light, or magnetic field [37,38]. Applications of nanoparticles in shape-memory nanocomposite polymers can increase thermal conductivity of the polymers [39,40]. These wires can also be made with clinically relevant levels of elastic stiffness. Once placed in the mouth, these polymers can be activated by the body temperature or photoactive nanoparticles activated by light and thus influence tooth movement. Future research directions in shape-memory nanocomposite polymers to produce esthetic orthodontic wires can be of interesting potential in orthodontic biomaterial research.

11.6.2 BioMEMS/NEMS for orthodontic tooth movement and maxillary expansion

Microelectromechanical systems (MEMS) devices are manufactured using similar microfabrication techniques as those used to create integrated circuits. They often have moving components that allow a physical or analytical function to be performed by the device in addition to their electrical functions. The biological MEMS (bioMEMS) are made up of micromachined elements usually on silicon substrates, including gears, motors, and actuators with linear and rotary motion for applications to biological systems. Implantable bioMEMS have been used as biosensors for in vivo diagnostics of diseases and as drug delivery microchips [41–43]. Nanoelectromechanical systems (NEMS) are devices integrating electrical and mechanical functionality on the nanoscale level.

Evidence suggests that orthodontic tooth movement can be enhanced by supplementing the mechanical forces with electricity [44,45]. Animal experiments indicated that when 15−20 microamperes of low direct current (dc) was applied to the alveolar bone by modifying the bioelectric potential, osteoblasts and periodontal ligament cells demonstrated increased concentrations of the second messengers cAMP (adenosine-3′,5′-cyclic monophosphate) and cGMP (cyclic guanosine monophosphate). These findings suggest that electric stimulation enhanced cellular enzymatic phosphorylation activities, leading to synthetic and secretory processes associated with accelerated bone remodeling. However, the intraoral source of electricity is a major problem that has to be addressed.

It has been recently proposed that microfabricated biocatalytic fuel cells (enzyme batteries) can be used to generate electricity to aid orthodontic tooth movement [46]. An enzymatic microbattery, when placed on the gingiva near the alveolar bone, might be a possible electrical power source for accelerating orthodontic tooth movement. It is proposed that this device uses organic compound (glucose) as the fuel and is noninvasive, and non-osseointegrated. The enzyme battery can be fabricated with the combination of two enzyme electrodes and biocatalysts such as glucose oxidase or formate dehydrogenase to generate electricity (Figure 11.6) [46]. However, there are several issues like soft tissue biocompatibility, effect of food with different temperature and pH range on the output of such microfabricated enzyme battery that need to be addressed. The use of microenzyme batteries has issues like enzyme stability, electron transfer rate, and enzyme loading which result in shorter lifetime and poor power density.

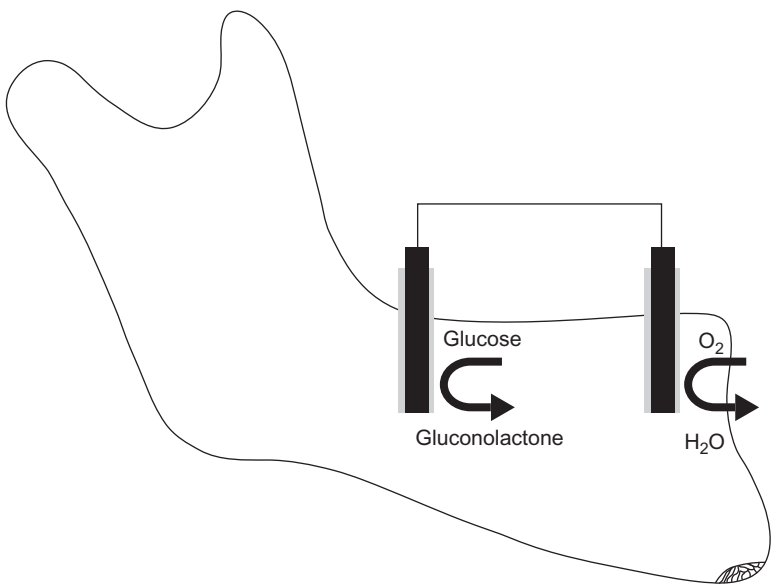

FIGURE 11.6

A schematic diagram of an oral biocatalytic fuel cell. In this system, the following reaction generating electricity for enhancing orthodontic tooth movement occurs: Glucose + O_2 → gluconolactone + H_2O/H_2O_2 [46].

Nanotechnology has offered nanostructured materials like mesoporous media, nanoparticles, nanofibers, and nanotubes, which have been demonstrated as efficient hosts of enzyme immobilization. When nanostructured conductive materials are used, the large surface area of these nanomaterials can increase the enzyme loading and facilitate reaction kinetics, and thus improve the power density of the biofuel cells. It is expected that the MEMS/NEMS based system will be applied over the next few years to develop biocompatible powerful biofuel cells, which can be safely implanted in the alveolus of the maxilla or mandible or in the palate to enhance orthodontic tooth movement or rapid maxillary expansion.

11.6.3 Nanorobot delivery for oral anesthesia and improved oral hygeine

In 2000, Robert A Freitas Jr. [47] suggested that dental nanorobots can be utilized to induce oral anesthesia. These nanorobots can be controlled by an onboard nanocomputer that executes preprogrammed instructions and can be delivered as colloidal suspension containing millions of active analgesic micrometer-sized nanorobot particles on the patient's gingiva. The nanorobots might use specific motility mechanisms to travel through human tissues with navigational precision, acquire energy, and sense and manipulate their surroundings. They might also achieve safe cytopenetration and use any of a multitude of techniques to monitor, interrupt, or alter nerve-impulse traffic in individual nerve cells [48]. Freitas also proposed that these nanorobots can be guided painlessly through the gingival sulcus, lamina propria, cementodentinal junction, dentinal tubules, and finally reach the pulp. Moreover, this journey can be directed by a combination of chemical gradients, temperature differentials, and even positional navigation, all under the control of the onboard nanocomputer.

In turn, the nanocomputer would be directed by the dentist to induce anesthesia, for example, in a specific tooth that requires treatment. More futuristic applications have been proposed by Freitas on utilizing nanorobots to treat carious lesions, dentin hypersensitivity, and dentifrobots (nanorobots in dentifrices). These could be delivered through mouthwash or toothpaste and could patrol supra- and subgingival surfaces of teeth, performing continuous plaque/calculus removal and metabolize trapped organic matter into harmless and odorless vapor [47]. He has also suggested that orthodontic nanorobots could directly manipulate periodontal tissues allowing rapid, painless tooth movement and repositioning within minutes to hours. However, it should be noted that inflammation and bone modeling govern the rate of orthodontic tooth movement. The idea of achieving orthodontic tooth movement within minutes to hours looks futuristic considering the time required for the biological adaptation and remodeling processes of the periodontium that accompanies orthodontic treatment.

11.7 Temporary anchorage devices

While TADs have become increasingly utilized by orthodontic professionals to assist in the process of moving teeth, commercially available TADs exhibit a success rate of 60−75% [49−51]. Currently, TADs are manufactured with smooth titanium surfaces (pure titanium or titanium alloy (Ti−6Al−4V)) because complete osseointegration is a disadvantage that complicates their removal. On the other hand, lack of osseointegration is also one of the factors for the failure of TADs.

The success of TADs also depends on other factors like proper initial mechanical stability and loading quality and quantity. Clinically there are difficulties encountered in the removal of TADs due to increased osseointegration even on the smoother surface TADs. Therefore, it is postulated that the balance lies in the fabrication of an ideal surface that could stimulate initial osseointegration and facilitate its removal once the TAD is no longer needed. Biocompatible coatings like titanium nanotubes should be studied to evaluate if the nanotubular layer can enhance initial osseointegration and can serve as an interfacial layer between the newly formed bone and the TAD.

11.8 Conclusions

The applications of nanotechnology and nanoparticles have offered the biomaterial scientists the opportunity to fabricate materials with improved physical and mechanical properties. The field of dental biomaterials is constantly evolving. The addition of such nanoparticles to currently available materials enhances their properties and clinical use. The applications of nanotechnology in orthodontic materials have been reported in the literature over the past few years. However, the number of studies specifically addressing orthodontics and nanotechnology are small. The authors expect that the next decade will bring an increase in the amount and quality of research that will help unveil the next generation of nanomaterials for orthodontic treatment. There are many avenues yet to be explored that would help move MEMS/NEMS based systems in orthodontics from the drawing board to the bench top and clinical study arena. The utilization of nanoparticles for improving the TADs should be one such avenue.

References

[1] R.P. Feynman, There is plenty of room at the bottom, Eng. Sci. 23 (1960) 22–36.
[2] N. Taniguchi, On the basic concept of 'NanoTechnology', Proc. ICPE Tokyo 2 (1974) 18–23.
[3] D. Mijatovic, J.C. Eijkel, A. van den Berg, Technologies for nanofluidic systems: top-down vs. bottom-up—a review, Lab Chip 5 (5) (2005) 492–500.
[4] M. Lazzari, et al., Self-assembly: a minimalist route to the fabrication of nanomaterials, J. Nanosci. Nanotechnol. 6 (4) (2006) 892–905.
[5] S.I. Stupp, et al., Supramolecular materials: self-organized nanostructures, Science 276 (5311) (1997) 384–389.
[6] M.C. Roco, Nanotechnology: convergence with modern biology and medicine, Curr. Opin. Biotechnol. 14 (3) (2003) 337–346.
[7] S.K. Sahoo, V. Labhasetwar, Nanotech approaches to drug delivery and imaging, Drug Discov. Today 8 (24) (2003) 1112–1120.
[8] G. Binning, C. Quate, C. Gerber, Atomic force microscope, Phys. Rev. Lett. 12 (1986) 930.
[9] R.P. Kusy, J.Q. Whitley, Effects of surface roughness on the coefficients of friction in model orthodontic systems, J. Biomech. 23 (9) (1990) 913–925.
[10] C. Bourauel, et al., Surface roughness of orthodontic wires via atomic force microscopy, laser specular reflectance, and profilometry, Eur. J. Orthod. 20 (1) (1998) 79–92.
[11] J.P. Alcock, et al., Nanoindentation of orthodontic archwires: the effect of decontamination and clinical use on hardness, elastic modulus and surface roughness, Dent. Mater. 25 (8) (2009) 1039–1043.

[12] G.J. Lee, et al., A quantitative AFM analysis of nano-scale surface roughness in various orthodontic brackets, Micron 41 (7) (2010) 775–782.
[13] M. Redlich, et al., Improved orthodontic stainless steel wires coated with inorganic fullerene-like nanoparticles of WS(2) impregnated in electroless nickel-phosphorus film, Dent. Mater. 24 (12) (2008) 1640–1646.
[14] A. Katz, M. Redlich, L. Rapoport, H.D. Wagner, R. Tenne, Self-lubricating coatings containing fullerene-like WS2 nanoparticles for orthodontic wires and other possible medical applications, Triboil. Lett. 21 (2) (2006) 135–139.
[15] G.R. Samorodnitzky-Naveh, et al., Inorganic fullerene-like tungsten disulfide nanocoating for friction reduction of nickel-titanium alloys, Nanomedicine (Lond) 4 (8) (2009) 943–950.
[16] A. Moshaverinia, et al., Modification of conventional glass-ionomer cements with N-vinylpyrrolidone containing polyacids, nano-hydroxy and fluoroapatite to improve mechanical properties, Dent. Mater. 24 (10) (2008) 1381–1390.
[17] T. Uysal, et al., Are nano-composites and nano-ionomers suitable for orthodontic bracket bonding? Eur. J. Orthod. 32 (1) (2010) 78–82.
[18] S.J. Ahn, et al., Experimental antimicrobial orthodontic adhesives using nanofillers and silver nanoparticles, Dent. Mater. 25 (2) (2009) 206–213.
[19] R.R. Moraes, et al., Improved dental adhesive formulations based on reactive nanogel additives, J. Dent. Res. (2011).
[20] G. Rahilly, N. Price, Nickel allergy and orthodontics, J. Orthod. 30 (2) (2003) 171–174.
[21] A.L. Greppi, D.C. Smith, D.G. Woodside, Nickel hypersensitivity reactions in orthodontic patients. A literature review, Univ. Tor. Dent. J. 3 (1) (1989) 11–14.
[22] R. Lindsten, J. Kurol, Orthodontic appliances in relation to nickel hypersensitivity. A review, J. Orofac. Orthop. 58 (2) (1997) 100–108.
[23] C.A. Pazzini, et al., Allergy to nickel in orthodontic patients: clinical and histopathologic evaluation, Gen. Dent. 58 (1) (2010) 58–61.
[24] R.L. Bowen, Properties of a silica-reinforced polymer for dental restorations, J. Am. Dent. Assoc. 66 (1963) 57–64.
[25] J.L. Ferracane, Current trends in dental composites, Crit. Rev. Oral. Biol. Med. 6 (4) (1995) 302–318.
[26] S.B. Mitra, D. Wu, B.N. Holmes, An application of nanotechnology in advanced dental materials, J. Am. Dent. Assoc. 134 (10) (2003) 1382–1390.
[27] D.A. Terry, Direct applications of a nanocomposite resin system: Part 1—the evolution of contemporary composite materials, Pract. Proc. Aesthet. Dent. 16 (6) (2004) 417–422.
[28] A.D. Wilson, B.E. Kent, A new translucent cement for dentistry. The glass ionomer cement, Br. Dent. J. 132 (4) (1972) 133–135.
[29] C.M. Killian, T.P. Croll, Nano-ionomer tooth repair in pediatric dentistry, Pediatr. Dent. 32 (7) (2010) 530–535.
[30] Y. Korkmaz, et al., Influence of different conditioning methods on the shear bond strength of novel light-curing nano-ionomer restorative to enamel and dentin, Lasers Med. Sci. 25 (6) (2010) 861–866.
[31] M.M. O'Reilly, J.D.B. Featherstone, Demineralization and remineralization around orthodontic appliances: an in vivo study, Am. J. Orthod. Dentofacial Orthoped. 92 (1) (1987) 33–40.
[32] B. Øgaard, G. Rølla, J. Arends, Orthodontic appliances and enamel demineralization: Part 1. Lesion development, Am. J. Orthod. Dentofacial Orthop. 94 (1) (1988) 68–73.
[33] W.A. Wiltshire, Determination of fluoride from fluoride-releasing elastomeric ligature ties, Am. J. Orthod. Dentofacial Orthop. 110 (4) (1996) 383–387.
[34] W.A. Wiltshire, In vitro and in vivo fluoride release from orthodontic elastomeric ligature ties, Am. J. Orthod. Dentofacial Orthop. 115 (3) (1999) 288–292.

[35] K.K. Miura, et al., Anticariogenic effect of fluoride-releasing elastomers in orthodontic patients, Braz. Oral. Res. 21 (3) (2007) 228–233.
[36] G.T. Kluemper, et al., Efficacy of a wax containing benzocaine in the relief of oral mucosal pain caused by orthodontic appliances, Am. J. Orthod. Dentofacial Orthop. 122 (4) (2002) 359–365.
[37] S.I. Gunes, S.C. Jana, Shape memory polymers and their nanocomposites: a review of science and technology of new multifunctional materials, J. Nanosci. Nanotechnol. 8 (4) (2008) 1616–1637.
[38] M.A. Stuart, W.T. Huck, J. Genzer, M. Müller, C. Ober, M. Stamm, et al., Emerging applications of stimuli-responsive polymer materials, Nat. Mater. 9 (2010) 101–113.
[39] Q. Meng, J. Hu, A review of shape memory polymer composites and blends, Compos. A Appl. Sci. Manuf. 40 (11) (2009) 1661–1672.
[40] J. Leng, X. Lan, Y. Liu, S. Du, et al., Shape-memory polymers and their composites: stimulus methods and applications, Prog. Mater. Sci. 56 (7) (2011) 1077–1135.
[41] E.E. Nuxoll, R.A. Siegel, BioMEMS devices for drug delivery, IEEE Eng. Med. Biol. Mag. 28 (1) (2009) 31–39.
[42] B. Xu, BioMEMS enabled drug delivery, Nanomedicine 1 (2) (2005) 176–177.
[43] P.L. Gourley, Brief overview of BioMicroNano technologies, Biotechnol. Prog. 21 (1) (2005) 2–10.
[44] Z. Davidovitch, M.D. Finkelson, S. Steigman, J.L. Shanfeld, P.C. Montgomery, E. Korostoff, et al., Electric currents, bone remodeling, and orthodontic tooth movement. II. Increase in rate of tooth movement and periodontal cyclic nucleotide levels by combined force and electric current, Am. J. Orthod. 77 (1) (1980) 33–47.
[45] Z. Davidovitch, M.D. Finkelson, S. Steigman, J.L. Shanfeld, P.C. Montgomery, E. Korostoff, et al., Electric currents, bone remodeling, and orthodontic tooth movement. I. The effect of electric currents on periodontal cyclic nucleotides, Am. J. Orthod. 77 (1) (1980) 14–32.
[46] J. Kolahi, M. Abrishami, Z. Davidovitch, Microfabricated biocatalytic fuel cells: a new approach to accelerating the orthodontic tooth movement, Med. Hypotheses 73 (3) (2009) 340–341.
[47] R.A. Freitas Jr., Nanodentistry, J. Am. Dent. Assoc. 131 (11) (2000) 1559–1565.
[48] R.A.J. Freitas, Nanomedicine. Vol. 1. Basic Capabilities, vol. 2011, Landes Bioscience, Georgetown, TX, 1999.
[49] M. Schatzle, R. Männchen, M. Zwahlen, N.P. Lang, et al., Survival and failure rates of orthodontic temporary anchorage devices: a systematic review, Clin. Oral. Implants Res. 20 (12) (2009) 1351–1359.
[50] S. Miyawaki, I. Koyama, M. Inoue, K. Mishima, T. Sugahara, T. Takano-Yamamoto, et al., Factors associated with the stability of titanium screws placed in the posterior region for orthodontic anchorage, Am. J. Orthod. Dentofacial Orthop. 124 (4) (2003) 373–378.
[51] S. Kuroda, Y. Sugawara, T. Deguchi, H.M. Kyung, T. Takano-Yamamoto, et al., Clinical use of miniscrew implants as orthodontic anchorage: success rates and postoperative discomfort, Am. J. Orthod. Dentofacial Orthop. 131 (1) (2007) 9–15.

CHAPTER

Nanotechnology in Orthodontics—2: Facts and Possible Future Applications

12

Tarek El-Bialy

Departments of Dentistry and Biomedical Engineering, Division of Orthodontics, The University of Alberta, Edmonton, AB, Canada

CHAPTER OUTLINE

12.1 Introduction

Nanotechnology involves the creation, manipulation, and use of materials and devices at the size scale of < 100 nm. It describes the technique of creating and using devices and components comparable in size to molecules and intracellular architecture [1]. Nanotechnology is well progressing in many biological sciences including medicine, pharmacy, and dentistry. In general dentistry, nanotechnology has potential to be applied in management of teeth hypersensitivity, anesthesia, production of more enhanced dental products, and in orthodontic treatment [2]. This chapter presents the current status of the use of nanotechnology and nanoanalysis and three possible future applications in orthodontics. These applications involve nanoscale study of the topography of different orthodontic materials to evaluate their nanocharacteristics or nanomechanical properties. The possibility of nanogene therapy to enhance generation or to modify growth of different craniofacial structures is discussed. In addition, a nanofabricated ultrasound device for orthodontics is a future direction that would change the profile of dentofacial regeneration including possible prevention and treatment of orthodontically induced root resorption or dentoalveolar fracture.

Nanobiomaterials in Clinical Dentistry.

12.2 Nanoscale in orthodontics

One of the known challenges in orthodontics is bond failure of orthodontic attachments including orthodontic brackets and tubes. In order to minimize bond failure, many attempts have been introduced to enhance the strength of orthodontic bonding composites. One of these attempts was to introduce nanocomposite and nanoionomer [3]. The introduction of nanofiller components originally was introduced to enhance some physical properties of the hardened restorative composites. Because of the decreased dimension of the particles in the nanofillers, a wide size distribution and increased filler load is achieved, which decreases polymerization shrinkage [4], and increases mechanical strength and resistance to fracture. In addition, it has been reported that nanocomposites had a good marginal seal to enamel and dentin compared with total-etch adhesives [5]. Since these nanofiller-containing resin-modified glass ionomer cements (Ketac N100) were reported to have improved physical properties, as well as increased fluoride release than other restorative materials, it has been suggested to be used as a bonding material for orthodontic attachments. The increased fluoride release by nanofiller-bonding materials compared to other restorative materials make them more attractive in orthodontics since demineralization of the labial surfaces of teeth during orthodontic therapy is one of the major challenges facing orthodontists and orthodontic patients, especially in patients with compromised oral hygiene. However, although the results of using such nanocomposite and nanoionomer bonding system may be suitable for bonding since they fulfill suggested ranges for clinical acceptability, they are inferior to a conventional orthodontic composite [3]. There may be ongoing attempts to enhance bonding strength of these nanocomposite and nanoionomer bonding systems to utilize their high fluoride release property in order to make them at least comparable in bond strength to conventional orthodontic bonding systems.

Because of the increased awareness of enamel demineralization around orthodontic attachments, different materials have been used to minimize enamel demineralization. The effectiveness of these materials has been evaluated using atomic force microscopy (AFM) measurements that quantitatively evaluate nanoscale enamel surface roughness after using these materials [6] (Figure 12.1).

Orthodontic treatment may involve removal of some teeth to alleviate dental crowding or to treat some types of malocclusions. Closing extraction spaces usually requires moving bracketed teeth along arch wires made from different types of materials using sliding (also known as arch-guided) tooth movement. The friction between orthodontic brackets and wires, especially with a combination of metals, sometimes affects the efficiency of tooth movement. Also, friction in orthodontics has contributed to loss of anchorage due to application of increased forces to overcome friction between the brackets and wires. Increased friction between orthodontic wires and bracket surfaces has been attributed to micro/nanoasperities or mechanical interlocking at the micro- or nanolevels [7] (Figure 12.2).

For this purpose, nanotechnology has been introduced to study different orthodontic wires and bracket slots to evaluate nanomechanical properties and topographic pattern of these materials in order to understand factors affecting friction between orthodontic wires and brackets. However, the exact measurements of these micro/nanoasperities have only been evaluated using AFM. AFM allows for quantitative evaluation of the nanoscale surface roughness of various orthodontic bracket slots before and after sliding movement of archwire in vitro and in vivo [8].

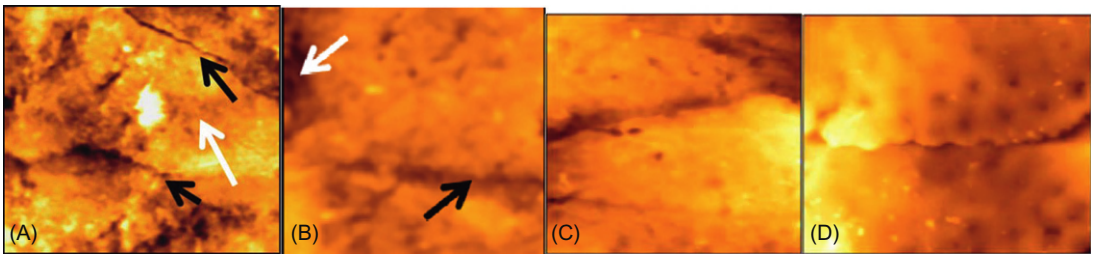

FIGURE 12.1

AFM of human enamel treated by acid etching only showing narrow grooves (black arrows) and flattened perikymata ridges (white arrow) with cracks and many destructed areas of nontreated enamel surface (A); enamel treated with acid etching and fluoride varnish showing moderately wide perikymata groove (black arrow) and localized areas of destruction (white arrow) (B); enamel treated with acid etching and unfilled sealant group showing wide perikymata grooves and flattened perikymata ridges (C); and enamel treated with acid etching followed by proseal showing perikymata ridge and groove with obvious focal holes (frames are $50 \times 50\ \mu m$)

From Ref. [6].

FIGURE 12.2

Because all surfaces have irregularities that are large on a molecular level, real contact occurs only at peaks of irregularities, called asperities. When interlocking occurs between the peaks and bottoms of the asperities, resistance to movement occurs [7].

12.3 Nanotechnology and gene therapy in orthodontics

Mandibular underdevelopment has been attributed to a variable interaction of genetic and environmental factors, which is believed to be difficult to manipulate or stimulate. Bite jumping appliances, also known as functional appliances (FAs), have long been claimed and used to enhance mandibular growth in cases with deficient mandibles (mandibular retrognathism). A recent study systematically reviewed reports on the effectiveness of FAs and concluded that the analysis of the effect of treatment with FAs versus an untreated control group showed skeletal changes that were statistically significant in the short term but unlikely to be clinically significant [9].

It has been reported that rat condylar growth can be significantly increased by local gene therapy with recombinant adenovirus associated virus (rAAV)-mediated vascular endothelial growth factor (VEGF), which is an important angiogenic mediator in vascularization and endochondral ossification [10]. Although rAAV vector for gene delivery is proven to be a strong and effective vector, its use in human patients is facing controversial and ethical issues. There is a growing emphasis on nanotechnology in cancer detection and treatment (http://nano.cancer.gov). For example, nanovector liposomes have been used successfully in breast cancer therapy [11]. Regardless of its successful use, nanobiotechnology is still at its early stage of development and its use in treatment of diseases other than cancer could be especially challenging. The challenges facing these nanovectors might not have viable applications, especially in mandibular growth stimulation and could end up on the "technology shelf" in the future [12].

12.4 Nanofabricated ultrasound device for orthodontics

In translational research, proof of concept is usually the first step in testing the viability of new technology for potential treatment of any disease. We and other researchers have shown in proof of principle the efficacy of utilizing Low Intensity Pulsed Ultrasound (LIPUS) in stimulating mandibular growth in growing animals and in human patients [13–16]. One of the main challenges we faced when a pilot clinical trial was conducted to stimulate mandibular growth in humans with hemifacial microsomia was that the patients (young adults) needed to hold the LIPUS transducers (applicators) to their mandibular condyles for 20 min every day for at least 1 year in order to achieve clinical improvement of the deficient side of the mandible. This created a great challenge and burden on the parents to do this for that extended period of time. In order to minimize errors in LIPUS application and maximize consistency in treatment, a noncompliant LIPUS application is in high demand. In addition, we have shown that LIPUS application to orthodontically moving teeth can minimize root resorption [17]. External apical root resorption (EARR) concurrent with orthodontic treatment is widely accepted as a risk in all types of orthodontic treatment appliances. Challenges in using LIPUS intraorally in treatment of EARR concurrent with orthodontic treatment is that the size of commercially available LIPUS transducers are quite large (3.5 cm^3), difficult to adjust, and larger than any human tooth. In addition, the patients have to hold the LIPUS transducers tightly against the gingiva of the corresponding tooth/teeth for 20 min/day for at least 4 weeks in order to achieve clinically noticeable decrease in EARR concurrent with orthodontic treatment. Because of these challenges there are needs for noncompliant LIPUS devices that can be inserted into the patient's mouth and deliver the predesigned LIPUS treatment to the tooth/teeth in question. In order to build an intraoral LIPUS device that is independent of power supply or patient compliance, a nanocircuit design has been incorporated in order to nanofabricate the main operation circuit as well as LIPUS transducer controller. In addition, a nanofabricated battery is required in a nanoscale intraoral LIPUS device. The first step in this nanodesigned LIPUS device was the nanofabrication of the operation circuit that delivers the required signal to the LIPUS transducer. This step has been developed by our group and tested for its validity to be potentially used for future nanofabricated LIPUS transducers and devices [18]. A future nanofabricated LIPUS device is compared to the original large-scaled device in the following figure (Figure 12.3).

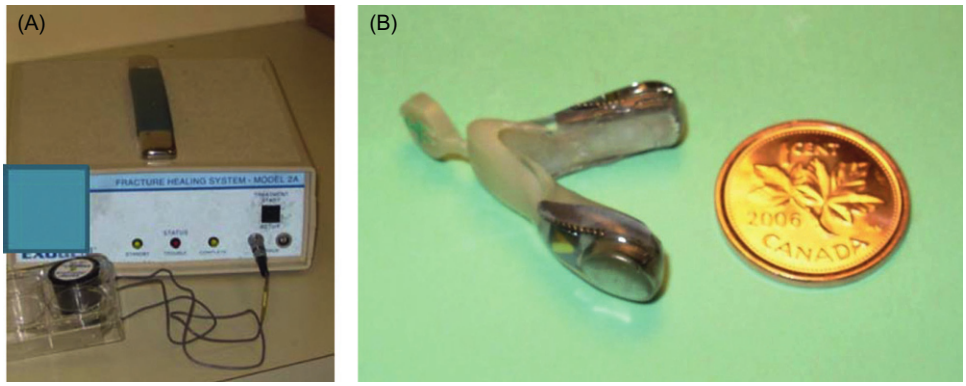

FIGURE 12.3

(A) Large-scaled LIPUS device and (B) future nanofabricated intraoral LIPUS device.

12.5 Nanomechanical sensors for orthodontic forces and moments measurement

Orthodontic forces and moments are an undetermined force system due to many factors that are involved, including the orthodontic wire materials (that affect its modulus of elasticity) and geometry (that affects its stiffness). Both modulus of elasticity and geometry are important in determining wire stiffness according to the following equation:

$$K\ (\text{stiffness}) = E \times I\ (E \text{ is the modulus of elasticity and } I \text{ is the area moment of inertia})$$

For round wire (Figure 12.4). Where d is the diameter of the round wire

$$I = \pi(d^4)/64$$

For rectangular wire (Figure 12.5). Dimensions of the rectangular wire where (b) is the wire base in the in-out direction; and (h) is the wire height in the up-down direction

$$I = b(h^3)/12$$

In addition, wire stiffness is also dependent on the wire length, which is determined intraorally by the interbracket distance. The smaller the bracket width, the greater the interbracket distance and lower the wire stiffness according to the following equation:

$$K\ (\text{stiffness}) \alpha 1/L^3$$

where L is the interbracket distance or wire length (Figure 12.6).

All the above factors affect the stiffness of the wire and consequently the force applied to the teeth. Since any small changes in wire length or diameter/cross section can change the wire stiffness and consequently the applied force by this wire, it is almost impossible to predict the exact amount of force applied by the same wire to two different patients due to the difference in

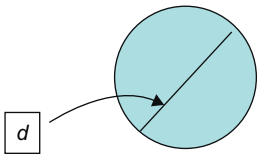

FIGURE 12.4

Diameter of round wires (*d*).

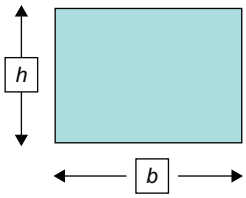

FIGURE 12.5

Rectangular wires' dimension base (*b*) and height (*h*).

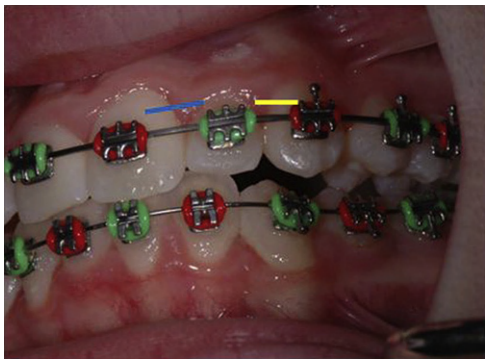

FIGURE 12.6

Interbracket distance between the maxillary left canine and maxillary left lateral incisor (yellow line) is less than that between maxillary left central incisor and maxillary left lateral incisor (blue line). The longer wire segment is more flexible than the shorter one. (For interpretation of the references to color in this figure legend, the reader is referred to the web version of this book.)

teeth crown widths, resulting in variation in interbracket wire lengths, and consequently applying different forces using the same type, shape, and size of wire. What complicates this process further is that the moments applied to the teeth are the resultant of multiplication of the magnitude of force times the perpendicular distance between the centers of resistance of the tooth to the line of action of the applied force (Figure 12.7).

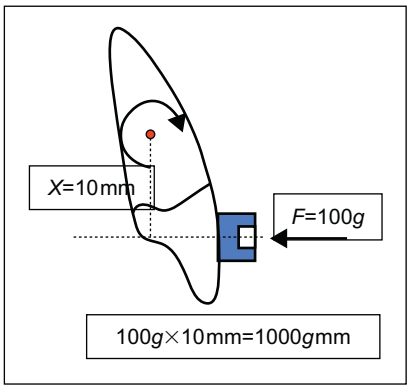

FIGURE 12.7

The moment produced by the force (*F*) equals the magnitude of the force *F* (100*g*) multiplied by the perpendicular distance between the center of resistance and the line of action of the force (*X* = 10 mm).

Since the teeth root lengths are different among individuals, this consequently changes the length of the moment arms and the applied moments using similar forces. In order to apply biologically tolerable forces and moments to the teeth to efficiently move teeth with minimal adverse effects such as EARR depending on the individual's intrinsic susceptibility, researchers have been working to develop brackets that can carry three-dimensional mechanical sensors in the bracket bases to measure in three dimensions the real-time forces and moments applied to the teeth. This would facilitate the orthodontist adjusting these forces should they exceed biologically acceptable limits.

In order to achieve this, microsensors have been proposed in the recent literature. Lapatki et al. in 2007 reported on the introduction of a "smart" bracket for multidimensional force and moment measurement [19,20]. They reported on a large-scale prototype bracket that utilized microsystem chip encapsulation. Development of a nanosystem chip that can be encapsulated into small low-profile contemporary bracket systems with reduced mesiodistal and occlusogingival dimensions will allow clinical testing of the utilization of this technology.

12.6 Future applications of nanotechnology in orthodontics

Although nanotechnology application in orthodontics is considered to be in its infancy, there is a huge potential application of nanotechnology in orthodontics including nanodesigned orthodontic bonding materials, possible nanovector for gene delivery for mandibular growth stimulation, and nano-LIPUS devices. Also, nanomechanical sensors can be fabricated and be incorporated into the base of orthodontic brackets and tubes in order to provide real-time feedback about the applied orthodontic forces. This real-time feedback allows the orthodontist to adjust the applied force to be within a biological range to efficiently move teeth with minimal side effects. In a fast growing world of nanotechnology, the hope would be to get these technologies into clinical application

sooner than later. However, financial burden in developing and applying such technologies is a road block that requires special funding programs from major funding agencies and organizations.

12.7 Conclusions

In conclusion, the future in orthodontic treatment will rely mainly on nanotechnology should all the current attempts succeed to its clinical application at a reasonable cost to the orthodontist and patients. It is recommended that appropriate research funds be allocated to orthodontic and dentistry nanotechnology research and development to help take these technologies to the clinical trial phase.

Acknowledgment

The author would like to thank all those who provided permission to use figures from their publications in this chapter.

References

[1] M.A. Zarbin, C. Montemagno, J.F. Leary, R. Ritch, Nanomedicine in ophthalmology: the new frontier, Am. J. Ophthalmol. 150 (2010) 144−162.e2.
[2] F.J. Leary, Nanotechnology: what is it and why is small so big? Can. J. Ophthalmol. 45 (5) (2010) 449−456.
[3] T. Uysal, A. Yagci, B. Uysal, G. Akdogan, Are nano-composites and nano-ionomers suitable for orthodontic bracket bonding? Eur. J. Orthod. 32 (2010) 78−82.
[4] N. Moszner, U. Salz, New developments of polymeric dental composites, Program. Polym. Sci. 26 (2001) 535−576.
[5] S. Geraldeli, J. Perdigao, Microleakage of a new restorative system in posterior teeth, J. Dent. Res. (2003) 126 (Abstract).
[6] S.F. Shinaishin, S.A. Ghobashy, T.H. El-Bialy, Efficacy of light-activated sealant on enamel demineralization in orthodontic patients: an atomic force microscope evaluation, Open. Dent. J. 5 (2011) 179−186.
[7] W. Proffit, Contemporary Orthodontics, fifth ed., 2012, p. 329.
[8] G.J. Leea, K.H. Parkc, Y.G. Parkc, H.K. Park, A quantitative AFM analysis of nanoscale surface roughness in various orthodontic brackets, Micron 41 (2010) 775−782.
[9] E. Marsico, E. Gatto, M. Burrascano, G. Matarese, G. Cordasco, Effectiveness of orthodontic treatment with functional appliances on mandibular growth in the short term, Am. J. Orthod. Dentofacial Orthop. 139 (1) (2011) 24−36 (Review).
[10] A.B. Rabie, J. Dai, R. Xu, Recombinant AAV-mediated VEGF gene therapy induces mandibular condylar growth, Gene Ther. (2007).
[11] J.W. Park, Liposome-based drug delivery in breast cancer treatment, Breast Cancer Res. 4 (3) (2002) 95−99.
[12] P. Fortina, L.J. Kricka, S. Surrey, P. Grodzinski, Nanobiotechnology: the promise and reality of new approaches to molecular recognition, Trends Biotechnol. 23 (4) (2005) 168−173.

[13] R. Oyonarte, M. Zárate, F. Rodriguez, Low-intensity pulsed ultrasound stimulation of condylar growth in rats, Angle Orthod. 79 (5) (2009) 964−970.
[14] T. El-Bialy, I. El-Shamy, T.M. Graber, Growth modification of the rabbit mandible using therapeutic ultrasound: is it possible to enhance functional appliance results? Angle Orthod. 73 (6) (2003) 631−639.
[15] T.H. El-Bialy, A. Hassan, T. Albaghdadi, H.A. Fouad, A.R. Maimani, Growth modification of the mandible using ultrasound in baboons: a preliminary report, Am. J. Orthod. Dentofacial Orthop. 130 (10) (2006) 435e7−435e14.
[16] T. El-Bialy, A.H. Hassan, A. Alyamani, T. Albaghdadi, Treatment of hemifacial microsomia by therapeutic ultrasound and hybrid functional appliance. A non-surgical approach, Open. Access J. Clin. Trials 2 (2010) 29−36.
[17] T. El-Bialy, I. El-Shamy, T.M. Graber, Repair of orthodontically induced root resorption by ultrasound in humans, Am. J. Orthod. Dentofacial Orthop. 126 (2) (2004) 186−193.
[18] W.T. Ang, C. Scurtescu, W. Hoy, T. El-Bialy, Y.Y. Tsui, J. Chen, Design and implementation of therapeutic ultrasound generating circuit for dental tissue formation and tooth-root healing, IEEE Trans. Biomed. Circuits Syst. 2 (2010) 49−61.
[19] B.G. Lapatki, O. Paul, Smart brackets for 3D-force-moment measurements in orthodontic research and therapy—developmental status and prospects, J. Orofac. Orthop. 68 (5) (2007) 377−396.
[20] B.G. Lapatki, J. Bartholomeyczik, P. Ruther, I.E. Jonas, O. Paul, Smart bracket for multi-dimensional force and moment measurement, J. Dent. Res. 86 (1) (2007) 73−78.

CHAPTER

Nanoparticle Coating of Orthodontic Appliances for Friction Reduction

13

Meir Redlich[a] **and Reshef Tenne**[b]

[a]*NanoMediCOT™ (Nanotechnologies for medical and healthcare applications) Israel*

[b]*Department of Materials Research, Weizmann Institute, Rehovot 76100*

CHAPTER OUTLINE

Nanobiomaterials in Clinical Dentistry.

13.1 Introduction

Orthodontics deals with prevention and correction of malaligned teeth in the jaws as well as the proper positioning of jaws in the face (dentofacial orthopedics). Esthetics and function are the main reasons to seek orthodontic treatment. Since the beginning of the twentieth century, orthodontic tooth movement has been performed by the metal appliances available. These consisted of attachments bonded onto the tooth (brackets) and wires engaged within a specific slot incorporated within the brackets. This clinical setup is also referred to as fixed orthodontic appliances. Until the emergence of etching-bonding procedures on the tooth enamel [1,2], metal bands were cemented onto the teeth. This setup allows the orthodontist to control tooth movement during the entire course of treatment. In the early 1900s, orthodontists used gold, platinum, silver, steel, gum rubber, vulcanite, and occasionally zinc, copper, and brass. During the 1950s, stainless steel (SS) was introduced in orthodontics and became the popular material for making brackets and archwires. In the early 1970s, nickel−titanium (Ni−Ti) archwire was used for the first time in orthodontics [3] which originated from the Ni−Ti alloys developed at the Naval Ordnance Laboratory by Buehler [4]. Currently, orthodontists are mostly using SS brackets and archwires made of SS and Ni−Ti metal alloys with different size and shape (round and rectangular) for archwires. There are also wires made of cobalt−chromium−nickel and β-titanium, available for use in orthodontics.

In order to initiate orthodontic tooth movement, force has to be applied on the tooth. This force is exerted either by the archwires engaged into the bracket's slots or by springs and elastics which are attached to the brackets or by extra-oral devices such as headgear. Apart from the metallurgical aspect of orthodontics, teeth movement is entirely dependent on the biological changes occurring within the tissues encircling the teeth, mainly the periodontal ligament and the alveolar bone. Consequently, biomechanics is considered as the basis for orthodontic treatment. There are additional principles which will assure successful orthodontic therapy such as proper diagnosis and treatment plan, successful bonding, prevention of caries formation and root resorption (shortening the length of the tooth), patient's compliance, and retention protocol. However, the level of the orthodontic force is the core of the treatment. Force magnitude of 40−60 g exerted directly on the tooth for an adequate continuous period, without the metal fixed appliance setup, is sufficient to move the tooth in the jaw. However, application of orthodontic force using fixed appliances requires a significant increase in the force level in order to overcome the friction created at the bracket-wire interface [5].

13.2 Friction in orthodontics

Friction is defined as the *force* resisting the relative motion of solid surfaces, fluid layers, and material elements sliding against each other. There are two types of friction: static friction which occurs between two objects that are not moving relative to each other and it prevents an object from sliding down, and kinetic friction which occurs when two objects are moving relative to each other and its value is usually less than the static friction for the same material. In orthodontics, the kinetic friction is irrelevant because tooth movement is not a continuous motion of the tooth along the wire. It is a series of tipping and root uprighting movements resulting from the biological response of the bone, a pseudostatic condition. The orthodontist encounters friction during two

phases of fixed appliance treatment. At the beginning, during the initial alignment stage, a light, low-module Ni−Ti archwire is used. Engaging the flexible shape memory Ni−Ti alloy into malaligned teeth/brackets activates the wire and creates internal forces. Upon deactivation, an internal shear force drives wire straightening and force is applied on the teeth. As a result, the wire slides through the neighboring brackets and at this point, the important role of friction forces. As treatment progresses the Ni−Ti wires are replaced by rigid SS archwires. At this stage, tooth movement occurs by sliding motion of the tooth over the wire and the orthodontic force needs to overcome the friction resistance to their sliding motion. In some cases, a group of teeth are being translated (i.e., retracting incisors distally) and the orthodontic force makes the SS wire slide through the slots of the posterior teeth. The concept of friction force in orthodontics was re-emphasized in 1997 by Kusy and Whitley [5]. Mathematically, friction resistance to sliding (RS) is described as an additive effect of classical friction (FR), binding (BI), and physical notching (NO).

$$RS = FR + BI + NO$$

The FR is the result of the contact between the wire and the slot walls during the sliding motion. This force directly reduces the effective force delivered to the tooth. When initial tooth movement occurs, an angle (θ) forms between the slot and the wire (Figure 13.1). At the point where the wire first contacts the edges of the slot walls, the BI component starts contributing to the RS and this point is called the critical contact angle for binding (θ_c). From this point on, as θ increases the BI component grows and the term FR becomes negligible. At a higher angle (θ_z), notching begins and the NO component takes a major role in RS (Figure 13.2), causing notches in the wire due to plastic deformation that stop the sliding completely.

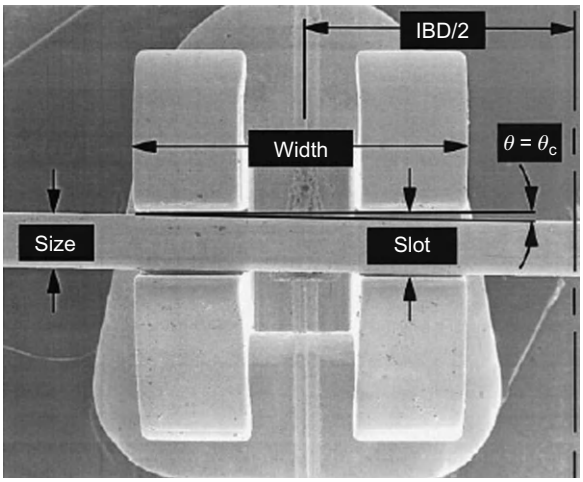

FIGURE 13.1

Photograph of an archwire engaged in a bracket showing the geometric parameters that are important to adequately describe orthodontic sliding mechanics: the archwire size (Size), the bracket slot (Slot), the bracket width (Width), the interbracket distance (IBD), and the angulation (θ) that corresponds to the critical contact angle of second-order angulation [6].

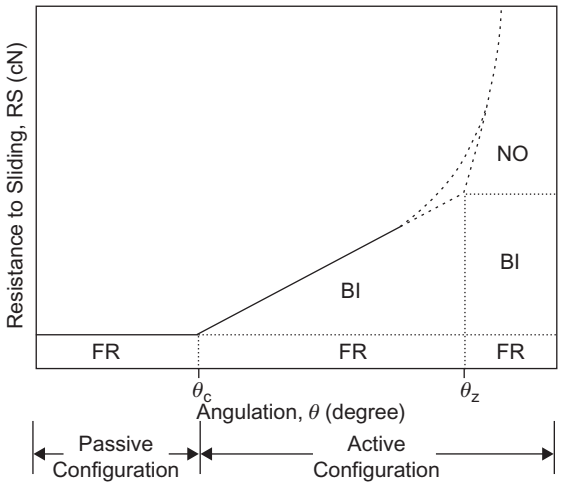

FIGURE 13.2

Schematic diagram showing the partition of the resistance to sliding (RS) into classical friction (FR), elastic binding (BI), and physical notching (NO) within the passive and active configurations with important boundary conditions (θ_c and θ_z) delineated [6].

Following are the number of factors that may influence the RS components directly and indirectly:

1. The archwire: size, shape, material, surface roughness.
2. The bracket: material, size, and shape of the slot and its edges, surface of slot and the angle formed between the wire and the slot.
3. Ligation of the wire in the slot: elastic module, metal wire ligature, and self-ligating brackets.
4. Intraoral factors: saliva, plaque, and corrosion.
5. Other factors: distance between teeth and direction of the applied force.

Over the years, attempts have been made by researchers and manufacturers to reduce the friction. The problem was approached from different aspects:

1. A method for ligating the wire to the slot can theoretically reduce the friction. This was shown to be true with the self-ligating brackets at a 0 angle (clinically not relevant), but higher friction was recorded once the wire contacted the slot walls [7–9].

   The massive advertisement campaign by most orthodontic manufacturers during the last decade in favor of the self-ligating brackets to reduce friction and reduce treatment time was not scientifically and clinically proven [9,10].
2. Surface modification like ion implantation at the wire–bracket interface can minimize friction during tooth movement. However, limited studies to date have evaluated the frictional characteristics of wires and brackets which have received this surface treatment [11].
3. Recently, diamond-like carbon (DLC) coatings showed a significant reduction in friction forces [12]. Such DLC coatings have been also applied on orthodontic wires and brackets,

showing great beneficial effect in terms of reducing friction [13]. However, these experiments were conducted under dry conditions and the behavior of the DLC coatings in similar wet environment should be evaluated.

These attempts and many others were successful to some extent but did not fully overcome the problem. The improvements were mainly directed at the beginning of tooth movement where lower friction was recorded, but the main impediment of the movement is encountered at the angles where BI and NO are the components mainly responsible for the RS. Hence significant reduction of friction at BI might reduce the excessive orthodontic force. Overcoming this inevitable frictional force means using excessive orthodontic force than what is actually needed to move a tooth. Some investigators found that 40−60% of the orthodontic force is aimed at overcoming the frictional resistance.

The use of excessive orthodontic forces has several disadvantages especially on the anchor unit usually desired to remain stable during treatment and it might increase the risk of root resorption. It is assumed that the reduction in frictional resistance could enhance the alignment and the space closure and therefore could lead to reduced treatment time. Thus, reducing frictional forces during orthodontic tooth movement will significantly contribute to successful treatment outcome.

13.3 Materials considerations: fullerene-like nanoparticles

The search for material technologies may lead to significant reduction of friction coefficient in orthodontic devices, self-lubricating coatings have been contemplated and a new technology for applying these coatings on the wires was thus developed. To explain this technology, the concept of inorganic fullerene-like (IF) nanoparticles (NP) and inorganic nanotubes (INT) is described below.

13.3.1 Prelude: inorganic fullerene-like nanoparticles of WS_2 and MoS_2

Hollow closed-cage carbon structures, the fullerenes (C_{60}) and carbon nanotubes are known for some-time. Research into similar structures from other (inorganic) layered compounds started soon after. Thus, IF NP and INT of tungsten disulfide (WS_2) first and subsequently of molybdenum disulfide (MoS_2) were discovered in 1992 [14−16], and elicited considerable interest ever since in this emerging field [17−21]. This observation is surprising in view of the fact that the chemical bond is not stable beyond a few angstroms and hence structures with hollow spaces of a few nanometer and above were initially thought to be unfavorable. The formation of such hollow closed cages can be attributed to the inherent instability of the planar nanostructures of layered compounds. In graphite, the carbon atoms are bonded in flat sp^2 bonds forming a hexagonal network (Figure 13.3A). The graphene sheets are stacked together via weak van der Waals forces. In the case of MS_2 (Figure 13.3B), where M stands for a metal atom like molybdenum or tungsten, the molecular sheet is made up of a layer of M atoms sandwiched between two outer sulfur layers. Each M atom binds to six sulfur atoms forming a lattice with trigonal biprism (octahedral) coordination. In analogy to graphite, weak van der Waals forces are responsible for the stacking of the S−M−S layers together. Therefore, these compounds are highly anisotropic with respect to many

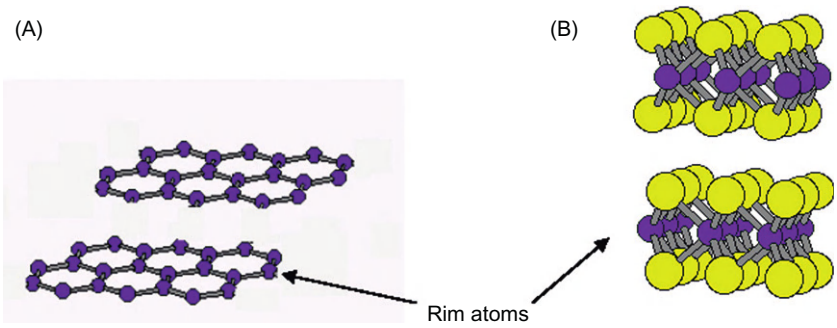

FIGURE 13.3

Schematic presentation of (A) graphite (the C-atoms in purple) and (B) MoS_2 with the Mo atoms in purple and sulfur atoms in yellow.

of their physical and chemical properties. The basal (van der Waals) surfaces of the crystal, which are perpendicular to the *c*-axis, consist of sulfur atoms that form bonds to three underlying W/Mo atoms. These sulfur atoms are chemically inert. However, rim W (or Mo) and S atoms (Figure 13.3), that is, atoms on edge of the layer, which are abundant in the nanostructure, are only four- and twofold bonded, respectively, making the planar form unstable and forcing it to fold and close on itself. Therefore, by folding the molecular sheet and stitching the rim atoms together, seamless and stable nanotubular (one dimensional) and spherical (zero-dimensional fullerene-like) structures with all W/Mo and S atoms being six- and threefold bonded, respectively, are produced [14–17]. Initially, only the transition metal chalcogenides of WS_2 and MoS_2 were known in the form of closed-cage structures and nanotubes. However, over the years this family has been expanded considerably and it now encompasses a large number of other compounds like oxides, hydroxides, nitrides, chlorides, sulfides, selenides, and even pure elements like bismuth, arsine, and phosphorus.

13.3.2 Synthesis

The most useful method for the synthesis of IF-WS_2 NP and WS_2 nanotubes (INT-WS_2) is the sulfidization of WO_3 NP at elevated temperatures (850°C) [22–25]. Thereafter the initial route for large-scale synthesis of IF NP and INT of WS_2 involved the use of oxides as the starting materials. After a clear understanding of the growth mechanism was established, large-scale synthesis of IF-WS_2 NP and INT-WS_2 was realized by using the fluidized-bed reactor (FBR) [23–25], which has significant advantages over the previous synthetic approaches. It resulted in IF NP with a more perfect crystalline structure compared with the product of the previous synthetic systems (which used horizontal reactors). This observation can be attributed to the fact that much of the reaction takes place in the gas phase, where an isotropic environment for the reaction prevails. The vertical posture of the oven allows continuous addition of oxide powder into the chamber during the reaction, thereby increasing the output of the reactor. Moreover, the fluidized-bed concept lends itself to further scale-up and to produce larger amounts of a pure IF/INT phases with little or no compromise on the quality of the synthesized NP.

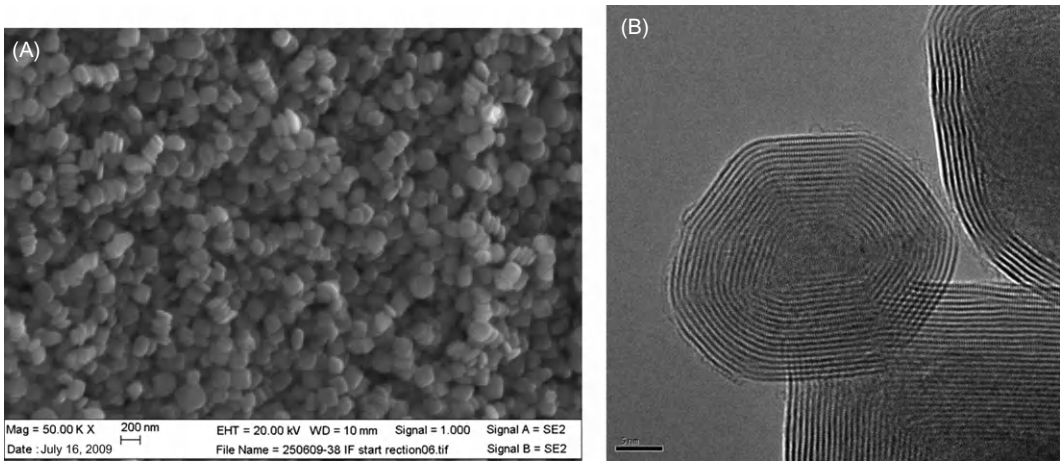

FIGURE 13.4

(A) SEM micrograph of assortment of IF-MoS_2 nanoparticles (scale bar is 200 nm); (B) TEM micrograph of one such nanoparticle (scale bar 5 nm). Note the (nested) closed MoS_2 layers.

The synthesis of IF-MoS_2 NP from MoO_3 powder was found to be more complex. The reason for these difficulties was the high volatility of the oxide powder above 700°C. Following a concerted effort to elucidate the growth mechanism of IF-MoS_2 NP [26], a new vertical (FBR-like) reactor was erected and used [26], which allowed synthesis of about 0.5 g/day of high-quality IF-MoS_2 NP. Figure 13.4A and B shows typical scanning electron microscope (SEM) and transmission electron microscope (TEM) images of such NP, respectively. The NP assume the form of oblate structure having many (>20) closed walls and small hollow core. The diameter of such NP spans in the range of 60−150 nm with mean value of about 80 nm. When added to lubricating fluids, these NP were found to exhibit excellent tribological behavior [27,28].

A more recent accomplishment was the synthesis of rhenium (Re) doped IF/INT NP [29]. Rhenium, being one-column to the right of W (Mo) on the periodic table, has five valence electrons in its outer shell compared to four for molybdenum or tungsten. Thus, substituting about 100 Re atoms in the IF-MoS_2 nanoparticle ($\sim 10^6$ atoms) induces negative surface charge on the nanoparticle surface. Such NP behave quite differently from the undoped NP. For example, the doped NP disperse well and form stable suspensions in various fluids. They also exhibit enhanced conductivity and may find electronic applications in the future. Most importantly, adding small amounts of such NP to lubricating fluids (poly-alpha olephin: type 4, i.e., PAO-4) leads to a precipitous reduction in the friction and wear [29,30] as shown in Figure 13.5. These findings make the IF NP and particularly the doped ones, very suitable for some medical applications, as explained below.

13.3.3 Self-lubricating surfaces

The idea of making self-lubricating surfaces, i.e., hard surfaces which do not require any fluid to lubricate the contact area, is not new and has been pursued by many groups before; see for example

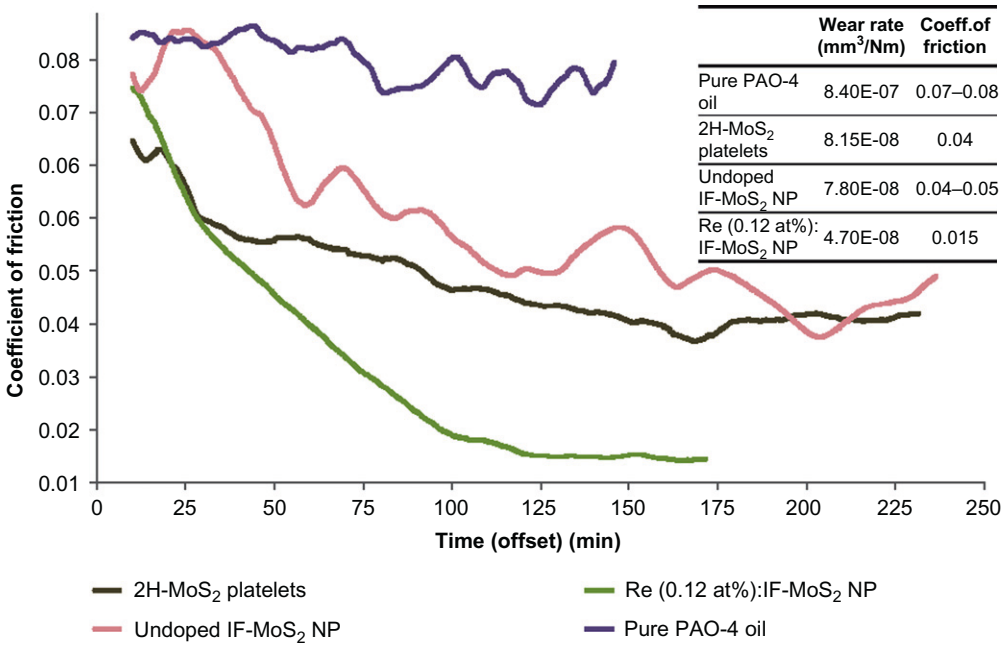

	Wear rate (mm^3/Nm)	Coeff.of friction
Pure PAO-4 oil	8.40E-07	0.07–0.08
2H-MoS_2 platelets	8.15E-08	0.04
Undoped IF-MoS_2 NP	7.80E-08	0.04–0.05
Re (0.12 at%): IF-MoS_2 NP	4.70E-08	0.015

FIGURE 13.5

Friction coefficient of different lubricating fluids based on PAO-4: pure purple; formulated with 2H-MoS_2 (dark brown); IF-MoS_2 (undoped—light brown) and Re-doped IF-MoS_2 (green). Wear rate of the different lubricants are shown in the inset table. (For interpretation of the references to color in this figure legend, the reader is referred to the web version of this book.)

Refs. [31–34]. Therefore, it was almost natural, once the IF NP were known to have superior solid lubrication behavior, to try to incorporate them in metallic coatings. This would be expected to endow such films the genuine behavior of a very hard coating which is nonetheless also self-lubricating. A series of articles, where electroless or electroplating baths containing IF NP are used to prepare self-lubricating surfaces, were thus reported quite recently [35–38]. Different kinds of films and substrates were used. While their potential applications go beyond dentistry or medical devices, the focus of much of the present authors was in this direction.

13.4 Orthodontic appliances coated with nanoparticles

13.4.1 Challenges in designing the experimental setup

The study of medical devices in a materials laboratory, like the present one requires special considerations. Once a medical issue addressable with the present technology has been identified and evaluated, the next most intricate issue is to design a working model to be used for the experiments. This working model should reflect the salient features of the medical problem being studied.

At the same time, the studied model should conform to the measurement techniques used in materials science laboratories like electron microscopes, X-ray diffraction, tensile tests, and pin on disk friction testing device. This dilemma was encountered in all the measurements reported here and beyond. In fact, for most of the experiments done in the present laboratory, the time spent on designing, constructing, and readapting the experimental models was by far the longest compared to the data collection and analysis.

13.4.2 Coating process and tribological measurements

13.4.2.1 SS wires with IF-WS_2 impregnated in electroless nickel–phosphorous film

Orthodontic wires (Ormco, California 0.019×0.025 in.^{2} rectangular SS) were coated by electroless process with a uniform and smooth nickel–phosphorous (Ni–P) film using 100 mL solution (ENPLATE Ni-425, Enthone Inc.) [35]. The orthodontic wires (or SS plate substrate) were inserted into the electroless Ni–P bath (88°C, pH = 4.8, magnetic stirring) for 30 min. The plating resulted in a shiny smooth Ni–P layer. To another electroless solution, 200 mg of agglomerated IF-WS_2 powder with average particle size of 120 nm was added together with a cationic surfactant (cetyl-trimethylammoniumbromide: CTAB). A short (1 min) sonication (Sonifaier 150, Branson-30 Watts) was used to disperse the agglomerates and ensure the stability of the suspension. A special procedure was developed to deposit a uniform and relatively smooth composite Ni–P + IF film and secure its adequate adherence to the underlying archwire. Following hydorfluoric acid etching, a pure Ni film was electron-beam deposited onto the substrate; then Ni–P film was deposited from the electroless solution. Finally, a composite Ni–P + IF film was deposited. In several cases, the coated samples were annealed in nitrogen gas atmosphere at 400°C.

13.4.2.2 SS wires with IF-WS_2 impregnated in electrocodeposition nickel film

The IF-WS_2 NP were dispersed in an aqueous solution of nickel salt ($NiCl_2 \times 6H_2O$) and plated on a wire with a cross section of 0.019×0.025 in^2 and made of SS 110 mm in length (provided by Ormco Corporation, Orange, CA) [38]. The coating was produced by the electrochemical codeposition process with a direct current of 0.02 A and exposure of 20 min for every wire piece at 25°C. To minimize the agglomeration of the IF NP in the bath, a combination of ultrasonic treatment and the CTAB surfactant was used.

13.4.2.3 Ni–Ti wires with cobalt and IF-WS_2 film by electroplating procedure

Ni–Ti (Nitinol) wires were supplied by the following companies: Orthonol (CO, USA); Ormco (CA, USA), Nitinol Classic (CA, USA); Dentsply (NY, USA). Codeposition of cobalt and IF-WS_2 NP film was carried out from a cobalt chloride + IF solution buffered by boric acid and CTAB as surfactant [39]. The film was deposited at 55°C by galvanostatic plating with a current density of 15 mA/cm^2. In order to assure proper adhesion of the film to the substrate, Ti (10 nm) and Ni (20 nm) films were deposited onto the cleaned Ni–Ti wires by electron-beam evaporation prior to the electrodeposition process. Uniformity of the coating was achieved by rotating the sample.

The effects of cobalt coatings of endodontic files with impregnated fullerene-like WS_2 NP on file fatigue and failure were also examined. Dynamic X-ray diffraction (XRD), nanoindentation, and torque measurements all indicate a significant improvement in the fatigue resistance and consequently delay in the time to breakage of the coated files. This observation was attributed to

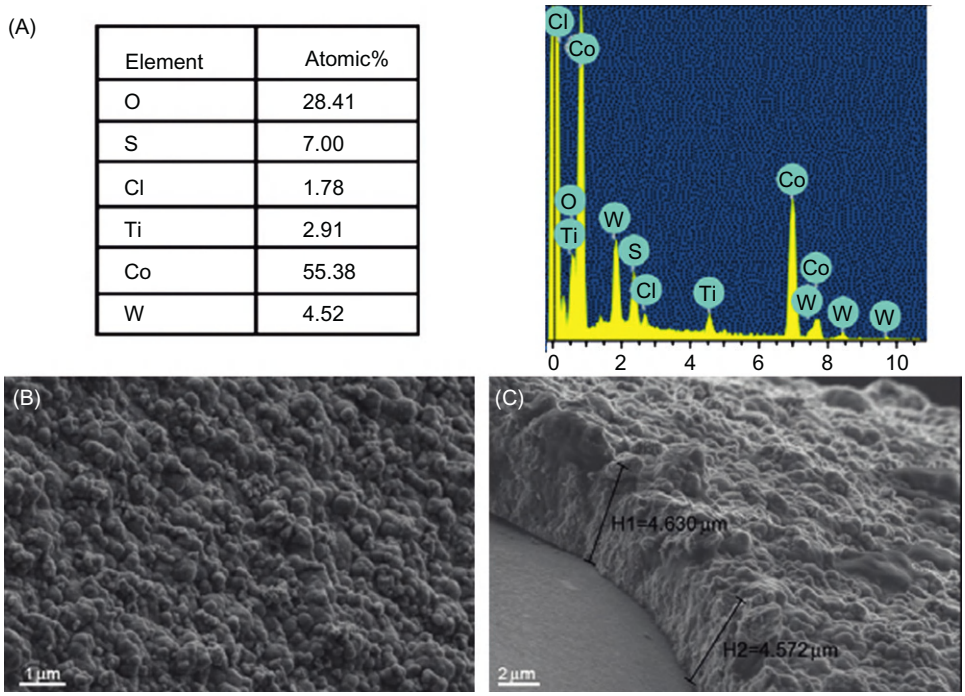

FIGURE 13.6

SEM/EDS analysis of the electrodeposited cobalt film onto Ni−Ti surface.

the reduced friction between the coated file and the surrounding. These methods are possibly also applicable to a variety of other Ni−Ti-based medical devices where fatigue and consequent failure are of relevance [38]. Figure 13.6 shows the SEM/EDS (energy dispersive X-ray analysis mounted on scanning electron microscope) analysis of such coatings. A uniform coating a few microns thick was thus obtained. The atomic ratio of W/Co ~12.5 indicates that substantial amount of IF-WS_2 NP was incorporated into these coatings. The surface is rather rough which suggests that the partition of the IF NP along the Co-film coating is possibly not uniform and the film surface is enriched with respect to the NP. XRD of the film (Figure 13.7) shows again a distinct (0002) peak of the IF-WS_2 at 14.2°.

13.4.3 Coating adhesion and wear

The adhesion of the cobalt coating to the Ni−Ti orthodontic wires was determined by inspecting the folded wire, which showed excellent integrity of the film (see Figure 13.8).

Figure 13.9 shows a scratch test of the Co + IF coating with nanoindenter. The test is done by profiling the surface of the Ni−Ti file surface coated with Co + IF film. This is followed by scratching it with increasing loads up to a maximal value of 30 mN. As a test of the quality of the coated surface, a final surface profiling shows little variation with respect to the original file surface.

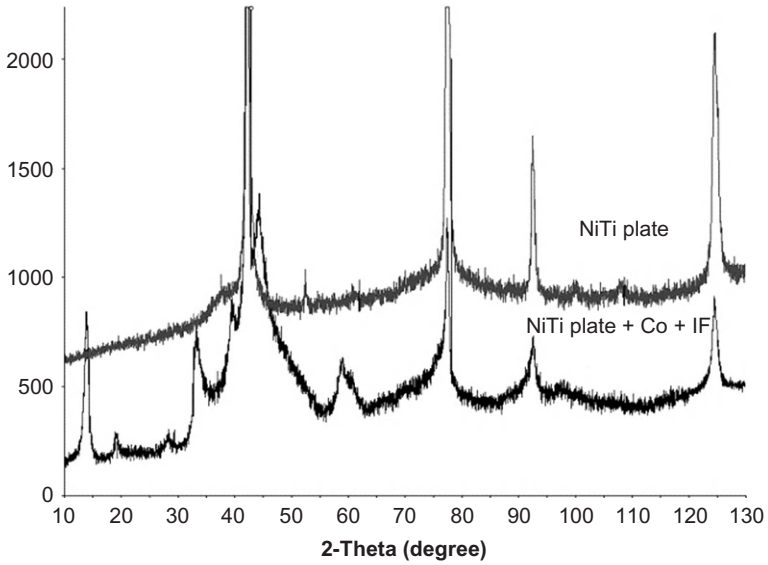

FIGURE 13.7

Diffraction patterns of Ni–Ti plate and a plate coated with Co + IF-WS_2 film.

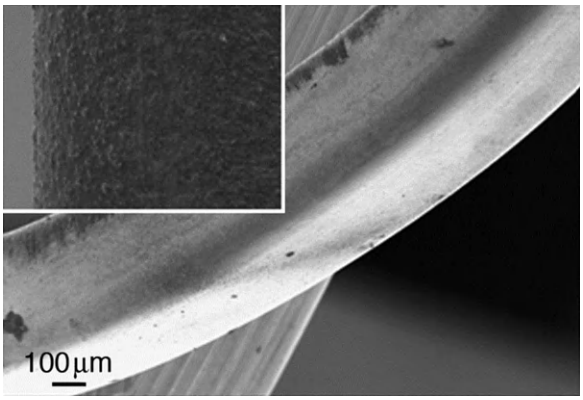

FIGURE 13.8

Electron micrograph of a Ni–Ti wire after adhesion test of the coating. The straight wire was coated with Co + IF film and then folded, exhibiting excellent adhesion as demonstrated in the figure. The high-magnification micrograph of the film not seen shows a uniform film Co + IF.

13.4.4 In vitro friction force tests

The validity and the significance of the results obtained in an experiment of friction force rely on the resemblance of the in vitro setup of the bracket and wire to the relevant clinical situation. However, the numerous in situ factors affecting orthodontic tooth movement cannot be

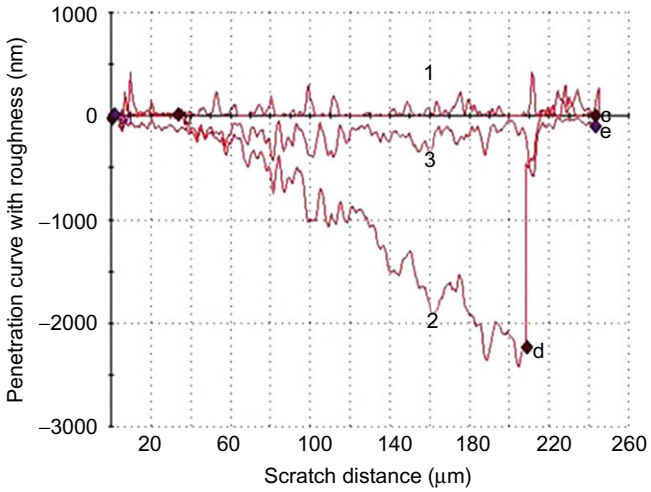

FIGURE 13.9

Scratch test performed using the nanoindenter showing an almost complete recovery of the Co + IF-coated file after release of the load. (1) Surface profile of the pristine surface, (2) scratch test with increasing force, up to 30 mN, and (3) surface profiling after the pressure release.

fully duplicated in the laboratory. Nevertheless, these experiments were conducted in various best-fit models.

The following sections describe various experimental friction models used to evaluate the effect of IF coatings of orthodontic wires on the friction force.

13.4.4.1 SS wires with IF-WS_2 NP impregnated in electroless Ni–P film

In the first set of experiments, a system which simulated the sliding of a tooth along an archwire, described previously by Redlich et al. [40] was utilized. Upper incisor SS brackets were bonded to aluminum plates by a bracket-mounting apparatus. This apparatus ensured the accurate and similar positioning of the brackets on the plates. The plates were then connected to the base of a universal mechanical testing apparatus (Instron 4502) through a device with three different notches angulated at 0°, 5°, and 10° to the long axis of the device (Figure 13.10). Angulations represent the contact angle between the wire and bracket during the movement of the tooth.

In this setup, the tensile tester was set to move the bracket down along the wire at a constant speed of 10 mm/min to a distance of 5 mm. The test begins with a steady increase in the force and reaches a maximum when movement begins on the wire. This maximum force represents the static friction and it is the force that is of interest in this case. A run-in period was needed before testing the coated wires with Instron. The run-in was carried out by repeated back and forth movements of the wire in a bracket slot before connecting the wire to the Instron. A new bracket was used for each testing. The highest angle was tested in the dry and wet mode. Deionized water was used to simulate the wet conditions in the mouth. Table 13.1 summarizes the results of the mechanical

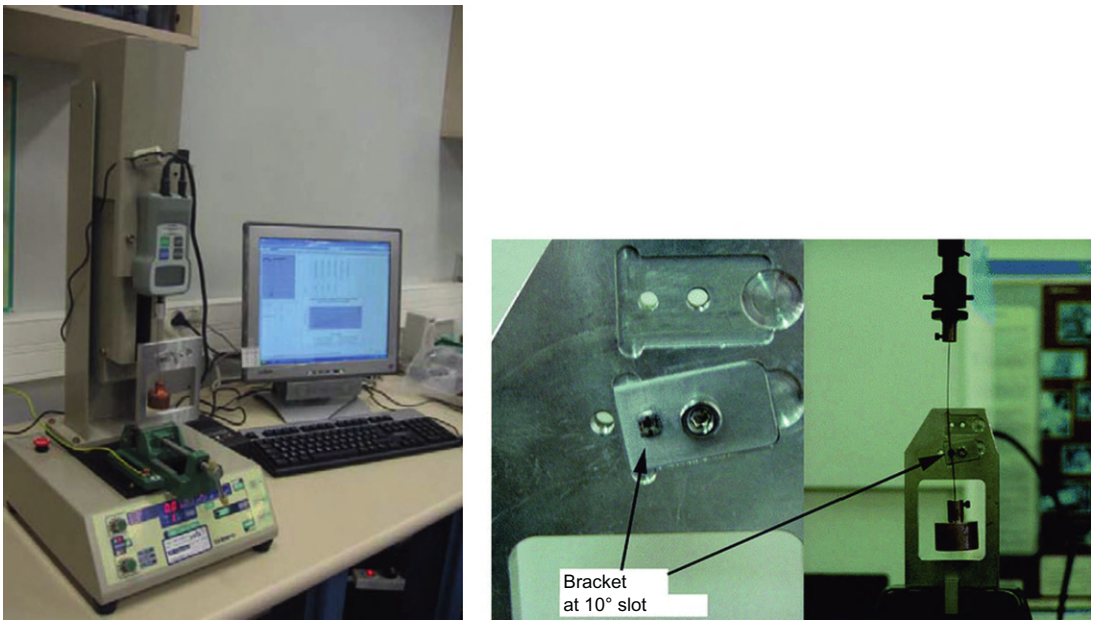

FIGURE 13.10

A photograph showing the device used to mount the brackets and orthodontic wires onto the Instron setup for the simulation of the archwire functioning in the mouth. About 12-cm segments of the orthodontic wires (coated and uncoated) were attached, on their upper part, to a 10-Newton load cell and the lower end was connected to a 150 g weight. The wires were then inserted into the slots in the brackets and ligated with an elastomeric module to all four wings of the brackets with 10° angulation. The 150 g weight was used to restraighten the wire following its insertion into the bracket similar to the clinical situation [41].

Table 13.1 Summary of the Results of the Tribological Tests of SS Orthodontic Wires (N ± SD)

Angle/Coating	0°	5°	10°
Noncoated wire	1.32 ± 0.12	2.95 ± 0.09	4.00 ± 0.19 dry 3.35 ± 0.21 wet
Ni–P + IF-coated wire	1.10 ± 0.06	1.58 ± 0.25	1.85 ± 0.21 dry 1.57 ± 0.23 wet

measurements. Each data point is an average of five different measurements. The results of these series of experiments are summarized in Table 13.1.

The mechanism by which the reduced friction of the coated wire is achieved can be explained by the models suggested in Refs. [36] and [42]. At the first stage, when there is no angle between the slot and wire, the IF NP act as spacers and reduce the number of metal asperities that come into contact, resulting in a lower coefficient of friction. As the angle grows, the load at the edges of the

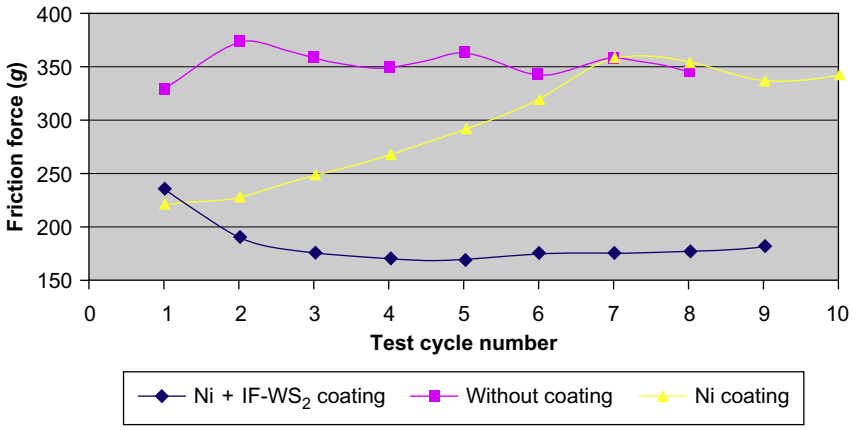

FIGURE 13.11

Dependence of the friction force between bracket and SS archwire on the test cycle number (10° angulation).

slot increases causing a higher friction at the surface of uncoated wire. It is probably at this point on the coated wire that the release of a few IF NP from the film into the tribological interface and their rolling and exfoliation occurs, resulting in the formation of a solid lubricant film on the sliding wire. The higher load at this point brings the asperities of the mating surfaces in straight contact causing the fluid (saliva in the mouth) to be squeezed out of the gap between the wire and slot, relying on the excellent tribological behavior of the solid lubricant film to allow the sliding of the archwire. When the two materials are made of SS, as is the case with the uncoated wire a high friction coefficient is obtained. The presence of WS_2 nanosheets at the interface under high loads leads to a very facile sliding between these sheets thereby reducing the coefficient of friction.

13.4.4.2 SS wires with IF-WS_2 impregnated in electrocodeposition of nickel film

Coated and uncoated SS rectangular archwires were engaged into brackets, which were attached to a special device set at 10° angulations to the wire (Figure 13.10). The wire is connected on the top to the load gauge and on the bottom to the 150 g (1.5 N) weight. The device is connected to the base of a testing machine and pulled down at a constant speed of 10 mm/min to a distance of 5 mm. The tests results showed (Figure 13.11) that friction forces between the rectangular archwire and the self-ligating bracket were reduced on the coated wire by up to 60% compared to the uncoated at the 10° angulation. Therefore, coated SS archwires with a composite Ni + IF-WS_2 offers an opportunity to substantially reduce the friction force during orthodontic tooth movement [41].

13.4.4.3 Ni–Ti wires with cobalt and IF-WS_2 film by electroplating procedure

Friction measurements of the coated Ni–Ti wires were made using a device designed to simulate sliding movement within a bracket system assembled to a Twin Column Testing Machine LR10K with 10 kN load cell Instron system [43,44] (Figure 13.12). The simulation device consisted of a horizontal mobile plate bearing SS brackets. The tested Ni–Ti rectangular wire (7 cm long),

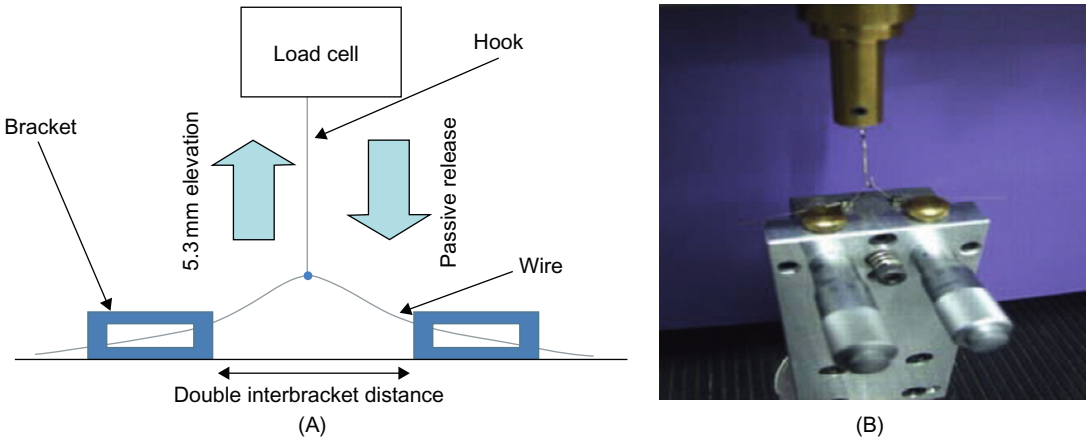

FIGURE 13.12

(A) Three-point bending test scheme; (B) a photograph of the assembling device with two brackets mounted on its upper surface; the wire is engaged into the brackets and elevated to a given height.

Table 13.2 Summary of the Friction Measurements of Cobalt + IF-Coated Ni–Ti Wires

Wire	Instantaneous Force (N)	Static Coefficient	Kinetic Force (N)	Kinetic Coefficient
Ni–Ti uncoated (2°)	1.541 ± 0.3	0.103 ± 0.02	1.555 ± 0.3	0.103 ± 0.02
Ni–Ti coated (2°)	1.253 ± 0.2	0.083 ± 0.01	1.154 ± 0.2	0.077 ± 0.01
Percentage of friction force reduction (2°)	19	20	26	30
Ni–Ti uncoated (3.8°)	1.640 ± 0.2	0.109 ± 0.02	1.487 ± 0.2	0.099 ± 0.01
Ni–Ti coated (3.8°)	1.290 ± 0.3	0.086 ± 0.02	0.990 ± 0.2	0.066 ± 0.01
Percentage of friction force reduction (3.8°)	21	22	34	34
Ni–Ti coated (5°)	1.207 ± 0.4	0.080 ± 0.02	0.927 ± 0.2	0.061 ± 0.01

vertically positioned was slotted through the moveable bracket and connected to a load cell on one end and to a counterweight mass of 1.5 N on the other. The friction force was measured as the tested wire was drawn up with a constant speed of 5 mm/min while slotted in the bracket for a distance of 5 mm. The bracket was set throughout the experiment at the same position using utility fork designed for this manner and bonded to the mobile plate using dental resin cement. In order to simulate different levels of frictional force, the mobile plate was moved horizontally creating angulations of 2° and 3.8° between the wire and the bracket. Tests were repeated 10 times for each angle both with coated and uncoated wires. Data were obtained and analyzed using NEXYGEN™ MT Materials Test and Data Analysis Software.

Results of the friction measurements using the Instron system are given in Table 13.2. Friction measurements in 2° angle showed a reduction of 20% in the static coefficient and about 30% of the

kinetic coefficient of friction. When enlarging the distance between the bracket and the long axis of the Instron system, thus creating a contact angle of 3.8° and simulating superior load applied onto the wire, a decrease in both static and kinetic coefficients was noted at the coated wire. This decline in static and kinetic coefficients was of 22% and 34%, respectively, with respect to the uncoated wire. In an additional series of measurements made only on the Co + IF coated wire in a contact angle of 5°, a static coefficient of 0.08 and kinetic friction coefficient of 0.061 were observed. The trend of the frictional force reduction as the load rises sustained throughout the entire series of experiments. The unique coating of IF-WS_2 NP embedded in cobalt matrix demonstrated a significant friction reduction of the Ni−Ti alloy.

The reduction in the friction as a result of the Co/IF-WS_2 coatings can be attributed to the release of minute amounts of IF-WS_2 NP which are impregnated in the cobalt coating. WS_2 and MoS_2 are known to provide efficient lubrication even in bulk (platelets) form. These kind of compounds are typified by the strong covalent bonds between sulfur and metal (tungsten) atoms within each plane while only weak van der Waals forces exist between planes; thus, low interplanar shear strength exists and permits sliding of two adjacent planes [31−34]. The WS_2 NP prevent asperity contact between the bracket and wire surfaces. Their round shape suggests that a rolling friction scenario is also possible in this case. Furthermore, elastic deformations of the NP augment their resilience and diminish the energy dissipation associated with friction and wear under the load [16]. In addition, the IF-WS_2 NP act as a protection against oxidation of the metal surface [37]; hence, it could be suggested that the coating also reduces or even obstructs nickel (cobalt) release, which is a known allergen, from the Ni−Ti wire.

13.5 Safety: toxicity and biocompatibility

The ongoing emergence and spread of nanoscale man-made materials for medical applications aroused the awareness of the scientists, the regulatory agencies, and the public to their safety. Safety, in terms of health-care use is determined by both nontoxic response and biocompatibility. Briefly, toxicity is the degree to which the material can harm humans and animals. The local and systemic responses of the host to the mode and the period of material exposure are evaluated [45]. Biocompatibility has recently been defined as *the ability of a biomaterial to perform its desired function with respect to a medical therapy, without eliciting any undesirable local or systemic effects in the recipient or beneficiary of that therapy, but generating the most appropriate beneficial cellular or tissue response in that specific situation, and optimizing its clinically relevant performance* [46].

The toxicity of the IF-WS_2 NP, manufactured by "NanoMaterials," for industrial applications, was tested at various modes of exposure by three authorized laboratories. The results showed no apparent toxic effect of IF-WS_2 after oral administration, dermal application, and inhalation tests in rats [47−49]. Toxicity tests, initially performed on animals, conducted in compliance with the OECD (Organisation for Economic Co-operation and Development) Principles of Good Laboratory Practice, are a prerequisite for further biocompatibility evaluations toward medical use. These tests are done on the as-prepared NP while biocompatibility of the medical device will be evaluated afterward in conjunction with all the other components comprising the NP coating of the device.

Recently, two acute toxicity tests (oral and dermal) using the Re-doped IF-MoS_2 NP were conducted [50,51]. The objective of the first study was to assess the acute oral toxicity of Re-doped IF-MoS_2 NP (Re:IF-MoS_2) following single administration of 2000 mg/kg, by oral gavage to mice, using prespecified fix doses, based on the identification of the dose(s) mortality and/or moribund status of the animals. The results showed no mortality in any of the animals throughout the entire 14-day study period. No noticeable clinical signs in reaction to dosing were evident in any of the animals. Mean group body weight gain at the end of the 14-day study period was noted in all groups. No gross pathological findings were evident in any of the animals at the time of their scheduled necropsy. Histopathologic findings revealed no treatment related changes in all the organs examined. Based on the lack of observed adverse reactions Re:IF-MoS_2 may be regarded as not causing acute toxicity risk through this route of administration and is classified as hazard Category 5 according to the Globally Harmonized Classification System [50] (Figures 13.13 and 13.14).

A second acute dermal toxicity of Re-doped MoS_2 was assessed on the basis of the testing procedure recommended by the OECD Guideline for the Testing of Chemicals. A single limit dose level corresponding to 2000 mg/kg of Re:IF-MoS_2 was topically applied for 24-h exposure duration to mice, for the purpose of evaluating health hazards likely to arise from short-term exposure in consideration of its projected use as a coating on medical devices. The results showed no mortality prior to the scheduled sacrifice. No clinical signs were observed in any of the animals at the immediate time postdosing. The body weight gain of all animals at the end of the 14-day observation period was within the normal limits. No abnormalities were detected in any of the animals at the time of their scheduled necropsy, at 14-days postdosing. Based on the results obtained following a single dermal application of Re:IF-MoS_2 dose level corresponding to 2000 mg/kg, it may be concluded that Re-doped MoS_2 NP do not represent an acute toxic risk by this route of administration [51].

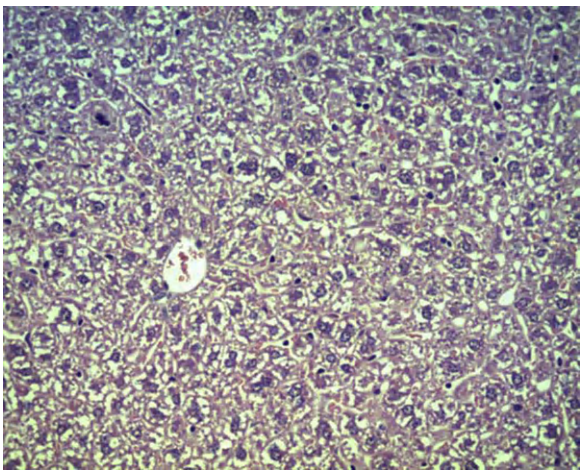

FIGURE 13.13

Liver centrilobular region. No abnormality detected 14 days after single administration of 2000 mg/kg of Re-doped IF-MoS_2 nanoparticles (*Hematoxylin and eosin* (H&E), ×20).

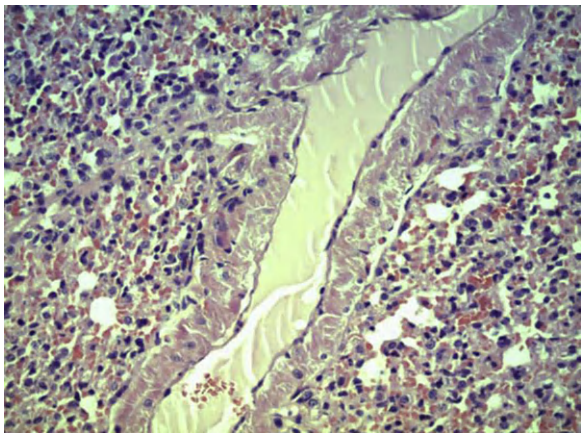

FIGURE 13.14

Lung section. No abnormality detected 14 days after single administration of 2000 of Re-doped IF-MoS_2 nanoparticles mg/kg (H&E, ×20).

In addition to these animal tests, recent reports demonstrated no cytotoxic effect of IF NP on the vitality and proliferation rate of human culture cells. Wu [52] et al. tested the effect of MoS_2 NP dispersed within cell medium, on two types of human cells: A549 cells (lung adenocarcinoma cells) and K562 cells (leukemic cells). The results showed that the MoS_2 NP were reasonably nontoxic and biocompatible up to the given concentrations. Furthermore, there was no obvious change of the morphologies of A549 cells treated with MoS_2 NP for 2 days even at the highest concentration.

Another study [53] examined the effect of WS_2 nanotubes of (INT-WS_2) on human salivary gland cell line. The cells were cultured and subjected to three different concentrations of INT-WS_2 with and without INT-WS_2. Cell viability, growth, and morphologic features were examined until reaching cell confluence. The results showed no significant differences between all the various cell concentrations groups. The authors concluded that INT-WS_2 do not affect salivary gland cells' viability, growth rate, or morphology.

13.6 Conclusions: from the lab to the clinic

The route of the archwires and the brackets, as well as other similar dental and medical devices, coated with IF-NP from the laboratory bench to the orthodontic patients is a multi-stage process.

This route starts with extensive laboratory work to choose the appropriate IF NP for the coating and subsequently determining the coating process. Thereafter, comprehensive in vitro tests are to be conducted, using the proper stimulatory models, to validate the efficacy of the IF-coated orthodontic materials.

The next stage is pursuing biocompatibility approval from the relevant regulatory agencies. At this stage, the product will be available for initial clinical evaluation and finally commercial manufacturing and sales in the orthodontic market.

Acknowledgments

We are grateful to "NanoMaterials" Ltd. for supplying the nanopowders. Collaboration with the following people is gratefully acknowledged: Dr. Alon Katz, Dr. Gili Naveh, Mrs. Adi Ram Adini, Prof. Abraham Nyska, Dr. Doron Aframian, Dr. Rita Rosentsveig, and Mrs. Lena Yadgarov. R.T. gratefully acknowledges the support of ERC (project INTIF 226639), the Israel Science Foundation, the Harold Perlman Foundation, The GMJ Schmidt Minerva Center for supramolecular chemistry, and the Irving and Cherna Moskowitz Center for Nano and Bio-Nano Imaging. R.T. is the Drake Family Chair in Nanotechnology and director of the Helen and Martin Kimmel Center for Nanoscale Science.

References

[1] M.G. Buonocore, A simple method of increasing the adhesion of acrylic filling materials to enamel surface, J. Dent. Res. 34 (1955) 849–853.
[2] G.V. Newman, Bonding plastic orthodontic attachments to tooth enamel, N. J. Dent. Soc. 35 (1964) 346–358.
[3] G.F. Andreasen, H. Bigelow, J.G. Andrews, 55 Nitinol wire: force developed as a function of "elastic memory", Aust. Dent. J. 24 (1979) 146–149.
[4] W.J. Buehler, J.V. Gilfrich, R.C. Wiley, Effects of temperature phase changes on the mechanical properties of alloys near composition NiTi, J. Appl. Phys. 34 (1963) 1475–1484.
[5] R.P. Kusy, J.Q. Whitley, Friction between different wire-bracket configurations and materials, Semin. Orthod. 3 (1997) 166–177.
[6] R.P. Kusy, Ongoing innovations in biomechanics and materials for the new millennium, Angle Orthod. 70 (2000) 366–376.
[7] M. Hain, A. Dhopatkar, P. Rock, The effect of ligation method on friction in sliding mechanics, Am. J. Orthod. Dentofacial Orthop. 123 (2003) 416–422.
[8] G.A. Thorstenson, R.P. Kusy, Resistance to sliding of self-ligating brackets versus conventional stainless steel twin brackets with second-order angulation in the dry and wet (saliva) states, Am. J. Orthod. Dentofacial Orthop. 120 (2001) 361–370.
[9] P. Scott, A.T. DiBiase, M. Sherriff, M.T. Cobourne, Alignment efficiency of Damon3 self-ligating and conventional orthodontic bracket systems: a randomized clinical trial, Am. J. Orthod. Dentofacial Orthop. 134 (2008) 470e1–470e8.
[10] S.J. Burrow, Friction resistance to sliding in orthodontics: a critical review, Am. J. Orthod. Dentofacial Orthop. 135 (2009) 442–447.
[11] A. Wichelhaus, M. Geserick, R. Hibst, F.G. Sander, The effect of surface treatment and clinical use on friction in NiTi orthodontic wires, Dent. Mater. 21 (2005) 938–945.
[12] M. Zolgharni, B.J. Jones, R. Bulpett, A.W. Anson, J. Franks, Energy efficiency improvements in dry drilling with optimized diamond-like carbon coatings, Diamond Relat. Mater. 17 (2008) 1733–1737.
[13] T. Muguruma, M. Iijima, W.A. Brantley, I. Mizoguchi, Effects of a diamond-like carbon coating on the frictional properties of orthodontic wires, Angle Orthod. 81 (2011) 143–150.
[14] R. Tenne, L. Margulis, M. Genut, G. Hodes, Polyhedral and cylindrical structures of tungsten disulphide, Nature 360 (1992) 444–446.
[15] L. Margulis, G. Salitra, R. Tenne, M. Talianker, Nested fullerene-like structures, Nature 365 (1993) 113–114.
[16] Y. Feldman, E. Wasserman, D.J. Srolovitz, R. Tenne, High-rate, gas-phase growth of MoS_2 nested inorganic fullerenes and nanotubes, Science 267 (1995) 222–226.

[17] R. Tenne, Inorganic nanotubes and fullerene-like materials, Nat. Nanotechnol. 1 (2006) 103−111.
[18] H.J. Fan, U. Goesele, M. Zacharias, Formation of nanotubes and hollow nanoparticles based on Kirkendall and diffusion processes: a review, Small 3 (2007) 1660−1671.
[19] A. Enyashin, S. Gemming, G. Seifert, Nanosized allotropes of molybdenum disulfide, Eur. Phys. J. 149 (2007) 103−125.
[20] C.N.R. Rao, A. Govindaraj, Synthesis of inorganic nanotubes, Adv. Mater. 21 (2009) 4208−4233.
[21] M.N. Tahir, A. Yella, J.K. Sahoo, H. Annal-Therese, N. Zink, W. Tremel, Synthesis and functionalization of chalcogenide nanotubes, Phys. Status Solidi B 247 (2010) 2338−2363.
[22] Y. Feldman, G.L. Frey, M. Homyonfer, V. Lyakhovitskaya, L. Margulis, H. Cohen, et al., Bulk synthesis of inorganic fullerene-like MS_2 (M = Mo, W) from the respective trioxides and the reaction mechanism, J. Am. Chem. Soc. 118 (1996) 5362−5367.
[23] Y. Feldman, A. Zak, R. Popovitz-Biro, R. Tenne, New reactor for production of tungsten disulfide onion-like (inorganic fullerene-like) nanoparticles, Solid State Sci. 2 (2000) 663−672.
[24] R. Rosentsveig, A. Margolin, Y. Feldman, R. Popovitz-Biro, R. Tenne, WS_2 nanotube bundles and foils, Chem. Mater. 14 (2002) 471−473.
[25] A. Zak, L. Sallacan-Ecker, A. Margolin, M. Genut, R. Tenne, Insight into the growth mechanism of WS_2 nanotubes in the scaled-up fluidized bed reactor, Nano 4 (2009) 91−98.
[26] A. Zak, Y. Feldman, V. Alperovich, R. Rosentsveig, R. Tenne, Growth mechanism of MoS_2 fullerene-like nanoparticles by the gas phase synthesis, J. Am. Chem. Soc. 122 (2000) 11108−11116.
[27] R. Rosentsveig, A. Margolin, A. Gorodnev, R. Popovitz-Biro, Y. Feldman, L. Rapoport, et al., Synthesis of fullerene-like MoS_2 nanoparticles and their tribological behavior, J. Mater. Chem. 19 (2009) 4368−4374.
[28] R. Rosentsveig, R. Tenne, A. Gorodnev, N. Feuerstein, H. Friedman, N. Fleischer, et al., Fullerene-like MoS_2 nanoparticles and their tribological behavior, Tribol. Lett. 36 (2009) 175−182.
[29] L. Yadgarov, R. Rosentsveig, G. Leitus, A. Albu-Yaron, A. Moshkovith, V. Perfilyev, et al., Controlled doping of MS_2 (M = W, Mo) nanotubes and fullerene-like nanoparticles, Angew. Chem. 51 (2012) 1148−1151.
[30] L. Rapoport, A. Moshkovith, V. Perfiliev, A. Laikhtman, I. Lapsker, L. Yadgarov, et al., High lubricity of Re-doped fullerene-like MoS_2 nanoparticles, Tribol. Lett. 45 (2012) 257−264.
[31] P.D. Fleischauer, J.R. Lince, A comparison of oxidation and oxygen substitution in MoS_2 solid film lubricants, Tribol. Int. 32 (1999) 627−636.
[32] M. Chhowalla, G.A.J. Amaratunga, Thin films of fullerene-like MoS_2 nanoparticles with ultra-low friction and wear, Nature 407 (2000) 164−167.
[33] A.A. Voevodin, J.S. Zabinski, Supertough wear-resistant coatings with "chameleon" surface adaptation, Thin Solid Films 370 (2000) 223−231.
[34] I.L. Singer, S. Fayeulle, P.D. Ehni, Wear behavior of triode-sputtered MoS_2 coatings in dry sliding contact with steel and ceramics, Wear 195 (1996) 7−20.
[35] W.X. Chen, Z.D. Xu, R. Tenne, R. Rosenstveig, W.L. Chen, H.Y. Gan, et al., Wear and friction of Ni−P electroless composite coating including inorganic fullerene-like WS_2 nanoparticles, Adv. Eng. Mater. 4 (2002) 686−690.
[36] A. Katz, M. Redlich, L. Rapoport, H.D. Wagner, R. Tenne, Self-lubricating coatings containing fullerene-like WS_2 nanoparticles for orthodontic wires and other possible medical applications, Tribol. Lett. 21 (2006) 135−139.
[37] H. Friedman, O. Eidelman, Y. Feldman, A. Moshkovith, V. Perfiliev, L. Rapoport, et al., Fabrication of self-lubricating cobalt coatings on metal surfaces, Nanotechnology 18 (2007) 1−8.
[38] A.R. Adini, Y. Feldman, S.R. Cohen, L. Rapoport, A. Moshkovith, M. Redlich, et al., Alleviating incidental and fatigue-related failure of NiTi root canal files by self-lubricating coatings, J. Mater. Res. 26 (2011) 1234−1242.

[39] G.R. Samorodnitzky-Naveh, M. Redlich, L. Rapoport, Y. Feldman, R. Tenne, Inorganic fullerene-like tungsten disulphide nanocoating for friction reduction of nickel–titanium alloys, Nanomedicine 4 (2009) 943–950.
[40] M. Redlich, A. Gorodnev, Y. Feldmean, I. Kaplan-Ashiri, R. Tenne, N. Fleischer, et al., Friction reduction and wear resistance of electro-co-deposited inorganic fullerene-like WS_2 coating for improved orthodontic stainless steel wires, J. Mater. Res. 23 (2008) 2909–2915.
[41] M. Redlich, Y. Mayer, D. Harari, I. Lewinstein, In vitro study of frictional forces during sliding mechanics of "reduced-friction" brackets, Am. J. Orthod. Dentofacial Orthop. 124 (2003) 69–73.
[42] (a) L. Cizaire, B. Vacher, T. Le Mogne, J.M. Martin, L. Rapoport, A. Margolin, et al., Mechanisms of ultra-low friction by hollow inorganic fullerene-like MoS_2 nanoparticles, Surf. Coat. Technol. 160 (2002) 282–287. (b) L. Joly-Pottuz, F. Dassenoy, M. Belin, B. Vacher, J.M. Martin, N. Fleischer, Ultralow-friction and wear properties of IF-WS_2 under boundary lubrication, Tribol. Lett. 18 (2005) 477–485.
[43] N. Reznikov, G. Har-Zion, Y. Abed, I. Barkana, M. Redlich, Measurement of friction forces between stainless steel wires and "reduced friction" self-ligating brackets, Am. J. Orthod. Dentofacial Orthop. 138 (2010) 330–338.
[44] N. Reznikov, G. Har-Zion, Y. Abed, I. Barkana, M. Redlich, Influence of friction resistance on superelastic properties of initial NiTi wires in "reduced friction" and conventional bracket systems, J. Dent. Biomech. (2010) 613142.
[45] S. Singh, H.S. Nalwa, Nanotechnology and health safety—toxicity and risk assessment of nanostructure materials on human health, J. Nanosci. Nanotech. 7 (2007) 3048–3070.
[46] D.F. Williams, On the mechanism of biocompatibility, Biomaterial 29 (2008) 2941–2953.
[47] H. Tsabari, Inorganic fullerene-like nano-spheres (IF-$\mathbf{WS_2}$): acute oral toxicity, acute toxic class method in the rat, Final report, Batch no. HP6, Harlan Biotech, Israel, 2005.
[48] I. Haist, Test for sensitization (local lymph node assay—LLNA) with inorganic fullerene-like $\mathbf{WS_2}$ nanospheres, Project no. 052052, BSL Bioservice, Germany, 2005.
[49] G.E. Moore, Acute inhalation toxicity study in rats–limit test, Product safety laboratories, Study no. 18503, Dayton, NJ, 2006.
[50] B. Nachshon, Single dose response acute oral toxicity in the mouse, IF-MO (R_e) $\mathbf{S_2}$, Batch no. 200910–2, Harlan Biotech, Israel, 2011.
[51] B. Nachshon, Acute dermal toxicity in mice, IF-MO(R_e)S_2, Batch No. 241111–1, Harlan Biotech, Israel, 2012.
[52] H. Wu, R. Yang, B. Song, Q. Han, J. Li, Y. Zhang, et al., Biocompatible inorganic fullerene-like molybdenum disulfide nanoparticles produced by pulsed laser ablation in water, ACS Nano 5 (2011) 1276–1281.
[53] E. Goldman, A. Zak, R. Tenne, Y. Neumann, A. Palmon, A.H. Hovav, et al., Biocompatibility examination of inorganic nanotubes (INT-WS_2) on A5 salivary gland cell line, NanoIsrael, Third International Nanotechnology Conference, Poster presentation no. 135, 2012.

CHAPTER

14 Characterization of Silver Nanoparticles Incorporated Acrylic-Based Tissue Conditioner with Antimicrobial Effect and Cytocompatibility

Ki Young Nam[a] **and Chul Jae Lee**[b]

[a]*Department of Dentistry, College of Medicine, Keimyung University, Daegu, Korea*
[b]*School of Chemical Industry, Yeungnam College of Science & Technology, Daegu, Korea*

CHAPTER OUTLINE

14.1 Introduction

Tissue conditioners have been commonly used to enhance the recovery of denture-bearing tissues from trauma, damage, or residual ridge resorption usually caused by ill-fitting dentures (Figures 14.1 and 14.2). However, these materials are degenerated and are easily degradable with time. The surfaces of acrylic gel polymer are susceptible to colonization by microorganisms [1], and microbial growth from the adherence of microbial cells is promoted by its rough surface and adhesive interactions between *Candida* species and oral bacteria, mostly *Candida albicans* (*C. albicans*) and oral

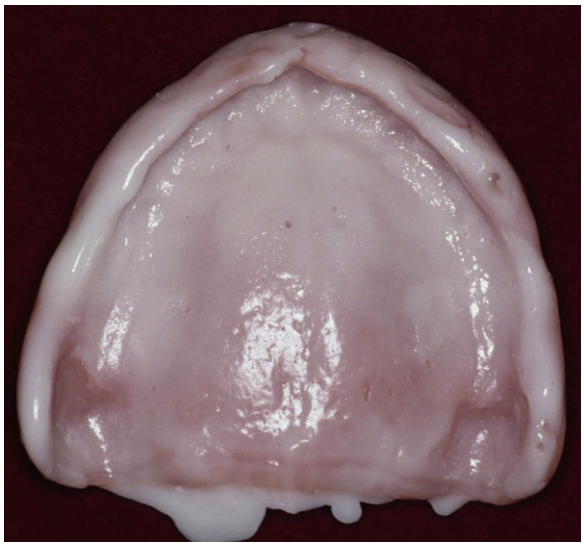

FIGURE 14.1

Clinical application of acrylic-based tissue conditioner on maxillary full denture.

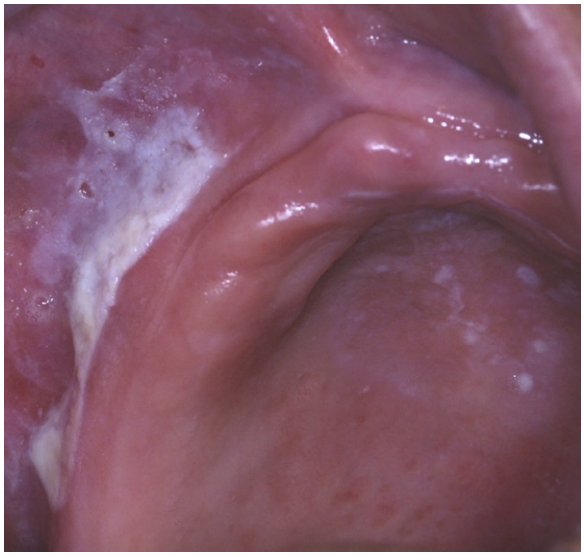

FIGURE 14.2

Denture-induced stomatitis related with fungal infection on palate and vestibule of maxilla.

streptococci [2,3]. Moreover, *Staphylococcus aureus* (*S. aureus*), giving rise to pharyngeal and respiratory infections, has been isolated from dentures and the oral cavity in elderly patients with decreased immunological activity [4,5]. Therefore, the maintenance of tissue conditioner and the prevention of the accumulation of microorganisms on such materials are of great importance. Tissue conditioners could be kept clean by mechanical and chemical methods. However, it is also known that these methods can cause considerable damage to tissue conditioner [6,7] and to some geriatric or hospitalized patients, even denture cleansing might be compromised owing to cognitive impairment, reduced motor dexterity, and memory loss. Though systemic or local antibiotic agents have been prescribed for eliminating the microbial population, considering the microbial resistance and the increase in health-care cost, the research on latent antimicrobial material may be needed [8,9]. Several in vitro and in vivo studies have shown the beneficial effects of antimicrobial agents combined in tissue conditioners [10–12]. However, bacteria may induce stomatitis [13,14] and no potentially effective and persistent antimicrobial agent that can be incorporated in tissue conditioners has yet been developed. Silver (Ag) has been well known for its antimicrobial properties and has a long history of application in medicine with well-tolerated tissue response and low toxicity profile [15]. Ag is more toxic than many other metals against a broad spectrum of sessile bacteria and fungi which colonize on plastic surfaces [16,17]. Such antibacterial characteristics of Ag has drawn attention recently due to the emergence of antibiotic resistant bacteria as a result of overuse of antibiotics and far lower propensity to induce microbial resistance than antibiotics. Ag-contained materials have been already used in various medical fields, such as in vascular graft, central venous catheter, and wound dressing [18,19]. Particularly, silver nanoparticles (Ag°), the nanosized (nm) inorganic particle form of Ag, with its rapid and broad-spectrum efficacy and sustained release of silver cation (Ag^{+}) [18,19] appear to be more effective means of prophylaxis than microsized (μm) Ag powder which shows lower antimicrobial activity owing to its limited surface [19,20].

Evaluating the biocompatibility of an antimicrobial material is an essential step toward the clinical application of the material in addition to testing its physical properties. Through minute elution of Ag^{+}, the cations may accumulate in oral epithelial cells or when large areas of oral mucosa are exposed to Ag° compounds over an extended period, it can possibly cause argyria or disruption of normal microflora [21,22].

The following sections of this chapter discuss the in vitro (i) synthesis of Ag° dental acrylic gel polymer and (ii) the antimicrobial effect and cytocompatibility of the modified acrylic tissue conditioner containing Ag°.

14.2 Preparation and identification of silver nanoparticles

Ag° was prepared using the following procedure. Aqueous silver sol was prepared with 10.0 mM of analytical grade $AgNO_3$ in distilled water and 2.0% polyvinyl pyrrolidon was used as stabilizer. All solutions were deaerated by bubbling with argon gas for 1 h and then were irradiated in the field of 20KGy ^{60}Co Gamma-ray sources. The transmission electron microscope (TEM) image of prepared Ag° nanoparticles shows that the average size of the Ag° is about 50–80 nm (Figure 14.3). The UV-vis spectrum of the Ag° is shown in Figure 14.4, the peak at 409.7 nm is the surface plasmon band of the Ag° synthesized by the gamma irradiation reduction.

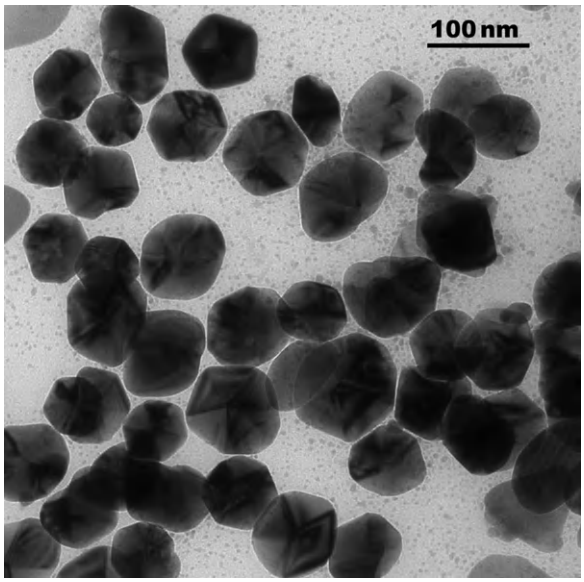

FIGURE 14.3

TEM view of a prepared Ag° used in this study. The average size of silver nanoparticles is approximately 50–80 nm.

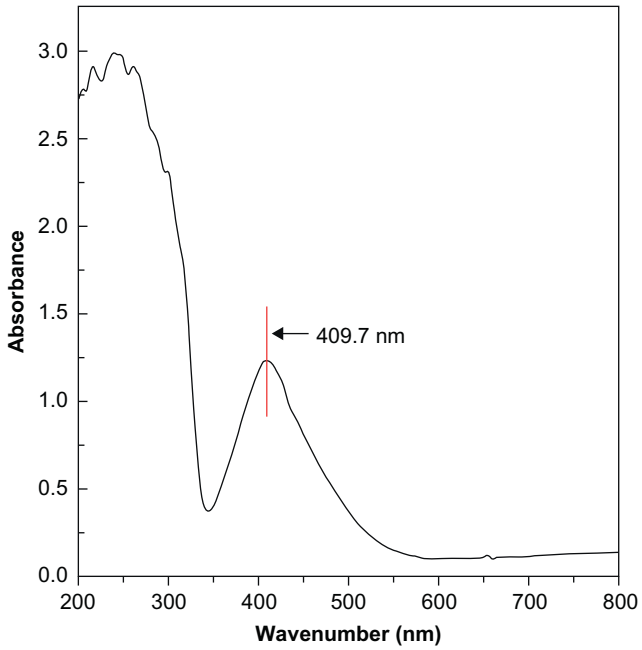

FIGURE 14.4

UV-vis spectrum of Ag° prepared by the gamma irradiation reduction method.

14.3 Acrylic tissue conditioner combined with silver nanoparticles

14.3.1 Fabrication of Ag°-tissue conditioner composites

The acrylic tissue conditioner selected for this study was Soft-Liner® supplied as powder and liquid. Colloidal Ag° was preliminary combined and homogenized with the conditioner liquid in a sterile glass beaker at concentrations ranging from 0 (control), 0.1, 0.5, 1.0, and 2.0% (vol/vol%: colloidal Ag°/conditioner liquid), respectively. The conditioner powder was immediately added and mixed for 30 s at designated powder/liquid ratio by manufacturer's instruction. In order to fabricate samples into uniform shape with regular surface, the mixed paste of conditioner was poured onto a custom-made brass mold with dimensions of 20 mm diameter $\times$3.0 mm depth. The mixed paste was sandwiched between glass slides until it was solidified under humid condition. Before microbial assay, all samples were sterilized with ethylene oxide gas for 24 h to ensure their initial sterility.

14.3.2 In vitro antimicrobial effects on *S. aureus, Streptococcus mutans*, and *C. albicans*

Three standard strains of microorganisms were used: *S. aureus* (ATCC 6538), *S. mutans* (ATCC 10449), and *C. albicans* (ATCC 14053). These microbial species tested are currently recommended to test the efficacy of antiseptic drugs [23]. *S. aureus*, a pathogen causing respiratory infections, has often been isolated from dentures and the oral cavity [4,24], and dentures have recently been reported to be a carriage of this pathogen [25]. *S. mutans* has been associated closely with the pathogenesis of dental caries, which is of limited clinical significance for denture wearers [26]. However, extensive plaque formation on denture might also contribute to the decay of residual natural teeth and can cause inflammation of gingival tissue adjacent to the denture [26]. *C. albicans* has been regularly isolated, suggesting a pathogenic association between bacteria and fungi related with denture-induced stomatitis.

Microbial suspensions were obtained from single colony isolated on agar plates and inoculated in appropriate broth for overnight cultures. Bacterial strains were grown in brain–heart infusion (BHI) broth and plated on agar plates at 37°C while *C. albicans* strain was grown in Schaedler broth and plated on agar plates at 30°C. After incubating microbial cells at 37°C overnight, optical density (OD) of the microbial suspension at 600 nm was adjusted to 1.0 using a spectrophotometer. The suspension was diluted with phosphate-buffered saline (pH 7.4) to 1:100 and suspended to final concentration of 1.0×10^7 cells/mL [14,27]. Each disc sample of Ag°-tissue conditioner and control were placed on multiwell culture plate with 22.1 mm diameter. Initial microbial suspensions (100 μL) in 1.0 mL of Sabouraud broth were inoculated to each well and incubated at 37°C. A small volume of microbial suspension (100 μL) was used and the microbes were adjusted to the stationary phase to be suspended in broth. The oral microbe would appear to be in a stationary phase rather than in growing phase, when the nutrition is limited in the presence of antibodies and antimicrobial enzymes in the oral cavity [28]. The assays with samples immersed in large suspension volume could not reproduce in vivo tissue conditioner which is closely in contact with the gingival mucosa [11]. Microbes in suspension (planktonic phase) are sensitive to lower antiseptic concentrations than microbes colonizing surfaces protected by a biofilm [29].

After an incubation period of 24 h and extended 72 h, suspension (100 μL) was withdrawn, viable cells colony forming unit (CFU) in the suspension was determined by using the spread plate method at a level of detection within 500 CFU per plate through serial dilution. As no standard of the antimicrobial effect on dental material has been established so far, the concept of minimum bactericidal concentration of antibiotics was adopted as the antimicrobial concentration at more than 99.9% elimination of the microbes [30,31].

The antimicrobial effects of Ag°-tissue conditioner against *S. aureus, S. mutans*, and *C. albicans* were demonstrated as the mean viable cells after 24 and 72 h of incubation (Table 14.1). When compared to initial CFU at 0 h, control group (0% Ag°) did not exhibit any microbial inhibitory effect against all of the strains, though the tissue conditioner itself possesses antimicrobial effects due to ingredients such as plasticizers and ethanol [32]. Some studies have shown that the antimicrobial effect of these ingredients was at variance and has little antimicrobial effect [1,33]. For two bacterial strains, *S. aureus* and *S. mutans*, Ag° incorporated samples showed the minimal bactericidal effects at the dose above 0.1% and no viable cells were detected from the conditions of 1.0% above. For fungal strain *C. albicans*, the minimal fungicidal concentration was shown at the dose of above 0.5% and no CFU was detected in 2.0%. It is reported that Ag and Ag-based compounds are highly toxic to prokaryotic cells showing strong biocidal effects on bacterial species [17], while Ag showed less effect on eukaryotic cells such as mold and yeasts [34]. The mechanism of antimicrobial effect of silver supported compound has not been fully explained yet. It was suggested that as a result of catalytic action of Ag, oxygen is converted into active oxygen (including hydroxyl

Table 14.1 Antimicrobial Effect of Ag°-Tissue Conditioner Samples (0–2.0%) Against *S. aureus*, *S. mutans*, and *C. albicans* at 24 and 72 h of Incubation Periods

Strain[a]	Incubation Period (h)	Ag° Dose (Vol%)				
		0 (Control)	0.1	0.5	1.0	2.0
S. aureus (10^7)	24	$5.4 \times 10^8 \pm (6 \times 10^7)$	**$7.1 \times 10^3 \pm (5 \times 10^2)$**	**48 ± (66)** **12 ± (4)**	**0** **0**	**0** **0**
	72	$8.7 \times 10^7 \pm (2 \times 10^6)$	**$9.7 \times 10^2 \pm (5 \times 10^2)$**			
S. mutans (10^7)	24	$1.2 \times 10^7 \pm (3 \times 10^6)$	**$3.6 \times 10^3 \pm (6 \times 10^2)$**	**30 ± (75)** **7 ± (11)**	**0** **0**	**0** **0**
	72	$3.5 \times 10^6 \pm (4 \times 10^5)$	**$5.4 \times 10^2 \pm (4 \times 10^2)$**			
C. albicans (10^7)	24	$4.3 \times 10^7 \pm (9 \times 10^6)$	$2.6 \times 10^5 \pm (9 \times 10^4)$	**$2.2 \times 10^2 \pm (3 \times 10^2)$**	**10 ± (25)** **20 ± (34)**	**0** **0**
	72	$5.2 \times 10^7 \pm (9 \times 10^6)$	$5.5 \times 10^4 \pm (9 \times 10^3)$	**$1.2 \times 10^2 \pm (75)$**		

Results are expressed in mean CFU with standard deviation (sd). Data in bold represent values statistically different from control ($P < 0.01$).
[a]*Starting inoculums: 10^7 CFU.*

radicals) by the action of light energy and/or H_2O in the air or water only at polar surfaces [19]. These active oxygen radicals caused the structural damage in bacteria and lead to the damage or even the death of the microorganisms, the so-called "oligodynamic action of silver" [19,35].

14.3.3 Cytotoxic test on human gingival cell line

Human gingival fibroblasts (HGF; ATCC 2014) were used to evaluate the cytotoxicity of Ag°-tissue conditioner by MTT (tetrazolium-based 3-(4,5-dimethylthiazol-2-yl)-2,5 diphenyltetrazolium bromide) assay. The cells were grown and subcultured for 24 h at 37°C in an atmosphere of 5% CO_2 in air and 100% relative humidity. HGF cell suspension was prepared at a concentration of 4×10^4 cells/mL and dispensed (180 μL/well) onto 96-well cell-culture plates. The multiwell plates were incubated at 37°C and 5% CO_2 in air for 24 h. The culture medium was removed from the wells and 20 μL of the extracts from experimental Ag°-tissue conditioner (0%, 0.1%, 0.5%, 1.0%, and 2.0%) were added into each well and incubated for 2, 8, 24, 48, and 72 h at 37°C and 5% CO_2 in air. Then, 10% MTT (100 μL) was added to each well and kept in a dark environment for 4 h at 37°C and after MTT was aspirated, 100 μL of dimethyl sulfoxide was added to each well. OD for each group was measured using ELISA reader under the absorbance at 570 nm. Cell viability (CV (%)) was calculated using the following equation:

$$C_v(\%) = \frac{\text{Sample optical density}}{\text{Control optical density}} \times 100$$

and cytotoxicity was evaluated by the cell viability as highly cytotoxic when less than 25% and less than 50−25% were qualified as moderately cytotoxic [36].

It is generally accepted that Ag° express their toxicity through the generation of reactive oxygen species (ROS) [37]. Increased cellular ROS levels are associated with the induction of genetically programmed cell death (apoptosis), as well as necrotic cell death in several cell lines [38]. Kim et al. [39] reported the subchronic oral toxicity and tissue accumulation of Ag° in rats for 90 days and highlighted that Ag° have significant toxic effects on cells that primarily occur in a dose-dependent manner. The results indicated that 2.0% Ag° group was expressed as highly cytotoxic effect to HGF at 24 and 72 h incubation periods while control (0%) and 0.1% and 0.5% groups were graded as noncytotoxic at all incubation periods even though the 0.5% group showed significant decrease in cell viability at 24 and 72 h over the control group (Figure 14.5). Phthalates and other esters of aromatic carboxylic acids are used as plasticizers in Soft-Liner® and they have been reported to elute from the conditioners during masticatory force and to possibly be toxic [40,41]. However, control group, an acrylic tissue conditioner "Soft-Liner®" without Ag° revealed no cytotoxic effect to HGF at all incubation periods. This result could be related to in vitro, static experimental condition for tested samples unlike normal functioning of tissue conditioner in oral cavity [41].

14.4 Characterization of Ag°-tissue conditioner composites

14.4.1 Determination of eluted Ag^+ from the specimens

For Ag^+ determination, atomic absorption spectrophotometer and shaking incubator were utilized. Ag°-tissue conditioner (0.5%, 1.0%, and 2.0%) specimens were put into 100 mL of sterile distilled water. After storage at 37°C under agitation, the concentration of released Ag^+ determined at every

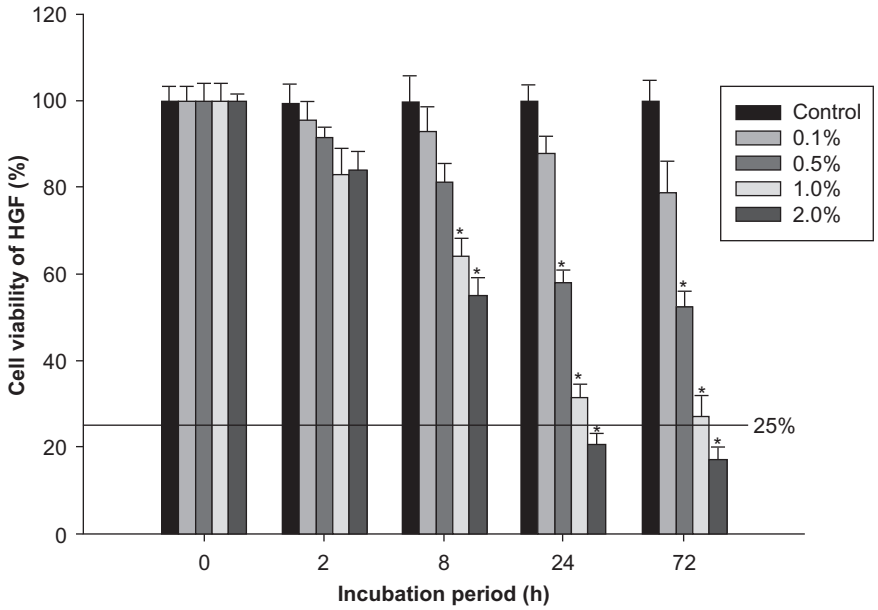

FIGURE 14.5

Cell viabilities (%) for tissue conditioner with varying concentrations in the range of 0–2.0% of Ag° at 2–72 h of incubation. * represents values statistically different from control ($P < 0.01$).

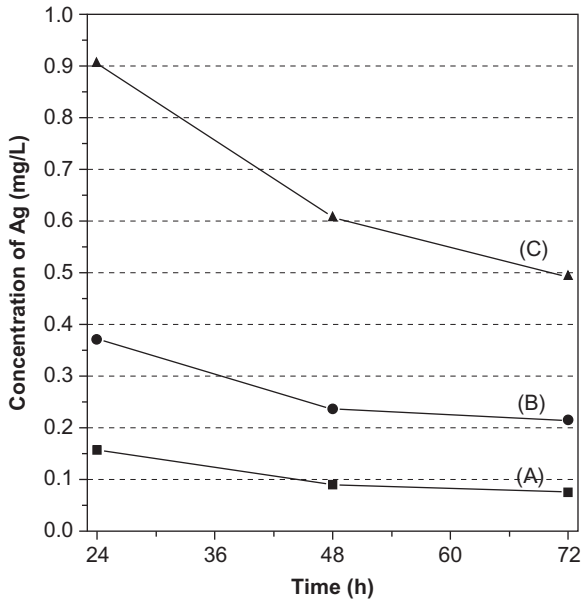

FIGURE 14.6

The quantities of Ag^+ releasing from Ag°-tissue conditioner composites according to concentrations of Ag° incorporated: (A) 0.5%, (B) 1.0%, and (C) 2.0%.

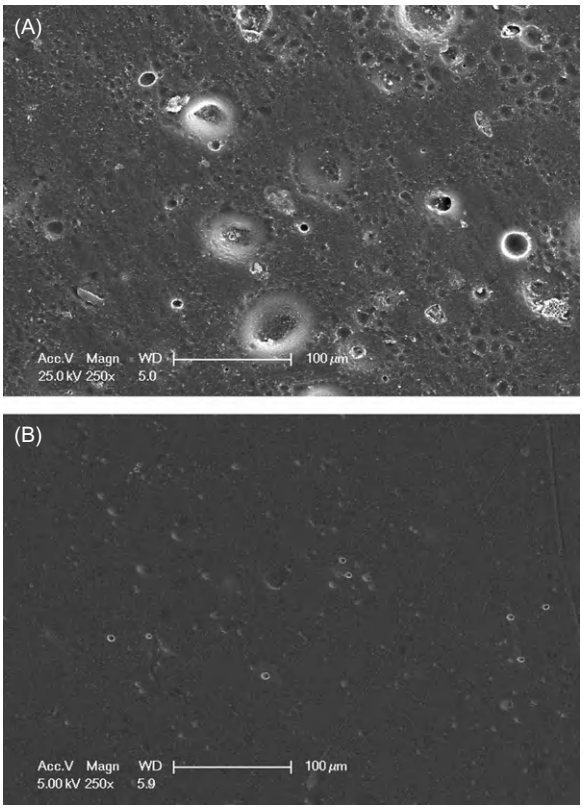

FIGURE 14.7

SEM image of 2.0% Ag°-tissue conditioner (A) as compared to control and (B) similar surface texture with large porosity is seen (×250).

6 h with replacement of new distilled water from 24 to 72 h of storage. The quantity (mg/L) of Ag^+ was expressed as the amounts of Ag^+ in the solution per unit of surface area of the disc (cm^2). The quantities of released Ag^+ were dose dependent and decreased in all tested specimens as time elapsed (Figure 14.6). The amount of eluted Ag^+ followed a steady state of approximately 0.08 mg/L in 0.5% of Ag° and 0.21 mg/L in 1.0% of Ag° after 48-h storage. In 2.0% Ag°-tissue conditioner, eluted Ag^+ was detected as approximately 0.49 mg/L at 72 h with a steeper decrease as compared to others. Considering in vivo tissue conditioners closely fitting the oral mucosa, further investigation would be needed to clarify the main action of Ag°-embedded gel polymer whether the antimicrobial effects resulted from Ag^+ elution or due to direct contact [42–44] or mixed effects.

14.4.2 Microstructure of Ag°-tissue conditioner composites

The microstructure of obtained Ag°-tissue conditioner was studied by scanning electron microscope (SEM) equipped with energy dispersion spectroscopy. The Ag° loaded tissue conditioner was gold

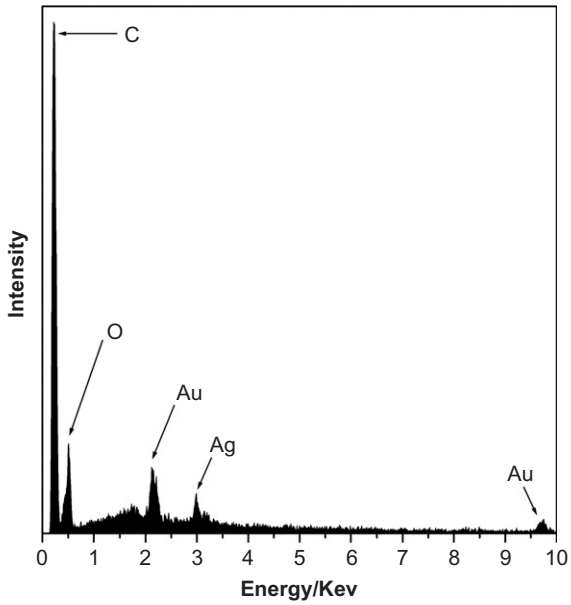

FIGURE 14.8

In EDX analysis of Ag°-loaded tissue conditioner, the spectrum shows the characteristic peak for Ag at 3 Kev. Unassigned peaks originate from polymer or external contaminants.

sputtered under high vacuum before the analysis. SEM image of 2.0% Ag°-tissue conditioner (Figure 14.7A) exhibited similar surface texture some enlarged porosities as compared to control (Figure 14.7B). Energy dispersive X-ray (EDX) studies were also performed for Ag°-tissue conditioner to identify the Ag° in the composites. EDX analysis identified Ag peak clearly which shows that Ag° were successfully immobilized into the Ag°-tissue conditioner (Figure 14.8).

14.5 Conclusions

Experimental acrylic tissue conditioner containing silver nanoparticles (Ag°-tissue conditioner) was characterized in regards to its antimicrobial effect and cytocompatibility. Formations of silver nanoparticles (50−80 nm) were evaluated by TEM, UV-vis spectroscopy (409.7 nm), and the identification of Ag° in the compound was confirmed by EDX analysis. The prepared Ag°-tissue conditioner has the great bactericidal/fungicidal activity with reduction of 99.9% of *S. aureus, S. mutans* at 0.1% of Ag° incorporated, and *C. albicans* at 0.5% of Ag° combined over the control (0% of Ag°) value. Up to 0.5% Ag° showed no cytotoxic influence on HGF. Thus, this chapter concludes that within the limitations of the present in vitro study, Ag°-loaded acrylic tissue conditioner could be a possible candidate for a novel antimicrobial tissue conditioner with uncompromised cytocompatibility.

References

[1] N. Okita, D. Ørstavik, J. Ørstavik, K. Østby, In vivo and in vitro studies on soft denture materials: microbial adhesion and tests for antibacterial activity, Dent. Mater. 7 (1991) 155–160.

[2] D.R. Radford, S.J. Challacombe, J.D. Walter, Denture plaque and adherence of *Candida albicans* to denture-base materials in vivo and in vitro, Crit. Rev. Oral. Biol. Med. 10 (1999) 99–116.

[3] R.G. Nair, L.P. Samaranayake, The effect of oral commensal bacteria on candidal adhesion to denture acrylic surfaces. An in vitro study, APMIS 104 (1996) 339–349.

[4] C. Wilkieson, L.P. Samaranayake, T.W. MacFarlane, P.-J. Lamey, D. MacKenzie, Oral candidosis in the elderly in long term hospital care, J. Oral. Pathol. Med. 20 (1991) 13–16.

[5] T. Rossi, J. Laine, E. Eerola, P. Kotilainen, R. Peltonen, Denture carriage of methicillin-resistant *Staphylococcus aureus*, Lancet 345 (1995) 1557.

[6] A. Harrison, R.M. Basker, I.S. Smith, The compatibility of temporary soft materials with immersion denture cleansers, Int. J. Prosthod. 2 (1989) 254–258.

[7] H. Nikawa, H. Iwanaga, T. Hamada, S. Yuhta, Effects of denture cleansers on direct soft denture lining materials, J. Prosthet. Dent. 72 (1994) 657–662.

[8] L.M. De Visschere, L. Grooten, G. Theuniers, J.N. Vanobbergen, Oral hygiene of elderly people in long-term care institutions—a cross sectional study, Gerodontology 23 (2006) 195–204.

[9] L.A. Casemiro, C.H. Gomes Martins, C. Pires-de-Souza Fde, H. Panzeri, Antimicrobial and mechanical properties of acrylic resins with incorporated silver–zinc zeolite—Part I, Gerodontology 25 (2008) 187–194.

[10] D.M. Quinn, The effectiveness, in vitro, of miconazole and ketoconazole combined with tissue conditioners in inhibiting the growth of *Candida albicans*, J. Oral. Rehabil. 12 (1985) 177–182.

[11] M.R. Truhlar, K. Shay, P. Sohnle, Use of a new assay technique for quantification of antifungal activity of nystatin incorporated in denture liners, J. Prosthet. Dent. 71 (1994) 517–524.

[12] C.K.W. Chow, D.W. Matear, H.P. Lawrence, Efficacy of antifungal agents in tissue conditioners in treating candidiasis, Gerodontology 16 (1999) 110–118.

[13] A.S.F. Koopmans, N. Kippuw, J. de Graaff, Bacterial involvement in denture-induced stomatitis, J. Dent. Res. 67 (1988) 1246–1250.

[14] E. Budtz-Jørgensen, E. Theilade, J. Theilade, H.A. Zander, Method for studying the development, structure and microflora of denture plaque, Scand. J. Dent. Res. 89 (1981) 149–156.

[15] J. Fu, J. Ji, D. Fan, J. Shen, Construction of antibacterial multilayer films containing nanosilver via layer-by-layer assembly of heparin and chitosan-silver ions complex, J. Biomed. Mater. Res. A 79 (2006) 665–674.

[16] R.M. Slawson, H. Lee, J.T. Trevors, Bacterial interactions with silver, Biometals 3 (1990) 151–154.

[17] G. Zhao, S.E. Stevens Jr., Multiple parameters for the comprehensive evaluation of the susceptibility of *Escherichia coli* to the silver ion, Biometals 11 (1) (1998) 27–32.

[18] V. Alt, T. Bechert, P. Steinrücke, M. Wagener, P. Seidel, E. Dingeldein, et al., An in vitro assessment of the antibacterial properties and cytotoxicity of the nanoparticles silver bone cement, Biomaterials 25 (2004) 4383–4391.

[19] U. Samuel, J.P. Guggenbichler, Prevention of catheter-related infections: the potential of a new nano-silver impregnated catheter, Int. J. Antimicrob. Agents 23 (2004) 75–78.

[20] J.B. Wright, K. Lam, D. Hansen, R.E. Burrell, Efficacy of topical silver against fungal burn wound pathogens, Am. J. Infect. Control. 27 (1999) 344–350.

[21] H.G. Petering, Pharmacology and toxicology of heavy metals: silver, Pharmacol. Therapeut. 1 (1976) 127–130.

[22] G. Ramage, K. Vande Walle, B.L. Wickes, J.L. Lopez-Ribot, Standardized method for in vitro antifungal susceptibility testing of *Candida albicans* biofilms, Antimicrob. Agents Chemother. 45 (2001) 2475−2479.
[23] M.E. Reverdy, A. Martra, J. Fleurette, Application of a micromethod to the study of the bactericidal activity of 2 antiseptics based on chlorhexidine gluconate, Pathol. Biol. 34 (1986) 688−693.
[24] D. Steinberg, S. Eyal, Early formation of *Streptococcus sobrinus* biofilm on various dental restorative materials, J. Dent. 30 (2002) 47−51.
[25] J. Satou, A. Fukunaga, A. Morikawa, I. Matsumae, N. Satou, H. Shintani, Streptococcal adherence to uncoated and saliva-coated restoratives, J. Oral. Rehabil. 18 (1991) 421−429.
[26] S. Hahnel, M. Rosentritt, R. Bürgers, G. Handel, Adhesion of *Streptococcus mutans* NCTC 10449 to artificial teeth: an in vitro study, J. Prosthet. Dent. 100 (4) (2008) 309−315.
[27] J. Chandra, P.K. Mukherjee, S.D. Leidich, F.F. Faddoul, L.L. Hoyer, L.J. Douglas, et al., Antifungal resistance of candidal biofilms formed on denture acrylic in vitro, J. Dent. Res. 80 (3) (2001) 903−908.
[28] Y. Abe, M. Ishii, M. Takeuchi, M. Ueshige, S. Tanaka, Y. Akagawa, Effect of saliva on an antimicrobial tissue conditioner containing silver−zeolite, J. Oral. Rehabil. 31 (2004) 568−573.
[29] P.C. Baehni, Y. Takeuchi, Anti-plaque agents in the prevention of biofilm-associated oral diseases, Oral. Dis. 9 (2003) 23−29.
[30] W. Bruns, H. Keppeler, R. Bancks, Suppression of intrinsic resistance to penicillins in *Staphylococcus aureus*, by polidocanol, a dodecyl polyethyleneoxid ether, Antimicrob. Agents Chemother. 27 (1985) 632−639.
[31] A.G. Gristina, R.A. Jennings, P.T. Naylor, Q.N. Myrvik, L.X. Webb, Comparative in vitro antibiotic resistance of surface-colonizing coagulase-negative staphylococci, Antimicrob. Agents Chemother. 33 (1989) 813−816.
[32] T. Matsuura, Y. Abe, Y. Sato, M. Okamoto, M. Ueshige, Y. Akagawa, Prolonged antimicrobial effect of tissue conditioners containing silver-zeolite, J. Dent. 25 (1997) 373−377.
[33] E. Mäkilä, V.K. Hopsu-Havu, Mycotic growth and soft denture lining materials, Acta Odontol. Scand. 35 (1977) 197−205.
[34] M. Christensen, J. Rungby, S.C. Mogensen, Effects of selenium on toxicity and ultrastructural localization of mercury in cultured murine macrophages, Toxicol. Lett. 47 (3) (1989) 259−270.
[35] Q.L. Feng, J. Wu, G.Q. Chen, F.Z. Cui, T.N. Kim, J.O. Kim, A mechanistic study of the antibacterial effect of silver ions on *Escherichia coli* and *Staphylococcus aureus*, J. Biomed. Mater. Res. 52 (2000) 662−668.
[36] International Organization for Standardization (ISO 10993-5), Biological evaluation of medical devices—Part 5, tests for cytotoxicity: in vitro methods, 1992.
[37] R. Foldbjerg, P. Olesen, M. Hougaard, D.A. Dang, H.J. Hoffmann, H. Autrup, PVP-coated silver nanoparticles and silver ions induce reactive oxygen species, apoptosis and necrosis in THP-1 monocytes, Toxicol. Lett. 190 (2009) 156−162.
[38] M. Ott, V. Gogvadze, S. Orrenius, B. Zhivotovsky, Mitochondria, oxidative stress and cell death, Apoptosis 12 (2007) 913−922.
[39] Y.S. Kim, M.Y. Song, J.D. Park, K.S. Song, H.R. Ryu, Y.H. Chung, Subchronic oral toxicity of silver nanoparticles, Part Fibre Toxicol. 7 (2010) 20−31.
[40] D.W. Jones, E.J. Sutow, G.C. Hall, W.M. Tobin, B.S. Graham, Dental soft polymers: plasticizer composition and leachability, Dent. Mater. 4 (1988) 1−7.
[41] B.S. Graham, D.W. Jones, E.J. Sutow, An in vivo and in vitro study of the loss of plasticizer from soft polymer-gel materials, J. Dent. Res. 70 (5) (1991) 870−873.

[42] C. Pesci-Bardon, T. Fosse, D. Serre, L. Madinier, In vitro antiseptic properties of an ammonium compound combined with denture base acrylic resin, Gerodontology 23 (2006) 111–116.
[43] K. Yoshida, M. Tanagawa, M. Atsuta, Characterization and inhibitory effect of antibacterial dental resin composites incorporating silver-supported materials, J. Biomed. Mater. Res. 47 (1999) 516–522.
[44] S. Imazato, N. Ebi, U. Takahashi, T. Kaneko, S. Ebisu, R.R.B. Russel, Antibacterial activity of bactericide-immobilized filler for resin-based restoratives, Biomaterials 24 (2003) 3605–3609.

CHAPTER

Bioactive Glass Nanoparticles for Periodontal Regeneration and Applications in Dentistry

15

Sandhra M. Carvalho, Agda A.R. Oliveira, Elke M.F. Lemos and Marivalda M. Pereira

Metallurgical and Materials Engineering Department, Federal University of Minas Gerais, Belo Horizonte, Minas Gerais, Brasil

CHAPTER OUTLINE

15.1 Introduction

Bioactive glasses were first developed by Hench et al. in 1969, and represent a group of reactive materials that are able to bond to mineralized bone tissue in physiological environment. Bioactive glasses are widely used in the biomedical area. Early applications of bioactive glasses were in the form of solid pieces for small bone replacement in middle ear surgery [1,2]. Later, several applications of bioactive glasses have been proposed, including the dental field. Recently, bioactive glasses have been widely studied for potential application in tissue engineering and regenerative medicine.

A range of bioactive glasses with attractive properties, like biocompatibility and bioactivity, and synthesized by newer methods have been developed. Various investigations have been undertaken to obtain bioactive glasses in different forms, such as bulk, powder, composites, and porous scaffolds.

Nanobiomaterials in Clinical Dentistry.

Nanotechnology offers a new strategy to develop bioactive glasses with a higher surface area. Nanotechnology is defined as a science that involves the development of materials and devices at the nanoscale. Specific properties of bioactive glasses can be improved and controlled when synthesized in nanometer scale. Therefore, nanosized biomaterials have greater biocompatibility and bioactivity. This new approach is important both for bioactive glasses used in particulate form as well as for coatings on biomedical devices or as fillers in composite materials.

Over time, bioactive glasses have been applied in various specialties of dentistry such as periodontics, endodontics, and implantology. This chapter describes the importance and applications of bioactive glass in dentistry and periodontics.

15.2 Composition and synthesis of bioactive glass nanoparticles

Bioactive glass when in contact with body fluids induces a specific biological response at the interface of the material, resulting in the formation of a carbonated hydroxyapatite (HA) layer on its surface and, through this layer, binding to the mineralized tissue. The bioactivity of bioactive glass is not an absolute concept determined only by the composition but is also affected by the size and shape of the material. The formation of this HA layer is essential for synthetic materials to exhibit bioactivity [3,4].

There is an advance in research on bioactive glasses for newer applications in tissue engineering, and therefore new routes of synthesis of bioactive glass have been proposed. A high surface area silica-rich is crucial for the formation of HA layer. Sol−gel glasses exhibited increasing specific surface area and pore volume compared with the glasses produced by conventional melting process, which enhanced their biocompatibility and bioactivity by accelerating the deposition process of HA [3,4]. One approach to improve the properties of bioactive glass material is their development at the nanoscale. Reducing the size of bioactive glass granules can accelerate the formation of HA layer and also provide more active sites for cell attachment. Compared with microparticles, nanoparticles have significantly higher surface area, and this drastically changes the material characteristics such as surface energy, wettability, surface topography, and surface chemistry. Furthermore, studies have shown that nanoscale materials have higher biocompatibility [5,6]. Ostomel et al. (2006) also showed that the reduction of bioactive glass particles to nanoscale could stimulate their bioactivity [7]. Bioactive glasses are capable of forming a HA layer, and the osseointegration to bone tissue is performed through this layer. The rate of osseointegration to the mineralized tissue depends on the rate of formation of HA layer, which depends on the composition of the bioactive glass [4,8].

The basic components of most bioactive glasses are SiO_2, Na_2O, CaO, and P_2O_5. However, among the sol-gel-derived bioactive glasses, the composition of 60% SiO_2, 36% CaO, and 4% P_2O_5 (by weight) has a high level of bioactivity, showing great potential for engineering applications of mineralized tissues [9]. In the past decade, several studies have been directed at the development of bioactive glass nanoparticles. Recently, Brunner et al. (2006) reported on the preparation of bioactive glass nanopowders using flame synthesis, a process that requires a high-temperature environment [10]. By contrast, sol-gel technology is a low-temperature preparation method, and the glasses prepared by the sol-gel method contain a porous structure with a higher surface area.

The sol-gel route is based on controlled hydrolysis and condensation of alkoxides to form a suspension of colloidal particles (sol), which upon polycondensation forms an interconnected network structure (gel). However, the particle size of the traditional sol-gel-derived bioactive glasses was larger than 1 μm.

The synthesis of bioactive glass uses typical precursors like tetraethyl orthosilicate (TEOS), calcium nitrate (CN), and triethylphosphate (TEP). Particle diameter can be controlled by fine-tuning variable parameters, such as reagent concentration and reaction temperature. According to Bogush and Zukoski (1991), five parameters play an important role in the size and distribution of silica nanoparticles: (i) concentration of TEOS, (ii) concentration of ammonia, (iii) concentration of water, (iv) alcohol effect, and (v) reaction temperature [11,12]. Hong et al. (2009) developed bioactive glass nanoparticles by combining the sol−gel method and co-precipitation. In that study, the mixture of precursor was hydrolyzed in acidic medium and condensed under alkaline conditions separately [13,14].

Stöber et al. (1968) reported on a pioneering method for the synthesis of spherical and monodisperse silica nanoparticles from aqueous alcohol solution of silicon alkoxides in the presence of ammonia as a catalyst from which different sizes of silica particles were obtained [15]. The Stöber method can be modified to produce particles with composition different from those of pure silica. Oliveira (2011) synthesized bioactive glass nanoparticles based on the Stöber method [16] (Figure 15.1).

Chen et al. (2009) investigated the effects of different morphologies on the in vitro bioactivity of nanosized bioactive glass particles in the system $CaO-P_2O_5-SiO_2$ by using lactic acid in the sol−gel method and concluded that not only the surface area but also the surface morphology play an important role in bioactivity of the material [17].

Nanosized particles contain a large surface area that results in high interfacial energy and thermodynamic instability. In general, these particles tend to agglomerate during the synthesis of the particles in an attempt to minimize the free energy of the system. To maintain the stability of the particles, some studies focused on obtaining spherical bioactive glass particles to create a bioactive material with dispersion capability under dilute aqueous and alcoholic conditions [18]. Spherical bioactive glass nanoparticles developed and characterized by Oliveira (2011) are shown in Figure 15.2 [16].

Several techniques were developed in which $SiO_2-CaO-P_2O_5$ bioactive glass nanoparticles were prepared. The best bioactivity results were from ternary systems with spherical particles below 50 nm produced with a pH of 11.5. El-Kady et al. (2010) prepared particles, comprised of 60 wt% SiO_2, 36 wt% CaO, and 4 wt% P_2O_5, with sizes less than 100 nm using alkali-mediation with the application of moderate ultrasound dispersion combined with mechanical agitation as well as the addition of ethanol as a dispersant [19]. Previous studies have shown that low concentrations of TEOS and water provide monodispersed uniform-sized nanoparticles [11,12,15,20−25]. The size of the nanoparticles was found to increase with TEOS and with increasing concentrations of water and ammonia of up to 7 M and 2 M, respectively [20]. Particles prepared in methanol solutions are the smallest, and the particle sizes increase with the increasing chain length of alcohol. The particle size distribution also becomes broader when longer chain alcohols are used as solvents. Particles prepared in methanol and ethanol-glycerol solutions resulted in a stable sol. However, when butanol and ethanol are used, precipitation could easily be observed [11,12,20,24,26].

The ammonia-catalyzed reactions of TEOS in ethanol with water (Stöber method) can be used for the preparation of monodispersed spherical nanoparticles bioactive glass. Alcohol is added to prevent the liquid−liquid phase separation during the initial phase of the hydrolysis reaction [27]. Methanol is chosen as the solvent medium to act as a surfactant and promote the production of

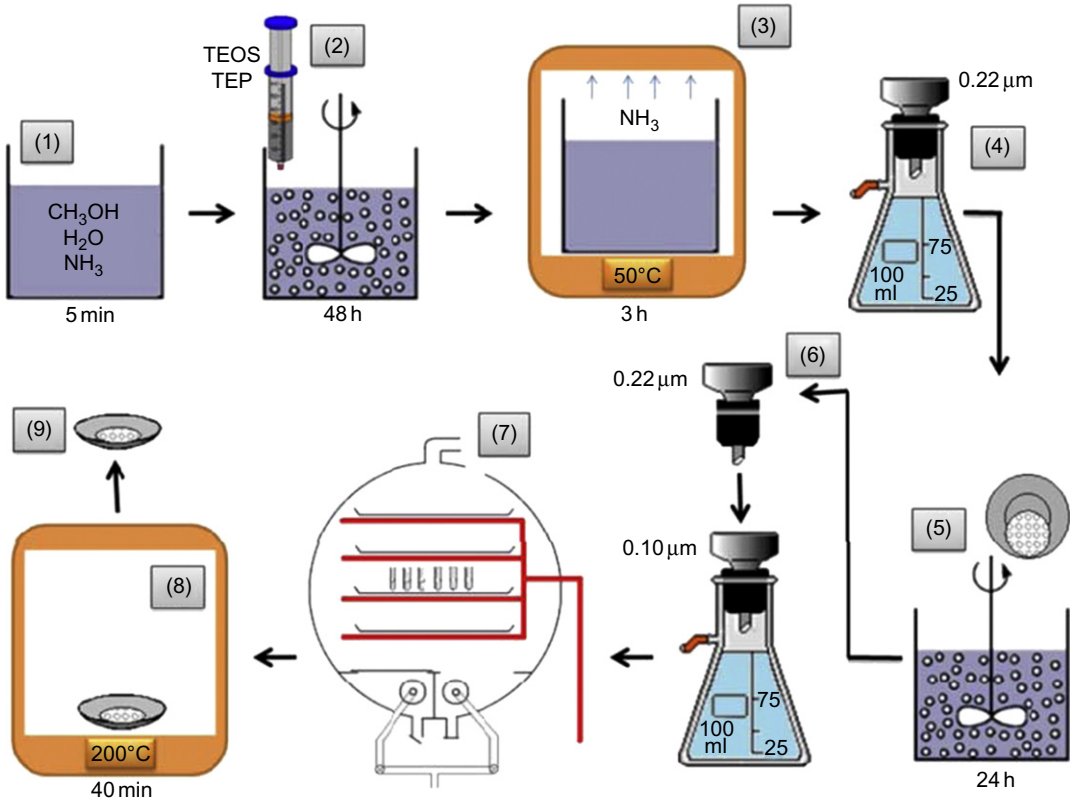

FIGURE 15.1

Schematic representation of bioactive glass nanoparticles synthesis based on the Stöber method: (1) Reaction medium; (2) Alkoxide hydrolysis and condensation; (3) The formed sol; (4) BGNP filtration; (5) Addition of calcium nitrate; (6) BGNP filtrations; (7) BGNP freeze drying; (8) Thermal treatment and (9) BGNP powder.

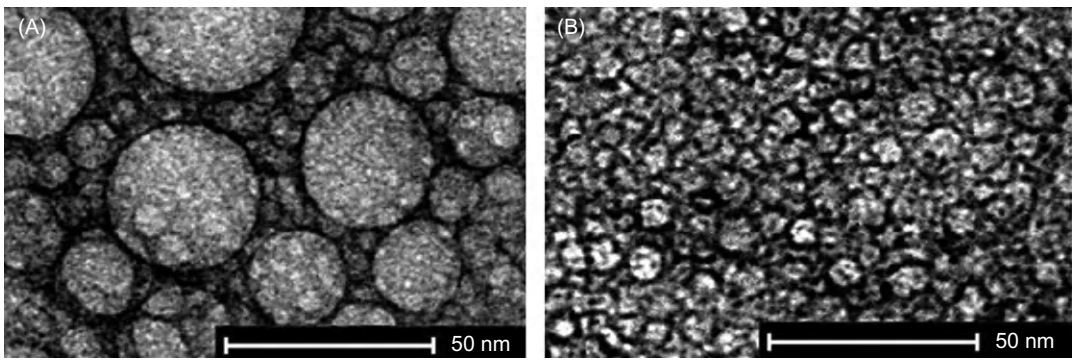

FIGURE 15.2

TEM images of bioactive glass nanoparticles. Images (A) and (B) show the difference between the particle sizes.

dispersed particles with nanometric diameter [26]. In general, the hydrolysis reaction of TEOS can be expressed by the following simple equation [27]:

$$Si(OR)_4 + 2H_2O \rightarrow SiO_2 + 4ROH \quad (15.1)$$

In fact, the controlled hydrolysis process produces the singly hydrolyzed monomer [$(OR)_3Si(OH)$]:

$$Si(OR)_4 + xH_2O + NH_3 \rightarrow (-0)_xSi(OR)_{4-x} + xROH + NH_4^+ \quad (15.2)$$

These intermediate reaction products participate in the condensation reactions, Eqs (15.3) and (15.4), in turn forming silica nanoparticles.

$$Si(OR)_4 + (OH)Si(OR)_3 \rightarrow (OR)_3Si - O - Si(OR)_3 + ROH \quad (15.3)$$

$$(OR)_3Si(OH) + (OH)Si(OR)_3 \rightarrow (OR)_3Si - O - Si(OR)_3 + H_2O \quad (15.4)$$

15.3 Bioactivity of glass nanoparticles

Numerous responses can be observed when a biomaterial comes in contact with living cells and tissues, and these responses depend on the type of material used. If this material is biologically active and induces a specific response, leading to formation of a continuous interface between the material and living tissue, it is called bioactive. Bioactive glasses have this unique feature and when they come in contact with the body, form a layer of carbonated HA on the surface of the material, which permits the interaction of biomaterials especially with mineralized tissue (Figure 15.3).

The complex process of HA formation has been extensively studied in the literature [27]. A sequence of interfacial reactions, which begin immediately after bioactive glass is soaked in simulated body fluid, is interpreted in terms of the electrostatic interaction of the functional groups with the ions in the fluid. The reaction is divided into four steps [9,27,28]:

1. Initially, the surface becomes negative, attributed to the silanols (Si−OH) formed on bioactive glass particles upon being soaked in simulated body fluid, by two mechanisms: (i) The −OH formation occurs due to release of calcium ions (Ca^{2+}) from their surfaces by means of exchange with H_3O^+, Na^+, and K^+ ions in simulated body fluid and (ii) a loss of soluble silica to solution, in $Si(OH)_4$ form, causing the breakdown of Si−O−Si bonds and silanols formation. As a result, many Si−OH groups are formed on their surfaces and a local supersaturation of Ca^{2+} ions is established.
2. As time passes, there occurs a selective combination of OH^- charged surface with the Ca^{2+} ions from the simulated body fluid solution. As the calcium ions accumulate on the surface, the surface gradually gains an overall positive charge.
3. The pH of simulated body fluid solution, where the concentration of HPO_4^{2-} is much larger than that of PO_4^{3-}, favors the incorporation of HPO_4^{2-} ions in the bioactive glass surface and the migration of PO_4^{3-} ions from the bulk to the surface of the glass. The result leads to calcium deficiency, and the surface once again becomes negatively charged.
4. The calcium ions combine with the phosphate ions (PO_4^{3-} and HPO_4^{2-}) and form amorphous calcium phosphates ($Ca_3(PO_4)_2$ and $CaHPO_4$). These calcium phosphates spontaneously transform into the apatite through the incorporation of OH^- and CO_3^{2-} anions from the solution

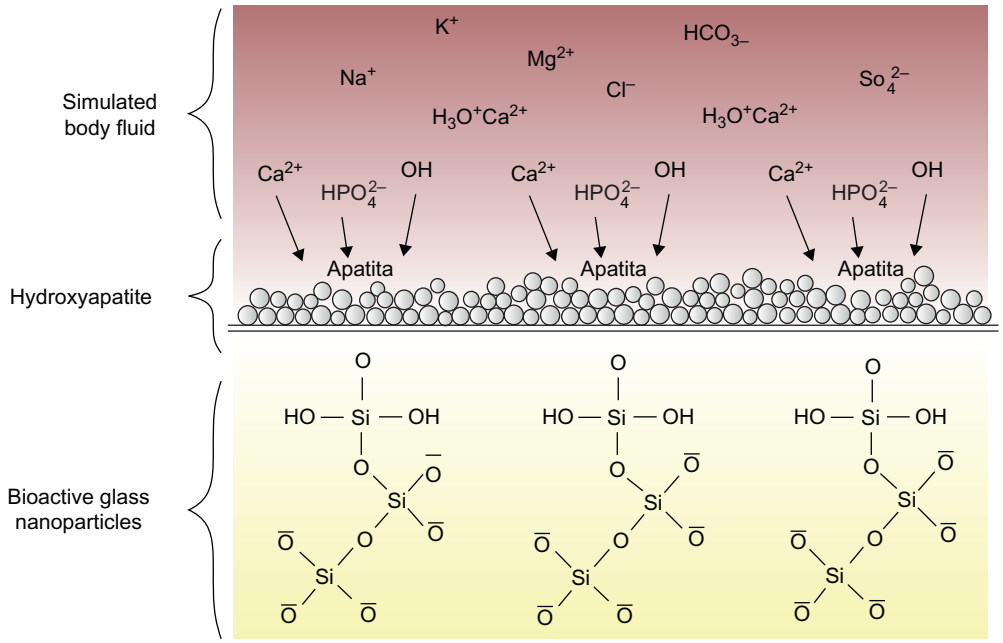

FIGURE 15.3

Schematic drawing of the formation process of hydroxyapatite layer. It shows the formation of hydroxyapatite layer after interaction of the bioactive glass with simulated body fluid.

to form hydroxyl carbonate apatite (HCA) $Ca_5(PO_4CO_3)_3(OH)$ layers. Once apatite nuclei forms, crystals grow by consuming calcium and phosphate ions from the simulated body fluid.

Several in vitro and in vivo studies show that a series of reactions occur that lead to the formation of a carbonated HA layer on the bioactive glass surface (Figure 15.4). Parameters such as surface charge, composition, structure, and morphology will be important in the formation of the Ca/P layer as well as in the interaction between the material surface and the surrounding medium, proteins, and cells [9,28–33].

Several theories have been proposed to explain the formation of this layer. The HA layer is spontaneously formed in the surface of bioactive glass of the $CaO–SiO_2–P_2O_5$ system after exposure to body fluids [27–30,34,35]. Studies have shown that apatite is preferentially formed on a surface material composed mainly of CaO and SiO_2 because the Ca^{2+} ions released from the glass increase the degree of saturation of the apatite in relation to surrounding fluid. In addition, the Si–OH groups of the hydrated silica gel formed on the surface induce a heterogeneous nucleation of apatite. These crystals grow by consuming calcium and phosphate ions from the body fluid and those that migrate from the bulk to the surface of the glass.

Compared with microparticles, bioactive glass nanoparticles have advantages in bone repair and regeneration, with the decrease in grain size promoting an increase in cellular adhesion, enhanced osteoblast proliferation and differentiation, and an increase in the biomineralization process

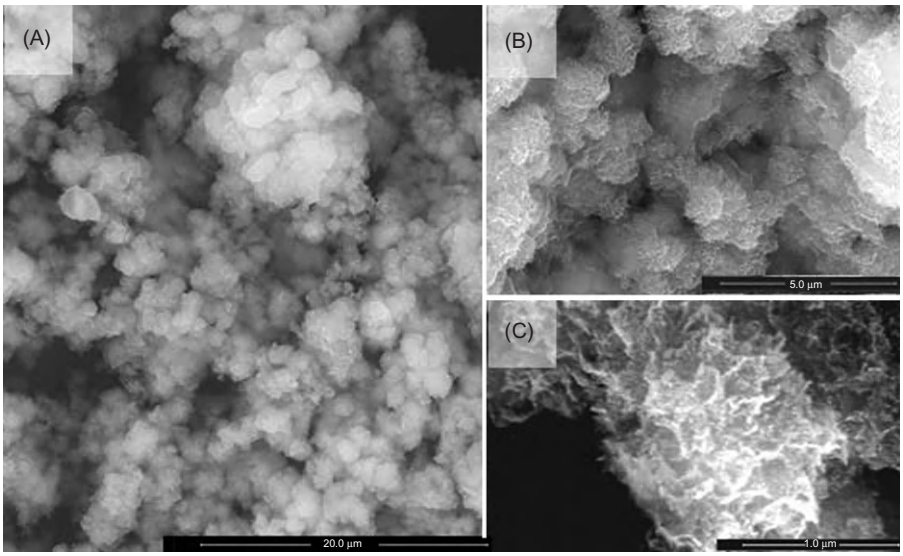

FIGURE 15.4

SEM images of bioactive glass nanoparticles. It shows the formation of the carbonated HA layer on the surface of bioactive glass nanoparticles. Images (B) and (C) are magnifications of image (A).

[36,37]. The use of nanosized particles may provide a means for a more rapid release of Ca and P [15,23] and low negative zeta potential in biological medium, which has important effects in vivo [24] and promotes cell attachment and proliferation [25,26].

Doostmohammadi et al. (2011) studied bioactive glass nanoparticles 63S (<40 nm) produced through the sol-gel method [38]. The small particle size (high surface area) and apatite surface layer suggest that a given mass of these particles will release Ca and P ions and be absorbed faster than the same mass of larger bioactive glass particles. Webster et al. (1999) showed that a significant increase in protein adsorption and osteoblast adhesion could be observed on nanoscale ceramic materials, as compared with microscale ceramic materials [39]. Nanoceramics have been reported to demonstrate enhanced in vitro osteoblast proliferation, osteoblast activity, and long-term functions on particles of size lesser than 100 nm [40,41].

Recently, the concept of biological surface modification has opened new insights into biomaterial engineering. The biological response refers to the ability of the material to directly stimulate cell behavior via proper biochemical signals. Bioactive glasses induce HA precipitation in physiological fluids. Thus, by anchoring to specific surface biomolecules, it is possible to improve tissue regeneration around implants, from both a chemical and biological point of view.

15.4 Bioactive glass in dentistry

Bioactive glasses of the $SiO_2-Na_2O-CaO-P_2O5$ system are of potential interest in dentistry because of their antimicrobial properties [42] and their ability to remineralize dentin [43].

Bioactive glasses are interesting materials for use as bone grafts, implant coatings, bone cements, toothpaste, and various other applications in dentistry.

The application of bioactive glass in dentistry began in the mid-1980s when Dr. Clark, Dr. Stanley, and Dr. Hall tested the bioactive glass and have been successful in preserving the alveolar ridge in edentulous patients. These results have led to regulatory approval for commercial use of Bioglass®. In this decade, not only the pioneer brand Bioglass® but also several new bioactive glass types have been increasingly studied and applied in various areas of dentistry. Perioglass®, for example, is widely used in implant dentistry and periodontics [4].

In the following sections, the impacts and applications in dentistry of this new strategy of development of nanoscale bioactive glasses will be discussed. Further research will be presented and the future of bioactive glass nanoparticles in dentistry will be discussed.

Nanoscale bioactive glasses have been gaining attention due to their reported superior bioactivity when compared with conventional micron-sized bioactive glass materials. There is evidence in the literature of a more rapid mineralization in bones and teeth when in contact with bioactive glass nanoparticles [44].

Evidence shows that surface properties of the bioactive glass may affect cellular response. Bioactive glass on the nanoscale shows excellent properties, such as surface energy, surface wettability, surface topography, and surface chemistry. This improvement is due to the increased surface area of the material at the nanoscale.

The events occurring at the interface of bioactive glass with cells attempt to mimic the natural interaction of cells with extracellular matrix. Biomaterials do not directly interact with living tissue but with a layer of adsorbed proteins such as fibronectin, vitronectin, fibrinogen, collagen, and laminins called soluble proteins of the matrix. Cells recognize proteins of the matrix through a family of cell surface receptors called integrins [45,46]. When these receptors are sensed, they group together and form adhesion complexes that provide anchoring cells to the bioactive glass surface and unleash subsequent cellular responses. Therefore, the initial interaction of the cell material is a complex process that begins with the adsorption of proteins followed by adhesion, spreading, cell differentiation, and ends with the full operation of the cell [46]. So the improvement of surface properties of bioactive glass has a direct influence on the adsorption of specific proteins, thus causing an increase in bioactivity and biocompatibility of the material.

There are several applications for bioactive glass nanoparticles in dentistry; for example, various products with bioactive glass nanoparticles have been developed to control the formation of oral biofilm, such as toothpaste and mouth rinses. These products are designed to decrease bacterial adhesion thereby reducing the formation of biofilms. Although bioactive glasses have been used in bone regeneration for many years, only recently studies on their antimicrobial properties have gained focus.

A further application of the antibacterial properties of bioactive glass nanoparticles is in the endodontic area. Disinfection of a complex root canal system is essential for long-term success in endodontics. However, even after the chemical and mechanical treatment of the channels is sometimes impossible to achieve complete disinfection. Microbiological studies have demonstrated the presence of resistant microorganisms such as *Enterococcus faecalis* and *Candida albicans* in persistent infections of the channel. Microorganisms remaining in the root canals are the major cause of treatment failure in the root canal. An ideal drug for endodontic treatment should achieve a wide-spectrum antimicrobial, be biocompatible, be able to reduce inflammation, and induce repair of mineralized tissue [47–50].

Calcium hydroxide, originally designed as a channel disinfectant and filler material by Hermann in 1920, remains a topical antiseptic widely used. The suspension of calcium hydroxide releases Ca ions that results in alkalinization of the environment. Similarly, the antibacterial properties of bioactive glasses are based on the potential of increasing the pH in aqueous suspensions [51] resulting from the exchange of sodium ions and protons of the glass matrix in an aqueous environment [52].

The broad-spectrum antimicrobial effect of bioactive glass in different oral microorganisms has been reported, which justifies its use as an intracanal medication endodontic therapy [42]. The increase in specific surface area of bioactive glass nanoparticles improves the area of active release of ions, resulting in the improvement of antibacterial properties of the material. *E. faecalis* is one of the more resistant microorganisms in endodontic therapy and is often associated with treatment failure. However, research has shown that particles of 20−50 nm bioactive glass increased antibacterial properties against *E. faecalis* in direct contact model [43].

Bioactive glasses are known for osteoconductivity and bonding to bone through the release of ions and formation of a layer of apatite [53]. Because of these characteristics, bioactive glasses are widely used for bone reconstruction and tissue engineering, but are also interesting candidates for the mineralization in dentistry. In the past decades, bioactive glass nanoparticles have been used on studies about the specific effects of remineralization of dentin, due to their excellent regenerative properties in mineralized tissues.

Dentin is a permeable tubular structure representing most of the dental tissue composed of the organic matrix embedded in a crystalline matrix of apatite, having about 70% of apatite, 20% of collagen, and 10% of water. Although there is a physiological balance between demineralization and remineralization of dental hard tissues in the oral cavity, some factors such as an acidic diet or the presence of plaque can cause disequilibrium, which results in tooth demineralization.

Several studies suggest that bioactive glass has potential as an agent of dentin mineralization and restorative filling [54,55]. As explained above, bioactive glass when in contact with body fluids interacts with the environment, releasing ions and subsequently forming a layer of apatite. Saliva is also a body fluid that will stimulate the interaction of bioactive glass with the environment and release of ions and the formation of apatite. However, the mineralization process is long, which impedes the use of bioactive glass in dental practices. A possible acceleration of this process is the use of bioactive glass nanoparticles, since the high specific surface area of the nanoparticles may facilitate the dissolution of ions from the glass and thus accelerate the dentin mineralization [10]. Vollenweider et al. (2007) showed that after treatment with bioactive glass nanoparticles for 30 days, there was a pronounced increase in the mineral content of the dentin samples [53]. In addition, bioactive glass nanoparticles can be used in minimally invasive cavity preparation teeth. However, it is still necessary to create alternatives that allow effective use of bioactive glass nanoparticles in this procedure.

Another application of the ability of remineralization of bioactive glass is related to the dentin sensitivity. Dentin hypersensitivity is characterized by sharp, localized, non-spontaneous pain occurring in response to some stimulus. This pain is caused by loss of the tooth structure, resulting in exposure of dentinal tubules to the oral environment. The currently accepted theory for hypersensitive dentin is the hydrodynamic theory, which proposes that external stimuli such as cold, hot, pressure, or tactile when applied to exposed dentin causes movement within the dentinal tubules [56]. This movement of fluid stimulates mechanoreceptors near the dentinal tubule and can trigger a pain response. This theory is based on the understanding that open tubules allow fluid flow through the tubules, which results in pressure changes that excite the nerve endings in the tooth

pulp. Therefore, it is coherent with the observation that occluded tubules can treat and reduce dentinal sensitivity [55,57,58]. Occlusion of dentinal tubules is an approach currently used in the treatment of dentin hypersensitivity, and numerous products using active ingredients may occlude the dentinal tubule. Although there are advantages on the use of products in terms of availability and cost to the consumer, a great disadvantage is the time. They may take up to 2–4 weeks for efficacy of the relief symptoms [58].

The majority of the bioactive glasses used today are based on the original composition developed by Hench et al. [4]. Silica is the key component of bioactive glass, and acts as a nucleation site for the precipitation of calcium and phosphate ions in the formation of HA. Research indicates that bioactive glass nanoparticles induce formation of apatite in dentin, indicating that it is a potential material to be used for the treatment of dentin hypersensitivity. The occlusion of dentin tubules may reduce or eliminate hypersensitivity by restricting dentinal fluid movement. This process of remineralization of dentin tubes is quicker when using products with bioactive glass nanoparticles, since the larger surface area associated with nanoscale particles leads to a more efficient ion release (Figure 15.5).

As previously mentioned, bioactive glasses are widely used for bone restoration; therefore, there are several studies about its application in oral and craniofacial surgery. Every year, millions of people worldwide suffer bone loss in the region of the face resulting from trauma, tumor, or bone diseases. Bone grafting procedures are required frequently in oral and maxillofacial surgery. One of the traditional bone-filling treatments is the autograft using autogenous materials. The autogenous bone appears as an excellent biological alternative. However, the need for a donor site and a surgical procedure represent additional factors that can limit their use.

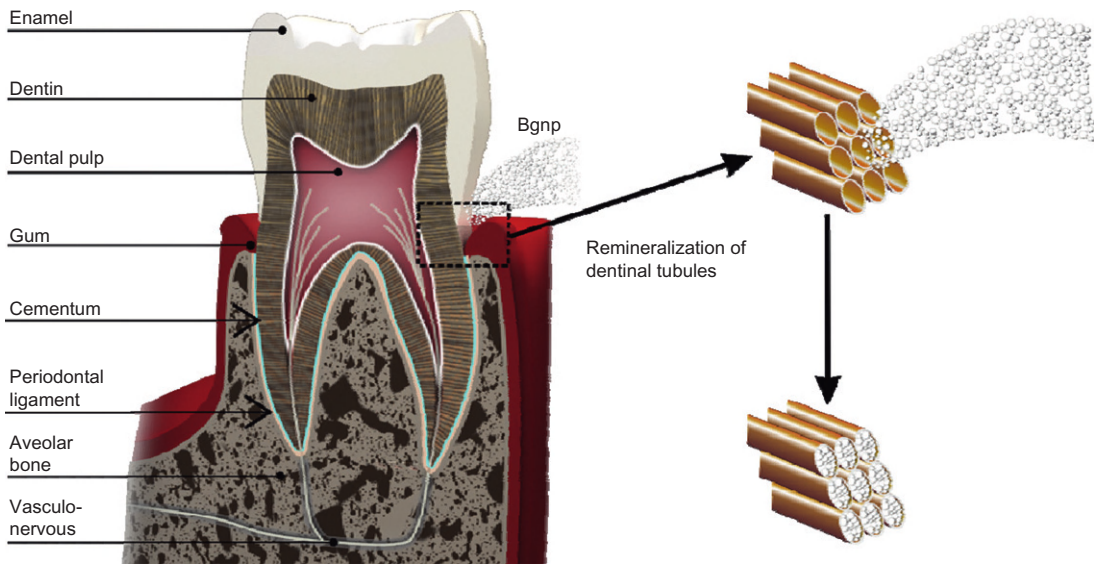

FIGURE 15.5

Schematic drawing of treatment of dentinal hypersensitivity. It shows the mineralization of dentinal tubules after treatment with bioactive glass nanoparticles.

Another procedure is allograft, which is made between different individuals of the same species. However, this procedure also has limitations such as need for donors and the possible transmission of antigenic proteins among others. Another alternative that has been widely used is the use of alloplastic material, and among them bioactive glass is one of the most researched.

Bone tissue is a complex of organic and inorganic materials organized in a global architecture of several length scales, including the nanoscale. Therefore, the applications of glass nanoparticles in bone grafts have the dual aim of improving the mechanical properties as well as incorporating nanotopographic features that mimic properties of bone.

The purpose of tooth replacement is the restoration of function and esthetics without affecting the mineralized structures and soft tissues of the oral cavity. One of the challenges in implantology is to achieve and maintain the osseointegration as well as the epithelial junction of the gingival tissue with implants [59]. Bone regeneration is required for many clinical issues in the dental area. The autogenous graft is always a choice, but sometimes the host tissue is thin and cannot be modeled with the desired shape.

Metals and alloys have wide application in the area of implant dentistry, and the most commonly used are titanium alloys. Titanium implants have excellent mechanical properties, but do not exhibit bioactivity; that is, they are not capable of binding to the living tissue. Unlike them, bioactive glasses are able to cause specific biological responses. Therefore, coating of implants with bioactive glasses is a way to combine good titanium mechanical properties and bioactivity of the glasses. Various techniques for surface treatment are applied to modify the surface of titanium.

Many studies have shown that implants coated with bioactive glasses have a higher rate of integration and increased bone fixation, faster when compared with uncoated implants [60,61]. Development of new technologies is also very important to improve the properties and applications of biomaterials. Application of bioactive glass coatings using nanoparticles is a promising alternative for increasing the interaction of glass with the implant surface.

The bioactive glass material is one of the most studied and widely used to treat bone periodontal defects due to its bioactive properties, so in the next section this topic will be discussed more extensively.

15.5 Bioactive glass nanoparticles in periodontal regeneration

Periodontium is a complex structure, consisting of epithelial tissue (gum) and connective (periodontal ligament) and mineralized tissue (cementum and alveolar bone) (Figure 15.6). To achieve success in periodontal therapy, the sealing of the junctional epithelium, the insertion of new connective tissue fibers, the formation of new cementum, and the alveolar bone restoration are needed. The main aims of periodontal therapy are to eliminate the disease by infection control and correct anatomical defects through regeneration of the tissues supporting the teeth.

Although Hench started to develop bioactive glass in 1969, only from the 1990s that material was first applied in studies ‘in vivo’ in periodontal lesions. These studies evaluated histological efficacy of bioactive glass, and the results were positive compared with conventional treatments [62]. At this time, bioactive glass was clinically approved for use both in dense form—for

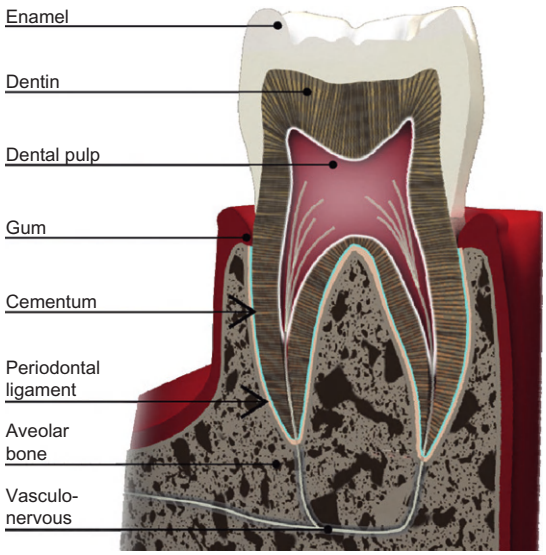

FIGURE 15.6

Structures forming part of the organ dental and periodontal tissue.

application as middle ear prostheses and as bone implants for alveolar ridge maintenance after extraction—and in particulate form, for the treatment of periodontal bone defects [63,64].

Based on these studies, bioactive glasses have been widely applied in dentistry for the treatment of periodontal defects, probably due to its properties of bone formation by osteoconduction and osteoinduction. The clinical use of bioactive glass in the particulate form of the brand Perioglass® has shown, over the years, positive results, with a good adaptation to the bone defects and maintaining a good clot. Several studies and clinical reports indicate the glass as a material of easy handling with excellent bioactivity and biocompatibility. Histological studies show that the use of bioactive glasses can induce formation of new cementum and the formation of a new insertion [63].

Schepers et al. (1991) also showed that bioactive glass particles have the property of stimulating the formation of bone tissue in the treatment of bone lesions created surgically in the jaws of dogs [65]. In a histological study conducted in the tibia of rabbits, MacNeill et al. (1999) confirmed the study of Schepers et al. (1991) [66].

Studies in humans evaluated the use of bioactive glass compared with the scrape surgery in the treatment of intrabony periodontal defects. Results demonstrated significant clinical improvements, such as an increase in radiographic density and a decrease in probing depth [62].

Some clinical studies have shown beneficial effects of using platelet-rich plasma (PRP) associated with bioactive glass in periodontal therapy. Periodontal regeneration involves a complex series of events, and the recruitment of progenitor cells to the injured site and growth factors are vital during this process. These factors are responsible for the migration, proliferation, and differentiation of periodontal progenitor cells. PRP is derived from a platelet concentrate that contains high concentrations of growth factors. Some studies have encouraged the association between the use of PRP with bioactive glass for periodontal regeneration [67].

In recent decades, there is an advance in the study of new therapies for complete periodontal regeneration. Regenerative procedures are forms of treatment aimed to reconstruct the lost structure or damaged periodontal tissue. The periodontal regeneration involves a sequence of biological events including adhesion, migration, proliferation, and differentiation [68,69]. Numerous methods of therapies have been tested to achieve periodontal regeneration.

The complete regeneration of periodontal tissues has not yet been achieved, but significant progress has been achieved through the use of autogenous bone grafts, bone allografts, guided tissue regeneration (GTR), the implantation of alloplastic materials, and use of cellular factors.

Autogenous bone grafts are transplanted from one place to another in the same individual. Because of their osteogenic potential, autogenous bone grafts have been widely used in periodontal therapy. They can be from intra- or extra-oral sources. However, the necessity of a second surgical site, which can complicate post-surgery, is a disadvantage that has been associated with their use.

Allografts are transplanted between genetically different individuals of the same species. Iliac bone marrow, lyophilized bone graft, freeze-dried bone allograft (FDBA), and decalcified FDBA are the types of bone allografts widely available in commercial tissue banks [70]. However, despite the approval of bone tissue banks, the real osteogenic potential of these transplants is questionable.

In dentistry, GTR is often used in the reconstruction of periodontal defects. GTR technique is based on the use of biocompatible membranes in order to prevent accelerated migration of the epithelium to the injured site, and allows conditions for the regeneration of all periodontal attachment apparatus. The use of GTR has shown favorable results on the periodontal regeneration when applied in some specific kinds of bony defects. It is used in different types of barriers, such as membranes, expanded polytetrafluoroethylene, collagen [71], cellulose, and polylactic acid [72–74].

Although polymeric products show positive results, there are still major challenges to overcome in their use in periodontal regeneration. Research attempting to overcome these challenges include the use of ceramic nanoparticles, and among them, bioactive glass nanoparticles incorporated into GTR membranes are of particular interest because they induce a significant increase in cellular uptake and cell adhesion compared with bioactive glass microscale [75,76].

Alloplastic materials are synthetic, bioactive, and biocompatible, and may act as a substitute for living tissue. Recently, bioactive materials have shown to be an excellent alternative for periodontal structure regeneration, stimulating the infiltration of responsive cells, promoting cell differentiation, and formation of bone tissue. Research shows that the bioactive materials are capable of stimulating periodontal healing. Among these materials, bioactive glass has been widely researched in periodontal regeneration.

As mentioned previously, bioactive glass nanoparticles have been widely studied due to its superior bioactivity compared with conventional bioactive glasses. So this justifies the development of new systems with bioactive glass nanoparticles that can be used in the periodontal regeneration.

Cell therapy for periodontal regeneration is a new option; studies suggest that periodontal ligament consists of different cells in various stages and that these cells when necessary may differentiate into cementoblasts, osteoblasts, or fibroblasts of the periodontal ligament [77]. The discovery of these called progenitor cells suggests the possibility of repair of damaged periodontal tissue.

Recent studies have shown that periodontal ligament cells in direct contact with bioactive glass nanoparticles exhibited increased proliferation and cell viability and also an increase in alkaline phosphatase activity [78] (Figure 15.7).

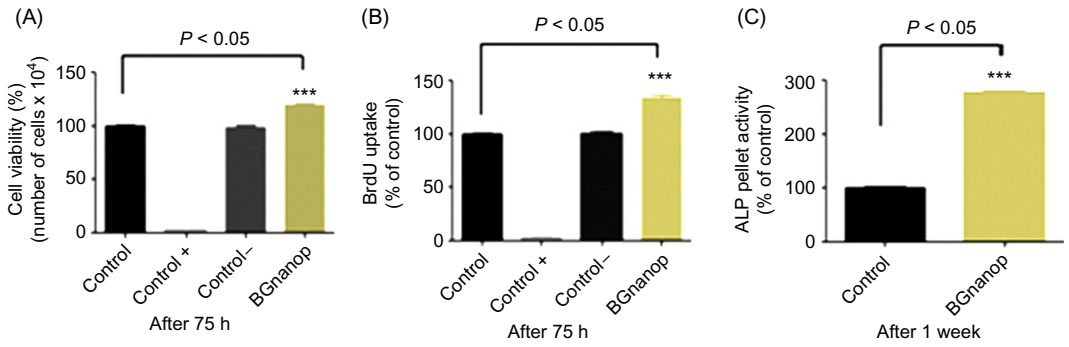

FIGURE 15.7

Cell viability, cell proliferation, and alkaline phosphatase activity. A significant increase in cell viability, cell proliferation, and ALP activity was observed in the presence of bioactive glass nanoparticles when compared with the control group.

Another study examined the behavior of cementoblasts in contact with the bioactive glass nanoparticles, and it also demonstrated an increase in cell viability and proliferation [79]. Together, these results show that the bioactive glass nanoparticles are capable of inducing cell proliferation of periodontal ligament, especially cementoblast, indicating that it is a potential material for use in periodontal tissue regeneration by tissue engineering (Figure 15.8).

15.6 Bioactive glass nanocomposites

The combination of biodegradable polymers and bioactive ceramic creates a new type of material for tissue engineering applications. The association of ceramic and polymeric materials has been used to produce composites in order to create materials with special properties that do not exist in the isolated materials. The aim of these composite materials is to improve strength and bioactivity given by the inorganic component while maintaining the polymer properties such as flexibility. However, to maximize interaction between the components of the composite, increasing the number of surfaces and interfaces is required. From this observation arose the concept of development of nanocomposites.

The particle size of the inorganic phase is an important parameter that affects the mechanical properties of composite materials. The introduction of filler materials at the nanoscale usually increases the strength and stiffness of composites, as compared with the properties of the pure polymer or composites.

Nanocomposites can be developed by several ways: (i) a combination of polymers and inorganic phase, (ii) a combination of functionalized copolymers and an inorganic phase, (iii) a precipitation of nanoparticles in the polymer phase, among others.

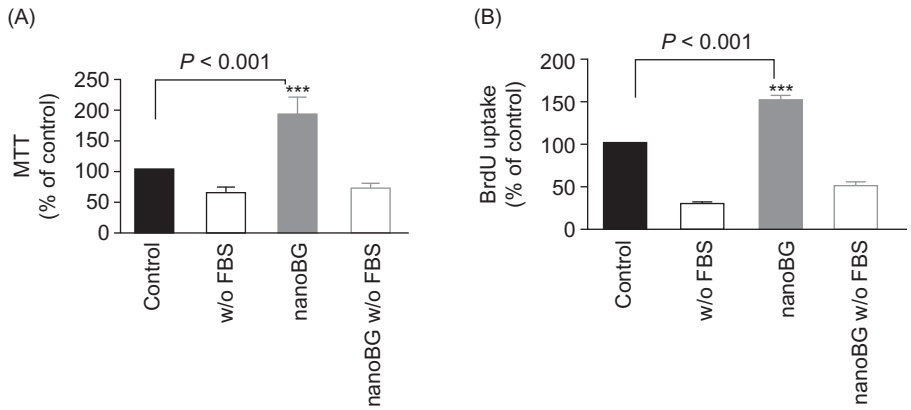

FIGURE 15.8

Cell viability and cell proliferation. The MTT assay and cell proliferation BrdU assay were used to evaluate the behavior of cementoblasts in direct contact with particles. A significant increase in cell viability and cell proliferation in the presence of bioactive glass nanoparticles was observed when compared with the control group.

Bioactive glasses, especially when processed as porous scaffolds, have inferior mechanical properties. In particular, the low toughness values limit their use in situations where there is a load application. Different concepts for the structural design of composites have been proposed to overcome the inherent fragility of bioactive glasses, and advances in nanotechnology have stimulated the creation of composite biomaterials with improved properties and functions.

One approach to improve the mechanical properties of the bioactive glass is the production of organic/inorganic hybrid in which an inorganic phase, with nanometric dimensions, is inserted into a polymeric matrix. The sol-gel process is potentially useful in enabling the combination of polymers with ceramic materials at the nanometer scale. It allows for the preparation of ceramic materials at temperatures compatible with the polymer processing. Bioactive glass composites have been developed based on this strategy [8,16,19,80–85].

The use of bioactive glass nanoparticles in a polymer matrix mimics the structure of natural bone, which contains nano-scaled-size HA cristallites. Webster et al. (2001) reported a significant increase in protein adsorption and osteoblast adhesion on ceramic nanocomposites in comparison with ceramic microcomposites [76].

Several synthetic or natural polymers, such as polyvinyl alcohol (PVA), chitosan, polyethylene glycol (PEG), gelatin, collagen, poly(caprolactone) (PCL), and polyurethanes, are used to construct nanocomposites for tissue engineering applications. Biopolymers have the advantage of being biodegradable and present similar structure to the extracellular matrix components. The polymer phase plays a fundamental role in the final properties of the composite.

Misra et al. (2008) reported the successful preparation of poly(3hydroxybutyrate) (P(3HB))/bioactive glass nanoparticle composite. The addition of nanoparticles has shown a significant effect on the mechanical properties of the material. Moreover, they demonstrated in vitro degradation (30 days) in simulated body fluid and an increase in bioactivity [86].

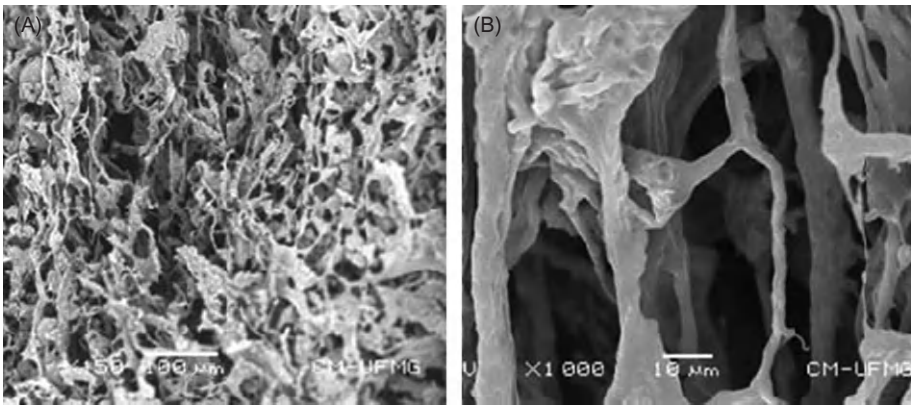

FIGURE 15.9

SEM image of composite scaffold PU/PVA/bioactive glass nanoparticles: (A) the structure of the nanocomposite with 2% of bioactive glass nanoparticles and (B) magnification of image.

Oliveira et al. (2011) synthesized and characterized bioactive glass nanoparticles/polyurethane nanocomposites for tissue engineering applications. The materials presented good cell viability and HA layer formation upon immersion in simulated body fluid [16] (Figure 15.9). Currently, there is great interest in materials with biodegradable polyurethanes for use in medical and dental areas because of its versatility and biocompatibility. Pereira et al. (2009) developed polyurethane/montmorillonite nanocomposite to function as membrane for GTR to treat periodontal disease. The composition, morphology, and mechanical properties of the biomaterials were evaluated. The cellular viability, proliferation, and morphology changes of rat culture cementoblasts were also investigated.

El-Kady et al. (2010) developed scaffolds of nanocomposite bioactive glass/poly(L-lactide) by sol-gel method. The addition of bioactive glass nanoparticles improved the bioactivity of the material in vitro. Marelli et al. (2011) developed composites scaffolds of nanofibrillar collagen with bioactive glass nanoparticles for use in bone tissue engineering [87]. Therefore, those nanocomposites of bioactive glass have the potential to be applied in tissue engineering.

15.7 Bioactive glass nanocomposite applications in bone regeneration and dental implants

Several natural and synthetic materials or a combination of them are being developed for tissue engineering in dentistry. Among the natural polymers, chitosan has been widely studied for applications in dentistry. Chitosan is a biopolymer (polysaccharide) derived from partial deacetylation of chitin. Chitin is a polysaccharide found abundantly in nature and which constitutes the exoskeletons of insects and crustaceans. Chitosan is considered as an appropriate functional material for biomedical applications because of its high biocompatibility, biodegradability, and antibacterial properties. Due to its antibacterial properties [9], chitosan becomes a material suitable for the design of scaffolds for the regeneration of the alveolar bone since these areas are highly susceptible to bacterial infection [88,89].

Peter et al. (2010) developed chitosan-gelatin/bioactive glass nanoparticles composite scaffolds for alveolar bone tissue engineering. Studies of mineralization had higher amounts of mineral deposits in the nanocomposite scaffold. Cell viability assays with osteoblast lineage showed the biocompatibility of the material, indicating that the material has the potential for alveolar bone regeneration applications [80].

Sowmya et al. (2011) synthesized and characterized β-chitin hydrogel/bioactive glass nanoparticles nanocomposite scaffolds for periodontal regeneration. The porosity, swelling, degradation 'in vitro', biomineralization, toxicity, cell attachment, and cell proliferation were evaluated. The nanocomposite scaffolds were found to be satisfactory in all aspects. Therefore, these nanocomposites are promising candidates for the treatment of periodontal lesions [90].

Another application of nanocomposites is the coating of dental implants. Current research focuses on improving the mechanical performance and biocompatibility of Ti-based systems through variations in alloy composition, microstructure, and surface treatment. A method that allows changing the biological properties of Ti alloy is a modification of the chemical composition. Surface modification methods such as chemical etching and coating by plasma spraying are often used to improve the ability of osseointegration of titanium dental implants [91,92].

Another method that may allow a change in biological properties of Ti alloy is the development of a nanocomposite Ti/bioactive glass, which will combine the favorable mechanical properties of titanium and the excellent biocompatibility and bioactivity of the glass [64]. Jurczyk et al. (2011) synthesized and characterized nanocomposite Ti/45S5 Bioglass for use in dental implants [93].

In summary, there are several points that favor the use of nanocomposites of bioactive glass in dentistry, including best cellular response, biocompatibility, and bioactivity.

15.8 The future of bioactive glass nanoparticles in dentistry

Nanotechnology has as a principle the ambitious challenge to precisely control individual particles in the nanometer range. Some of these results, relevant and of great impact on human life, are already in use in modern dentistry, helping in the recovery of the smile of people in need of oral rehabilitation.

The dental regenerative medicine results from the integration of several appropriate areas such as cell biology, molecular genetics, and materials engineering. Recent advances in dental tissue engineering, materials science, and cell culture suggest that in the near future the total regeneration of the teeth will not be a utopian concept but can become a reality [94,95].

The understanding of mechanisms involved in wound healing and tissue formation, together with recent advances in materials science and stem cell research, are helping to find the ways that lead to tissue regeneration. More and more evidence has shown that regeneration of affected dental tissues is becoming possible, and this breakthrough can be developed for use in future clinical treatments. Progress in research on regeneration in the dental field coincides with the advancement of tissue engineering. This multidisciplinary field aims to regenerate tissues and organs that have been injured or lost due to trauma, cancer resection, congenital deformities, or degenerative diseases.

The concept of tissue regeneration depends on the development of biomimetic materials, growth factors, and sources of specific cells that can regenerate lost tissues. Therefore, it is an ideal that, in

the future, tissue engineering can provide a variety of products such as stem cells, smart scaffolds, and growth factors for clinical therapies in dentistry.

In this context, new and different conceptions of nanostructured materials have been developed for use in the dental field. An interesting alternative for use in tissue engineering is the development of injectable systems containing bioactive glass nanoparticles. Smart materials that respond to specific stimuli have been extensively described in literature. In particular, the hydrogel polymer systems have many advantages: (i) They have adequate permeability for the transport of cell nutrients and metabolites, (ii) they exhibit biocompatibility and biodegradability, and (iii) some formulations are thermoresponsive. These bioactive gelling systems can be used as injectable materials for small bone defects, and may also be combined with three-dimensional scaffolds to enhance mechanical properties (Figure 15.10).

Couto et al. (2009) developed and characterized an injectable system containing bioactive glass nanoparticles [96]. This system could be used, for example, in periodontal bone lesions where cells and cellular factors could be injected directly into the periodontal tissue.

Another approach for the bioactive glass nanoparticles is their use in systems for drug delivery. Bioactive glasses have ideal characteristics for these systems; they can carry an active dose of drug molecules to target sites without any leak and premature negative effect on other areas. Generally, high specific surface area and high porosity are prerequisites for drug delivery systems.

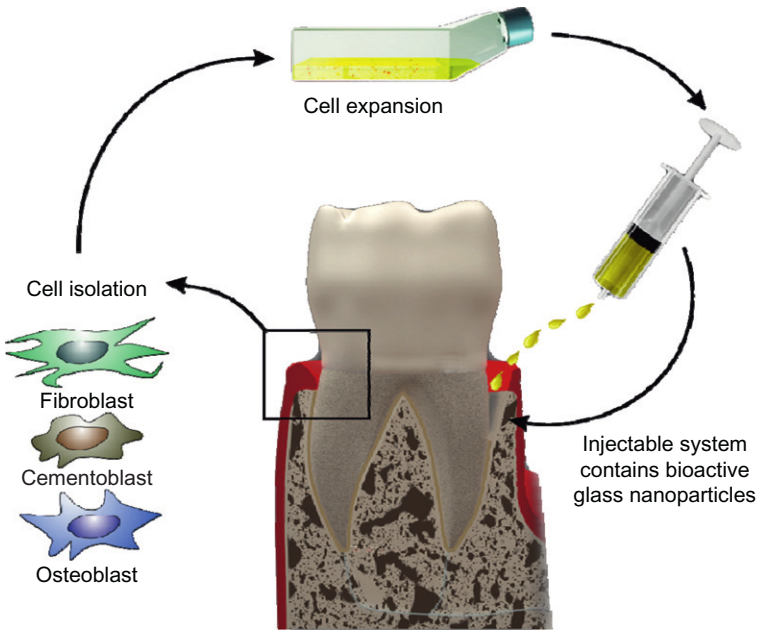

FIGURE 15.10

Schematic representation of injectable system. The figure shows cells removed from the periodontal tissue, expanded and injected into the injured tissue.

The functionalization of the system can also be performed using metal nanoparticles such as gold, copper, and silver. These systems can act as therapeutic agents directly or carry biologically active molecules. An indication of use of these systems in dentistry is the treatment of head and neck tumors that needs controlled release of drugs at specific sites [97–99]. Bonici et al. (2012) synthesized and characterized bioactive glasses functionalized with Cu nanoparticles and organic molecules for use in drug delivery systems [99].

Recent decades have seen the development of regenerative therapies based on stem cells and molecular factors. Tissue regeneration is oriented by stimulus and regulatory factors such as different growth factors and extracellular matrix of the molecular factors that promote specific responses to the target cells.

As mentioned above, the bioactive glass because of its bioactivity has been responsible for increasing the proliferation and differentiation of osteoprogenitor cells. Understanding the role of growth factors, their mechanisms of action, and molecular signaling pathways suggest the way stem cells could be used as regenerative therapeutics in dentistry.

Bioactive glasses at the nanoscale are emerging as a powerful approach of last generation of bioactive materials for applications in dentistry. There are substantial advantages of such systems compared with the conventional scale, allowing the use of these materials in more sophisticated applications.

15.9 Conclusions

The use of nanotechnology in tissue engineering expands continuously, but pragmatic challenges have hampered the clinical use of emerging nanobiomaterials. Many research groups are active in this area to increase the versatility of this technology. On the other hand, the increase in the development of new devices in the dental field and its regenerative applications require a thorough analysis of how they can be assessed before clinical use in humans. The progress in dental therapy using nanobiomaterials strongly depends on the selection of a preclinical model suitable to evaluate the safety and efficacy of therapies in humans.

The scientific challenge of tissue engineering involves the understanding of cellular mechanisms as well as the development of appropriate biomaterials that act as supports for adhesion, migration, and cell proliferation.

Bioactive glass nanoparticles have shown advantages over (micron-sized) conventional glass due to their large surface area and increased bioactivity. These nanomaterials inspired researchers to investigate new routes of synthesis and applications in tissue engineering. However, many tests are still needed in vivo to complete clinical validation of these materials.

Acknowledgments

The authors are grateful to Rodolfo Cunha Santos for his contribution to the preparation of figures and authors are also grateful to CNPq for the financial support.

References

[1] L.L. Hench, Bioceramics and the origin of life, J. Biomed. Mater. Res. 23 (1989) 685–703.

[2] V. Mourino, A.R. Boccaccini, Bone tissue engineering therapeutics: controlled drug delivery in three-dimensional scaffolds, J. R. Soc. Interface 7 (2010) 209–227.

[3] F. Balas, M. Kawashita, T. Nakamura, T. Kokubo, Formation of bone-like apatite on organic polymers treated with a silane-coupling agent and a titania solution, Biomaterials 27 (2006) 1704–1710.

[4] L.L. Hench, The story of Bioglass, J. Mater. Sci. Mater. Med. 17 (2006) 967–978.

[5] T.J. Webster, C. Ergun, R.H. Doremus, R.W. Siegel, R. Bizios, Enhanced functions of osteoblasts on nanophase ceramics, Biomaterials 21 (2000) 1803–1810.

[6] T.J. Webster, C. Ergun, R.H. Doremus, R.W. Siegel, R. Bizios, Specific proteins mediate enhanced osteoblast adhesion on nanophase ceramics, J. Biomed. Mater. Res. 51 (2000) 475–483.

[7] T.A. Ostomel, Q. Shi, C.K. Tsung, H. Liang, G.D. Stucky, Spherical bioactive glass with enhanced rates of hydroxyapatite deposition and hemostatic activity, Small 2 (2006) 1261–1265.

[8] M.M. Pereira, J.R. Jones, R.L. Orefice, L.L. Hench, Preparation of bioactive glass-polyvinyl alcohol hybrid foams by the sol-gel method, J. Mater. Sci. Mater. Med. 16 (2005) 1045–1050.

[9] T. Kokubo, H.M. Kim, M. Kawashita, Novel bioactive materials with different mechanical properties, Biomaterials 24 (2003) 2161–2175.

[10] T.J. Brunner, R.N. Grass, W.J. Stark, Glass and bioglass nanopowders by flame synthesis, Chem. Commun. (Camb.) (2006) 1384–1386.

[11] G.H. Bogush, C.F. Zukoski, The kinetics of the precipitation of uniform silica particles through the hydrolysis and condensation of silicon alkoxides, J. Colloid Interface Sci. 142 (1991) 1–18.

[12] D.L. Green, J.S. Lin, Y.F. Lam, M.Z. Hu, D.W. Schaefer, M.T. Harris, Size, volume fraction, and nucleation of Stober silica nanoparticles, J. Colloid Interface Sci. 266 (2003) 346–358.

[13] W. Xia, J. Chang, Preparation and characterization of nano-bioactive-glasses (NBG) by a quick alkali-mediated sol-gel method, Mater. Lett. 61 (2007) 3251–3253.

[14] Z. Hong, R.L. Reis, J.F. Mano, Preparation and in vitro characterization of novel bioactive glass ceramic nanoparticles, J. Biomed. Mater. Res. A 88 (2009) 304–313.

[15] W. Stöber, A. Fink, E. Bohn, Controlled growth of monodisperse silica spheres in the micron size range, J. Colloid Interface Sci. 26 (1968) 62–69.

[16] A.A.R. Oliveira. New method to obtain bioactive glass nanoparticles, biodegradable polyurethanes and their composites for biomedical applications. Tese de doutorado. Universidade Federal de Minas Gerais, Belo Horizonte, Minas Gerais, Brasil (2011). English version avaliable online at http://www.ppgem.eng.ufmg.br/tese_detalhes.php?aluno=1016.

[17] X. Chen, B. Lei, Y. Wang, N. Zhao, Morphological control and in vitro bioactivity of nanoscale bioactive glasses, J. Non-Cryst. Solids 355 (2009) 791–796.

[18] S. Labbaf, O. Tsigkou, K.H. Muller, M.M. Stevens, A.E. Porter, J.R. Jones, Spherical bioactive glass particles and their interaction with human mesenchymal stem cells in vitro, Biomaterials 32 (2011) 1010–1018.

[19] A.M. El-Kady, A.F. Ali, M.M. Farag, Development, characterization, and in vitro bioactivity studies of sol-gel bioactive glass/poly(L-lactide) nanocomposite scaffolds, Mater. Sci. Eng. C 30 (2010) 120–131.

[20] C.J. Brinker, G.W. Scherer, The Sol-Gel Science the Physics and Chemistry of Sol-Gel Processing, Academic Press, ISBN 0-12-134970-5, 1990.

[21] Z. Hong, R.L. Reis, J.F. Mano, Preparation and in vitro characterization of scaffolds of poly(L-lactic acid) containing bioactive glass ceramic nanoparticles, Acta Biomater. 4 (2008) 1297–1306.

[22] Z. Hong, E.G. Merino, R.L. Reis, J.F. Mano, Novel rice-shaped bioactive ceramic nanoparticles, Adv. Eng. Mater. 11 (2009) 25–29.

[23] M. Hosokawa, K. Nogi, M. Naito, T. Yokoyama, Nanoparticle Technology Handbook, Elsevier, ISBN 9780444531223, 2007.
[24] K.S. Rao, K. El-Hami, T. Kodaji, K. Matsushige, A novel method for synthesis of silica nanoparticles, J. Colloid Interface Sci. 289 (2005) 125–131.
[25] X.-D. Wang, Z.-X. Shen, T. Sang, X.-B. Cheng, M.-F. Li, L.-Y. Chen, et al., Preparation of spherical silica particles by Stöber process with high concentration of tetra-ethyl-orthosilicate, J. Colloid Interface Sci. 341 (2010) 23–29.
[26] J.S. Park, H.J. Hah, S.M. Koo, Y.S. Leea, Effect of alcohol chain length on particle growth in a mixed solvent system, J. Ceram. Proc. Res. 7 (1) (2006) 83–89.
[27] M.M. Pereira, L.L. Hench, Mechanisms of hydroxyapatite formation on porous gel-silica substrates, J. Sol-Gel Sci. Technol. 7 (1996) 59–68.
[28] T. Kokubo, H. Kushitani, C. Ohtsuki, S. Sakka, Chemical reaction of bioactive glass and glass-ceramics with a simulated body fluid, J. Mater. Sci.: Mater. Med. 3 (1992) 79–83.
[29] P. Ducheyne, P. Bianco, S. Radin, E. Schepers, Bioactive materials: mechanisms and bioengineering considerations, in: Bone Bonding, Reed Healthcare Communications, 1992, pp. 1–12.
[30] P. Li, C. Ohtsuki, T. Kokubo, K. Nakanishi, N. Soga, K. De Groot, The role of hydrated silica, titania, and alumina in inducing apatite on implants, J. Biomed. Mater. Res. 28 (1994) 7–15.
[31] H. Lu, S.R. Pollack, P. Ducheyne, Particle electrophoresis of 45S5 bioactive glass particles in simulated physiological electrolyte solutions, Proc. Surf. Biomater. 24 (1995).
[32] K. Yamashita, N. Oikawa, T. Umegaki, Acceleration and deceleration of bone-like crystal growth on ceramic hydroxyapatite by electric poling, Chem. Mater. 8 (1996) 2697–2700.
[33] M. Ueshima, S. Nakamura, K. Yamashita, Huge, millicoulomb charge storage in ceramic hydroxyapatite by bimodal electric polarization, Adv. Mater. 14 (2002) 591–594.
[34] M.M. Pereira, A.E. Clark, L.L. Hench, Homogeneity of bioactive sol-gel derived glasses in the system SiO2-CaO-P2O5, J. Mater. Synth. Proc. 2 (3) (1994) 189–195.
[35] M.B. Coelho, M.M. Pereira, Sol-gel synthesis of bioactive glass scaffolds for tissue engineering: effect of surfactant type and concentration, J. Biomed. Mater. Res. Part B: Appl. Biomater. 75B (2005) 451–456.
[36] T. Pauloin, M. Dutot, J.M. Warnet, P. Rat, *In vitro* modulation of preservative toxicity: high molecular weight hyaluronan decreases apoptosis and oxidative stress induced by benzalkonium chloride, Eur. J. Pharm. Sci. 34 (2008) 263–273.
[37] M.S. Tung, F.C. Eichmiller, Dental applications of amorphous calcium phosphates, J. Clin. Dent. 10 (1999) 1–6.
[38] A. Doostmohammadi, A. Monshi, R. Salehi, M.H. Fathi, Z. Golnyia, A.U. Daniels, Bioactive glass nanoparticles with negative zeta potential, Ceram. Int. 37 (2011) 2311–2316.
[39] T.J. Webster, R.W. Siegel, R. Bizios, Osteoblast adhesion on nanophase ceramics, Biomaterials 20 (1999) 1221–1227.
[40] E. Palin, H. Liu, T.J. Webster, Mimicking the nanofeatures of bone increases bone-forming cell adhesion and proliferation, Nanotechnology 16 (2005) 1828–1835.
[41] O.D. Schneider, S. Loher, T.J. Brunner, L. Uebersax, M. Simonet, R.N. Grass, et al., Cotton wool-like nanocomposite biomaterials prepared by electrospinning: *in vitro* bioactivity and osteogenic differentiation of human mesenchymal stem cells, J. Biomed. Mater. Res. Part B Appl. Biomater. 84 (2008) 350–362.
[42] P. Stoor, E. Soderling, J.I. Salonen, Antibacterial effects of a bioactive glass paste on oral microorganisms, Acta Odontol. Scand. 56 (1998) 161–165.
[43] T. Waltimo, T.J. Brunner, M. Vollenweider, W.J. Stark, M. Zehnder, Antimicrobial effect of nanometric bioactive glass 45S5, J. Dent. Res. 86 (2007) 754–757.

[44] Z. Hong, G.M. Luz, P.J. Hampel, M. Jin, A. Liu, X. Chen, et al., Mono-dispersed bioactive glass nanospheres: preparation and effects on biomechanics of mammalian cells, J. Biomed. Mater. Res. A 95 (2010) 747–754.
[45] A.G. Arroyo, D. Taverna, C.A. Whittaker, U.G. Strauch, B.L. Bader, H. Rayburn, et al., In vivo roles of integrins during leukocyte development and traffic: insights from the analysis of mice chimeric for alpha 5, alpha v, and alpha 4 integrins, J. Immunol. 165 (2000) 4667–4675.
[46] R.O. Hynes, Q. Zhao, The evolution of cell adhesion, J. Cell Biol. 150 (2000) F89–F96.
[47] B.S. Chong, T.R. Pitt Ford, The role of intracanal medication in root canal treatment, Int. Endod. J. 25 (1992) 97–106.
[48] B.R. Oguntebi, Dentin tubule infection and endodontic therapy implications, Int. Endod. J. 27 (1994) 218–222.
[49] V. Ballal, M. Kundabala, S. Acharya, M. Ballal, Antimicrobial action of calcium hydroxide, chlorhexidine and their combination on endodontic pathogens, Aust. Dent. J. 52 (2007) 118–121.
[50] P. Mehrvarzfar, H. Akhavan, H. Rastgarian, N.M. Akhlagi, R. Soleymanpour, A. Ahmadi, An in vitro comparative study on the antimicrobial effects of bioglass 45S5 vs. calcium hydroxide on *Enterococcus faecalis*, Iran. Endod. J. 6 (2010) 29–33.
[51] I. Allan, H. Newman, M. Wilson, Antibacterial activity of particulate Bioglass® against supra- and subgingival bacteria, Biomaterials 22 (2001) 1683–1687.
[52] L.L. Hench, J. Wilson, Surface-active biomaterials, Science 226 (1984) 630–636.
[53] M. Vollenweider, T.J. Brunner, S. Knecht, R.N. Grass, M. Zehnder, T. Imfeld, et al., Remineralization of human dentin using ultrafine bioactive glass particles, Acta Biomater. 3 (2007) 936–943.
[54] A.P. Forsback, S. Areva, J.I. Salonen, Mineralization of dentin induced by treatment with bioactive glass S53P4 in vitro, Acta Odontol. Scand. 62 (2004) 14–20.
[55] D.G. Gillam, J.Y. Tang, N.J. Mordan, H.N. Newman, The effects of a novel Bioglass® dentifrice on dentin sensitivity: a scanning electron microscopy investigation, J. Oral Rehabil. 29 (2002) 305–313.
[56] M. Brannstrom, A. Astrom, The hydrodynamics of the dentin; its possible relationship to dentinal pain, Int. Dent. J. 22 (1972) 219–227.
[57] D.G. Gillam, H.S. Seo, J.S. Bulman, H.N. Newman, Perceptions of dentin hypersensitivity in a general practice population, J. Oral Rehabil. 26 (1999) 710–714.
[58] D.G. Gillam, A. Aris, J.S. Bulman, H.N. Newman, F. Ley, Dentin hypersensitivity in subjects recruited for clinical trials: clinical evaluation, prevalence and intra-oral distribution, J. Oral Rehabil. 29 (2002) 226–231.
[59] S. Lavenus, G. Louarn, P. Layrolle, Nanotechnology and dental implants, Int. J. Biomater. (2010) 915327
[60] L.L. Hench, I.D. Xynos, J.M. Polak, Bioactive glasses for in situ tissue regeneration, J. Biomater. Sci. Polym. Ed. 15 (2004) 543–562.
[61] L.L. Hench, Biomaterials, Science 208 (1980) 826–831.
[62] J.S. Zamet, U.R. Darbar, G.S. Griffiths, J.S. Bulman, U. Bragger, W. Burgin, et al., Particulate Bioglass® as a grafting material in the treatment of periodontal intrabony defects, J. Clin. Periodontol. 24 (1997) 410–418.
[63] N. Neto, T. Deliberador, C. Storrer, A. Sousa, A. Campos, T. Lopes, The use of the bioactive glass in the regenerative periodontal therapy—a literature review, RSBO 5 (2008) 81–89.
[64] L.L. Hench, Bioactive ceramics, Ann. N.Y. Acad. Sci. 523 (1988) 54–71.
[65] E. Schepers, M. De Clercq, P. Ducheyne, R. Kempeneers, Bioactive glass particulate material as a filler for bone lesions, J. Oral Rehabil. 18 (1991) 439–452.

[66] S.R. Macneill, C.M. Cobb, J.W. Rapley, A.G. Glaros, P. Spencer, In vivo comparison of synthetic osseous graft materials. A preliminary study, J. Clin. Periodontol. 26 (1999) 239−245.
[67] B.C. Vasconcelos Gurgel, P.F. Goncalves, S.P. Pimentel, G.M. Ambrosano, F.H. Nociti Jr., E.A. Sallum, et al., Platelet-rich plasma may not provide any additional effect when associated with guided bone regeneration around dental implants in dogs, Clin. Oral Implants. Res. 18 (2007) 649−654.
[68] W.V. Giannobile, R.A. Hernandez, R.D. Finkelman, S. Ryan, C.P. Kiritsy, M. D'andrea, et al., Comparative effects of platelet-derived growth factor-BB and insulin-like growth factor-I, individually and in combination, on periodontal regeneration in *Macaca fascicularis*, J. Periodontal Res. 31 (1996) 301−312.
[69] W.V. Giannobile, Periodontal tissue engineering by growth factors, Bone 19 (1996) S23−S37.
[70] H.L. Wang, J. Cooke, Periodontal regeneration techniques for treatment of periodontal diseases, Dent. Clin. North Am. 49 (2005) 637−659, vii.
[71] R.L. Van Swol, R. Ellinger, J. Pfeifer, N.E. Barton, N. Blumenthal, Collagen membrane barrier therapy to guide regeneration in Class II furcations in humans, J. Periodontol. 64 (1993) 622−629.
[72] A.M. Polson, G.L. Southard, R.L. Dunn, A.P. Polson, G.L. Yewey, D.D. Swanbom, et al., Periodontal healing after guided tissue regeneration with Atrisorb barriers in beagle dogs, Int. J. Periodontics Restorative Dent. 15 (1995) 574−589.
[73] A.M. Polson, S. Garrett, N.H. Stoller, G. Greenstein, A.P. Polson, C.Q. Harrold, et al., Guided tissue regeneration in human furcation defects after using a biodegradable barrier: a multi-center feasibility study, J. Periodontol. 66 (1995) 377−385.
[74] A.M. Polson, G.L. Southard, R.L. Dunn, A.P. Polson, J.R. Billen, L.L. Laster, Initial study of guided tissue regeneration in Class II furcation defects after use of a biodegradable barrier, Int. J. Periodontics Restorative Dent. 15 (1995) 42−55.
[75] G. Balasundaram, M. Sato, T.J. Webster, Using hydroxyapatite nanoparticles and decreased crystallinity to promote osteoblast adhesion similar to functionalizing with RGD, Biomaterials 27 (2006) 2798−2805.
[76] T.J. Webster, C. Ergun, R.H. Doremus, R.W. Siegel, R. Bizios, Enhanced osteoclast-like cell functions on nanophase ceramics, Biomaterials 22 (2001) 1327−1333.
[77] C.A. Mcculloch, E. Nemeth, B. Lowenberg, A.H. Melcher, Paravascular cells in endosteal spaces of alveolar bone contribute to periodontal ligament cell populations, Anat. Rec. 219 (1987) 233−242.
[78] S.M. Carvalho, A.A.R. Oliveira, L.M. Andrade, M.F. Leite, M.M. Pereira., The effect of bioactive glass nanoparticles on the behavior of human periodontal ligament cells, Dent. Mater. 27 (2011) 42−43.
[79] S.M. Carvalho, A.A.R. Oliveira, C.A. Jardim, C.B.S. Melo, D.A. Gomes, M. De Fátima Leite, et al., Characterization and induction of cementoblast cell proliferation by bioactive glass nanoparticles, J. Tissue Eng. Regen. Med. (2011).
[80] M. Peter, N.S. Binulal, S.V. Nair, N. Selvamurugan, H. Tamura, R. Jayakumar, Novel biodegradable chitosan—gelatin/nano-bioactive glass ceramic composite scaffolds for alveolar bone tissue engineering, Chem. Eng. J. 158 (2010) 353−361.
[81] Oliveira A.A.R., V. Ciminelli, Dantas M.S.S., H.S. Mansur, M.M. Pereira, Acid character control of bioactive glass/polyvinyl alcohol hybrid foams produced by sol-gel, J. Sol-Gel Sci. Technol. (2008) doi: 10.1007/s10971-008-1777-1.
[82] H.S. Costa, E.F. Stancioli, M.M. Pereira, R.L. Orefice, H.S. Mansur, Synthesis, neutralization and blocking procedures of organic/inorganic hybrid scaffolds for bone tissue engineering applications, J. Mater. Sci.: Mater. Med. 20 (2009) 529−535.
[83] T. Niemela, H. Niiranen, M. Kellomaki, Self-reinforced composites of bioabsorbable polymer and bioactive glass with different bioactive glass contents. Part II: in vitro degradation, Acta Biomater. 4 (2008) 156−164.

[84] K. Rezwan, J.J. Blaker, A.R. Boccaccini, Biodegradable and bioactive porous polymer/inorganic composite scaffolds for bone tissue engineering, Biomaterials 27 (2006) 3413−3431.
[85] R. Ravarian, F. Moztarzadeh, M. Solati Hashjin, S.M. Rabiee, P. Khoshakhlagh, M. Tahriri, Synthesis, characterization and bioactivity investigation of bioglass/hydroxyapatite composite, Ceram. Int. 36 (2010) 291−297.
[86] S.K. Misra, D. Mohn, T.J. Brunner, W.J. Stark, S.E. Philip, I. Roy, et al., Comparison of nanoscale and microscale bioactive glass on the properties of P(3HB)/Bioglass® composites, Biomaterials 29 (2008) 1750−1761.
[87] B. Marelli, C.E. Ghezzi, D. Mohn, W.J. Stark, J.E. Barralet, A.R. Boccaccini, et al., Accelerated mineralization of dense collagen-nano bioactive glass hybrid gels increases scaffold stiffness and regulates osteoblastic function, Biomaterials 32 (2011) 8915−8926.
[88] R. Jayakumar, R. Ramachandran, V.V. Divyarani, K.P. Chennazhi, H. Tamura, S.V. Nair, Fabrication of chitin—chitosan/nano TiO2-composite scaffolds for tissue engineering applications, Int. J. Biol. Macromol. 48 (2011) 336−344.
[89] R. Muzzarelli, R. Tarsi, O. Filippini, E. Giovanetti, G. Biagini, P.E. Varaldo, Antimicrobial properties of N-carboxybutyl chitosan, Antimicrob. Agents Chemother. 34 (1990) 2019−2023.
[90] S. Sowmya, P.T. Sudheesh Kumar, K.P. Chennazhi, S.V. Nair, H. Tamura, R. Jayakumar, Biocompatible β-chitin hydrogel/nanobioactive glass ceramic nanocomposite scaffolds for periodontal bone regeneration, Trends Biomater. Art. Organs 25 (2011) 1−11.
[91] W. Xue, X. Liu, X. Zheng, C. Ding, In vivo evaluation of plasma-sprayed titanium coating after alkali modification, Biomaterials 26 (2005) 3029−3037.
[92] L. Le Guehennec, P. Layrolle, G. Daculsi, A review of bioceramics and fibrin sealant, Eur. Cell Mater. 8 (2004) 1−10.
[93] K. Jurczyk, K. Niespodziana, M.U. Jurczyk, M. Jurczyk, Synthesis and characterization of titanium-45S5 Bioglass nanocomposites, Mater. Des. 32 (2011) 2554−2560.
[94] M.P. Young, P. Sloan, A.A. Quayle, D.H. Carter, A survey of clinical members of the association of dental implantology in the United Kingdom. Part II. The use of augmentation materials in dental implant surgery, Implant. Dent. 10 (2001) 149−155.
[95] M.P. Young, D.H. Carter, P. Sloan, A.A. Quayle, Survey of clinical members of the association of dental implantology in the United Kingdom: Part I. Levels of activity and experience in oral implantology, Implant. Dent. 10 (2001) 68−74.
[96] D.S. Couto, Z. Hong, J.F. Mano, Development of bioactive and biodegradable chitosan-based injectable systems containing bioactive glass nanoparticles, Acta Biomater. 5 (2009) 115−123.
[97] A.J. Salinas, S. Shruti, G. Malavasi, L. Menabue, M. Vallet-Regi, Substitutions of cerium, gallium and zinc in ordered mesoporous bioactive glasses, Acta Biomater. 7 (2011) 3452−3458.
[98] V. Aina, T. Marchis, E. Laurenti, E. Diana, G. Lusvardi, G. Malavasi, et al., Functionalization of sol gel bioactive glasses carrying Au nanoparticles: selective Au affinity for amino and thiol ligand groups, Langmuir 26 (2010) 18600−18605.
[99] A. Bonici, G. Lusvardi, G. Malavasi, L. Menabue, A. Piva, Synthesis and characterization of bioactive glasses functionalized with Cu nanoparticles and organic molecules, J. Eur. Ceram. Soc. 30 (2012).

CHAPTER

Impact of Nanotechnology on Dental Implants

16

Sandrine Lavenus[a,b,c], Julie Rozé[a], Guy Louarn[b] and Pierre Layrolle[c]

[a]*INSERM, U791, Laboratory for Osteoarticular and Dental Tissue Engineering Faculty of Dental Surgery, University of Nantes, Nantes, France*

[b]*CNRS, UMR6502, Institut des Matériaux Jean Rouxel (IMN), University of Nantes, Nantes, France*

[c]*Inserm U957, Bone Resorption Physiopathology and Primary Bone Tumors Therapy, Faculty of Medicine, University of Nantes, Nantes, France*

CHAPTER OUTLINE

16.1 Introduction

Implants are commonly used in dental surgery for restoring teeth. One of the challenges in implantology is to achieve and maintain the osseointegration as well as the epithelial junction of the gingival with implants. An intimate junction of the gingival tissue with the neck of dental implants may prevent bacterial colonizations leading to periimplantitis while direct bone bonding may ensure a biomechanical anchoring of the artificial dental root (Figure 16.1).

The first step of the osseointegration of implants is called primary stability and is related to the mechanical anchorage, design of implants, and bone structure [1]. This primary interlock decreases with time at the benefit of the secondary anchorage, which is characterized by a biological bonding at the interface between bone tissues and implant surface. Between the primary mechanical and

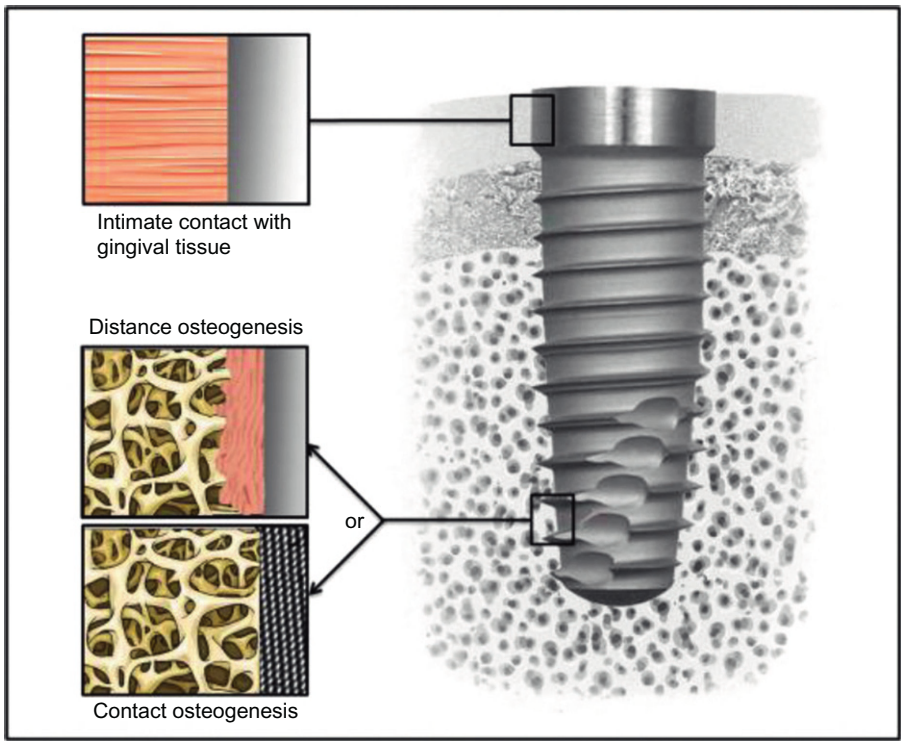

FIGURE 16.1

Tissue integration of dental implant. Note the intimate contact with gingival tissue in the upper part and the desired contact osteogenesis in the tapered lower part rather than distance osteogenesis.

secondary biological anchorage, a decreased implant stability could be observed. Many studies have attempted to enhance the osseointegration of implants by various surface modifications. The aim is to provide metal implants with surface biological properties for the adsorption of proteins, the adhesion and differentiation of cells, and tissue integration. These biological properties are related to chemical composition, wettability, and roughness of metal implant surfaces. However, the control of these surface properties at the protein and cell levels, thus in the nanometer range, remains a challenge for researchers and dental implant manufacturers.

Nanotechnologies may produce surfaces with controlled topography and chemistry that would help understanding biological interactions and developing novel implant surfaces with predictable tissue-integrative properties [2–4]. Various processing methods derived from the electronic industry such as lithography, ionic implantation, anodization, and radio frequency plasma treatments may be applied to the surfaces of dental implants to produce controlled features at the nanometer scale. These surfaces may then be screened by using high throughput biological assays in vitro. For instance, specific protein adsorption, cell adhesion, and differentiation of stem cells should be studied in relation to the surface properties. This approach may define the ideal surface

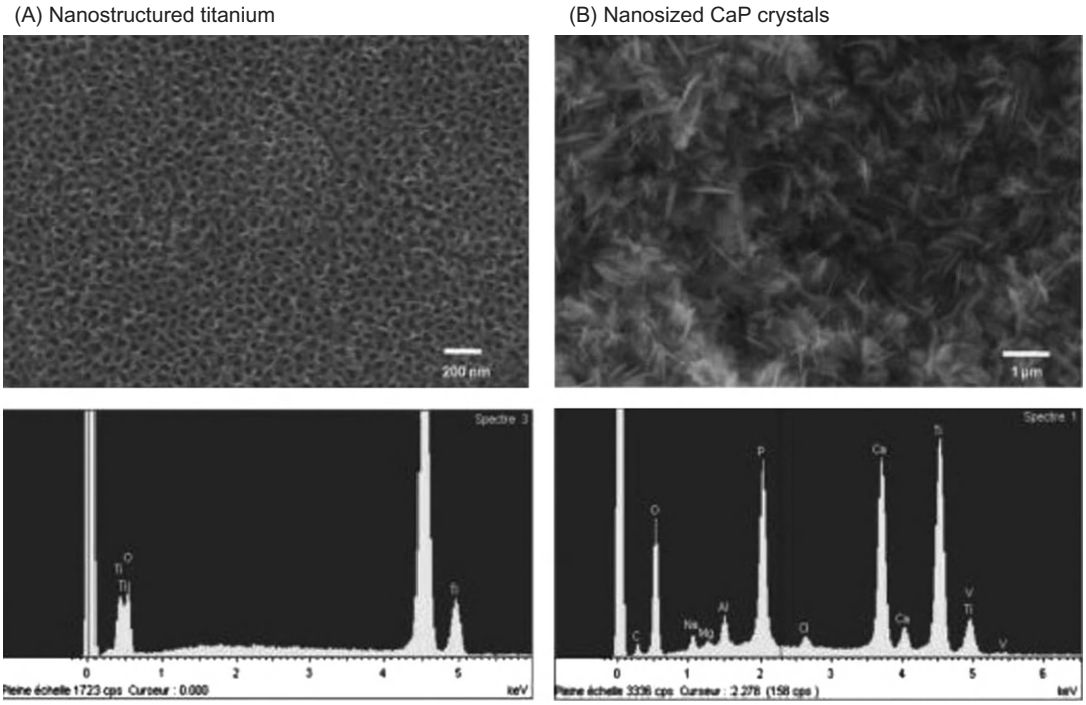

FIGURE 16.2

Scanning electron micrographs and energy dispersive analysis for X-ray of (A) nanostructured titanium surface obtained by anodization and (B) nanosized thin CaP coating on titanium produced by electrochemical deposition. Note the regular array of TiO_2 nanopores of approximately 100 nm in diameter and the nanosized CaP crystals on titanium surfaces.

for a specific biological response. Following in vitro screening, nanostructured surfaces may then be tested in animal models to validate hypothesis in a complex in vitro environment.

New coating technologies have also been developed for applying hydroxyapatite (HA) and related calcium phosphates (CaP), the mineral of bone, onto the surface of implants (Figure 16.2). Many studies have demonstrated that these CaP coatings provided titanium implants with an osteoconductive surface [5,6]. Following implantation, the dissolution of CaP coatings in the periimplant region increased ionic strength and saturation of blood leading to the precipitation of biological apatite nanocrystals onto the surface of implants. This biological apatite layer incorporates proteins and promotes the adhesion of osteoprogenitor cells that would produce the extracellular matrix of bone tissue. Furthermore, it has been also shown that osteoclasts, the bone resorbing cells, are able to degrade the CaP coatings through enzymatic ways and can create resorption pits on the coated surface [6]. Finally, the presence of CaP coatings on metals promotes an early osseointegration of implants with a direct bone bonding as compared to noncoated surfaces. The challenge is to produce CaP coatings that would dissolve at a similar rate than bone apposition in order to get a direct bone contact on implant surfaces.

This chapter reviews the different steps of the interactions between biological fluids, cells, tissues, and surfaces of implants. Recent nanoscale surface modifications and CaP coating technologies of dental implants are discussed. The sequence of biological events in relation to surface properties is related. Mechanisms of interaction with blood, platelets, and hematopoietic and mesenchymal stem cells (MSCs) on the surface of implants are described. These early events have shown to condition the adhesion, proliferation, and differentiation of cells as well as the osseointegration of implants. Future implant surfaces may improve the tissue-integrative properties and long-term clinical success for the benefits of patients.

16.2 Nanoscale surface modifications

Surface properties play a determinant role in biological interactions. In particular, the nanometer-sized roughness and the chemistry have a key role in the interactions of surfaces with proteins and cells. These early interactions will in turn condition the late tissue integration. In this prospect, different methods have been reported for enhancing bone healing around metal implants [2,7]. Modifying surface roughness has been shown to enhance the bone to implant contact and improve their clinical performance [8,2]. Grit blasting, anodization, acid etching, chemical grafting, and ionic implantation were the most commonly used methods for modifying surface roughness of metal implants. Combinations of these techniques could be used such as acid etching after grit blasting in order to eliminate the contamination by blasting residues on implant surfaces. This grit-blasting residue may interfere with the osseointegration of the titanium dental implants [9–11]. It has been shown that grit blasting with biphasic calcium phosphate (BCP) ceramic particles gave a high average surface roughness and particle-free surfaces after acid etching of titanium implants. Studies conducted both in vitro and in vivo have shown that BCP grit-blasted surfaces promoted an early osteoblast differentiation and bone apposition as compared to mirror-polished or alumina grit-blasted titanium [12,13]. Anodization is a method commonly used to obtain nanoscale oxides on metals including titanium [14,15]. By adjusting the anodization condition such as voltage, time, and shaking, nanoscale properties could be controlled. Shankar et al. [16] have reported that the diameters of the nanotubes could be modified to a range from 20 to 150 nm in modifying voltage conditions. On the other hand, Kang et al. [17] found that TiO_2 nanotube arrays were more uniform on electro-polished than machined titanium. Moreover, TiO_2 nanotubes on Ti improved the production of alkaline phosphatase (ALP) activity by osteoblastic cells. In particular, nanotubes with a diameter of 100 nm upregulated the level of ALP activity as compared to nanotube surfaces with a diameter of 30–70 nm [18]. Since ALP is a marker of osteogenic differentiation, these surfaces may demonstrate enhanced bone tissue-integrative properties.

Another approach for improving osseointegration of dental implants is to apply a CaP coating having osteoconductive properties [19–21]. Different methods such as plasma spraying, biomimetic, and electrophoretic deposition have been developed to coat metal implants with CaP layers. Nevertheless, plasma-sprayed HA-coated dental implants have been related to clinical failures due to coating delimitation and heterogeneous dissolution rate of deposited phases. An electrochemical process which consists of depositing CaP crystals from supersaturated solutions has been proposed for coating titanium implants with CaP layers [22,23]. Upon implantation, these CaP coatings dissolve and release Ca^{2+} and HPO_4^{2-} increasing saturation of blood in the periimplant region. This dissolution led to the precipitation of biological apatite nanocrystals with the incorporation of various

proteins. This biological apatite layer will promote cell adhesion, differentiation into osteoblast, and the synthesis of mineralized collagen, the extracellular matrix of bone tissue. In addition to dissolution, osteoclast cells are also able to resorb the CaP coatings and activate osteoblast cells to produce bone tissue. As a result, these CaP coatings promote a direct bone-implant contact without an intervening connective tissue layer leading to a proper biomechanical fixation of dental implants.

16.3 Interactions of surface dental implants with blood

During surgery, blood vessels are injured and thus, dental implant surfaces interact with blood components (Figure 16.3). Various plasma proteins get adsorbed on the material surface within a minute. Platelets from blood also interact with the implant surface. Plasma proteins modify the surface while activated platelets are responsible for thrombus formation and blood clotting. Subsequently, the various cell types that are migrated to the injured site interact with the surface through membrane integrin receptors. These early events occur prior to periimplant tissue healing.

Plasma contains dissolved substances such as glucose, amino acids, cholesterols, hormones, urea, and various ions (Figure 16.4). Most of these components are needed for the viability of cells and tissues. All of these blood substances could interact with implant surface thus modifying their chemical properties like charge or hydrophobicity.

Blood interactions with implants lead to protein adsorption, which is dependent on the surface properties of the material and occurs through a complex series of adsorption and displacement steps

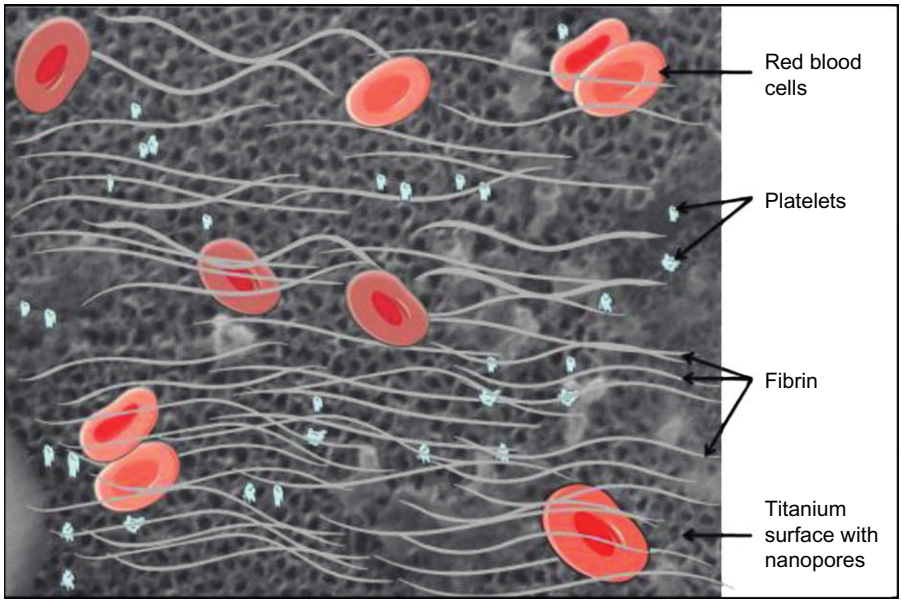

FIGURE 16.3

Interactions of surface of dental implants with blood. Note the numerous proteins, red blood cells, and activated platelets that lead to blood clotting on implants.

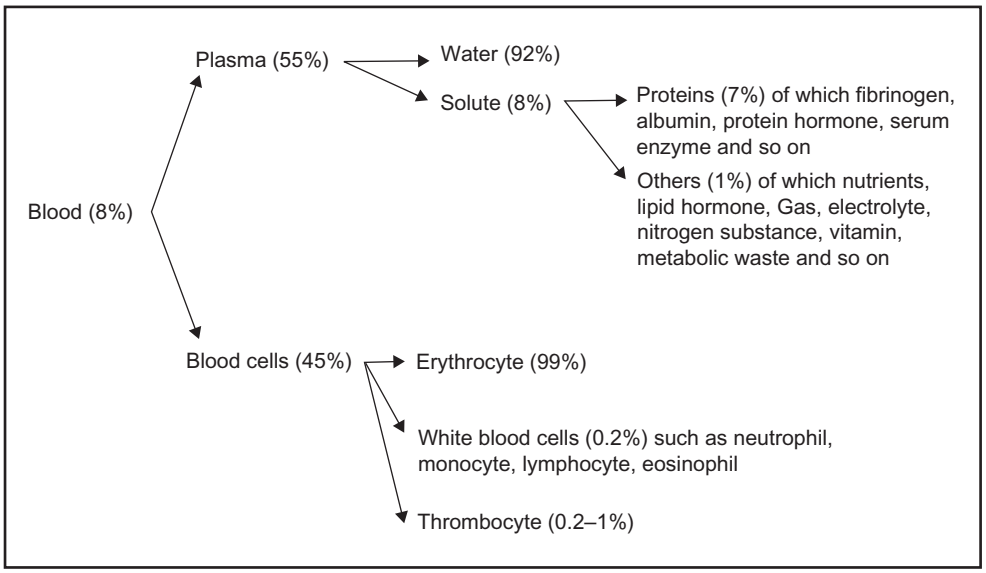

FIGURE 16.4

Scheme showing blood composition and components that primarily interact with surface of dental implants.

known as the Vroman effect [24]. A hydrophilic surface is better for blood coagulation than a hydrophobic surface. Consequently, dental implant manufacturers have developed high hydrophilic and rough implant surfaces which in turn exhibited better osseointegration than conventional ones [25]. Adsorption of proteins such as fibronectin, vitronectin on surface of dental implants could promote cell adhesion by cell-binding RGD (Arg−GlyAsp) domain. This RGD sequence interacts with integrin present on the cell membrane [26]. Interactions between cell membrane integrins and proteins coated onto implant surface play a key role in adhesion of many cell types. After proteins absorption, the osseointegration is characterized by platelets adhesion and fibrin clots formation at the injured blood vessels site. It has been shown that implants in contact with platelet-rich plasma (PRP) with a platelet concentration of approximately 1,000,000 protein/μL have a positive effect on osseointegration. At lower concentrations of PRP, the effect was not optimal, while higher concentrations resulted in a paradoxically inhibitory effect of bone regeneration. Other studies were not in agreement with this PRP's beneficial effect on the osseointegration of dental implants [27]. The assessment of bioactivity of surface-treated dental implants should be tested in vitro using biological fluids containing blood components [2].

16.4 Interactions between surfaces and mesenchymal stem cells

Following blood clotting around dental implants, several cells interact with surfaces for tissue healing. MSCs attracted to the injured site by chemotactic factors have a determinant role in peri-implant tissue healing.

16.4.1 Origin of mesenchymal stem cells

MSCs are stem cells derived from somatic tissues which can be differentiated into mesenchymal lineages such as bone, cartilage, fat, and skin. In addition, MSCs are present in many connective tissues and blood at low concentrations serving as a sort of internal repair system. MSCs are distinguished from other cell types by two important characteristics. First, they are unspecialized cells able to renew themselves through cell division, sometimes after long periods of inactivity. Second, under certain physiologic or experimental conditions, they can be induced to become tissue- or organ-specific cells with special functions. MSCs have high proliferative and multipotent capacity leading to differentiated cells under the guidance of various cues or niches. MSCs are conventionally defined as adherent, non-hematopoietic cells expressing markers such as CD13, CD29, CD44, CD54, CD73, CD90, CD105, and CD166, and being negative for CD14, CD34, and CD45 [28,29]. While originally identified in the bone marrow [30] MSCs have been extracted from numerous tissues including adipose [31,32], heart [33], dental pulp [34], peripheral blood [35], and cord blood [36]. One of the major properties of MSCs is their ability to differentiate into various cells like adipocytes [37], chondrocytes [31], osteoblasts [38], neurons [39,40], muscles [40,41], and hepatocytes [42] in vitro after treatment with induction agents.

16.4.2 Migration, adhesion, and proliferation

The integration of implant with neighboring bone and gingival tissue depends on successful cross talk between old tissue and implant surface. The challenge in dental implant research is the capability of the surface to guide cells' colonization and differentiation. Cell migration, adhesion, and proliferation on implant surfaces are a prerequisite to initiate the tissue regeneration (Figure 16.5). Authors have shown that some factors present in tissues and secreted during the inflammatory phase are able to attract MSCs to the injured site [43,44]. MSCs migration and proliferation were stimulated in vitro by many growth factors including Platelet-derived growth factor (PDGF) [45,46], Epidermal growth factor (EGF) [46,47], Vascular endothelial growth factor (VEGF) [48], Transforming growth factor (TGF-β) [45,49], Bone morphogenetic protein-2 (BMP-2) and BMP-4 [45,48]. These factors are certainly released in the injured sites by cells involved in tissue healing. Furthermore, plasma clot serves as storage to fibrin molecules and release system for a variety of bioactive factors including growth factors that attract and differentiate MSCs into specific lineages [50−52]. The platelet factors are well known to stimulate the proliferation of MSCs [53]. The formation of a clot matrix with a potent chemo-attractive factor like PDGF, EGF, or fibrin may further enhance MSCs numbers and periimplant tissue healing surface. Moreover, the plasma clot in contact with implant surface represents a three-dimensional microporous structure that allows diffusion of regulatory factors [54,55] and is involved in the migration, proliferation, and differentiation of MSCs. After MSCs recruitment in the injured site, cells adhere on the local extracellular matrix as well as on the implant surface beginning an extensive proliferation in order to build up new tissue. Again, surface modifications of implants in the nanometer range condition the biological responses.

16.4.3 Differentiation

In the microenvironment, MSCs are stimulated by some specific factors to differentiate into the adequate cell line. Under the influence of these factors, MSCs switch to osteoblastic cells in contact

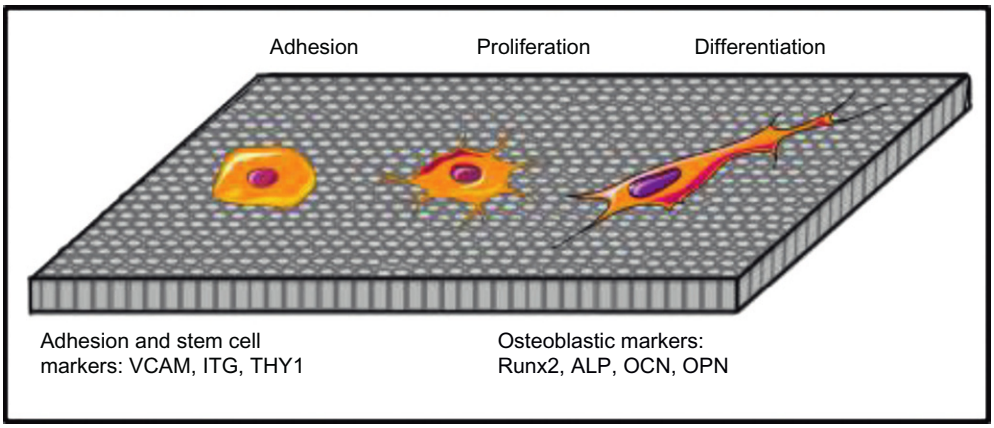

FIGURE 16.5

The adhesion, proliferation, and differentiation of mesenchymal stem cells on nanostructured surfaces. The adhesion of stem cells is characterized by the expression of cell surface markers (VCAM, ITG, THY1) while phenotypic markers (Runx2, ALP, OCN, OPN) are specific to their osteoblastic differentiation. OCN, osteocalcin; OPN, osteopontin.

to bone tissue while they differentiate into fibroblastic lineage in the gingival tissue region. These two differentiation pathways are in concurrence around dental implants. In some cases, implants are encapsulated by fibrous tissue due to the proliferation and differentiation of MSCs into fibroblastic cells. In response to cytokine, fibroblasts migrate and generate a capsule of collagen, which is the first step in the generation of gingival tissue or rejection on contact to bone. This fibrous capsule prevents bonding between implant surface and juxtaposed bone and caused implant failure [56]. On the other hand, both the differentiation of MSCs into fibroblastic lineage and the fibroblastic adhesion are desired in the gingival upper part of dental implants. Fibroblasts adhesion has been shown to be lower on nanoscale surface compared to conventional surfaces [57]. Moreover, nanometer-size features have been shown to decrease fibroblast adhesion and proliferation [58,59]. The micro- and nanoscale surface properties of metal implant including chemistry, roughness, and wettability, could affect bone formation [60]. Numerous treatment such as machining, grit blasting, Ti/HA plasma spray, chemical etching, and anodization are available to modify the implant surface. Research has specifically demonstrated that nanorough Ti [61] and nanostructured Ti can enhance osteoblast adhesion and differentiation compared to their nanosmooth control [62]. Furthermore, surface with micro- and nanopores has been shown to greatly enhance osseointegration [63,64]. Surface properties may control the steps of adhesion, proliferation, and differentiation of MSCs, and thus condition tissue integration.

16.5 Tissue integration

Branemark et al. [65] described the osseointegration as a direct structural and functional bone to implant contact under load. As previously discussed, the biological events occurring at the tissue-

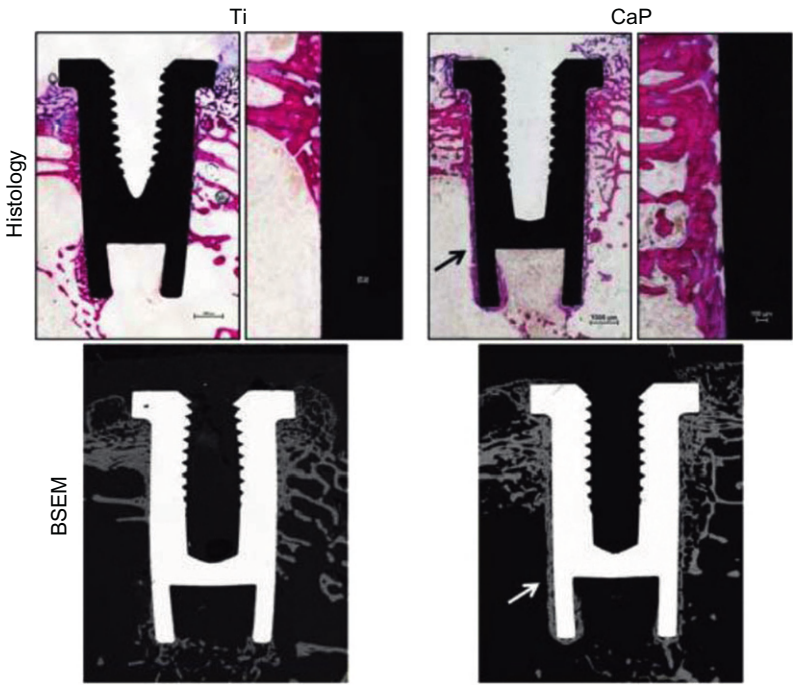

FIGURE 16.6

Micrographs showing the osseointegration of bare titanium (Ti) and CaP-coated implants after implantation in femoral condyles of rabbits for 4 weeks. Note the direct bone apposition on CaP-coated implants (arrows) on both histology (basic fuchsine, toluidine blue staining) and back-scattered electron microscopy (BSEM) images.

implant interface are influenced by the chemistry, topography, and wettability of dental implant surfaces. The challenge in developing new implant surface is increasing the clinical success rate as well as decreasing the tissue healing time for immediate loading of implants, particularly in esthetic situations [66–68]. One of the objectives is to develop implant surfaces having predictable, controlled, and guided tissue healing. For instance, surfaces that promote contact osteogenesis rather than distance osteogenesis would be desired in bone site while intimate fibrous tissue healing would be in the gingival tissue (Figure 16.1). In order to enhance this intimate contact between tissues and implant, surface treatments at the nanometer scale have been performed on metal implants and tested in various animal models. Implant surface with various roughness has been used to increase the total area available for osteoapposition. Kubo et al. [66] observed a substantial increase by 3.1 times in bone–titanium interfacial strength by Ti nanotube (300 nm) at 2 weeks of implantation in femur of rats. These results suggest the establishment of nanostructured surfaces for improved osteoconductivity. Moreover, Ogawa et al. [69] have prepared Ti nanostructure by physical vapor deposition and tested their osseointegration in femur of rats. They found an increased surface area by up to 40% and a greater strength of osseointegration for the nanostructured compared to an

acid-etched surface. Some authors have correlated the initial events in bone formation adjacent to surface with the long-term tissue response to these materials in humans [70,71].

By mimicking the chemical composition of natural bone, HA and CaP coatings on Ti greatly enhance osseointegration. As shown in Figure 16.6, a greater direct bone apposition was observed on CaP coated than on bare Ti implants. During the bone healing process, calcium and phosphate ions are released from the CaP coating in the periimplant region and saturate body fluids to precipitate a biological apatite, which serves as a substrate for osteoblastic cells producing bone tissue. Several authors have shown the benefit of using CaP-coated titanium implants for improving the osseointegration [72,73]. In particular, Le Guehennec et al. [21] have studied the osseointegration of four implant surfaces in the femoral epiphyses of rabbits after 2 and 8 weeks of healing. In this study, the bone-implant contact and bone growth inside the chambers were compared for four different implant surfaces and it was shown that biomimetic coating method may enhance the bone apposition onto titanium. In order to prevent coating delamination and implant loosening, the CaP coating should dissolve or degrade under osteoclastic activity at a similar rate than bone apposition. The final result should be a direct bone-implant coating without the presence of fibrous tissue. Another advantage of these CaP coatings is related to their preparation by biomimetic methods at physiological temperature and pH from simulated body fluids. CaP crystals have characteristics that resemble bone mineral in terms of size and composition. Furthermore, it is possible to incorporate biologically active drugs such as antibiotics or growth factors during the precipitation of CaP coatings on Ti implants [74]. These molecules could be locally and gradually released in the periimplant region for either preventing bacterial infections or stimulating bone growth.

16.6 Conclusions

Many reports have shown that nanometer-controlled surfaces have a great effect on early events such as the adsorption of proteins, blood clot formation, and cell behaviors occurring upon implantation of dental implants. These early events have an effective impact on the migration, adhesion, and differentiation of MSCs. Nanostructured surfaces may control the differentiation pathways into specific lineages and ultimately direct the nature of periimplant tissues. Despite an active research in dental implants, the ideal surface for predictive tissue integration remains a challenge.

Acknowledgments

The authors are grateful to Jean-Charles Ricquier for contribution in figures preparation. We acknowledge the pharmaceutical company SERVIER for allowing us to use some drawings taken from their Web site.

References

[1] J. Rozé, S. Babu, A. Saffarzadeh, M. Gayet-Delacroix, A. Hoornaert, P. Layrolle, Correlating implant stability to bone structure, Clin. Oral Implants Res. 20 (2009) 1140–1145.

[2] L. Le Guéhennec, A. Soueidan, P. Layrolle, Y. Amouriq, Surface treatments of titanium dental implants for rapid osseointegration, Dent. Mater. 23 (2007) 844–854.
[3] S. Lavenus, J.-C. Ricquier, G. Louarn, P. Layrolle, Cell interaction with nanopatterned surface of implants, Nanomedicine 5 (2010) 937–947.
[4] S. Lavenus, G. Louarn, P. Layrolle, Nanotechnology and dental implants, Int. J. Biomater. 2010 (2010) 915327.
[5] R.G.T. Geesink, Osteoconductive coatings for total joint arthroplasty, Clin. Orthop. Relat. Res. (2002) 53–65.
[6] S. Leeuwenburgh, et al., Osteoclastic resorption of biomimetic calcium phosphate coatings in vitro, J. Biomed. Mater. Res. 56 (2001) 208–215.
[7] R.G. Geesink, K. de Groot, C.P. Klein, Chemical implant fixation using hydroxyl-apatite coatings. The development of a human total hip prosthesis for chemical fixation to bone using hydroxyl-apatite coatings on titanium substrates, Clin. Orthop. Relat. Res. (1987) 147–170.
[8] M.M. Shalabi, J.G.C. Wolke, J.A. Jansen, The effects of implant surface roughness and surgical technique on implant fixation in an in vitro model, Clin. Oral Implants Res. 17 (2006) 172–178.
[9] M. Esposito, J.M. Hirsch, U. Lekholm, P. Thomsen, Biological factors contributing to failures of osseointegrated oral implants. (I). Success criteria and epidemiology, Eur. J. Oral Sci. 106 (1998) 527–551.
[10] M. Esposito, J.M. Hirsch, U. Lekholm, P. Thomsen, Biological factors contributing to failures of osseointegrated oral implants. (II). Etiopathogenesis, Eur. J. Oral Sci. 106 (1998) 721–764.
[11] W.-D. Müeller, et al., Evaluation of the interface between bone and titanium surfaces being blasted by aluminium oxide or bioceramic particles, Clin. Oral Implants Res. 14 (2003) 349–356.
[12] L. Le Guehennec, et al., Osteoblastic cell behaviour on different titanium implant surfaces, Acta Biomater. 4 (2008) 535–543.
[13] A. Citeau, et al., In vitro biological effects of titanium rough surface obtained by calcium phosphate grid blasting, Biomaterials 26 (2005) 157–165.
[14] S. Oh, et al., Stem cell fate dictated solely by altered nanotube dimension, Proc. Natl. Acad. Sci. U. S. A. 106 (2009) 2130–2135.
[15] L. Zhang, Y. Han, Effect of nanostructured titanium on anodization growth of self-organized TiO_2 nanotubes, Nanotechnology 21 (2010) 55602.
[16] K. Shankar, et al., Highly-ordered TiO_2 nanotube arrays up to 220 μm in length: use in water photoelectrolysis and dye-sensitized solar cells, Nanotechnology (2007).
[17] S.H. Kang, H.S. Kim, J.-Y. Kim, Y.-E. Sung, An investigation on electron behavior employing vertically-aligned TiO_2 nanotube electrodes for dye-sensitized solar cells, Nanotechnology 20 (2009) 355307.
[18] K.S. Brammer, et al., Improved bone-forming functionality on diameter-controlled TiO(2) nanotube surface, Acta Biomater. 5 (2009) 3215–3223.
[19] N.C. Geurs, R.L. Jeffcoat, E.A. McGlumphy, M.S. Reddy, M.K. Jeffcoat, Influence of implant geometry and surface characteristics on progressive osseointegration, Int. J. Oral Maxillofac. Implants 17 (2002) 811–815.
[20] J.E. Davies, Understanding peri-implant endosseous healing, J. Dent. Educ. 67 (2003) 932–949.
[21] L. Le Guehennec, et al., Histomorphometric analysis of the osseointegration of four different implant surfaces in the femoral epiphyses of rabbits, Clin. Oral Implants Res. 19 (2008) 1103–1110.
[22] M.A. Lopez-Heredia, P. Weiss, P. Layrolle, An electrodeposition method of calcium phosphate coatings on titanium alloy, J. Mater. Sci. Mater. Med. 18 (2007) 381–390.
[23] R.Z. LeGeros, Properties of osteoconductive biomaterials: calcium phosphates, Clin. Orthop. Relat. Res. (2002) 81–98.

[24] R. Miller, Z. Guo, E.A. Vogler, C.A. Siedlecki, Plasma coagulation response to surfaces with nanoscale chemical heterogeneity, Biomaterials 27 (2006) 208−215.
[25] T. Sawase, et al., Photo-induced hydrophilicity enhances initial cell behavior and early bone apposition, Clin. Oral Implants Res. 19 (2008) 491−496.
[26] G. Balasundaram, M. Sato, T.J. Webster, Using hydroxyapatite nanoparticles and decreased crystallinity to promote osteoblast adhesion similar to functionalizing with RGD, Biomaterials 27 (2006) 2798−2805.
[27] G. Weibrich, T. Hansen, W. Kleis, R. Buch, W.E. Hitzler, Effect of platelet concentration in platelet-rich plasma on peri-implant bone regeneration, Bone 34 (2004) 665−671.
[28] W. Richter, Mesenchymal stem cells and cartilage *in situ* regeneration, J. Intern. Med. 266 (2009) 390−405.
[29] T.E. Ichim, et al., Mesenchymal stem cells as anti-inflammatories: implications for treatment of Duchenne muscular dystrophy, Cell. Immunol. 260 (2010) 75−82.
[30] A.J. Friedenstein, K.V. Petrakova, A.I. Kurolesova, G.P. Frolova, Heterotopic of bone marrow. Analysis of precursor cells for osteogenic and hematopoietic tissues, Transplantation 6 (1968) 230−247.
[31] A.C.W. Zannettino, et al., Multipotential human adipose-derived stromal stem cells exhibit a perivascular phenotype in vitro and in vivo, J. Cell. Physiol. 214 (2008) 413−421.
[32] M.Q. Wickham, G.R. Erickson, J.M. Gimble, T.P. Vail, F. Guilak, Multipotent stromal cells derived from the infrapatellar fat pad of the knee, Clin. Orthop. Relat. Res. (2003) 196−212, doi:10.1097/01.blo.0000072467.53786.ca.
[33] M.J. Hoogduijn, et al., Human heart, spleen, and perirenal fat-derived mesenchymal stem cells have immunomodulatory capacities, Stem Cells Dev. 16 (2007) 597−604.
[34] Y.-Y. Jo, et al., Isolation and characterization of postnatal stem cells from human dental tissues, Tissue Eng. 13 (2007) 767−773.
[35] Q. He, C. Wan, G. Li, Concise review: multipotent mesenchymal stromal cells in blood, Stem Cells 25 (2007) 69−77.
[36] W. Oh, D.-S. Kim, Y.S. Yang, J.K. Lee, Immunological properties of umbilical cord blood-derived mesenchymal stromal cells, Cell. Immunol. 251 (2008) 116−123.
[37] D.L. Morganstein, et al., Human fetal mesenchymal stem cells differentiate into brown and white adipocytes: a role for ERRalpha in human UCP1 expression, Cell Res. 20 (2010) 434−444.
[38] L. Marinucci, et al., Effects of hydroxyapatite and Biostite® on osteogenic induction of hMSC, Ann. Biomed. Eng. 38 (2010) 640−648.
[39] G. Lepski, et al., Limited Ca^{2+} and PKA-pathway dependent neurogenic differentiation of human adult mesenchymal stem cells as compared to fetal neuronal stem cells, Exp. Cell Res. 316 (2010) 216−231.
[40] A.J. Engler, S. Sen, H.L. Sweeney, D.E. Discher, Matrix elasticity directs stem cell lineage specification, Cell 126 (2006) 677−689.
[41] Y. Liu, et al., Flk-1 + adipose-derived mesenchymal stem cells differentiate into skeletal muscle satellite cells and ameliorate muscular dystrophy in mdx mice, Stem Cells Dev. 16 (2007) 695−706.
[42] M. Chivu, et al., In vitro hepatic differentiation of human bone marrow mesenchymal stem cells under differential exposure to liver-specific factors, Transl. Res. 154 (2009) 122−132.
[43] H. Agis, B. Kandler, M.B. Fischer, G. Watzek, R. Gruber, Activated platelets increase fibrinolysis of mesenchymal progenitor cells, J. Orthop. Res. 27 (2009) 972−980.
[44] J.P. Vogel, et al., Platelet-rich plasma improves expansion of human mesenchymal stem cells and retains differentiation capacity and in vivo bone formation in calcium phosphate ceramics, Platelets 17 (2006) 462−469.
[45] Y. Mishima, M. Lotz, Chemotaxis of human articular chondrocytes and mesenchymal stem cells, J. Orthop. Res. 26 (2008) 1407−1412.

[46] Y. Ozaki, et al., Comprehensive analysis of chemotactic factors for bone marrow mesenchymal stem cells, Stem Cells Dev. 16 (2007) 119–129.
[47] S.A. Kuznetsov, A.J. Friedenstein, P.G. Robey, Factors required for bone marrow stromal fibroblast colony formation in vitro, Br. J. Haematol. 97 (1997) 561–570.
[48] J. Fiedler, F. Leucht, J. Waltenberger, C. Dehio, R.E. Brenner, VEGF-A and PIGF-1 stimulate chemotactic migration of human mesenchymal progenitor cells, Biochem. Biophys. Res. Commun. 334 (2005) 561–568.
[49] H. Jian, et al., Smad3-dependent nuclear translocation of beta-catenin is required for TGF-beta1-induced proliferation of bone marrow-derived adult human mesenchymal stem cells, Genes Dev. 20 (2006) 666–674.
[50] I. Catelas, J.F. Dwyer, S. Helgerson, Controlled release of bioactive transforming growth factor beta-1 from fibrin gels in vitro, Tissue Eng. Part C Methods 14 (2008) 119–128.
[51] C. Wong, E. Inman, R. Spaethe, S. Helgerson, Fibrin-based biomaterials to deliver human growth factors, Thromb. Haemost. 89 (2003) 573–582.
[52] M.W. Mosesson, Fibrinogen and fibrin structure and functions, J. Thromb. Haemost. 3 (2005) 1894–1904.
[53] G. Rock, D. Neurath, M. Lu, A. Alharbi, M. Freedman, The contribution of platelets in the production of cryoprecipitates for use in a fibrin glue, Vox Sang. 91 (2006) 252–255.
[54] I. Catelas, et al., Human mesenchymal stem cell proliferation and osteogenic differentiation in fibrin gels in vitro, Tissue Eng. 12 (2006) 2385–2396.
[55] T. Schildhauer, D. Seybold, J. Gebmann, G. Muhr, M. Koller, Fixation of porous calcium phosphate with expanded bone marrow cells using an autologous plasma clot, Mater. Sci. Eng. Technol. (2007) 1012–1014.
[56] J.A. Hobkirk, Progress in implant research, Int. Dent. J. 33 (1983) 341–349.
[57] E. Eisenbarth, J. Meyle, W. Nachtigall, J. Breme, Influence of the surface structure of titanium materials on the adhesion of fibroblasts, Biomaterials 17 (1996) 1399–1403.
[58] A. Cohen, P. Liu-Synder, D. Storey, T. Webster, Decreased fibroblast and increased osteoblast functions on ionic plasma deposited nanostructured Ti coatings, (2007) 385–390.
[59] D. Miller, R. Vance, A. Thapa, T. Webster, K. Haberstroch, Comparaison of fibroblast and vascular cell adhesion to nanostructured poly(lactic co glycolic acid) films, Appl. Bion. Biochem. (2005) 1–7.
[60] R.M. Streicher, M. Schmidt, S. Fiorito, Nanosurfaces and nanostructures for artificial orthopedic implants, Nanomedicine 2 (2007) 861–874.
[61] S. Puckett, R. Pareta, T.J. Webster, Nano rough micron patterned titanium for directing osteoblast morphology and adhesion, Int. J. Nanomed. 3 (2008) 229–241.
[62] C. Yao, E.B. Slamovich, T.J. Webster, Enhanced osteoblast functions on anodized titanium with nanotube-like structures, J. Biomed. Mater. Res. A 85 (2008) 157–166.
[63] K.-H. Frosch, et al., Growth behavior, matrix production, and gene expression of human osteoblasts in defined cylindrical titanium channels, J. Biomed. Mater. Res. A 68 (2004) 325–334.
[64] S.H. Oh, R.R. Finõnes, C. Daraio, L.-H. Chen, S. Jin, Growth of nano-scale hydroxyapatite using chemically treated titanium oxide nanotubes, Biomaterials 26 (2005) 4938–4943.
[65] P.I. Brånemark, et al., Osseointegrated titanium fixtures in the treatment of edentulousness, Biomaterials 4 (1983) 25–28.
[66] K. Kubo, et al., Cellular behavior on TiO_2 nanonodular structures in a micro-to-nanoscale hierarchy model, Biomaterials 30 (2009) 5319–5329.
[67] R.Z. LeGeros, R.G. Craig, Strategies to affect bone remodeling: osteointegration, J. Bone Miner. Res. 8 (Suppl. 2) (1993) S583–S596.
[68] R.M. Pilliar, Cementless implant fixation—toward improved reliability, Orthop. Clin. N. Am. 36 (2005) 113–119.

[69] T. Ogawa, L. Saruwatari, K. Takeuchi, H. Aita, N. Ohno, Ti nano-nodular structuring for bone integration and regeneration, J. Dent. Res. (2008) 751−756.
[70] B.D. Boyan, Z. Schwartz, J.C. Hambleton, Response of bone and cartilage cells to biomaterials in vivo and in vitro, J. Oral Implantol. 19 (1993) 116−122; (Discussion 136−137).
[71] D. Kohavi, et al., Effect of titanium implants on primary mineralization following 6 and 14 days of rat tibial healing, Biomaterials 13 (1992) 255−260.
[72] M.K. Jeffcoat, E.A. McGlumphy, M.S. Reddy, N.C. Geurs, H.M. Proskin, A comparison of hydroxyapatite (HA)-coated threaded, HA-coated cylindric, and titanium threaded endosseous dental implants, Int. J. Oral Maxillofac. Implants 18 (2003) 406−410.
[73] E.A. McGlumphy, L.J. Peterson, P.E. Larsen, M.K. Jeffcoat, Prospective study of 429 hydroxyapatite-coated cylindric omniloc implants placed in 121 patients, Int. J. Oral Maxillofac. Implants 18 (2003) 82−92.
[74] Y. Liu, K. de Groot, E.B. Hunziker, BMP-2 liberated from biomimetic implant coatings induces and sustains direct ossification in an ectopic rat model, Bone 36 (2005) 745−757.

CHAPTER

17 Titania Nanotube Coatings on Dental Implants with Enhanced Osteogenic Activity and Anti-Infection Properties

Lingzhou Zhao[c], Kaifu Huo[a,b] and Paul K. Chu[b]

[a]*School of Materials and Metallurgy, Wuhan University of Science and Technology, Wuhan, China*

[b]*Department of Physics and Materials Science, City University of Hong Kong, Tat Chee Avenue, Kowloon, Hong Kong, China*

[c]*Department of Periodontology and Oral Medicine, School of Stomatology, The Fourth Military Medical University, West Changle Road, Xi'an, China*

CHAPTER OUTLINE

17.1 Introduction

Dental implants are an ideal option for people in good general oral health who have lost a tooth or teeth due to periodontal disease, an injury, or some other reasons. Titanium (Ti) and its alloys are

Nanobiomaterials in Clinical Dentistry.

widely used as dental implant materials due to their good mechanical properties, excellent corrosion resistance, and biocompatibility. The long-term normal functions of dental implants are related to their early and rigid osseointegration. Although the spontaneously formed thin TiO_2 passive layer provides some corrosion resistance and biocompatibility for the Ti implant, it is not able to induce bone formation effectively. Providing that the natural extracellular matrix (ECM) has a hierarchical nanostructure [1], the formation of a nanostructured surface on an implant is a good strategy to achieve enhanced osseointegration. Grit blasting, anodization, acid etching, chemical grafting, and ion implantation are some common techniques used to modify Ti implants to enhance bone–implant contact (BIC) and improve their clinical performance. Anodization is a newly developed method to form an oxide nanotube (NT) coating on metals including Ti [2–5]. By adjusting the anodization conditions such as the voltage and time, nanoscale properties can be controlled [2,3]. The nanotubular topography mimics the dimensions of collagen fibril in bones to some extent [6] and has elasticity similar to that of bones [7]. The NT coatings on Ti have been found to foster the growth of nanostructured hydroxyapatite in simulated body fluids (SBF) [8,9], enhance ECM secretion, mineralization, and other functionalities of osteoblasts, and even induce the commitment of mesenchymal stem cells (MSCs) toward bone lineage in the absence of extra osteogenic supplements (OS) [2,3,10–12]. Emerging in vivo evidence also suggests the ability of the NT coatings to enhance osseointegration [13–16].

Implant-associated infection which is another issue impairing the normal function of dental implants is usually difficult to treat and sometimes requires implant removal and repeated revision of surgeries [17]. Various means such as thorough sterilization and stringent aseptic surgical protocols have been proposed to mitigate bacterial contamination. However, bacterial invasion usually occurs after surgery, and complications can arise from infection of nearby tissues or a hematogenous source at a later time [18]. Infections associated with dental implants are characterized by bacterial colonization and biofilm formation on the implanted device and infection of the adjacent tissues (periimplantitis). Bacteria in the biofilm are far more resistant to antibiotics resulting in persistent infection despite aggressive antibiotic therapy [19]. As emerging antibiotic resistance becomes more challenging, developing novel implants or surface modification methods with dual functions of excellent bone-bonding ability and long-lasting antibacterial ability through a procedure ready for industrial production and clinical application is the need for the hour in implant dentistry.

NTs on dental Ti implants not only provide a nanotopographical surface to induce bone formation effectively but also serve as a good drug loading and delivering platform for various targeted agents to attain extra functions. Many kinds of agents including antibacterial agents, bone growth favoring agents, and anti-inflammatory agents have been incorporated into NTs to enhance the implants in clinical applications. It is our belief that NTs are more suitable for loading and delivery of the inorganic agents that are stable and have very low effective doses. Hence, we have loaded silver [5], strontium [20], zinc and so on into the NTs to achieve long-term functions concerning antibacterial ability and osteogenesis induction.

In this chapter, we summarize the latest progress on TiO_2 NT coatings and review the factors influencing the NT bioactivity, the effects of the NTs on bone cell functionalities in vitro, osseointegration in vivo, and drug loading and delivery. This chapter will not describe in detail the preparation and mechanism of TiO_2 NT by anodization because there are already some reviews in the literature regarding the fabrication of anodized NT arrays on Ti implants.

17.2 Fabrication of NTs on Ti

Uniform and highly ordered NT arrays can be readily fabricated by anodization of a Ti foil in F-containing electrolytes. The as-anodized NTs, which grow in situ on the Ti substrate, are highly oriented perpendicular to the Ti surface [21]. The NTs are generally fabricated in the aqueous hydrofluoric acid (HF) electrolyte in a two-electrode electrochemical cell at a constant potential between 5 and 35 V [4,8,10]. At a low anodization voltage of 5 V, the morphology of the anodized film is sponge-like with a typical pore size of 25 nm. At 20 V, hollow and cylindrical tube-like features with an inner diameter of 80 nm form (Figure 17.1). Besides the HF/H_2O electrolyte, many other aqueous electrolytes have also been developed to fabricate NTs, for example, H_2SO_4/NaF/

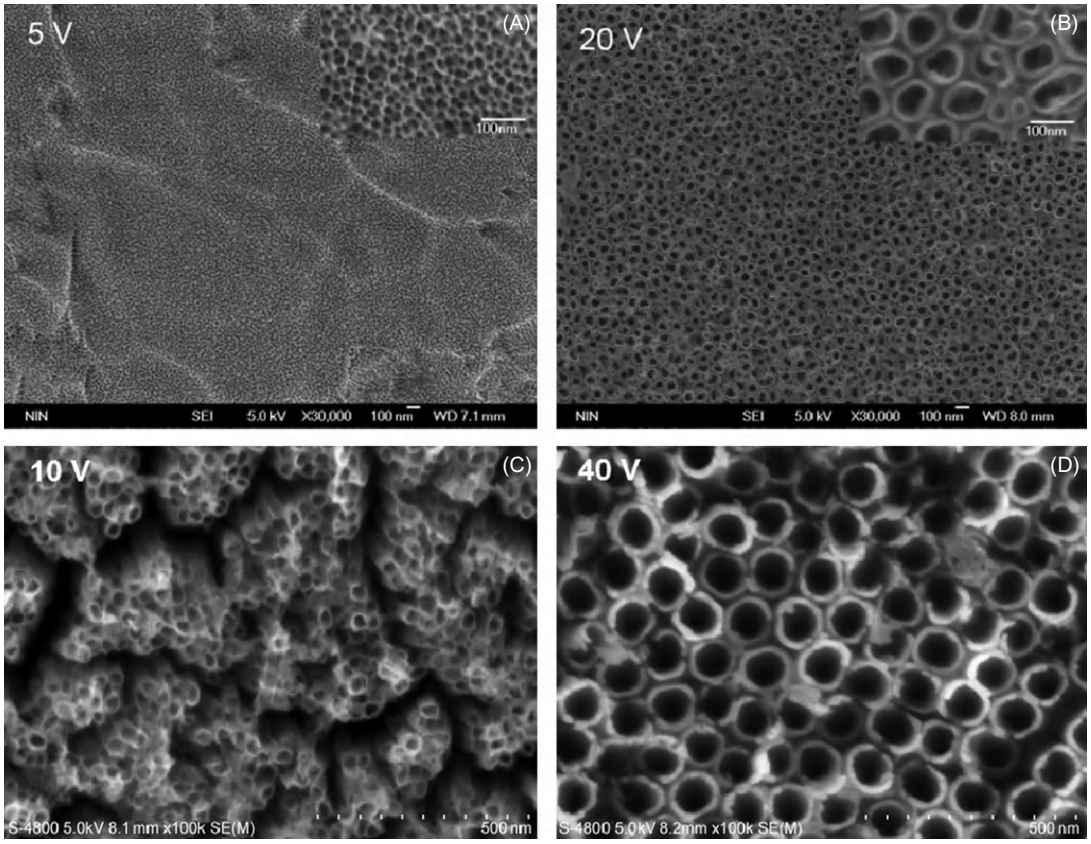

FIGURE 17.1

(A and B) NTs formed at 5 and 20 V in 0.5 wt% aqueous HF solution with tube diameters of 25 and 80 nm, respectively. (C and D) NTs formed at 10 and 40 V in an EG solution with 0.5 wt% NH_4F, 5 vol% CH_3OH, and 5 vol% H_2O with tube diameters of 30 and 80 nm, respectively.

Reprinted with permission from Ref. [4].

H_2O [7], NaH_2PO_4/HF [9], and Na_2SO_4/HF [9]. The diameter of the NTs can be regulated to vary from 15 to 140 nm and the length can range from 200 to 1000 nm by adjusting the electrolyte content and anodization voltage [21]. When using polar organic electrolytes, much longer NTs of hundreds of micrometers can be fabricated [22]. Ethylene glycol (EG) is the commonly used organic solvent to fabricate NTs. The typical NTs formed by anodization of a Ti foil in an EG solution with 0.5 wt% NH_4F, 5 vol% CH_3OH, and 5 vol% H_2O at 10 V for 1 h and 40 V for 40 min are shown in Figure 17.1C and D, respectively.

17.3 Factors influencing the bioactivity of the NTs

Various factors can influence the bioactivity of the NTs during their preparation and cell culture process. A better understanding of these factors helps to optimize the NTs for better biological performance. Here, we summarize the factors such as the sterilization process, phenotype of cells, protein concentration in the culture medium, and smoothness of the top ends of the tube walls that affect the bioactivity of the NTs.

17.3.1 Influence of sterilization on the bioactivity of the NTs

Sterilization process is essential for the in vitro bioactivity assay and finally in vivo applications of dental implants. However, many researchers choose sterilization methods arbitrarily when studying the biocompatibility of NTs. In some experiments, autoclaving is used [10–13,23], whereas in some others, ultraviolet (UV) irradiation or ethanol immersion is used [24–26]. Sterilization methods can be considered as a posttreatment of the samples, and the various sterilization methods can change the surface properties of the samples and corresponding bioactivity. We have compared the effects of three commonly used sterilization methods, namely autoclaving, UV irradiation, and ethanol immersion on the bioactivity of NTs.

We have found that the sterilization process can modify the surface of the biomaterials. Strong discoloration of samples is occasionally observed after autoclaving, but it is usually not found after UV or ethanol sterilization. The most significantly modified characteristics after sterilization are surface chemistry and wettability. Autoclaving decreases the surface free energy of biomedical implants, but contrarily UV treatment dramatically enhances that of Ti (Figure 17.2A). The decrease in hydrophilicity by autoclaving is related to the deposition of hydrophobic contaminants on the implant surfaces [27]. The enhancement in the surface free energy of Ti by UV treatment is associated with the molecular structure alteration of surface titania with abundant Ti–OH group formation and removal of surface hydrophobic contaminants especially hydrocarbons [28,29]. The changes in the surface properties subsequently lead to differential cell responses. UV and ethanol sterilizations induce higher initial adherent cell numbers (Figure 17.2B) and cell proliferation than autoclaving, and UV irradiation leads to the best cell functionalities including adhesion, proliferation, as well as differentiation represented by related gene expressions. UV sterilization appears to be the optimal sterilization method from the viewpoint of eliminating surface contamination.

Oh et al. [30] have investigated the influence of two sterilization methods of wet autoclaving versus dry autoclaving on the functionalities of osteoblasts cultured on the NTs. Their results

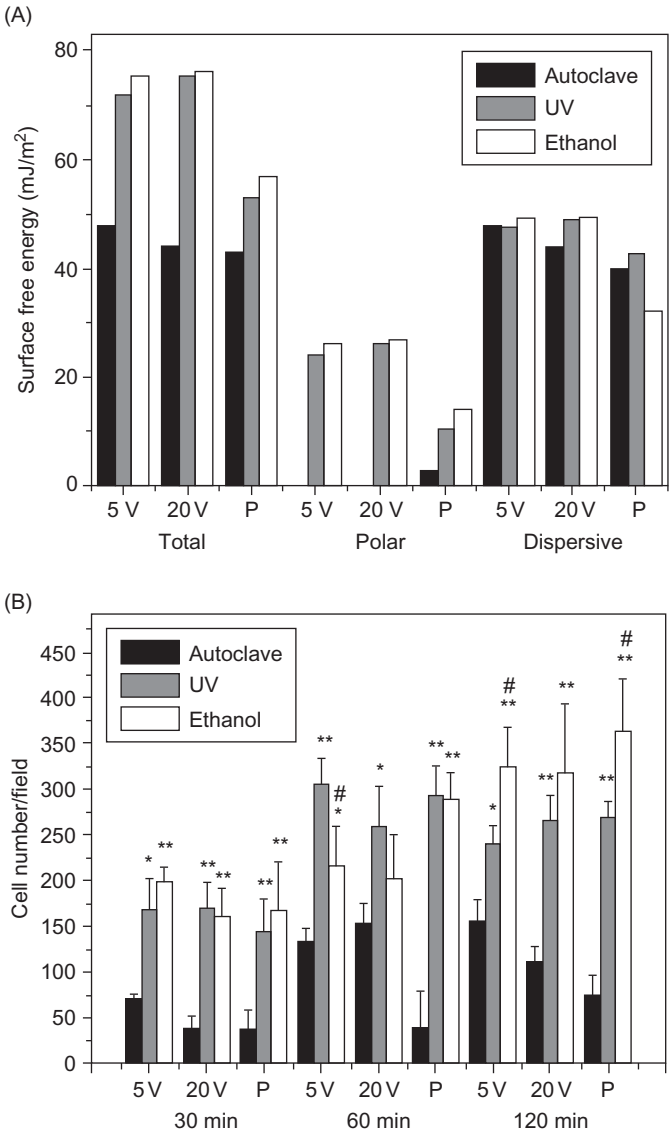

FIGURE 17.2

(A) Values of surface free energy (mJ/m^2) and (B) initial osteoblast adhesion of 5 V NTs, 20 V NTs, and polished Ti after sterilized by autoclaving, UV irradiation, and ethanol immersion. The samples sterilized by UV and ethanol generate higher surface free energy and thus initial adherent cell numbers. $*p<0.05$ and $**p<0.01$ compared with the autoclave-sterilized of each surface, $\#p<0.05$ compared with the UV-sterilized of each surface.

Reprinted with permission from Ref. [4].

indicate that the adhesion, proliferation, and alkaline phosphatase (ALP) activity of osteoblasts cultured on the larger 70 and 100 nm NTs are dramatically changed by the different sterilization conditions at a low cell seeding density of 10,000 cells/well in 12-cell culture well. The different autoclaving methods create huge differences in cell adherence on 70 and 100 nm NTs compared to 30 and 50 nm NTs. These results reveal that the nanofeatures of proteins adhered on the NTs can be altered by different sterilization methods.

17.3.2 Influence of cell phenotype on the bioactivity of the NTs

NTs have been assayed for various biological purposes such as bone implants [2,3,10–12,31], transcutaneous part of the implants [32], and vascular prostheses [24]. There is much evidence from the various primary cell phenotypes including primary osteoblasts, osteoblast cell lines, MSCs, endothelial cells (ECs), vascular smooth muscle cells (VSMCs), dermal fibroblasts, and epidermal keratinocytes suggesting that different cell phenotypes respond differently to the NTs. We have observed differential responses of primary rat calvarial osteoblasts to the NTs compared to those of the osteoblast cell lines [10,31]. Our results to some degree corroborate the report by Brammer et al. [33]. They have compared the effects of TiO_2 and C-coated NT surface chemistries on osteoblast and osteoprogenitor cell behaviors. The TiO_2 NT surface induces an increase in osteoblast functionalities in terms of ALP activity. In contrast, it is the carbon chemistry that results in increased bone mineral deposition and bone matrix protein expression of osteoprogenitor cells. More significant evidence unambiguously demonstrating the phenotypic dependence of cell responses to the NTs is obtained from ECs/VSMCs and dermal fibroblasts/epidermal keratinocytes. Peng et al. [24] have found that the NTs significantly enhance EC proliferation but decrease VSMC proliferation (Figure 17.3). Smith et al. [32] have reported increased dermal fibroblast and decreased epidermal keratinocyte adhesion, proliferation, and differentiation on the NTs.

The evidence reminds us that when comparing the reports on the bioactivity of the NTs from different sources, it should be borne in mind that the responses of cells to the NTs are phenotypic dependent. In addition, the differential response of the different cell phenotypes to the NTs provides a good approach for tissue specific implants that selectively benefit from the desired tissue integration while simultaneously inhibiting the unwanted response.

17.3.3 Influence of protein concentration in culture medium on the bioactivity of the NTs

The proteins adsorbed to the implant surface play a key role in cell/implant interactions. We have compared the influence of the serum concentration in the culture medium on the change in the protein adsorption amount and the consequent initial cell spreading on the NTs and flat Ti [2]. Different serum concentrations do not influence cell adhesion on flat Ti control and 25 nm NTs but seriously affect that on 80 nm NTs (Figure 17.4). The cells attach and spread well on the 80 nm NTs when cultured with 5% or 10% serum while 2% serum leads to poor cell adhesion. This phenomenon can be explained by the cell adhesion mechanism. A requirement for normal cell functionalities on biomaterials is stable adhesion or else cell apoptosis will occur [34]. Therefore, the amount of adsorbed proteins is very important for the biological performance of biomaterials. The amounts of proteins on the nanostructured surface increase with serum concentrations from

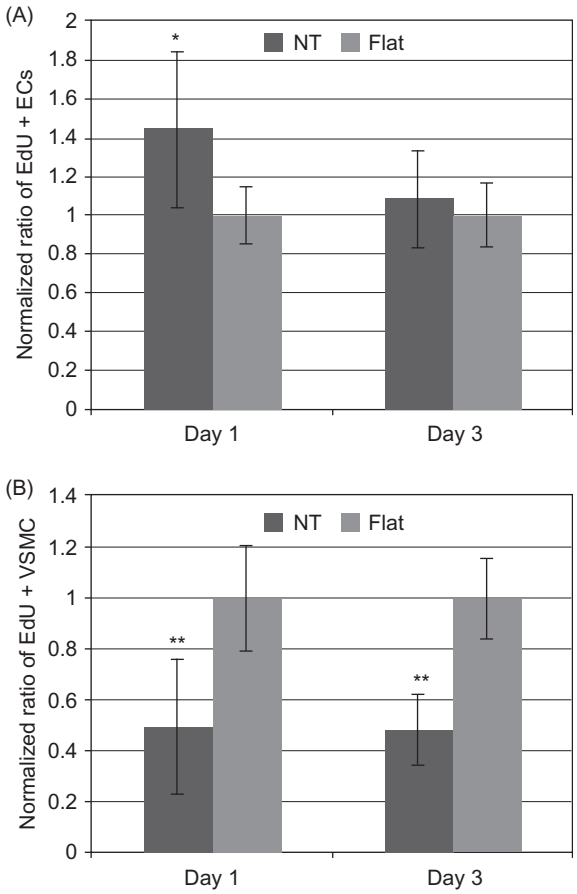

FIGURE 17.3

Ratio of 5-*ethynyl*-2′-deoxyuridine (EdU) positive (A) ECs and (B) VSMCs on flat or NT substrate normalized by the average proportion of positive cells on flat surfaces on day 1 and 3. Data are presented as average±standard deviation. $*P<0.05$, $**P<0.01$ versus same day flat control.

Reprinted with permission from Ref. [24].

2% to 10% (Figure 17.4B, F, G, J, and K). With regard to the flat surface and 25 nm NTs, because large microscale focal adhesion can form, the cells can attach and spread well in 10%, 5%, or 2% serum. As for the large NTs with size of 50−100 nm, because they constrain cell focal adhesion to the top of the tube walls, high quality is needed for the small focal adhesion to support stable cell adhesion. As shown in Figure 17.4G, H, K, and L), when cultured in 10% or 5% serum, the adsorbed proteins not only widen the intertubular areas but also provide adequate integrin adhesion sites, thus giving rise to enough high-quality focal adhesion and good cell adhesion. In 2% serum, the smaller amount of adsorbed proteins results in narrow tube walls, a low density of integrin adhesion sites, low-quality small focal adhesion, and poor cell adhesion (Figure 17.4C and D).

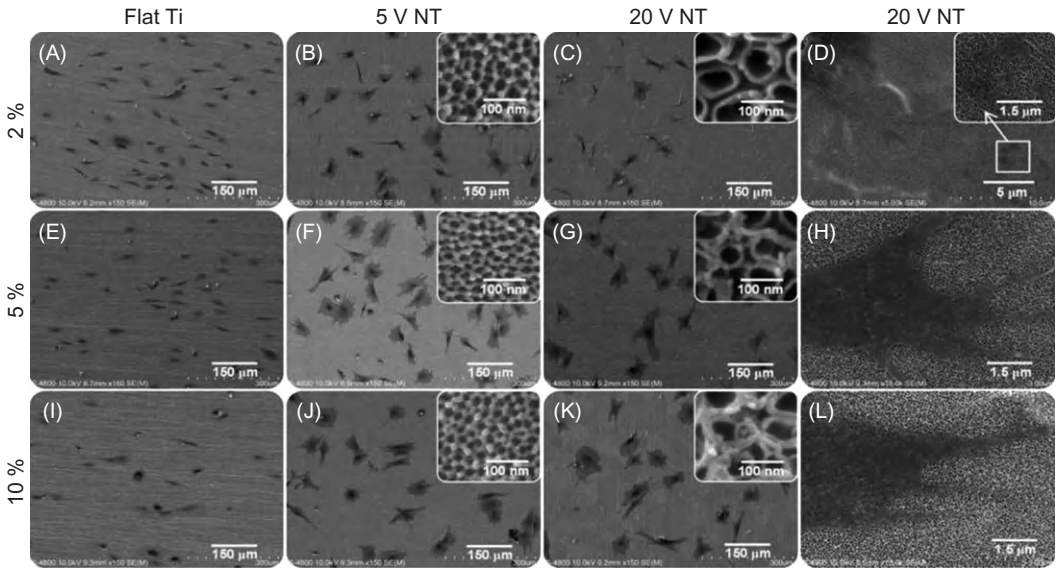

FIGURE 17.4

Cell shape on flat Ti, 25 and 80 nm NTs cultured with 2%, 5% or 10% serum for 12 h. The insets in (B), (C), (F), (G), (J), and (K) show the ECM deposition along the nanotopographies.

Reprinted with permission from Ref. [2].

Long and thin cell fillopodia are observed on 80 nm NTs cultured in 2% serum indicating that cells cannot form stable adhesion (Figure 17.4D), while strong and thick lamellipodia are observed from cells cultured in 5% or 10% serum demonstrating stable cell adhesion (Figures 17.4H and L). We have also observed many cell fragments on 80 nm NTs in 2% serum on the cell retraction path (Figure 17.4D). This may partly account for cell apoptosis on the surface. In Park et al.'s [25,35] experiments, a low-medium serum concentration of 2% is used in cell cultures and should account for the unfavorable effect of larger NTs on MSC functions observed by them. Since there are abundant proteins in vivo, the results obtained from 10% serum should reflect the in vivo performance of the NTs more accurately. Our results indicate the influence of protein concentration in the culture medium on the evaluated bioactivity of the NTs, which should be of concern when comparing different reports on the NTs bioactivity.

17.3.4 Influence of protein distribution pattern on the bioactivity of the NTs

As aforementioned, the proteins adsorbed onto the biomaterials mediate cell adhesion and follow functions on the biomaterials and play a crucial role in conveying the biological effects of the topographical cue. Besides the amount, other aspects of the adsorbed proteins such as species, conformation, and orientation have also been reported to influence the cell/biomaterials interaction. We notice that the NTs formed in an inorganic electrolyte have relatively flat top ends of NT walls

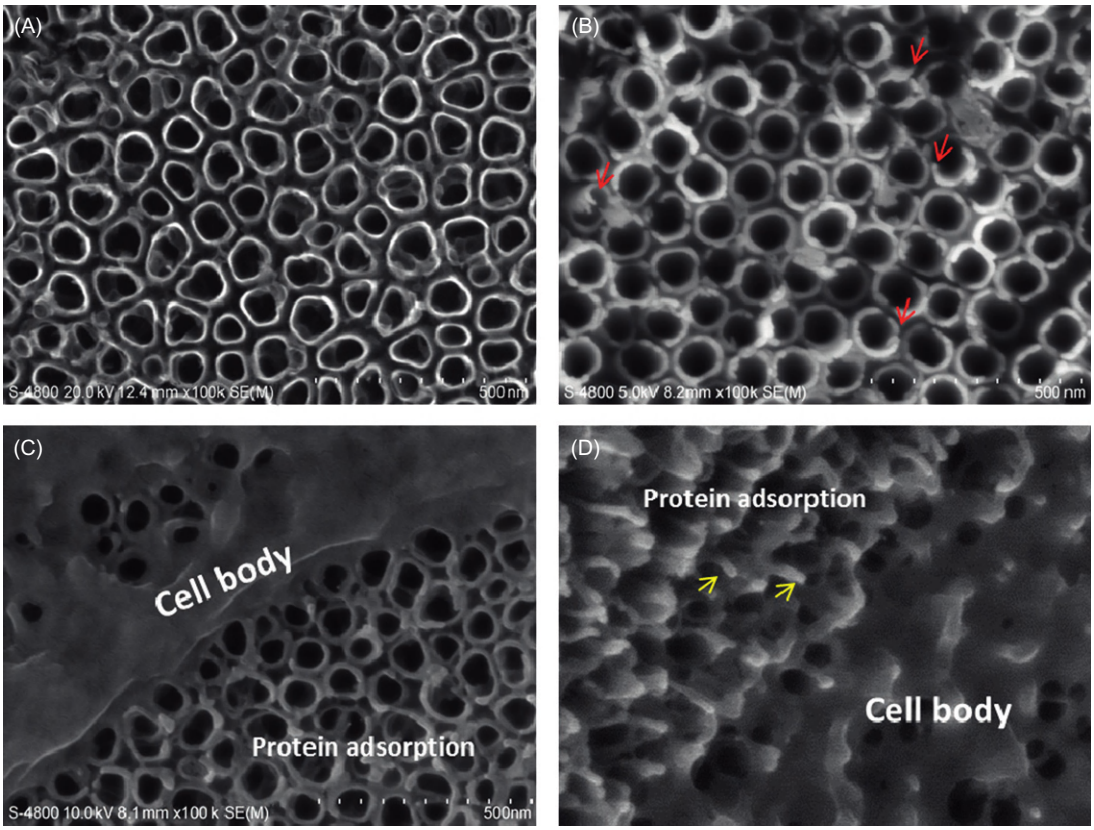

FIGURE 17.5

(A) NTs formed at 20 V in 0.5 wt% HF aqueous solution; (B) NTs formed at 40 V in an EG solution with 0.5 wt % NH_4F, 5 vol% CH_3OH, and 5 vol% H_2O. Red arrows indicate the unsmooth top ends of nanotube walls with flakes; (C) protein adsorption on the NTs shown in (A) and the detail of cell interaction with them; (D) protein adsorption on the NTs shown in (B) and details of cell interaction with them. Yellow arrows show the protein pillars formed on them. (For interpretation of the references to color in this figure legend, the reader is referred to the web version of this book.)

Parts of the figure are reprinted with permission from Ref. [2].

(Figure 17.5A), and consequently induce an even distribution of proteins along the tube walls and intimate cell attachment (Figure 17.5C). On contrary, for the NTs formed in an EG solution with 0.5 wt% NH_4F, 5 vol% CH_3OH, and 5 vol% H_2O, the top ends of the NT walls are not completely smooth and have flakes (Figure 17.5B). Although the NTs formed in the EG solution induce more protein deposition forming thicker protein layers, the adsorbed proteins do not distribute evenly but form pillars (Figure 17.5D). Tall protein pillars with relatively small top dimensions mostly <50 nm are distributed at a certain distance from each other. The uneven protein distribution can be ascribed to the unsmooth top ends of the NT walls with flakes, which provide local nucleation

sites for protein aggregation leading to pillar formation. Collectively, the evidence demonstrates that even subtle changes in the nanotopography can lead to dramatic alteration in the protein deposition pattern. The immediate substrate that cells interact with is the adsorbed proteins rather than the primitive nanotopographies. The notably uneven protein deposition will change the nanotopography and make the ultimate topographical cues exposed to cells to be quite different from the primitive nanotopographies, thereby altering the biological performance. The uneven protein distribution consequently leads to compromised cell focal adhesion and following functions including proliferation and differentiation. It is thus strongly suggested that the protein adsorption pattern should also be carefully inspected when studying the bioactivity of nanoscale biomaterials.

17.4 In vitro bioactivity of the NTs and in vivo osseointegration

17.4.1 In vitro bioactivity of the NTs

NTs can foster the growth of nanostructured hydroxyapatite. Oh et al. [8] have treated the NTs with NaOH solution to investigate their bioactivity. NTs induce the growth of extremely fine-scale (~8 nm feature) nanofibers of bioactive sodium titanate on the top edge of the ~15 nm thick NT wall. After immersion in a SBF, the nanoscale sodium titanate can induce the nucleation and growth of nanodimensioned HA phase. The kinetics of HA formation can be significantly accelerated by the presence of the NTs. Pittrof et al. [9] have developed micropatterned NT layers surrounded by compact oxide via an optimized process. By immersing such patterns in SBF, selective and dense apatite deposition occurs only on the NT surfaces (Figure 17.6). These results verify the strong ability of the NTs to induce apatite deposition. Although there is still debate whether SBF can predict the bioactivity of biomaterials [36], the strong ability of the NTs to foster nanostructured hydroxyapatite deposition to a certain degree demonstrates their bone formation favoring properties.

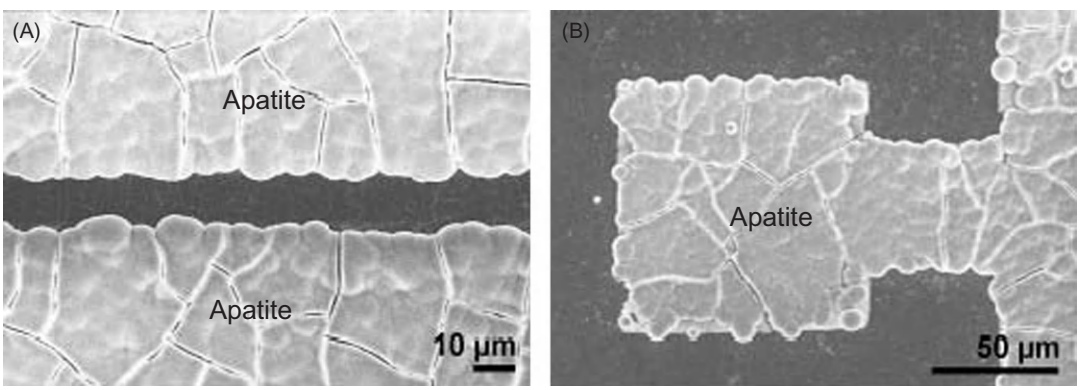

FIGURE 17.6

Patterned samples after immersion in 1.5× SBF. (A and B) Field emission scanning electron microscopy (FE-SEM) micrographs showing selective apatite nucleation exclusively on nanotube regions.

Reprinted with permission from Ref. [9].

Osteoblasts are responsible for bone formation, and the effects of NTs on osteoblast functions have been widely observed on primary rat calvarial osteoblasts [3,4,31] and MC3T3-E1 mouse osteoblasts [10,26]. There is some controversy on the effects of the NTs on some of the osteoblast functions due to the differential experimental conditions in the literature. However, it seems that the NTs are effective in promoting ECM secretion and mineralization. The NTs with diameters of 25 and 80 nm formed in 0.5 wt% aqueous HF solution can induce more collagen secretion and mineral deposition in primary rat calvarial osteoblast cultures [4]. Hierarchical hybrid micro/nanotextured titanium surface topographies with NTs produced by our group by simple acid etching followed by anodization mimic the hierarchical structures of bone tissues, thereby inducing more collagen secretion compared to the microrough and flat Ti surfaces (Figure 17.7) [3].

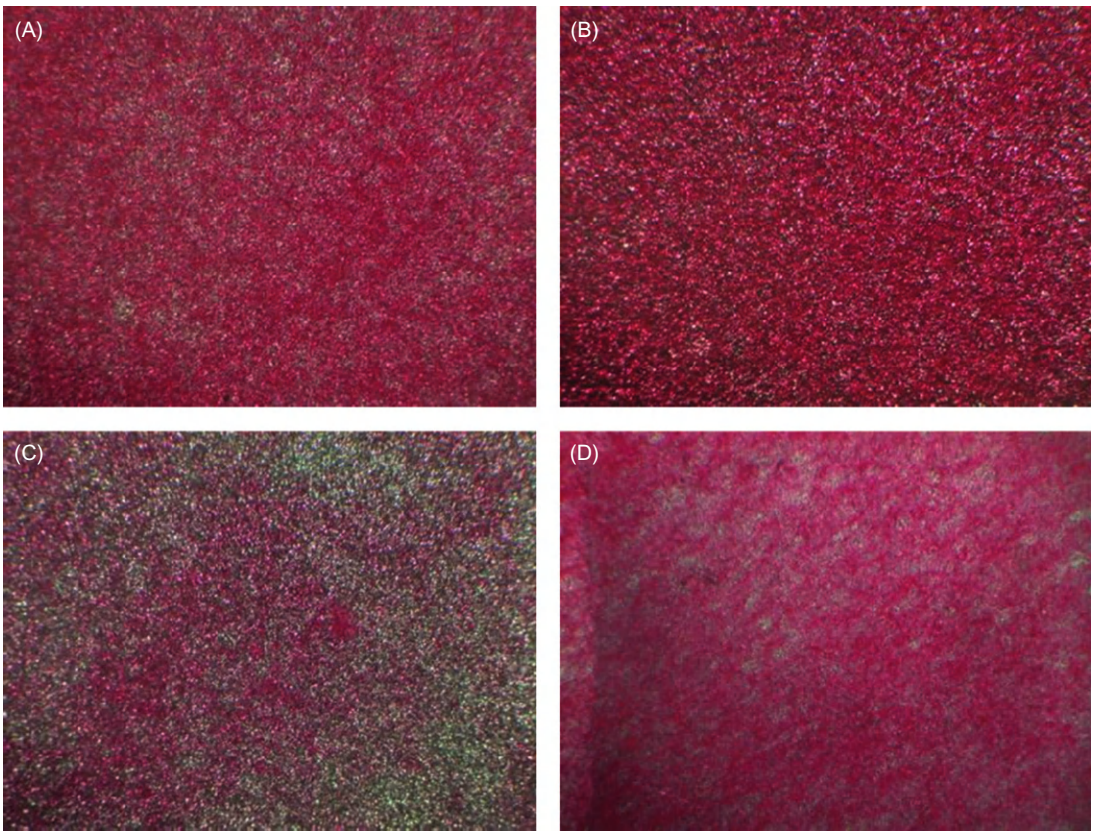

FIGURE 17.7

Collagen secretion by osteoblasts on samples after 7 days of incubation. (A) Hierarchical hybrid micro/nanotextured surface with 15 nm NTs, (B) hierarchical hybrid micro/nanotextured surface with 80 nm NTs, (C) acid-etched microstructured surface, and (D) flat Ti surface.

Reprinted with permission from Ref. [3].

MSCs play a crucial role in bone regeneration and bony fixation of implanted biomaterials. Most of the osteoblastic cells that colonize the implant surface to induce bone growth originate from MSCs and hence, in order to accomplish good osseointegration, it is critical to induce the differentiation of MSCs preferentially toward osteogenitor cells and then into osteoblasts in lieu of other cell lineages. We find that the NTs significantly promote MSC attachment and spreading (Figure 17.8), collagen secretion and ECM mineralization (Figure 17.9), as well as osteogenesis-related gene expression in the absence of extra OS [2]. The osteogenesis-inducing ability of the 80 nm NTs is higher than that of the 25 nm ones. Oh et al. [37] have also observed that small 30 nm NTs promote MSC adhesion without noticeable differentiation whereas larger ones of 70−100 nm elicit selective MSC differentiation to osteoblasts. Moon et al. [38] have recently assessed the size effect of NTs on the behavior and osteogenic functionality of human MSCs. After incubation for 2 weeks, expression of ALP, osteopontin, integrin-β, and protein kinase R-like endoplasmic reticulum kinase genes are significantly higher in cells cultured on 70 nm NTs than those cultured on 30, 50, and 100 nm NTs and Ti. The evidence demonstrates that NTs with a suitable tube size have osteogenesis-inducing ability.

The osteogenesis-inducing ability of the NTs arises from their modulating effect on cell shape and focal adhesion. This will lead to changes in the mechanotransduction including the indirect one, that is integrin-dependent signal pathways, and the direct one that is gene expression originating from the cell nucleus distortion by force transferred via the cytoskeleton [39,40]. The shape of stem cells on biomaterials is closely related to the high cytoskeletal tension such as the well-spread stem cell and that with the proper aspect ratio undergoing osteogenesis with the poorly spread stem cell becoming adipocytes [41]. Therefore, the effects of the NTs on promoting MSC spreading constitute an important mechanism for the osteogenesis-inducing ability. The higher osteogenesis-inducing ability rendered by the 80 nm NTs than the 25 nm ones can be explained by the influence of the nanotopography on the cell focal adhesion size, distribution, and related mechanotransduction. The presentation of integrin ligation sites at a distance larger than a certain value (about 50−70 nm) perturbs integrin clustering, focal adhesion assembly, and organization of the actin stress fiber anchored to the focal adhesion [42]. Accordingly, the 25 nm NTs do not, or slightly, influence the integrin clustering and focal adhesion formation. Instead, the 80 nm NTs constrain the cell focal adhesion to the intertubular area. In this way, the 80 nm NTs modulate the size, shape, and distribution of focal adhesion to a nanoscale periodic occurrence. On one hand, it triggers more integrin-related signals, and on the other hand, it induces a nanoscale periodic distribution of the cytoskeletal actin and stress leading to extensive nucleus distortion and related direct mechanotransduction signals.

17.4.2 In vivo osseointegration of the NTs

The good bone-favoring properties of the NTs with suitable size have also been verified by various in vivo studies. Bjursten et al. [13] have investigated the in vivo bone bonding between 80 nm NTs and grit-blasted TiO_2. Four weeks after implantation into rabbit tibias, the NTs improve the bone bonding strength by as much as ninefolds compared to the grit-blasted TiO_2 surface. The histological analysis confirms greater BIC areas, new bone formation, and calcium and phosphorus levels on the NTs. Von Wilmowsky et al. [14] have reported that a NT structured implant surface with a diameter of 30 nm can influence bone formation and bone development by enhancing the osteoblast functionalities and the NT coatings resist shearing forces evoked by implant insertion. They have recently reported a significantly higher value of the BIC for the 50, 70, and 100 nm NTs

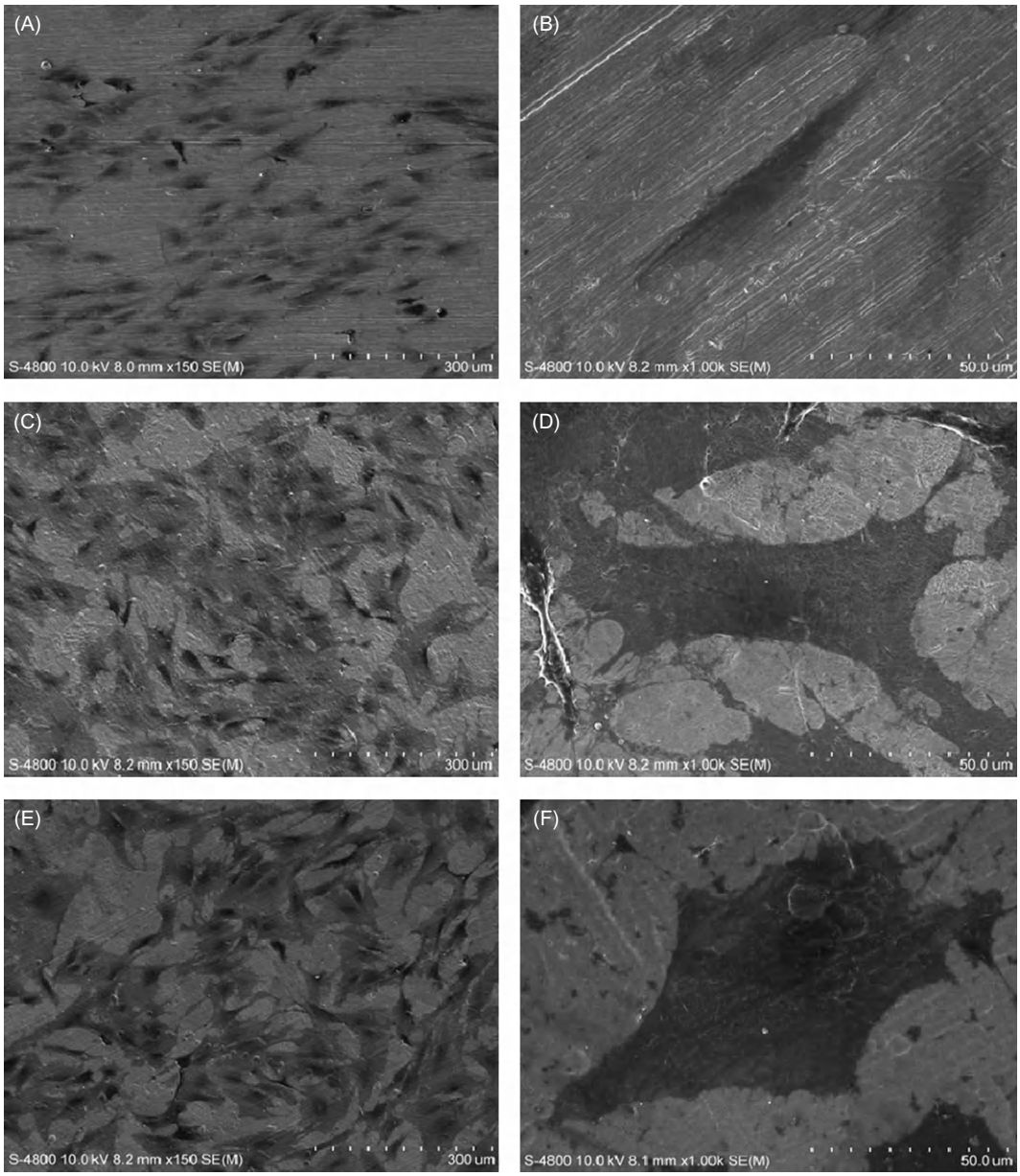

FIGURE 17.8

SEM pictures showing the morphology of cells after 2 days of culture on samples. (A and B) flat Ti control; (C and D) 25 nm NTs; (E and F) 80 nm NTs.

Reprinted with permission from Ref. [2].

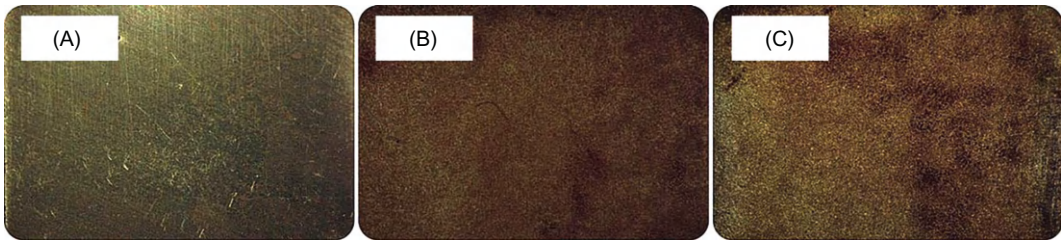

FIGURE 17.9

ECM mineralization on different samples after 2 weeks culturing of MSCs. (A) Flat Ti control, (B) 25 nm NTs, and (C) 80 nm NTs.

Reprinted with permission from Ref. [2].

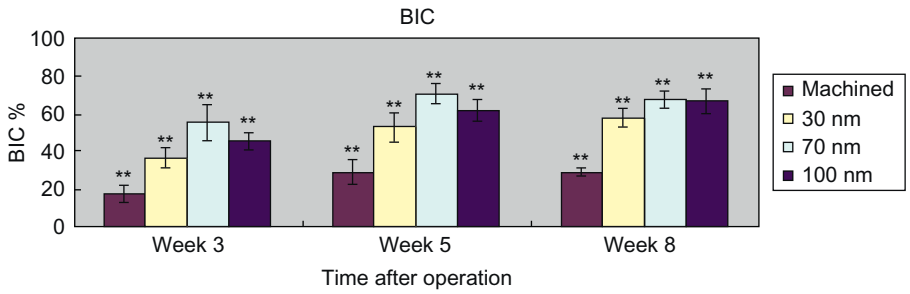

FIGURE 17.10

Values of BIC for all implant surfaces at 3, 5 and 8 weeks after implantation. Asterisk (*) shows significant difference in comparison with machined implant ($P < 0.05$). Double asterisks (**) show a significant difference in comparison with all other groups in experiment ($P < 0.05$).

Reprinted with permission from Ref. [16].

compared to the pristine Ti controls [15]. The bone morphogenetic protein 2 (BMP-2) expression within the 50, 70, and 100 nm groups is statistically different compared to the control group. In addition, a significant difference is found from the osteocalcin expression in the 70 nm group. Wang et al. [16] have investigated the effects of the NTs with different diameters of 30, 70, and 100 nm on the biological attachment mechanism of implants to bone in vivo. When comparing to machined Ti implants, a significant increase in BIC (Figure 17.10) and gene expression level is found in the bone attached to implants with the NTs, especially with the 70 nm diameter ones. The evidence demonstrates the strong ability of the NTs to induce better osseointegration, and the NTs with a size of about 70 nm may be the optimal ones for osseointegration.

17.5 Drug-loading NTs for better bioactivity and antibacterial properties

The nanotubular structure of the NTs provide space for drug loading, thereby opening the possibility of endowing the implant surface with extra properties by loading targeted agents. Desai's group

first tested the suitability of the NTs to serve as a potential drug loading and delivering platform [43,44]. They used bovine serum albumin and lysozyme as model proteins to investigate the loading and release efficiencies from the NT platforms. They demonstrated the efficacy of using NTs as drug eluting coatings for implantable devices. Various amounts of drugs can be incorporated into the NTs and their release can be adjusted by varying the tube length, diameter, and wall thickness [43]. Another report demonstrated that the NTs can control small molecule delivery within weeks and larger molecules in months [44]. Various agents have been experimentally loaded into the NTs to attain better bioactivity and extra properties such as antibacterial ability. There are many reports on the incorporation of growth factors or antibiotics to the NTs and certain bioactivity and antibacterial ability. However, we believe that the NTs are ideal for loading and delivering targeted inorganic agents such as silver (Ag), strontium (Sr), and zinc (Zn). First of all, these are much smaller molecules than growth factors and antibiotics and function at very low doses. Long-lasting activity can be achieved by increasing the loaded amounts and controlling the release rate appropriately. Secondly, these agents are stable due to their inorganic nature, thereby facilitating the use of loading processes and loading methods that tend to have harsh conditions. Thirdly, the stable properties of the agents may also permit relatively long storage after fabrication of the implants and it is important to commercial adoption.

As mentioned in the introduction section, postoperation infection remains one of the most common and serious complications for a dental implant, and so a surface boasting long-term antibacterial ability is highly desirable in order to prevent implant-associated infection. We have fabricated Ag nanoparticles incorporated NTs (NT−Ag) on Ti implants to achieve this purpose [5]. The Ag nanoparticles adhere tightly to the wall of the NTs prepared by immersion in a $AgNO_3$ solution followed by UV light irradiation (Figure 17.11). The amount of Ag introduced to the NTs can be controlled by changing the processing parameters such as the $AgNO_3$ concentration and immersion time. The NT−Ag can kill all the planktonic bacteria in the suspension during the first several days, and the ability of the NT−Ag to prevent bacterial adhesion is maintained without obvious decline for 30 days, which are normally long enough to prevent postoperation infection in the early and intermediate stages and perhaps even late infection around the implant. The ability of the NT−Ag to prevent viable bacterial colonization is vividly displayed by fluorescence staining (Figure 17.12). After 7 days of repeated bacterial invasion every 24 h, there are large amounts of viable bacteria on the flat Ti and smaller amounts on the TiO_2−NTs. In comparison, the amounts of viable bacteria are obviously smaller on the NT−Ag samples due to the Ag loading amount. Although the NT−Ag structure shows some cytotoxicity, it can be reduced by properly controlling the Ag release rate. This NT−Ag structure with relatively long-term antibacterial ability has promising applications in bone implants after eradicating the cytotoxicity by properly controlling the Ag release.

Sr shows the effect to modulate bone turnover toward osteogenesis by enhancing osteoblast functions and inhibiting osteoclast functions, and so Sr-loaded nanotubular structures (NT−Sr) that allow controlled and long-term Sr release are expected to yield favorable osteogenic effects. Well-ordered $SrTiO_3$ NT arrays capable of Sr release at a small rate and for a long time have been successfully fabricated on titanium by simple hydrothermal treatment of anodized titania NTs (Figure 17.13) [20]. This surface architecture combines the functions of nanoscale topography and Sr release to enhance osseointegration while at the same time leaving space for loading of other functional substances. In vitro experiments reveal that the $SrTiO_3$ NT arrays possess good biocompatibility (Figure 17.13) and

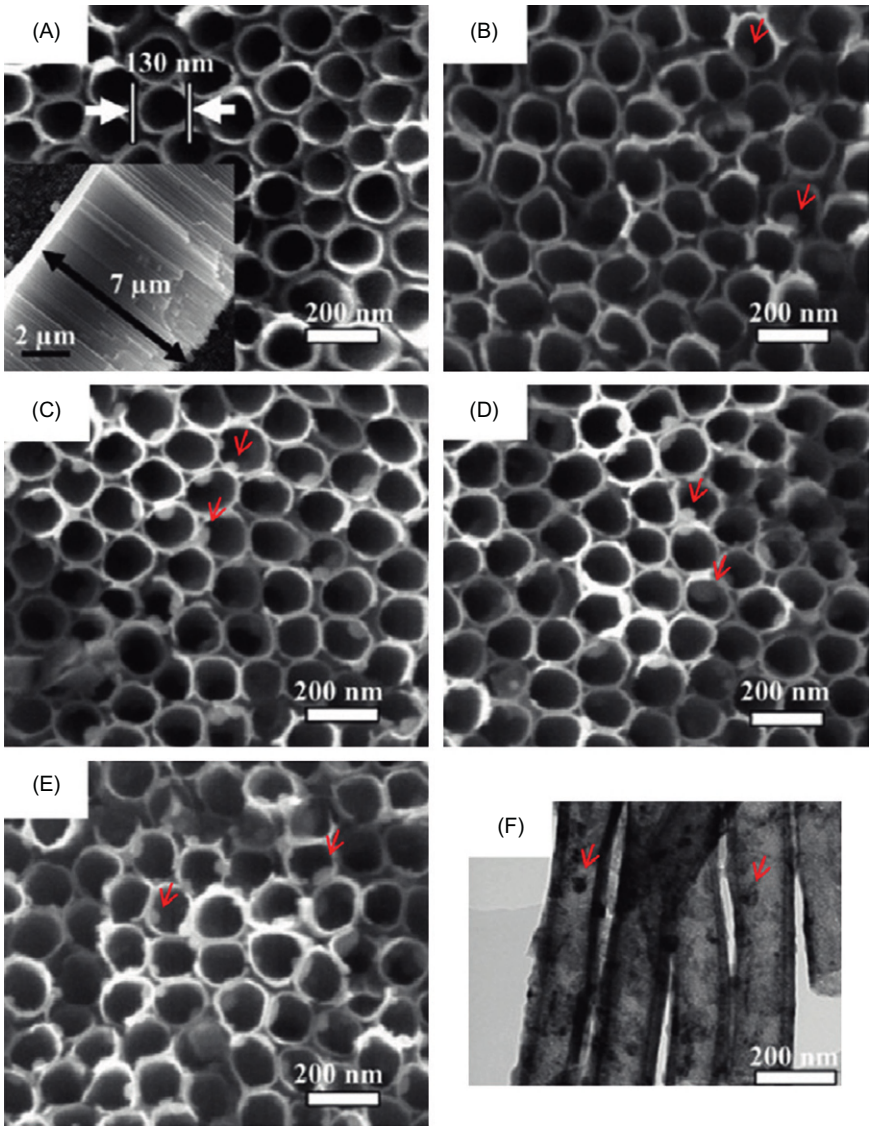

FIGURE 17.11

SEM images of the samples. (A) NTs, (B–E) Ag incorporating NTs formed in $AgNO_3$ solutions of different concentrations (0.5, 1, 1.5, and 2 M). The inset in (A) is the side-view SEM image revealing that the length of the nanotubes is about 7 μm. The red arrows in (B–E) indicate the Ag nanoparticles. (F) TEM image acquired from the Ag incorporating NTs formed in 1 M $AgNO_3$ shows that the Ag nanoparticles attached to the inner wall of the NTs have a diameter of about 10–20 nm. (For interpretation of the references to color in this figure legend, the reader is referred to the web version of this book.)

Reprinted with permission from Ref. [5].

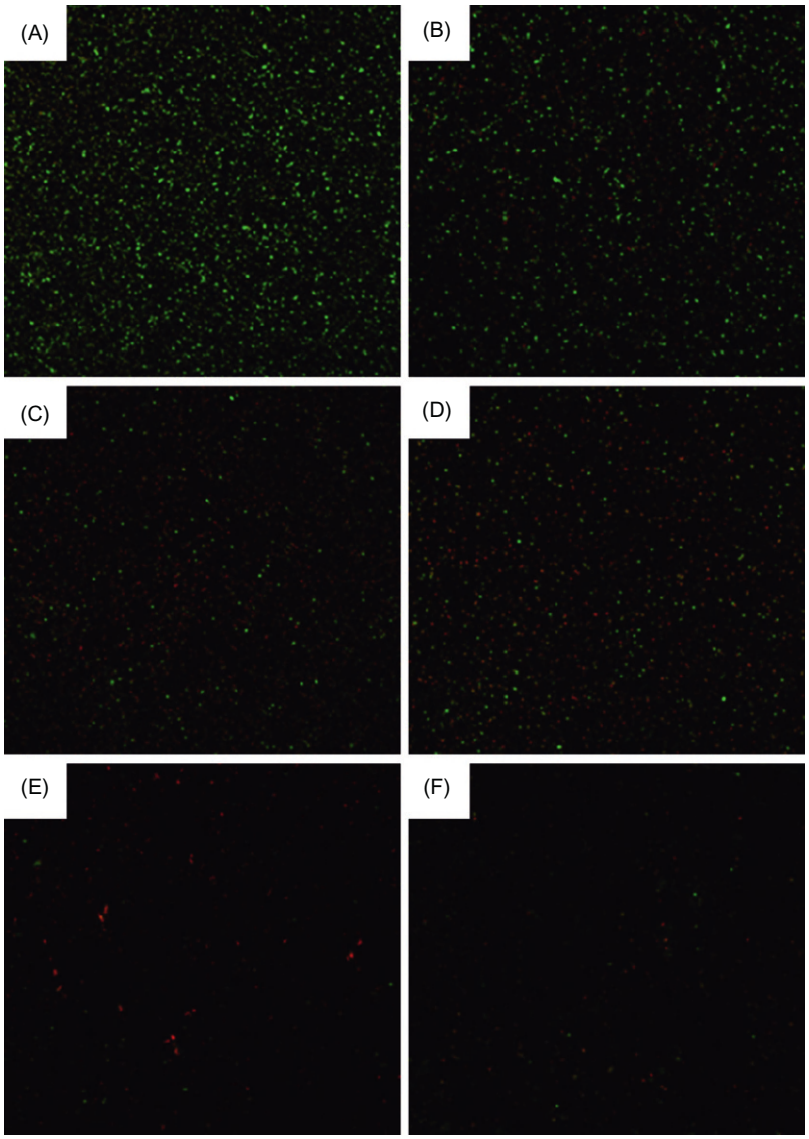

FIGURE 17.12

Representative images showing viability of the bacteria after 7 days of incubation on samples: (A) Ti, (B) NTs, (C–F) Ag incorporating NTs formed in $AgNO_3$ solutions of different concentrations (0.5, 1, 1.5, and 2 M). Live bacteria appear green while dead ones appear orange. (For interpretation of the references to color in this figure legend, the reader is referred to the web version of this book.)

Reprinted with permission from Ref. [5].

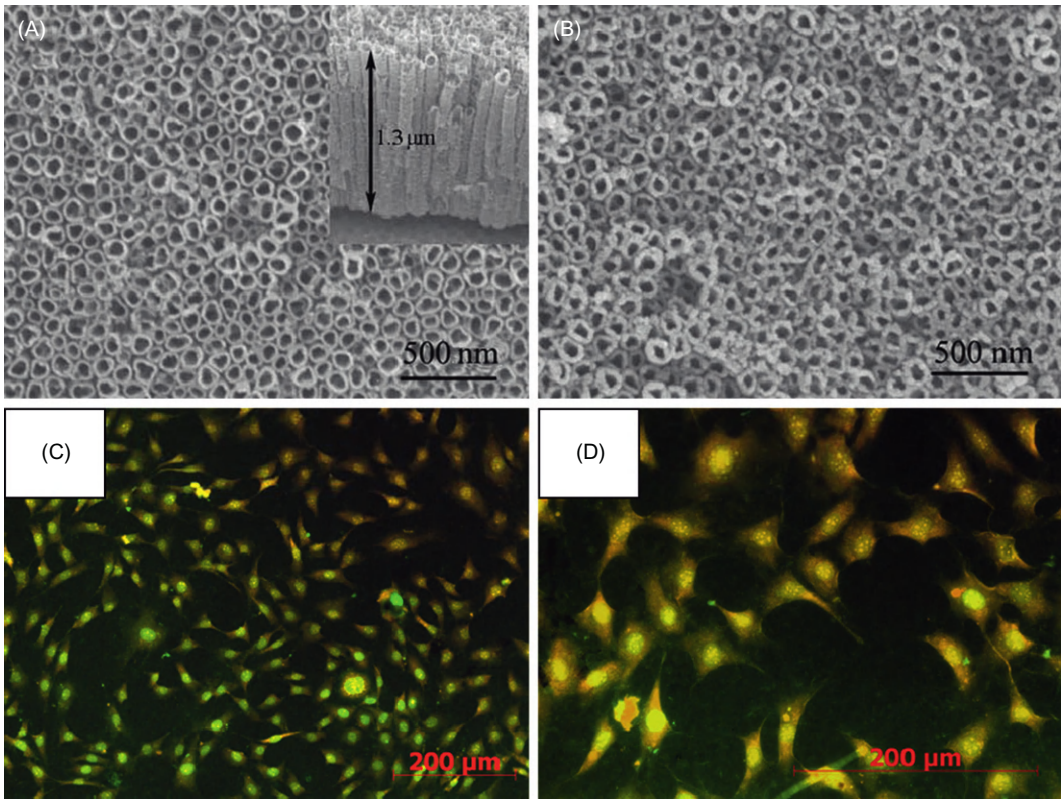

FIGURE 17.13

SEM micrographs of (A) titania nanotube arrays and (B) $SrTiO_3$ nanotube arrays. Cell morphology on $SrTiO_3$ nanotube arrays after 5 days of culturing: (C) low magnification and (D) high magnification.

Reprinted with permission from Ref. [20].

can induce precipitation of hydroxyapatite from SBF. Recently, we have found that the NT−Sr coating can dramatically improve MSC spreading as well as proliferation and enhance MSC differentiation toward osteogenitor cells and subsequently osteoblasts. The inorganic NT−Sr gives rise to good osteogenic activity without the need to apply foreign complex biomolecules. The materials are easy to fabricate and have good stability that would facilitate large-scale industrial production, storage, transport, sterilization, and clinical use. They are thus very attractive to bone implants, especially osteoporotic bone implants for clinical applications.

In addition to Sr, there are many other agents showing attractive properties in bone−implant applications, e.g., Zn. Besides the effects of positively regulating bone turnover, Zn has good antibacterial activity and anti-inflammation ability. Hence, Zn is a good candidate for implant surface loading and long-term release to attain better clinical performance. We have also developed Zn loaded NTs (NT−Zn) using a method similar to that of NT−Sr. The NT−Zn can also promote

MSC attachment and spread and induce MSC osteogenic differentiation. In addition, the NT−Zn samples also exhibit excellent antibacterial effects to prevent bacterial colonization.

17.6 Conclusions

Many reports have revealed the effectiveness of NTs in promoting the functions of osteoblasts and MSCs and MSC osteogenic differentiation in vitro and enhancing implant osseointegration in vivo. Our studies demonstrate the suitability of the NTs to load and deliver some inorganic bioactive agents such as Ag, Sr, and Zn to achieve antibacterial- and/or osteogenesis-inducing abilities. The NT surfaces, especially those loaded with suitable inorganic bioactive agents, have huge promise in fabricating dental implants with better clinical performance.

Acknowledgments

This work was jointly supported by National Natural Science Foundation of China Nos. 50902104 and 31200716, City University of Hong Kong Applied Research Grant (ARG) No. 9667066, and the Opening Project of State Key Laboratory of High Performance Ceramics and Superfine Microstructure (SKL201103SIC).

References

[1] J.Y. Rho, L. Kuhn-Spearing, P. Zioupos, Mechanical properties and the hierarchical structure of bone, Med. Eng. Phys. 20 (1998) 92−102.
[2] L. Zhao, L. Liu, Z. Wu, Y. Zhang, P.K. Chu, Effects of micropitted/nanotubular titania topographies on bone mesenchymal stem cell osteogenic differentiation, Biomaterials 33 (2012) 2629−2641.
[3] L. Zhao, S. Mei, P.K. Chu, Y. Zhang, Z. Wu, The influence of hierarchical hybrid micro/nano-textured titanium surface with titania nanotubes on osteoblast functions, Biomaterials 31 (2010) 5072−5082.
[4] L. Zhao, S. Mei, W. Wang, P.K. Chu, Z. Wu, Y. Zhang, The role of sterilization in the cytocompatibility of titania nanotubes, Biomaterials 31 (2010) 2055−2063.
[5] L. Zhao, H. Wang, K. Huo, L. Cui, W. Zhang, H. Ni, et al., Antibacterial nano-structured titania coating incorporated with silver nanoparticles, Biomaterials 32 (2011) 5706−5716.
[6] M. Tzaphlidou, The role of collagen in bone structure: an image processing approach, Micron 36 (2005) 593−601.
[7] G.A. Crawford, N. Chawla, K. Das, S. Bose, A. Bandyopadhyay, Microstructure and deformation behavior of biocompatible TiO_2 nanotubes on titanium substrate, Acta Biomater. 3 (2007) 359−367.
[8] S.H. Oh, R.R. Finones, C. Daraio, L.H. Chen, S.H. Jin, Growth of nano-scale hydroxyapatite using chemically treated titanium oxide nanotubes, Biomaterials 26 (2005) 4938−4943.
[9] A. Pittrof, S. Bauer, P. Schmuki, Micropatterned TiO_2 nanotube surfaces for site-selective nucleation of hydroxyapatite from simulated body fluid, Acta Biomater. 7 (2011) 424−431.
[10] K.S. Brammer, S. Oh, C.J. Cobb, L.M. Bjursten, H.V. Heyde, S. Jin, Improved bone-forming functionality on diameter-controlled TiO_2 nanotube surface, Acta Biomater. 5 (2009) 3215−3223.
[11] K. Das, S. Bose, A. Bandyopadhyay, TiO_2 nanotubes on Ti: influence of nanoscale morphology on bone cell-materials interaction, J. Biomed. Mater. Res. A 90 (2009) 225−237.

[12] S. Oh, C. Daraio, L.H. Chen, T.R. Pisanic, R.R. Finones, S. Jin, Significantly accelerated osteoblast cell growth on aligned TiO_2 nanotubes, J. Biomed. Mater. Res. A 78A (2006) 97–103.
[13] L.M. Bjursten, L. Rasmusson, S. Oh, G.C. Smith, K.S. Brammer, S. Jin, Titanium dioxide nanotubes enhance bone bonding in vivo, J. Biomed. Mater. Res. A 92 (2010) 1218–1224.
[14] C. von Wilmowsky, S. Bauer, R. Lutz, M. Meisel, F.W. Neukam, T. Toyoshima, et al., In vivo evaluation of anodic TiO_2 nanotubes: an experimental study in the pig, J. Biomed. Mater. Res. B Appl. Biomater. 89 (2009) 165–171.
[15] C. von Wilmowsky, S. Bauer, S. Roedl, F.W. Neukam, P. Schmuki, K.A. Schlegel, The diameter of anodic TiO_2 nanotubes affects bone formation and correlates with the bone morphogenetic protein-2 expression in vivo, Clin. Oral Implants Res. 23 (2012) 359–366.
[16] N. Wang, H. Li, W. Lu, J. Li, J. Wang, Z. Zhang, et al., Effects of TiO_2 nanotubes with different diameters on gene expression and osseointegration of implants in minipigs, Biomaterials 32 (2011) 6900–6911.
[17] L. Zhao, P.K. Chu, Y. Zhang, Z. Wu, Antibacterial coatings on titanium implants, J. Biomed. Mater. Res. B Appl. Biomater. 91 (2009) 470–480.
[18] T.P. Schmalzried, H.C. Amstutz, M.K. Au, F.J. Dorey, Etiology of deep sepsis in total hip arthroplasty. The significance of hematogenous and recurrent infections, Clin. Orthop. Rel. Res. 280 (1992) 200–207.
[19] T.F. Mah, G.A. O'Toole, Mechanisms of biofilm resistance to antimicrobial agents, Trends Microbiol. 9 (2001) 34–39.
[20] Y. Xin, J. Jiang, K. Huo, T. Hu, P.K. Chu, Bioactive $SrTiO_3$ nanotube arrays: strontium delivery platform on Ti-based osteoporotic bone implants, ACS Nano 3 (2009) 3228–3234.
[21] L. Yang, S. Luo, Q. Cai, S. Yao, A review on TiO_2 nanotube arrays: fabrication, properties, and sensing applications, Chin. Sci. Bull. 55 (2010) 331–338.
[22] K. Shankar, G.K. Mor, H.E. Prakasam, S. Yoriya, M. Paulose, O.K. Varghese, et al., Highly-ordered TiO_2 nanotube arrays up to 220 μm in length: use in water photoelectrolysis and dye-sensitized solar cells, Nanotechnology 18 (2007) 065707.
[23] C. Yao, E.B. Slamovich, T.J. Webster, Enhanced osteoblast functions on anodized titanium with nanotube-like structures, J. Biomed. Mater. Res. A 85 (2008) 157–166.
[24] L. Peng, M.L. Eltgroth, T.J. LaTempa, C.A. Grimes, T.A. Desai, The effect of TiO_2 nanotubes on endothelial function and smooth muscle proliferation, Biomaterials 30 (2009) 1268–1272.
[25] J. Park, S. Bauer, K. von der Mark, P. Schmuki, Nanosize and vitality: TiO_2 nanotube diameter directs cell fate, Nano Lett. 7 (2007) 1686–1691.
[26] K.C. Popat, M. Eltgroth, T.J. Latempa, C.A. Grimes, T.A. Desai, Decreased *Staphylococcus epidermis* adhesion and increased osteoblast functionality on antibiotic-loaded titania nanotubes, Biomaterials 28 (2007) 4880–4888.
[27] R.E. Baier, A.E. Meyer, C.K. Akers, J.R. Natiella, M. Meenaghan, J.M. Carter, Degradative effects of conventional steam sterilization on biomaterial surfaces, Biomaterials 3 (1982) 241–245.
[28] Y. Han, D. Chen, J. Sun, Y. Zhang, K. Xu, UV-enhanced bioactivity and cell response of micro-arc oxidized titania coatings, Acta Biomater. 4 (2008) 1518–1529.
[29] R. Wang, K. Hashimoto, A. Fujishima, M. Chikuni, E. Kojima, A. Kitamura, et al., Photogeneration of highly amphiphilic TiO_2 surfaces, Adv. Mater. 10 (1998) 135–138.
[30] S. Oh, K.S. Brammer, K.-S. Moon, J.-M. Bae, S. Jin, Influence of sterilization methods on cell behavior and functionality of osteoblasts cultured on TiO_2 nanotubes, Mater. Sci. Eng. C 31 (2011) 873–879.
[31] L. Zhao, S. Mei, W. Wang, P.K. Chu, Y. Zhang, Z. Wu, Suppressed primary osteoblast functions on nanoporous titania surface, J, Biomed. Mater. Res. A 96 (2011) 100–107.
[32] B.S. Smith, S. Yoriya, T. Johnson, K.C. Popat, Dermal fibroblast and epidermal keratinocyte functionality on titania nanotube arrays, Acta Biomater. 7 (2011) 2686–2696.

[33] K.S. Brammer, C. Choi, C.J. Frandsen, S. Oh, G. Johnston, S. Jin, Comparative cell behavior on carbon-coated TiO_2 nanotube surfaces for osteoblasts vs. osteo-progenitor cells, Acta Biomater. 7 (2011) 2697−2703.
[34] L. Zhao, L. Hu, K. Huo, Y. Zhang, Z. Wu, P.K. Chu, Mechanism of cell repellence on quasi-aligned nanowire arrays on Ti alloy, Biomaterials 31 (2010) 8341−8349.
[35] J. Park, S. Bauer, P. Schmuki, K. von der Mark, Narrow window in nanoscale dependent activation of endothelial cell growth and differentiation on TiO_2 nanotube surfaces, Nano Lett. 9 (2009) 3157−3164.
[36] T. Kokubo, H. Takadama, How useful is SBF in predicting in vivo bone bioactivity? Biomaterials 27 (2006) 2907−2915.
[37] S. Oh, K.S. Brammer, Y.S. Li, D. Teng, A.J. Engler, S. Chien, et al., Stem cell fate dictated solely by altered nanotube dimension, Proc. Natl. Acad. Sci. U. S. A. 106 (2009) 2130−2135.
[38] K.-S. Moon, S.-H. Yu, J.-M. Bae, S. Oh, Biphasic osteogenic characteristics of human mesenchymal stem cells cultured on TiO_2 nanotubes of different diameters, J. Nanomater. (2012) doi: 10.1155/2012/252481.
[39] A.S. Curtis, M. Dalby, N. Gadegaard, Cell signaling arising from nanotopography: implications for nanomedical devices, Nanomedicine 1 (2006) 67−72.
[40] L.E. McNamara, R.J. McMurray, M.J. Biggs, F. Kantawong, R.O. Oreffo, M.J. Dalby, Nanotopographical control of stem cell differentiation, J. Tissue Eng. (2010) 120623.
[41] R. McBeath, D.M. Pirone, C.M. Nelson, K. Bhadriraju, C.S. Chen, Cell shape, cytoskeletal tension, and RhoA regulate stem cell lineage commitment, Dev. Cell 6 (2004) 483−495.
[42] E.A. Cavalcanti-Adam, T. Volberg, A. Micoulet, H. Kessler, B. Geiger, J.P. Spatz, Cell spreading and focal adhesion dynamics are regulated by spacing of integrin ligands, Biophys. J. 92 (2007) 2964−2974.
[43] K.C. Popat, M. Eltgroth, T.J. LaTempa, C.A. Grimes, T.A. Desai, Titania nanotubes: a novel platform for drug-eluting coatings for medical implants? Small 3 (2007) 1878−1881.
[44] L. Peng, A.D. Mendelsohn, T.J. LaTempa, S. Yoriya, C.A. Grimes, T.A. Desai, Long-term small molecule and protein elution from TiO_2 nanotubes, Nano Lett. 9 (2009) 1932−1936.

CHAPTER

Carbon Nanomaterials for Implant Dentistry and Bone Tissue Engineering

18

Qing Cai[a], Karthikeyan Subramani[b], Reji Mathew[c] and Xiaoping Yang[a]

[a]*State Key Laboratory of Organic-Inorganic Composites, College of Materials Science and Technology, Beijing University of Chemical Technology, Beijing, People's Republic of China*

[b]*Department of Orthodontics, University of Kentucky, Lexington, KY, USA*

[c]*Department of Oral and Maxillofacial Radiology, Midwestern University, Downers Grove, IL, USA*

CHAPTER OUTLINE

18.1 Introduction

In natural tissues or organs, cells directly interact with nanostructured extracellular matrices (ECM), which are mainly composed of nanofibrous collagen fibrils. Nanomaterials, resembling the natural ECM in some features and possessing unique physiochemical properties, play a key role in stimulating cell growth as well as guide tissue regeneration [1]. Carbon nanotubes (CNTs) are essentially cylindrical molecules made of carbon atoms. CNTs can be considered as made from graphene sheets rolled into a seamless cylinder that can be open ended or capped, and have a high

Nanobiomaterials in Clinical Dentistry.

aspect ratio with diameters as small as 1 nm and length of several micrometers. CNTs made from a single graphene sheet result in single-walled carbon nanotubes (SWCNT), while several graphene sheets make up multiwalled carbon nanotubes (MWCNTs). Ever since their discovery in 1991 by Iijima [2], there has been intense interest in these allotropes of carbon due to their unique physical and chemical properties and potential applications in a wide range of fields, from electronic devices and sensors to nanocomposite materials of high strength and low weight. On the other hand, CNFs are long, thin strands of material with diameters about 10−1000 nm, which are also mostly composed of carbon atoms but bonded together in microscopic crystals and aligned parallel to the long axis of the fiber. The crystal alignment makes the CNFs exceptionally strong for their size. These two kinds of three-dimensional carbon nanomaterials are also viewed as a class of biomaterials with high potential for biomedical applications [3,4] (Figure 18.1).

CNTs are well-ordered, hollow nanostructures consisting of carbon atoms bonded to each other via sp^2 (hybrid orbital comes from 1 S and 2 P orbital) bonds, which are stronger than sp (hybrid orbital comes from 1 S and 1 P orbital) and sp^3 (hybrid orbital comes from 1 S and 3 P orbital) bonds. These features are exactly the key factors rendering CNTs excellent mechanical strength and high electrical and thermal conductivity.

In a biomimetic viewpoint, the three-dimensional CNTs/CNFs resemble the nanofibrous network of natural ECM. SWCNTs have an average diameter of 1.5 nm, and their length varies from several hundred nanometers to several micrometers. In contrast, the diameter of MWCNTs typically ranges between 10 and 100 nm [8]. These were envisioned to be good candidates for bone tissue engineering. Studies have demonstrated that CNTs/CNFs were superior for bone regeneration due to their osteoconductivity [9]. One of the underlying mechanisms might be the electrochemical interactions between CNTs/CNFs and cells. A study had reported that electroconductive MWCNTs were less cytotoxic as compared to MWCNTs [10]. Moreover, conductive MWCNTs affected significantly the mitochondrial membrane polarity, the intracellular pH, and the reorganization of cytoskeleton actin filaments, and cell functions were strictly dependent on electrochemical interactions [10]. Another study stated that CNTs/CNFs with cell favorable surface properties might promote

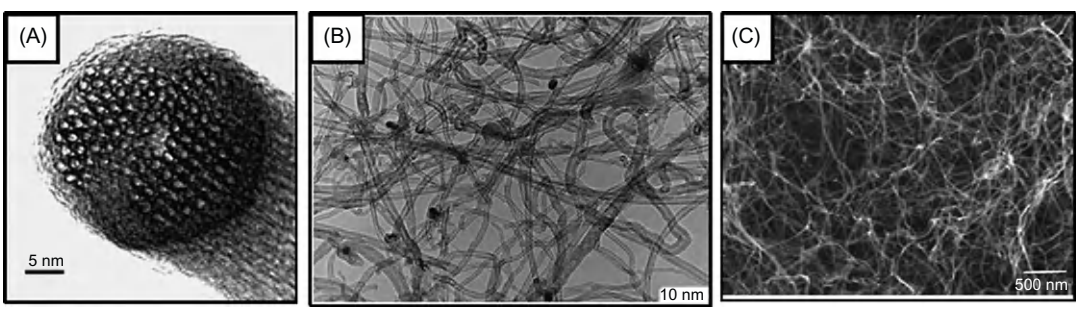

FIGURE 18.1

(A) High-resolution TEM micrograph of a SWNT bundle, (B) TEM image of MWCNT, and (C) SEM image of CNFs.

Part (A) reproduced with permission from Ref. [5], Part (B) reproduced with permission from Ref. [6], and Part (C) reproduced with permission from Ref. [7]

adsorption and specific protein interactions when they were compared with conventional materials [11]. Obviously, this would efficiently stimulate new bone growth, and this was thought to be the underlying mechanism behind why carbon nanomaterials were excellent for bone regeneration [11].

Moreover, the unique mechanical, physical, and chemical properties of CNTs/CNFs categorize them as outstanding reinforcement additives in polymeric nanocomposites. With the extraordinary stiffness and strength, CNTs/CNFs are deemed as ideal materials to provide structural reinforcement for bone tissue scaffold, especially for those load-bearing defect reparations [12]. Thus, CNTs/CNFs have been used in two main areas of bone tissue engineering: for structural and electrical enhancement of polymer and ceramic composites, and for nanostructured coatings to improve the bioactivity of titanium implant surfaces [13].

However, pristine CNTs/CNFs tend to bundle up and are insoluble in most types of solvents, making them difficult to be used in biological systems [14]. It was only after the development of strategies to functionalize them with organic groups and render them soluble that had opened the way to bio-applications of CNTs/CNFs. Moreover, there are conflicting data concerning the safety and biocompatibility of CNTs/CNFs. Although in some cases, like gene delivery, CNTs/CNFs were used without significant toxicity, other cytotoxic effects have been observed, including induction of intracellular reactive oxygen species (ROS), DNA damage, and apoptosis (cell death) [15]. Usually, the cytotoxicity of pristine CNTs/CNFs is due to the residual metal catalysts resulting from production methods and also the insolubility of pristine CNTs [16]. Therefore, to integrate CNTs/CNFs into biological systems, CNTs/CNFs need to be functionalized and purified by the removal of residual metal catalysts to improve their solubility and biocompatibility properties.

Having a high aspect ratio (i.e., the length to diameter ratio) and high surface area with many dangling bonds on the side walls, CNTs/CNFs are capable of adsorbing or conjugating a wide variety of therapeutic molecules [17,18]. Thus, CNTs/CNFs can be surface engineered (i.e., functionalized) and utilized as carriers of biomolecular motifs. In this chapter, attempts on CNTs/CNFs for implant dentistry and bone regeneration application are reviewed.

18.2 Enhanced functions of osteoblasts on carbon nanomaterials

Efforts on bone regeneration by using cells/scaffold construction have been tried for decades, aiming at replacing the use of autographs and allographs in bone transplantation [19]. Various materials, including synthetic polymers, biopolymers, and ceramics, have been investigated as substrates to grow bone-related cells (osteoblasts, bone-marrow-derived stromal cells (BMSCs), fibroblasts) and induce bone formation both in vitro and in vivo.

When designing a material to be used as a bone scaffold, one criterion concerning the mechanical properties of the materials is usually the first consideration because bone is a hard tissue providing mechanical support to the body and protecting internal organs. With the excellent mechanical strength (Young's modulus, 0.2−1 TPa; tensile strength, 11−63 GPa) [20] and diameters close to the size of the triple helix of collagen fibrils (which are 1.5 nm in width and 300 nm in length and have a periodicity of 67 nm) [21], CNTs/CNFs are naturally ideal candidates as reinforcing agents in bone scaffolds. Lahiri et al. [22] proposed the use of CNTs as reinforcements to increase the mechanical properties of a polylactide-caprolactone copolymer (PLC) matrix. Addition of 2 wt %

CNTs showed a uniform dispersion in the copolymer matrix, whereas severe agglomeration occurred at 5 wt % CNTs due to CNT entanglement and resulted in high porosity. The mechanical properties of PLC composite with 2 wt % CNTs increased remarkably, and an increase in elastic modulus by 100% and tensile strength by 160% were detected without any adverse effect on the ductility of PLC up to 240% elongation. An in vitro biocompatibility study on the PLC−CNT composites showed an increase in the viability of human osteoblast cells compared with the PLC matrix, which was attributed to the combined effect of CNT content and surface roughness of the composite films. Mattioli-Belmonte et al. [23] reported the mechanical, thermal, and biological characterization of a solid free form microfabricated polycaprolactone (PCL)−CNT composite. By changing the ratio of CNTs to PCL, the elastic modulus of the nanocomposites varied between 10 MPa and 75 MPa (Figure 18.2). When the CNT concentration in the composite reached 12.5 mg/ml, the elastic modulus achieved the maximum point. If CNT concentrations were high, their inhomogeneous dispersion in the composite materials would lead to an abrupt decrease of elastic modulus as well as an increase in fragility. Pan et al. [24] fabricated MWCNT/PCL composite scaffolds by the solution evaporation technique. Their results also showed that mechanical properties of the composite scaffolds were improved with the addition of MWCNTs (0.25−2 wt %).

Sitharaman et al. [25] examined the suitability of various nanocomposite materials made of poly(propylene fumarate) (PPF) and SWCNT for potential use as bone tissue engineering scaffolds. They demonstrated that SWCNTs, especially ultra-short SWCNTs (US-tube), could significantly

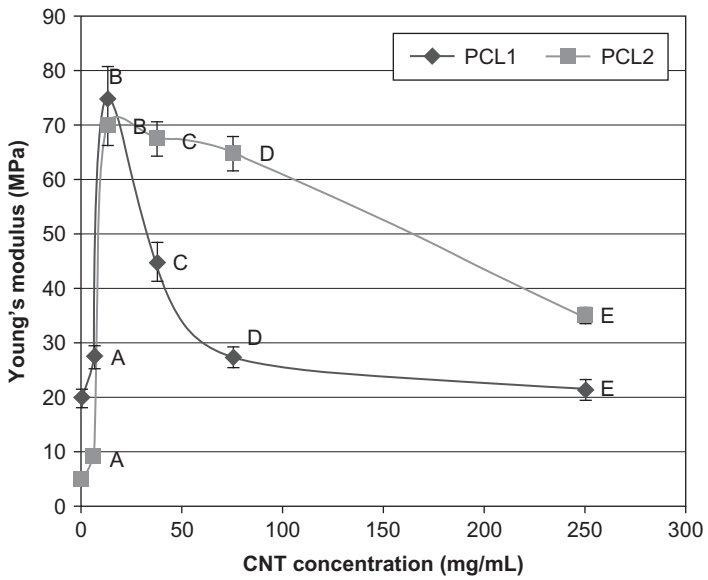

FIGURE 18.2

Elastic modulus of composite spin coated films as function of CNT concentration. The errors are of the order of 4%. The PCL (MW65,000) polymer was dissolved in chloroform to give 0.1 g/ml and 0.2 g/ml solutions (w/v), referred to as solutions PCL1 and PCL2, respectively.

Reproduced with permission from Ref. [23].

reinforce PPF to cover the limitations of inferior mechanical properties of PPF for use in load-bearing applications. On the other hand, many reports have revealed that the incorporation of CNTs into polymeric matrix could render nanocomposite scaffolds with some osteogenic and bioactive properties. Pan et al. [24] found that the scaffolds with low concentration (0.5 wt %) of MWCNTs were able to enhance the proliferation and differentiation of rat BMSCs. Sitharaman et al. [26] evaluated the in vivo biocompatibility of US-tube-reinforced PPF scaffolds in a rabbit model. US-tube nanocomposite scaffolds and control polymer scaffolds were implanted in rabbit femoral condyles and in subcutaneous pockets. At 4 and 12 weeks after implantation, examinations showed that the porous US-tube nanocomposite scaffolds exhibited favorable hard and soft tissue responses at both time points. At 12 weeks, US-tube nanocomposite scaffolds had promoted a three-fold greater bone tissue ingrowth than control polymer scaffolds. As shown in Figure 18.3, both PPF

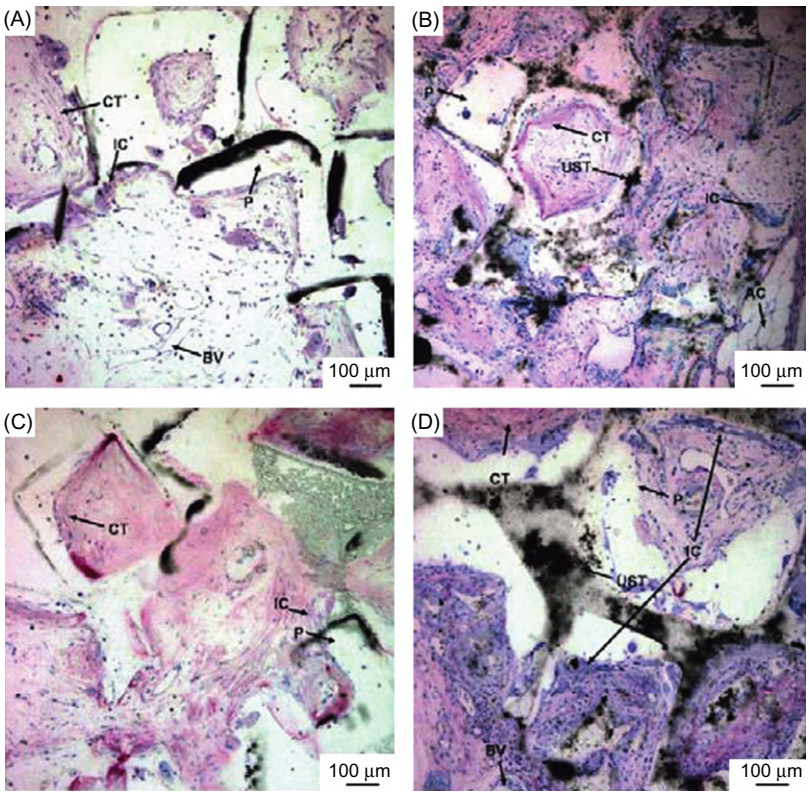

FIGURE 18.3

Representative histological sections of scaffolds implanted subcutaneously: (A) a PPF scaffold 4 weeks after implantation, (B) a US-tube/PPF scaffold after 4 weeks, (C) a PPF implant after 12 weeks, and (D) a US-tube/PPF implant after 12 weeks. The images are presented at 10× magnification. P: PPF scaffold, UST: US-tubes, CT: connective tissue, AC: adipose cells, BV: blood vessels, IC: inflammatory cells.

Reproduced with permission from Ref. [26].

and US-tube/PPF scaffolds exhibit a diffuse cell density at the earlier (4 week) time point and a denser cell population at the later (12 week) time point. Lin et al. [27] prepared biodegradable poly (lactic-*co*-glycolic acid) (PLGA)/carboxyl-functionalized MWCNT (c-MWCNT) nanocomposites via solvent casting technique and assessed the biocompatibility of the nanocomposites in vitro by using rat BMSCs. The presence of c-MWCNTs not only increased the mechanical properties of the nanocomposites but also promoted cell adhesion, viability, and production levels of alkaline phosphatase (ALP). These results demonstrated that CNT-modified polymer composites were beneficial for promoting cell growth and inducing BMSCs to differentiate into osteoblasts.

In addition to use of CNTs as reinforcement, some studies intended to culture cells directly on CNT films or scaffolds. An earlier study on metabolic activity and adhesion of human osteoblasts on SWCNT films demonstrated that the SWCNT films were nontoxic for osteoblast activity and adhesion, which were in the same range as Ti6Al4V alloy control group used in the study [28]. When the maturation of human osteoblast-like SaoS-2 cells on MWCNT compact substrate was evaluated using assays for osteonectin, osteopontin, and osteocalcin gene expression, total protein (TP) amount, and ALP activity, the results indicated that the CNTs induced osteogenic maturation of the osteoblasts [29]. Zanello et al. [9] prepared CNT-coated glass coverslips by spraying different CNT dispersions onto preheated (ca. 80°C) glass coverslips. These coverslips were used for cell culture after dry sterilization directly. The CNTs in the study included as-prepared CNTs (AP-CNTs), as well as nitric acid-treated SWNTs (SWNT-COOH), poly(*m*-aminobenzene sulfonic acid) functionalized SWNTs (SWNT-PABS), and poly(ethylene glycol) (PEG) functionalized SWNTs (SWNT-PEG), on the basis of their net negative, zwitterionic, and neutral electric charge, respectively, at the pH of the experiment. The authors studied osteoblastic ROS 17/2.8 cells proliferation on these CNTs in 5-day-old cultures and found that the CNTs supported ROS 17/2.8 cell growth in the order of electrically neutral AP-CNTs and SWNT-PEG, and then the negative SWNT-COOH and zwitterionic SWNT-PABS. The results suggested the surface charge of CNTs was a vital property necessary for adequate secretion of bone matrix, although one could not say that it alone was responsible for osteoblast growth. Furthermore, the cells cultured on SWNTs produced plate-shaped crystals (100−1000 nm in length and approximately 20 nm in thickness) similar in shape to hydroxyapatite (HA) crystals found in woven bone, which aggregated in clusters. These results indicated that SWNTs could facilitate the deposition of mineralized matrix (Figure 18.4).

To make CNTs, which are of relatively short aspect ratio, into three-dimensional scaffolds, Zhang et al. [30] wrapped natural polysaccharides such as amylose (AMY), alginate (ALG), and chitosan (CHI) onto SWCNTs to give a series of SWCNT scaffolds. The polysaccharide-wrapped SWCNTs well mimicked the natural nanofibrous ECM and significantly enhanced cell adhesion and proliferation. The surface properties of the SWCNT scaffolds, such as functional groups, surface charge, and hydrophilicity, directly influenced the protein adsorption, which led to significant changes in the expression of cellular focal adhesion kinase (FAK) and thus affected the mammalian cell morphology and proliferation. Hirata et al. [31] coated 3-D collagen scaffold surface with MWCNTs to obtain porous structures (MWCNT-coated sponge) for bone tissue engineering. They cultured rat primary osteoblasts on MWCNT-coated sponge in a 3-D dynamic flow cell culture system and measured differentiation markers. The measurements showed that ALP activity, calcium and osteopontin contents of cells on the MWCNT-coated sponges at 7 days were significantly higher than those on uncoated ones. This confirmed the earlier differentiation of osteoblasts on the MWCNT-coated sponges. By using 12-week-old Wistar rats as the animal model, the bone

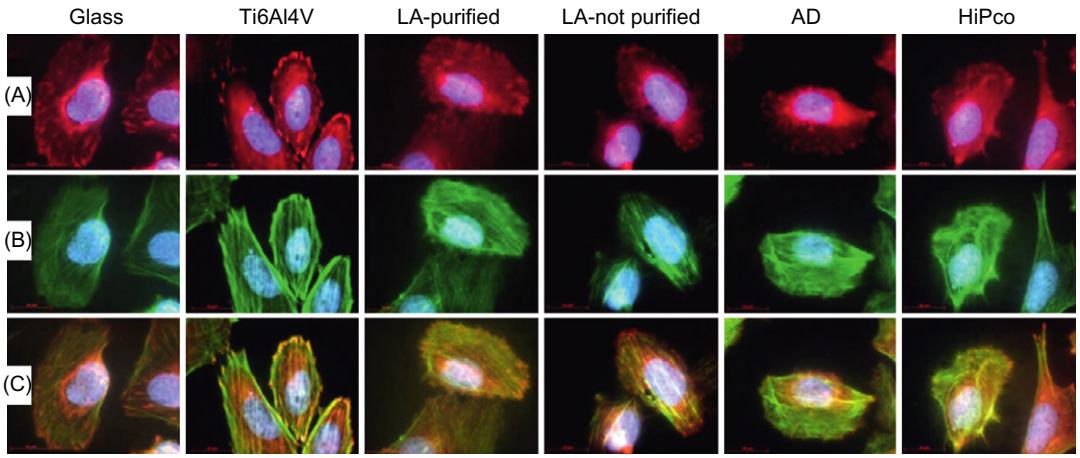

FIGURE 18.4

Fluorescent staining of osteoblasts adherent to glass, titanium alloy, and differently prepared SWCNTs (SWCNT films prepared by laser ablation (LA) (purified and not purified), by arc discharge (AD), and by HiPco processes) after 48 h. (A) Visualization of vinculin (red) and nucleus (blue), (B) visualization of actin (green) and nucleus (blue), (C) visualization of vinculin (red), actin (green), and nucleus (blue). (For interpretation of the references to color in this figure legend, the reader is referred to the web version of this book.)

Reproduced with permission from Ref. [28].

defects (1.5×1.5 mm) in the left femur regenerated more effectively by implanting MWCNT-coated sponges in comparison with pure collagen sponges. At 28 and 56 days after implantation, new bone attachment to MWCNTs was observed (Figure 18.5).

As for using CNFs in scaffolds for tissue regeneration, many literatures have referred to Elias et al.'s [32] study as the first report. In 2002, Elias et al. studied the in vitro culture of osteoblasts on CNF compacts with different fiber dimensions (i.e., 100 nm or less or conventional CNFs with dimensions larger than 100 nm). They analyzed functions of osteoblasts, like proliferation, synthesis of intracellular proteins, ALP activity, and deposition of calcium-containing mineral, to evaluate the effect of CNFs dimension on cell behaviors. After 3−21 days of culture, it was interesting to find that proliferation and differentiation of osteoblasts were enhanced on CNFs with smaller diameters. This study provided the first evidence of the size of the CNFs playing an important role in increasing osteoblast functions because those CNFs used in their study were not functionalized with bioactive molecules and were in their raw state. In another study, Price et al. [33] tested the effect of some select properties of carbon fibers (specifically, dimension, surface energy, and chemistry) on osteoblasts and osteoblast competitive cell line (e.g., fibroblasts, chondrocytes, and smooth muscle cells) adhesion. In the study, researchers dispersed CNFs in polycarbonate urethane (PCU) to create PCU/CNF composites. They found that the composites with smaller scale (i.e., nanometer dimension) carbon fibers promoted osteoblast adhesion but decreased the adhesion of other cells. Surface energy of CNFs was considered as another material property to have influenced the initial adhesion of competitive cells and that these cells' adhesion decreased when CNF surface energy was increased. Similarly, CNT-incorporated polymer composites also showed such cell selectivity. Mei et al. [34] electrospun MWCNTs into PLLA

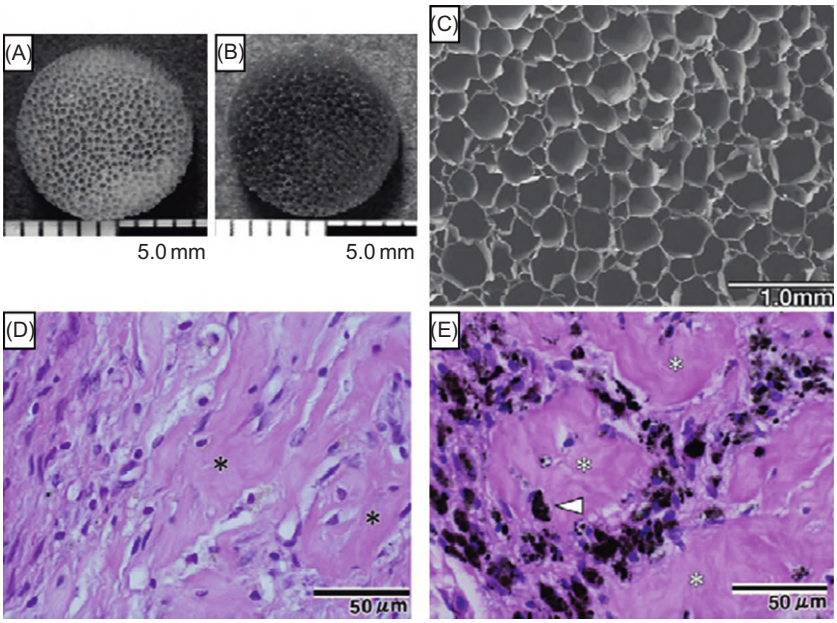

FIGURE 18.5

(A) The whole shape of the uncoated collagen sponge honeycomb and (B, C) MWCNT-coated sponge. Histology at 28 days after implantation of each sponge with osteoblasts cultured for 1 day in the subcutaneous tissue. (A) After implantation of the uncoated sponge, flattened bone-like tissue is observed. (B) The bone formed in the transplanted sponge coated with MWCNTs maintains the original shape of the sponge even after the sponge walls have been absorbed. Some of the MWCNTs (white arrowhead) are attached to the bone tissue (white asterisk) directly.

Reproduced with permission from Ref. [31].

nanofibers. Histologic examinations showed that periodontal ligament cells (PDLCs) attached on the membranes functioned well in vivo, while the growth of gingival epithelial cells (GECs) was prohibited on electrospun PLLA/MWCNT/HA membranes. In orthopedic applications, early cellular events (such as cell adhesion) are critical since subsequent cell functions are influenced by such early events. Therefore, this selectivity in the initial stages of cellular interaction with high surface energy CNTs/CNFs may give such materials an advantage over current orthopedic/dental materials.

CNFs/CNTs can influence cell behaviors in many ways, and this effect is governed by surface area, energy, chemistry, and roughness. Although the exact mechanism of why and how cell functions are affected by CNTs/CNFs remains unclear, protein adsorption and conformation on CNF/CNT materials clearly play an important role in increasing their bioactivity. Myoblastic mouse cells (C2C12) are a multipotent cell line that is capable of differentiating toward different phenotypes under the action of specific proteins, chemical, or biological factors. Li et al. [35] cultured them on MWCNT and graphite compacts, respectively. They found that the ALP activity by C2C12 cells on MWCNTs was significantly higher than on graphite, suggesting that MWCNTs were able to induce C1C12 cells to differentiate into osteogenic cells more than graphite. The authors had observed

increased protein adsorption on MWCNTs and proposed it be the underlying mechanism for the enhanced functions of C2C12 cells. Li et al. [36] also evaluated attachment, proliferation, osteogenic gene expression, ALP/DNA, protein/DNA, and mineralization of human adipose-derived stem cells cultured in vitro on MWCNT and graphite compacts with the same dimension. They placed the compacts in culture medium with 50% fetal bovine serum (FBS) before cell culture. With the adsorption of the protein in advance, the increments of the ALP/DNA and protein/DNA for the MWCNT compacts were found to be significantly more than the increments of those for the graphite compacts.

It has been generally believed that matrixes interacted with proteins existing in culture medium first and then attracted cells to attach and spread [37], suggesting that the larger amount of protein adsorbed on matrixes is crucial. Using this feature, CNTs/CNFs might stimulate inducible cells in soft tissues to form bone by concentrating more proteins, including bone-inducing proteins. Some reports showed that nano-roughness alone was sufficient to modulate cellular behavior and early stage of stem cell lineage recruitment without the aid of an induction medium [38]. This phenomenon was also found on CNT compacts. Tay et al. [39] cultured human MSCs on a thin mesh-like layer of carboxylic-functionalized SWCNTs with a vertical height of less than 100 nm. It was observed that the cells spread better on a SWCNT film as compared to cover slip, resulting in larger cell area and having higher occurrence of filopodia (microspikes) at the cell boundaries. Cytoskeleton arrangement was observed to be less orientated in the cells cultured on a SWCNT film as compared to control. According to Khang et al. [40], it should be the contribution of nanoscale surface roughness on the adsorption of one key cell adhesive protein, fibronectin, that promoted cell differentiation. Khang et al. prepared various surface energies by creating different nanosurface roughness features via mixing MWCNTs and PCU. Specifically, independent contributions of surface chemistry (70%) and surface nano-roughness (30%) were found to mediate fibronectin adsorption. The results clarified one of the important reasons why MWCNTs/PCU composites enhance cellular functions and tissue growth, which was their physical nano-roughness on promoting the adsorption of fibronectin, a protein well known to be critical for mediating the adhesion of anchorage-dependent cells.

All these studies indicate that the CNTs/CNFs and their composites can serve as osteogenic scaffolds with good cytocompatibility properties, reinforced mechanical properties, and improved electrical conductivity to effectively enhance bone tissue growth. In addition to those controversial issues on cytotoxicity, however, another point needs to be stated, which is CNTs/CNFs are nonbiodegradable. CNT/CNF scaffolds are quite unlike the conventional biodegradable polymeric scaffolds, which are able to disappear as the new bone grows. The nonbiodegradable CNTs/CNFs would behave as inert matrixes, on which cells proliferate and deposit new live matrix, and finally integrate into functional, normal bone. Therefore, more studies are needed to address how the body will interact with nonbiodegradable CNTs/CNFs, more specifically the reaction of the immune system, before we can fully take advantage of their promising applications in bone regeneration.

18.3 CNT/CNF applications in dentistry

One potential area in dentistry for carbon nanomaterial applications might be the carbon-fiber-reinforced epoxy resin posts, for their close elastic modules to dentin, no erosion, less time-consuming, and less expensive clinical procedures than conventional procedures for cast metal posts [41]. Another application is carbon/graphite fiber-reinforced poly(methyl methacrylate) (PMMA) denture resin to

fulfill the mechanical requirements [42,43]. However, an important clinical problem related to carbon material–incorporated products in oral application is the poor esthetics because of their black color. As a phenomenon, with the fast development of nanocomposites application in dentistry [44], sparse report can be found on using CNTs/CNFs in oral cavity.

Zhang et al. [45] have developed a process to improve the application of SWCNTs in dental resin-based composites. To achieve uniform dispersion of SWCNTs in matrix, they deposited a thin shell of nano-SiO_2 onto the oxidized surface of SWCNTs, and then surface modified this SWCNTs/SiO_2 with organosilane (allyl triethoxysilane, ATES). Finally, the authors blended this SWCNTs/SiO_2/ATES into a resin monomer. Although the composite resin specimens with the modified SWCNTs exhibited improved flexural strength, the nanocomposite resin specimens prepared as described above were still grayish black, which was disharmonious with the color of natural teeth and was therefore not suitable for direct oral use. The authors suggested the application of other inorganic additives such as sol-gel-based opalescent fillers or chromophoric xerogel pigment particles to achieve the desired esthetic requirements. In one of our previous studies, a composite fibrous network consisting of poly(L-lactic acid) (PLLA), MWCNTs, and HA (PLLA/MWCNT/HA) was fabricated to develop novel guided tissue regeneration (GTR) membranes for periodontal defects [34]. Its unique feature is the selective promotion of attachment and proliferation of PDLCs, while inhibition of GECs making it a potential candidate for GTR application, which is suggested as the inner layer of functional-graded membranes to face the periodontal defects directly (Figure 18.6).

For application in implant dentistry, CNTs also can be used as a coating on titanium implants. An earlier study showed that osteoblasts synthesized more ALP and calcium on the surfaces of nonfunctionalized MWCNTs grown from anodized nanotubular titanium surface than on anodized nanotubular titanium without MWCNTs and currently used unanodized commercial titanium surface for implant manufacturing [46]. This study concluded that bone growth could possibly be enhanced on currently used titanium implants coated with MWCNTs. In a recent study, titanium plates were aminated and coated with collagen. Carboxylated MWCNTs were coated onto this collagen surface and mouse osteoblasts were cultured on the nanotubes. The results of this study showed increased cell proliferation and adhesion on the MWCNTs [47]. The reason for these results was thought due to the similarity of the dimensions of SWCNTs/MWCNTs to that of the triple helix collagen fibers in bone, which makes these nanotubes ideal candidates as substrates for bone growth and as a coating on titanium implants.

Another possible application of CNTs/CNFs in dentistry might be the use of CNT/CNF-reinforced ceramic to improve fracture toughness. Over the past three decades, considerable research has been devoted to the development of HA acting as a coating material for titanium or other metals used as implants. The metal substrates are able to provide mechanical properties, while the biocompatibility is usually rendered by HA coating. Although plasma-sprayed HA coatings have successfully improved the aspects of bone attachment and integration of the implants, the long-term stability of these coatings is still a very challenging issue since these coatings tend to have uncontrollable dissolution and sometimes exhibit insufficient fracture toughness and bond strength to the metal substrate [48,49]. Due to their outstanding mechanical properties and excellent chemical stability, introducing small amounts of CNTs to ceramic are envisioned to produce tougher ceramic materials [50–52]. Kobayashi et al. [51] used CNFs as reinforcement for HA composites. The fracture toughness values for CNF/HA composites were around 1.6 times higher than those obtained

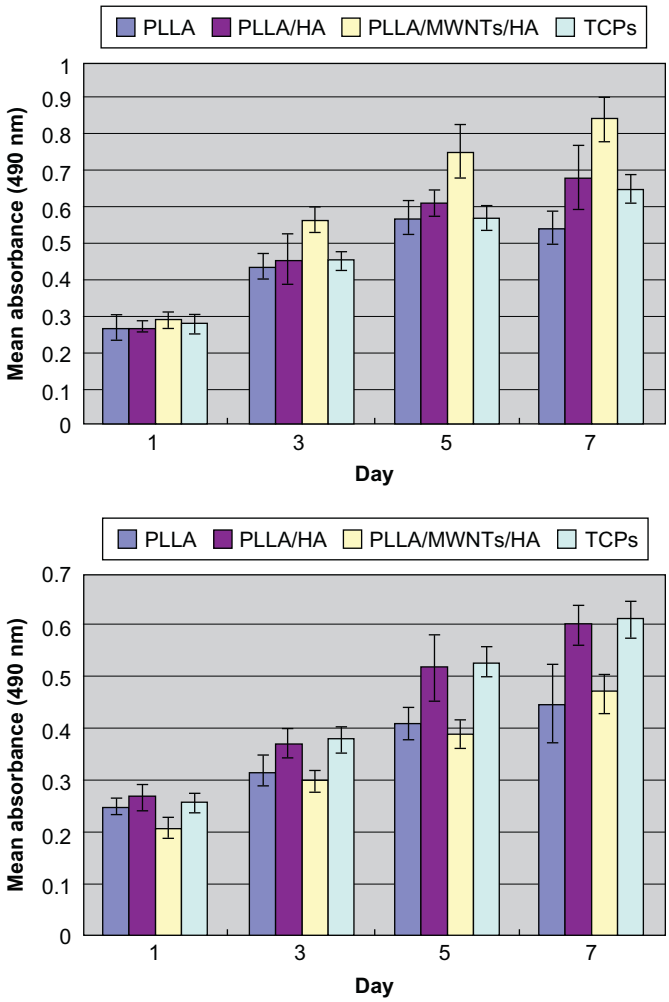

FIGURE 18.6

Effect of nanofibrous membranes with different compositions on the adhesion and proliferation of periodontal ligament cells (PDLCs, top) and gingival epithelial cells (GECs, bottom) determined by MTT assay. Standard deviations are shown as bars.

Reproduced with permission from Ref. [34].

for HA. Equal bioactivity was obtained for CNF/HA composites and HA by being evaluated by immersion tests in simulated body fluid (SBF). Chen et al. [52] introduced MWCNTs into HA coatings using laser surface alloying. Scratching test results indicated that the as-alloyed HA composite coatings exhibited improved wear resistance and lower friction coefficient by increasing the amount of CNTs in the precursor material powders (Figure 18.7). These composites have

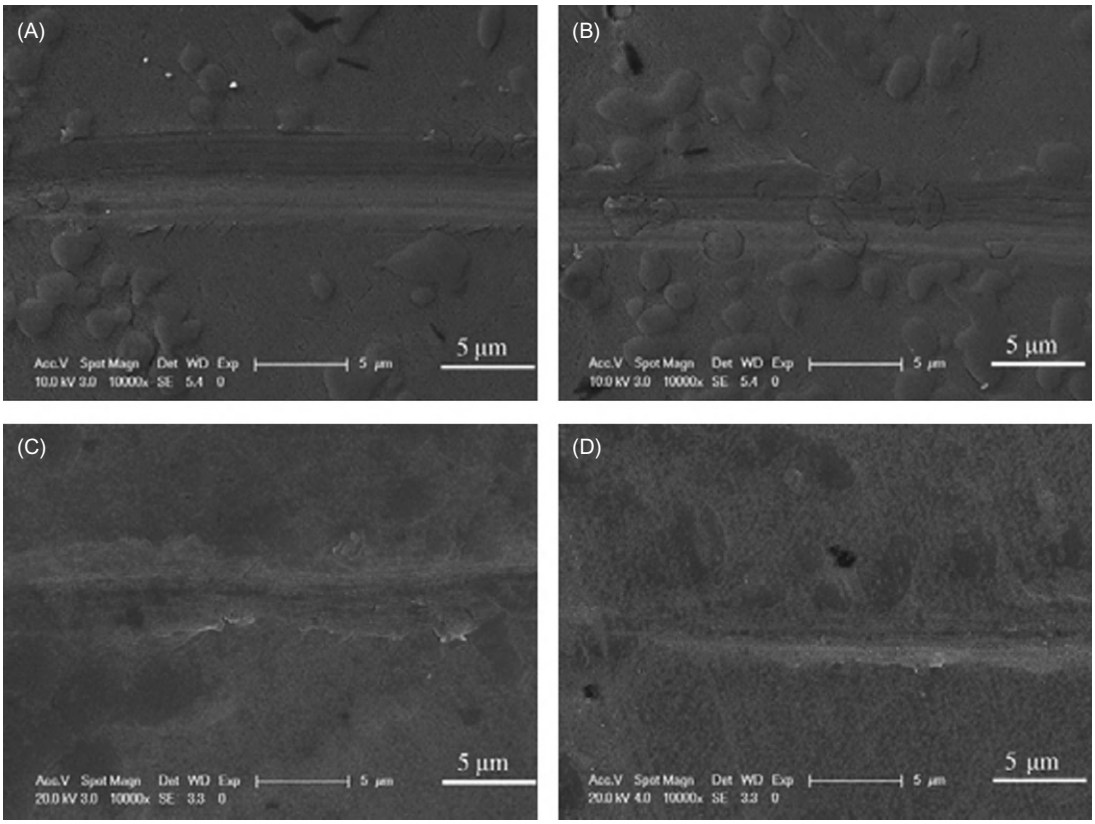

FIGURE 18.7

Field-emission SEM images of morphologies of the scratch tracks (scratch performed from left to right) of as-alloyed HA coatings containing different amount of CNTs at the bottom stage during scratching: (A) CNT-free coating, (B) HA-5% CNT coating, (C) HA-10% CNT coating, and (D) HA-20% CNT coating.

Reproduced with permission from Ref. [52].

potential applications in the field of coating materials for metal implants under high load-bearing conditions. In addition, titanium substrates with such a coating can increase the surface roughness at the nanoscale level and enhance osteoblast response. Such surfaces can be of immense use in dental implants and orthodontic mini-implants (TADs).

18.4 Fabrication of carbon nanomaterials

The fabrication of CNTs has been extensively discussed in the previous chapter. Conventionally, CNTs are fabricated by several methods, such as electric arc vaporization, laser vaporization, gas phase catalytic growth from carbon monoxide, and chemical vapor deposition (CVD) from

hydrocarbons [53]. With a similar growth mechanism, CNFs also can be synthesized by the above methods [54]. But with the fast development of electrospinning, CNFs fabricated from polymer solution electrospinning and carbonization has been preferred [55]. To date, therefore, CVD and electrospinning are the most promising ones among many techniques used for the synthesis of CNTs and CNFs, respectively.

18.4.1 Carbon nanotubes (CNTs)

CNTs were discovered as a microscopic miracle in the cathode deposits obtained in the arc evaporation of graphite [56]. Since then, arc discharge, laser ablation, and CVD have been well developed as the three main and modified methods to obtain good yields of both MWCNTs and SWCNTs. The arc discharge and laser ablation employ solid-state carbon precursors to provide carbon sources needed for nanotube growth and require high temperatures (thousands of degrees Celsius) to vaporize carbon. And in the procedure, large amounts of by-products are associated [5]. CVD technique utilizes hydrocarbon gases as sources for carbon atoms and metal catalyst particles as "seeds" for nanotube growth, which can take place at relatively lower temperatures (500−1000°C) [53]. The synthesis of CNTs by CVD generally involves heating a catalyst material in a furnace and passing a hydrocarbon gas through the tube reactor for a period of time. The catalytic species are transition-metal nanoparticles that serve as seeds to nucleate the growth of nanotubes. Briefly, supersaturation occurs when carbon is dissolved in a transition metal that melts to form a carbon−iron solid-state solution, and carbon atoms will precipitate out from the nanoparticle, leading to the growth of a nanotube to a maximum length (typically 50 μm) [2]. Over patterned catalyst arrays, organized nanotube structures can be synthesized for nanotubes growing from specific sites on surfaces. The most effective metals have been shown to be iron, nickel, and cobalt. Typically, the as-prepared CNTs contain metal particles, metal clusters coated with carbon, amorphous carbon, and in some cases fullerenes, with a 30 wt % abundance of CNT ropes. Thus, the pristine CNTs cannot be used directly in biomedical applications without purification and functionalization.

18.4.2 Carbon nanofibers (CNFs)

With a similar growth mechanism to CNTs, CNFs also can be synthesized by methods like vapor growth, arc discharge, laser ablation, and CVD [53]. Among them, CVD is commonly used for its lower process temperature. For example, Ağiral et al. [57] developed nickel thin-film catalyst coated inside a closed channel fused silica microreactor in order to grow CNFs on Ni/alumina. By directly flowing reactant gases over a catalytic coating inside the microchannels, a mechanically stable and porous CNF−alumina composite was formed with high surface area (160 m^2/g). Mori et al. [58] reported a catalyst-free low-temperature growth of CNFs by microwave plasma-enhanced CVD, whose diameter was about 50−100 nm and growth rate about 5 nm/s. The maximum length of CVD produced CNFs was around tens of microns. However, these are very expensive processes due to low product yield and the expensive equipment required. To produce relatively long and continuous CNFs at low cost, the rapidly developing technology of electrospinning has provided a unique opportunity [55]. In this technique, a polymer precursor for producing CNFs is dissolved in organic solvent and electrospun into fibers of several hundreds of nanometers under the application of an electrostatic force. The applied electric field and solution conductivity

are important parameters that influence the fiber diameter during the spinning, in addition to parameters such as the jet length, solution viscosity, surrounding gas, flow rate, and the geometry of the collector assembly [59,60]. Then the polymeric nanofibers are subjected to thermal treatment (oxidative stabilization and carbonization) to obtain CNFs [61].

Among the various precursors for producing CNFs, polyacrylonitrile (PAN) is the most commonly used and important polymer, mainly due to its high carbon yield (up to 56%), flexibility for tailoring the structure of the final CNF products, and the ease of obtaining stabilized products due to the formation of a ladder structure via nitrile polymerization [55]. In the oxidative stabilization treatment (200°C−300°C), cyclization of nitrile groups and cross-linking of the chain molecules occurs upon heating to prevent PAN fibers melting during subsequent carbonization. In the following carbonization procedure, usually 1000°C−1500°C, noncarbonized components would be removed in the form of H_2O, NH_3, CO, HCN, CO_2, and N_2 gases. It is noteworthy that applying tension during stabilization and carbonization is crucial for preparation of CNFs with high mechanical strength [62]. Unlike CNTs or conventional CNFs, which are produced by bottom-up methods, the CNFs produced by electrospinning are through a top-down nanomanufacturing process, which results in low-cost, continuous nanofibers that do not require further expensive purification and that are also easy to align, assemble, and process for many applications.

18.5 Cytotoxicity of carbon nanomaterials

However promising a new technology or material might be for biomedical applications, it must be safe. It is crucial to understand its response to a foreign substance when it is introduced into the body at any time. There are debates in numerous literatures regarding the cytotoxicity of CNTs and CNFs [63]. There are two types of in vitro studies done on evaluating the cell response to CNTs/CNFs: one with CNTs/CNFs dispersed in the cell culture and the second with CNTs/CNFs held in a substrate in contact with the cell culture. The studies with CNTs/CNFs dispersed in the cell culture showed low biocompatibility [6,64], whereas the other studies showed an obvious preference of osteoblasts or neurons cell growth on a CNT/CNF surface [9,65,66].

With such high specific surface areas, CNTs/CNFs have high interfacial chemical and physical reactivity that translate to biological reactivity. Can a CNT/CNF pierce through a phospholipid bilayers of living cell? Do the catalytic metal impurities in CNTs/CNFs and poor CNT dispersion in aqueous media cause toxicity? Great efforts have been made to clarify their cytotoxicity; however, it is still a controversial topic in the literature. The results should be considered carefully because the CNTs/CNFs applied for cytotoxicity study were in different size, shape, surface area, surface chemistry, etc. The first source of toxicity in CNTs/CNFs comes from the catalyst metal residuals, such as Co, Ni [16]. These metals are known to be toxic to biological systems if the pristine products were used. It has been shown that SWCNTs decreased keratinocyte [67] and HEK293 cell (human embryonic kidney cells) survival significantly [64], thus raising important concerns about their biocompatibility. This disadvantage has been eliminated by now for most CNTs/CNFs used for biomedical application have been chemically modified to improve solubility and biological properties, a process during which metal ions have been removed with oxidative treatment [14,18]. The chemically functionalized CNTs have been shown to be biocompatible on different types of

cells like neurons and osteoblasts [9,68]. MWCNTs that were chemically functionalized with carboxylic acid, ethylene diamine, or poly-*m*-aminobenzene sulfonic acid were shown to be biocompatible and were observed to provide a substrate for neurite extension [68]. A study on mouse fibroblast cell attachment on MWCNTs chemically functionalized with carboxylic acid group (−COOH) reported no cytotoxicity with elongated cytoplasmic projections onto the MWCNTs [9].

The second source of toxicity in CNTs/CNFs might come from their needle-like, long fibrous structures because their clearance by macrophage engulfment is hindered and therefore resulting in cell and tissue injuries [69,70]. According to such a viewpoint, some researchers believe that making CNTs/CNFs smaller and shorter will make them less toxic. Those chemically modified CNTs/CNFs with surface −COOH or −OH groups, or functionalized ones with bioactive molecules, dispersed well in aqueous solution, and were believed to have better clearance from systemic blood circulation through the renal excretion routes and reduced accumulation in tissues [71−73]. Fraczek et al. [74] studied the in vivo behavior of two types of CNTs (SWCNTs and MWCNTs) by implanting them into the skeletal rat muscle. It was observed that MWCNTs were found to form large aggregates within the living tissue, while distinctly smaller particles consisting of SWCNTs were easily phagocytosed by macrophages and transported to local lymph nodes. Mutlu et al. [75] treated lung sections from mice with dispersed SWCNTs, and the results revealed uptake of SWCNTs by macrophages and gradual clearance over time. They concluded that the toxicity of SWCNTs in vivo was attributable to the aggregation of the nanomaterial rather than the large aspect ratio of the individual nanotubes. However, some others thought that, with the increase in dispersity, the modified CNTs/CNFs would show higher cytotoxicity compared to untreated ones. Cells would be exposed to higher concentration of free CNTs/CNFs if they dispersed well in a solution, compared to those pristine CNTs aggregation [76,77]. Thus, the particle dimension or surface area of carbon nanomaterials might also be a potential cytotoxicity. Jia et al. [78] reported that the degree of cytotoxicity caused by carbon nanomaterials followed a mass basis with SWNTs > MWCNTs > quartz > C60. Tian et al. [77] also tested the cytotoxicity of five forms of carbon materials on human fibroblasts. They found that all five types of carbon materials decreased cell survival, and the steepest decrease was in cells treated with SWCNT. Pogodin et al. [79] recently calculated the energy cost associated with the insertion of a CNT into a model phospholipid bilayer using the single-chain mean field theory. The results of their calculation of different diameters of nanotubes suggested that the thinner a nanotube, the less an energy barrier it became. Thus, it might be concluded that larger objects, such as MWCNTs having diameters more than 4 nm, will have an even larger energy barrier, which requires the application of an external force to pierce through the bilayer. In this case, other energy-dependent translocation mechanisms like endocytosis might be responsible for the CNTs penetrating the living cell.

Some other researchers were concerned if CNT electrical properties affected the so-called "charge-sensitive" cell parameters, interacting with cellular electrical activity. Fiorito et al. [10] compared the cytotoxicity of two kinds of MWCNTs to neuronal and bone cells. One was as-prepared and the other was purified by annealing at 2400°C to get better electroconductive properties (a-MWCNT). Their findings showed that a-MWCNTs were less cytotoxic as compared to as-prepared MWCNTs. Moreover, only annealed and better conductive a-MWCNTs could significantly affect the mitochondrial membrane polarity, the intracellular pH, and the reorganization of cytoskeleton actin filaments, demonstrating cell functions were strictly dependent on electrochemical mechanisms. To investigate the in vitro effects of SWCNTs in cells of the oral

cavity, Cicchetti et al. [80] exposed human gingival fibroblasts to 50, 75, 100, 125, 150 μg/ml SWCNTs for 24 h and investigated genotoxicity, cytotoxicity, oxidative stress, and stress response. They found that SWCNTs produced genotoxic effects at all doses, but the two highest doses induced a strong decrease of the cell proliferation and cell survival, causing apoptosis.

18.6 Fabrication of carbon nanomaterials with improved osteogenic bioactivity

Although the toxicity of carbon nanomaterials remains a controversial topic, researchers are still very much interested in using them for bone regeneration due to their unique mechanical properties and special enhancement on bone-related cells' response. How further to reduce their toxicity and increase their osteogenic activity has long been an important issue for bone tissue engineering [81]. The as-produced CNTs tend to entangle and bundle up. They are insoluble in most types of solvents; particularly, their poor dispersion in aqueous environment makes them difficult to be used in biological systems [82]. As stated above, the CNTs aggregation might cause cytotoxicity. Besides, the residual metal catalysts in pristine CNTs are another source of cytotoxicity. For applications as scaffolds for bone regeneration, CNTs/CNFs should further support new bone growth and initiate apatite formation, while pristine CNTs/CNFs have little functional groups and are hard to meet these demands. To integrate CNTs/CNFs into biological systems, therefore, functionalization of CNTs/CNFs is necessary.

The most common functionalization strategy of CNTs is through oxidation. In this method, CNTs are refluxed in strong acids (usually sulfuric acid and nitric acid) to bring some carboxylic groups to the caps and sidewalls of CNTs through an oxidation process. The introduction of hydrophilic carboxylic groups not only helps the stable dispersion of CNTs in aqueous solutions but also provides bonding sites for other suitable chemicals [14,17,18,83]. Meanwhile, it allows better capacity to attract calcium cations to enhance nucleation and formation of apatite in vitro and in vivo, making CNTs bioactive and osteoconductive. CNFs can be chemically modified similarly to CNTs, except that the reactions can only take place on fiber surface [84]. Calcium phosphate (CaP) compounds are key structural materials of natural bones and teeth [85]. Among different forms of CaP compound, HA and β-tricalcium phosphate (β-TCP) are the two most important and well-known biomaterials used for bone substitution and reconstruction. They demonstrate high bioaffinity owing to their chemical composition, crystal structure, and Ca/P ratio similar to apatite found in the human skeletal system. Integrating CaP compounds into or onto CNT/CNF scaffolds, possessing good mechanical properties, and excellent osteogenicity can be valuable for bone regenerative applications [86].

18.6.1 Biomineralization

By different ways, HA/CNT composites have been prepared, such as electrophoretic deposition [87], in situ CVD [88], inclusion of CNTs in a CaP sol-gel matrix [89], and biomineralization [90]. Among them, biomineralization by immersing CNTs/CNFs in SBFs or applying an alternative soaking process are simple, quick, and efficient, and by which apatite layers form on CNT/CNF surface. The surface chemistry of CNTs/CNFs plays a vital role in these biomineralization

processes. Various SBFs have been developed for biomineralization study. The conventional SBF mimics the human blood plasma in the ion concentrations of Ca^{2+}, HPO_4^{2-}, Na^+, Cl^-, K^+, Mg^{2+}, and SO_4^{2-}, except with a significant deficiency in its HCO_3^- concentration (4.2 mM). From this conventional SBF, the SBF-induced biomimetic process is rather slow and takes normally up to a few weeks to induce the nucleation of CaP mineralites. It has been known that the biomineralization induced by SBF includes two steps of nucleation and particle growth. One way to accelerate the nucleation is to use supersaturated SBFs (e.g., 1.5, 2.5, 5, and even 10 times SBF). Another way is to use the surface functional groups, usually negative carbonyl groups, to attract calcium cations and induce nucleation [91].

Using a revised supersaturated SBF (r-SBF), Akasaka et al. [92] found that needle-like apatite crystallites directly grew starting from the surface of HCl-purified MWCNTs after immersion for 2 weeks, considering the MWCNTs might be acting as core for initial crystallization of the apatites. However, in this condition, the reproducibility of sizes and shapes of apatites formed on MWCNTs were poor because the r-SBF was highly supersaturated and was difficult to handle. Instead of using supersaturated SBF, Liao et al. [93] applied solutions of 0.5 M $CaCl_2$ and 0.5 M H_3PO_4 (Ca/P = 1.66) to coat HCl-treated MWCNTs. They gradually added the solutions to MWCNT dispersions through separate tube pumps. In these procedures, fibril-like nHA polycrystals were formed and oriented at a certain angle to the long axis of the CNTs. The defects were analogous to edge dislocations along the surface of CNTs. Having served as the nucleation sites for nHA, these defects had been functionalized principally into carboxylic groups. Aryal et al. [94] immersed carboxylated CNTs in conventional SBF for 7−21 days and found that MWCNT-COOH was capable of nucleating HA crystals from SBF within 7 days, which resulted in the formation of hierarchy assemblies. The large surface area of nanotubes enabled the interaction of SBF and carboxyl group and the nucleation of HA initiated through the carboxyl group.

But some researchers thought CNTs-COOH itself are not efficient for inducing the formation of apatite. They used the carbonyls on CNTs to do some additional modification. Xiao et al. [95] prepared two types of prefunctionalized MWNTs, which were acid-oxidized MWCNTs and covalently modified MWCNTs with PEG. The influences of the acid-oxidization duration, prephosphorylation, and PEGylation of MWCNTs on in situ growth of HA were further investigated in SBF with ionic concentrations of 2, 5, and 10 times, respectively, at 37°C for 24 h. The results exhibited that all these factors had positive effects on the HA crystals growth; especially the PEGylation of MWCNTs played a key role during the deposition (Figure 18.8). The binding affinity between the HA crystals and the PEG-MWCNT surface was strong enough by the ionic and hydrogen bond interactions, which was very helpful to improve the dispersion ability and biocompatibility of nanotubes. Yan et al. [96] coated CNTs with polydopamine by a simple and feasible route, and then its in vitro bioactivity and cytocompatibility was assessed by immersion study in SBF. As a result, it had been demonstrated that the introduction of polydopamine coating could greatly enhance the bioactivity, which was attributed to the good combination of catecholamine structure of polydopamine. Tan et al. [97] functionalized MWCNTs with surfactant sodium dodecyl sulfate (SDS) and conducted mineralization by alternately dispersing the SDS-MWNTs into aqueous solutions of $CaCl_2$ and Na_2HPO_4 each for 30 min. SDS could provide some negative charges as nucleation sites for HA on the tube surface.

Mineralization study on CNFs is relatively sparse. Wan et al. [7] prepared 3-D CNFs by carbonization under inert conditions with 3-D bacterial cellulose nanofibers as starting carbon sources. The resulting CNFs showed 3-D fibrous structural features with diameter ranging from 10 nm to

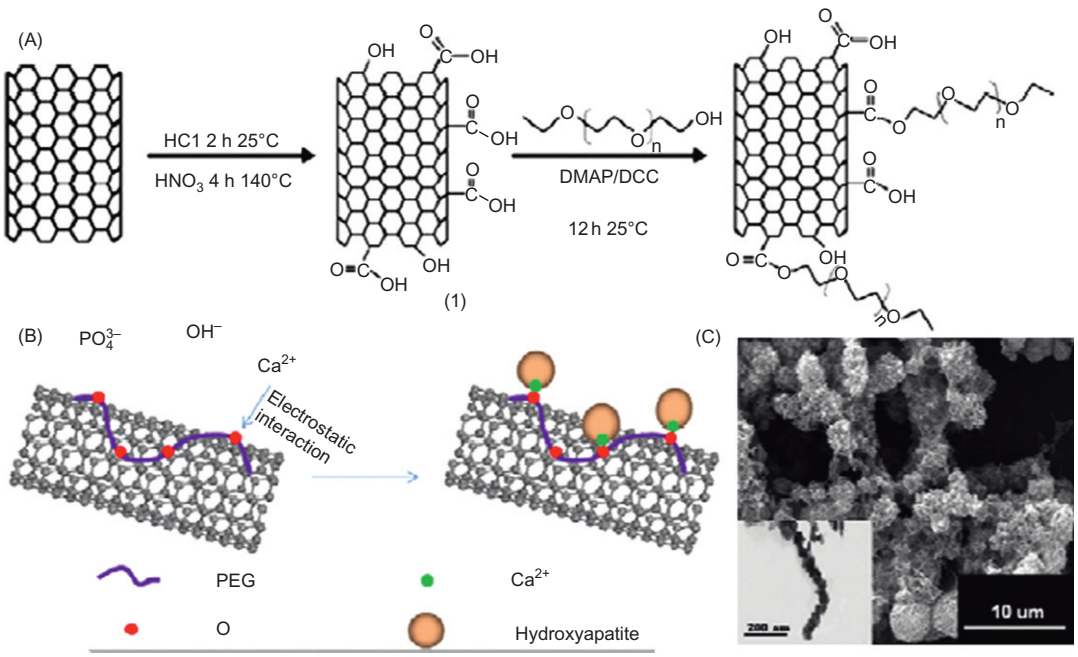

FIGURE 18.8

(A) Scheme of synthetic route for the preparation of PEG-MWCNT, (B) scheme of biomineralization mechanism of the preparation of HA-PEG-MWCNT, and (C) SEM and inserted TEM images of HA-PEG-MWCNT.

Reproduced with permission from Ref. [95].

20 nm. In vitro biomineralization process was performed on the surface-treated 3-D CNFs. The results showed that surface treatment of CNFs in nitric acid promoted the mineralization on CNFs.

18.6.2 Sol–gel/electrospinning

Another method to fabricate CaP/CNF hybrid is the preparation of CaP nanoparticles embedded CNFs, produced in our lab, by combining sol–gel and electrospinning techniques [98,99]. Among the different techniques available for the production of CaP compounds, including co-precipitation, solid-state reactions, hydrothermal reactions, and electrochemical deposition, the sol–gel technique is the simplest and most versatile to produce ceramic materials with high homogeneity [85,100]. The sol-gel technique is generally based on hydrolysis reaction followed by the condensation of the precursors to achieve the formation of colloidal particles (sol) and subsequent formation of a three-dimensional network (gel). Calcination, sintering, or chemical conversion of the precursor into the desired ceramic at an elevated temperature is conducted with concomitant removal of all organic components from the precursor fibers. To produce CaP compounds, like HA and β-TCP, calcium nitrate and triethyl phosphate (TEP) are usually used as the precursors. A feasible way to produce ceramic nanofibers is to electrospin the above sol–gel solution and subsequently calcinize

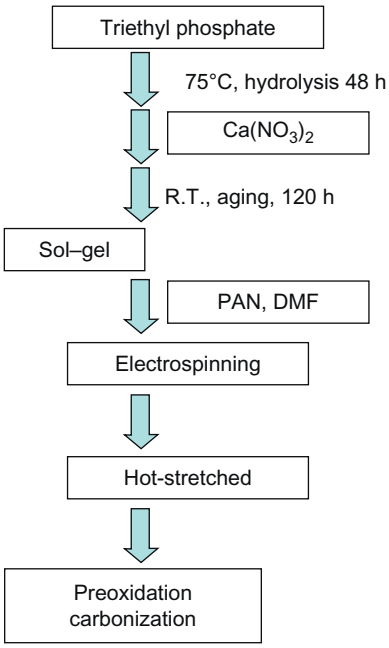

FIGURE 18.9

Schematic illustration for the preparation of β-TCP@/CNF membranes.

[101,102]. However, the inappropriate rheological properties and rapid hydrolysis rates of precursors make it very hard to control the electrospinning process because an inorganic sol is a thermostatically unstable system. To make the solution spinnable, one method is to introduce a polymer into the solution to regulate the rheological properties. This is very easy and involves simply co-dissolving the precursor and polymer in a cosolvent. Poly(vinyl pyrolidone) (PVP) is one of the most popular polymers employed as a matrix. Other polymers, such as poly(vinyl alcohol) (PVA), poly(vinyl acetate) (PVAc), PAN, PMMA, and poly(acrylic acid) (PAA) have also been widely used. Inorganic/polymer composite nanofibers are obtained via electrospinning from the above solutions. In the following steps of calcinations, the organic phase is burnt out while the nanofibers evolve into ceramic nanofibers [103,104]. As we have learnt, a popular and simple way to produce CNFs is from electrospinning the PAN/DMF solution, followed by oxidation and carbonization. This has provided us an excellent opportunity to modify CNFs. If we add PAN as the matrix to CaP precursor sol−gel solution to modify rheological properties, the electrospun CaP precursor/PAN composite nanofibers can be envisioned into CaP ceramic/CNF hybrids under proper calcination condition. In the calcination process, the precursors transform into CaP ceramic like HA or β-TCP depending on the feeding ratio of Ca/P, and meanwhile PAN transforms into CNFs. This is such an easy way to embed bioactive CaP nanoparticles into CNFs, to improve their biological properties.

Our lab has done some work on preparing β-TCP or bioglass-embedded CNFs via sol−gel/electrospinning. As shown in Figure 18.9, to produce β-TCP@CNFs, TEP is dissolved in distilled water and hydrolyzed first, followed by dissolving calcium nitrate tetrahydrate into the hydrolyzed

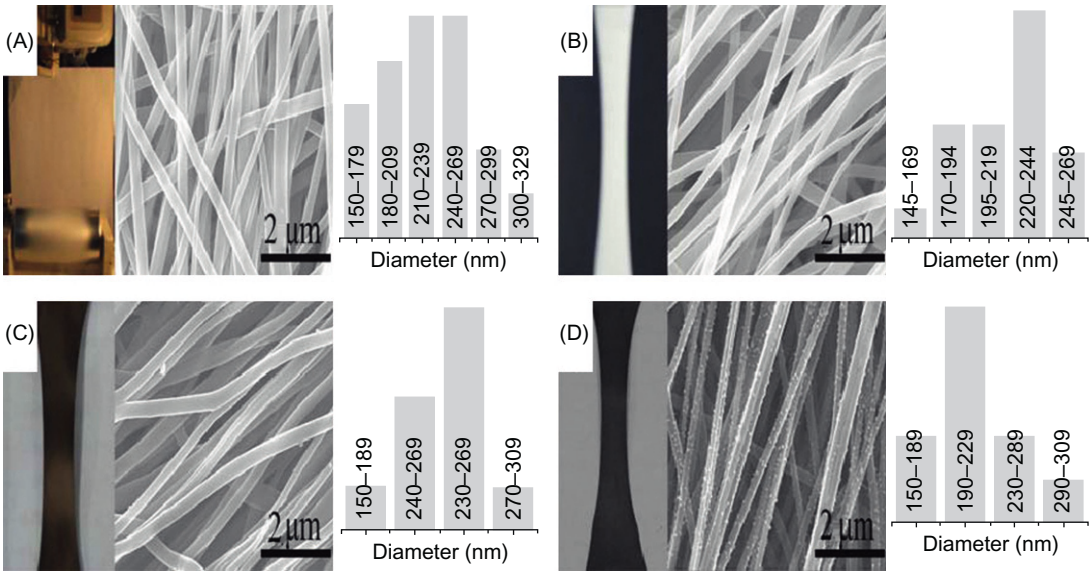

FIGURE 18.10

Change of fiber morphology and diameter at different stages of preparation of β-TCP@CNFs: (A) as-spun nanofiber, (B) after 100% hot-stretched, (C) after preoxidation, and (D) after carbonization.

TEP solution. The solution is stirred at room temperature for a certain time to generate a CaP complex. Then a certain amount of the prepared sol−gel solution is added to the pre-prepared PAN/DMF solution and stirred to obtain a homogeneous solution. This solution is then electrospun and the as-spun nanofibrous membranes are collected in an aluminum roller. The as-spun nanofibrous membranes are stabilized at 533 K for 30 min in air and then carbonized at 1373 K for 2 h in N_2 surrounding to obtain the β-TCP@CNF hybrid nanofibers.

In Figure 18.10, the macroscopic and microscopic changes of β-TCP@CNFs in different stages of preparation process are shown. It can be seen clearly that the average fiber diameters continue to decrease as the as-spun composite fibers are treated with hot-stretching, pre-oxidation, and finally carbonization. The pre-oxidation is performed at the temperature range of 250−300°C, cyclization takes place in the procedure, and some hydrogen atoms are released. Therefore, the white PAN mats change into brown and the average fiber diameter further decreases. As the temperature is further increased above 600°C, denitrogenation will happen and CNFs are formed. At the same time, the CaP crystals will result from the precursors with the removal of organic component. After carbonization, nanoparticles can be observed on the fiber surface in the SEM photos (Figure 18.11). Via TEM observation, numerous nanoparticles can be seen inside the fibers.

To further reveal the crystallographic microstructures of CNFs and β-TCP nanoparticles in hybrid CNFs, HR-TEM characterizations are performed. The HR-TEM image of a typical CNF distinctly shows the disordered lattice structure with low degree of crystallization. The presence of two well-resolved concentric diffuse rings (Figure 18.12A), corresponding to the (0 0 2) and the

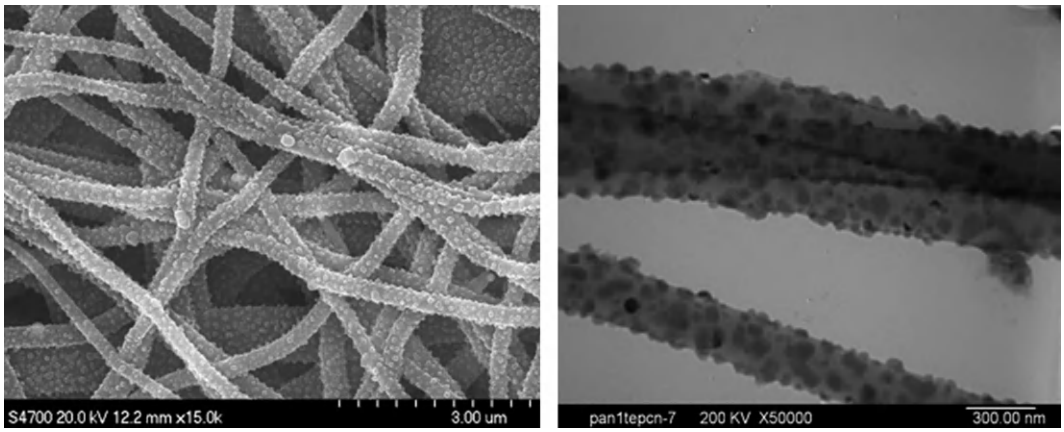

FIGURE 18.11

SEM and TEM images of the β-TCP nanoparticles on CNFs carbonized at 1373 K.

Reproduced with permission from Ref. [98].

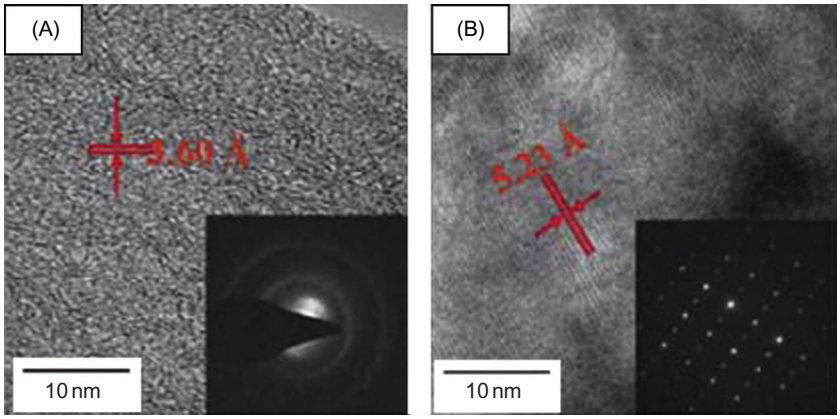

FIGURE 18.12

(A) HR-TEM images and SAED patterns (inset) of CNFs and (B) β-TCP nanoparticles in the β-TCP@CNFs.

Reproduced with permission from Ref. [99].

(1 0 1) planes of graphite (Figure 18.13A), as well as the absence of specific discrete diffraction spots are observed in the selected area electron diffraction (SAED) pattern of the CNFs [105]. With the incorporation of β-TCP, it displays well-defined lattice fringes with a d-spacing of 5.23 Å, which can be assigned to the (1 1 0) lattice plane of rhombohedral (R3c) β-TCP (Figure 18.12B and Figure 18.13B). The homologous interplanar spacing indicates the high crystallization of β-TCP nanoparticles [106].

With a similar method, bioglass@CNF hybrids can also be prepared by adding a ratio of tetraethyl orthosilicate into CaP precursor solution. By varying their molar ratios, different bioglass-like 45S, 58S, 68S, etc. can be incorporated. Also, ion-doped CaP compounds embedded CNFs can be fabricated. Considering the important role of Mg^{2+} and Zn^{2+} in bone growth [107], we have also incorporated different amounts of Mg^{2+} and Zn^{2+} into β-TCP to achieve better osteoinductivity (Figure 18.14). All these alterations have provided a powerful way to produce CNFs with significantly improved biological properties.

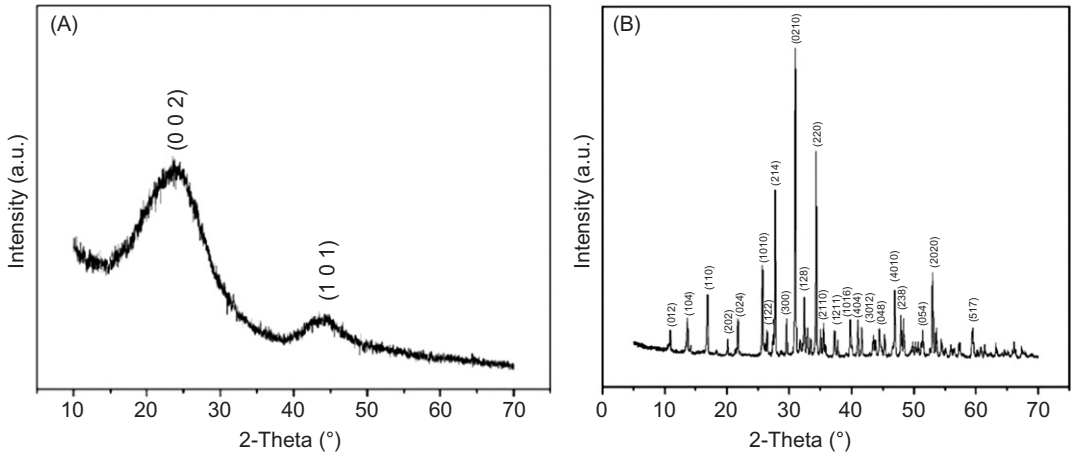

FIGURE 18.13

XRD patterns of (A) CNFs and (B) β-TCP@CNFs carbonized at 1373 K in N_2 for 2 h.

Reproduced with permission from Ref. [99].

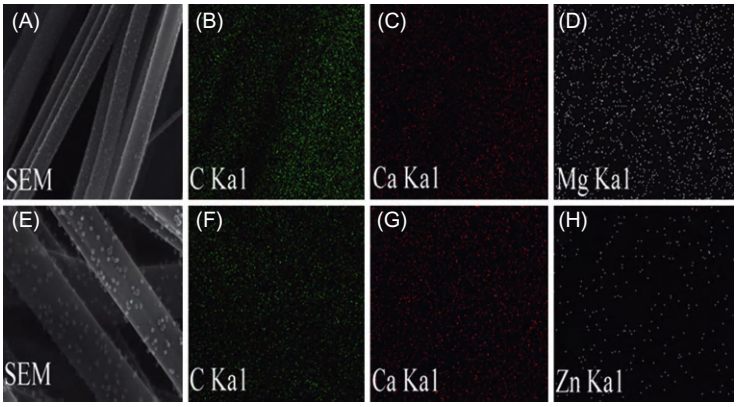

FIGURE 18.14

Element mapping analysis of ion-doped β-TCP@CNFs: (A–D) $Ca_{2.97}Mg_{0.03}(PO_4)_2$@CNFs and (E–H) $Ca_{2.99}Zn_{0.01}(PO_4)_2$@CNFs.

18.7 Unique properties of CaP nanoparticles–embedded CNFs for bone tissue engineering

According to Kokubo's definition [91], a "bioactive" compound is a material that accelerates heterogeneous apatite crystallization in a solution supersaturated toward HA. In recent years, there are some contradictory reviews pointing out that the use of SBF for bioactivity testing leads to false positive and false negative results [108,109]. Despite these criticisms, the use of an in vitro protocol for testing the bone bonding potential of a material remains a very attractive concept, although it must be contemplated very carefully. In a parallel test, by using the same SBF and soaking for the same period, we believe the apatite-forming ability of pure CNFs and β-TCP@CNFs still can give us some proof to show their difference in osteogenic activity. By immersing them in 1.5 times SBF at 37°C for just 2 days, the apatite formation on pure CNFs and β-TCP@CNFs were observed to be significantly different. As shown in Figure 18.15, the β-TCP-embedded CNFs have enhanced the apatite nucleation and growth on fiber surface, compared to pure CNFs. The driving force was thought to be coming from the initial dissolving of β-TCP, which served as the site for nucleation.

PDLCs were cultured on CNFs and β-TCP@CNF membranes, and their proliferation was evaluated (Figure 18.16). The PDLCs adhered on both CNFs and β-TCP/CNF membranes with proliferating preference along the aligned longitudinal direction of nanofibers. After 7 days of culture, the cells proliferated on the membrane surfaces with increasing coverage areas. It was of interest to note that the PDLCs were more actively extended on the β-TCP/CNF membrane than those on the CNF membrane. This behavior was attributed to more adhesion sites for PDLCs provided by the β-TCP nanoparticles on the nanofiber external surfaces.

In addition to improved biological properties of CNFs, more importantly, the incorporation of β-TCP can give CNFs some "biodegradability." That is to decrease the aspect ratio of continuous CNFs via the dissolution of inorganic component and to favor its clearance from body. In an accelerating degradation test, we immersed the pure and the β-TCP-decorated CNFs in diluted hydrogen chloride acid solutions for 24 h (Figure 18.17). Observed with SEM and TEM, it could be seen that

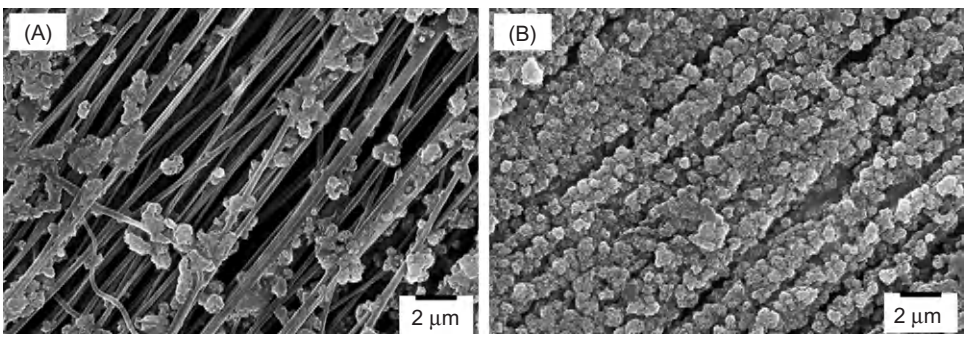

FIGURE 18.15

Mineral deposition on pure CNFs (A) and β-TCP@CNFs (B) by immersing in 1.5 times SBF at 37°C for 2 days.

Unpublished data from our lab.

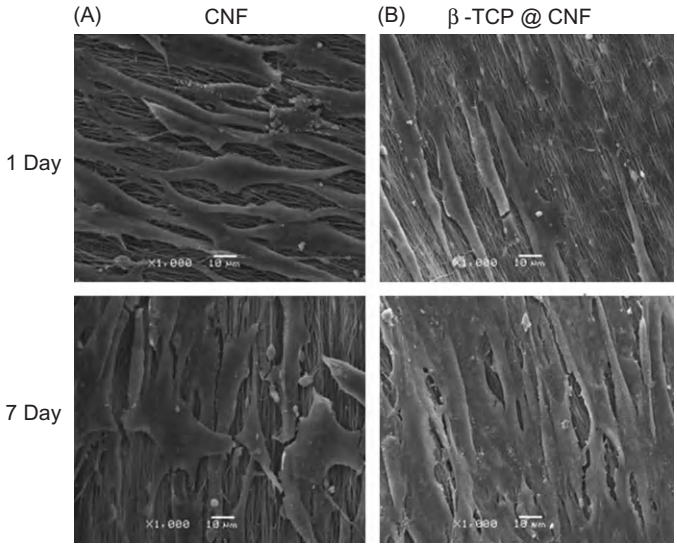

FIGURE 18.16

SEM images of PDLCs cultured on (A) CNFs and (B) β-TCP@CNF membranes for 1 day and 7 days.

Reproduced with permission from Ref. [99].

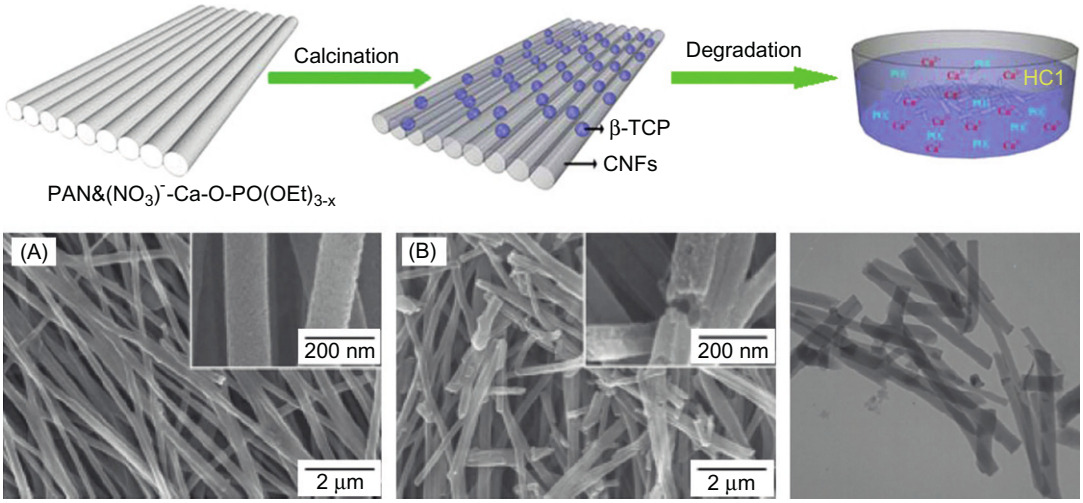

FIGURE 18.17

Schematic degradation of β-TCP@CNF procedure and observations of (A) HCl-treated pure CNFs and (B) β-TCP@CNFs.

Reproduced with permission from Ref. [99].

the pure CNFs remained in their initial morphology after acid treatment. This is similar to the results reported by R.H. Hurt, who found no degradation occurring to normal carbon materials under the acid treatment [110]. The β-TCP-decorated CNF have broken into short segments due to the dissolution of β-TCP nanoparticles. The shortened CNFs and the release of calcium cations and phosphate anions as nutrient mineral salts may be advantageous to improve the physiochemical compatibility of CNF-based scaffold. As compared to conventional large aspect ratio CNFs, these short CNFs maybe more easily eliminated from systemic blood circulation through the renal excretion routes, which can be potentially used as the degradable scaffold [72,73].

18.8 Conclusions

This chapter discussed some of the researches concerning the modification of CNTs and CNFs to improve their biocompatibility and bioactivity properties and highlighted their applications in bone regeneration and implant dentistry. These nanomaterials are becoming increasingly attractive as they can be modified to be integrated into human body for promoting tissue regeneration. Despite the tremendous potential CNTs and CNFs can bring, the presence of unreacted catalysts in CNTs/CNFs is a key factor promoting their toxicity, so care should be taken when synthesizing CNTs/CNTs. Inorganic nanoparticles embedded CNFs, which was developed in our lab, provided a promising method to produce CNFs with bioactivity and biocompatibility, while without using any catalyst. However, the toxicity of these materials is one of the issues that remain further investigation, to see if they can really be safe to be used for applications discussed in this chapter.

References

[1] L.J. Zhang, T.J. Webster, Nanotechnology and nanomaterials: promises for improved tissue regeneration, Nano Today 4 (2009) 66–80.
[2] S. Iijima, Helical microtubules of graphitic carbon, Nature 354 (1991) 56–58.
[3] P.A. Tran, L.J. Zhang, T.J. Webster, Carbon nanofibers and carbon nanotubes in regenerative medicine, Adv. Drug Deliv. Rev. 61 (2009) 1097–1114.
[4] B.S. Harrison, A. Atala, Carbon nanotube applications for tissue engineering, Biomaterials 28 (2007) 344–353.
[5] C.T. Kingston, Z.J. Jakubek, S. Dénommée, B. Simard, Efficient laser synthesis of single-walled carbon nanotubes through laser heating of the condensing vaporization plume, Carbon 42 (2004) 1657–1664.
[6] J. Chłopek, B. Czajkowska, B. Szaraniec, E. Frackowiak, K. Szostak, F. Béguin, In vitro studies of carbon nanotubes biocompatibility, Carbon 44 (2006) 1106–1111.
[7] Y. Wan, G. Zuo, F. Yu, Y. Huang, K. Ren, H. Luo, Preparation and mineralization of three-dimensional carbon nanofibers from bacterial cellulose as potential scaffolds for bone tissue engineering, Surf. Coat. Technol. 205 (2011) 2938–2946.
[8] Y. Lin, S. Taylor, H. Li, K.A.S. Fernando, L. Qu, W. Wang, et al., Advances toward bioapplications of carbon nanotubes, J. Mater. Chem. 14 (2004) 527–541.
[9] L.P. Zanello, B. Zhao, H. Hu, R.C. Haddon, Bone cell proliferation on carbon nanotubes, Nano Lett. 6 (2006) 562–567.

[10] S. Fiorito, M. Monthioux, R. Psaila, P. Pierimarchi, M. Zonfrillo, E. D'Emilia, et al., Evidence for electro-chemical interactions between multi-walled carbon nanotubes and human macrophages, Carbon 47 (2009) 2789–2804.
[11] J. Du, C. Ge, Y. Liu, R. Bai, D. Li, Y. Yang, et al., The interaction of serum proteins with carbon nanotubes depend on the physicochemical properties of nanotubes, J. Nanosci. Nanotechnol. 11 (2011) 10102–10110.
[12] K. Sahithi, M. Swetha, K. Ramasamy, N. Srinivasan, N. Selvamurugan, Polymeric composites containing carbon nanotubes for bone tissue engineering, Int. J. Biolog. Macromole. 46 (2010) 281–283.
[13] T.J. Webster, M.C. Waid, J.L. McKenzie, R.L. Price, J.U. Ejiofor, Nano-biotechnology: carbon nanofibres as improved neural and orthopaedic implants, Nanotechnology 15 (2004) 48–54.
[14] K.A. Worsley, I. Kalinina, E. Bekyarova, R.C. Haddon, Functionalization and dissolution of nitric acid treated single-walled carbon nanotubes, J. Am. Chem. Soc. 131 (2009) 18153–18158.
[15] W.H. Suh, K.S. Suslick, G.D. Stucky, Y.H. Suh, Nanotechnology nanotoxicology and neuroscience, Prog. Neurobiol. 87 (2009) 133–170.
[16] O. Vittorio, V. Raffa, A. Cuschieri, Influence of purity and surface oxidation on cytotoxicity of multiwalled carbon nanotubes with human neuroblastoma cells, Nanomed. Nanotechnol. Med. 5 (2009) 424–431.
[17] B.I. Kharisov, O.V. Kharissova, H.L. Gutierrez, U.O. Méndez, Recent advances on the soluble carbon nanotubes, Ind. Eng. Chem. Res. 48 (2009) 572–590.
[18] K.A. Wepasnick, B.A. Smith, K.E. Schrote, H.K. Wilson, S.R. Diegelmann, D.H. Fairbrother, Surface and structural characterization of multi-walled carbon nanotubes following different oxidative treatments, Carbon 49 (2011) 24–36.
[19] R. Cancedda, P. Giannoni, M. Mastrogiacomo, A tissue engineering approach to bone repair in large animal models and in clinical practice, Biomaterials 28 (2007) 4240–4250.
[20] J.N. Coleman, U. Khan, W.J. Blau, Y.K. Gun'ko, Small but strong: a review of the mechanical properties of carbon nanotube-polymer composites, Carbon 44 (2006) 1624–1652.
[21] B. Zhao, H. Hu, S.K. Mandal, R.C. Haddon, A. Bone Mimic, Based on the self-assembly of hydroxyapatite on chemically functionalized single-walled carbon nanotubes, Chem. Mater. 17 (2005) 3235–3241.
[22] D. Lahiri, F. Rouzaud, S. Namin, A.K. Keshri, J.J. Valdés, L. Kos, et al., Carbon nanotube reinforced polylactide-caprolactone copolymer: mechanical strengthening and interaction with human osteoblasts in vitro, Appl. Mater. Interfaces 1 (2009) 2470–2476.
[23] M. Mattioli-Belmonte, G. Vozzi, Y. Whulanza, M. Seggiani, V. Fantauzzi, G. Orsini, et al., Composites for bone tissue engineering scaffolds, Mater. Sci. Eng. 32 (2012) 152–159.
[24] L. Pan, X. Pei, R. He, Q. Wan, J. Wang, Multiwall carbon nanotubes/polycaprolactone composites for bone tissue engineering application, Colloids Surf., B 93 (2012) 226–234.
[25] X. Shi, B. Sitharaman, Q.P. Pham, F. Liang, K. Wu, W.E. Billups, et al., Fabrication of porous ultrashort single-walled carbon nanotube nanocomposite scaffolds for bone tissue engineering, Biomaterials 28 (2007) 4078–4090.
[26] B. Sitharaman, X. Shi, X.F. Walboomers, H. Liao, V. Cuijpers, L.J. Wilson, et al., In vivo biocompatibility of ultra-short single-walled carbon nanotube/biodegradable polymer nanocomposites for bone tissue engineering, Bone 43 (2008) 362–370.
[27] C. Lin, Y. Wang, Y. Lai, W. Yang, F. Jiao, H. Zhang, et al., Incorporation of carboxylation multiwalled carbon nanotubes into biodegradable poly(lactic-*co*-glycolic acid) for bone tissue engineering, Colloids Surf. B 83 (2011) 367–375.
[28] M. Kalbacova, M. Kalbac, L. Dunsch, U. Hempel, Influence of single-walled carbon nanotube films on metabolic activity and adherence of human osteoblasts, Carbon 45 (2007) 2266–2272.
[29] X. Li, H. Gao, M. Uo, Y. Sato, T. Akasaka, S. Abe, et al., Maturation of osteoblast-like SaoS2 induced by carbon nanotubes, Biomed. Mater. 4 (2009) 015005.

[30] X. Zhang, L. Meng, Q. Lu, Cell behaviors on polysaccharide-wrapped single-wall carbon nanotubes: a quantitative study of the surface properties of biomimetic nanofibrous scaffolds, ACS Nano 3 (2009) 3200−3206.
[31] E. Hirata, M. Uo, H. Takita, T. Akasaka, F. Watari, A. Yokoyama, Multiwalled carbon nanotube-coating of 3D collagen scaffolds for bone tissue engineering, Carbon 49 (2011) 3284−3291.
[32] K.L. Elias, R.L. Price, T.J. Webster, Enhanced functions of osteoblasts on nanometer diameter carbon fibers, Biomaterials 23 (2002) 3279−3287.
[33] R.L. Price, M.C. Waid, K.M. Haberstroh, T.J. Webster, Selective bone cell adhesion on formulations containing carbon nanofibers, Biomaterials 24 (2003) 1877−1887.
[34] F. Mei, J. Zhong, X. Yang, X. Ouyang, S. Zhang, X. Hu, et al., Improved biological characteristics of poly(L-lactic acid) electrospun membrane by incorporation of multiwalled carbon nanotubes/hydroxyapatite nanoparticles, Biomacromolecules 8 (2007) 3729−3735.
[35] X. Li, H. Gao, M. Uo, Y. Sato, T. Akasaka, Q. Feng, et al., Effect of carbon nanotubes on cellular functions in vitro, J. Biomed. Mater. Res. A 91 (2009) 132−139.
[36] X. Li, H. Liu, X. Niu, B. Yu, Y. Fan, Q. Feng, et al., The use of carbon nanotubes to induce osteogenic differentiation of human adipose-derived MSCs in vitro and ectopic bone formation in vivo, Biomaterials 33 (2012) 1−10.
[37] M.A. Cole, N.H. Voelcker, H. Thissen, H.J. Griesser, Stimuli-responsive interfaces and systems for the control of protein-surface and cell-surface interactions, Biomaterials 30 (2009) 1827−1850.
[38] M.J. Dalby, N. Gadegaard, R. Tare, A. Andar, M.O. Riehle, P. Herzyk, et al., The control of human mesenchymal cell differentiation using nanoscale symmetry and disorder, Nat. Mater. 6 (2007) 997−1003.
[39] C.Y. Tay, H. Gu, W.S. Leong, H. Yu, H. Li, B. Heng, et al., Cellular behavior of human mesenchymal stem cells cultured on single-walled carbon nanotube film, Carbon 48 (2010) 1095−1104.
[40] D. Khang, S.Y. Kim, P. Liu-Snyder, G.T.R. Palmore, S.M. Durbin, T.J. Webster, Enhanced fibronectin adsorption on carbon nanotube/poly(carbonate)urethane: independent role of surface nano-roughness and associated surface energy, Biomaterials 28 (2007) 4756−4768.
[41] M. Fredriksson, J. Astbäck, M. Pamenius, K. Arvidson, A retrospective study of 236 patients with teeth restored by carbon fiber-reinforced epoxy resin posts, J. Prosthet. Dent. 80 (1998) 151−157.
[42] K. Ekstrand, I.E. Ruyter, H. Wellendorf, Carbon/graphite fiber reinforced poly(methylmethyacrylate): properties under dry and wet conditions, J. Biomed. Mater. Res. 21 (1987) 1065−1080.
[43] W.R. Larson, D.L. Dixon, S.A. Aquilino, J.M. Clancy, The effect of carbon graphite fiber reinforcement on the strength of provisional crown and fixed partial denture resins, J. Prosthet. Dent. 66 (1991) 816−820.
[44] A. Mihranyan, N. Ferraz, M. Strøme, Current status and future prospects of nanotechnology in cosmetics, Prog. Mater. Sci. 57 (2012) 875−910.
[45] F. Zhang, Y. Xia, L. Xu, N. Gu, Surface modification and microstructure of single-walled carbon nanotubes for dental resin-based composites, J. Biomed. Mater. Res. B Appl. Biomater. 86B (2008) 90−97.
[46] S. Sirivisoot, C. Yao, X. Xiao, B.W. Sheldon, T.J. Webster, Greater osteoblast functions on multiwalled carbon nanotubes grown from anodized nanotubular titanium for orthopedic applications, Nanotechnology 18 (2007) 365102−365107.
[47] M. Terada, S. Abe, T. Akasaka, M. Uo, Y. Kitagawa, F. Watari, Multiwalled carbon nanotube coating on titanium, Biomed. Mater. Eng. 19 (2009) 45−52.
[48] J.F. Kay, Calcium phosphate coatings for dental implants, Dent. Clin. North Am. 36 (1992) 1−18.
[49] H.T. Zeng, W.F. Lacefield, XPS, EDX and FTIR analysis of pulsed laser deposited calcium phosphate bioceramic coatings: the effects of various process parameters, Biomaterials 21 (2000) 23−30.
[50] F. Lupo, R. Kamalakaran, C. Scheu, N. Grobert, M. Ruhle, Microstructural investigations on zirconium oxide-carbon nanotube composites synthesized by hydrothermal crystallization, Carbon 42 (2004) 1995−1999.

[51] S. Kobayashi, W. Kawai, Development of carbon nanofiber reinforced hydroxyapatite with enhanced mechanical properties, Compos. Part A 38 (2007) 114–123.
[52] Y. Chen, T.H. Zhang, C.H. Gan, G. Yu, Wear studies of hydroxyapatite composite coating reinforced by carbon nanotubes, Carbon 45 (2007) 998–1004.
[53] H. Dai, Carbon nanotubes: synthesis integration and properties, Acc. Chem. Res. 35 (2002) 1035–1044.
[54] N.M. Rodriguez, A review of catalytically grown carbon nanofibers, J. Mater. Res. 8 (1993) 3233–3250.
[55] S.K. Nataraj, K.S. Yang, T.M. Aminabhavi, Polyacrylonitrile-based nanofibers—a state-of-the-art review, Prog. Polym. Sci. 37 (2012) 487–513.
[56] R. Andrews, D. Jacques, D. Qian, T. Rantell, Multiwall carbon nanotubes: synthesis and application, Acc. Chem. Res. 35 (2002) 1008–1017.
[57] A. Ağiral, L. Lefferts, J.G.E. (Han) Gardeniers, In situ CVD of carbon nanofibers in a microreactor, Catal. Today 150 (2010) 128–132.
[58] S. Mori, M. Suzuki, Catalyst-free low-temperature growth of carbon nanofibers by microwave plasma-enhanced CVD, Thin Solid Films 517 (2009) 4264–4267.
[59] D.H. Reneker, A.L. Yarin, Electrospinning jets and polymer nanofibers, Polymer 49 (2008) 2387–2425.
[60] N. Bhardwaj, S.C. Kundu, Electrospinning: a fascinating fiber fabrication technique, Biotechnol. Adv. 28 (2010) 325–347.
[61] Z. Zhou, C. Lai, L. Zhang, Y. Qian, H. Hou, D.H. Reneker, et al., Development of carbon nanofibers from aligned electrospun polyacrylonitrile nanofiber bundles and characterization of their microstructural electrical and mechanical properties, Polymer 50 (2009) 2999–3006.
[62] J. Liu, Z.R. Yue, H. Fong, Continuous nanoscale carbon fibers with superior mechanical strength, Small 5 (2009) 536–542.
[63] W.H. Suh, K.S. Suslick, G.D. Stucky, Y.H. Suh, Nanotechnology, nanotoxicology and neuroscience, Prog. Neurobiol. 87 (2008) 133–170.
[64] D. Cui, F. Tian, C.S. Ozkan, M. Wang, H. Gao, Effect of single wall carbon nanotubes on human HEK293 cells, Toxicol. Lett. 155 (2005) 73–85.
[65] M.A. Correa-Duarte, N. Wagner, J. Rojas-Chapana, C. Morsczeck, M. Thie, M. Giersig, Fabrication and biocompatibility of carbon nanotube-based 3D networks as scaffolds for cell seeding and growth, Nano Lett. 4 (2004) 2233–2236.
[66] T. Gabay, E. Jakobs, E. Ben-Jacob, Y. Hanein, Engineered self-organization of neural networks using carbon nanotube clusters, Phys. A: Stat. Mech. Appl. 350 (2005) 611–621.
[67] A.A. Shvedova, V. Castranova, E.R. Kisin, D. Schwegler-Berry, A.R. Murray, V.Z. Gandelsman, et al., Exposure to carbon nanotube material: assessment of nanotube cytotoxicity using human keratinocyte cells, J. Toxicol. Environ. Health Part A 66 (2003) 1909–1926.
[68] H. Hu, Y. Ni, V. Montana, R.C. Haddon, V. Parpura, Chemically functionalized carbon nanotubes as substrates for neuronal growth, Nano Lett. 4 (2004) 507–511.
[69] S. Hirano, S. Kanno, A. Furuyama, Multi-walled carbon nanotubes injure the plasma membrane of macrophages, Toxicol. Appl. Pharmacol. 232 (2008) 244–251.
[70] Y.B. Zhang, Y. Xu, Z.G. Li, T. Chen, S.M. Lantz, P.C. Howard, et al., Mechanistic toxicity evaluation of uncoated and PEGylated single-walled carbon nanotubes in neuronal PC12 cells, ACS Nano 5 (2011) 7020–7033.
[71] K. Kostarelos, The long and short of carbon nanotube toxicity, Nat. Biotechnol. 26 (2008) 774–776.
[72] R. Singh, D. Pantarotto, L. Lacerda, G. Pastorin, C. Klumpp, M. Prato, et al., Tissue biodistribution and blood clearance rates of intravenously administered carbon nanotube radiotracers, PNAS 103 (2006) 3357–3362.

[73] A. Abarrategi, M.C. Gutiérrez, C. Moreno-Vicente, M.J. Hortigüela, V. Ramos, J.L. Lòpez-Lacomba, et al., Multiwall carbon nanotube scaffolds for tissue engineering purposes, Biomaterials 29 (2008) 94−102.
[74] A. Fraczek, E. Menaszek, C. Paluszkiewicz, M. Blazewicz, Comparative in vivo biocompatibility study of single and multi-wall carbon nanotubes, Acta Biomater. 4 (2008) 1593−1602.
[75] G.M. Mutlu, G.R.S. Budinger, A.A. Green, D. Urich, S. Soberanes, S.E. Chiarella, et al., Biocompatible nanoscale dispersion of single-walled carbon nanotubes minimizes in vivo pulmonary toxicity, Nano Lett. 10 (2009) 1664−1670.
[76] A. Magrez, S. Kasas, V. Salicio, N. Pasquier, J.W. Seo, M. Celio, et al., Cellular toxicity of carbon-based nanomaterials, Nano Lett. 6 (2006) 1121−1125.
[77] F. Tian, D. Cui, H. Schwarz, G.G. Estrada, H. Kobayashi, Cytotoxicity of single-wall carbon nanotubes on human fibroblasts, Toxicol. In Vitro 20 (2006) 1202−1212.
[78] G. Jia, H. Wang, L. Yan, X. Wang, R. Pei, T. Yan, et al., Cytotoxicity of carbon nanomaterials: single-wall nanotube, multi-wall nanotube, and fullerene, Environ. Sci. Technol. 39 (2005) 1378−1383.
[79] S. Pogodin, V.A. Baulin, Can a carbon nanotube pierce through a phospholipid bilayer? ACS Nano 4 (2010) 5293−5300.
[80] R. Cicchetti, M. Divizia, F. Valentini, G. Argentin, Effects of single-wall carbon nanotubes in human cells of the oral cavity: geno-cytotoxic risk, Toxicol. In Vitro 25 (2011) 1811−1819.
[81] R.H. Hurt, M. Monthioux, A. Kane, Toxicology of carbon nanomaterials: status, trends, and perspectives on the special issue, Carbon 44 (2006) 1028−1033.
[82] Y. Sun, K. Fu, Y. Lin, W. Huang, Functionalized carbon nanotubes: properties and applications, Acc. Chem. Res. 35 (2002) 1096−1104.
[83] E.L. Bakota, L. Aulisa, D.A. Tsyboulski, R.B. Weisman, J.D. Hartgerink, Multidomain peptides as single-walled carbon nanotube surfactants in cell culture, Biomacromolecules 10 (2009) 2201−2206.
[84] K.L. Klein, A.V. Melechko, T.E. McKnight, S.T. Retterer, P.D. Rack, J.D. Fowlkes, et al., Surface characterization and functionalization of carbon nanofibers, J. Appl. Phys. 103 (2008) 061301−061326.
[85] H. Zhou, J. Lee, Nanoscale hydroxyapatite particles for bone tissue engineering, Acta Biomater. 7 (2011) 2769−2781.
[86] S. Jalota, S.B. Bhaduri, A.C. Tas, Using a synthetic body fluid (SBF) solution of to make bone substitutes more osteointegrative, Mater. Sci. Eng. C 28 (2008) 129−140.
[87] K. Grandfield, F. Sun, M. FitzPatrick, M. Cheong, I. Zhitomirsky, Electrophoretic deposition of polymer-carbon nanotube−hydroxyapatite composites, Surf. Coat. Technol. 203 (2009) 1481−1487.
[88] H. Najafi, Z.A. Nemati, Z. Sadeghian, Inclusion of carbon nanotubes in a hydroxyapatite Sol-Gel matrix, Ceram. Int. 35 (2009) 2987−2991.
[89] H. Li, L. Wang, C. Liang, Z. Wang, W. Zhao, Dispersion of carbon nanotubes in hydroxyapatite powder by in situ chemical vapor deposition, Mater. Sci. Eng. B 166 (2010) 19−23.
[90] L. Niu, H. Kua, D.H.C. Chua, Bonelike apatite formation utilizing carbon nanotubes as template, Langmuir 26 (2010) 4037−4069.
[91] T. Kokubo, H. Takadama, How useful Is SBF in predicting in vivo bone bioactivity? Biomaterials 27 (2006) 2907−2915.
[92] T. Akasaka, F. Watari, Y. Sato, K. Tohji, Apatite formation on carbon nanotubes, Mater. Sci. Eng. C 26 (2006) 675−678.
[93] S. Liao, G. Xu, W. Wang, F. Watari, F. Cui, S. Ramakrishna, et al., Self-assembly of nano-hydroxyapatite on multi-walled carbon nanotubes, Acta Biomater. 3 (2007) 669−675.
[94] S. Aryal, S.R. Bhattarai, R. Bahadur, M.S. Khil, D.R. Lee, H.Y. Kim, Carbon nanotubes assisted biomimetic synthesis of hydroxyapatite from simulated body fluid, Mater. Sci. Eng. A 426 (2006) 202−207.

[95] Y. Xiao, T. Gong, S. Zhou, The functionalization of multi-walled carbon nanotubes by in situ deposition of hydroxyapatite, Biomaterials 31 (2010) 5182−5190.
[96] P. Yan, J. Wang, L. Wang, B. Liu, Z. Lei, S. Yang, The in vitro biomineralization and cytocompatibility of polydopamine coated carbon nanotubes, Appl. Surf. Sci. 257 (2011) 4849−4855.
[97] Q. Tan, K. Zhang, S. Gu, J. Ren, Mineralization of surfactant functionalized multi-walled carbon nanotubes (MWNTs) to prepare hydroxyapatite/MWNTs nanohybrid, Appl. Surf. Sci. 255 (2009) 7036−7039.
[98] H.Y. Liu, Q. Cai, P.F. Lian, Z. Fang, S. Duan, X.P. Yang, et al., β-tricalcium phosphate nanoparticles adhered carbon nanofibrous membrane for human osteoblasts cell culture, Mater. Lett. 64 (2010) 725−728.
[99] H.Y. Liu, Q. Cai, P.F. Lian, Z. Fang, S. Duan, S. Ryu, et al., The biological properties of carbon nanofibers decorated with β-tricalcium phosphate nanoparticles, Carbon 48 (2010) 2266−2272.
[100] F. Wang, M.S. Li, Y.P. Lu, Y.X. Qi, A simple sol-gel technique for preparing hydroxyapatite nanopowders, Mater. Lett. 59 (2005) 916−919.
[101] Y.Q. Dai, W.Y. Liu, E. Formo, Y.M. Sun, Y.N. Xia, Ceramic nanofibers fabricated by electrospinning and their applications in catalysis, environmental science, and energy technology, Polym. Adv. Technol. 22 (2010) 326−338.
[102] D. Li, J.T. McCann, Y.N. Xia, Electrospinning: a simple and versatile technique for producing ceramic nanofibers and nanotubes, J. Am. Ceram. Soc. 89 (2006) 1861−1869.
[103] Y. Wu, L. Hench, J. Du, K. Choy, J. Guo, Preparation of hydroxyapatite fibers by electrospinning technique, J. Am. Ceram. Soc. 87 (2004) 1988−1991.
[104] X. Dai, S. Shivkumar, Electrospinning of PVA-calcium phosphate sol precursors for the production of fibrous hydroxyapatite, J. Am. Ceram. Soc. 90 (2007) 1412−1419.
[105] E. Zussman, X. Chen, W. Ding, L. Calabri, D.A. Dikin, J.P. Quintana, et al., Mechanical and structural characterization of electrospun PAN-derived carbon nanofibers, Carbon 43 (2005) 2175−2185.
[106] J. Tao, W. Jiang, H. Zhai, H. Pan, X. Xu, R. Tang, Structural components and anisotropic dissolution behaviors in one hexagonal single crystal of β-tricalcium phosphate, Cryst. Growth Des. 8 (2008) 2227−2234.
[107] V. Zaichick, S. Zaichick, V. Karandashev, S. Nosenko, The effect of age and gender on Al, B, Ba, Ca, Cu, Fe, K, Li, Mg, Mn, Na, P, S, Sr, V, and Zn contents in rib bone of healthy humans, Biol. Trace. Elem. Res. 129 (2009) 107−115.
[108] M. Bohner, J. Lemaitre, Can bioactivity be tested in vitro with SBF solution? Biomaterials 30 (2009) 2175−2179.
[109] H.B. Pan, X.L. Zhao, B.W. Darvell, W.W. Lu, Apatite-formation ability—predictor of "bioactivity"? Acta Biomater. 6 (2010) 4181−4188.
[110] X. Liu, L. Guo, D. Morris, A.B. Kane, R.H. Hurt, Targeted removal of bioavailable metal as a detoxification strategy for carbon nanotubes, Carbon 46 (2008) 489−500.

CHAPTER

Nanoceramics for Bone Regeneration in the Oral and Craniomaxillofacial Complex

19

R. Dziak[a], K. Mohan[a], B. Almaghrabi[a] and Y. Park[b]

[a]*Department of Oral Biology, State University of New York at Buffalo, NY, USA*

[b]*Department of Prosthodontics Yonsei University College of Dentistry, Seoul, Korea*

CHAPTER OUTLINE

19.1 Introduction

The goal of tissue engineering is to develop biological substitutes that maintain, improve, or restore tissue and organ functionality damaged through disease, trauma, or congenital abnormalities [1]. Bone tissue engineering in particular aims to replace critical bone loss due to trauma or disease. In the oral cavity and craniofacial region, bone tissue engineering approaches are used in clinical procedures such as restoration of alveolar bone after periodontal disease, sinus augmentation, peri-implantitis, as well as reconstructive surgery after trauma or conditions such as cancer.

Although there have been tremendous advances in the development of tissue engineering approaches for bone that involve specific aspects of the bone regenerative process, basically the goal of all strategies is to provide at the site of defect, an environment in which the appropriate cells such as stem cells or more immediate osteoblastic precursors can migrate and attach to

Nanobiomaterials in Clinical Dentistry.

scaffolds that can provide mechanical support as well as signaling factors to optimize the cells' osteogenic functions (Figure 19.1).

Recent reviews have focused on cell sources for bone regeneration [2] and delivery of growth factors [3] in tissue engineering. The requirements of scaffolds are complex and specific to the structure and function of the site of interest. Generally accepted characteristics of scaffolds have the properties listed in Table 19.1.

As noted by Hollister and Murphy the technical requirements of scaffolds can also be qualitatively described as the 4 Fs: Form, Function, Fixation, and Formation [5]. Form is the requirement that scaffolds fill complex three-dimensional (3D) osseous defects. Function is the requirement that scaffolds provide temporary mechanical load bearing within the defects. Fixation is the requirement that scaffolds are securely attached to bone at the defect margins, with formation requiring that scaffolds enhance bone formation by providing the appropriate growth environments, allowing perfusion of needed nutrients and delivering osteoinductive factors, including cells, proteins, and/or genes [5].

Nanotechnology has been very pivotal in the fabrication of materials with properties that support the cellular processes involved in bone regeneration and repair and provide a scaffold for optimal 3D tissue formation. This chapter will discuss some of the recent advances in the

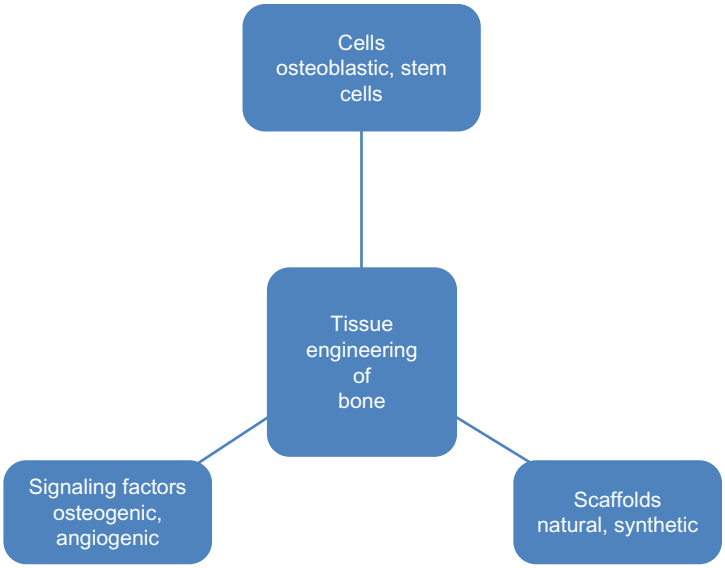

FIGURE 19.1

Basic components for tissue engineering of bone. The design of optimal bone tissue engineering for bone regeneration in specific sites such as in the craniofacial/oral cavity regions requires the attraction of the appropriate endogenous osteogenic cells or the addition of exogenous cells to scaffolds that will support the bone regenerative processes with the addition of growth factors that will enhance osteogenesis as well as support angiogenesis.

Table 19.1 Design Criteria for Bone Tissue Engineering Scaffolds

1. Ability to deliver and/or mediate appropriate cellular interactions	The material should not only be biocompatible, but also foster attachment, differentiation, and proliferation of osseous and vascular cells as needed.
2. Osteoconductivity with host bone	An ideal scaffold should not only eliminate the formation of fibrous tissue encapsulation but also result in a strong bond between the scaffold and host bone.
3. Biodegradability	The composition of the material, combined with the porous structure of the scaffold, should result in biodegradation in vivo at rates appropriate to tissue regeneration.
4. Mechanical properties	The mechanical strength of the scaffold should be sufficient to provide mechanical stability in load bearing sites before the synthesis of new extracellular matrix by cells is completed.
5. Porous structure	The scaffold should have an interconnected porous structure with porosity >90% and diameters between 300–500 μm for cell penetration, tissue ingrowth and vascularization, and nutrient delivery.
6. Fabrication	The material should possess desired fabrication capability, e.g., being readily produced into irregular shapes of scaffolds that match the defects in bone of individual patients.
7. Translational potential	The fabrication of the scaffold should be suitable for commercialization and approval for use in specified clinical procedures.

(Adapted from Ref. [4])

development of nanoceramics that fulfill many of the desired qualities for a bone scaffold and have great clinical potential in bone regenerative procedures in dentistry.

19.2 Nanoceramics and bone repair

Many investigations of nanophase materials to date have illustrated their general characteristics for bone repair. For example, increased bone forming osteoblast adhesion on nanograined materials in comparison to conventional (micron-grained) materials has been reported [6,7]. Osteoblast proliferation in vitro and long-term functions were also enhanced on ceramics with grain or fiber sizes less than 100 nm [7,8]. In addition to osteoblast responses, reports of modified behavior of bone resorptive osteoclastic cells have also been documented on nanophase ceramics [6] and in vivo studies have demonstrated increased new bone formation on metals coated with nanohydroxyapatite compared to conventional apatite [9].

The significance of nanotechnology is that it creates materials that mimic the natural nanostructure of living human tissues. With specific reference to bone, it is important to note that this tissue is a natural nanostructured composite material composed of intimately connected inorganic (bone apatite) and organic compounds (mainly collagen but also noncollagenous proteins). Due to the

hierarchical nature of bone with the lowest level of osseous materials in the nanoscale range, materials with nanometer structures are logically natural choices for fabrication of optimal bone implants and graft materials for osseous regeneration [10].

When considering bioceramics for bone tissue engineering it is essential to consider the degree of biodegradability (resorption) as well as the mechanical strength of the materials. For example, porous hydroxyapatite (HA) and tricalcium phosphate (TCP) have been shown to have excellent osteoconductive properties, but their biodegradation is poor [10]. Nanotechnology has been shown to play an important role in the development of porous bioceramics with high mechanical strength and enhanced bioactivity and resorbability [11,12].

19.3 Hydroxyapatite

Nanosized HA is the main component of mineral bone in the form of nanometer-sized needlelike crystals of approximately 5−20 nm width by 60 nm length [10]. Since synthetic HA has been shown to possess exceptional biocompatibility and bioactivity properties, it has been widely used clinically in the form of powders, granules, dense and porous blocks, and various composites. Most recently, for tissue engineering applications the trend is to develop nanosized HA with properties closer to those of living bone. Nanophase HA properties such as surface grain size, pore size, and wettability can be modulated for optimal osteoblast adhesion and long-term osteoconductivity [11].

nanOss® bone void filler originally from Angstrom Medica is considered to be the first nanotechnology medical device to receive clearance by the US Food and Drug Administration in 2005. According to that original developing company and Pioneer Surgical Technology Inc. that now markets the material, nanOss® is an innovative structural biomaterial that is highly osteoconductive and remodels over time into human bone with applications in the sports medicine, trauma, spine, and general orthopedics markets. It is formulated by precipitating nanoparticles of calcium phosphate in aqueous phase and the resulting white powder is compressed and heated to form a dense, transparent, and nanocrystalline material. It is claimed to be the first material that duplicates the microstructure, composition, and performance of human bone.[1] Pioneer Surgical Technology Inc. presently has commercially available nanOss Bioactive Loaded®, a prefilled mixing syringe with nanOss mixed with a collagen-based biopolymer, designed for use in minimally invasive orthopedic surgical procedures as well as nanOss Bioactive 3D bone graft that utilizes the nanocrystalline HA suspended in a porous gelatin-based foam to promote bone growth in the posterolateral spine.[1]

Another commercially available product for use in oral maxillofacial applications, Ostim®, also is comprised of nanocrystalline particles of HA. This material which is available in a syringe as a ready-to-use paste (Heraeus Kutzer, Hanau, Germany) and contains approximately 65% water and 35% nanoscopic HA particles has been used for augmentation procedures in osseous defects [13]. It should be noted that Ostim® does not harden in situ upon mixing with blood or the spongiosa material at the osseous defect site [14]. In a case series to evaluate the healing potential of intrabony peri-implantitis the application of the nano-HA material resulted in clinically significant

[1] http://www.pioneersurgical.com/#

reductions in periodontal depth and gains in clinical attachment 6 months after therapy [15]. These improvements in periodontal healing were comparable to those obtained in patients treated in the same series with a bovine-derived xenograft (Bio-Oss®) in combination with a collagen membrane (Bio-Gide®) (Figure 19.2).

Although the clinical improvement noted in the nanomaterial group appeared to be within the range of other regenerative treatment procedures in this as well as other studies, there were some reported difficulties with the material. The material seemed to compromise initial adhesion of the mucoperiosteal flaps in all of the patients treated with it and the low consistency seemed to lead to collapse of these flaps into the intrabony defect and to migration of inflammatory cells to the area of the wound [15]. Although no histological data were available from this study, another study with the nanosized material did provide some information regarding the tissue composition of augmented intraoral sites 6–7 months after the application of the material in patients needing lateral ridge augmentation [16] {Figure 19.3}.

Histological analyses showed the presence of small pieces of the nanocrystalline HA in biopsy cores after 6 months without any signs of inflammatory reactions. Moreover, upon

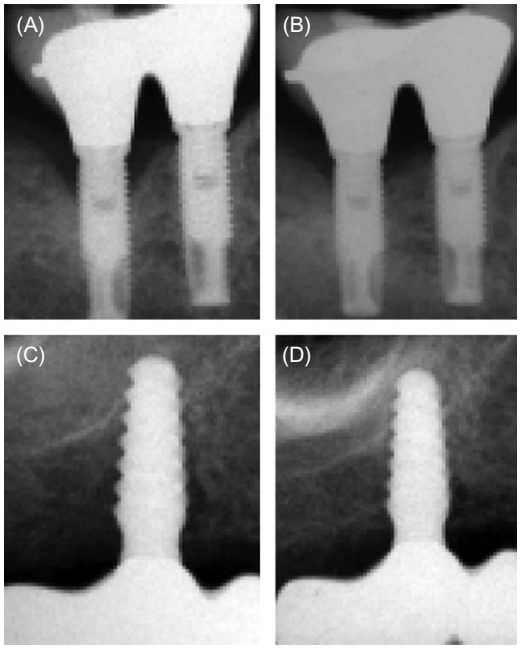

FIGURE 19.2

Case study comparing nano-HA Ostim® to calcium phosphate xenograft and collagen membrane for treatment of intrabony peri-implantitis. (A) Radiograph immediately before application of bovine-derived xenograft in combination with a collagen membrane. (B) Postoperative radiograph at 6 months. (C) Radiograph immediately before application of nanocrystalline HA. (D) Postoperative radiograph at 6 months.

Figure from Ref. [15] with permission from publisher.

clinical and radiographic analysis, it was determined that significant alveolar ridge width gain occurred with the material providing an appropriate site for placement of a primary stable implant. The histological assessment of the action of nano-HA material in this study was fairly consistent with studies of the material in various animal models such as the critical size calvarial defect in the adult domestic pig and metaphyseal defects in the Gottinger Minipig [14]. Although in the pig calvarial defect model it was reported that complete resorption of the nano-sized material occurred after 12 weeks [13], in the Gottinger Minipig metaphyseal model, there was still incomplete resorption after 1 year despite a period of robust resorption during the first

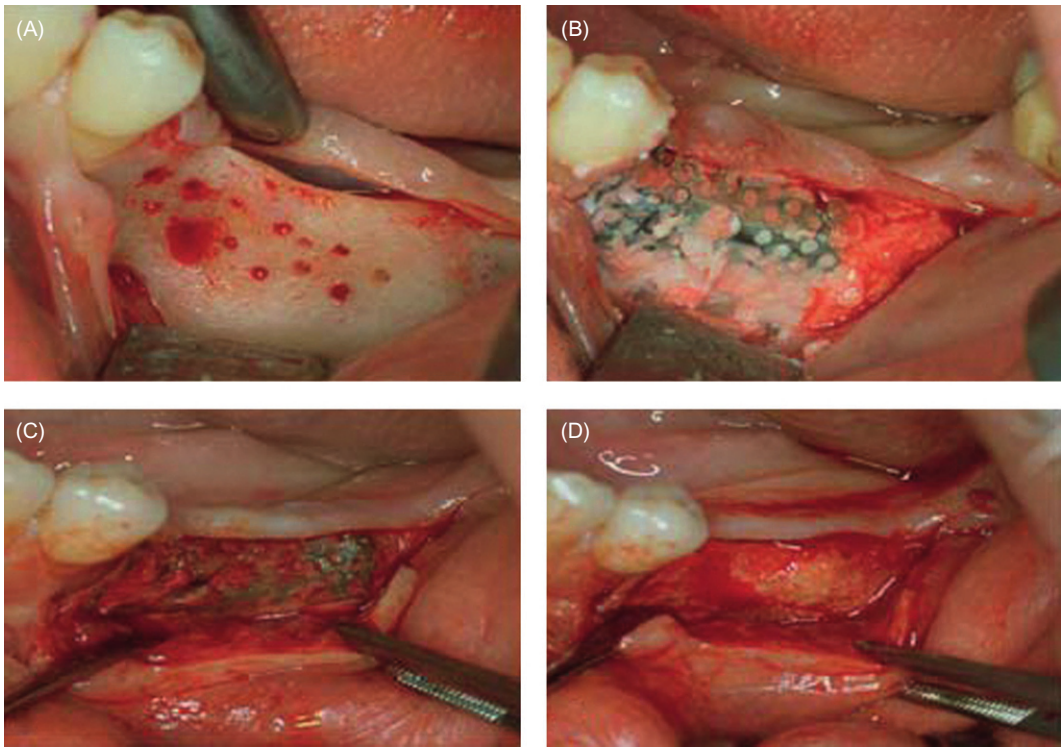

FIGURE 19.3

Overview of treatment course with nano-HA for lateral ridge augmentation. (A) A full-thickness flap was elevated and the augmentation area of future implant sites for replacement of the left mandibular second premolar and the first and second molars was prepared with additional cortical perforations. (B) The titanium mesh was fixed and the nano-HA bone substitution material is in place. (C) After elevating a full-thickness flap at reentry 6 months post augmentation, a dense hard tissue gain was found with a thin layer of soft tissue directly underneath the titanium mesh. (D) After removal of the titanium mesh, a gain in alveolar ridge width due to defect regeneration by hard tissue formation was noted.

Figure from Ref. [15] with permission from publisher.

6 weeks after implantation. In this minipig model there was also indication of extensive bioactivity 6 weeks after the placement of the nanomaterial with osseous deposition and extensive contact of osteoblasts with the material that appeared to act as a scaffold. There was also indication of resorption with polynucleated cells in close contact to the material's surface. Vascularization at the implant site was also histologically identified from the 6 week time period onward [14]. Based on the handling characteristics as well as the chemical properties of this nanosized HA material, it was concluded in this study that despite the fact that full resorption did not occur even after 12 months postoperatively, Ostim® is suited for minimally invasive applications into defect sites that are stable or that need to be surgically augmented [14]. Although there are several reports of successful osseointegration with the use of nano-HA products such as Ostim® and nanOss®, it is still difficult to ascertain if these nanoproducts yield significantly more optimal bone remodeling properties than the conventional materials without nanosized properties. For example, a study by Huber et al. [17] designed to evaluate the Ostim® paste and a solid HA ceramic, Cerabone®, for treatment of critical size bone defects in rabbits found only slightly more significant increases in bone ingrowth with Ostim® in comparison to Cerabone® and reported similarly excellent results for Ostim® and a group in which a Cerabone® core was surrounded by the Ostim® paste. No doubt, however, that different osseous defect models might produce relatively different results depending upon such parameters as the size, shape, and location of the defect and so care must be taken in the interpretation of results from various animal models that might not truly represent the clinical conditions in which the grafts are intended to be used.

There have been recent published reports of two randomized controlled clinical studies designed to assess the efficacy of Ostim® after open flap debridement (OFD) on healing of intrabony periodontal defects [18,19]. The results of these studies have indicated statistically significantly higher clinical improvements following OFD and subsequent defect fill with the nano paste compared to OFD alone [18,19]. However, since these studies did not provide histological data, it has been difficult to definitively assess the effect of the nanomaterial on bone regeneration in the treated individuals. In a very recent study [20], the Ostim® material was further evaluated, both clinically and histologically, in six patients, each of them displaying very advanced intrabony defects around teeth scheduled for extraction due to advanced chronic periodontitis and further prosthodontics considerations. Seven months following surgery, there was a significant reduction in probing pocket depth and clinical attachment level gain similar to other studies with the material. However, histological analysis of the surrounding hard and soft tissue around the teeth extracted after end of the regeneration period revealed a healing predominantly characterized by epithelial down growth with only limited formation of new cementum (NC) and bone regeneration in three of the six biopsies (Figure 19.4).

There was resorption of the nano-HA in four out of the six biopsies with a few remnants of the graft particles (either surrounded by newly formed mineralized tissue or encapsulated in connective tissue) in two biopsies. On the basis of these results and with the recognition that the teeth selected for this study displayed very advanced destruction of the periodontal supporting apparatus and possible limited regenerative potential, the investigators in this study concluded that this nanomaterial has only limited potential for periodontal healing of intrabony defects [20]. Therefore, clinical outcomes obtained following surgery with OFD and the nano-HA may not always be indicative of actual periodontal regeneration.

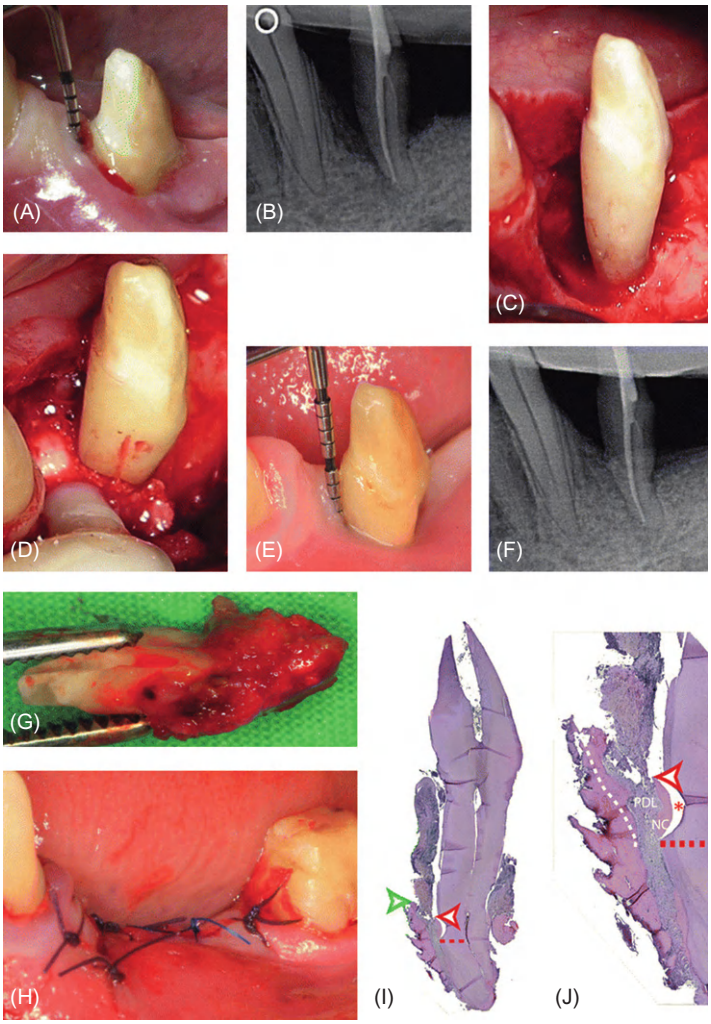

FIGURE 19.4

Clinical study with nano-HA (Ostim®) used for advanced intrabony defects. (A) Mesial aspect of tooth 34 prior to surgery with OFD + nano-HA depicting a probing depth of 10 mm. (B) Preoperative radiograph demonstrating the presence of a deep intrabony defect. (C) Following removal of granulation tissue and thorough scaling and root planing, the intraoperative situation revealed a deep one- and two-wall intrabony defect. (D) The intrabony component was filled with nano-HA. (E) At 7 months following surgery, a substantial reduction of probing depth was measured. (F) At 7 months, the intraoral radiograph revealed a hard tissue fill of the intrabony component. (G) Removed biopsy. (H) Complete flap closure, immediately after biopsy removal. (I) The histological evaluation revealed a healing predominantly characterized by a long junctional epithelium and limited regeneration of cementum and bone. *Red arrowhead*: coronal extension of NC,

19.4 Nano-HA–collagen composites

In addition to nano-HA preparations, in an attempt to mimic natural bone even more closely, several researchers have fabricated nano-HA–collagen composites (nano-HA/collagen) [21–23]. In particular, one laboratory has prepared a hierarchical structure resembling natural bone by allowing self-assembly of collagen triple helices and the formation of nano-HA crystals on the surface of these fibrils [23]. In this technique, nano-HA crystals grow on the surface of collagen fibrils such that their *c*-axes orient along the longitudinal axes of the collagen fibrils and the mineralized fibrils become aligned parallel to each other forming mineralized collagen fibers as in situ in bone. In vitro studies have shown that this composite supports osteoblastic cell growth and new bone formation [24,25]. The nano-HA/collagen-based scaffolds have now been successfully used in many clinical cases requiring various types of bone repair [26] with wound healing and no abnormalities found in local and systematic examinations during long-term follow-up [27].

19.5 Hydrogels and nano-HA

Other studies, although recognizing the advantages of nano-HA for bone regenerative purposes, have made efforts to improve some of the properties of this material with respect to controlling its biodegradability and porosity for better bioactivity. Because of the inherent ability of hydrogels to swell in aqueous media and to permit the transport of enzymes and nutrients to and through various supporting ceramic scaffolds, there has been increasing interest in the use of hydrogels with ceramics in tissue engineering [28,29].

Chitosan is a promising hydrogel material for bone regeneration because it is biocompatible and biodegradable with a degradation rate that is dependent on factors such as degree of deacetylation and crystallinity [30]. It can also be easily formed into beads, fibers, or more complex structures [31,32]. In another recent study [33], β chitin hydrogel/nano-HA composite scaffolds were synthesized and shown to have improved porosity, swelling ability, protein adsorption, and retention as well as biomineralization properties for use as a potential candidate for bone tissue engineering applications. Although it appears to date that only in vitro studies and a preliminary in vivo study in a rat calvarial defect model [30] have been conducted with this type of nanocomposite scaffolds, there have been a series of studies that have tested the combination of polymers such as chitin with traditional-sized HA. These earlier studies which do include in vivo experiments suggest that the composites support bony ingrowths into the implant as the matrix gradually resorbs [34–36].

◀ *green arrowhead*: coronal extension of new bone, *red dotted line*: apical extension of the notch. Original magnification ×5. (J) Higher magnification of the defect shown in (I). Formation of NC and new periodontal ligament (PDL) was confined to the area of the notch. *Red arrowhead*: coronal extension of NC, *red dotted line*: apical extension of the notch, *white dotted line*: margin between the newly formed bone and old bone, *red asterisk*: artifact. Original magnification ×25. (For interpretation of the references to color in this figure legend, the reader is referred to the web version of this book.)

Figure from Ref. [20] with permission from publisher.

The composites may have optimal porosity to support the attachment and growth of osteoblastic cells with sufficient retention of plasticity for ease of filling defects while maintaining sufficient mechanical strength for support.

Metallic nanoparticles such as copper and zinc have high antibacterial activity, low toxicity, and chemical stability. Moreover, zinc has been shown to be an important trace element in bone [37], required for cell proliferation [38] and it has been suggested to play an important role in collagen production and biomineralization [39,40]. Because of these properties, these metals have been utilized in the fabrication of materials for bone tissue engineering. The addition of nanocopper and zinc has been recently shown to significantly increase swelling, decrease degradation, increase protein adsorption, and increase antibacterial activity in chitosan/nano-HA scaffolds [41]. These composites have been shown to have no toxicity toward osteoprogenitor cells and have therefore been postulated to have advantages over the chitosan nano-HA scaffolds without added metals for use in osseous regeneration in many critical sites such as in the oral cavity where antimicrobial effects might be particularly useful [41]. Although to date it does not appear that clinical studies with chitosan/nano-HA composites of this type have been reported, the experimental in vitro studies do target them as promising scaffolds for use in oral bone tissue engineering. Their development should be further pursued in order to optimize the bioresorbability and mechanical strength properties of the scaffold material for various craniofacial bone and periodontal intrabony defect sites.

19.6 Chitosan and nano-bioactive glass composites

Other variations of chitosan and nanoceramics have recently been developed and tested for bone tissue engineering. In particular, a chitosan−gelatin/nano-bioactive glass ceramic composite has been shown to have many excellent properties for use in alveolar bone tissue regeneration [42]. This composite extends the valuable characteristics of chitosan discussed above with the blending of gelatin, a unique sequence of amino acids such as glycine, proline, and hydroxyproline that enhances cell attachment and nanoparticles of glass ceramics that are osteoconductive and biodegradable. Bioactive glass particles, particularly those synthesized by a sol−gel process, have been shown to bond to hard tissues because of their ability to form a surface layer of hydroxycarbonate apatite and produce no local or systemic toxicity or inflammatory or foreign-body response [6,43,44]. A composite of chitosan−gelatin and nanoglass ceramic can be fabricated to have pore sizes in the range of 150−300 μm which should be optimal for migration of cells into the interior of the scaffold and osseous ingrowths and vascularization [45]. The degradation and swelling behavior of the composite scaffold also appeared optimized for cell attachment and spreading with biomineralization occurring with the formation of an apatite layer on the surface of the composite [42]. These properties point to the usefulness of these composites in tissue engineering applications in bone regeneration.

19.7 Nanocalcium sulfate

Calcium sulfate (CS) is another highly biocompatible material with a long clinical history as a synthetic ceramic material. The hemihydrate form of CS, also known as plaster of Paris, is one of the

simplest synthetic bone-like grafts with a report in 1892 by Dreesman, as described by Peltier, showing its use to fill bone cavities which later were found to be filled with solid bone [46]. CS has been further demonstrated in many animal and clinical studies to be an effective osteoconductive scaffold that enhances bone regeneration [47]. In our laboratory, CS has been shown to adsorb platelet-derived growth factor (PDGF-BB) and to support enhanced human osteoblastic cell proliferation in vitro when treated with the growth factor [48]. Although CS is a desirable osteoconductive material and potential carrier of osteoinductive factors in its presently available state, it has some deficiencies, including slow and variable degradation rate and weak mechanical properties [49]. In an attempt to use nanotechnology to improve some of the properties of CS, our laboratory has been working to fabricate a nanocalcium sulfate (nCS) scaffold material. We recently presented our studies on the use of a cryo-vacuum technique to process dihydrate CS into dihydrate nCS, which was then subjected to oven drying to produce a hemihydrate nCS. The cryo-vacuum process for preparing CS dihydrate nanocrystals was based on that previously demonstrated by Salvadori et al. [50]. The advantages of this cryo-vacuum technique are that it is simple and avoids the introduction of any surfactants or other components beyond CS and water.

The nCS synthesized in this manner was sterilized by glow discharge treatment, a practical method for most clinical situations. Electron microscopy showed that the nCS powder consists of aggregates of closely arranged acicular crystals, approximately 30−80 nm in width, 400−600 nm in length and approximately 80−100 nm in diameter, providing a surface area as determined by Brunauer, Emmett, and Teller surface area analysis using a Micromeretics Model 2000 ASAP nitrogen physisorption apparatus, to be about 10 times that of conventional CS. Physicochemical characterization confirmed the composition and phase of the material. Surface microhardness testing showed that the nCS was stronger than conventional CS and may provide an additional advantage to the scaffolding properties of the material. Cell viability/metabolic activity assays with human osteoblastic and PDL cells verified the safety and biocompatibility of nCS and alkaline phosphatase assays showed that the material supports the differentiation of osteoblastic cells [49].

Studies from our lab as well as many others point to the potential use of scaffold materials as carriers that can release and maintain levels of growth factors to aid in their ability to facilitate bone repair [51]. Release kinetics for adsorbed PDGF and bone morphogenetic protein-2 (BMP-2) [49] suggested that nCS may serve as an appropriate vehicle for slow release delivery of these agents that have been approved for clinical use in a number of bone regenerative procedures [52,53].

Our laboratory has found that when human recombinant BMP-2 (rhBMP-2) was mixed with CS (conventional size, medical-grade calcium sulfate) or nCS and allowed to dry into disks of equal weight and proportion, there was a significantly greater amount of the BMP-2 released from the nCS disks at 37°C over a 7-day period as measured with a specific immunoassay for the growth factor. However, when a mixture of 10% alginate, a natural polysaccharide, and nCS was mixed with the BMP-2, there was a much faster and significantly greater release of the BMP-2 compared to nCS alone with a significant amount released after 2 h that did not change for up to 7 days. This study suggests that the use of alginate can significantly improve the properties of an nCS scaffold at least with respect to the release of growth factors (Figure 19.5).

However, although these data suggest that nCS has release characteristics for growth factors different than conventional-sized CS and that they can be modified with the use of alginate, they do not provide sufficient information to predict how this nCS material will function as a vehicle

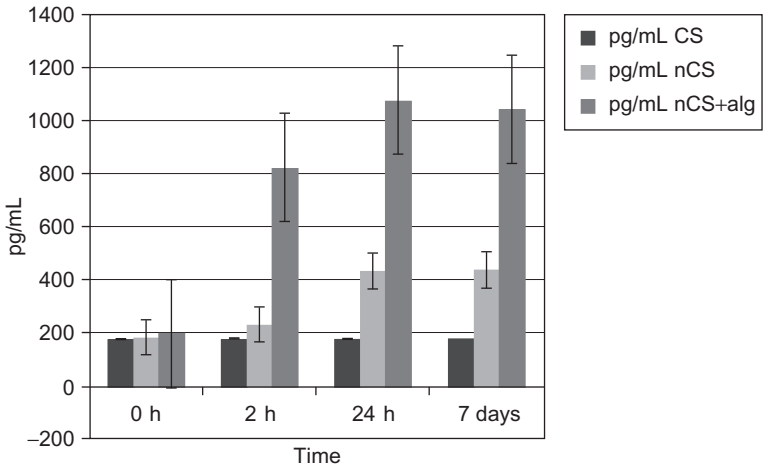

FIGURE 19.5

Release of rhBMP-2 from nCS alone, nCS + 10% alginate in comparison to CS. Disks were fabricated from the scaffold materials with rhBMP-2 (Prospec, Rehovot, Israel), added at a final concentration of 1 μg/disk. BMP-2 released from the disks at 37°C was measured with a specific immunoassay (Quantikine Kit, R&D Systems). Values are the mean ± standard deviation of four samples in each group.

delivery agent in various in vivo situations where bone formation is the desired end function. Although our in vitro data suggest that nCS releases only a small percentage of absorbed BMP-2, an effective dose cannot be predicted since the in vivo conditions in a particular site may significantly alter the kinetics of release and availability of the growth factor at that site. The complexities involved in the delivery of growth factors to in vivo sites in tissue engineering strategies have been reviewed [54,55] and it must be recognized that extrapolation from in vitro studies to a particular in vivo model is extremely limited.

Therefore, as an extension of these in vitro studies, most recently, we also tested nCS in the rat calvarial defect model, which is a well-studied model that allows in vivo testing of the bone regenerative ability of a material [56,57]. All protocols used here were approved by the Institutional Animal Care and Use Committee of State University of New York at Buffalo, New York, USA. Basically the technique involved creating an 8 mm critical size defect using a low-speed hand piece and trephine drill in the calvaria of adult male Sprague-Dawley rats. The cranial defect created in each rat was then filled with a constant amount (100 mg) of either nCS alone, or nCS mixed with 10 or 50% alginate with and without PDGF-BB or rhBMP-2. In some other rats, the defect was filled with Capset® which was a commercially available conventional-sized CS, or GEM21®, a commercially available (Osteohealth) mixture of beta TCP and PDGF, or DFDBA (demineralized freeze-dried bone allograft, commercially available, Dentsply). In the negative control group, the defects were left untreated. There were a minimum of four animals in each treatment and control group. In all animals, the overlying tissues were closed in layers with resorbable 4–0 Vicryl® sutures. As shown in Figure 19.6, radiographic analysis using Image J software to measure bone filling in the calvaria from the margin of defect after 2 weeks of treatment, revealed that were no

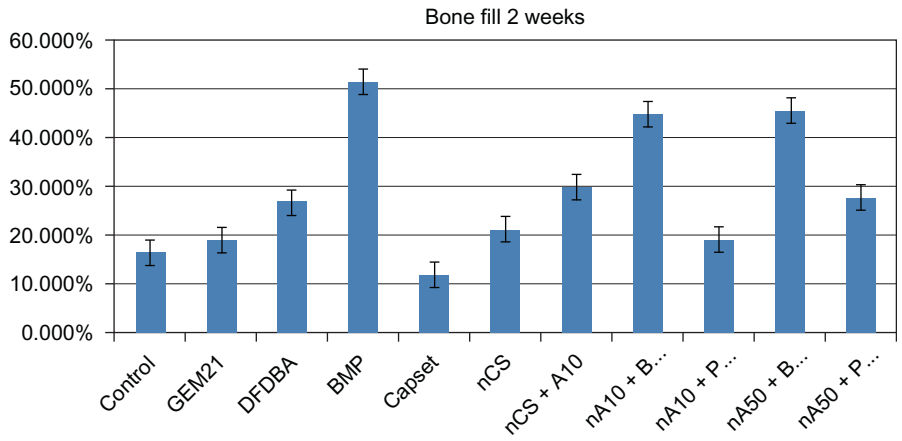

FIGURE 19.6

Bone fill in rat calvarial defects. Rat calvarial defects were filled with either GEM21® (300 μg/mL PDGF in sterile water mixed 1 to 1 with solid TCP), DFDBA, Capset® (medical-grade CS), BMP (1500 μg BMP-2/mL deposited on a collagenous sponge matrix), nCS alone, nCS + A10 (nCS with 10% alginate), nA10 + B (nCS + 10% alginate + BMP-2 [900 μg/g nCS]) and nA10 + P (nCS + 10% alginate + PDGF-BB[180 μg/g nCS]), nA50 + B (nCS + 50% alginate + BMP-2 [900 μg/g nCS]), nA50 + P (nCS + 50% alginate + PDGF-BB [180 μg/g nCS]). The controls were nonfilled defect. There were four animals/treatment group. The mixtures of alginate and nCS increased the bone fill compared to nCS alone. The bone fill was significantly greater with the combination of nCS + alginate and BMP-2 compared to GEM21®, DFDBA, but was not significantly different than with BMP-2 applied on a collagenous sponge.

significant differences between control and Capset®, GEM21® and nCS. However, there were significant increases compared to control with DFDBA, BMP-2 alone and all nCS samples that included BMP-2. It is also interesting to note that the combination of nCS with alginate resulted in greater bone fill than nCS alone and comparison of the samples treated with nCS to those with Capset® did show a greater fill with nCS although at this time period, neither resulted in significantly greater effects compared to untreated controls. It can also be observed that under these conditions, PDGF-BB either added as a part of the GEM21® treatment or with the nCS did not produce increases in bone fill. This experiment suggested that a combination of nCS with alginate might enhance the bone-filling properties of the material at least with respect to some critical bone defects sites and lead to further studies on the manner in which alginate might be modifying the properties of the nanomaterial.

Alginate, a natural polysaccharide extracted from brown sea algae, has been extensively used in various aspects of tissue engineering because it is biocompatible, hydrophilic, and biodegradable under normal physiological conditions [58]. It forms stable hydrogels in the presence of certain divalent cations (e.g., Ca^{2+}) in low concentrations [59]. When scaffolds containing alginate are placed in a liquid milieu, there is uncontrolled degradation of ionically cross-linked alginate due to loss of divalent cations. This leads to formation of pores inside the scaffold. In the in vivo experiment described above, alginate was added to nCS powder to induce in situ pore formation and

optimize the properties of the implant scaffold to lead to enhanced bone fill at the defect site. A previous study with an alginate/HA composite had shown that scaffolds of this type have a porous structure that supports osteoblastic cell attachment and growth [60]. It appears the addition of alginate to nCS optimizes the conditions to enable more osteoblastic cell growth and thus more bone fill in the rat calvarial model, however, more studies are needed to understand the nature of alginate's effects in this system.

In order to better understand the nature of the scaffold created by combining nCS and alginate the microscopic structure and cell-material interaction of different proportions of nCS and alginate were studied in our laboratory. Samples of different proportions of alginate (5%, 10%, 15%, 20%, and 50% by weight) and nCS were incubated in water for 24 h. It was noted that once the scaffolds were placed in water, they started to absorb water and swell, with the loss of divalent cations in the surrounding liquid causing dissolution of the ionically cross-linked alginate. The integrity of the 50%, 20%, and 15% alginate scaffolds was lost completely after 24 h. Although the 10% and 5% alginate scaffolds still kept their shape, their mechanical properties were weakened (Figure 19.7). Scanning electron microscope (SEM) analysis showed increased roughness on the surface which may be due to the sponge-like consistency of the scaffold (Figure 19.8). The alginate absorbed water and became gelatinous with the gel layer isolating nanoparticles of CS and covering the

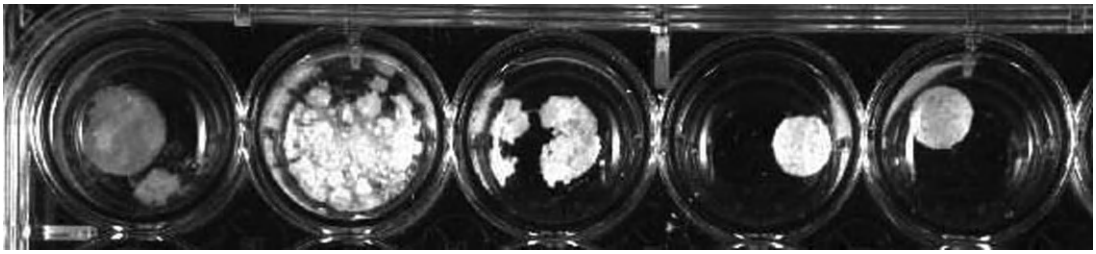

FIGURE 19.7

Dissolution behavior of nCS and alginate composite scaffolds after 24 h incubation in water. From left to right: nCS:alginate = 50:50, 80:20, 85:15, 90:10, and 95:5.

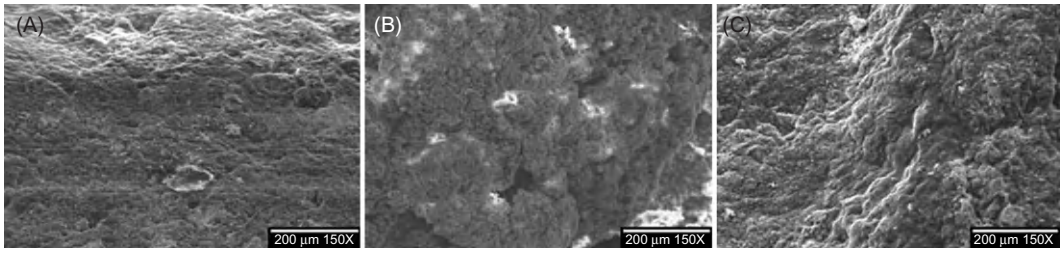

FIGURE 19.8

(A)–(C) SEM images of nCS and alginate samples after 24 h of incubation in water at 150× magnification. (A) nCS:alginate = 95:5, (B) nCS:alginate = 90:10, and (C) nCS:alginate = 50:50.

space in between the clustered crystals of nCS (Figure 19.9) and creating macropores within the scaffold.

The integrity of the 50%, 20% and 15% alginate, nCS scaffolds was lost completely after 24 h. Although the 10% and 5% alginate, nCS scaffolds still kept their shape, their mechanical properties were weakened.

Cell attachment studies were conducted by seeding human PDL cells on the nCS + alginate samples and incubating for 24 h under standard conditions with MEM media. SEM studies revealed that the cells attached to 95 nCS:5 alginate and the 90 nCS:10 alginate scaffolds but not to the 50:50 scaffolds with the greatest attachment to the 95:5 scaffolds. Also it was observed that the cells attached to the nCS:alginate scaffolds were spherical rather than elongated like those attached to the nCS alone scaffolds (Figure 19.10). Cell viability assays, however, revealed no significant differences among cells cultured on the nCS:alginate scaffolds although the 95 nCS:5 alginate group did possess the highest values of viability compared to the other two composite groups and nCS alone (Figure 19.11).

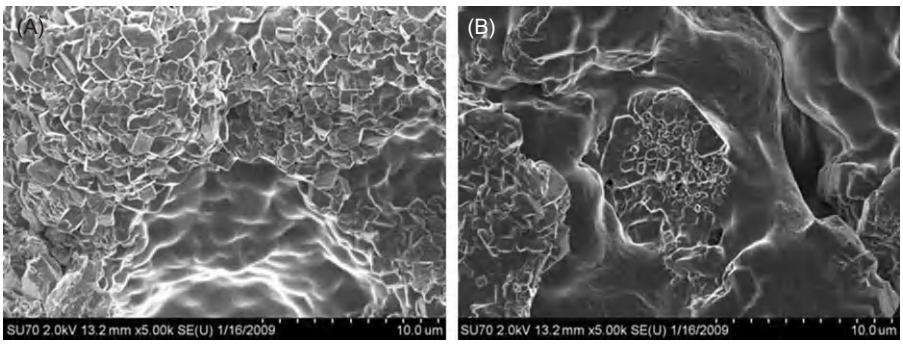

nCS:alginate (90:10) nCS:alginate (50:50)

FIGURE 19.9

SEM images of nCS and alginate samples after setting without incubation: (A) Alginate layer wraps around the cluster of crystals of nCS. (B) More alginate layers than separate clusters of nCS particles.

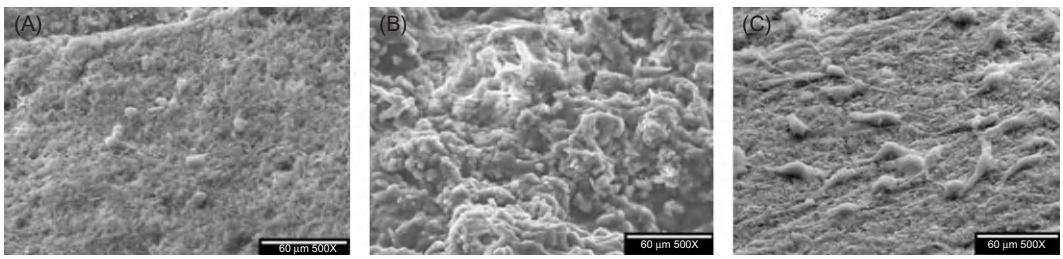

FIGURE 19.10

SEM images of periodontal cell attachment on nCS scaffolds after 24 h of incubation (500 ×). (A) 95 nCS:5 alginate; (B) 50 nCS:50 alginate; (C) nCS alone.

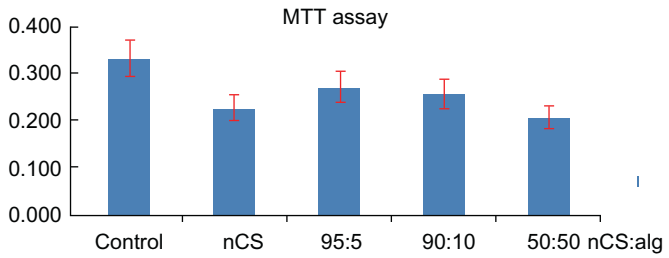

FIGURE 19.11

Periodontal cell viability tests with nCS and nCS alginate scaffolds. The MTT (3-(4,5-dimethyl-thiazol-2-yl)-2,5-diphenyl tetrazolium bromide) cell assay was conducted according to the method described previously to measure the metabolic cell activity as an assessment of viability in the presence of the nCS-alginate scaffolds [49]. Control represents cells grown in tissue culture wells without added scaffolds. Viability data are expressed as average OD ± standard deviation with $n = 4$ samples per group.

Although the nCS + alginate scaffold developed in our laboratory has not been yet tested in clinical studies, on the basis of the in vitro work and the in vivo animal studies, there are no apparent reasons why the material should not be biocompatible and effective in supporting bone regeneration in the craniofacial as well as other bony sites. We are presently in the process of optimizing conditions of the nCS + alginate mixture so that it can be used as an injectable product with or without growth factors in a variety of clinical conditions.

Presently, there is a different nCS product that is available for clinical use. This material is marketed and sold as NanoGen® (Orthogen) and has been approved for clinical use in the United States. Since it is a proprietary product, the exact conditions of its fabrication are not known. However, according to Orthogen's website,[2] it has unique microscopic structure and properties. Although the material is described as a "nanocrystalline calcium sulfate bone graft," it is also stated on the company's website that in the fabrication of the material microcrystalline CS is converted to grains of CS in the range of 200−900 nm that are then compressed to form granulates in the sizes ranged from 400−1000 μm, clearly not in the range of nanosized particles as they are usually defined. Although to date there does not appear to be studies yet published documenting the claims, the website,[2] also states that NanoGen® undergoes controlled degradation over a period of 12 weeks in contrast to the 4−6 weeks for traditional CS. Moreover, there are claims that the material is completely replaced with regenerated vital bone, critical to its success as a bone graft. The material is purposed to be used as a stand-alone bone graft material, in combination with other bone graft materials or to serve as a resorbable barrier over other bone grafts in postextraction sites, periodontal infra-osseous defects, apicoectomy, root perforations, dehiscence and fenestrations, mini and great sinus lifting. There is a published case report in which the NanoGen® material has been shown to be effective in regeneration of bone in an extraction socket of a 55-year-old female patient with histomorphometric analysis of the bone core extracted from the regenerated socket 6 months after grafting showing 47% vital bone volume with osteoclasts and osteoblastic remodeling involvement [61]. Although this one case does suggest that the properties of the CS product

[2] http://www.orthogencorp.com/

Table 19.2 Nanoceramics with Bone Scaffold Characteristics—Available for Clinical Use

Product Name	Material Composition	Approved Clinical Applications	Special Considerations
nanOss®	Nano-HA	Orthopedics	Intended for bony voids or gaps that are not intrinsic to the stability of bony structure
nanOss™ Bioactive Loaded nanOss™ Bioactive 3D	Nanohydroxyapatite plus collagen-based biopolymer nano-HA suspended in a gelatin-based foam	Orthopedics	Indicated to be gently packed into bony voids or gaps in the spine in conjunction with bone marrow aspirate or bone marrow aspirate and autograft bone; to be used in osseous defects surgically created or from traumatic injury
Ostim®	Nano-HA + water paste	Craniomaxillofacial (intrabony periodontal defects; lateral ridge augmentation)	Histological evidence for incomplete resorption 7 months postsurgery and limited healing potential [20]
Nanogen®	Nanocrystalline CS compressed granules of nanosized CS to form particles ranging from 400–1000 μm	Craniomaxillofacial (stand-alone bone graft, in combination with or a resorbable barrier over other bone grafts, periodontal intraosseous defects, apicoectomy, root perforations, dehiscence and fenestrations, sinus lifting)	Manufacturer's website[2] claims (data not yet published) of controlled degradation over 12 weeks compared to 4–5 weeks of traditional CS; case report of good bone regeneration at extraction sites 6 months post grafting [61]; no published clinical studies to date

used here result in favorable bone regeneration at extraction sites, additional studies are warranted to ascertain if the surface area and degradation properties of NanoGen® are suitable for other sites where regeneration of bone is the desired endpoint. Since the ultimate goal of most bone grafting procedures is the restoration of the defect site with vital bone and the complete resorption of the grafting material as the bone regenerative processes ensue, development of processes that lead to a controlled degradation of a biocompatible, osteoconductive material such as CS, are critically important for clinical advances in the field of bone tissue engineering.

19.8 Conclusions

Some recent papers have addressed the difficulties in achieving translation of bone tissue engineering from concept and laboratory studies to clinical therapies [5,62,63]. It has been argued that

despite over 25 years of research with extensive funding and over 12,000 papers on bone tissue engineering and over 2000 papers on bone scaffolds alone in the past 10 years, there are very limited numbers of bone tissue engineering clinical products and auto or allo bone grafts remain the gold standard and treatment of choice, for large defects, especially in craniomaxillofacial reconstruction [5]. For any therapy to be successfully adapted for clinical use, there are significant technical, business, and philosophical barriers that must be overcome. It has been argued that the technical challenges for scaffold translation alone are significant in that the materials must fill the "Form, Fixation, Function and Formation needs" [5] of repair of bony defects. However, it has also been noted that this can be best accomplished by targeting specific clinical applications and then developing a material as a modular system with increasing levels of complexity as needed [5]. This is the approach that appears to be emerging with the development of nanoceramics bone tissue engineering therapies in the craniomaxillofacial and oral cavity (Table 19.2).

As pointed out in this chapter, nanohydroxyapatite is presently commercially available for clinical use as Ostim® and nanOss® with complexity to the material recently introduced with nanOss Bioactive® bone graft that utilizes a collagen- or gelatin-based biopolymer in addition to the nano-HA material.[3] As further discussed here, nanomaterials such as the HA as well as bio active glass and CS can be further fabricated with materials such as chitosan and alginate to modify the porosity and growth factor delivery properties of the nanoscaffold for a more optimal functional form designed for a particular clinical procedure. Although there are many components such as cell sources, growth factors, and signaling pathways, in addition to the scaffold material, that have to be considered in the fabrication of an ideal bone tissue engineered product, there is an ever increasing body of basic and preclinical studies that suggest that nanoceramics will continue to play an important role in the development of sound clinical therapeutics for repair of critical defects in the craniofacial region as well as throughout the skeleton.

Acknowledgment

The authors are grateful for the clinical insight of Dr. Sebastiano Andreana throughout our work with CS and especially during the preparation of this paper.

References

[1] R. Langer, J.P. Vacanti, Tissue engineering, Science 260 (1993) 920–926.
[2] P.G. Robey, Cell sources for bone regeneration: the good, the bad, and the ugly (but promising), Tissue Eng. 17 (2011) 423–430.
[3] F.-M. Chen, M. Zhang, Z.-F. Wu, Toward delivery of multiple growth factors in tissue engineering, Biomaterials 31 (2010) 6279–6308.
[4] Q. Chen, J.A. Roether, A.R. Boccaccini, Bioactive glass and composite materials, in: W. Ashammakhi, R. Reis, F. Chiellini (Eds.), Topics in Tissue Engineering, vol. 4, 2008, pp. 1–27. Chapter 6

[3] http://www.prweb.com/releases/2012/5/prweb9555762.htm

[5] S.J. Hollister, W.L. Murphy, Scaffold translation: barriers between concept and clinic, Tissue Eng. Part B 17 (2011) 459–474.
[6] T.J. Webster, C. Ergun, R.H. Doremus, R.W. Siegel, R. Bizios, Enhanced functions of osteoblasts on nanophase ceramics, Biomaterials 21 (2000) 1803–1810.
[7] Z. Shi, X. Huang, Y. Cai, R. Tang, D. Yang, Size effect of hydroxyapatite nanoparticles on proliferation and apoptosis of osteoblast-like cells, Acta Biomater. 5 (2009) 338–345.
[8] H. Liu, T.J. Webster, Nanomedicine for implants: a review of studies and necessary experimental tools, Biomaterials 28 (2007) 354–369.
[9] P. Li, Biomimetic nano-apatite coating capable of promoting bone ingrowth, J. Biomed. Mater. Res. A 66 (2003) 79–85.
[10] N. Tran, T.J. Webster, Nanotechnology for bone materials, WIREs nanomed, Nanobiotechnol 1 (2008) 336–351.
[11] G.M. Cunniffe, F.J. O'Brien, S. Partap, T.J. Levingstone, K.T. Staton, G.R. Dickson, The synthesis and characterization of nanophase hydroxyapatite using a novel dispersant-aided precipitation method, J. Biomed. Mater. Res. 95A (2010) 1142–1149.
[12] P.N. Kumta, C. Sfeir, D.H. Lee, D. Olton, D. Choi, Nanostructured calcium phosphates for biomedical applications: novel synthesis and characterization, Acta Biomater. 1 (2005) 65–83.
[13] M. Thorwarth, S. Schultze-Mosgau, P. Kessler, J. Wiltfang, K.A. Schlegel, Bone regeneration in osseous defects using a resorbable nanoparticular hydroxyapatite, J. Oral Maxillofac. Surg. 63 (2005) 1626–1633.
[14] C. Spies, S. Shnurer, T. Gotterbarm, S. Breusch, Animal study of the bone substitute material Ostim within osseous defects in Gottinger minipigs, Z. Orthop. Unfall. 145 (2008) 64–69.
[15] F. Schwarz, K. Bieling, T. Latz, E. Nuesry, J. Becker, Healing of intrabony peri-implantitis defects following application of a nanocyrstalline hydroxyapatite (Ostim) or a bovine-derived xenograft (Bio-Oss) in combination with a collagen membrane (Bio-Gide). A case series, J. Clin. Periodontol. 33 (2006) 491–499.
[16] F.P. Strietzel, P.A. Reichart, H.L. Graf, Lateral alveolar ridge augmentation using a synthetic nanocrystalline hydroxyapatite bone substitution material (Ostim®). Preliminary clinical and histological results, Clin. Oral Implants Res. 18 (2007) 743–751.
[17] F.X. Huber, N. McArthur, J. Hillmeier, H.J. Kock, M. Baier, M. Diwo, et al., Void filling of tibia compression fracture zones using a novel resorbable nanocrystalline hydroxyapatite paste in combination with a hydroxyapatite ceramic core: first clinical results, Arch. Orthop. Trauma. Surg. 126 (2006) 533–540.
[18] A. Kasaj, B. Rhrig, G.G. Zafiropoulos, B. Willershausen, Clinical evaluation of nanocrystalline hydroxyapatite paste in the treatment of human periodontal bony defects–a randomized controlled clinical trial: 6-month results, J. Periodontol. 79 (2008) 394–400.
[19] B. Heinz, A. Kasaj, M. Teich, S. Jepsen, Clinical effects of nanocrystalline hydroxyapatite paste in the treatment of intrabony periodontal defects: a randomized controlled clinical study, Clin. Oral Invest. 14 (2010) 525–531.
[20] A. Horváth, A. Stavropoulos, P. Windisch, L. Lukács., I. Gera, A. Sculean, Histological evaluation of human intrabony periodontal defects treated with an unsintered nanocrystalline hydroxyapatite paste, Clin. Oral Invest. (2012) (published online, May 12).
[21] J. Aizenberg, J.C. Weaver, M.S. Thanawala, V.C. Sundar, D.E. Morse, P. Fratzl, Skeleton of *Euplectella* sp.: structural hierarchy from the nanoscale to the macroscale, Science 309 (2005) 275–278.
[22] M.C. Chang, T. Ikoma, M. Kikuchi, J. Tanaka, Preparation of a porous hydroxyapatite/collagen nanocomposite using glutaraldehyde as a crosslinkage agent, J. Mater. Sci. Lett. 20 (2001) 1199–1201.

[23] W. Zhang, S.S. Liao, F.Z. Cui, Hierarchical self-assembly of nanofibrils in mineralized collagen, Chem. Mater. 15 (2003) 3221−3226.
[24] C. Du, F.Z. Cui, W. Zhang, Q.L. Feng, X.D. Zhu, K. de Groot, Formation of calcium phosphate/collagen composites through mineralization of collagen matrix, J. Biomed. Mater. Res. 50 (2000) 518−527.
[25] S.S. Liao, F.Z. Cui, W. Zhang, Q.L. Feng, Hierarchically biomimetic bone scaffold materials: nano-HA/collagen/PLA composite, J. Biomed. Mater. Res. B Appl. Biomater. 69 (2004) 158−165.
[26] Z. Chen, H. Liu, X. Liu, F.Z. Cui, Injectable calcium sulfate/mineralized collagen-based bone repair materials with regulable self-setting properties, J. Biomed. Mater. Res. Part A 99A (2011) 554−563.
[27] X. Yu, L. Xu, L.Y. Bi, Y. Qu, D.B. Zheng, X. Cao, Posterolateral fusion using nano-crystal/collagen bone materials in lumbar spine, Orthop. J. China 13 (2005) 586−588.
[28] K. Gkioni, S.C.G. Leeuwenburgh, T.E.L. Douglas, A.G. Mikos, J.A. Jansen, Mineralization of hydrogels for bone regeneration, Tissue Eng.: Part B 16 (2010) 577−585.
[29] H. Tamura, T. Furuike, S.V. Nair, R. Jayakumar, Biomedical applications of chitin hydrogel membranes and scaffolds, Carbohydr. Polym. 84 (2011) 821−825.
[30] B.M. Chesnutt, Y. Yuan, K. Buddington, W.O. Haggard, J.D. Bumgardner, Composite chitosan/nano-hydroxyapatite scaffolds induce osteocalcin production by osteoblasts in vitro and support bone formation in vivo, Tissue Eng. Part A 15 (2009) 2571−2579.
[31] A. Di Martino, M. Sittinger, M.V. Risbud, Chitosan: a versatile biopolymer for orthopaedic tissue-engineering, Biomaterials 26 (2005) 5983−5990.
[32] E. Khor, Chitosan: Fulfilling a Biomaterial's Promise, Elsevier, Oxford, UK, 2001.
[33] R. Jayakumar, K.P. Chennazhi, S. Srinivasan, S.V. Nair, T. Furuike, H. Tamura, Chitin scaffolds in tissue engineering, Int. J. Mol. Sci. 12 (2011) 1876−1987.
[34] S. Higashi, T. Yamamuro, T. Nakamura, Y. Ikada, S.H. Hyon, K. Jamshidi, Polymer-hydroxyapatite composites for biodegradable bone filler, Biomaterials 7 (1986) 183−187.
[35] M. Ito, *In vitro* properties of a chitosan-bonded hydroxyapatite bone-filling paste, Biomaterials 12 (1991) 41−45.
[36] A.C.A. Wan, E. Khor, G.W. Hastings, Hydroxyapatite modified chitin as potential hard tissue substitute material, J. Biomed. Mater. Res. 38 (1997) 235−241.
[37] H.W. Kim, H.E. Kim, V. Salihi, Stimulation of osteoblast responses to biomimetic nanocomposites of gelatin−hydroxyapatite for tissue engineering scaffolds, Biomaterials 26 (2005) 5221−5230.
[38] G. Wei, P. Ma, Structure and properties of nano-hydroxyapatite/polymer composite scaffolds for bone tissue engineering, Biomaterials 25 (2004) 4749−4757.
[39] M. Yamaguchi, H. Oishi, Y. Suketa, Stimulatory effect of zinc on bone formation in tissue culture, Biochem. Pharmacol. 22 (1987) 4007−4012.
[40] D. Chen, L. Waite, W.M. Pierce Jr, In vitro effects of zinc on markers of bone formation, Biol. Trace Elem. Res. 68 (1999) 225−234.
[41] A. Tripathi, S. Saravanan, S. Pattnaik, A. Moorthi, N.C. Partridge, N. Selvamurugan, Bio-composite scaffolds containing chitosan/nano-hydroxyapatite/nano-copper−zinc for bone tissue engineering, Int. J. Biol. Macromol. 50 (2012) 294−299.
[42] M. Peter, N. Ganesh, N. Selvamurugan, S.V. Nair, T. Furuike, H. Tamura, et al., Preparation and characterization of chitosan-gelatin/nanohydroxyapatite composite scaffolds for tissue engineering applications, Carbohydr. Polym 80 (2010) 687−694.
[43] M. Vogel, C. Voigt, U.M. Gross, C.M. Mai, In vivo comparison of bioactive glass particles in rabbits, Biomaterials 22 (2001) 357−362.
[44] W. Xia, J. Chang, Preparation and characterization of nano-bioactive-glasses (NBG) by a quick alkali-mediated sol−gel method, Mater. Lett. 61 (2007) 3251−3253.

[45] V. Karageorgiou, D. Kaplan, Porosity of 3D biomaterial scaffolds and osteogenesis, Biomaterials 26 (2005) 5474–5491.
[46] L.F. Peltier, The use of plaster of Paris to fill defects in bone, Clin. Orthopedics 21 (1961) 1–29.
[47] M.P. Sidqui, P. Collin, C. Vitte, N. Forest, Osteoblast adherence and resorption activity of isolated osteoclasts on calcium sulphate hemihydrate, Biomaterials 16 (1995) 1327–1332.
[48] J. Bateman, G. Intini, J. Margarone III, S. Goodloe III, P. Bush, S.E. Lynch, et al., Platelet-derived growth factor enhancement of two alloplastic bone matrices, J. Periodontol. 76 (2005) 1833–1841.
[49] Y.B. Park, K. Mohan, A. Al-Sanousi, B. Almaghrabi, R.J. Genco, M.T. Swihart, et al., Synthesis and characterization of nanocrystalline calcium sulfate for use in osseous regeneration, Biomed. Mater. 6 (2011) 055007.
[50] B. Salvadori, G. Capitani, M. Mellini, L. Dei, A novel method to prepare inorganic water-soluble nanocrystals, J. Colloid Interface Sci. 298 (2006) 487–490.
[51] Q. Zhang, Q.F. He, T.H. Zhang, X.L. Yu, Q. Liu, F.L. Deng, Improvement in the delivery system of bone morphogenetic protein-2: a new approach to promote bone formation, Biomed. Mater. 7 (2012) 045002.
[52] J.O. Hollinger, C.E. Hart, S.N. Hirsch, S. Lynch, G.E. Friedlaender, Recombinant human platelet derived growth factor: biology and clinical applications, J. Bone Joint Surg. Am. 80 (2008) 48–54.
[53] D.H.R. Kempen, L. Lu, T.E. Hefferan, L.B. Creemers, A. Maran, K.L. Classic, et al., Retention of in vitro and in vivo BMP-2 bioactivities in sustained delivery vehicles for bone tissue engineering, Biomaterials 29 (2008) 3245–3252.
[54] H. Uludag, T. Gao, T.J. Porter, W. Friess, J.M. Wozney, Delivery systems for BMPs: factors contributing to protein retention at an application site, J. Bone Joint Surg. Am. 83A (2001) S128–S135.
[55] M. Nakashima, A. Reddi, The application of bone morphogenetic proteins to dental tissue engineering, Nat. Biotechnol. 21 (2003) 1025–1032.
[56] H. Perinpanayagam, T. Martin, V. Mithal, M. Dahman, N. Marzec, J. Lampasso, et al., Alveolar bone osteoblast differentiation and Runx2/Cbfa1 expression, Arch. Oral Biol. 51 (2006) 406–415.
[57] M.A. Rauschmann, T.A. Wichelhaus, V. Stirnal, E. Dingeldein, L. Zichner, R. Schnettler, Nanocrystalline hydroxyapatite and calcium sulphate as biodegradable composite carrier material for local delivery of antibiotics in bone infections, Biomaterials 26 (2005) 2677–2684.
[58] A.D. Augst, H.J. Kong, D.I. Mooney, Alginate hydrogels as biomaterials, Macromol. Biosci. 6 (2006) 623–633.
[59] X. Qi, J. Ye, Y. Wang, Alginate/poly (lactic-*co*-glycolic acid)/calcium phosphate cement scaffold with oriented pore structure for bone tissue engineering, J. Biomed. Mater. Res. 89A (2009) 980–987.
[60] H.-R. Lin, Y.-J. Yeh, Porous alginate/hydroxyapatite composite scaffolds for bone tissue engineering: preparation, characterization, and *in vitro* studies, J. Biomed. Mater. Res. 71B (2004) 52–65.
[61] Z. Mazor, R. Horowitz, J. Ricci, H. Alexander, I. Chesnoiu-Matei, S. Mamidwar, The use of novel nanocrystalline calcium sulfate for bone regeneration in extraction socket, J. Implant Adv. Clin. Dent. 3 (2011) 39–49.
[62] R. O'Keefe, J. Mao, Bone tissue engineering and regeneration: from discovery to the clinic—an overview, Tissue Eng. Part B 17 (2011) 389–392.
[63] C.H. Evans, Barriers to the clinical translation of orthopedic tissue engineering, Tissue Eng. Part B 17 (2011) 437–441.

CHAPTER

Biomimetics Using Nanotechnology/Nanoparticles in Dental Tissue Regeneration

20

Shengbin Huang[a,b], Tingting Wu[a,b] and Haiyang Yu[a,b]

[a]*State Key Laboratory of Oral Diseases, Chengdu, People's Republic of China*

[b]*West China Hospital of Stomatology, Sichuan University, Chengdu, People's Republic of China*

CHAPTER OUTLINE

20.1 Introduction

Tissue engineering is a multidisciplinary field by nature bringing together biology, engineering, and clinical sciences with the goal of generating new tissues and organs [1]. This field builds on the interface between material science and biocompatibility, and integrates cells, natural or synthetic scaffolds, and specific signals to create new tissues. Nowadays, regenerative dentistry is viewed synonymous to tissue engineering in dentistry. Continuous research is going on in this field at both preclinical and clinical levels; remarkable and promising results are also being obtained. However, the high demand for esthetics of dental tissue structures and the complex atmosphere pose special challenges in this area [2]. Nanotechnology is described as science and techniques which control and manipulate matter at a nanometric level. It has progressed tremendously in the last few decades. Nanomaterials are materials with basic structural units, grains, particles, fibers or other constituent components smaller than 100 nm in at least one dimension [3] and have great potential in disease prevention, diagnosis, and treatment. To date, advances in this field have led to significant

Nanobiomaterials in Clinical Dentistry.

progress in tissue repair and regeneration. With the help of nanotechnology it is possible to interact with cell components, to manipulate cell proliferation and differentiation, and in the production and organization of extracellular matrices. New nanomaterials are leading to a range of emerging dental treatments that utilize more biomimetic materials that closely duplicate natural tooth structure. The uses of nanostructures that will work in harmony with the body's own regenerative processes are moving into dental clinical practice. In this chapter, we will focus on the recent progress of the applications of nanotechnology in dental tissue regeneration, the contributions of these new technologies in the development of innovative biomimetic materials and their potential clinical applications.

20.2 Nanotechnology for craniofacial bone and cartilage tissue engineering

Craniofacial bone defects secondary to trauma, infection, cancer, and congenital disorders represent a major health problem. Current strategies aimed at replacing bony defects include the utilization of autografts, allografts, and synthetic biomaterials. Despite the fact that these substitutes restore stability and function to a reasonable degree, however, they still have limitations. Tissue engineering is considered as an optimal approach for various tissue repairs including craniofacial defect repair [4]. Biomaterials, acting as scaffolds for tissue engineering, play an essential role in the process of tissue regeneration. Moreover, incorporation of nanotechnology into scaffold design and manufacture will further enhance the quality and function of regenerated tissues. Due to the biomimetic features and excellent physicochemical properties, nanomaterials have been shown to improve adhesion, proliferation, and differentiation of cells, which would finally guide tissue regeneration (Figure 20.1) [5].

Within the craniofacial tissue engineering field, the major types of materials used are natural and synthetic polymers, ceramics, composite materials, and electrospun nanofibers. Synthetic and natural polymers are excellent candidates for bone/cartilage tissue engineering application due to their biodegradability and ease of fabrication. Numerous studies have shown successful bone formation with nanofibrous synthetic and natural polymer scaffolds such as electrospun polycaprolactone [6], poly(lactic-*co*-glycolic acid) (PLGA) [7], polyvinyl alcohol/type I collagen blend [8], and many others [9]. Nanofibrous scaffolds would be an advantageous microenvironment for bone tissue formation by mimicking the type I collagen fibers that are a major component of bone and provide a cellular platform for bone formation [10].

Nanophase ceramics are popular as bone substitutes, coatings, and filler materials due to their dimensional similarity to bone/cartilage tissue and unique surface properties including surface topography, surface chemistry, surface wettability, and surface energy. Numerous in vitro studies have revealed that nano-hydroxyapatite (HA) significantly enhances osteoblast adhesion and function [11–13]. In vivo studies have also demonstrated that nanostructured HA can improve cell attachment and mineralization suggesting that nanosized HA may be a better candidate for clinical use in terms of bioactivity [14–19]. In general, nanostructured ceramics offer much improved performances compared to their larger particle-sized counterparts due to their huge surface-to-volume

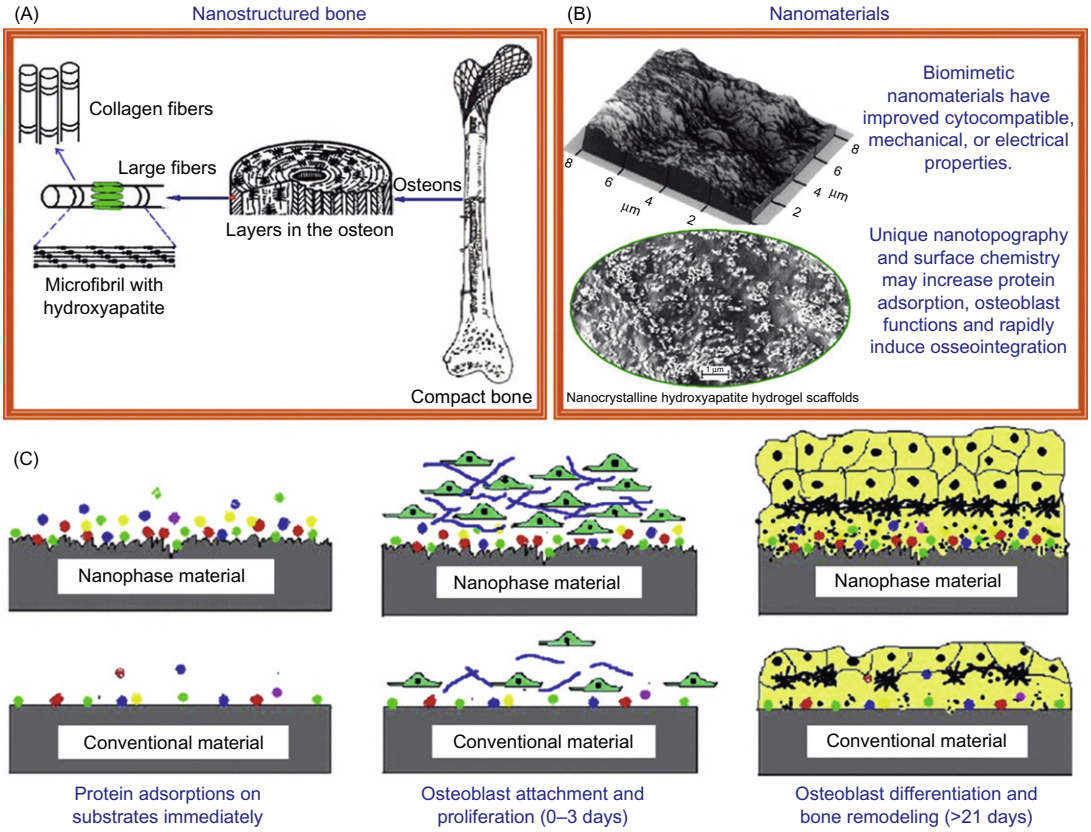

FIGURE 20.1

The biomimetic advantages of nanomaterials. (A) The nanostructured hierarchal self-assembly of bone. (B) Nanophase titanium (top, the atomic force microscopy image) and nanocrystalline HA/HRN hydrogel scaffold (bottom, the SEM image). (C) Schematic illustration of the mechanism by which nanomaterials may be superior to conventional materials for bone regeneration. The bioactive surfaces of nanomaterials mimic those of natural bones to promote greater amounts of protein adsorption and efficiently stimulate more new bone formation than conventional materials.

Adapted from Ref. [5]. Reprinted with permission from Elsevier.

ratio and unusual chemical synergistic effects. Nanosized HA is expected to have a better bioactivity than coarser crystals [20–22]. Similar tendencies have been reported for other nanoceramics including alumina, zinc oxide, and titania. Osteoblast adhesion increased by 146% and 200% on nanophase zinc oxide (23 nm) and titania (32 nm) compared to microphase zinc oxide (4.9 μm) and titania (4.1 μm), respectively [23,24].

Commercial formulations (nano-bone) have also been developed and extensively used in clinic. nanOss® bone void filler from Angstrom Medica Inc. is considered as the first nanotechnological medical device receiving clearance by the US Food and Drug Administration (FDA) in 2005.

Its major composition is calcium orthophosphate nanoparticles, which mimics the nanostructure, composition, and performance of human bone. nanOss® is remodeled over time into human bone with applications in sports medicine, trauma, spine, and general orthopedics [25]. Ostim® (Osartis GmbH & Co. KG, Obernburg, Germany) is another popular commercial formulation. It is a ready-to-use injectable paste that received CE (Conformite Europeans) approval in 2002. Ostim® is a suspension of synthetic nano-HA in water, prepared by a wet chemical reaction [26]. Ostim® can be used to treat metaphyseal fracture and cysts, alveolar ridge augmentation, osteotomies, etc. [25,27–37].

Although inorganic and organic substances show potential to promote bone regeneration, they have inferior mechanical properties. Bone is composed of both collagen (mainly type I) and mineralized substance (mainly HA), therefore, a biomimetic scaffold should contain both inorganic and organic components. Kim et al. [38] demonstrated that a rapid screening tool for potential biomimetic analogs of collagen mineralization and the nanoscopic protocol could accelerate the application of Collagen-HA in bone regeneration. Recently, another study showed that chondroitin sulfate (CS) combined with nano-HA exhibited the potential to mimick native bone extracellular matrix (ECM) to promote bone regeneration [39]. These findings show that tissue engineering based on the nanotechnology can become a breakthrough approach to reconstructing bone deformities in a more effective and less traumatic way.

As it relates to craniofacial reconstruction, the design of polymer scaffolds with defined mechanical and degradative properties has opened a new avenue to cartilage reconstruction. Cartilage destruction is associated with trauma and with degenerative articular cartilage destruction at the temporomandibular joint. The limited capacity of cartilaginous tissue to regenerate and the lack of inductive molecules have focused interest among researchers and manufacturers in developing engineered cartilage. Cartilage itself is avascular and has relatively limited ability for intrinsic repair. A pilot clinical study showed that a newly developed biomimetic osteochondral scaffold with nucleating collagen fibrils along with HA nanoparticles could be used to repair femoral condyle defects of knee joints. Magnetic resonance imaging (MRI) demonstrated good short-term stability of the scaffold. Histologic analysis showed the formation of subchondral bone without the presence of biomaterials. This result is encouraging and should be a cue for TMJ defects repair [40]. Gene therapy approaches based on nanotechnology are promising for growth factor signaling mediated cartilage regeneration. As shown by Erisken et al. [41], osteochondral tissue regeneration could be induced with nanofibrous scaffolds fabricated with two different layers that were respectively conjugated with insulin (for chondrogenic differentiation) or with A-glycerophosphate (for osteogenic differentiation). After being seeded on this mimetic scaffold, adipose-derived stem cells could be induced to chondrogenic cells at insulin-rich location and to osteogenic cells at a A-glycerophosphate-released region. This approach may also be applied for regenerating complex craniofacial tissues such as TMJ [41].

20.3 Nanotechnology for periodontal regeneration

Periodontal disease leads to destruction of the periodontium: alveolar bone, cementum, the periodontal ligament, and gingiva. Effective treatment for periodontal tissue regeneration

plays an important role in the normal function of craniofacial and systemic system. However, a logical various conventional therapies (open flap debridement (OFD), guided tissue regeneration (GTR), and bone replacement grafts, provided either alone or in a combination) for periodontal tissue regeneration have shown limited and variable clinical outcomes (Figure 20.2) [42].

To accelerate clinical translation, there is an ongoing need to develop therapeutics based on endogenous regenerative technology (ERT), which can stimulate latent self-repair mechanisms in patients and harness the host's innate capacity for regeneration. ERT in periodontics applies the patient's own regenerative "tool," i.e. patient-derived growth factors and fibrin scaffolds, sometimes in association with commercialized products (e.g., Emdogain and Bio-OSS), to create a materials niche in an injured site where the progenitor/stem cells from neighboring tissues can be recruited for in situ periodontal regeneration. The selection and design of materials influence therapeutic potential and the number and invasiveness of the associated clinical procedures [42]. This has shifted the focus from the attempt to recreate tissue replacement/constructs ex vivo to the development of biofunctionalized biomaterials that incorporate and release regulatory signal in a precise and near-physiological fashion to achieve in situ regeneration. Therefore, certain artificially designed scaffold features such as porosity, pore size, and interpore connectivity are necessary for optimal tissue engineering applications (accelerated/expedited tissue regeneration) no matter which biomaterial scaffold is proposed [43].

In this regard, a biomimetic scaffold mimicking certain features such as nanoscale topography and biological cues of natural ECM is advantageous for facilitating cell recruitment, seeding, adhesion, proliferation, differentiation, and neo tissue genesis [42]. Thus, as mentioned above, biomimetic features and excellent physicochemical properties of nanomaterials play a key role in stimulating cell growth and guiding tissue regeneration. Nanotechnology is expected to play an important role in the design and application of biofunctionalized biomaterials in the periodontal tissue repair process. For example, alginate/nano bioactive glass ceramic (nBGC) (synthesis of nBGC particles) composite scaffolds were successfully fabricated using lyophilization technique and characterized. The scaffolds were found to have characteristic materialistic and biological properties essential to facilitate periodontal regeneration [44]. The composite scaffolds had a pore size of about 100−300 μm, controlled porosity and swelling ability, limited degradation and enhanced biomineralization, due to the presence of nBGC in the alginate scaffold. Incorporation of nBGC did not alter the viability of MG-63 and hPDLF cells and also helped to attain good protein adsorption, cell attachment, and cell proliferation onto the scaffolds. The hPDLF cells also showed distinct osteoblast-like behavior with enhanced alkaline phosphatase activity. All these results suggested that alginate/nBGC composite scaffold serves as an appropriate bioactive matrix for periodontal tissue regeneration, thus indicating signs of another successive outbreak in the field of periodontal tissue engineering. In another study, Yang et al. [45] developed an electrospun nano-apatite/PCL composite membrane for GTR/GBR application, the results showed that the electrospun membrane incorporating nano-apatite is strong, enhances bioactivity and supports osteoblast-like cell proliferation and differentiation. The membrane system can be used as a prototype for the further development of an optimal membrane for clinical use.

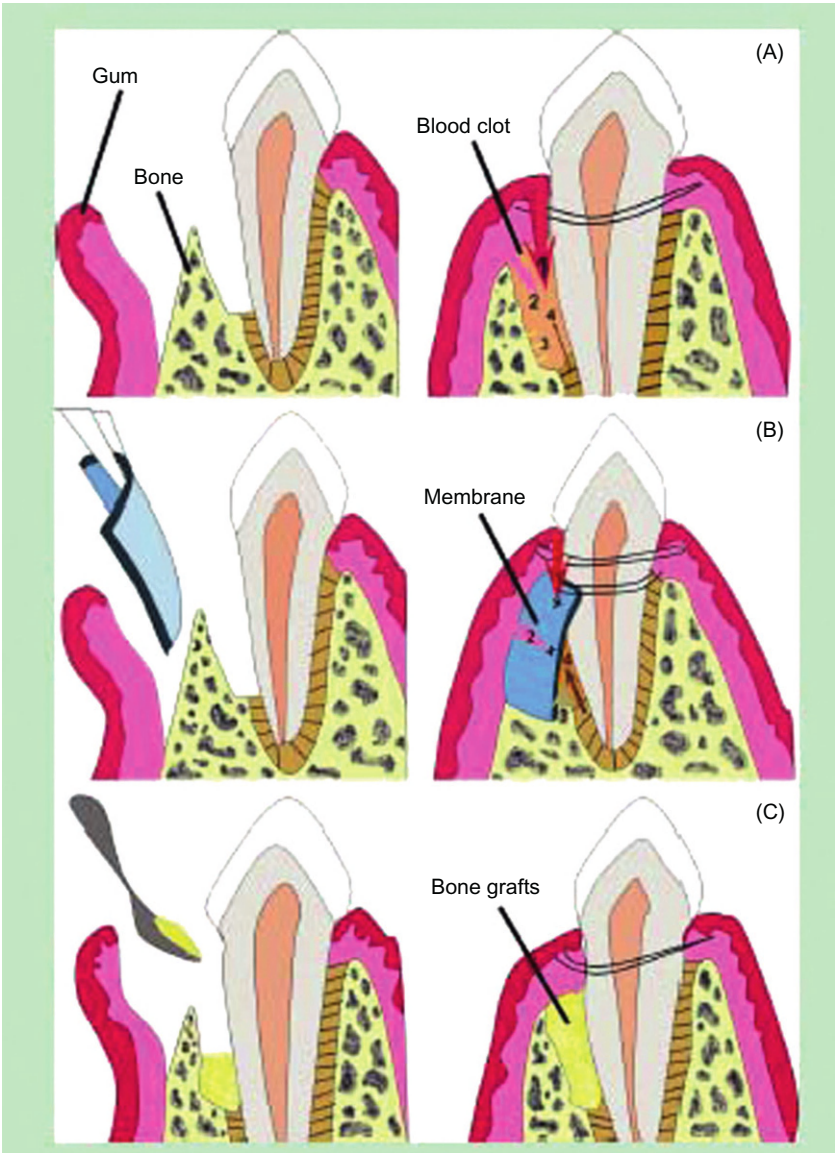

FIGURE 20.2

Schematic diagrams of several techniques commonly used in periodontal surgery. (A) OFD procedure involves the periodontal surgeon lifting the gum away from the tooth and surrounding bone, providing increased access for scaling and root planning. However, periodontal defects, if left empty after OFD, fill with the first cells to reach the area, i.e., epithelial cells (1) and fibroblasts (2), after cell proliferation, which generates core of fibro-epithelial tissues that attach to the root surface, hence bone (3) and periodontal

20.4 Nanotechnology for tooth regeneration

Tooth regeneration has long been the dental profession's aspiration; however, the combination of tissue bioengineering along with the development of genetically designed trigger nanoparticles, which are biomimetic with mineralized tissues, have begun to bear fruit in the manufacturing of in vitro teeth.

Mao and coworkers, the pioneer researchers in the dental regeneration, suggested that the regeneration of teeth can be divided into several specific areas as follows [46]:

1. Regeneration or de novo formation of an entire, anatomically correct tooth;
2. Regeneration of the root;
3. Regeneration of dental pulp;
4. Regeneration of dentin that may either act as reparative dentin to seal off an exposed pulp chamber or as a replacement of current synthetic materials;
5. Regeneration of cementum as a part of periodontium regeneration or for loss of cementum and/or dentin resulting from orthodontic tooth movement;
6. Regeneration of periodontium including cementum, periodontal ligament, and alveolar bone;
7. Regeneration or synthesis of enamel-like structures that may be used as biological substitute for enamel;
8. Remineralization of enamel and dentin.

For tooth regeneration, biomaterials have served primarily as a scaffold for (1) transplanted stem cells and/or (2) recruitment of endogenous stem cells. It is indispensable for the regeneration of tooth root, tooth crown, dental pulp, or an entire tooth. Nanomaterials, which can mimic surface properties of natural tissues, have been highlighted as promising candidates for improving traditional dental tissue engineering materials. The various forms of tooth tissue engineering related to nanotechnology and nanomaterials are described in the following sections.

20.4.1 Nanomaterials in biomimetic enamel regeneration

Enamel is the hardest material formed by vertebrates and is the most highly mineralized skeletal tissue present in the body. Mature enamel is composed of 95–97% carbonated HA by weight with less than 1% organic material. Mature dental enamel has a complex form, providing a striking example of a highly mineralized structure exquisitely adapted to absorb essential mechanical and abrasive stresses throughout the lifetime of the organism (Figure 20.3) [47].

◀ ligament (3) regeneration are cumbered. (B) GTR is a surgical procedure that utilizes a barrier membrane which is placed under the gum and over the remaining bone to prevent epithelial down-growth (1) and fibroblast trans-growth (2) into the wound space, thereby maintaining a space for true periodontal tissue regeneration (3 and 4). (C) The use of bone grafts is a surgical procedure that replaces missing bone with materials from the patient's own body (autogenous bone) or an artificial, synthetic, or natural substitute. Bone growth may be stimulated by the grafts and new bone fills the defect which may provide support for the tooth.

Adapted from Ref. [42]. Reprinted with permission from Elsevier.

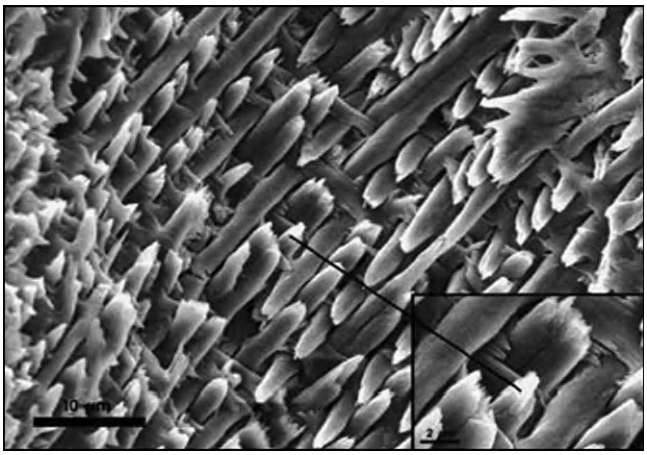

FIGURE 20.3

The organization of dental enamel. Scanning electron micrograph of the surface of an acid-etched ground section of mature mouse incisal dental enamel. Ordered arrays of enamel prisms are each constructed of parallel bundles of carbonated HA enamel crystallites.

Adapted from Ref. [47]. Reprinted with permission from Elsevier.

However, enamel cannot heal itself by a cellular repair as enamel is both acellular and avascular. It loses mineral substances due to caries, trauma, and erosion. Restorations of damaged tooth tissues with artificial materials represent the traditional therapeutic solutions. Although many sophisticated materials are now available for restoration, their use is not yet completely satisfactory. A combination of tissue bioengineering with the development of genetically designed trigger nanoparticles which are biomimetic with mineralized tissues, have begun to bear fruit in the manufacturing of in vitro teeth tissue even the whole teeth. For example the amelogenin gene has been manipulated to adhere to HA nanoparticles. When these are directly shot to pluripotential cells encapsulated in nanohydrogels they begin to work on the formation of the enamel tissue [48]. The previous attempts to engineer enamel focused mainly on chemical synthesis. Chen et al. [49] synthesized and modified the HA nanorod surface with monolayers of surfactants to create specific surface characteristics that allowed the nanorods to self-assemble into an enamel prism-like structure at a water/air interface. The size of the synthetic HA nanorods can be controlled, and synthesized nanorods were similar in size to both human and rat enamel crystals. In other studies, prism-like structures, consisting of fluoroapatite crystals similar to the dimensions of those seen in human enamel have been synthesized using hydrothermal method [50]. This method is a widely adopted nanotechnology to create nanorods, nanowires, and whiskers and has already been shown to be an effective way to create different kinds of nanomaterials [51–53]. However, the majority of these synthesis methods were developed using high temperature, high pressure, and extremely acidic pH or in the presence of a concentrated solution of surfactants. It is generally accepted that the biomimetic synthesis of enamel-like apatite structures under physiological condition is an alternative restorative pathway. Recently, Li et al. [54] reported that a bioinspired cooperative effect of an amino acid (glutamic acid, Glu) and nano-apatite particles can result in the regeneration of

enamel-like structure under physiological conditions. Importantly, the mechanical characteristics of the repaired enamel are well maintained by using this feasible enamel remodel. These successful approaches of enamel regeneration implies a potential of material-inspired strategy of nano assembling in biomedical application and opens the possibility that in the future dental practice might drastically change, allowing the manufacturing of teeth in the dental practice office.

20.4.2 Nanomaterial in enamel and dentine remineralization

The prevention of tooth decay and the treatment of lesions and cavities are ongoing challenges in dentistry. In recent years, biomimetic approaches have been used to develop nanomaterials for the remineralization of early enamel lesions [55]. Nowadays, nano-HA is widely studied as a biomimetic material for the reconstruction of tooth enamel suffering from mineral loss and as an effective anticaries agent because of its unique potential for remineralization [56–63]. Our previous studies demonstrated that nano-HA has the potential to remineralize initial enamel caries lesions under dynamic pH cycling conditions. In addition, a concentration of 10% nano-HA may be optimal for remineralization of early enamel caries in vitro [64]. In further research, however we found that nano-HA helped mineral deposition predominantly in the outer layer of the lesion and only had a limited capacity to reduce lesion depth. Nevertheless, the remineralization effect of nano-HA increased significantly when the pH was less than 7.0 [65]. Further, our research showed that there was a significant synergistic effect of combined GCE and nano-HA treatment on promoting the remineralization of initial enamel lesion [66]. When GCE was added with nano-HA, significant higher volume percent mineral was present in the body of lesion, it would not completely inhibit the deposition of nano-HA on the out layer of lesion in the remineralization process, so full remineralization on the initial enamel lesion was obtained. The SEM images showed that the crystals of surface layer in the GCE + nano-HA group were arranged regularly and densely uniform structure was formed (Figure 20.4E), whereas, irregularly arranged crystals were present in the nano-HA group (Figure 20.4C).

Accumulated evidence has demonstrated that the average size of the calcium phosphate crystals play an essential role in the formation of hard tissues and has a significant influence on its intrinsic properties, including solubility and biocompatibility [67,68]. An in vitro study demonstrated that evenly sized nano-apatite particles (20-nm-sized HA and building blocks of biological apatite of dental enamel) could simultaneously repair and prevent initial erosive lesions in enamel compared with conventional HA crystals that are hundreds of nanometers in length [62]. Our in vitro study also demonstrated that nano-HA provides better remineralization than micro-HA. Generally, these studies suggest that analogs of nanobuilding blocks of biominerals should be highlighted in the entire subject of biomineralization.

In summary, the remineralization effect of nano-HA on caries lesions is clear, but the mechanism of action is still open to debate. A number of researchers have proposed that nano-HA promotes remineralization through excellent deposition onto etched enamel [62] or by depositing apatite nanoparticles in the defects on demineralized enamel. Other researchers, however, have suggested that nano-HA acts to deliver a calcium source to the mouth, which can increase oral calcium levels, and has the potential to limit acid challenges by reducing enamel demineralization while promoting enamel remineralization [56–58]. Based on these theories combined with our current results, we propose that the mechanism of remineralization is that HA acts as a calcium phosphate

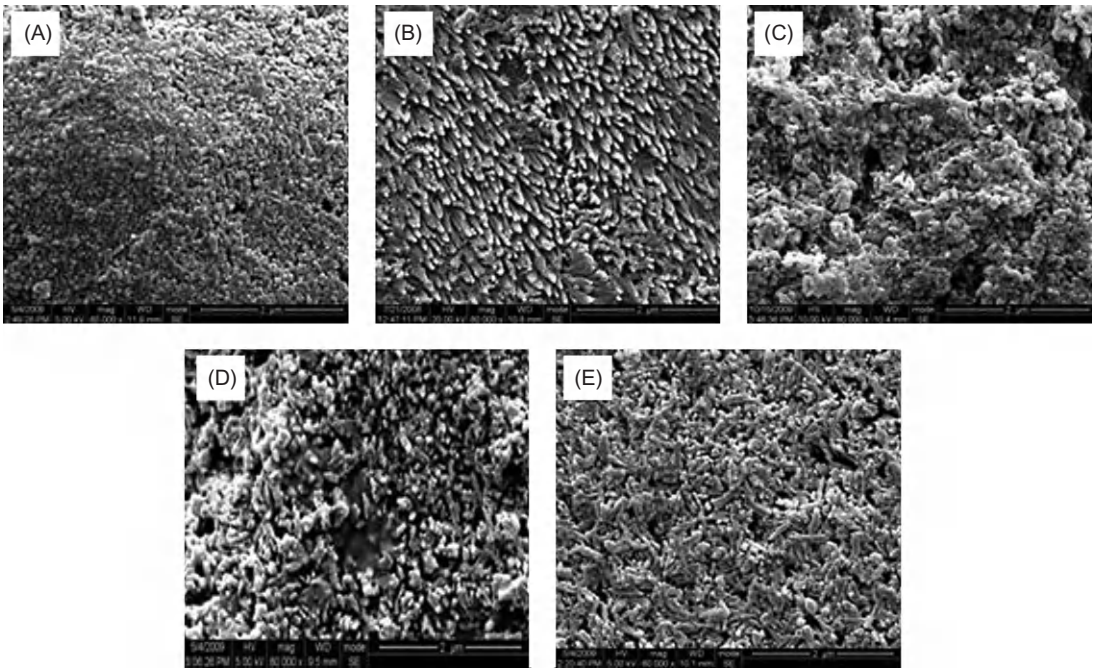

FIGURE 20.4

SEM images of the enamel surfaces in different groups (60,000×). Many micropores and honeycomb structures were apparently on enamel surface in DDW group (B), however, after application of nano-HA, acicular crystals had sedimented on the lesion surface and the cavities and microspores significantly decreased, meanwhile, the surface of the demineralized enamel appeared to be covered by crystal, arranged in a thick and homogenous apatite layer (C). Some fingerlike crystals disorderly distributed on the surface of enamel after being treated with GCE, a honeycomb structure still remained in some regions on the surface of lesion (D). In GCE + nano-HA group, the surface morphology was similarly to that in the nano-HA group, however, the crystals were arranged regularly and dense layer was also obtained after addition of GCE (E). Different sized globules were formed on the lesion surface in the NaF group (A).

reservoir, helping to maintain a state of supersaturation with respect to enamel minerals, thereby depressing enamel demineralization and enhancing remineralization; this is in accordance with the classic paradigm of "top-down" ion-mediated crystalline growth to account for the intricate biomineralization strategies identified in nature [69]. Nano-HA, however, shows promising remineralization efficacy on enamel lesions in view of its unique characteristics, including excellent deposition properties, which are in good agreement with the "bottom-up" concept of particle-mediated nanoprecursor assembly and mesocrystalline transformation in the biomineralization process [70].

Other biomimetic approaches for remineralization of initial submicrometer enamel erosions and lesions are based on nanosized casein phosphopeptide-amorphous calcium phosphate (CPP-ACP). The CPP-ACP prevents demineralization and promotes remineralization of initial enamel lesions in laboratory, animal, human experiments and in randomized, controlled clinical trials [71–79].

The CPP-ACP literature has been reviewed by several authors [80–82] with the most recent being a systematic meta-analysis concluding that there is sufficient clinical evidence demonstrating enamel remineralization and caries prevention by regular use of products containing CPP-ACP (82). The CPPs stabilize calcium and phosphate ions through the formation of amorphous nanocomplexes, which would be expected to enter the porosities of an enamel subsurface lesion and diffuse down concentration gradients into the body of the subsurface lesion. Once present in the enamel subsurface lesion, the CPP-ACP would release the weakly bound calcium and phosphate ions which then deposits into crystal voids [83]. Further, the CPP-ACP nanocomplexes have also been demonstrated to bind onto the tooth surface and into supragingival plaque to significantly increase the level of bioavailable calcium and phosphate ion [84]. In all of the remineralization technologies currently available commercially, the CPP-ACP and CPP-ACFP technology has the most evidence to support its use.

Except for the nano-HA and CPP-ACP, other nanosized calcium phosphates have also been considered as remineralization agents due to their unique properties. For nanodimensional DCPA, decreasing of DCPA particle dimensions were found to increase the Ca^{2+} and PO_4^{3-} ions release from DCPA-based biocomposites. Nano-DCPA-based biocomposites, possessing both a high strength and good release of Ca^{2+} and PO_4^{3-} ions, may therefore provide the needed and unique combination of stress-bearing and caries-inhibiting capabilities suitable for dental applications [85]. A positive influence of adding nanodimensional β-TCP against acid demineralization and promoted remineralization of enamel surface was also detected [86]. In another in vitro study, nanosized amorphous calcium carbonate particles applied twice a day for 20 days promoted remineralization of artificial white-spot enamel lesions [87].

Dentine remineralization is clinically significant for the prevention and treatment of dentine caries, root caries, and dentine hypersensitivity. Dentine remineralization is, however, more difficult than enamel remineralization due to the abundant presence of organic matrix in dentine. An accepted notion is that dentine remineralization occurs neither by the spontaneous precipitation nor by the nucleation of mineral on the organic matrix (mainly type I collagen) but by the growth of residual inorganic crystals in the lesions [88]. Reconstitution and remineralization of dentine using nanosized bioactive glass particles and betatricalcium phosphate was also tested in vitro, however, the mechanical properties of original dentine could not be reproduced [89,90]. Fortunately, the biomimetic remineralization scheme provides a proof of concept for the adoption of nanotechnology as an alternative strategy to remineralization of dentine. Metastable ACP nanoprecursors were generated when polyacrylic acid was included in the phosphate-containing fluid. The nanoprecursors were attracted to the acid-demineralized collagen matrix and transformed into polyelectrolyte-stabilized apatite nanocrystals that assembled along the microfibrils (intrabrillar remineralization) and surface of the collagen fibrils (interfibrillar remineralization) to achieve dentine remineralization [91]. The results revealed that guided tissue remineralization based on nanotechnology is potentially useful in the remineralization of acid-etched dentine that is incompletely infiltrated by dentine adhesives, and partially demineralized caries-affected dentine.

20.4.3 Nanomaterial in dentin–pulp complex regeneration

Restorative dentistry is looking for techniques and materials to regenerate the dentin–pulp complex in a biological manner. This showed the great potential in the treatment of our most common oral

health problem and cavities. There is evidence suggesting that odontoblasts (cells that produce dentin), dental pulp stem cells (DPSC) and stem cells from human exfoliated deciduous teeth (SHED) are able to produce pulp/dentin-like tissues when seeded on specific condition or scaffolds [92–95]. In the process, advanced biomimetic scaffolding materials are versatile enough to provide a suitable 3D network to accommodate these cells and guide their growth, organization, and differentiation. One important step toward regenerative endodontics was achieved when SHED mixed with nanofiber peptide scaffold and injected into full-length root canals were able to generate a dental pulp. Figure 20.5 shows the presence of a pulp tissue fulfilling the hollow passageway of the root canal, with proliferative activity and blood network maturity comparable to the ones observed in a young human dental pulp [96].

Another in vitro study showed that peptide–amphiphile molecules provide a nanostructured, cell-responsive matrix that is specifically conducive to dental stem cells. The SHED and DPSC seeded in PA hydrogels show difference in morphology, proliferation, and differentiation behavior.

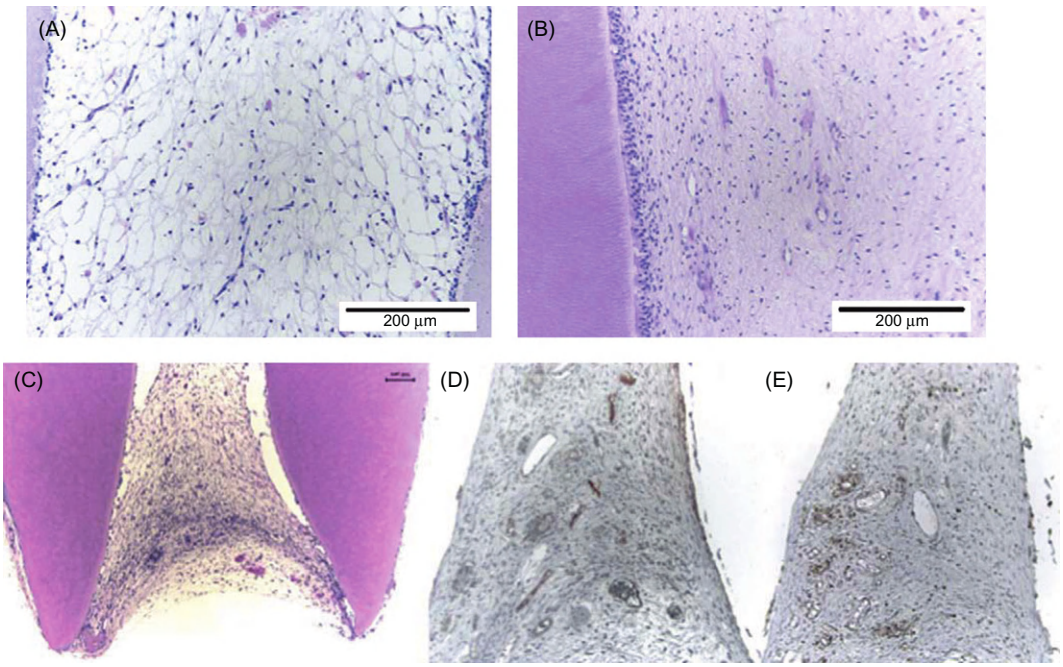

FIGURE 20.5

Dental pulp tissue engineered for 35 days inside root canal using SHED cells (A) and natural dental pulp from premolar (B). It is possible to observe the formation of a healthy tissue without inflammatory signs and a densification of odontoblast-like cell along dentin walls in the SHED originated tissue similar to the control. The engineered tissue occupies the whole apical portion (C) and immunohistochemistry with proliferating cell nuclear activity and factor VIII show a proliferative tissue with well-established and mature blood network (D) and (E).

Adapted from Ref. [96]. Reprinted with permission from Elsevier.

SHED seem to be a suitable tool for soft tissue regeneration, such as dental pulp, whereas DPSC might be useful for engineering mineralized tissues like dentin [97]. Further development and successful application of these strategies to regenerate dentin and dental pulp could one day revolutionize the treatment of our most common oral health problem and cavities.

20.5 Conclusions

Despite the challenges in dental tissue regeneration that lie ahead, significant evidence exists to support the premise that recent advances in nanotechnology, acting as biomimetic tools, show great potential to overcome the challenges and promise for improved the dental tissue regeneration. Nanomaterials tailored for engineering dental tissues are continually being introduced and yield numerous clinical dental benefits. These include improved treatments for periodontal defects, enhanced maxillary and mandibular bone regeneration, perhaps more biological methods to repair teeth after carious damage and possibly even regrowing lost teeth. In the near future, advances in bioengineering research will lead to the wide application of the regenerative dentistry into general dental practice to produce wonderful treatments and dramatically improve patients' quality of life.

References

[1] R. Langer, J.P. Vacanti, Tissue engineering, Science 260 (1993) 920−926.
[2] S. Yildirim, S.Y. Fu, K. Kim, H. Zhou, C.H. Lee, A. Li, et al., Tooth regeneration: a revolution in stomatology and evolution in regenerative medicine, Int. J. Oral Sci. 3 (2011) 107−116.
[3] R.W. Siegel, G.E. Fougere, Mechanical properties of nanophase metals, Nanostruct. Mater. 6 (1995) 205.
[4] S.M. Warren, K.D. Fong, C.M. Chen, E.G. Loboa, C.M. Cowan, H.P. Lorenz, et al., Tools and techniques for craniofacial tissue engineering, Tissue Eng. 9 (2003) 187−200.
[5] L.J. Zhang, T.J. Webster, Nanotechnology and nanomaterials: promises for improved tissue regeneration, Nano Today 4 (2009) 66−80.
[6] H. Yoshimoto, Y. Shin, H. Terai, J. Vacanti., A biodegradable nanofiber scaffold by electrospinning and its potential for bone tissue engineering, Biomaterials 24 (2003) 2077−2082.
[7] M. Jose, V. Thomas, Y. Xu, S. Bellis, E. Nyairo, D. Dean, Aligned bioactive multi-component nanofibrous nanocomposite scaffolds for bone tissue engineering, Macromol. Biosci. 10 (2010) 433−444.
[8] A. Asran, S. Henning, G. Michler, Polyvinyl alcohol-collagen-hydroxyapatite biocomposite nanofibrous scaffold: mimicking the key features of natural bone at the nanoscale level, Polymer 51 (2010) 868−876.
[9] J. Venugopal, M. Prabhakaran, Y. Zhang, S. Low, A.S. Choon, S. Ramakrishna, Biomimetic hydroxyapatite-containing composite nanofibrous substrates for bone tissue engineering, Philos Transact. A Math Phys. Eng. Sci. 368 (2010) 2065−2081.
[10] M.J. Gupte, P.X. Ma, Nanofibrous scaffolds for dental and craniofacial applications, J. Dent. Res. 91 (2012) 227−234.
[11] T.J. Webster, C. Ergun, R.H. Doremus, R.W. Siegel, R. Bizios, Specific proteins mediate enhanced osteoblast adhesion on nanophase ceramics, J. Biomed. Mater. Res. 51 (2000) 475−483.
[12] T.J. Webster, C. Ergun, R.H. Doremus, R.W. Seigel, R. Bizios, Enhanced osteoclast-like cell functions on nanophase ceramics, Biomaterials 22 (2001) 1327−1333.

[13] S.P. Nukavarapu, S.G. Kumbar, J.L. Brown, N.R. Krogman, A.L. Weikel, M.D. Hindenlang, et al., Polyphosphazene/nano-hydroxyapatite composite microsphere scaffolds for bone tissue engineering, Biomacromolecules 9 (2008) 1818−1825.
[14] M. Sato, M.A. Sambito, A. Aslani, N.M. Kalkhoran, E.B. Slamovich, T.J. Webster, Increased osteoblast functions on undoped and yttrium-doped nanocrystalline hydroxyapatite coatings on titanium, Biomaterials 27 (2006) 2358−2369.
[15] E.S. Thian, J. Huang, S.M. Best, Z.H. Barber, R.A. Brooks, N. Rushton, et al., The response of osteoblasts to nanocrystalline silicon-substituted hydroxyapatite thin films, Biomaterials 27 (2006) 2692−2698.
[16] K.U. Lewandrowski, S.P. Bondre, D.L. Wise, D.J. Trantolo, Enhanced bioactivity of a poly(propylene fumarate) bone graft substitute by augmentation with nano-hydroxyapatite, Biomed. Mater. Eng. 13 (2003) 115−124.
[17] E.S. Thian, Z. Ahmad, J. Huang, M.J. Edirisinghe, S.N. Jayasinghe, D.C. Ireland, et al., Bioactivity of nanoapatite produced by electrohydrodynamic atomization, J. Bionanosci. 1 (2007) 60−63.
[18] S. Pezzatini, R. Solito, L. Morbidelli, S. Lamponi, E. Boanini, A. Bigi, et al., The effect of hydroxyapatite nanocrystals on microvascular endothelial cell viability and functions, J. Biomed. Mater. Res. A 76A (2006) 656−663.
[19] S. Pezzatini, L. Morbidelli, R. Solito, E. Paccagnini, E. Boanini, A. Bigi, et al., Nanostructured HA crystals up-regulate FGF-2 expression and activity in microvascular endothelium promoting angiogenesis, Bone 41 (2007) 523−534.
[20] S.I. Stupp, G.W. Ciegler, Organoapatites: materials for artificial bone. I. Synthesis and microstructure, J. Biomed. Mater. Res. 26 (1992) 169−183.
[21] T.J. Webster, C. Ergun, R.H. Doremus, R.W. Siegel, R. Bizios, Enhanced osteoclast-like cell functions on nanophase ceramics, Biomaterials 22 (2001) 1327−1333.
[22] J. Huang, S.M. Best, W. Bonfield, R.A. Brooks, N. Rushton, S.N. Jayasinghe, et al., In vitro assessment of the biological response to nanosized hydroxyapatite, J. Mater. Sci. Mater. Med. 15 (2004) 441−445.
[23] G. Colon, B.C. Ward, T.J. Webster, Increased osteoblast and decreased *Staphylococcus epidermidis* functions on nanophase ZnO and TiO_2, J. Biomed. Mater. Res. A 78 (2006) 595−604.
[24] T.J. Webster, E.L. Hellenmeyer, R.L. Price, Increased osteoblast functions on theta + delta nanofiber alumina, Biomaterials 26 (2005) 953−960.
[25] W. Paul, C.P. Sharma, Nanoceramic matrices: biomedical applications, Am. J. Biochem. Biotechnol. 2 (2006) 41−48.
[26] F.X. Huber, N. McArthur, J. Hillmeier, H.J. Kock, M. Baier, M. Diwo, et al., Void filling of tibia compression fracture zones using a novel resorbable nanocrystalline hydroxyapatite paste in combination with a hydroxyapatite ceramic core: first clinical results, Arch. Orthop. Trauma Surg. 126 (2006) 533−540.
[27] R. Smeets, G. Jelitte, M. Heiland, A. Kasaj, M. Grosjean, D. Riediger, et al., Hydroxylapatit-Knochenersatzmaterial (Ostim®) bei der Sinusbodenelevation, Schweiz Monatsschr. Zahnmed. 118 (2008) 203−208.
[28] K.L. Gerlach, D. Niehues, Die Behandlung der Kieferzysten mit einem neuartigen nanopartikulären Hydroxylapatit, Mund Kiefer GesichtsChir 11 (2007) 131−137.
[29] F. Schwarz, K. Bieling, T. Latz, E. Nuesry, J. Becker, Healing of intrabony periimplantitis defects following application of a nanocrystalline hydroxyapatite (Ostim™) or a bovine-derived xenograft (Bio-Oss™) in combination with a collagen membrane (Bio-Gide™). A case series, J. Clin. Periodontol. 33 (2006) 491−499. Materials 2 (2009) 2037
[30] F.P. Strietzel, P.A. Reichart, H.L. Graf, Lateral alveolar ridge augmentation using a synthetic nanocrystalline hydroxyapatite bone substitution material (Ostim®). Preliminary clinical and histological results, Clin. Oral Implants Res. 18 (2007) 743−751.

[31] C. Spies, S. Schnürer, T. Gotterbarm, S. Breusch, Tierexperimentelle Untersuchung des Knochenersatzstoffs OstimTM im knöchernen Lager des Göttinger Miniaturschweins, Z. Orthop. Unfall. 146 (2008) 64–69.
[32] M. Thorwarth, S. Schultze-Mosgau, P. Kessler, J. Wiltfang, K.A. Schlegel, Bone regeneration in osseous defects using a resorbable nanoparticular hydroxyapatite, J. Oral Maxillofac. Surg. 63 (2005) 1626–1633.
[33] J. Brandt, S. Henning, G. Michler, M. Schulz, A. Bernstein, Nanocrystalline hydroxyapatite for bone repair, Key Eng. Mater. 361–363 (2008) 35–38.
[34] F.X. Huber, J. Hillmeier, L. Herzog, N. McArthur, H.J. Kock, P.J. Meeder, Open reduction and palmar plate-osteosynthesis in combination with a nanocrystalline hydroxyapatite spacer in the treatment of comminuted fractures of the distal radius, J. Hand Surg. Br. 31B (2006) 298–303.
[35] F.X. Huber, J. Hillmeier, N. McArthur, H.J. Kock, P.J. Meeder, The use of nanocrystalline hydroxyapatite for the reconstruction of calcaneal fractures: preliminary results, J. Foot Ankle Surg. 45 (2006) 322–328.
[36] M.W. Laschke, K. Witt, T. Pohlemann, M.D. Menger, Injectable nanocrystalline hydroxyapatite paste for bone substitution: in vivo analysis of biocompatibility and vascularization, J. Biomed. Mater. Res. B Appl. Biomater. 82B (2007) 494–505.
[37] C.K.G. Spies, S. Schnürer, T. Gotterbarm, S. Breusch, The efficacy of Biobon™ and Ostim™ within metaphyseal defects using the Göttinger Minipig, Arch. Orthop. Trauma Surg. 129 (2009) 979–988.
[38] Y.K. Kim, L.S. Gu, T.E. Bryan, J.R. Kim, L. Chen, Y. Liu, et al., Mineralisation of reconstituted collagen using polyvinylphosphonic acid/polyacrylic acid templating matrix protein analogues in the presence of calcium, phosphate and hydroxyl ions, Biomaterials 31 (2010) 6618–6627.
[39] Y. Zhang, V.J. Reddy, S.Y. Wong, X. Li, B. Su, S. Ramakrishna, et al., Enhanced biomineralization in osteoblasts on a novel electrospun biocomposite nanofibrous substrate of hydroxyapatite/collagen/chitosan, Tissue Eng. Part A 16 (2010) 1949–1960.
[40] E. Kon, M. Delcogliano, G. Filardo, D. Pressato, M. Busacca, B. Grigolo, et al., A novel nanocomposite multilayered biomaterial for treatment of osteochondral lesions: technique note and an early stability pilot clinical trial, Injury 41 (2010) 693–701.
[41] C. Erisken, D.M. Kalyon, H. Wang, C. Ornek-Ballanco, J. Xu, Osteochondral tissue formation through adipose-derived stromal cell differentiation on biomimetic polycaprolactone nanofibrous scaffolds with graded insulin and Beta-glycerophosphate concentrations, Tissue Eng. Part A 17 (2011) 1239–1252.
[42] F.M. Chen, J. Zhang, M. Zhang, Y. An, F. Chen, Z.F. Wu, A review on endogenous regenerative technology in periodontal regenerative medicine, Biomaterials 31 (2010) 7892–7927.
[43] P.X. Ma, Biomimetic materials for tissue engineering, Adv. Drug. Deliv. Rev. 60 (2008) 184–198.
[44] S. Srinivasan, R. Jayasree, K.P. Chennazhi, S.V. Nair, R. Jayakumar, Biocompatible alginate/nano bioactive glass ceramic composite scaffolds for periodontal tissue regeneration, Carbohydr. Polym. 87 (2012) 274–283.
[45] F. Yang, S.K. Both, X. Yang, X.F. Walboomers, J.A. Jansen, Development of an electrospun nano-apatite/PCL composite membrane for GTR/GBR application, Acta Biomater. 5 (9) (2009) 3295–3304.
[46] Z. Yuan, H. Nie, S. Wang, C.H. Lee, A. Li, S.Y. Fu, et al., Biomaterial selection for tooth regeneration, Tissue Eng. Part B Rev. 17 (2011) 373–388.
[47] A.G. Fincham, J. Moradian-Oldak, J.P. Simmer, The structural biology of the developing dental enamel matrix, J. Struct. Biol. 126 (1999) 270–299.
[48] Z. Huang, T.D. Sargeant, J.F. Hulvat, A. Mata, P. Bringas, S.I. Ch Koh, et al., Bioactive nanofibers instruct cells to proliferate and differentiate during enamel regeneration, J. Bone Mineral Res. 23 (2008) 1995–2006.
[49] H.F. Chen, B.H. Clarkson, K. Sun, J.F. Mansfield, Self-assembly of synthetic hydroxyaptite nanorods into enamel prism like structure, J. Colloid Interface Sci. 188 (2005) 97–103.

[50] H.F. Chen, Z.Y. Tang, J. Liu, K. Sun, S.R. Chang, M.C. Peters, et al., Acellular synthesis of a human enamel-like microstructure, Adv. Mater. 18 (2006) 1846−1851.
[51] Y. Fujishiro, A. Fujimoto, T. Sato, A. Okuwaki, Coating of hydroxyapatite on titanium plates using thermal-dissociation of calcium-EDTA chelate complex in phosphate solutions under hydrothermal conditions, J. Colloid Interface Sci. 173 (1995) 119−127.
[52] W. Suchannek, M. Yoshimura, Processing and properties of hydroxyapatite-based biomaterials for use as hard tissue replacement implants, J. Mater. Res. 13 (1998) 94−117.
[53] M. Cao, Y. Wang, C. Guo, Y. Qi, C. Hu, Preparation of ultrahigh-aspect-ratio hydroxyapatite nanofibers in reverse micelles under hydrothermal conditions, Langmuir 20 (2004) 4784.
[54] L. Li, C. Mao, J. Wang, X. Xu, H. Pan, Y. Deng, et al., Bio-inspired enamel repair via Glu-directed assembly of apatite nanoparticle: an approach to biomaterials with optimal characteristic, Adv. Mater. 23 (2011) 4695−4701.
[55] M. Hannig, C. Hannig, Nanomaterials in preventive dentistry, Nat. Nanotechnol. 5 (2010) 565−569.
[56] K. Onuma, K. Yamagishi, A. Oyane, Nucleation and growth of hydroxyapatite nanocrystals for non-destructive repair of early caries lesions, J. Cryst. Growth 282 (2005) 199−207.
[57] Y. Yamagishi, K. Onuma, T. Suzuki, F. Okada, J. Tagami, M. Otsuki, et al., A synthetic enamel for rapid tooth repair, Nature 433 (2005) 819.
[58] K.L. Lv, J.X. Zhang, X.C. Meng, X.Y. Li, Remineralization effect of the nano-HA toothpaste on artificial caries, Key Eng. Mater. 330−332 (2007) 267−270.
[59] M.Y. Kim, H.K. Kwon, C.H. Choi, B.I. Kim, Combined effects of nano-hydroxyapatite and NaF on remineralization of early caries lesion, Key Eng. Mater. 330−332 (2007) 1347−1350.
[60] N. Roveri, E. Battistella, I. Foltran, E. Foresti, M. Iafisco, M. Lelli, et al., Synthetic biomimetic carbonate-hydroxyapatite nanocrystals for enamel remineralization, Adv. Mater. Res. 47−50 (2008) 821−824.
[61] N. Roveri, E. Battistella, C.L. Bianchi, I. Foltran, E. Foresti, M. Lafisco, et al., Surface enamel remineralization: biomimetic apatite nanocrystals and fluoride ions different effects, J. Nanomater. (2009) 10.1155/2009/746383.
[62] L. Li, H.H. Pan, J.H. Tao, X.R. Xu, C.Y. Mao, X.H. Gu, et al., Repair of enamel by using hydroxyapatite nanoparticles as the building blocks, J. Mater. Chem. 18 (2008) 4079−4084.
[63] P. Tschoppe, D.L. Zandim, P. Martus, A.M. Kielbassa, Enamel and dentine remineralization by nano-hydroxyapatite toothpastes, J. Dent. 3 (2011) 430−437.
[64] S.B. Huang, S.S. Gao, H.Y. Yu, Effect of nano-hydroxyapatite concentration on remineralization of initial enamel lesion in vitro, Biomed. Mater. 4 (2009) 034104.
[65] S. Huang, S. Gao, L. Cheng, H. Yu, Remineralization potential of nano-hydroxyapatite on initial enamel lesions: an in vitro study, Caries Res. 45 (2011) 460−468.
[66] S. Huang, S. Gao, L. Cheng, H. Yu, Combined effects of nano-hydroxyapatite and Galla chinensis on remineralization of initial enamel lesion in vitro, J. Dent. 38 (2010) 811−819.
[67] G. Balasundaram, M. Sato, T.J. Webster, Using hydroxyapatite nanoparticles and decreased crystallinity to promote osteoblast adhesion similar to functionalizing with RGD, Biomaterials 27 (2006) 2798−2805.
[68] Q. Hu, Z. Tan, Y. Liu, J. Tao, Y. Cai, M. Zhang, et al., Effect of crystallinity of calcium phosphate nanoparticles on adhesion, proliferation, and differentiation of bone marrow mesenchymal stem cells, J. Mater. Chem. 17 (2007) 4690−4698.
[69] S. Mai, Y.K. Kim, M. Toledano, L. Breschi, J.Q. Ling, D.H. Pashley, et al., Phosphoric acid esters cannot replace polyvinylphosphonic acid as phosphoprotein analogs in biomimetic remineralization of resin-bonded dentin, Dent. Mater. 25 (2009) 1230−1239.
[70] A.W. Xu, Y.R. Ma, H. Colfen, Biomimetic mineralization, J. Mater. Chem. 17 (2007) 415−449.

[71] E.C. Reynolds, Remineralization of enamel subsurface lesions by casein phosphopeptide-stabilized calcium phosphate solutions, J. Dent. Res. 76 (1997) 1587–1595.
[72] M.V. Morgan, G.G. Adams, D.L. Bailey, C.E. Tsao, S.L. Fischman, E.C. Reynolds, The anticariogenic effect of sugar-free gum containing CPP-ACP nanocomplexes on approximal caries determined using digital bitewing radiography, Caries Res. 42 (2008) 171–184.
[73] F. Cai, D.J. Manton, P. Shen, G.D. Walker, K.J. Cross, Y. Yuan, et al., Effect of addition of citric acid and casein phosphopeptide amorphous calcium phosphate to a sugar-free chewing gum on enamel remineralization in situ, Caries Res. 41 (2007) 377–383.
[74] Y. Iijima, F. Cai, P. Shen, G. Walker, C. Reynolds, E.C. Reynolds, Acid resistance of enamel subsurface lesions remineralized by a sugar-free chewing gum containing casein phosphopeptide-amorphous calcium phosphate, Caries Res. 38 (2004) 551–556.
[75] A.M. Al-Mullahi, K.J. Toumba, Effect of slow-release fluoride devices and casein phosphopeptide/amorphous calcium phosphate nanocomplexes on enamel remineralization in vitro, Caries Res. 44 (2010) 364–371.
[76] J.D. Bader, Casein phosphopeptide-amorphous calcium phosphate shows promise for preventing caries, Evid. Based Dent. 11 (2010) 11–12.
[77] G.D. Walker, F. Cai, P. Shen, G.G. Adams, C. Reynolds, E.C. Reynolds, Casein phosphopeptide-amorphous calcium phosphate incorporated into sugar confections inhibits the progression of enamel subsurface lesions in situ, Caries Res. 44 (2010) 33–40.
[78] N. Srinivasan, M. Kavitha, S.C. Loganathan, Comparison of the remineralization potential of CPP-ACP and CPP-ACP with 900 ppm fluoride on eroded human enamel: an in situ study, Arch. Oral Biol. 55 (2010) 541–544.
[79] H. Hamba, T. Nikaido, G. Inoue, A. Sadr, J. Tagami, Effects of CPP-ACP with sodium fluoride on inhibition of bovine enamel demineralization: a quantitative assessment using micro-computed tomography, J. Dent. 39 (2011) 405–413.
[80] E.C. Reynolds, Anticariogenic complexes of amorphous calcium phosphate stabilized by casein phosphopeptides: a review, Spec. Care Dent. 18 (1998) 8–16.
[81] C. Llena, L. Forner, P. Baca, Anticariogenicity of casein phosphopeptide-amorphous calcium phosphate: a review of the literature, J. Contemp. Dent. Prac. 10 (2009) 1–9.
[82] V. Yengopal, S. Mickenautsch, Caries preventive effect of casein phosphopeptide-amorphous calcium phosphate (CPP-ACP): a metaanalysis, Acta Odontol. Scand. 21 (2009) 1–12.
[83] N.J. Cochrane, F. Cai, N.L. Huq, M.F. Burrow, E.C. Reynolds, New approaches to enhanced remineralization of tooth enamel, J. Dent. Res. 89 (2010) 1187–1197.
[84] E.C. Reynolds, F. Cai, P. Shen, G.D. Walker, Retention in plaque and remineralization of enamel lesion by various forms of calcium in a mouthrinse or sugar-free chewing gum, J. Dent. Res. 82 (2003) 206–211.
[85] H.H.K. Xu, M.D. Weir, L. Sun, Nanocomposites with Ca and PO4 release: effects of reinforcement, dicalcium phosphate particle size and silanization, Dent. Mater. 23 (2007) 1482–1491.
[86] Y.W. Hong, J.H. Kim, B.H. Lee, Y.K. Lee, B.J. Choi, J.H. Lee, et al., The effect of nano-sized β-tricalcium phosphate on remineralization in glass ionomer dental luting cement, Key Eng. Mater. 361–363 (2008) 861–864.
[87] S. Nakashima, M. Yoshie, H. Sano, A. Bahar, Effect of a test dentifrice containing nano-sized calcium carbonate on remineralization of enamel lesions in vitro, J. Oral Sci. 51 (2009) 69–77.
[88] K. Kawasaki, J. Ruben, I. Stokroos, O. Takagi, J. Arends., The remineralization of EDTA-treated human dentine, Caries Res. 33 (1999) 275–280.

[89] Y. Shibata, L.H. He, Y. Kataoka, T. Miyazaki, M.V. Swain, Micromechanical property recovery of human carious dentin achieved with colloidal nano-betatricalcium phosphate, J. Dent. Res. 87 (2008) 233−237.
[90] M. Vollenweider, T.J. Brunner, S. Knecht, R.N. Grass, M. Zehnder, T. Imfeld, et al., Remineralization of human dentin using ultrafine bioactive glass particles, Acta Biomater. 3 (2007) 936−943.
[91] F.R. Tay, D.H. Pashley, Biomimetic remineralization of resin-bonded acid-etched dentin, J. Dent. Res. 88 (2009) 719−724.
[92] V.T. Sakai, Z. Zhang, Z. Dong, K.G. Neiva, M. Machado, S. Shi, et al., SHED differentiate into functional odontoblast and endothelium, J. Dent. Res. 89 (2010) 791−796.
[93] M.M. Cordeiro, Z. Dong, T. Kaneko, Z. Zhang, M. Miyazawa, S. Shi, et al., Dental pulp tissue engineering with stem cells from exfoliated deciduous teeth, J. Endod. 34 (2008) 962−969.
[94] V. Rosa, T.M. Botero, J.E. Nör, Regenerative endodontics in light of the stem cell paradigm, Int. Dent. J. 61 (2011) 23−28.
[95] G. Huang, T. Yamaza, L.D. Shea, F. Djouad, N.Z. Kuhn, R.S. Tuan, et al., Stem/progenitor cell-mediated de novo regeneration of dental pulp with newly deposited continuous layer of dentin in an in vivo model, Tissue Eng. Part A 16 (2009) 605−615.
[96] V. Rosa, A. Della Bona, B.N. Cavalcanti, J.E. Nör, Tissue engineering: from research to dental clinics, Dent. Mater. 28 (2012) 341−348.
[97] K.M. Galler, A. Cavender, V. Yuwono, H. Dong, S. Shi, G. Schmalz, et al., Self-assembling peptide amphiphile nanofibers as a scaffold for dental stem cells, Tissue Eng. Part A 14 (2008) 2051−2058.

CHAPTER

Scope of Nanotechnology in Endodontics

21

Sami M.A. Chogle[a,b], Bassam M. Kinaia[c,d] and Harold E. Goodis[e]

[a]*Associate Professor and Program Director, Graduate Endodontics, Henry M. Goldman School of Dental Medicine, Boston University, Boston, MA, USA,*

[b]*Adjunct Associate Professor, Department of Endodontics, School of Dental Medicine, Case Western Reserve University, Cleveland, OH, USA,*

[c]*Assistant Professor in Periodontology, Director of Continuing Education, The European University, Dubai Health Care City, Dubai, UAE,*

[d]*Adjunct Assistant Professor, Department of Periodontology and Dental Hygiene, School of Dentistry, University of Detroit Mercy, Detroit, MI, USA,*

[e]*Professor Emeritus, Department of Endodontics, University of California School of Dentistry, San Francisco, CA, USA*

CHAPTER OUTLINE

Nanobiomaterials in Clinical Dentistry.

21.1 Introduction

Root canal treatment is a highly predictable procedure with success rates of up to 96% [1,2]. The success of the treatment primarily depends on proper cleaning and shaping to disrupt the microbial ecology, disinfecting the root canal system, and finally sealing it to prevent microleakage. Although the treatment has a high success rate, failure still occurs due to inadequate cleaning and shaping in anatomically complex root canal systems and/or continued microbial leakage due to lack of adequate sealing material characteristics [3–5]. Current materials possess certain limitations such as shrinkage, solubility in oral environment, and moisture intolerance. Therefore, development of proper material for cleaning and shaping as well as sealing the root canal system are essential for long-term root canal treatment success.

Newer advances, including developments in armamentarium such as the use of the dental operating microscope and improved materials, have influenced the outcome of periradicular surgery, according to some studies [6–10]. Although success rates have increased incrementally, the option to extract teeth and replace them with dental implants has grown in popularity. Outcomes of primary endodontic treatment, which have the highest success rate of endodontics procedures, have been compared to implants [11–13]. Because of the "predictable" option to replace a tooth with a dental implant when endodontic treatment has failed, the perceived benefit of endodontic treatment depends on the continued improvement and refinement in the physical characteristics of materials, techniques, and armamentarium.

One such focus in both the medical and dental fields is the clinical applications of nanotechnology. Nanomaterial research has initiated a new era in material development for improved clinical outcomes. Nanotechnology is defined as the creation of functional materials with structures sized 100 nm or smaller [14]. In the field of endodontics, a fair amount of research is underway in an attempt to enhance every step in clinical procedures from files to filling materials. The smaller sized nanomaterials, more resistant to wear and fatigue, are being suggested for surface modifications of currently used rotary nickel–titanium files for root canal treatment to help reduce the incidence of instrument failure. The antimicrobial properties of some nanoparticles may be able to enhance the efficacy of irrigants and intracanal medicaments due to their size and possible dispersion in complex root canal anatomies.

Apart from these, a more concentrated effort has been ongoing to develop "nanomodified" materials. Dispersion of these particles into current and novel materials could fortify the sealing ability of obturating and sealer materials, as well as root-repair/root-end filling materials. For example, nanocomposites constitute a relatively new class of materials with the dispersed phase having at least one ultrafine dimension, typically a few nanometers as demonstrated in Figure 21.1. They include polymeric materials composed of nanoparticles like carbon nanotubes (CNTs), organically-modified clays (organoclays), or other nanoscale materials. Because of the nanoscale structure and huge interfacial area between polymer and organoclay, polymer–clay nanocomposites exhibit enhanced mechanical and thermal properties. Polymer–clay nanocomposites are particularly attractive for potential applications where enhanced barrier properties as well as physical properties are desired.

CNTs are predicted to have unique mechanical properties including high stiffness and axial strength as a result of their cylindrical graphitic structure. Experimental studies have shown that isolated CNTs possess exceptionally high Young's moduli in the terapascal range which are much higher than those typically found in stainless steel and carbon fibers [15]. Carbon fibers

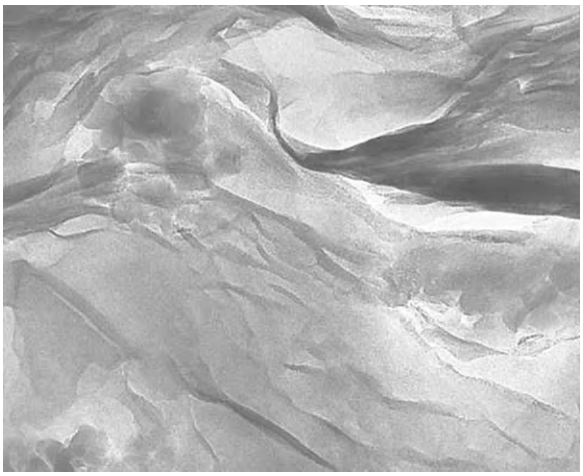

FIGURE 21.1

TEM demonstrating exfoliation of organoclay nanoparticles (dark aggregates) in a monomer matrix (100,000× magnification (50 nm scale)).

have already found applications in reinforced composites where there is a need for high-strength and light-weight materials [16]. The smaller diameters and larger aspect ratios found for CNTs is expected to lead to even higher strength composites. Recently, CNTs have been incorporated into methyl methacrylate-based resins and found to substantially enhance their load-bearing mechanical characteristics [17]. These studies suggest that the addition of CNTs in dental implant materials will prevent fatigue and failure caused by forces in the oral cavity and extend the life of dental restorations.

Another application of nanotechnology gaining significant interest is the use of nanoscaffolds for pulp regeneration. At the nanolevel, these scaffolds may eventually prove to be applicable to therapies ranging from pulp capping to complete pulp-dentin complex regeneration. This chapter aims to review these uses of nanotechnology for current and future clinical applications in endodontics.

21.2 Clinical applications

21.2.1 Instrument modifications

Rotary instruments, especially those made of nickel–titanium (Ni–Ti) alloys, are widely used by clinicians in everyday dental practice. Ni–Ti alloys possess many favorable characteristics such as resistance against corrosion and more importantly super-elasticity and excellent shape memory that allow it to navigate complex root canal systems for proper cleaning and shaping [18]. Despite these favorable characteristics of rotary Ni–Ti instruments, fatigue and failure of Ni–Ti alloys occur leading to possible intracanal instrument fracture. Although a disarticulated instrument in the canal may not directly result in failure of the endodontic procedure, the inability to clean beyond the fractured instrument (Figure 21.2) may result in persistent endodontic disease requiring surgical

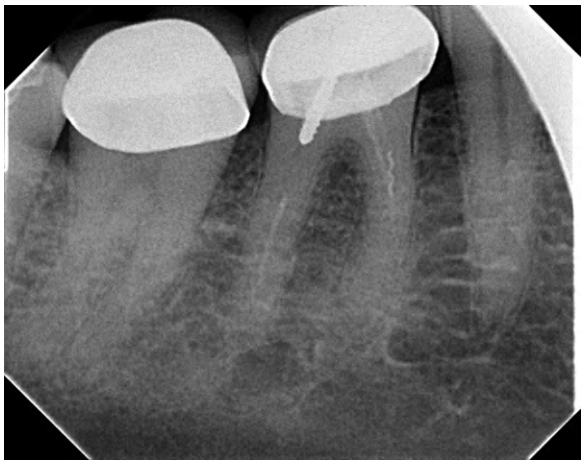

FIGURE 21.2

Periapical radiograph demonstrating a disarticulated file in the mesial canal of the first molar preventing further apical cleaning and shaping and obturation.

intervention [19]. Therefore, to reduce instrument fatigue and failure, reports have suggested changes in instrument design, instrumentation protocol, and more recently the use of nanomaterials for surface modifications of the currently used rotary Ni−Ti instruments.

Recent studies have attempted to modify the instrument surface by coating the Ni−Ti surface with different nanomaterials to overcome these characteristic shortcomings. Adini et al. [20] examined the effects of cobalt coatings with impregnated fullerene-like WS_2 nanoparticles on file fatigue and failure of Ni−Ti files. The addition of these nanoparticles significantly improved the fatigue resistance and time to breakage of the coated files as observed under dynamic X-ray diffraction. The authors attributed the improvement to the reduced friction between the file and the surrounding tissue with the nanoparticles coating [20]. In another study, the distal end of the file was modified by selective coating of endodontic files. The selective coating of the files distributed the nanoparticles nonuniformly along the surface of the file leaving only a part of the file coated and thereby having a higher torque making it more resistant to fatigue and failure [21]. Thus the use of nanoparticles for surface coatings of the instruments may significantly enhance their performance with less potential for fatigue and failure.

21.2.2 Enhancement of canal disinfection

A number of solutions and medications are used for disinfecting the root canal system and may be broadly classified under irrigants and medicaments. While irrigants usually signify high volume with low contact time within the canal system, medicaments are relatively more passive but rely on a longer contact time to exert their disinfecting properties. Both of these categories are being investigated for nanoparticle enhancement to help improve disinfection and sealing of the root canal system.

21.2.2.1 Irrigants

The main idea for cleaning and shaping of the root canal system is to disrupt and eradicate the microbial biofilms in the root canal system. Even though a lot of emphasis is placed on instrumentation of canals, it is well documented that irrigants play the central role in disinfection of the root canal system [22,23]. Irrigants can augment mechanical debridement by flushing out debris, dissolving tissue, and disinfecting the root canal system. This is especially needed for teeth with complex internal anatomy such as fins or other irregularities that might be missed by instrumentation [24]. According to Torabinejad et al. [25], the desired functions of an irrigating solution include (i) complete removal of the smear layer, (ii) disinfection of dentin and its tubules, (iii) sustained antibacterial effect after use, (iv) penetration of antimicrobial agents present in the solution into the dentinal tubules, (v) nonantigenic, nontoxic, and noncarcinogenic, (vi) no adverse effects on the physical properties of exposed dentin, (vii) no adverse effect on the sealing ability of filling material, (viii) not discoloring the tooth, (ix) convenient application, and (x) relatively inexpensive.

The main concern with irrigating techniques and irrigating fluids is the ability to reach all areas of the root canal system and removal of debris (i.e., smear layer) and biofilms without damage to host tissues. Different irrigants and techniques both manual and machine assisted are being used to disinfect the root canal system. Recent reports have investigated the types of nanoparticles to enhance the root canal disinfection properties as well as the tissue reaction to their use.

Over the last decade, silver nanoparticles have been used in various applications from electronics to antibacterial/antifungal agents in biotechnology and bioengineering including dental applications. In an animal study, Gomes-Filho et al. [26] observed the tissue response to implemented polyethylene tubes filled with fibrin sponge embedded with either 47 or 23 ppm silver nanoparticles dispersion material and compared them to plain fibrin sponges and those imbedded with 2.5% sodium hydrochloride used as controls over a 90-day period. The results of the study concluded that silver nanoparticles dispersion material at 23 ppm concentration appeared biocompatible compared to the rest of the groups. However, health concerns have been raised and toxicological reviews have reported that exposure to silver nanoparticles may be associated with "inflammatory, oxidative, genotoxic, and cytotoxic consequences" [27]. Further investigations are warranted to dictate the safe use of these nanoparticles in medical and dental applications.

Another way of root canal disinfection that is being investigated is the nanoparticle-based antimicrobial photodynamic therapy. Preliminary studies seem promising. In one study, Pagonis et al. [28] studied the in vitro effects of poly(lactic-co-glycolic acid) (PLGA) nanoparticles loaded with the photosensitizer methylene blue (MB) and light against *Enterococcus faecalis* by transmission electron microscopy (TEM). The nanoparticles were found to be concentrated mainly on cell walls of the microorganisms. The synergism of light and MB-loaded nanoparticles led to approximately 2 and 1 log 10 reduction of colony-forming units (CFUs) in planktonic phase and root canals, respectively. In both cases, mean log 10 CFU levels were significantly lower than controls and MB-loaded nanoparticles without light. The authors concluded that the utilization of PLGA nanoparticles encapsulated with photoactive drugs may be a promising adjunct in antimicrobial endodontic treatment. In another similar study, the cationic photosensitizer was able to inactivate the microbial biofilm bacteria (*E. faecalis*) and disrupt the biofilm structure [29,30]. Thus these therapies may provide a new alternative to conventional irrigants used in endodontic treatment.

21.2.2.2 Medicaments

For endodontic procedures that require more than one visit to complete, the remaining bacteria within the system can grow and reinfect the root canal space between appointments [31]. Historically, placement of intracanal medicaments became a popular method of preventing bacterial regrowth. Some form of calcium hydroxide (CaOH) is an intracanal medicament often used between visits. Although *E. faecalis* is an insignificant organism in infected but untreated root canals [32], it is extremely resistant to most of the intracanal medicaments used, particularly to the calcium hydroxide-containing dressings [33]. It can also survive in root canals as monoinfection, without any synergistic support from other bacteria [32,34]. Thus *E. faecalis* is a recalcitrant candidate among the causative agents of failed endodontic treatments.

Nanoparticulates such as chitosan (CS-np) and zinc oxide (ZnO-np) have been shown to possess significant antibacterial properties. Shrestha et al. in their study [35] tested the efficacy of fresh and aged CS-np and ZnO-np in disinfecting and disrupting *E. faecalis* biofilms. Using confocal laser scanning microscopy, total elimination of planktonic bacteria was observed in contrast to the biofilm bacteria, which survived even after 72 h. There was a significant reduction in the thickness of biofilm after nanoparticulate treatment and the authors concluded that the rate of bacterial killing by the nanoparticulates depended on the concentration and time of interaction and that aging for 90 days did not affect their antibacterial properties. Although these findings need to be further investigated and confirmed in animal and in vivo studies, the preliminary reports seem promising.

21.2.3 Material modifications

21.2.3.1 Obturating materials

The American Association of Endodontists published "Appropriateness of Care and Quality Assurance Guidelines" [36] regarding contemporary endodontic treatment. In that publication, root canal obturation is defined and characterized as:

> *The three-dimensional filling of the entire root canal system as close to the cementodentinal junction as possible. Minimal amounts of root canal sealers, which have been demonstrated to be biologically compatible, are used in conjunction with the core-filling material to establish an adequate seal.*

Although a number of materials have been advocated over the last 150 years for root canal obturation, gutta-percha has remained as the material of choice. Gutta-percha has satisfied a number of the tenets for an ideal root filling material highlighted by Grossman [37]. However, its main disadvantages cited include lack of rigidity and adhesiveness, ease of displacement under pressure, minimal antimicrobial property, and shrinkage if thermo-plasticized. Proper adaptation of obturating materials to the cleaned and shaped root canal walls and in increased antimicrobial activity would be important to reduce gaps and microleakage.

The incorporation of nanoparticles may increase the surface area between the dentin and the obturating material leading to enhanced adaptation. Bioactive glass 45S5 is one of the recent nanoparticles used in endodontic therapy. It has amorphous nanoparticles of 20−60 nm in size. The smaller particle size increases the contact surface area and thereby possesses a higher antimicrobial effect than the macrosized material. The clinical antimicrobial efficacy of bioactive glass 45S5 was

evaluated in persisting root canal infections containing isolates of *Enterococci*. The killing efficacy against the bacteria was significantly better with the nanosized treatment material [38].

Bioactive glass 45S5, similarly to CaOH, has also been used for treatment of traumatized front teeth with open apices. The conventional treatment with CaOH may affect mechanical dentin properties by decreasing its flexural strength over time. Recently, Marending et al. [39] used suspensions of nanoparticulate bioactive glass 45S5 as dressing material and compared it to CaOH in traumatized front teeth with open apices. The results showed a 35% drop in dentin mean flexural strength values with CaOH and a 20% drop with bioactive glass 45S5 indicating superiority of the latter. However, these results should be interpreted with caution since the affected dentin was mainly in the superficial layers. Furthermore, Mohn et al. [40] prepared nanosized particles of bioactive glass and modified it with bismuth oxide to obtain radiopaque properties. They evaluated the performance of it as a filling material. Based on scanning electron microscopy (SEM), the authors concluded that bioactive glass modified with bismuth oxide is a radiopaque bioactive root canal filling material.

21.2.3.2 Sealers

Sealer materials used during obturation are grouped based on their prime constituent, such as zinc oxide-eugenol, calcium hydroxide, resins, glass ionomers, or silicones. The use of a sealer during root canal obturation is essential and enhances the possible attainment of an impervious seal and serves as filler for canal irregularities and minor discrepancies between the root canal wall and gutta-percha. Sealers are often expressed through lateral or accessory canals, and they can assist in microbial control should there be microorganisms left on the root canal walls or in the tubules [41–43]. Sealers can also serve as lubricants to assist in the thorough seating of the core-filling material during compaction. In canals where the smear layer has been removed, many sealers demonstrate increased adhesive properties to dentin (in addition to flowing into the patent tubules) [44–46].

As stated by Gutmann and Witherspoon [47], the future directions for the ideal sealer should focus on materials that (i) penetrate the patent dentinal tubules, (ii) bind intimately to both the organic and inorganic phases of dentin, (iii) neutralize or destroy microorganisms and their products, (iv) predictably induce a cemental regenerative response over the apical foramen, and (v) strengthen the root system. Since the size of nanoparticles can penetrate the dentinal tubules to ensure that all the spaces have been sealed effectively, the development of a sealer based on nanotechnology may be an important step to achieve a better sealer material in endodontics. Chen et al. [48] in their study used a new root canal filling sealer primarily composed of nanohydroxyapatite crystals in 279 nm after setting in an extracted tooth model. The sealer demonstrated superior antimicrobial activity (*Actinomyces naeslundii, Peptostreptococcus anaerobius, Porphyromonas gingivalis, Porphyromonas endodontalis,* and *Fusobacterium nucleatum*) as well as minimal microleakage compared to two other materials.

Another preliminary report [49] demonstrated that nanocrystalline tetracalcium phosphate had significantly higher antimicrobial potency in an agar-diffusion test. The formation of amorphous $Ca(OH)_2$ during setting was thought to increase the pH value in the agar gel around the specimens yielding a zone of inhibition. However, a similar study reported contradictory results. Masudi et al. [50] evaluated the apical sealing ability of an experimental NHA (40–60 nm) resin-based endodontic sealer and compared it to a commonly used resin-based sealant material. Teeth in the first group were obturated using gutta-percha with AH26. The second group was obturated with the

experimental sealer. The results showed that there was no statistically significant difference in apical sealing ability when measuring penetration of the dye using stereo microscope. Taken together, the above three reports may indicate promising initial reports that with further research may yield superior materials.

21.2.3.3 Retro-filling and root-repair materials

Numerous studies have demonstrated the importance of root-end filling placement during periapical surgery. According to Harty et al. [51], the most important factor in determining the success of an apicoectomy is the efficiency of the apical seal. Wu et al. [52] suggested that a tight and long-lasting seal of root-end fillings are of primary clinical importance. Several studies have indicated that the lack of a good root canal filling could compromise the surgical outcome [53,54]. In addition, a number of clinical studies on healing after periradicular surgery have confirmed the benefit of placing a high-quality root canal filling prior to surgery [55,56].

The properties of an ideal root-end filling material have been well documented in the scientific literature and are summarized as this material would adhere or bond to tooth tissue and ''seal'' the root end three dimensionally; not promote, and preferably inhibit, the growth of pathogenic microorganisms; be dimensionally stable and unaffected by moisture in either the set or unset state; be well tolerated by periradicular tissues with no inflammatory reactions; stimulate the regeneration of normal periodontium; be nontoxic both locally and systemically; not corrode or be electrochemically active; not stain the tooth or the periradicular tissues; be easily distinguishable on radiographs; have a long shelf life; and be easily handled. Although almost every available dental restorative material or cement has at one time or another been suggested for root-end filling, these properties have yet to be found in any one material. It may therefore be concluded that the ideal retrofill material does not yet exist [57].

Mineral Trioxide Aggregate (MTA) has become the material of choice of retrograde filling in spite of its handling and long setting time. To overcome these disadvantages, a very recent study by Saghiri et al. [58] evaluated a nanomodified MTA for enhanced physiochemical properties. They concluded that the increased surface area of powder by nanodispersion can reduce setting time and increase microhardness. This may help the MTA to set faster without losing its required hardness once set. Other studies are investigating new materials rather than modifications to current materials. A polymer nanocomposite (PNC) is a generalized term for polymeric materials that is loaded with minimal amount of nanoparticles such as clays and CNTs [59]. As opposed to conventional composites, the dispersed phase has a very high surface-to-volume ratio. PNCs have therefore shown greatly improved mechanical and thermal properties of the material even at very low filler content (typically between 0% and 5%). Previous studies have indicated substantial improvements in heat resistance, [59,60] dimensional stability [61], stiffness, [62,63], reduced electrical conductivity [64,65], and most uniquely, drug elution capabilities [66,67]. Recently, two such novel nanocomposites were investigated for initial apical seal along with a commonly used polymer-based compomer in an in vitro model [68]. Although one of the PNCs did not significantly reduce leakage, the results revealed that leakage of commercial compomer was more than 12 times more likely than the second PNC. SEM of these PNCs placed as root-end filling materials revealed a tight interface with the PNC entering into the dentinal tubules (Figure 21.3) [69]. This was corroborated with equal or greater values (Figure 21.4) of push-out force required when compared to MTA and Geristore® [70].

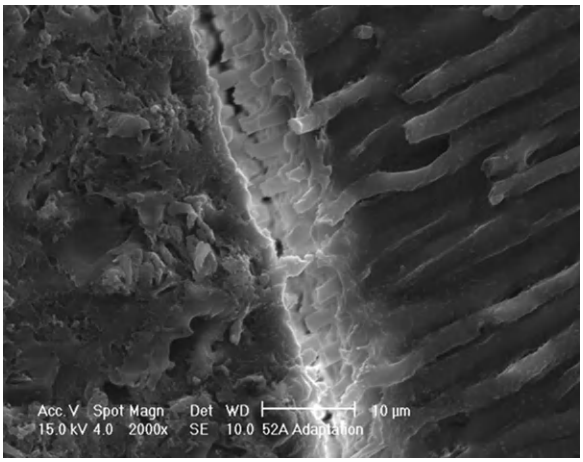

FIGURE 21.3

SEM image revealing the dentin–nanocomposite interface. The dentinal tubules (right) are seen to be penetrated by the nanocomposite fibers.

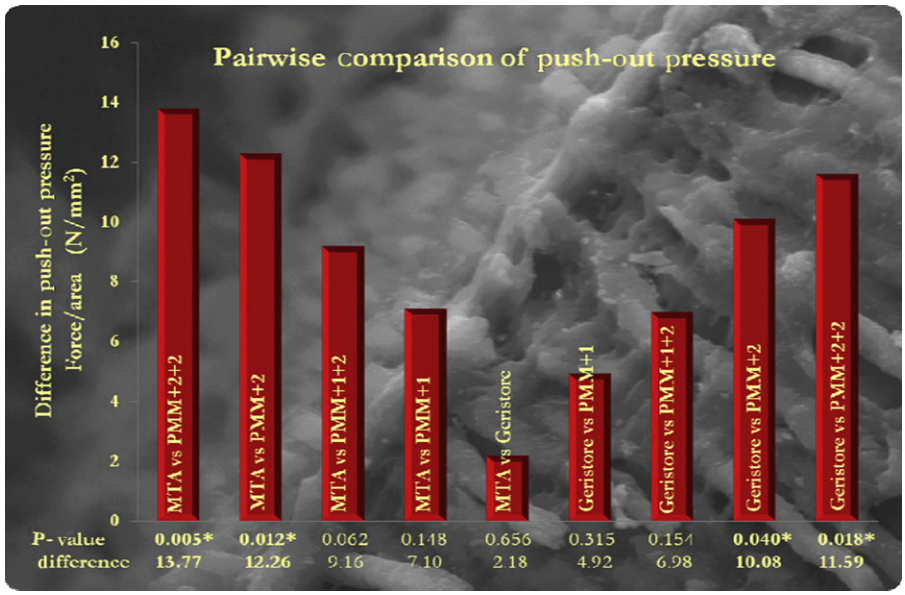

FIGURE 21.4

Bar chart comparing push-out force for nanocomposites Poly(methyl methacrylate) (PMM) containing varying quantities of organoclay nanoparticles (1–2%) with MTA and Geristore. The 2% nanocomposite groups performed significantly better than MTA and Geristore.

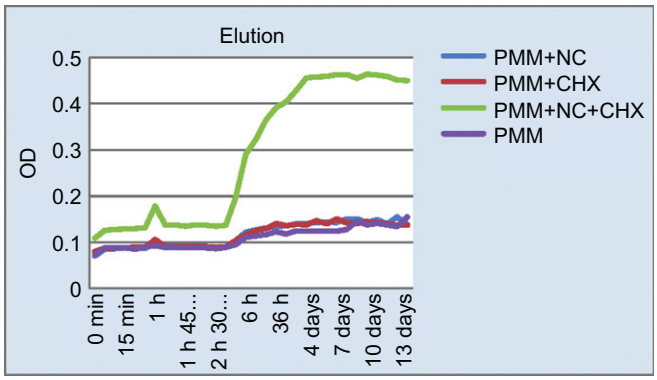

FIGURE 21.5

Histogram with plotted optical density values for CHX release over a 2-week time period. The nanocomposite group with CHX (PMM + NC + CHX) showed a consistently higher release with time compared to nanocomposite without CHX (PMM + NC), regular composite (PMM), and composite with CHX (PMM + CHX).

One significant property of nanocomposites is the ability for drug elution. Initial reports with dental composite materials such as 50/50 hydroxyethylmethacrylate, and urethane dimethacrylate have demonstrated antimicrobial release of chlorhexidine (CHX) despite polymerization shrinkage [71]. Unpublished pilot data of PNC containing CHX diacetate salt hydrate 2% indicated, based on optical density readings (Figure 21.5), that the PNC showed initiation of CHX elution at 3 h that peaked at 4 days and remained constant till the length of experiment (2 weeks) [Chogle et al., unpublished data]. The authors claim from ongoing experiments that the elution of CHX can also be controlled by certain factors. Although very nascent, the ability to create, place, and control a "smart" root-end filling material may be vital to counter primary, secondary, and refractory apical infections.

The cytotoxicity of such PNCs has been investigated as well. Modareszadeh et al. [72] evaluated polymer PNC resins with C-18 organoclay dispersed within the resin matrix and containing CHX diacetate salt hydrate 2% and compared it to that of two widely accepted commercially available materials, ProRoot® MTA and Geristore®. Elutes of materials extracted after 24 h and 1, 2, and 3 weeks were interacted with the mouse fibroblasts L-929 using a colorimetric cell viability assay Mitochondria-Targeting Sequence (MTS) which is based on mitochondrial dehydrogenases activity and differences in the mean bioactivity values were assessed. The results showed no statistically significant difference in cytotoxicity between ProRoot® MTA, Geristore®, and PNC resin C-18 at all-time intervals. Further investigations would be needed to confirm these in vitro findings.

21.3 Applications for repair and pulp regeneration

Repair and regeneration in endodontics deal with systems and mechanisms that maintain or restores original structures and functions of tissue by reproducing embryonic development. In the tooth, the main concern of researchers and ultimately clinicians is the maintenance or regeneration of the

dental pulp. The dental pulp is considered a low-compliance system that does not suffer disease or injury in a manner to retain those cells, connective tissue, nerve fibers, and blood vessels as they were originally formed embryonically and postbirth [73].

The dental pulp is a difficult tissue to access in humans without causing an inflammatory response. It is a result of its environment and the hard tissues (enamel, dentin) that surround it. From the standpoint of the possibility of repair and/or regeneration when the dental pulp is injured, infected, or necrosed, its nature must be understood before any treatment modalities are attempted. Another unusual aspect of the dental pulp is that it is a completely sensory tissue. That sensory design implies that the adult pulp is protective of that tissue throughout the life of the tooth. However, that same protective nature can be disturbed due to its location and its functions.

The following is a brief review of the nature of the dental pulp's location that mitigates against its ability to survive, repair itself, and regenerate a pulp-like tissue. First, the pulp has a terminal microvascular supply with few, if any, anastomoses (with the exception of multirooted teeth). Second, the dental pulp has a relatively large volume of tissue with a relatively small vascular supply. The largest vessels to enter and exit the tissue are arterioles and venules. Last, and probably the major deterrent to repair and regeneration in response to injury or infection occurs due to it being surrounded by a hard, unyielding tissue (dentin) and itself surrounded on the crown of the tooth by enamel and the root by cementum [74]. However, in spite of its environment, the pulp has in infinite capacity to repair itself.

21.4 Repair and regeneration

The main culprit in relation to untoward events occurring in the dental pulp is due to the onset of dental caries. The hard tissue surrounding the pulp is susceptible to the microorganisms that cause enamel and dentin to become infected, with extension into the pulp tissue. When caries begins on the outer surface of enamel, the effect pulpally is an inflammatory response. As caries develops deeper into the enamel and dentin, microorganisms and their toxins travel directly into the pulp tissue. If caries is removed early in the pulpal inflammation process, any damage occurring within the pulp will be repaired by specialized cells (odontoblasts). Another form of dentin matrix will be formed and mineralized. This repair process narrows the pulp space but is still considered protective. The tooth is eventually restored and, if there are no further insults, will remain in the mouth over the lifetime of the patient. However, if caries is not removed early enough, the pulp continues to create dentin matrix. Sensory nerves, connective tissue, and blood vessels are compromised and narrowing becomes profound. Reduction of the space occurs and function is lost. The repair process occurs due to materials placed near to or into the pulp which cause the replacement of the original cells with cells that function in a manner not unlike the original cells. Today, ongoing research indicates that repair and regeneration can occur in a low-compliance environment. By necessity, the greater numbers of studies utilize animals whose teeth function in a manner similar to human teeth. Furthermore, bench-top research also is used to test theories before turning to animals [75]. The ultimate aim of these studies is to generate a natural tooth, including its hard and soft tissues to replace a missing tooth. Unfortunately, there is still very much to learn about these tissues and the therapy needed to return them to normal form and function.

21.5 Nanotechnology applications for repair and pulp regeneration

In today's studies, concerns have been raised as to the ability to transfer results from the laboratories and animals in order to use what has already been developed in a confident manner. The mechanisms of stem and progenitor cell propagation [76], differentiation [77] and growth, types of scaffolds [78], neural and vascular regeneration [79], and signaling mechanisms and the proteins involved in signaling [80], all without changing the genetic makeup of the tissue and without tissue toxicity, appear to be overwhelming. In fact, the only thing that changes is the scope of the research to deliver an environment that is able to regenerate tissue.

While human cells are larger than many of the new materials being produced at the nanoscale, the incorporation of these materials may lead to the development and production of restorative materials and new techniques that will close the interface completely between the margin of a tooth preparation and the restorative material used to fill the preparation. If that occurs, microleakage of microorganisms and other toxic substances (reinfection) will be halted and the dental pulp will be protected with no need for treatment.

Five bonding systems were tested for microleakage using nanoparticles of silver ammoniacal nitrate and were observed in a field emission SEM in a Yttrium aluminum garnet (YAG) backscattered electron mode. Electron dispersive system analysis was carried out in parallel to identify the existence of silver particles. Three of the restorative systems showed clear silver uptake in the adhesive and hybrid layers [81]. A recent study examined nanostructured assemblies that would not be toxic to pulp tissue. Melanocortin peptides (alpha-Melanocyte-stimulating hormone (MSH)) possess anti-inflammatory properties. Pulpal fibroblasts proliferation was observed in this substance which was covalently coupled with a Poly-Glutamic Acid (PGA-alpha-MSH) in the absence of lipopolysaccharide. While the mechanisms for this effect have not been elucidated, PGA-alpha-MSH may have important regulatory functions to modulate pulp inflammation [82]. Another study demonstrated the use of caffeic acid phenyl ester inhibited endogenous matrix metalloproteinases that cause hybrid layer degradation. The in vitro experiment inhibited microleakage [83]. Mine et al. [84] found that the nanointeraction between a silorane composite (a slow shrinking, two-step adhesive) bonded to enamel and dentin in an adhesive thickness of 10−20 μm. A later study [85] used a self-adhesive composite material to examine the ultrastructure between the adhesive and the enamel/dentin. The resultant hybrid layer of a maximum of 100 nm was found. These types of studies are necessary to limit the amount of closure of root canal system space inherent to pulpal injury.

The aspect of using nanotechnological methods of measuring nano- and micromechanical properties of a biologic and mechanical tissue, such as dentin, has recently been reported. The study was undertaken to test the zone of dentin immediately beneath the enamel−dentin junction. The area appears to demonstrate a softer dentin than in other areas of a tooth and is thought to play an important role in tooth function, strain distribution, and fracture resistance. Results showed well-known gradual increases in mechanical properties with increasing distance from the dento-enamel junction. Control dentin showed a higher elastic modulus and hardness on the lingual side of teeth for all measurements, while root dentin was harder on the buccal side. This suggests that nano- and micro-mechanical properties vary with tooth side, agreeing with literature using macroscopic methods of analysis. The buccal−lingual ratios of hardness for both nano- and micromeasurements of hardness in opposite directions in crown and root dentin suggest compensatory functions [86].

Dentin as a biologic and mechanical tissue was thought to be more prone to brittleness if the dentin surrounding the pulp canal space had been exposed to the stress of cleaning and shaping, and to the use of irrigants, sealers, and core materials [87]. In a recent study Cheron et al. [88] found that while not knowing what irrigants were used in the endodontic techniques, patient (tooth) age may be correlated to higher fracture susceptibility. A nanoscope atomic force microscope (AFM) with a triboscope head used with a Bercovich diamond tip was used in the experiment [89,90]. Interestingly, results of the Cheron et al. study [88] demonstrated that there was no difference in the modulus of elasticity or hardness of radicular intertubular dentin when comparing root-treated dentin (root canal procedure) with normal root dentin. The use of the AFM was very helpful in the concluding that treated dentin appeared to be the same.

As previously stated, research into the use of nanotechnology in various phases of the repair and regeneration of the dental pulp has not frequently been seen. However, several papers have theorized as to where the technology must move. While theoretical, there has been movement to begin such studies. Kanaparthy and Kanaparthy [91] and Freitas [92] have speculated that nanorobots could be constructed from parts with dimensions in the range of 1−100 nm. This may allow the co-use of substances as nanosensors for the delivery of precise amounts of a therapeutic agents used with pulp capping materials and drugs, such as antibiotics, as previously proposed. There was great hope that new systems of dental restorative materials using nanoparticles would also be developed.

The hard tissue directly below enamel is dentin. Dentin has a tubular structure formed by pulp cells, the odontoblasts. The dentin tubules contain an arm-like soft tissue extension, the odontoblast process, and fluid composed mainly of various proteins. Pulp sensory neurons are found and may extend into the tubules some distance around the odontoblast process [93]. The odontoblast and its process is the principal cell that is responsible for formation of the dentin matrix, which itself mineralizes into two types of dentin. Primary dentin matrix is initiated once the dental pulp cells and other cells involved in enamel formation are completed embryonically. Mineralization occurs throughout the crown and roots to complete tooth formation. Each odontoblast is an end-stage cell that remains functional over the entire lifetime of the pulp, unless replaced by an odontoblast-like cell during infection or injury. Secondary dentin forms throughout the life of the tooth through the same mechanisms and same cells that produced primary dentin and is a normal physiologic process. Both dentins are tubular with the tubules of secondary dentin being roughly a continuation of the tubules of primary dentin [94]. The formation of secondary dentin is at the expense of the root canal space and its contents. Therefore, since it is physiologic, the eventual result, if one lives long enough, is to see a marked narrowing and shortening of the canal space. A third type of dentin also is formed, which is the tertiary dentin. It is formed in response to trauma, injury, or infection and is atubular. While also protective in the first instance, it narrows the pulp space and is sometimes spoken of as a pathologic process. In an unchecked carious lesion, when microorganisms or toxins enter the pulp space and tissue, odontoblasts in the area of inflammation and infection are killed. Repair and regeneration may be possible through several therapies that are available and studies to date indicate formation of an odontoblast-like cell in place of the original odontoblast. The resulting tertiary dentin is formed with an atubular structure [95]. This explanation is necessary to understand the role of nanotechnology in repair and regeneration since these processes are not the same as the embryologic processes that formed the tooth originally.

Presently, there are only a few studies of nanotechnology as to what has been demonstrated at a larger scale. Smith et al. [96] examined the development of nanostructured polymer scaffolds for regeneration and bioengineering. The study focused on nanofibrous (NF) scaffolds with the incorporation of other components. Since extracellular matrices (ECM) are composed of collagen fibers between 50 and 500 nm, a biodegradable polymer was cast into a porous scaffold resulting in a NF pore-wall structure with nanofibers of the same diameter as found in ECM. In both NF and composite control scaffolds, cell adhesion, proliferation, and differentiation improved. The creation of a synthetic replica of the naturally occurring ECM has the potential to promote new tissue formation and is a huge step in understanding the enhanced biological regulation of cell behavior for tissue repair and regeneration [96].

The behavior of dental pulp stem cells on NF/gelatin/nano-hydroxyapatite NHA scaffolds was investigated. Dental pulp stem cells (DPSCs) were seeded on electrospun poly(epsilon caprolactone)/gelatin scaffolds with or without nanohydroxyapatite (NHA). Various tests (in vitro DNA content, ALP activity, and osteocalcin measurements) showed that the scaffolds supported DPSC adhesion, proliferation, and odontoblast differentiation. The presence of NHA upregulated ALP activity and promoted OC expression. Both scaffolds seeded with DPSCs were subcutaneously implanted into immunocompromised nude mice. Controls consisted of scaffolds with NHA but not seeded with DPSCs. Results showed that the combination of NHA on scaffolds upregulated expression of specific odontogenic genes and NHAs on nanofibers enhanced DPSC differentiation toward and odontoblast-like phenotype (-like cell) both in vitro and in vivo [97]. Wang et al. [98] examined the odontogenic differentiation of human DPSCs on NF poly(L-lactic acid) PLLA scaffolds. Highly porous NF-PLLA scaffolds mimicking collagen, type-I fibers were fabricated and seeded with DPSCs with and without Bone Morphogenic Protein-7 (BMP-7) growth factors and DXM -Dexamethasone(DXM) medium containing an assortment of other molecules. The combination of BMP-7 and DXM induced odontogenic differentiation more effectively than DXM alone. The nanoscaffolds provide an excellent environment for DPSCs to regenerate dental pulp and dentin. In a recent review, Gupta and Ma [99] used a multiscale scaffold incorporating nanofibrous features to mimic ECM with a porous network for regeneration of tissues. Results showed that creation of a microenvironment using nanofibrous scaffolds led to the formation of cartilage, enamel, dentin, and periodontal ligament regeneration. The authors state, however, that more studies are needed to understand the mechanisms of the nanofiber effects. There remains a significant technical challenge for the synthetic integration of structural mechanisms with biologic mechanisms to achieve functional tissue regeneration.

21.6 Conclusion

As may be seen by the above text, the full impact of nanotechnology in endodontics is still not realized. There seems to be nanoapplication for all aspects of routine root canal procedures. Whether it is the instruments and irrigants that are used to clean and shape root canals, or materials used to seal the cleaned root canal system, nanomaterials show potential to further improve their physical and chemical characteristics. In addition to these physical and chemical improvements, perhaps a major outcome of nanoenhancement would be the development of "smart" materials. "Smart" by

virtue of the reactive abilities of the nanoparticle dispersed in the material. If preliminary studies are confirmed and successful in animal and human models, these "smart" materials would be able to react to the local environment and/or insults. For example, a "smart" root-end filling material may be loaded with an antimicrobial agent along with a pH-sensitive nanoparticle acting as a "release gate." Here in case of apical infection, the ensuing decrease in pH in the inflamed/infected apical region could activate the release of drug from the root-end restoration to counter the infection. However, this would have local and systemic implications that would need to be thoroughly investigated for clinical viability.

Another major impact of nanotechnology would be in the area of pulp regeneration. Original and new studies have explored the use of scaffolds at the nanolevel that may eventually prove applicable to therapies that will limit their effect to small areas of a tooth rather than to the whole tooth. Results of the use on nanofibrous constructs as scaffolds is forward looking but they have to be tested in animals more frequently if they are to be used in humans. The use of nanoparticles to move growth factors into areas that require regeneration or in understanding signaling processes need to be examined further. Production of a synthetic EMC is a powerful advance for cell-based therapy development. Nanotechnology is at the door step of the research areas that have to be explored. It is time that steps are taken to walk through the doorway.

Acknowledgments

The authors would like to thank Drs Sohel Shaikh, Syed Qutubuddin, Andre K. Mickel, Mohan Sankaran, and Saeed Al Hassan for their continuous help and guidance in the nanotechnology research. The authors would also like to thank all the students and residents who have worked on this project particularly Drs Sumesh Potluri, Craig Duhaime, Mahmoud Modareszadeh, Ryan Reese, Clara Rhieu, Jeff Beacham, Jason Graves, Andrew Langston, and Logan Hazard. Some of the research in the chapter is supported by a Presidential Research Initiative (PRI) grant from the Case Western Reserve University, Cleveland, OH.

References

[1] J. Rud, J.O. Andreasson, J.E. Jensen, A follow-up study of 1,000 cases treated by endodontic surgery, Int. J. Oral Surg. 1 (1972) 215–228.

[2] L.Z. Strindberg, The dependence of the results of pulp therapy on certain factors, Acta Odontol. Scand. 14 (1956) 1–175.

[3] L.M. Lin, J.E. Skribner, P. Gaengler, Factors associated with endodontic treatment failures, J. Endod. 18 (1992) 625–627.

[4] H.A. Ray, M. Trope, Periapical status of endodontically treated teeth in relation to the technical quality of the root filling and the coronal restoration, Int. Endod. J. 28 (1995) 12–18.

[5] D.E. Vire, Failure of endodontically treated teeth: classification and evaluation, J. Endod. 17 (1991) 338–342.

[6] R.A. Rubinstein, S. Kim, Short-term observation of the results of endodontic surgery with the use of a surgical operation microscope and super-EBA as a root-end filling material, J. Endod. 25 (1999) 43–48.

[7] T. Testori, M. Capelli, S. Milani, R.L. Weinstein, Success and failure in periradicular surgery: a longitudinal retrospective analysis, Oral Surg. Oral Med. Oral Pathol. Oral Radiol. Endod. 87 (1999) 493–498.

[8] M.L. Zuolo, M.O. Ferreira, J.L. Gutmann, Prognosis in periradicular surgery: a clinical prospective study, Int. Endod. J. 33 (2000) 91–98.
[9] M. Maddalone, M. Gagliani, Periapical endodontic surgery: a 3-year follow-up study, Int. Endod. J. 36 (2003) 193–198.
[10] B.S. Chong, T.R. Pitt Ford, M.B. Hudson, A prospective clinical study of mineral trioxide aggregate and IRM when used as root-end filling materials in endodontic surgery, Int. Endod. J. 36 (2003) 520–526.
[11] S.L. Doyle, J.S. Hodges, I.J. Pesun, A.S. Law, W.R. Bowles, Retrospective cross sectional comparison of initial nonsurgical endodontic treatment and single-tooth implants, J. Endod. 32 (2006) 822–827.
[12] S.L. Doyle, J.S. Hodges, I.J. Pesun, M.K. Baisden, W.R. Bowles, Factors affecting outcomes for single-tooth implants and endodontic restorations, J. Endod. 33 (2007) 399–403.
[13] M. Iqbal, S. Kim, Single-tooth implant versus root canal treatment and restoration for compromised teeth: a meta-analysis, Oral Maxillofac. Implants 21 (2007) 96–116.
[14] The American Heritage Science Dictionary, Houghton Mifflin Company, 2005.
[15] M.M.J. Treacy, T.W. Ebbesen, J.M. Gibson, Exceptionally high Young's modulus observed for individual carbon nanotubes, Nature 381 (1996) 678–680.
[16] P. Calvert, Strength in disunity, Nature 357 (1992) 365–366.
[17] D.A. Pienkowski, R.J. Andrews, US Patent No. 6, 872, 403, (2005).
[18] O. Peters, F. Paqué, Current developments in rotary root canal instrument technology and clinical use: a review, Quintessence Int. 41 (2010) 479–488.
[19] P. Parashos, H. Messer, Rotary NiTi instrument fracture and its consequences, J. Endod. 32 (2006) 1031–1043.
[20] A.R. Adini, Y. Feldman, S. Cohen, L. Rapoport, A. Moshkovich, M. Redlich, et al., Alleviating fatigue and failure of NiTi endodontic files by a coating containing inorganic fullerene-like WS2 nanoparticles, J. Mater. Res. 26 (10) (2011) 1234–1242.
[21] R. Tenne, M. Redlich, A. Ram-Adini, Y. Feldman, G. Samorodnitzky, J. Moshonov, et al., Endodontic files with coatings of metals and inorganic fullerene-like structures, PCT Int. Appl. (2011)WO 2011161676 A1 20111229.
[22] M. Haapasalo, Y. Shen, W. Qian, Y. Gao, Irrigation in endodontics, Dent. Clin. North Am. 54 (2010) 291–312.
[23] M. Zehnder, Root canal irrigants, J. Endod. 32 (2006) 389–398.
[24] N.A. Baker, P.D. Eleazer, R.E. Averbach, S. Seltzer, Scanning electron microscopic study of the efficacy of various irrigation solutions, J. Endod. 1 (1975) 127–135.
[25] M. Torabinejad, R. Handysides, A.A. Khademi, L.K. Bakland, Clinical implications of the smear layer in endodontics: a review, Oral Surg. Oral Med. Oral Pathol. Oral Radiol. Endod. 94 (2002) 658–666.
[26] J.E. Gomes-Filho, F.O. Silva, S. Watanabe, L.T. Cintra, K.V. Tendoro, L.G. Dalto, et al., Tissue reaction to silver nanoparticles dispersion as an alternative irrigating solution, J. Endod. 36 (2010) 1698–1702.
[27] H.J. Johnston, G. Hutchison, F.M. Christensen, S. Peters, S. Hankin, V. Stone, A review of the in vivo and in vitro toxicity of silver and gold particulates: particle attributes and biological mechanisms responsible for the observed toxicity, Crit. Rev. Toxicol. 40 (2010) 328–346.
[28] T.C. Pagonis, J. Chen, C.R. Fontana, H. Devalapally, K. Ruggiero, X. Song, et al., Nanoparticle-based endodontic antimicrobial photodynamic therapy, J. Endod. 36 (2010) 322–328.
[29] A. Kishen, M. Upadya, G.P. Tegos, M.R. Hamblin, Efflux pump inhibitor potentiates antimicrobial photodynamic inactivation of *Enterococcus faecalis* biofilm, Photochem. Photobiol. 86 (6) (2010) 1343–1349.
[30] M. Upadya, A. Shrestha, A. Kishen, Role of efflux pump inhibitors on the antibiofilm efficacy of calcium hydroxide, chitosan nanoparticles, and light-activated disinfection, J. Endod. 37 (2011) 1422–1426.

[31] B.S. Chong, T.R. Pitt Ford, The role of intracanal medication in root canal treatment, Int. Endod. J. 25 (1992) 97.
[32] G. Sundqvist, D. Figdor, S. Persson, U. Sjogren, Microbiologic analysis of teeth with failed endodontic treatment and the outcome of conservative re-treatment, Oral Surg. Oral Med. Oral Pathol. 85 (1998) 86.
[33] A. Bystrom, R. Claeson, G. Sundqvist, The antibacterial effect of camphorated paramonochlorophenol, camphorated phenol, and calcium hydroxide in the treatment of infected root canals phenol, Endod. Dent. Traumatol. 1 (1985) 170–175.
[34] L. Fabricius, G. Dahlen, S.C. Holm, A.J.R. Moller, Influence of combinations of oral bacteria on periapical tissues of monkeys, Scand. J. Dent. Res. 90 (1982) 200.
[35] A. Shrestha, Z. Shi, K.G. Neoh, A. Kishen, Nanoparticulates for antibiofilm treatment and effect of aging on its antibacterial activity, J. Endod. 36 (2010) 1030–1035.
[36] Appropriateness of Care and Quality Assurance Guidelines, fouth ed., American Association of Endodontics, 2004.
[37] L.I. Grossman, Endodontic Practice, tenth ed., Lea and Febiger, Philadelphia, PA, 1981.
[38] T. Waltimo, T.J. Brunner, M. Vollenweider, W.J. Stark, M. Zehnder, Antimicrobial effect of nanometric bioactive glass 45S5, J. Dent. Res. 86 (2007) 754–757.
[39] M. Marending, W.J. Stark, T.J. Brunner, J. Fischer, M. Zehnder, Comparative assessment of time-related bioactive glass and calcium hydroxide effects on mechanical properties of human root dentin, Dent. Traumatol. 25 (2009) 126–129.
[40] D. Mohn, M. Zehnder, T. Imfeld, W.J. Stark, Radio-opaque nanosized bioactive glass for potential root canal application: evaluation of radiopacity, bioactivity and alkaline capacity, Int. Endod. J. 43 (2010) 210–217.
[41] Z.Z. Al-Khatib, R.H. Baum, D.R. Morse, C. Yesilsoy, S. Bhambhani, M.L. Furst, The antimicrobial affect of various endodontic sealers, Oral Surg. Oral Med. Oral Pathol. Oral Radiol. Endod. 70 (1990) 784–790.
[42] I. Heling, N.P. Chandler, The antimicrobial effect within dentinal tubules of four root canal sealers, J. Endod. 22 (1996) 257.
[43] L.B. Peters, P.R. Wesselink, W.R. Moorer, The fate and role of bacteria left in root dentinal tubules, Int. Endod. J. 28 (1995) 95.
[44] B.M. Briseno, B. Willerhausen, Root canal sealer cytotoxicity on human gingival fibroblasts. 1. Zinc oxide-eugenol based sealers, J. Endod. 16 (1990) 383.
[45] B.H. Sen, B. Piskin, N. Baran, The effect of tubular penetration of root canal sealers on dye microleakage, Int. Endod. J. 29 (1996) 23.
[46] A. Wennberg, D. Orstavik, Adhesion of root canal sealers to bovine dentin and gutta-percha, Int. Endod. J. 23 (1990) 13.
[47] J. Gutmann, D. Witherspoon, Obturation of the Cleaned and Shaped Root Canal System: Pathways of the Pulp, eighth ed., Mosby Elsevier, St. Louis, MS, 2002.
[48] Z. Chen, W. Wei, Z. Feng, X. Liu, X. Chen, W. Huang, K.Y. Shanghai, Development and in-vitro experiment study of bio-type root canal filling sealer using calcium phosphate cement, 16 (2007) 530–533.
[49] U. Gbureck, O. Knappe, N. Hofmann, J.E. Barralet, Antimicrobial properties of nanocrystalline tetracalcium phosphate cements, J. Biomed. Mat. Res. Part B Appl. Biomat. 83B (2007) 132–137.
[50] S.M. Masudi, J.J. Alshakhshir, A. Hassan, Apical Sealing Ability of Nano Hybrid Resin Based Endodontic Sealer: In Vitro Evaluation of New Experimental Nano Hydrodroxyapatite-Filled Epoxy Resin, first ed., Lap Lambert Academic Publishing, 2010.
[51] F.J. Harty, B.J. Parkins, A.M. Wengraf, The success rate of apicectomy. A retrospective study of 1,016 cases, Br. Dent. J. 129 (1970) 407–413.

[52] M.K. Wu, E.G. Kontakiotis, P.R. Wesselink, Long-term seal provided by some root-end filling materials, J. Endod. 24 (1998) 557–560.
[53] H. Tassery, M. Remusat, G. Koubi, W.J. Pertot, Comparison of the intraosseous biocompatibility of Vitremer and Super EBA by implantation into the mandible of rabbits, Oral Surg. Oral Med. Oral Pathol. Oral Radiol. Endod. 83 (1997) 602–608.
[54] J. Rud, V. Rud, E.C. Munksgaard, Periapical healing of mandibular molars after root-end sealing with dentin-bonded composite, Int. Endod. J. 34 (2001) 285–292.
[55] J. Rud, J.O. Andreasen, A study of failures after endodontic surgery by radiographic, histologic and stereomicroscopic methods, Int. J. Oral Surg. 1 (1972) 311–328.
[56] O. Molven, A. Halse, B. Grung, Surgical management of endodontic failures: indications and treatment results, Int. Dent. J. 41 (1991) 33–42.
[57] B.S. Chong, T.R. Pitt Ford, Root-end filling materials: rationale and tissue response, Endod. Top. 11 (2005) 114–130.
[58] M.A. Saghiri, K. Asgar, M. Lotfi, F. Garcia-Godoy, Nanomodification of mineral trioxide aggregate for enhanced physiochemical properties, Int. Endod. J. 24 (2012) (e-pub).
[59] P.S. Krishnan, M. Joshi, P. Bhargava, S. Valiyaveettil, C. He, Effect of heterocyclic based organoclays on the properties of polyimide-clay nanocomposites, J. Nanosci. Nanotechnol. 5 (2005) 1148–1157.
[60] K. Tanaka, J. Tamura, K. Kawanabe, M. Nawa, M. Uchida, T. Kokuboe, T. Nakamura, Phase stability after aging and its influence on pin-on-disk wear properties of Ce-TZP/Al2O3 nanocomposite and conventional Y-TZP, J. Biomed. Mater. Res. 67 (2003) 200–207.
[61] V. Petkov, V. Parvanov, P. Trikalitis, C. Malliakas, T. Vogt, M.G. Kanatzidis, Three-dimensional structure of nanocomposites from atomic pair distribution function analysis: study of polyaniline and (polyaniline)(0.5)V(2)O(5) × 1.0 H(2)O, J. Am. Chem. Soc. 127 (2005) 8805–8812.
[62] A. Gaboune, S.S. Ray, A. Ait-Kadi, B. Riedl, M. Bousmina, Polyethylene/clay nanocomposites prepared by polymerization compounding method, J. Nanosci. Nanotechnol. 6 (2006) 530–535.
[63] J.K. Pandey, A.P. Kumar, M. Misra, A.K. Mohanty, L.T. Drzal, R.P. Singh, Recent advances in biodegradable nanocomposites, J. Nanosci. Nanotechnol. 5 (2005) 497–526.
[64] M.S. Cho, H.J. Choi, W.S. Ahn, Enhanced electrorheology of conducting polyaniline confined in MCM-41 channels, Langmuir 20 (2004) 202–207.
[65] X.G. Li, R.R. Zhang, M.R. Huang, Synthesis of electroconducting narrowly distributed nanoparticles and nanocomposite films of orthanilic acid/aniline copolymers, J. Com. Chem. 8 (2006) 174–183.
[66] S.H. Cypes, W.M. Saltzman, E.P. Giannelis, Organosilicate-polymer drug delivery systems: controlled release and enhanced mechanical properties, J. Contr. Release 24 (2003) 163–185.
[67] S. Shaikh, A. Birdi, S. Qutubuddin, E. Lakatosh, H. Baskaran, Ann. Biomed. Eng. 35 (2007) 2130–2137.
[68] S.M. Chogle, C.F. Duhaime, A.K. Mickel, S. Shaikh, R. Reese, J.H. Bogle, et al., Preliminary evaluation of a novel polymer nanocomposite as a root-end filling material, Int. Endod. J. 44 (2011) 1055–1060.
[69] J. Beacham, S.M. Chogle, S. Shaikh, J. Phark, A.K. Mickel, J. Graves, et al., Qualitative assessment of a nanocomposite-dentin interface using scanning electron microscopy, Poster Presentation at the American Association of Endodontists Annual Session, Orlando, FL, 2009.
[70] J. Graves, S.M. Chogle, S. Shaikh, J. Phark, J. Beacham, A.K. Mickel, et al., Evaluation of bond strength of a new nano-clay enhanced retrofill polymer material in endodontics, Poster presentation at the American Association of Endodontists Annual session, Orlando, FL, 2009.
[71] D. Leung, D.A. Spratt, J. Pratten, K. Gulabivala, N.J. Mordan, A.M. Young, Chlorhexidine-releasing methacrylate dental composite materials, Biomaterials 26 (2005) 7145–7153.
[72] M.R. Modareszadeh, S.A. Chogle, A.K. Mickel, G. Jin, H. Kowsar, N. Salamat, et al., Cytotoxicity of set polymer nanocomposite resin root-end filling materials, Int. Endod. J. 44 (2011) 154–161.
[73] S. Kim, Microcirculation of the dental pulp in health and disease, J. Endod. 11 (1985) 465–471.

[74] S. Kim, Regulation of pulpal blood flow, J. Dent. Res. (1985) 590–596.
[75] Regenerative endodontics, Dent. Clin. N. Am., 2012 (in press).
[76] K.M. Galler, R.N. D'Souza, Tissue engineering approaches for regenerative dentistry, Regen. Med. 6 (2011) 111–240.
[77] D. Tziafas, K. Kondonas, Differentiation potential of dental papilla, dental pulp and apical papilla progenitor cells, J. Endod. 36 (2010) 781–789.
[78] K.M. Galler, R.N. D'Souza, J.D. Hartgerink, et al., Scaffolds for dental pulp tissue engineering, Adv. Dent. Res. 23 (2011) 333–339.
[79] E.M. Mullane, Z. Dong, C. Sedgley, et al., Effects of VEGF and FGF2 on the revasculature of severed human dental pulps, J. Dent. Res. 87 (2008) 1144–1148.
[80] H. Lovschall, M. Tummers, I. Thesleff, et al., Activation of the NOTCH signaling pathways in response to pulp capping of rat molars, Eur. J. Oral Sci. 113 (2005) 312–317.
[81] Y. Yuan, Y. Shimada, S. Ichinose, et al., Qualitative analysis of adhesive interface nanoleakage using FE-SEM/EDS, Dent. Mater. 23 (2007) 561–569.
[82] F. Fioretti, C. Mendoza-Palomares, M.C. Avoaka-Boni, et al., Nanostructured assemblies for endodontic regeneration, J. Biomed. Nanotechnol. 7 (2011) 471–475.
[83] M. Dundar, M. Ozcan, M.E. Comlekoglu, et al., Nanoleakage inhibition within hybrid layer using new protective chemicals and their effect on adhesion, J. Dent. Res. 90 (2011) 93–98.
[84] A. Mine, J. De Munck, A. Van Ende, et al., TEM characterization if a silorane composite bonded to enamel/dentin, Dent. Mater. 26 (2010) 524–532.
[85] M. Hanabusa, A. Mine, T. Kuboki, et al., TEM interfacial characterization of an experimental self-adhesive material bonded to enamel/dentin, Dent. Mater. 27 (2011) 818–824.
[86] D.S. Brauer, J.F. Gilton, G.W. Marshall, et al., Nano- and micromechanical properties of dentin: investigation if differences with tooth side, J. Biomech. 44 (2011) 1626–1629.
[87] C. Sedgely, H.H. Messer, Are endodontically treated teeth more brittle? J. Endod. 18 (1992) 332–335.
[88] R.A. Cheron, G.W. Marshall, H.E. Goodis, Nanomechannical properties of endodontically treated teeth, J. Endod. 37 (2011) 1562–1565.
[89] J.H. Kinney, S.J. Marshall, G.W. Marshall, The nanomechanical properties of human dentin: a critical review and re-evalutation of the literature, Cri. Rev. Oral Bio. Med. (2003) 13–29.
[90] A. Nazari, B. Bajaj, D. Zhang, et al., Aging and reduction in fracture toughness of human dentin, J. Mech. Behav. Biomed. Mater. 2 (2009) 550–559.
[91] R. Kanaparthy, A. Kanaparthy, The changing face of dentistry: nanotechnology, Int. J. Neuromed. 6 (2011) 2799–2804.
[92] R.A. Freitas Jr., Nanodentistry, J. Am. Dent. Assoc. 131 (2000) 1559–1565.
[93] P.E. Murray, I. About, P. Lumley, et al., Odontoblast morphology and dentin repair, J. Dent. 31 (2003) 75–82.
[94] A.J. Smith, H. Lescof, Introduction and regulation of crown dentino-genesis: embryonic events as a template for dental tissue repair? Crit. Rev. Oral Bio. Med. 12 (2001) 425–437.
[95] A.J. Smith, N. Cassidy, H. Perry, Reactionary dentinogenesis, Int. J. Dev. Biol. 39 (1995) 273–280.
[96] I.O. Smith, X.H. Liu, L.A. Smith, et al., Nanostructured polymer scaffolds for tissue engineering and regenerative medicine, Wiley Interdisc. Rev. Nanomed. Nanobiotechnol. 1 (2009) 226–236.
[97] X. Yang, F. Yang, X.F. Walboomers, et al., The performance of dental pulp stem cells on nanofibrous PCL/gelatin/nHA scaffolds, J. Biomed. Mater. Res. A 93 (2010) 247–257.
[98] J. Wang, X. Liu, J. Xiaobing, et al., The odontogenic differentiation of human dental pulp cells on nanofibrous poly(L-lacticacid) scaffolds in vitro and in vivo, Acta Biomater. 6 (2010) 3856–3863.
[99] M.J. Gupta, P.X. Ma, Nanofibrous scaffolds for dental and craniofacial applications, J. Dent. Res. 91 (2012) 227–234.

CHAPTER

22

Saliva as an Emerging Biofluid for Clinical Diagnosis and Applications of MEMS/NEMS in Salivary Diagnostics

Chamindie Punyadeera[a,b] **and Paul D. Slowey**[c]

[a]*Saliva Translational Research Group, The Australian Institute for Bioengineering and Nanotechnology,*
[b]*School of Chemical Engineering, The University of Queensland, St. Lucia, Queensland, Australia*
[c]*Oasis Diagnostics® Corporation, Vancouver, WA, USA*

CHAPTER OUTLINE

Nanobiomaterials in Clinical Dentistry.

22.1 Introduction

22.1.1 Saliva—A miracle biofluid?

Diagnostic tests based on biological fluids in general utilize blood, cerebrospinal fluid, peritoneal fluid, drainage fluid, urine, feces, and seldomly use esoteric fluids such as saliva, sweat, and tear. One may even say that saliva's popularity has suffered because it lacks "the drama of blood", the "sincerity of sweat," and the "emotional appeal of tears" [1]. With regard to obtaining sufficient sample volumes for clinical biochemical analysis, sweat and tears pose sample volume issues and urine lacks the wider acceptance by patients due to privacy issues. Therefore, saliva by default becomes the biological fluid of interest.

Human saliva offers several advantages over traditional blood-based biochemical assays for clinical diagnostics due to its noninvasiveness and stress-free sample collection, ease and multiple sampling opportunities, reduced need for sample preprocessing, minimal risk of contracting infectious organisms such as human immunodeficiency virus (HIV) and hepatitis-B virus (HEP-B), and it is an ideal biofluid for developing countries in the world due to cost-effective sample collection and processing [2–4]. In addition, saliva is an ideal biological fluid for performing clinical assays in neonates and in the elderly due to its noninvasive properties and ease of collection. The question that comes to mind then is why are there no saliva-based tests at the doctor's office or in use at the clinical pathology laboratories to date? The answer is that the translation and advancement of saliva diagnostics is hindered by two major obstacles: the analyte concentration in saliva is typically 100^{th} to 1000^{th} fold less than in blood, therefore requiring sensitive detection technologies to discern the diagnostic wealth of knowledge trapped within a saliva sample, and up until now the dearth of available technologies for sample collection and processing.

Human saliva mirrors the body's health and well-being, and most of the biomolecules that are present in blood or urine can also be found in salivary secretions [5]. A recent study by Yan et al. [6] compared the human salivary proteome to the plasma proteome by using a peptide fractionation method coupled to a cation exchange and mass spectrometry (MS) technique and revealed a total of 3020 proteins in plasma, 597 (~20%) of which were also found in human saliva. This highlights the clinical usefulness of saliva for disease detection. When using a hexapeptide library to compress the dynamic range of proteins present in saliva (i.e., to enrich low abundant proteins), Bandhakavi et al. [7] identified 2340 salivary proteins using a single analysis platform. In contrast to the plasma proteome, in which 99% of the total protein content is made up of only 22 abundant proteins [8], the 20 most abundant proteins in human whole saliva (WS) constitute only 40% of the protein content [8] This implies that it should be feasible to detect biomolecules of clinical sensitivity and specificity in saliva with ease as compared to blood.

Saliva is a clinically informative biofluid that may be useful for early disease detection, disease prognosis, and risk stratification as well as monitoring treatment response in patients facilitating easy clinical management of diseases. However, most of the current attempts to discern biomolecules in saliva that are suitable for clinical applications (i.e., technologies with high sensitivity and high specificity) are in their infancy, and have not yet been translated from a research laboratory to the clinic. As an example, researchers have developed rapid immunoassays to measure salivary C-reactive protein (CRP) levels (an acute inflammation marker that is also associated with the development of ischemic heart disease (IHD) [9,10]), to detect coronary events at an early stage [11–13].

Saliva has been used as a biological fluid for the diagnosis and prognosis of periodontal disease [14], oral cancer [15–17], diabetes [3], and autoimmune disorders [18]. In addition, researchers have identified biomarkers in saliva for the detection of early stage pancreatic cancer [19]. Streckfus et al. [20,21] measured soluble c-erbB-2 (also known as Her2/neu and is a prognostic breast cancer marker assayed in tissue biopsies from women diagnosed with malignant tumors) levels in saliva collected from breast cancer patients and concluded that it may have potential use in the initial detection and/or follow-up screening to determine the recurrence of breast cancer, thus paving the way towards personalized medicine.

The barriers to widespread implementation of salivary diagnostics are primarily (a) the lack of understanding of saliva physiology, most importantly diurnal and circadian variation of molecules present in saliva; (b) age (age-related variations have emerged, with a particular focus on the pediatric age group), gender, and genetic differences; (c) lack of understanding of the modes of molecule transportation from blood capillaries to saliva; (d) limited functional characterization of specific salivary peptides and proteins; (e) the fact that many proteins in saliva (i.e., histatins, statherins, and proline-rich peptides) are highly polymorphic and undergo post-translational modifications (PTMs) leading to large inter-individual and intra-individual variations [22]; (f) the lack of standardization of appropriate saliva sampling collection methods and proper sampling procedures with minimal influence on downstream applications [23,24]; and (g) the lack of universally accepted normalization/reference calibrators. Further adding complexity to the above-mentioned challenges is the reality that the composition of saliva can change based on diet and fluid intake [25]. It is important to minimize these variables in a clinical setting by asking participants to refrain from eating or drinking 1 h prior to donating a saliva sample to obtain similar baseline values between individuals and to report the salivary analyte/protein concentrations as a function of salivary flow rate.

22.1.2 Saliva production and bimolecular transport

Human saliva is a plasma ultra-filtrate and contains proteins that are either synthesized in situ in the salivary glands or are derived from blood. Saliva is primarily produced by three major glands (parotid, submandibular, and sublingual) and about 400 minor glands that are located within the oral cavity. A healthy adult produces 500–1500 mL of saliva in general per day, at a rate of approximately 0.5 mL/min [24], but several physiological and pathological conditions can modify saliva production quantitatively and qualitatively. Smell and taste stimulate saliva production and secretion, as do chewing, psychological and hormonal status, drugs, age, hereditary influences, oral hygiene, and physical exercise [26]. Also, the composition of saliva may be affected by many physiological variables [27], of which the most important factors are the salivary flow rate [28], the type of saliva (e.g., stimulated versus unstimulated), genetic polymorphisms [29], nature and duration of the stimulus, and circadian and circannular rhythms [30,31]. As an example, salivary cortisol levels are highest in the morning, soon after awakening and lowest in the evening and at night, and one should take this factor into consideration when interpreting salivary cortisol measurements [32,33].

Salivary glands are made up of two types of epithelial cells, and these are acinar and ductal cells. Saliva is produced in the acinar cells and stored in the salivary granules until an appropriate stimulation occurs. Upon stimulation, the salivary fluid passes from the lumen of the acinar cells to a branching network of ducts, where it is collected and enters into the oral cavity. Upon release

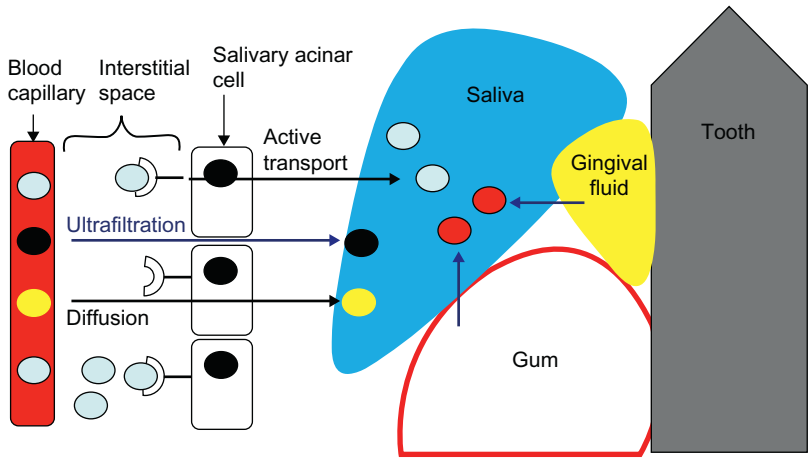

FIGURE 22.1

The transportation of biomolecules from blood capillaries (endothelium) to salivary acinar (epithelium) cells. Steroid hormones diffuse into saliva and other small molecules are filtered through the gap junctions. Large proteins are transported across the receptors present on the salivary acinar epithelial cells or through the gingival crevicular fluid.

into the oral cavity, the fluid is mixed with a number of exocrine, non-exocrine, cellular, and exogenous components, ultimately constituting WS. Human WS represents a mixture of secretions from salivary glands, gingival crevicular fluid (GCF), expectorated bronchial secretions, serum and blood cells from oral wounds, microorganisms, proteins from food debris, and desquamated epithelial cells. Therefore, the composition of WS is highly variable depending on the time and the nature of collection [34] and therefore represents a complex balance between local and systemic sources that can be of diagnostic use [35].

There are a number of mechanisms whereby molecules are transported from blood to saliva. Lipophilic molecules including steroid hormones such as testosterone, estrogens, and progesterone are transported into saliva by passive diffusion [36,37], while water and electrolytes filter from blood circulation through the pores of acinar cells. Various peptides from blood are transported through protein channels, while large proteins are transported into saliva via pinocytosis [4]. As an example, a molecule such as CRP (115 kDa) is too large to pass from the circulation to the salivary glands by diffusion or ultrafiltration [38], and it is hypothesized to enter into saliva, like many other serum proteins, as a component of GCF [39]. For a detailed description of molecular transportation mechanisms, refer to our review article [4] (see Figure 22.1 and Table 22.1).

22.2 Saliva as a biofluid for disease detection

In modern times, the early pioneers in oral diagnostics were two companies located in the Pacific Northwest region of the United States—Epitope, Inc. (Beaverton, Oregon) and Saliva Diagnostic

Table 22.1 Current Applications of Saliva in Research and/or Clinical Settings

Application	Salivary Biomolecules	References
Anxiety and stress	Cortisol and α-amylase	[40]
	3-methoxy-4-hydroxyphenylglycol	[41]
Aging	Mucin 1	[42]
	Proteomics	[43]
	Telomere length	[44]
Behavioral disorders	Testosterone	[45,46]
	Melatonin	[47]
Cancer (broader)	Breast cancer-HER-2	[48]
	Oral cancer	[17]
	Lung cancer	[49]
	Head and neck cancers	[15,50]
	Pancreatic cancer	[51]
	Prostate cancer	[52]
	Parotid tumors	[53]
Diabetes	Heat shock protein 60	[54]
	Glucose	[55]
	Matrix metalloproteinase	[56]
Environmental health	Copper levels	[57]
Fertility, infertility, and IVF	Oestradiol and progesterone	[58]
Hormone balance	Adiponectin	[59]
	DHEA	[60]
Helicobacter pylori	*Helicobacter pylori*	[61]
Inflammation	Cytokines	[62]
	C-reactive protein	[9]
Infection	Cytomegalovirus infection	[63]
	Human papilloma virus (HPV)	[64]
	Measles	[65]
	Polio	[66]
	Measles, mumps, rubella	[67]
Menopause	Salivary 17 beta estradiol	[68]
Nutrition	Moderate malnutrition (IgA)	[69]
	Zinc nutritional status (zinc concentration)	[70]
Obesity	Morbid obesity by proteomic analysis	[71]
Occupational health	Osteoarthritis	[72]
	(neuropeptides)	[73]
Physical training	Salivary IgA	[74]
	Saliva composition	[24]
Reproductive hormones	Total DHEA/free DHEA	[75]
	Estradiol	[76]
	Testosterone	[68]
Smoking status	Cotinine	[77]
		[78]
Social behavior and emotions	Salivary cortisol	[79]
	Salivary IgA	[80]

Systems, Inc. (SDS, Vancouver Washington). These two companies commercialized devices for saliva collection in the early 1990s, and these devices continue to be in widespread use for specific applications today. In addition, the products developed by these companies led to a much broader interest in saliva as a diagnostic fluid, and since then a plethora of new tools have become available that has greatly expanded the applications and opportunities for salivary diagnostics. This chapter attempts to cover the potential uses of saliva that have been explored so far and provides an indication of what can be expected in the future as the role of salivary diagnostics grows in an exponential fashion.

22.2.1 Saliva diagnostic assays in the market to date

22.2.1.1 HIV

Currently the OraSure® HIV-1 Oral Fluid Collection Device is available in conjunction with a newly FDA-approved HIV 1/2 ELISA kit from Avioq Diagnostics for laboratory HIV testing. A second oral-based test from Bio-Rad (the GS HIV 1/2 plus O ELISA) is also available for HIV diagnosis using saliva. In each case, results are confirmed by a definitive laboratory-based oral fluid (Western blot) test also manufactured by OraSure. Current markets for the OraSure HIV-1 test device include public health screening, surveillance, and a very large market in insurance risk assessment. In 2000, OraSure Technologies also launched the very first rapid diagnostic test for HIV diagnosis using oral fluid specimens. The OraQuick® HIV 1/2 device is an immunochromatographic test that delivers results in 20 min or less at the point of care. OraQuick® HIV 1/2 collects saliva around the gum line under the lip area, using a paddle-shaped device, which incorporates a proprietary test strip in the handle of the device ($>99.5\%$ sensitivity). This test may soon receive FDA approval for over-the-counter use (reference: *Washington Post*, May 14, 2012).

22.2.1.2 Drugs of abuse

OraSure Technologies is also a major player in the drugs of abuse area. The Intercept® Collection Device is used to collect saliva, which is immediately reflexed to a laboratory and tested for a range of drug entities using ELISA tests originally developed by the company. Currently, the predominant tests are the NIDA-5 series of drugs (cannabinoids (THC), opiates, amphetamines, cocaine, and phencyclidine (PCP)); however, there are now also applications for a number of drugs tested for by a variety of companies. One of the other most successful companies is Immunalysis, who provides a range of microplate ELISA assays that are optimized for oral fluid samples. Examples of other drugs of abuse in the market are tests for buprenorphine, methadone, and benzodiazepines, among others. In some cases it is parent drug that is detected, whereas in others it is a metabolite of the parent compound that is quantified. The current major applications include the workplace testing environment (including the Federal workplace), drug courts, methadone clinics, and military applications.

Newer devices are now entering the market, and these include the Versi•SAL® Saliva Collection Device (Oasis Diagnostics, www.4saliva.com, Vancouver, WA), which has been validated for use in the forensics area with ELISA test kits from Neogen Corporation (www.neogen.com, Lansing, MI) and its subsidiary company, International Diagnostic Systems (IDS, St. Joseph, MI) and the Greiner

Bio-One Saliva Collection System (www.grienerbioone.com, Vienna, Austria]. Neogen also has its own large method of collecting saliva known as UltraSal-2™, which has been validated to oral fluid specimens for multiple Neogen drug assays for the forensic market place. As well as traditional laboratory ELISA procedures, there are other technologies for drug screening that have moved to oral fluid testing. One such technology for rapid, high throughput testing is homogeneous immunoassay performed on large instrument platforms. Examples of companies providing such technologies includes Thermo Scientific (www.thermoscientific.com), who provide multiplex testing for the NIDA-5 drugs using the Oral-Eze Saliva Collection Device from Quest Diagnostics (www.questdiagnostics.com) and its own CEDIA reagents optimized for oral specimens. The Thermo Scientific reagents are optimized for a series of automated analyzers. A similar technology is available from Roche Diagnostics (www.roche-diagnostics.us), through collaboration with OraSure Technologies. In this instance, collection of specimens using the OraSure Intercept® Collection Device is followed by homogeneous immunoassay using Roche's KIMS (Kinetic Interaction of Micro-particles in Solution) technology. Four drug assays are now FDA cleared and on sale in the United States for multiple automated systems.

It is beyond the scope of this chapter to list all of the many available rapid oral drug screens, but some of the manual point-of-care tests that are available are shown in Table 22.2 for reference purposes.

There is a need and a market for roadside testing for drugs of abuse; however, currently available tools (mostly qualitative lateral flow-based systems) require additional improvements in order to provide value in law-enforcement decision making and these are as follows:

1. Improvement in the sensitivity for key drugs, for instance, marijuana (tetrahydrocannabinol, THC), where a cutoff close to the SAMHSA (Substance Abuse Mental Health Services Administration) cutoff of 4 ng/mL is needed
2. Linkage to a hand-held reading device to eliminate any subjectivity in reading test results

Table 22.2 List of Representative Rapid Oral Drugs of Abuse Tests/Manufacturers

Manufacturer	Web Site	Product Name
American Biomedica Corporation	www.abmc.com	OralStat
JAJ Scientific	www.jajinternational.com	QikTech
Innovacon (Alere)	www.innovaconinc.com	OrALert
Mavand	www.mavand.com	RapidSTAT
Envitec	www.envitec.com	SmartClip
Sun Biomedical	www.sunbiomed.com	OraLine
Branan Medical	www.brananmedical.com	Oratect XP
Ulti-med	www.ultimed.org	SalivaScreen
Varian	www.varian.com	OraLab 6
Securetec	www.securetec.net	DrugWipe 6

3. Provision of a hard copy of test results for evidentiary purposes
4. Faster acquisition of test results
5. Provision of a secondary ("B") sample for confirmation and anticorruption practices

Several companies have tried to solve the above problems and have met with limited commercial success. The most notable companies are Cozart Biosciences (United Kingdom, www.concateno.com, now Alere, Inc.), Securetec (Germany, www.securetec.net), and Mavand (Germany, www.mavand.com). While these companies have met with partial commercial success, additional improvements will allow these manufacturers to meet the requirements of an EU organization known as ROSITA (ROadSIde Testing Assessment) for use at the roadside (www.ROSITA.org). ROSITA is an independent body that evaluates all drug testing devices with potential application in law enforcement. ROSITA was set up to address the $164 billion annual cost in the European Union of "drivers who are under the influence of drugs." While all devices come under the scope of ROSITA, the strong preference is for oral-based tests that are user friendly and will be adopted by all police forces in the world.

22.2.1.3 Steroid hormones for general wellness

Saliva is an ideal medium for hormone assessment, and this has resulted in quite an "explosion" in the number of laboratories testing for specific hormones. Driven by naturopaths, herbalists, and nontraditional practicing physicians, a large and thriving market has developed where multiple laboratories provide "saliva collection kits" direct to consumers. Responding to advertisements in magazines focused on general health, nutrition, and fitness, customers are sent a kit in the regular mail that allows them to collect their own saliva (usually into a saliva cup) and send the sample back to a centralized laboratory where the results are evaluated for cortisol, testosterone, progesterone, estradiol, dehydroepiandrosterone (DHEA), and others and the results reported back to the individual as "normal" or "abnormal" together with recommendations on any follow-up actions. Perhaps this would include joining a fitness program or consulting a doctor because the level of a particular hormone is outside of the accepted "normal range," but since no diagnosis is given (just tips and recommendations related to general health status), these tests fall outside of the realm of "diagnostic tests." Among hormones tested clinically, cortisol is by far the largest due to the correlation of cortisol levels to stress and the growing hypothesis that stress is implicated in many chronic diseases, such as cardiovascular diseases, infectious diseases, and others.

Salimetrics Corporation (United States, www.salimetrics.com) has an FDA-cleared salivary cortisol (ELISA) assay kit and also sells a complete range of salivary hormone assays optimized to saliva specimens (Table 22.3).

22.2.1.4 Cotinine

Cotinine, the active metabolite of nicotine, is evaluated in smoking cessation programs and is used as a key indicator of risk in life insurance testing. Urine and salivary cotinine can be evaluated using a series of ELISA test kits. Available systems include the OraSure Collection device and

Table 22.3 Manufacturers of Salivary Hormone (ELISA) Test Kits

Company	Country	Web Site
DRG	United States	www.drg-international.com
IBL Hamburg	Germany	www.ibl-international.com
Hoelzel Diagnostika	Germany	www.hoelzel-biotech.com
Diametra	Italy	www.diametra.com
Alpco	United States	www.alpco.com
IBL America	United States	www.ibl-america.com

ELISA test kit from OraSure, the Immunalysis Quantisal™ Device and ELISA test kit, the Oasis Diagnostics® Versi•SAL® Device and Neogen/IDS ELISA microplate kits, as well as the Neogen UltraSal-2™ Collection Device and associated ELISA kit from Neogen.

22.2.1.5 Applications of saliva in molecular diagnostics

22.2.1.5.1 DNA

DNA Genotek (Ottawa, Canada, www.dnagenoetk.com) was the first company to commercialize a broad-based tool for the collection of saliva with subsequent application in genotyping, microarrays, and sequencing. Collection of (whole) mouth saliva into DNA Genotek's OraGene® device takes 10 min after which pure DNA is isolated from the stabilized sample and used in one of the above-mentioned downstream applications. Until recently, this device was used specifically for research applications; however, the device was recently cleared by the US FDA for clinical use in conjunction with the GenMark Diagnostics eSensor Assay for Warfarin sensitivity. The OraGene device has also found application in the high-profile "direct to consumer" area where companies such as 23 and Me, Navigenics, Complete Genomics, Knome, and Pathway Genomics offer "personal genome" testing to members of the public. Newer tools in this area include the DNA isolation and stabilization kits from Isohelix (www.isohelix.com) and Norgen Biotek Ontario Canada (www.norgenbiotek.com) and the DNA•SAL™ Salivary DNA Collection Device from Oasis Diagnostics® (Vancouver, United States, www.4saliva.com).

OralDNA Labs (www.oraldna.com), a subsidiary of Quest Diagnostics, offers a testing service in the United States for two tests in its Clinical Laboratory Implementation Act (CLIA)-approved testing facility in Brentwood, Tennessee. My PerioPath® is promoted as a "Salivary DNA Test that determines the risk of periodontal infections" and is based upon the detection of a series of bacterial pathogens in saliva. OraRisk HPV® is a "Salivary DNA Test that determines who is at increased risk for HPV-related oral cancers" and identifies various HPV subtypes as low, medium, or high risk as an indicator of overall risk for HPV-related oral carcinoma. Each patient gargles a solution, which harvests DNA, that is subsequently transferred by a funnel device into a transportation tube that is sent to the laboratory for downstream testing.

22.2.1.5.2 RNA

RNA can be isolated directly from saliva using a number of available "Salivary RNA Isolation" kits sold by Qiagen, GE Healthcare, Life Technologies, and others. Although the procedure to isolate RNA by this method is time consuming and costly, saliva has become a "trusted" medium for RNA research and development. There are no current tools available for direct RNA isolation; however, there are tools in development that will be useful for this purpose. Novel tools should be available within 1–2 years.

22.2.1.6 Applications of saliva in proteomics

Human saliva consists of a large number of proteins and peptides (the salivary proteome and peptidome) [81,82] that aids in maintaining oral homeostasis. Unlike the plasma proteome, the saliva proteome is highly susceptible to a variety of physiological and biochemical processes, and this presents a challenge for clinical salivary proteomics [29,83,84]. The dynamic range of proteins in saliva is another challenge. For instance, the abundant α-amylase in saliva is present at mg/mL concentrations, while the IL-6 and IL-8 cytokines of potential clinical relevance are present only at concentrations of pg/mL [85]. The saliva proteome also changes as a function of age. A loss of salivary acinar cell function was documented in healthy adults as a consequence of aging [86,87], while salivary production remained age stable in healthy adults. Such effects must be carefully considered in the development of salivary diagnostic assays, primarily by inclusion of appropriate control groups in assay development and validation.

22.2.2 Saliva research update

Saliva research expands from infectious disease detection, to dental research to assess gum diseases, to psychology and forensic sciences. As of today, a number of researchers are focusing on developing techniques and tools to discern the biomolecular composition of saliva with the aim of facilitating clinical translation. Saliva collection is a crucial step in the utilization of saliva for clinical purposes, so it is very important that saliva collection technique should not influence downstream applications. There are commercially available saliva collection devices suited for both the life science research as well as for diagnostic purposes, such as DNA Genotek (www.dnagenotek.com); Salimetrics oral swabs (http://www.salimetrics.com); Oasis Diagnostics® VerOFy®, Versi · SAL®, and DNA · SAL™ (http://www.4saliva.com); OraSure Technologies OraSure Oral Fluid Collection Device (http://www.orasure.com); Cozart® drugs of abuse collection devices (http://www.concateno.com), Immunalysis Quantisal™ Saliva Collection Device; and the Greiner Bio-One Saliva Collection System (http://www.gbo.com) [4]. These saliva sample collection technologies assist in obtaining either unstimulated or stimulated saliva.

Saliva collection procedures differ based on the type of saliva that one is interested in collecting. As an example, for ductal secretion collections, one can use Carlson–Crittenden cup [88,89] over the orifice of the Stenson's duct [90]. However, these methods are invasive and forfeit the noninvasive advantage of saliva for clinical use. It is important to determine experimentally which collection device is suited for a particular application before commencing any clinical trials. Standardization of saliva collection methods is also vital in translating saliva research from the lab to the clinic [91].

22.3 Applications of saliva for early detection of ischemic heart disease and in head and neck cancers

In this section, we will highlight a case study where saliva as a biological medium has been applied to diagnose IHD and head and neck squamous cell carcinoma (HNSCC) at an early stage.

22.3.1 Salivary C-reactive protein levels as a proxy to diagnose ischemic heart disease

C-reactive protein (CRP) is a marker of inflammation. CRP is a member of the class of acute-phase reactants that mediates innate and adaptive immunity [92]. It is produced by the hepatocytes in response to a variety of inflammatory cytokines [93] and may rise rapidly by as much as 1000-fold or more after an acute inflammatory stimulus [94]. CRP has been shown to be an independent predictor of cardiovascular events, and this biomolecule has also been proven to add prognostic value to cardiovascular risk [11,12].

We found that salivary CRP concentrations in 55 healthy volunteers ranged from 50.6 to 872.4 pg/mL. Using ranked statistical methods the derived reference interval in a healthy population was <824 pg/mL. The mean CRP level in the saliva of healthy human volunteers was 285 pg/mL and in cardiac patients was 1680 pg/mL ($P<0.01$). Analysis of CRP concentrations in paired serum and saliva samples from cardiac patients gave a positive correlation ($r^2 = 0.84$, $P<0.001$) (see Figure 22.2).

22.3.2 Salivary DNA methylation as a proxy to diagnose head and neck cancer

HNSCC is the fifth most common cancer in men with an incidence of about 780,000 new cases per year worldwide [95]. Despite advances in therapy, its prognosis has not markedly improved in the past 20 years [96]. This is mainly caused by the late diagnosis of HNSCC, when cancer cells may have metastasized to other parts of the body. HNSCC can affect the nasal passages, sinuses, mouth, throat, larynx (voice box), swallowing passages, salivary glands, and thyroid gland and arise from the surface epithelium. Tobacco use is a major risk factor for this type of cancer, and smoking kills over 1,000,000 people a year, causing 30% of all cancer-related deaths in western societies. Yet, one in three people worldwide is addicted to nicotine. In addition, 30% of HNSCC are a direct result of human papillomavirus (HPV) infections [97]. Of all HPV types, the high-risk strains HPV16 and, to a lesser extent, HPV18 are most commonly identified in oral squamous cell cancer biopsies [98].

22.3.2.1 Current clinical work flow for head and neck cancer

HNSCC detection is currently based on an expert clinical examination of the upper aerodigestive tract and histologic analysis of suspicious areas, but it may be undetectable in hidden sites, such as crypts of the tongue base or tonsils.

22.3.2.2 Current unmet clinical need in head and neck cancer patient management

At present, there are no early detection/screening tests for head and neck cancers. At the time of diagnosis of HNSCC, in 80% of the patients cancer cells may have already metastasized into other parts of the body, resulting in a low 5-year survival rate.

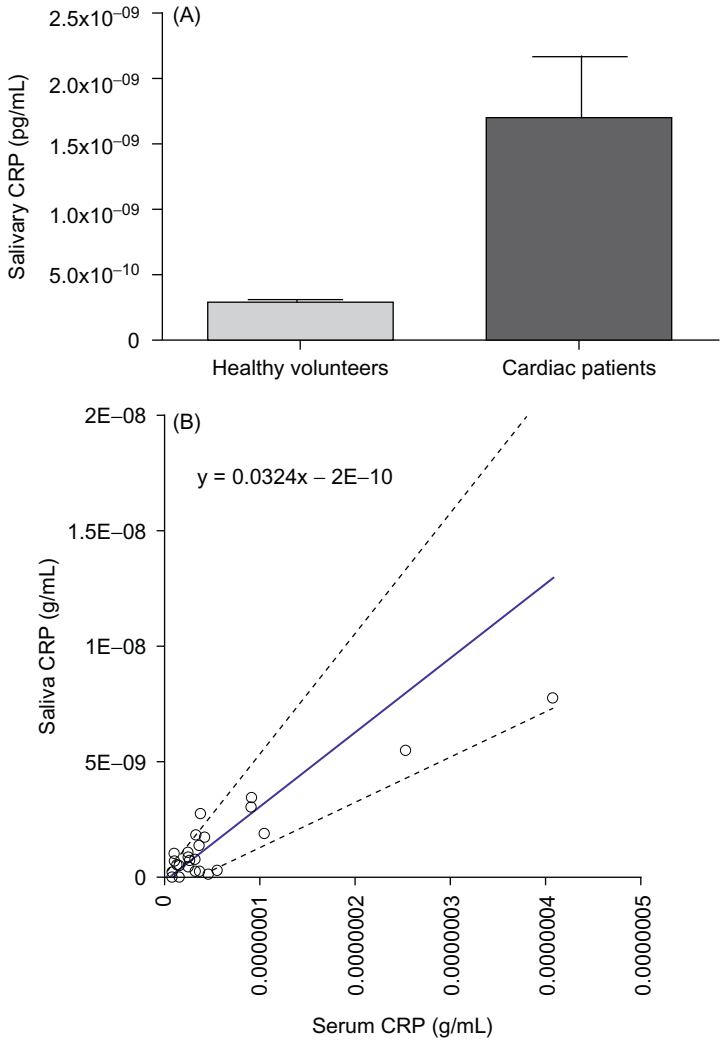

FIGURE 22.2

(A) Human salivary CRP levels in healthy volunteers ($n = 55$) and in cardiac patients ($n = 28$). (B) Correlation of salivary CRP levels to plasma CRP levels [9].

Early diagnosis of HNSCC holds the promise of improved prognosis but is currently impeded in many patients who delay seeking medical attention due to a number of factors associated with tobacco and alcohol intake. Moreover, if the tumors are tiny (unable to detect by modern cameras) and/or located in areas in the oral cavity that are not easily accessible, saliva offers the opportunity as a diagnostic medium for early detection since these tiny tumors secrete biomarkers that are indicative of a pathological condition. More so, the direct impact of smoking can clearly be seen in

the oral cavity due to its proximity; thus, human saliva is an ideal diagnostic medium for investigating smoking-related cancers.

The absence of definite early warning signs for most HNSCC suggests that sensitive and specific biomarkers are likely to be important for screening in high-risk patients [99]. DNA methylation in cells (the addition of methyl groups to cytosine residues on the DNA sequence) is an early event that occurs during tumor initiation [100]. In fact, promoter DNA hypermethylation is a more frequent mechanism of gene silencing than genetic mutation [101]. Unlike DNA mutations, DNA methylation abnormalities are reversible by drugs in a laboratory setting, and this reversal allows cancer cells to reactivate the silenced (da Silva, 2009 #3394) genes and produce tumor-suppressor proteins. Because DNA methylation normally leads to gene silencing (a negative biological event), a tumor-suppressor protein is not produced and thus protein detection methods cannot be used. For a diagnostic test to be implemented clinically, the test will ideally measure a positive event occurring in tumor cells de novo; therefore, by detecting DNA methylation in cells, one can turn a negative biological event into a positive clinical test. Understanding how abnormal DNA methylation arises in cancer cells, and how this change leads to silencing of genes, is extremely important in the development of treatments that could reverse this process as a strategy to prevent and/or treat cancer (Figures 22.3 and 22.4).

With the development of noninvasive early screening tools and strategies (such as the ones that are currently being developed in our laboratory) would enable the diagnosis of HNSCC at an earlier stage and render treatment strategies.

22.3.3 Applications of Micro Electromechanical Systems (MEMS)/Nano Electromechanical Systems (NEMS) in salivary diagnostics

Nanotechnology platforms are foreseen to change health care in a fundamental way by providing novel methods for disease diagnosis and prevention, therapeutics selection and administration, tailored to the patients' profile, drug delivery, and gene therapy. Nanotechnology is about manipulating matter atom by atom. Nanodentistry is defined as the science and technology of maintaining near-perfect oral health through the use of nanomaterials such as nano oral anesthesia inductions [102], nanodental techniques for major tooth repair, nano in-tooth repositioning, and nanorobotics [103].

Nanotechnology-based NEMS biosensors result in high sensitivity and specificity for analyte detection in complex matrices such as saliva, sensitivity of the detection system reaching down to single molecule levels. These convert (bio)chemical to electrical signal [104]. As an example, the Oral Fluid NanoSensor Test (OFNASET) technology is used for multiplex detection of salivary biomarkers for oral cancer. A previous study has demonstrated that the combination of two salivary proteomic biomarkers (thioredoxin and IL-8) [105] and four salivary mRNA biomarkers (SAT, ODZ, IL-8, and IL-1b) can be used to detect oral cancer with high specificity and sensitivity [106]. In addition, the optical nanobiosensor is a unique fiberoptics-based technology platform that allows minimally invasive analysis of intracellular components such as cytochrome c (which regulates apoptosis or programmed cell death and cellular energy production) [104]. Nanotechnology is not only providing information on diagnosing a disease but also provides treatment opportunities. As an example, BrachySilTM (Sivida, Australia) delivers 32P clinical trial for brachytherapy.

In summary, nanodentistry faces significant challenges in realizing its tremendous potential in revolutionizing the current dental care practice. Some of the obstacles in the advancement of nanodentistry

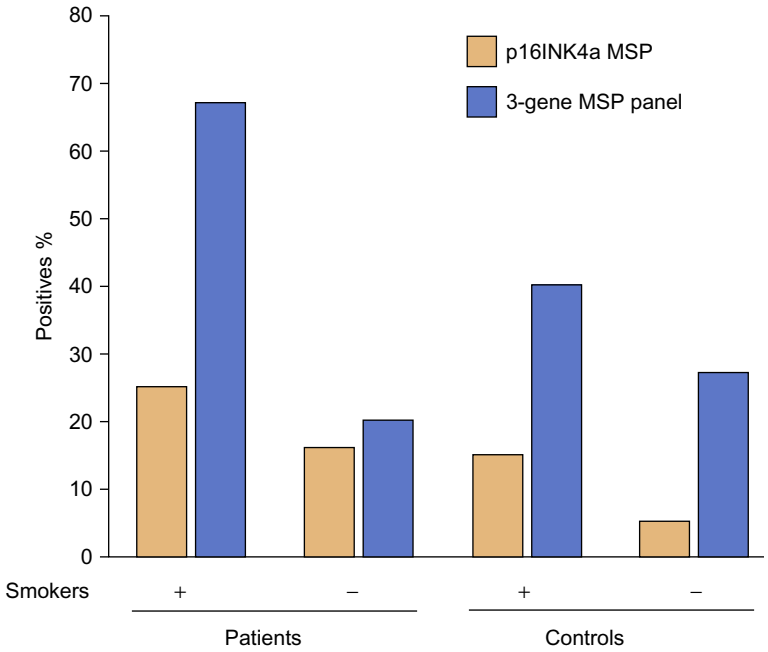

FIGURE 22.3

The DNA promoter hypermethylation of three tumor suppressor genes (DAPK1, RASSF1a, and p16) in saliva collected from a healthy control group ($n = 41$) and HNSCC patients ($n = 121$, both smokers and nonsmokers). On the *Y*-axis, if one of the genes is methylated that particular saliva sample is included in the data set [15].

include basic engineering problem from precise positioning and assembly of molecular-scale parts to biocompatibility issues, public acceptance, ethics, regulation, and human safety. When the issues raised above have been adequately addressed, nanodentistry will soon become a reality.

22.4 Future outlook and conclusions

There are many other areas where saliva may be used either as a replacement for traditional blood testing or as an adjunct to current testing methods. This section highlights some of the many possibilities that saliva may play a role in future clinical application. In each case, scholarly articles are readily available relating to the utility of saliva and serve as a solid basis for the development of future testing products. A series of biomarkers including CRP [9,23], α-amylase, and cortisol [65,66] have been used in the assessment of cardiovascular health, and rapid point-of-care test devices using saliva will in the near future be available to assess risk of CVD. In a related area LabNow, a company spearheaded by Dr. John McDevitt, a professor of biochemistry from the University of Texas at Austin, has developed a nano-biochip method that uses saliva to diagnose early heart attack. The

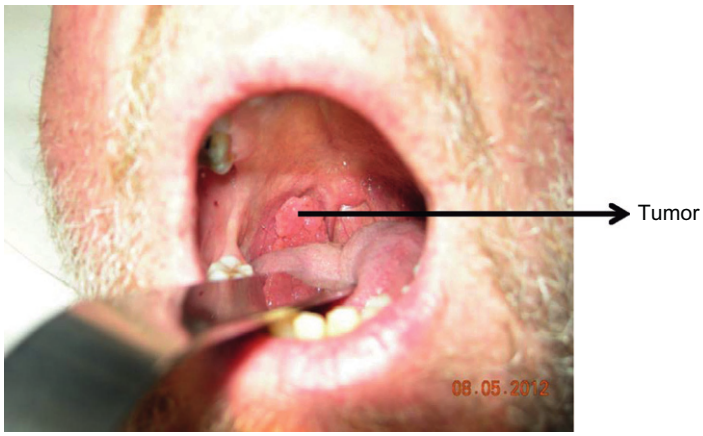

FIGURE 22.4

The patient is a 66-year-old gentleman—retired boatbuilder. He has been aware of a foreign-body sensation in the right side of his throat for up to 2 years. He had no pain, swallowing or voice problems. Dr. S. Coman staged this case as T2N0 SCC. Histology reports "moderately differentiated" squamous cell carcinoma. Stains for p16 are strongly evident.

(Photograph provided by Professor William B. Coman and Dr. S. Coman.)

method is reported to be more accurate than the standard EKG, which can miss up to 25% of potential heart attacks. In the oncology area, the use of saliva to isolate, characterize, and identify specific roles for various messenger RNAs and microRNAs has already been done, and the value of saliva as a tool to provide pure mRNA and pure miRNA for use in targeted therapies and general research will become increasingly important over the next several years. An early application for the use of miRNAs will be in the diagnosis of oral cancers, pancreatic cancer, and other malignancies, but the impact will not stop there. mRNAs and miRNAs have been reported in many disease processes, so it is expected that the role of RNA and salivary RNA in particular will expand dramatically.

Studies have also been performed confirming the detection of specific proteins such as Her-2/neu and tumor markers such as CA-125, CA 15−3 are possible, but to date no diagnostic tests have been developed using saliva specimens. Viral diseases represent another target area for salivary diagnostics with a number of major disease antibodies and antigens (hepatitis A, hepatitis B, hepatitis C, HHV-1 to HHV-8, EBV, CMV herpes, and influenza viruses) all detectable in saliva. Oral fluid samples have already proved useful in the evaluation of immunization efficacy, particularly in the developing world, where immune response to measles, mumps, polio, tetanus, and rubella vaccines have been routinely carried out. More recently, a company from the United Kingdom, MicroImmune, has developed a saliva-based point-of-care device for the detection of measles-specific IgM antibodies. The group made up of scientists from the Public Health Laboratory in Colindale (London) intend developing additional vaccine-specific rapid tests in the future.

The success of OralDNA Labs in the United States has spurred a "fever" of activity in the detection of bacterial infections using saliva specimens, and a number of companies are looking to target the dental office as the first line of attack in our general health. These companies will provide dental

tests or collection kits direct to practicing dentists, who in many instances see patients on a more routine basis than a general practice physician. In such circumstances, the dentist is well placed to identify the disease risk early on. Tests targeted for the dentist office that are in the development or available already include tests for dental caries, HPV, periodontal disease, and gingivitis.

The area of drug abuse is rapidly growing, but linked with this is an increase in the abuse of prescription drugs, particularly painkillers and antidepressants. With this comes a need to detect drug concentrations accurately and in real time. Saliva offers the best matrix in most cases to do this, and a number of companies with detection kits (ELISA tests) are evaluating options to use saliva as a specimen of choice to expand their product portfolios. As another example, the "designer" drug known as Spice (or K2) has led to several deaths in the United States and has been banned in many states. This and other such drugs will be logical targets for saliva test developers.

Lateral flow immunochromatography is a technique used to provide rapid diagnostic test results for multiple diseases using bodily fluids. Progress in manufacturing and development technology in the 1990s has been rapid, and this has resulted in the development of a whole series of rapid, point-of-care devices that initially were based upon the use of urine (the currently accepted mainstay for drug testing today) or blood specimens. In the area of drug testing, there has been a lot of work done to validate a number of multi-drug screening panels based on oral sampling. Up until now, most tests are qualitative in nature, i.e. provide a yes or no indication of drug presence. The opportunity to provide immediate results at the point-of-care using noninvasive samples is an attractive proposition; however, oral-based rapid tests for drugs of abuse have certain drawbacks that have limited the broader utilization of these devices to date. Potential problems include poor recovery of analytes (particularly marijuana (THC) from collection media), insufficient saliva delivery to the test strips, strip failure, and lack of sensitivity. Despite this, the "convenience factor" of oral testing has led to a proliferation of companies developing such tests and subsequent adoption of these tests in drug screening projects, criminal justice, employee screening, random testing, and other instances where immediate results can be beneficial. Further inroads into the market will be made once the above issues have been resolved.

Acknowledgments

The authors would like to acknowledge the financial support from the Queensland Government Smart Futures Fellowship Programme (QGSFF), the University of Queensland New Staff Research Funds (UQNSRSF 601252), and the University of Queensland Foundation Research Excellence Award Scheme. In addition, we would like to express our sincere gratitude to Professor William B. Coman and Dr. Scott Coman for providing us with the illustrations. In addition, we thank Mr. Jared Foo and Ms Ling Li Long for their technical assistance.

References

[1] D. Marmud, Saliva as a diagnostic fluid second now to blood? BMJ 305 (1992) 25.

[2] S. Hu, D.T. Wong, M. Arellano, P. Boontheing, J. Wang, H. Zhou, et al., Salivary Protein Biomarkers for Human Oral Cancer, Clin Cancer Research 14 (19) (2008) 6246–6252.

[3] P.V. Rao, A.P. Reddy, X. Lu, S. Dasari, A. Krishnaprasad, E Biggs, et al., Proteomic identification of salivary biomarkers of type-2 diabetes, J. Proteome Res. 8 (1) (2009) 239−245.
[4] T. Pfaffe, J. Cooper-White, P. Beyerlein, K. Kostner, C. Punyadeera, et al., Diagnostic potential of saliva: current state and future applications, Clin. Chem. 57 (5) (2011) 675−687.
[5] F. Bouwman, et al., 2D-electrophoresis and multiplex immunoassay proteomic analysis of different body fluids and cellular components reveal known and novel markers for extended fasting, BMC Med. Genomics 4 (1) (2011) 24.
[6] W. Yan, et al., Systematic comparison of the human saliva and plasma proteomes, Proteomics Clin. Appl. 3 (1) (2009) 116−134.
[7] S. Bandhakavi, et al., A dynamic range compression and three-dimensional peptide fractionation analysis platform expands proteome coverage and the diagnostic potential of whole saliva, J. Proteome Res. 8 (12) (2009) 5590−5600.
[8] J.A. Loo, et al., Comparative human salivary and plasma proteomes, J. Dent. Res. 89 (10) (2010) 1016−1023.
[9] C. Punyadeera, G. Dimeski, K. Kostner, P. Beyerlein, J. Cooper-White, et al., One-step homogeneous C-reactive protein assay for saliva, J. Immunol. Methods (2011).
[10] N. Christodoulides, M. Sanghamitra, M.S. Craig, L.M. Chris, N. Floriano, P.D. Priya, et al., Application of microchip assay system for the measurement of C-reactive protein in human saliva, Lab Chip 5 (3) (2005) 261−269.
[11] P.M. Ridker, C-reactive protein, inflammation, and cardiovascular disease: clinical update, Tex. Heart Inst. J. 32 (3) (2005) 384−386.
[12] P.M. Ridker, et al., Rosuvastatin to prevent vascular events in men and women with elevated C-reactive protein, N. Engl. J. Med. 359 (21) (2008) 2195−2207.
[13] H. Arima, et al., High-sensitivity C-reactive protein and coronary heart disease in a general population of Japanese: the Hisayama study, Arterioscler Thromb Vasc. Biol. 28 (7) (2008) 1385−1391.
[14] C.S. Miller, et al., Salivary biomarkers of existing periodontal disease: a cross-sectional study, J. Am. Dent. Assoc. 137 (3) (2006) 322−329.
[15] D.A. Ovchinnikov, M.A. Cooper, P. Pandit, W.B. Coman, J. Cooper-White, P. Keith, et al., Tumour-suppressor gene promoter hypermethylation in saliva of head and neck cancer patients. J. Trans. Oncol., September 2012.
[16] T. Shpitzer, et al., A comprehensive salivary analysis for oral cancer diagnosis, J. Cancer Res. Clin. Oncol. 133 (9) (2007) 613−617.
[17] D.T. Wong, Oral cancer and saliva diagnostics, in: National Oral Health Conference, 2007, Denver, CO.
[18] S. Hu, et al., Preclinical validation of salivary biomarkers for primary Sjögren's syndrome, Arthritis Care Res. 62 (11) (2010) 1633−1638.
[19] L. Zhang, J.J. Farrell, H. Zhou, D. Elashoff, D. Akin, N.-H. Park, et al., Researchers find biomarkers in saliva for detection of early-stage pancreatic cancer, Gastroenterology, (138) (2010) 949−957.
[20] C.F. Streckfus, et al., The presence of soluble c-erbB-2 in saliva and serum among women with breast carcinoma: a preliminary study, Clin. Cancer Res. 6 (6) (2000) 2363−2370.
[21] C.F. Streckfus, et al., Breast cancer related proteins are present in saliva and are modulated secondary to ductal carcinoma in situ of the breast, Cancer Invest. 26 (2) (2008) 159−167.
[22] M. Castagnola, P.M. Picciotti, I. Messana, C. Fanali, A. Fiorita, T. Cabras, et al., Potential applications of human saliva as diagnostic fluid, Acta Otorhinolaryngol Ital. 31 (6) (2011) 347−357.
[23] E. Topkas, et al., Evaluation of saliva collection devices for the analysis of proteins, Clin. Chim. Acta 413 (13−14) (2012) 1066−1070.
[24] J.L. Chicharro, et al., Saliva composition and exercise, Sports Med. 26 (1) (1998) 17−27.

[25] M.A. Anzano, A.J. Lamb, J.A. Olson, Impaired salivary gland secretory function following the induction of rapid, synchronous vitamin A deficiency in rats, J. Nutr. 111 (3) (1981) 496–504.
[26] N.P. Walsh, et al., Saliva flow rate, total protein concentration and osmolality as potential markers of whole body hydration status during progressive acute dehydration in humans, Arch. Oral Biol. 49 (2) (2004) 149–154.
[27] D.B. Ferguson, Current diagnostic uses of saliva, J. Dent. Res. 66 (2) (1987) 420–424.
[28] C. Dawes, Salivary flow patterns and the health of hard and soft oral tissues, J. Am. Dent. Assoc. 139 (Suppl. 2) (2008) 18S–24S.
[29] F.G. Oppenheim, et al., Salivary proteome and its genetic polymorphisms, Ann. N.Y. Acad. Sci. 1098 (2007) 22–50.
[30] I.D. Mandel, et al., Salivary studies in cystic fibrosis, Am. J. Dis. Child. 113 (4) (1967) 431–438.
[31] I.D. Mandel, Relation of saliva and plaque to caries, J. Dent. Res. 53 (2) (1974) 246–266.
[32] A.M. Hansen, A.H. Garde, R. Persson, Measurement of salivary cortisol—effects of replacing polyester with cotton and switching antibody, Scand. J. Clin. Lab. Invest. 68 (8) (2008) 826–829.
[33] A.M. Hansen, A.H. Garde, R. Persson, Sources of biological and methodological variation in salivary cortisol and their impact on measurement among healthy adults: a review, Scand. J. Clin. Lab. Invest. 68 (6) (2008) 448–458.
[34] E.J. Helmerhorst, F.G. Oppenheim, Saliva: a dynamic proteome, J. Dent. Res. 86 (8) (2007) 680–693.
[35] L. Caporossi, A. Santoro, B. Papaleo, Saliva as an analytical matrix: state of the art and application for biomonitoring, Biomarkers 15 (6) (2010) 475–487.
[36] M. Groschl, Current status of salivary hormone analysis, Clin. Chem. 54 (11) (2008) 1759–1769.
[37] M. Groschl, The physiological role of hormones in saliva, Bioessays 31 (8) (2009) 843–852.
[38] D.A. Granger, et al., Integration of salivary biomarkers into developmental and behaviorally-oriented research: problems and solutions for collecting specimens, Phys. Behav. 92 (4) (2007) 583–590.
[39] E. Megson, et al., C-reactive protein in gingival crevicular fluid may be indicative of systemic inflammation, J. Clin. Periodontol. 37 (9) (2010) 797–804.
[40] Y. Tanaka, et al., Salivary alpha-amylase and cortisol responsiveness following electrical stimulation stress in major depressive disorder patients, Prog. Neuropsychopharmacol. Biol. Psychiatry 36 (2) (2012) 220–224.
[41] S. Yamada, et al., Saliva level of free 3-methoxy-4-hydroxyphenylglycol (MHPG) as a biological index of anxiety disorders, Psychiatry Res. 93 (3) (2000) 217–223.
[42] W.-I. Chang, et al., MUC1 expression in the oral mucosal epithelial cells of the elderly, Arch. Oral Biol. 56 (9) (2011) 885–890.
[43] K.S. Ambatipudi, et al., Quantitative analysis of age specific variation in the abundance of human female parotid salivary proteins, J. Proteome Res. 8 (11) (2009) 5093–5102.
[44] E.J. Giltay, et al., Salivary testosterone: associations with depression, anxiety disorders, and antidepressant use in a large cohort study, J. Psychosomatic. Res. 72 (3) (2012) 205–213.
[45] I. Paclt, et al., Circadian rhythms of saliva melatonin in ADHD, anxious and normal children, Neuro Endocrinol. Lett. 32 (6) (2011) 790–798.
[46] M. Novakova, et al., Salivary melatonin rhythm as a marker of the circadian system in healthy children and those with attention-deficit/hyperactivity disorder, Chronobiol. Int. 28 (7) (2011) 630–637.
[47] C.F. Streckfus, D. Arreola, C. Edwards, L. Bigler, Salivary protein profiles among HER2/neu-receptor-positive and -negative breast cancer patients: support for using salivary protein profiles for modeling breast cancer progression, J. Oncol. 2012 (2012) 9.
[48] S. Punyani, R. Sathawane, Salivary level of interleukin-8 in oral precancer and oral squamous cell carcinoma, Clin. Oral Invest. (2012) 1–8.

[49] X. Li, T. Yang, J. Lin, Spectral analysis of human saliva for detection of lung cancer using surface-enhanced Raman spectroscopy, J. Biomed. Opt. 17 (2012) 3.
[50] T. Jarai, et al., Mass spectrometry-based salivary proteomics for the discovery of head and neck squamous cell carcinoma, Pathol. Oncol. Res. 18 (3) (2012) 623–628.
[51] L. Zhang, J.J. Farrell, H. Zhou, D. Elashoff, D. Akin, N.-H. Park, et al., Salivary transcriptomic biomarkers for detection of resectable pancreatic cancer, Gastroenterology 38 (2010) 949–957.
[52] N. Shiiki, et al., Association between saliva PSA and serum PSA in conditions with prostate adenocarcinoma, Biomarkers 16 (6) (2011) 498–503.
[53] G. Dyckhoff, et al., Carbohydrate antigen 19–9 in saliva, Otolaryngol. Head Neck Surgery 145 (5) (2011) 772–777.
[54] J. Yuan, P. Dunn, R.D. Martinus, Detection of Hsp60 in saliva and serum from type 2 diabetic and non-diabetic control subjects, Cell Stress Chaperones 16 (6) (2011) 689–693.
[55] A.C.U. Vasconcelos, et al., Comparative study of the concentration of salivary and blood glucose in type 2 diabetic patients, J. Oral Sci. 52 (2) (2010) 293–298.
[56] P.P. Costa, et al., Salivary interleukin-6, matrix metalloproteinase-8, and osteoprotegerin in patients with periodontitis and diabetes, J. Periodontol. 81 (3) (2009) 384–391.
[57] T. Thompson, et al., Copper levels in buccal cells of vineyard workers engaged in various activities, Ann. Occup. Hyg. 56 (3) (2012) 305–314.
[58] Y.F. Wong, L.E. Mao, K.R. Tam, P.P. Panesar, N.S. Neale, E. Chang, et al., Salivary oestradiol and progesterone after in vitro fertilization and embryo transfer using different luteal support regimens, Reprod. Fertil Dev. 2 (4) (1990) 351–358.
[59] E.-N. Akuailou, P. Vijayagopal, V. Imrhan, C. Prasad, Measurement and validation of the nature of salivary adiponectin, Acta Diabetol. 15 (1) (2012) 110–114.
[60] A. Oskis, A. Clow, L. Thorn, C. Loveday, F. Hucklebridge, Diurnal patterns of salivary cortisol and DHEA in adolescent anorexia nervosa, Stress 15 (6) (2012) 601–607.
[61] H. Momtaz, et al., Study of *Helicobacter pylori* genotype status in saliva, dental plaques, stool and gastric biopsy samples, World J. Gastroenterol. 18 (17) (2012) 2105–2111.
[62] K. Szczeklik, D. Owczarek, J. Pytko-Polończyk, B. Kęsek, T.H. Mach, Proinflammatory cytokines in the saliva of patients with active and non-active Crohn's disease, Pol. Arch. Med. Wewn. April 24 (2012) (pii: AOP79).
[63] E.J. Plosa, et al., Cytomegalovirus infection, Pediatr. Rev. 33 (4) (2012) 156–163 (quiz 163).
[64] D.O. Turner, et al., High-risk human papillomavirus (HPV) screening and detection in healthy patient saliva samples: a pilot study, BMC Oral Health 11 (2011) 28.
[65] R. Dantzer, N. Kalin, Psychoneuroendocrinology 34 (1) (2009).
[66] E.A. Shirtcliff, D.A. Granger, E. Schwartz, M.J. Curran, Use of salivary biomarkers in biobehavioral research: cotton-based sample collection methods can interfere with salivary immunoassay results. Psychoneuroendocrinology 26 (2) (2001) 165–173.
[67] D.J. Nokes, et al., Has oral fluid the potential to replace serum for the evaluation of population immunity levels? A study of measles, rubella and hepatitis B in rural Ethiopia, Bull. World Health Org. 79 (7) (2001) 588–595.
[68] F. Agha-Hosseini, et al., Relationship of stimulated saliva 17beta-estradiol and oral dryness feeling in menopause, Maturitas 62 (2) (2009) 197–199.
[69] D.N. McMurray, et al., Effect of moderate malnutrition on concentrations of immunoglobulins and enzymes in tears and saliva of young Colombian children, Am. J. Clin. Nutr. 30 (12) (1977) 1944–1948.
[70] T. Hovi, M. Stenvik, Selective isolation of poliovirus in recombinant murine cell line expressing the human poliovirus receptor gene, J. Clin. Microbiol. 32 (5) (1994) 1366–1368.
[71] R.S. Hobson, Challenges to future dental education, Br. Dent. J. 206 (3) (2009) 125–126.

[72] V.J. Howard, et al., Does sex matter? Thirty-day stroke and death rates after carotid artery stenting in women versus men: results from the Carotid Revascularization Endarterectomy versus Stenting Trial (CREST) lead-in phase, Stroke 40 (4) (2009) 1140–1147.
[73] H.P. Fischer, W. Eich, I.J. Russell, A Possible Role for Saliva as a Diagnostic Fluid in Patients with Chronic Pain, Elsevier, Seminars in Arthritis and Rheumatism 26 (6) 1998 348–359.
[74] V. Neville, M. Gleeson, J.P. Folland, Salivary IgA as a risk factor for upper respiratory infections in elite professional athletes, Med. Sci. Sports Exercise 40 (7) (2008) 1228.
[75] L.M. Swinkels, et al., Concentrations of total and free dehydroepiandrosterone in plasma and dehydroepiandrosterone in saliva of normal and hirsute women under basal conditions and during administration of dexamethasone/synthetic corticotropin, Clin. Chem. 36 (12) (1990) 2042–2046.
[76] C.M. Worthman, J.F. Stallings, L.F. Hofman, Sensitive salivary estradiol assay for monitoring ovarian function, Clin. Chem. 36 (10) (1990) 1769–1773.
[77] R.E. Latchaw, et al., Recommendations for imaging of acute ischemic stroke: a scientific statement from the American Heart Association, Stroke 40 (11) (2009) 3646–3678.
[78] G.P. Harris, et al., Three distinct amine receptors operating at different levels within the locomotory circuit are each essential for the serotonergic modulation of chemosensation in Caenorhabditis elegans, J. Neurosci. 29 (5) (2009) 1446–1456.
[79] R.P. Hobson, et al., How mothers with borderline personality disorder relate to their year-old infants, Br. J. Psychiatry 195 (4) (2009) 325–330.
[80] E.F. Nsutebu, R. Hobson, Is combination systemic therapy superior to monotherapy for enterococcal prosthetic joint infection? Clin. Infect. Dis. 48 (4) (2009) 495 (author reply 495–6).
[81] B.L. Schulz, J. Cooper-White, C.K. Punyadeera, Saliva proteome research: current status and future outlook, Crit. Rev. Biotechnol. (2012).
[82] C.-M. Huang, Comparative proteomic analysis of human whole saliva, Arch. Oral Biol. 49 (12) (2004) 951–962.
[83] C. Dawes, Considerations in the development of diagnostic-tests on saliva, Ann. N.Y. Acad. Sci. 694 (1993) 265–269.
[84] J.R. Whiteaker, et al., A targeted proteomics-based pipeline for verification of biomarkers in plasma, Nat. Biotechnol. 29 (7) (2011) 625–634.
[85] M.A. St John, et al., Interleukin 6 and interleukin 8 as potential biomarkers for oral cavity and oropharyngeal squamous cell carcinoma, Arch. Otolaryngol. Head Neck Surg. 130 (**8**) (2004) 929–935.
[86] E.M. Ghezzi, J.A. Ship, Aging and secretory reserve capacity of major salivary glands, J. Dent. Res. 82 (10) (2003) 844–848.
[87] A. Westermark, et al., Basic fibroblast growth factor in human saliva decreases with aging, Laryngoscope 112 (5) (2002) 887–889.
[88] M. Navazesh, S.K.S. Kumar, Measuring salivary flow: challenges and opportunities, J. Am. Dent. Assoc. 139 (Suppl. 2) (2008) 35S–40S.
[89] A.J. Carlson, A.L. Crittenden, The relation of ptyalin concentration to the diet and to the rate of secretion of the saliva, Am. J. Physiol. 26 (1) (1910) 169–177 (Legacy Content).
[90] M.W. Heft, B.J. Baum, Basic biological sciences unstimulated and stimulated parotid salivary flow rate in individuals of different ages, J. Dent. Res. 63 (10) (1984) 1182–1185.
[91] Mohamed, J.-L. Campbell, J. Cooper-White, G. Dimeski, C. Punyadeera, The impact of saliva collection and processing methods on CRP, IgE, and myoglobin immunoassays, J. Clin. Trans. Med. September, 5, (2012).
[92] S. Chomdej, et al., Detection of SNPs and linkage and radiation hybrid mapping of the porcine C-reactive protein (CRP) gene, Anim. Genet. 35 (6) (2004) 469–470.
[93] T.W. Du Clos, Function of C-reactive protein, Ann. Med. 32 (4) (2000) 274–278.

[94] S. Black, I. Kushner, D. Samols, C-reactive protein, J. Biol. Chem. 279 (47) (2004) 48487−48490.
[95] R. Sankaranarayanan, et al., An overview of cancer survival in developing countries, IARC Sci. Publ. (145) (1998) 135−173.
[96] A. Forastiere, et al., Head and neck cancer, N. Engl. J. Med. 345 (26) (2001) 1890−1900.
[97] D. Turner, et al., High-risk human papillomavirus (HPV) screening and detection in healthy patient saliva samples: a pilot study, BMC Oral Health 11 (1) (2011) 28.
[98] P. Goon, et al., HPV & head and neck cancer: a descriptive update, Head Neck Oncol. 1 (1) (2009) 36.
[99] Y. Li, et al., Salivary transcriptome diagnostics for oral cancer detection, Clin. Cancer Res. 10 (24) (2004) 8442−8450.
[100] R. Guerrero-Preson, et al., Global DNA methylation: a common early event in oral cancer cases with exposure to environmental carcinogens or viral agents, P. R. Health Sci. J. 28 (1) (2009) 24−29.
[101] P.M. Das, R. Singal, DNA methylation and cancer, J. Clin. Oncol. 22 (22) (2004) 4632−4642.
[102] P.E. Chandra Mouli, S. Manoj Kumar, S. Parthiban, Nanotechnology in dentistry—a review, Int. J. Biol. Med. Res. 3 (2) (2012) 1550−1553.
[103] R. Freitas Jr, Nanodentistry, J. Am. Dent. Assoc. 131 (11) (2000) 1559−1563.
[104] Y. Li, P. Denny, C.M. Ho, The oral fluid MEMS/NEMS Chip (OFMNC): diagnostic and translational applications, Adv. Dent. Res. 18 (2005) 3−5.
[105] M. Sundaram, Nanodentistry: a step ahead, JIDAT 4 (2012) 23−26.
[106] V. Gau, D. Wong, Oral fluid nanosensor test (OFNASET) with advanced electrochemical-based molecular analysis platform, Ann. N.Y. Acad. Sci. 1098 (2007) 401−410.

CHAPTER

Nanoparticles as Dental Drug-Delivery Systems

23

E. Piñón-Segundo[a], **N. Mendoza-Muñoz**[b] **and D. Quintanar-Guerrero**[b]

[a]*Laboratorio de Sistemas Farmacéuticos de Liberación Modificada (L-13), Unidad de Investigación Multidisciplinaria, Facultad de Estudios Superiores Cuautitlán, Universidad Nacional Autónoma de México, Estado de México, México.*

[b]*Laboratorio de Investigación y Posgrado en Tecnología Farmacéutica, Facultad de Estudios Superiores Cuautitlán, Universidad Nacional Autónoma de México, Estado de México, México.*

CHAPTER OUTLINE

23.1 Introduction

Until a few decades ago, it was uncommon to find words with the prefix *nano* (e.g., nanotechnology, nanomaterials, nanoparticles, nanoemulsions, and nanotubes). It is highly noticeable how the word *nano* has been dynamically incorporated into our scientific language and even into our day-to-day life. This can be explained by the evident advantages of working at nanoscale level compared with the traditional micro/macroscale level. The term *nanotechnology* was used for the first time in 1974 by Norio Taniguchi to describe the intimate engineering (atoms or molecules) of the matter. However, the basic and inspirational rules of nanotechnology probably come from the historical lecture *There is plenty of room at the bottom* given by Richard Feynman in the meeting of the American Physical Society in 1959. In this conference, Feynman established that there is no physical restriction that prevents tiny particles assembling, like several processes in nature. He pointed out that miniaturization is a challenge to be solved in the near future, and that it will be possible by assembling systems atom by atom. Due to these nearly prophetic predictions, Feynman is considered

by several scientific groups as the father of nanotechnology. It is important to point out that many current researchers are focused on bringing into reality the Feynman's "futuristic" ideas [1–3].

Nano comes from the Greek term *nanos*, which means "dwarf," and refers to things whose dimensions are a billion-fold smaller than the precedent unit, e.g., 1 nm represents a thousandth of a thousandth of a thousandth (0.000,000,001 or 10^{-9}) part of 1 m. It is important to point out that nature has designed several biological systems, including structures of the oral cavity, within the nanometer range. Figure 23.1 shows the different scales (macro-, micro- and nanoscale) and the dimensional sizes of some representative dental materials [4,5]. A nanometer is so small that it is very difficult to conceptualize it. Light microscopy cannot observe a nanosystem in its real size and the use of high-resolution microscopies is necessary (e.g., scanning or transmission electron microscopy, atomic force microscopy, scanning probe microscopy, etc.).

A material at the nanoscale is expected to have different properties and behavior than larger particles due to the fact that nanosystems have a much greater surface area. Less material can be used for specific important technological, economic, and environmental applications. The large surface area causes nanosystems to be more reactive than larger particles and some of the fundamental

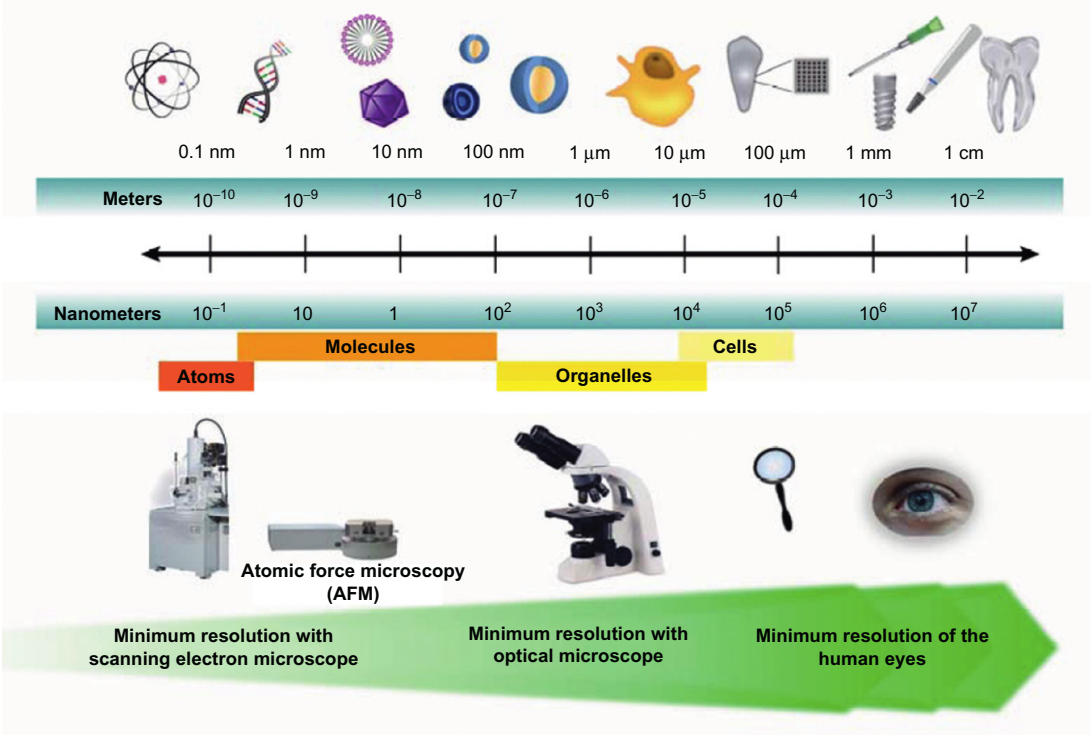

FIGURE 23.1

Representation of macro-, micro-, and nanoscales and the dimensional sizes of some representative dental systems.

chemical and physical properties change (e.g., transparency, color, and conductivity). In dentistry, these properties are beginning to be used to prepare more efficient materials and devices. Furthermore, the development of dental products tends toward more microscopic aspects; therefore, nanotechnology is positioning itself as a tool for important dental applications [6,7].

Several authors use the expression "top-down" to describe the preparation of nanosystems by the rupture (e.g. milling) of a material block. The expression "bottom-up" however relates to the fabrication of nanosystems by the assembly of basic components such as atoms or molecules [8,9]. The idea of encapsulating substances into nanosystems has different purposes; it can serve as a protection capable of preserving the functionality and bioavailability of encapsulated substances. Furthermore, encapsulation can be used for controlled release. Encapsulation can also modify the physical characteristics of the original material thus extending the therapeutic effect next to, or directly in contact with, the target site [10–12]. Representative nanomaterials used in dentistry are shown in Figure 23.2.

Nanocrystals are formed by the "top-down" approach using energy-intensive processes, where the active ingredient is directly fragmented (e.g., ball milling, high-shear homogenization, and ultrasonication) into submicron size from the bulk material [44]. Nanocrystals of potassium nitrate, poorly water-soluble calcium salts, calcium fluoride, and carbonate-substituted hydroxyapatite have been proposed as active substances for the treatment of dentine sensitivity, remineralization of tooth surfaces, and caries inhibition. These nanocrystals can be formulated as compounds for oral or dental hygiene such as solutions, suspensions, oils, resins, or other solid products. The enhanced effect of nanocrystals compared with their powders can be explained by their tiny size, which enables the nanocrystals to infiltrate and permeate the micronsized dentinal tubules or porous surfaces of the teeth forming a therapeutic depot [13,14,16,17].

Metal nanoparticles are submicron scale entities made of pure metals (e.g., gold, platinum, silver, titanium, zinc, cerium, iron, and thallium) or their compounds (e.g., oxides, hydroxides, sulfides, phosphates, fluorides, and chlorides) [44,45]. One of the most documented nanosystems in dentistry is silver nanoparticles. Due to their small size, they have a large area available for oxidation [38]. Silver nanoparticles, either as dispersion or incorporated into different materials, have shown different properties and applications in dental practice as antimicrobials, caries inhibitors, dental restorative materials, endodontic retrofilling cement, dental implants, and intraoral devices to prevent microbial accumulation (e.g., mouth guards) [33,38]. Metal oxide nanoparticles also have important dental applications. For example, Sevinç et al. [34] showed the antibacterial activity of zinc oxide nanoparticles by reducing the biofilm growth or plaque accumulation when they were included at 10% w/w in a resin-based formulation. Elsaka et al. [35] evaluated the addition of titanium oxide nanoparticles to a conventional glass ionomer and confirmed their potent antibacterial effect. Gold nanoparticles have also showed high bactericidal activity by a synergistic action with gallic acid. This promising antibacterial effect has attracted considerable interest from researchers and pharmaceutical companies due to their high microbial resistance to antibiotics and the development of resistant strains [31]. An interesting property of metal oxides is their photocatalytic capacity, which can be improved by increasing the surface area [10]. A recent patent [37] described the use of zinc oxide and titanium dioxide nanoparticles as bleaching agents. The dispersion is applied on the teeth and activated by a light source inducing a photocatalytic reaction promoting the bleaching. Similar results have been reported for selenium nanoparticles, which also removed smoking-induced dental stains and calculus [46]. An interesting approach with metal nanoparticles

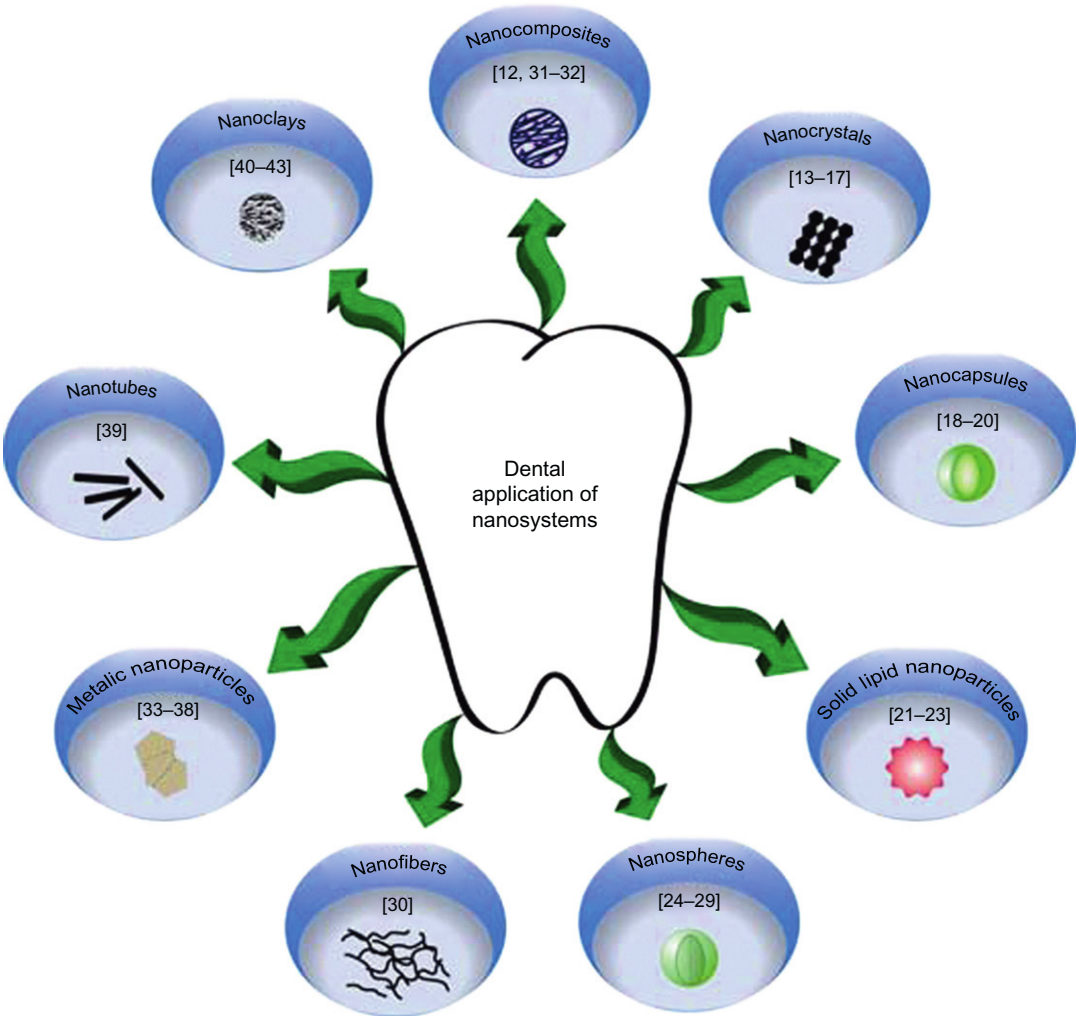

FIGURE 23.2

Examples of nanosystems with dental applications [13–43].

was proposed by Nagano et al. [41], who used platinum nanoparticles to prolong and increase the adhesive properties between tooth structure and adhesive resin. The administration of platinum nanoparticles before the application of composite resin prolonged bond durability by creating a higher conversion at the interface compared with conventional bonding procedures. Other effects attributed to metallic nanoparticles (e.g., zinc oxide nanoparticles) include antiplaque and antiodor effects, enhanced strength, and lower polymerization shrinkage, in addition to providing a good appearance and an esthetic surface [36,45].

Although nanotubes are some of the most thoroughly studied nanomaterials with important applications in several fields, their use in dentistry is still limited. Considering their extraordinary mechanical properties and ultra-high-tensile strength, carbon nanotubes have been proposed as composites in different formulations (e.g., dental resins). Zhang et al. [39] included single-walled carbon nanotubes coated with a thin shell of nano-SiO_2 in dental resin-based composites. It was concluded that the composite with modified carbon nanotubes exhibited an improved flexural strength. A similar use has been reported for TiO_2 nanotubes when introduced into alloys for dental materials. Recently, Ma et al. [47] proposed a sophisticated system with Ag nanoparticles/fibroblast growth factor 2 (FGF-2) deposited on a TiO_2 nanotubular surface, which has a large potential for use in dental implant abutment.

Nanoclays (natural silica) and their modified varieties (organoclays) are commonly used in dental products (e.g., toothpaste abrasives). Essentially they are nontoxic and nonirritant when used orally. In the last decade, silica nanoparticles (e.g., available under the trade names Aerosil (Degussa), HDK (Wacker), Cab-O-Sil (Cabot Corp.)) have been proposed as nanoscale fillers to enhance dental resins [40]. They can improve the rheological behavior, scratch/abrasion resistance, and surface hardness of the final products [41]. Gaikwad et al. [48] studied the roughness of the polished surfaces using atomic force microscopy after the use of different polishing materials, including silica nanoparticles. Significantly lower nanometer-scale roughness was obtained when silica nanoparticles were used to polish tooth surfaces, compared with conventional polishing pastes. Furthermore, silica nanoparticles are efficient at removing bacteria (e.g., *Streptococcus mutans*) from the polished areas. Silica nanoparticles demonstrate improved fixation of dental prostheses by increasing the strength, the adhesive ability and the resistance to oral fluid impact, and by reducing film thickness and heat emission in formulations based on zinc−phosphate cement [49]. Recently, an invention proposed by Müller and Wiens [43] combined hydroxyapatite and nano- or microspheres (e.g., silica) bound by an oligopeptide which can be used for sealing dental pits, fissures, and dentinal tubules to prevent tooth decay formation and to reduce dentin hypersensivity.

23.2 Definitions

The term nanoparticles will be used as the collective name to describe both nanospheres and nanocapsules [50] which differ in their morphology and architecture. Nanospheres are formed by a dense polymeric matrix, whereas nanocapsules are composed of an oil core surrounded by a polymeric membrane (see Figure 23.3). Nanoparticles show several advantages in relation to other materials including colloids used in the dental field, such as (i) better stability in biological fluids and during storage, (ii) easy preparation and diversity in preparation techniques, (iii) easy large-scale manufacturing, (iv) batch-to-batch reproducibility, and (v) controlled release. Nanoparticles also satisfy the purpose of encapsulating and delivering active substances to a target site (e.g., the dentogingival sac) known as carriers or vectors. Solid lipid nanoparticles and nanostructured lipid carriers are attractive modalities of nanoparticles. Both systems are solid at both room and body temperatures and are highly suitable for carrying lipophilic substances. Solid lipid nanoparticles are constituted only of solid lipids and nanostructured lipid carriers contain solid lipids and oils which increase their capacity to load active substances. The reasons for using lipids are their low toxicity, high biodegradability, and the possibility of modifying the bioavailability of some active substances [51].

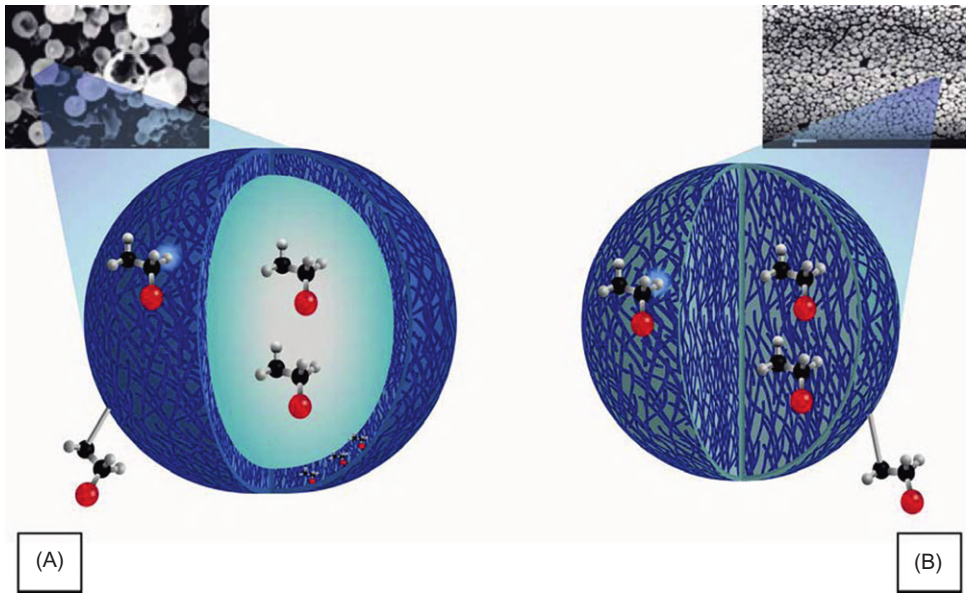

FIGURE 23.3

Schematic representation and microphotographies of nanoparticles: (A) nanocapsules and (B) nanospheres.

The "top-down" approach to prepare nanoparticles requires more process steps and, consequently, more control of the preparative variables. The materials are generally dissolved in a solvent to achieve a molecular solution that can be precipitated by solvent changes, e.g., pH, temperature, and addition of a nonsolvent, thus reducing its solubility. It is possible to prepare nanoparticles by polymerization of dispersed monomers, but their byproducts may not be completely biocompatible and toxic residues such as monomers, oligomers, and catalysts may persist. Consequently, their use in dental formulations is restricted. In general, it is preferable to use preformed materials, especially when polymers are involved. In this sense, another "top-down" technique is to disperse the molecular solution in an aqueous solution containing stabilizer in order to obtain a nanoemulsion, which by solvent removal forms nanoparticles. The nanoparticle preparation methods with high potential in dentistry from preformed polymers can be classified into five categories: (i) emulsification evaporation, (ii) salting out, (iii) solvent displacement, (iv) emulsification diffusion, and (v) spray drying [50]. They are summarized in Figure 23.4. These techniques have been broadly discussed elsewhere [50,52]. One of the main problems with these techniques is the poor encapsulation of water-soluble materials, which separate from the organic phase into the continuous aqueous phase. A double emulsion technique can be used to overcome this drawback.

In the case of solid lipid nanoparticles, the preferred method is high-pressure homogenization (HPH), in which high-efficiency devices are used to disperse the lipid in a stabilizer solution at high shear forces, breaking the particles into submicron sizes. This technique has two modalities: hot and cold homogenization (H-HPH and C-HPH); in both cases, if an active substance is included, it is necessary to melt the lipid to incorporate the drug (Figure 23.5) [51].

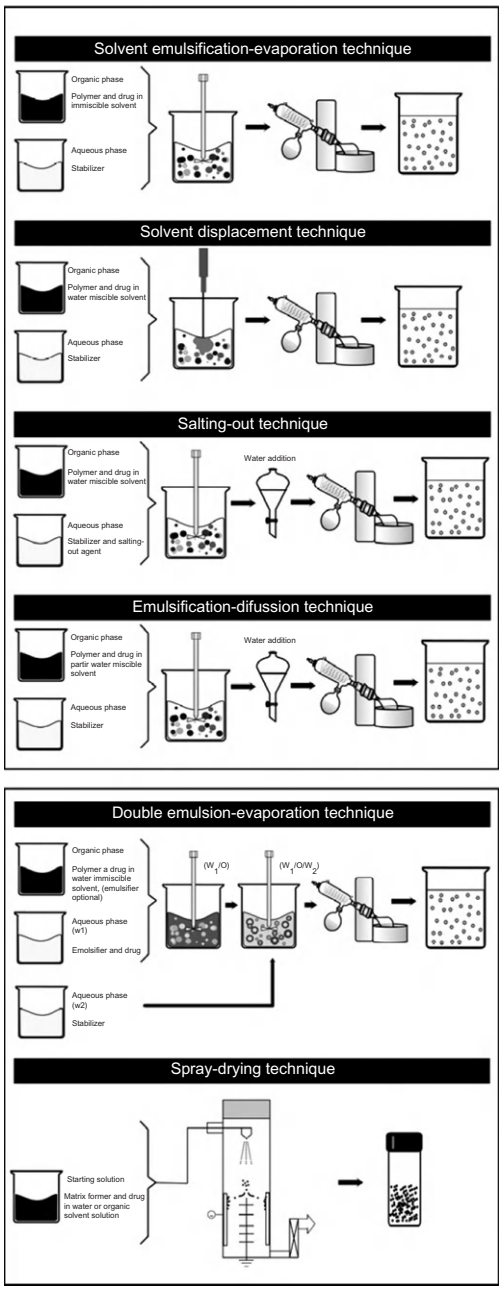

FIGURE 23.4

Methods used to prepare nanoparticles from preformed polymers.

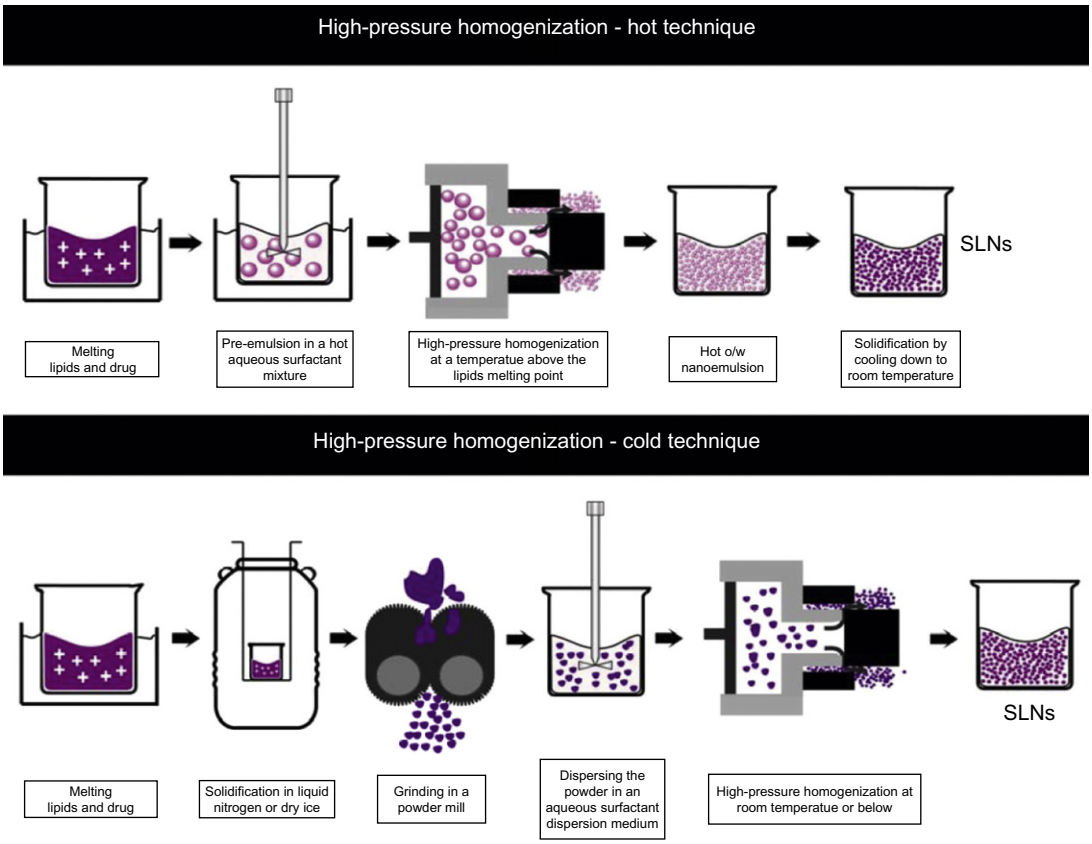

FIGURE 23.5

Modalities used to prepare solid lipid nanoparticles (SLNs) by HPH.

23.3 Dental applications of nanoparticles

Nanoparticles have been proposed as drug-delivery systems for caries control and restoration, tooth remineralization, management of dentinal hypersensivity, dental caries vaccine, oral biofilm management, root canal disinfection, local anesthesia, and periodontal infection. For example, nanoparticles can be used to improve treatments for diseases of dental and oral structures using the classical drugs. It is proposed that nanoparticles can be selectively delivered to target sites or cells. One of the most important applications of nanoparticles in dentistry is the treatment of periodontal disease.

Periodontal disease is a collective term that includes several pathological conditions characterized by degeneration and inflammation of the tissues surrounding and supporting the teeth: gum tissue (gingiva), periodontal ligament, alveolar bone, and dental cementum [7,8,53–57]. The relationship between the subgingival plaque and the development of periodontal disease is well established. This infectious process shows different grades of severity: (i) gingivitis, the early phase

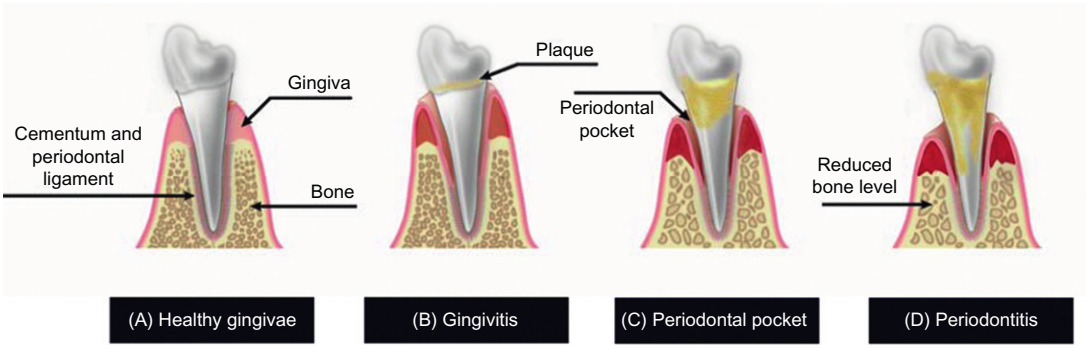

FIGURE 23.6

Schematic representation of the stages of periodontal diseases. (A) Healthy gum tissue, tooth anchored by periodontal structures. (B) Plaque formation (oral biofilm) causing gingivitis. (C) Formation of periodontal pocket (lesions between teeth and the junctional epithelium) and tooth connective tissue attachment gradually destroyed. (D) Periodontitis, destruction of gingiva, and bone that support the tooth and the cementum that protects the root.

of the disease that is confined to the gingiva, (ii) mild periodontitis, (iii) moderate periodontitis, and (iv) advanced periodontitis [53]. Periodontitis denotes inflammation of the gingival and adjacent deeper periodontal tissues, leading to gingival swelling, bleeding, and bad breath. In the last phase of the disease, the supporting structures of the periodontium are degenerated, alveolar bone begins to resorb, and the gingival epithelium migrates along the tooth surface, forming a periodontal pocket [7,56,58]. The periodontal pocket provides an excellent environment for the growth of pathogenic microorganisms, such as *Actinobacillus actinomycetemcomitans*, *Bacteroides* spp. (*B. gingivalis* and *B. intermedius*), *Wolinella recta*, *Eikenella* spp. *Porphyromonas gingivalis,* and *Provetella intermedia* [7,57,59]. Progressive pocket formation leads to the destruction of the supporting periodontal tissues and to loosening or exfoliation of the teeth [58]. Figure 23.6 shows the evolution patterns of periodontal disease from healthy gingiva to pathological periodontitis.

As soon as gingivitis with pocket formation occurs, the therapeutic approaches should be aimed at reducing the etiologic factors in order to decrease or eliminate inflammation and control the interaction between the plaque bacteria and the host response. The aim of periodontal therapy is to eliminate bacterial deposits or dental plaque (biofilm) from the tooth surface by mechanical treatment in combination with an adequate oral hygiene to prevent reinfection of the subgingival area by periodontopathic microorganisms and consequently to preserve the tooth [7,53,59]. Furthermore, various regenerative treatment options are available.

Local and/or systemic delivery of several antimicrobial and antibacterial agents has been effectively used to manage periodontal infections [54,56,57]. Systemic doses of antibiotics reach the periodontal tissues by transudation from the serum and then cross the crevicular and junctional epithelia to enter the gingival sulcus [54]. There are however, some disadvantages such as a rapid decline of the therapeutic plasma antibiotic concentration, the development of microbial resistance, and high peak plasma antibiotic concentrations, which may be associated with side effects such as gastrointestinal complaints, depression, and tachycardia [7,59]. The systemic administration of

drugs leads to therapeutic concentrations at the site of infection for short periods of time; therefore, forced repeated doses over longer periods are required [59]. In contrast, the use of local delivery of antibiotics specifically administered in the site of infection (periodontal pocket) could be very useful in eliminating pathogens, and thus enhancing the effect of conventional surgical therapy without the side effects of systemically administered antibiotics [53,60].

In addition to the antiinfective therapy to prevent the progression of periodontal disease, it is necessary to initiate a regenerative therapy to restore the structures destroyed by the disease [61]. In 2006, Kong et al. [2] published a review focusing on the development of nanomaterials and their potential use in the treatment of periodontal diseases, including diagnosis and treatment. Several regenerative options have since then been developed to treat diverse causes of periodontal diseases [62]. These include bone grafting, guided tissue regeneration, enamel matrix protein derivative, basic fibroblast growth factor, stem cell therapy, and photodynamic therapy (PDT) [55,62]. Due to the advances in biotechnology, progress in recombinant protein technology, protein- and/or gene based therapy, and tissue engineering has made it possible to use growth factors (GFs) and polynucleotides as effective drugs for facilitating wound healing and tissue regeneration [55]. Unquestionably, the localized delivery of GFs to the periodontium is an emerging and versatile therapeutic approach with the potential to regenerate the periodontium and the bone [63]. The half-lives of soluble GFs and other polynucleotides in the body are short because they are rapidly degraded and are typically deactivated by enzymes. They are also susceptible to other chemical and physical degradation reactions that occur in the body [55,63]. In order to preserve the GF bioactivity and control the GF release, several controlled release technologies are being explored, including the delivery of GFs by means of micro- or nanoscale particles, prefabricated scaffolds, injectable gels, composites, and so on. According to Chen et al. [55], carriers and delivery systems for GFs must be able to increase their retention at treatment sites for enough time to allow tissue regenerating cells to migrate to the area of injury and to proliferate and differentiate and eliminate loss of bioactivity. Furthermore, properties such as easy administration, targeted delivery, controlled release kinetics, and cell/tissue permeation enhancement are desirable.

23.3.1 Polymeric nanoparticles

Polymeric materials have been widely investigated for drug-delivery devices and tissue engineering [55]. Nonbiodegradable as well as biodegradable polymers have been used for the preparation of micro- and nanoparticles administered by the nasal, pulmonary, oral, or parenteral routes. These materials include synthetic or natural polymers and modified natural substances [7,53,59]. Biodegradable polymers, of natural or synthetic origin, have been widely used as drug-delivery systems for many bioactive compounds and are extensively employed in periodontal drug-delivery devices because of their biocompatibility, since they can be degraded into acceptable biocompatible products by chemical or enzymatic processes [53,55]. The devices manufactured with biodegradable materials do not require removal at the end of the treatment.

A number of drug-delivery systems for the treatment of periodontal diseases are being designed for targeted controlled drug release. Research has involved the use of local drug-delivery systems based on micro- and nanoparticles made from biocompatible or biodegradable polymers. A comprehensive review [53] has been recently published, where the use of drug-loaded microparticles in the management of endodontic and periodontal diseases was analyzed. Several

microparticulate systems were described, including microspheres or microcapsules as delivery systems for naproxen, succinyl sulfathiazole, histatins, alendronate, minocycline, chlorhexidine, doxycycline, or tetracycline. Polymers as alginate, chitosan, polyhydroxybutirate-*co*-hydroxyvalerate and polyester polymers such as poly(L-lactide), poly(D,L-lactide), poly(glycolide) and copolymers, polycaprolactones, and polyphosphazenes were used to obtain the particulate systems. Some of these carriers have the advantage that they can be incorporated into typical oral formulations as suspensions or toothpastes, or in hydrogels or novel bioadhesive drug-delivery systems, or they can even be directly injected into the periodontal pocket. Local polymeric-based drug-delivery systems, such as fibers, films, strips, gels, vesicular systems, microparticles, or nanoparticles have been used in dentistry for local drug delivery to provide adequate drug concentrations directly at the site of action. These systems are usually inserted into the periodontal pocket or injected in periodontal tissues to enhance the therapeutic effect of drugs and reduce the side effects of drugs associated with their systemic use [7,28,53,59,64]. Several specialized local delivery systems have been designed for the controlled release of drugs in periodontal tissues; however, the complexity of accessing periodontal tissues makes all of these systems only partially successful [25,28,59,60,65].

Compared to microparticles, nanoparticles offer several advantages, such as the ability to penetrate extracellular and intracellular areas that may be inaccessible to other delivery systems due to their small size, including the periodontal pocket areas below the gum line [7,28,61,66], as shown in Figure 23.7. The confocal laser scanning microscopy studies carried out by Ganem-Quintanar [67] established that biodegradable nanoparticles, when gently applied to the porcine gingival sulcular space, are able to penetrate into the junctional epithelium. Likewise, nanoparticles in the periodontal pocket could be a drug-delivery system that reduces the frequency of administration, in addition to providing an efficient active agent accumulation in the target sites over an extended period of time, maintaining an effective drug release rate [2,7,59]. Furthermore, nanoparticles have better stability in biological fluids. Unfortunately, there are very few studies on the preparation of antibacterial nanoparticles for periodontal therapy [28].

Poly(D,L-lactide) acid (PLA), poly(glycolic) acid, and poly(D,L-lactide-*co*-glycolide) acid (PLGA), have been the central focus in the development of nano/microparticles encapsulating therapeutic drugs in controlled release applications [68]. These materials offer several advantages, such as good biocompatibility and biodegradability, mechanical strength, and ease of administration via injection; in addition, the use of biodegradable materials allows sustained drug release within the target site over a period of days or even weeks [55,63,68].

In 2005, our research group [25] produced and characterized triclosan-loaded nanoparticles of less than 500 nm in diameter to obtain a novel intrapocket delivery system adequate for the treatment of periodontal disease. Triclosan (2,4,4′-trichloro-hydroxydiphenylether) (TCS) is a noncationic antimicrobial agent with a recognized efficacy against several plaque-forming bacteria. The nanoparticles are prepared using the previously patented emulsification−diffusion technique [69]. PLGA, PLA, and cellulose acetate phthalate were used as polymer and nanoparticles were stabilized with poly(vinyl alcohol). Different TCS/polymer ratios were used in order to analyze the effect of TCS on nanoparticle properties. Scanning electron microscopy and light scattering analysis indicated that high concentrations of TCS appear to cause an increase in nanoparticles mean size. Differential scanning calorimetry showed that solid TCS nanoparticles behaved as a homogeneous polymer matrix-type delivery system where the drug (TCS) is molecularly dispersed, suggesting that TCS could behave as a plasticizer. Additionally, a preliminary *in vivo* study was performed on dogs in which

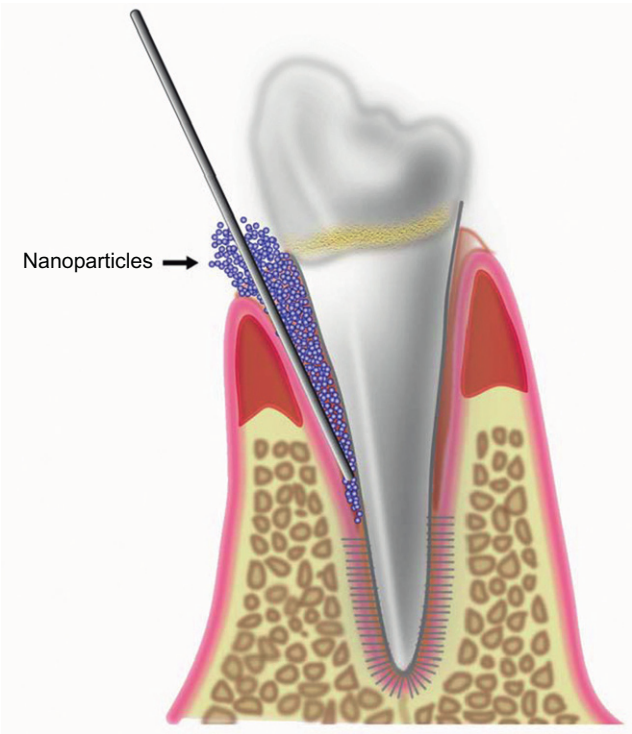

FIGURE 23.7

Schematic diagram of nanoparticles administered in periodontal pockets.

TCS-loaded PLGA nanoparticles (9.09% of TCS) were injected in the bottom of the experimental pockets; sterilized water was applied to the control periodontal pockets. After 15 days, a clear difference between control and experimental sites was detected. It was concluded that TCS nanoparticles diminished the inflammation at the experimental sites. Figure 23.8 shows photographs of the experimental sites 8 and 15 days after the administration of the nanoparticles.

Natural extracts have also been incorporated into polymeric nanoparticles for the treatment of dental caries and gingivitis infections [26]. The leaf extract of *Harungana madagascariensis* (a popular drug native to Africa and Madagascar) is known for its biological properties with mainly antibacterial, antifungal, and antiviral effects. The *in vitro* bactericidal activity of the ethyl acetate *H. madagascariensis* leaf extracts (HLE) on the main oral bacterial strains largely implicated in dental caries and gingivitis infections, and the possibility of potentialization of HLE antibacterial effects using the PLGA nanoparticles was analyzed. HLE/PLGA nanoparticles smaller than 300 nm were obtained by the solvent displacement technique. Encapsulation efficiencies were higher than 75%. The *in vitro* bactericidal activity results revealed that the incorporation of HLE into the biodegradable colloidal carrier increased the antimicrobial effects. When HLE was incorporated into PLGA nanoparticles, a reduction in the bactericidal concentration compared to HLE was observed.

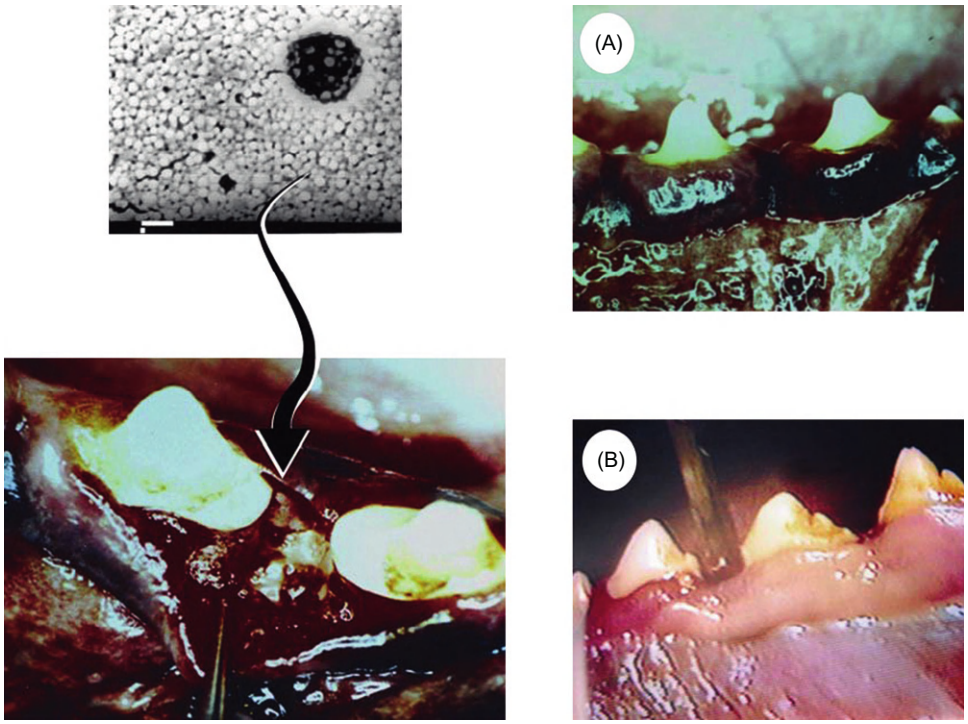

FIGURE 23.8

Experimental sites after the administration of TCS-loaded PLGA nanoparticles in dogs: (A) 8 and (B) 15 days.

This enhanced bactericidal activity of HLE/PLGA nanoparticles may be due to the bioadhesive property of the PLGA biopolymer, which remains on the bacterial cells for a prolonged period, thus extending the drug action.

A drug-delivery system for dental applications was proposed by Bakó et al. [27]. Biocompatible nanoparticles were obtained by free radical initiated copolymerization of the monomers 2-hydroxyethyl methacrylate and polyethylene glycol dimethacrylate in aqueous solution. This polymerization yielded a well-dispersible white powder material composed of nanoparticles with a size between 50 and 180 nm suitable for incorporation into a hydrogel matrix and to design new drug-delivery media for dental applications.

It is well recognized that minocycline is one of the broad-spectrum antibiotics frequently used for the treatment of periodontitis and related infections in periodontal diseases [53,54,64]. Recently, different methods, such as single emulsion (oil/water, modified oil/water and oil/oil) and double emulsion−solvent evaporation (water/oil/water), ion pairing, and nanoprecipitation were used to prepare both PLGA nanoparticles and PLGA with polyethylene glycol (PEG) nanoparticles (PEGylated PLGA nanoparticles) containing minocycline [28]. Almost all of the nanoparticles prepared from PLGA and PEG−PLGA under different conditions were less than 500 nm with a spherical shape and a smooth surface. The nanoparticles obtained by solid/oil/water ion pairing showed

higher entrapment efficiency (29.9%). Drug release studies using a dialysis technique were performed in phosphate buffer at pH 7.4, indicating a slow release of minocycline ranging from 3 days to several weeks. The antibacterial analysis against *Aggregatibacter actinomycetemcomitans* indicated that the minimum inhibitory concentration and minimum bactericidal concentration of nanoparticles were at least two times lower than that of the free drug. The results obtained by this group clearly showed that the antibacterial activity of minocycline-loaded nanoparticles was greater than that of the free drug, possibly due to a better penetration of nanoparticles into bacterial cells and to a better delivery of minocycline to the site of action.

Microbial biofilms in the oral cavity films are not only involved in causing caries, gingivitis, and periodontitis but are also involved in the etiology of various oral conditions, including oral malodor, denture stomatitis, candidiasis, and dental implant failure [70]. Chávez de Paz et al. [71] prepared nanoparticle complexes using chitosan of various molecular weights and degrees of deacetylation. These nanosystems were obtained by ion gelation with polyanionic sodium triphosphate. The penetrative antimicrobial effect on biofilms of *Streptococcus mutans* was assessed. Nanocomplexes prepared from low molecular weight chitosan showed the highest antimicrobial effect ($>95\%$ of cells damaged). The authors concluded that the effect of low molecular weight formulations affected the cell membrane integrity of *S. mutans* in a homogenous manner across the entire biofilm.

Previously, Liu et al. [72] had proposed the use of chitosan nanoparticles as the delivery vehicle through toothpaste. The chitosan nanoparticles were obtained by an emulsion dispersion technique, followed by glutaraldehyde cross linking, with NaF or cetylpyridinium chloride (CPC) as drugs. The nanoparticles between 100 and 500 nm in size showed good stability at neutral pH, while they precipitated quickly at alkaline conditions, increasing their sizes. The loaded drugs could be sustained released for at least 10 h, with a release percentage of 33% for CPC and 88% for NaF, respectively. Floccules were formed when the nanoparticles containing CPC were mixed with toothpaste lixivium. In contrast, nanoparticles with NaF showed very good stability in toothpaste lixivium after incubation at 60°C for 30 days. The authors concluded that the chitosan nanoparticles have a great potential to be used for the delivery of toothpaste actives and for *in situ* release of the actives in a sustained manner.

Additionally, chitosan was used to produce antisensitive oligonucleotide-loaded chitosan-tripolyphosphate nanoparticles [73]. Oligonucleotides form complexes with chitosan and the release of the former from nanoparticles is dependent on the loading methods and pH conditions. The percentage of oligonucleotides released from nanoparticles at pH 10.0 was higher than that under acidic conditions (pH 5.0). The results achieved suggested that the sustained release of oligonucleotides from chitosan nanoparticles may be suitable for the local therapeutic application in periodontal diseases.

Recently, Son et al. [74] have described the development of novel porous calcium phosphate (CaP) granules with an excellent drug-delivery system using drug-loaded biodegradable nanoparticles for bone regeneration. Dexamethasone (DEX)-loaded PLGA nanoparticles were prepared by the single oil in water emulsion−solvent evaporation technique. DEX was used as a model bioactive molecule because it induces osteoblastic differentiation *in vitro* and increases alkaline phosphatase activity. The DEX/PLGA nanoparticles produced were precoated with positively charged poly (ethyleneimmine) molecules and were then successfully incorporated and well dispersed in the microchannels of the CaP granules, which have a negative charge. *In vitro* release studies showed

that the nanoparticles were not released from the CaP granules, allowing a sustained release of DEX from the nanoparticle-based CaP granules over the course of 1 month. This work opens up new avenues of research to deliver bioactive drugs for bone regeneration using biodegradable nanoparticles incorporated into CaP granules.

Recently Dixon et al. [75] designed a nanoparticle-based targeted drug-delivery system for the treatment of bone loss containing an enantiomeric phenothiazine. Some of the proposed formulations describe the fabrication of PLGA nanoparticles and PLGA−PEG nanoparticles using the double emulsion−solvent evaporation method.

Another interesting alternative to antimicrobial treatments and mechanical removal of dental plaque is the PDT. PDT for human infections is based on the concept that an agent (a photosensitizer) which absorbs light can be preferentially taken up by bacteria and subsequently activated by light of the appropriate wavelength in the presence of oxygen to generate singlet oxygen and free radicals that are cytotoxic to microorganisms or cells of the target tissue [70,76].

There are some patent applications [77,78] related to the use of photosensitizing compounds for treating oral diseases, including inflammatory periodontal disease, by utilizing photosensitizing compounds in long-term effect or timed-release formulations and activating the photosensitizers with radiation to selectively destroy bacteria and other microbial bodies. These applications include the use of photosensitizers loaded in nanoparticles. The proposed formulations could be applied to the oral cavity, in periodontal pockets, or coated at the desired sites.

Pagonis et al. [79] proposed the incorporation of methylene blue (MB) into PLGA nanoparticles for antimicrobial endodontic treatment. MB is a well-established photosensitizer that has been used in PDT for targeting various gram-positive and gram-negative oral bacteria. MB/PLGA nanoparticles (150−200 nm in diameter) were obtained by the solvent displacement technique. The susceptibility of *Enterococcus faecalis* to PDT mediated by MB/PLGA nanoparticles was evaluated in experimentally infected root canals of extracted teeth. More recently, the *in vitro* effect of PDT on human dental plaque bacteria using MB-loaded PLGA nanoparticles with a positive or negative charge and red light at 665 nm was analyzed [76]. The surface properties of nanoparticles were modified with a cationic or anionic charge using cetyl trimethyl ammonium bromide or Pluronic® F-108, respectively. The results indicated that cationic MB/PLGA nanoparticles have the potential to be used as carriers of MB for the photodestruction of oral biofilms. The greater PDT bacterial killing by cationic MB-loaded nanoparticles showed the ability of nanocarriers to diffuse in biofilms and release the encapsulated drug in the active form. It is uncertain, however, whether the sufficient concentrations of MB were released in order to have the greatest possible effect in the eradication of the biofilm organisms. Even though additional studies are required, it is important to note that these nanoparticles are a promising area of research.

23.3.2 Nonpolymeric nanoparticles

A development of nanoparticle application for dental drug delivery was proposed in a recent patent by Shefer and Shefer [21]. These researchers suggest a biodegradable bioadhesive controlled release system of nanoparticles for oral-care products, which is useful for site specific delivery of biologically active ingredients or sensory markers over an extended period of time, targeting biological surfaces comprising the oral cavity and the mucous membranes of various tissues. Specifically, these nanoparticles can be used in hygiene products, such as toothpaste or mouthwash,

and for the treatment and prevention of periodontal diseases, considering their capacity to remain in the periodontal pocket. The system was prepared by dispersing and homogenizing candelilla wax in a cetylpirydinium chloride (bioadhesive) solution at 90°C. The uniform milk-like formulation was immediately cooled at room temperature by immersing it into an ice/water bath under continuous mixing. The solid lipid nanoparticles obtained showed high bioadhesiveness when evaluated by *in vitro* measurements (HeLa cells). The nanoparticle bioadhesiveness is attributed to the cationic surface, which can attach to tooth surfaces via complex interaction between the cationic portion of the material and the proteinaceous portion of the tooth in order to predispose the surface of the tooth to allow nanoparticles to adhere to the surface of the tooth. Different biologically active ingredients such as anticalculus ingredients, antimicrobials, anti-inflammatory agents, antibiotics, and local anesthetics can be entrapped in the solid lipid nanoparticles during the fusion of the wax.

The same authors [22] have proposed a multicomponent controlled release system with bioadhesive properties for oral care. In this invention, solid lipid nanoparticles are encapsulated into moisture-sensitive microspheres by spray drying. The dry system in contact with water or biological fluids disintegrates releasing the nanoparticles. The system can encapsulate different flavors, sensory markers, and active ingredients, or combinations. Holpuch et al. [23] have confirmed that solid lipid nanoparticles are internalized by monolayer-cultured human oral mucosal cell line explants and normal human oral explants, supporting the premise that solid lipid nanoparticles-based delivery results in higher final intracellular levels relative to bolus administration. Furthermore, the penetration and subsequent internalization of nanoparticles within the proliferating basal layer cells demonstrate the feasibility of nanoparticle formulations for local delivery and stabilization of oral chemopreventive compounds.

An interesting patent [80] proposes a complex controlled release system based on polymerizable resinous dental cement with porous nanoparticles of silica, chlorhexidine (antibacterial agent) and its salts, or inclusion compounds (cyclodextrines). The extended release can be defined by desorption of chlorhexidine from silica and the film formed.

The encapsulation of inorganic particles with polymers is a promising system for dental applications. These systems are known as core-shell nanoparticles and combine various properties in one entity consisting of different chemical components. Dong et al. [18] synthesized *N*-halamine functionalized silica-polymer core-shell nanoparticles via copolymerization with styrene, acrylate acid, methyl methacrylate, and vinyl acetate. These nanoparticles displayed a powerful antibacterial activity against gram-negative bacteria and gram-positive bacteria, and their antibacterial activities have been greatly improved compared to their bulk counterparts. This antibacterial effect can be applied in dental devices and dental office equipment.

Recombinant human platelet-derived GF is a potent and extensively investigated GF in the field of periodontal regeneration. This factor, however, has a high degree of variability, mainly due to the lack of a continual supply for a required period of time. Elangovan et al. [24] have suggested the use of CaP nanoparticles as vectors for platelet-derived GF to target fibroblasts. The results demonstrated that the nanoparticles synthesized have higher levels of biocompatibility and efficiently transfected platelet-derived GF plasmids into murine fibroblasts, indicating that CaP nanoparticles can be a potential candidate to deliver the genes of interest into fibroblasts, the major cell in the periodontium.

Recently, Kovtun et al. [81] synthesized chlorhexidine-loaded CaP nanoparticles for dental maintenance. Two effects are combined, the remineralization effect and the antibacterial effect,

the former being attributed to CaP and its improved adhesion by carboxymethyl cellulose and the latter to the controlled release of chlorhexidine. Nanoparticles can be applied either as dispersion (mouth rinse) or as a paste. The functionalized nanoparticles showed a higher adsorption on tooth surfaces (enamel and dentin) and the ability to close open dentin tubules. The authors concluded that these nanoparticles represent a very promising tool to improve oral hygiene and dental treatment in cases of common enamel and/or dentin erosion, dentin hypersensivity, gingivitis, and marginal periodontitis.

A novel patent [82] proposes the use of an organic dye-encapsulated silica shell nanosphere for minimizing color fading by oral-care compositions containing peroxide and fluoride ions. The methods to prepare the nanospheres include the water-in-oil microemulsion method, the condensation method using silica and dye precursors and the silicate crystal growth technique. The results clearly indicated that color loss due to a redox reaction between the peroxide species and the dye was minimized by using dye-encapsulated silica.

23.4 Future trends

Several nanomaterials have been proposed for dental applications showing clear advantages compared to their conventional formulations. A number of these have potential applications but further research is required in order to consolidate their real therapeutic effect. However, to date, there is insufficient information available to generalize the use of nanoparticles in dentistry and to allow the development of a plan for a wide range of other applications. The toxicological aspect about the safety of nanoparticles is a controversial issue in dentistry considering tissue properties and potential internalization. It is clear that these aspects should be critically examined. However, the research activity on nanotechnology in the dental field is gaining pace and several of these challenges will be solved in a short time, consolidating the transition of these products to the market.

Acknowledgments

This work was funded by PAPIIT/UNAM (Ref. IN222411-3, and IN224111-3), and CONACYT (Ref. 128799). N. Mendoza-Muñoz acknowledges a grant from CONACYT, México (Ref. 177414).

The authors are grateful to Mr. Rodolfo Robles for his technical assistance in obtaining the microphotographies (scanning electron microscopy) included in Figures 23.3 and 23.8.

References

[1] R.W. Kesall, I.W. Hamley, M. Geoghegan, Nanoscale Science and Technology, John Wiley & Sons, New Jersey, USA. 2005.

[2] L.X. Kong, Z. Peng, S.-D. Li, P.M. Bartold, Nanotechnology and its role in the management of periodontal diseases, Periodontology 40 (2006) 184–196.

[3] A. Nugent, Application of hebbian and anti-hebbian learning to nanotechnology-based physical neural networks, US20040162796, 2009

[4] K. Henry, Z. Bao, Methods of fabricating nanoscale-to-microscale structures, US20080038170, 2008.
[5] A. Renugalakshmi, T.S. Vinothkumar, D. Kandaswamy, Nanodrug delivery systems in dentistry: a review on current status and future perspectives, Curr. Drug Deliv. 8 (2011) 586−594.
[6] R. Shorr, R. Rodriguez, Pharmaceutical and diagnostic compositions containing nanoparticles useful for treating targeted tissues and cells, WO02102311, 2002.
[7] N. Jain, G.K. Jain, S. Javed, Z. Iqbal, S. Talegaonkar, F.J. Ahmad, et al., Recent approaches for the treatment of periodontitis, Drug Discov. Today 13 (2008) 932−943.
[8] S. Sharma, S.E. Cross, C. Hsueh, R.P. Wali, A.Z. Stieg, J.K. Gimzewski, Nanocharacterization in dentistry, Int. J. Mol. Sci. 11 (2010) 2523−2545.
[9] P.S. Kumar, S. Kumar, R.C. Savadi, J. John, Nanodentistry: a paradigm shift−from fiction to reality, J. Indian Prosthodont. Soc. 11 (2011) 1.6.
[10] R.P. Allaker, The use of nanoparticles to control oral biofilm formation, J. Dent. Res. 89 (2010) 1175−1186.
[11] S. Nugen, M. Hiorth, M. Rykke, G. Smistad, The potential of liposomes as dental drug delivery systems, Eur. J. Pharm. Biopharm. 77 (2011) 75−83.
[12] S.A. Saunders, Current practicality of nanotechnology in dentistry. Part I: Focus on nanocomposite restoratives and biomimetics, Clin. Cosm. Invest. Dent. 1 (2009) 47−61.
[13] G. Gazzaniga, N. Roveri, L. Rimondini, B. Palazzo, M. Lafisco, Biologically active nanoparticles of a carbonate-substituted hydroxyapatitte process for their preparation and compositions incorporating the same, WO137606A1, 2007.
[14] A.A.K. Henkel, Suthech GMBH Co. KG, A. Barth, C. Kropf, T. Poth, Oral and dental care product, WO020878A2, 2005.
[15] H.W.H. Lee, S.M. Colby, Process to form nano-sized materials, the compositions and uses thereof, WO140476A2, 2008.
[16] L. Cheng, M.D. Weir, K. Zhang, S.M. Xu, Q. Chen, X. Zhou, et al., Antibacterial nanocomposite with calcium phosphate and quaternary ammonium, J. Dent. Res. 91 (2012) 460−466.
[17] H.H.K. Xu, M.D. Weir, L. Sun, J.L. Moreau, S. Takagi, L.C. Chow, et al., Strong nanocomposites with Ca, PO_4, and F release for caries inhibition, J. Dent. Res. 89 (2010) 19−28.
[18] A. Dong, J. Huang, S. Lan, T. Wang, L. Xiao, W. Wang, et al., Synthesis of *N*-halamine-functionalized silica-polymer core-shell nanoparticles and their enhanced antibacterial activity, Nanotechnology 22 (2011) 1−9.
[19] M.L. Zambrano-Zaragoza, E. Mercado-Silva, E. Gutierrez Cortez, E. Castaño-Tostado, D. Quintanar-Guerrero, Optimization of nanocapsules preparation by the emulsification-diffusion method for food applications, LWT-Food Sci. Technol. 44 (2011) 1362−1368.
[20] J.P. Anais, N. Razzouq, M. Carvalho, C. Fernandez, A. Astier, M. Paul, et al., Development of α-tocopherol acetate nanoparticles: influence of preparative processes, Drug Dev. Ind. Pharm. 35 (2009) 216−223.
[21] A. Shefer, S. Shefer, Biodegradable bioadhesive controlled release system of nano-particles for oral care products, WO41765A2, 2002.
[22] A. Shefer, S.D. Shefer, Multi component controlled release system for oral care, food products, nutraceutical, and beverages, US0152629A1, 2003.
[23] A.S. Holpuch, G.J. Hummel, G.A. Seghi, P. Pei, P. Ma, R.J. Mumpr, et al., Nanoparticles for local drug delivery to the oral mucosa: proof of principle studies, Pharm. Res. 27 (2010) 1224−1236.
[24] S. Elangovan, S. Jain, P.C. Tasi, H.C. Margolis, M. Amiji, Nano-sized calcium phosphate particles for periodontal gene therapy, J. Periodont. (2012) DOI: 10.1902/jop.2012.120012 Posted online on March 13, 2012.
[25] E. Piñón-Segundo, A. Ganem-Quintanar, V. Alonso-Pérez, D. Quintanar-Guerrero, Preparation and characterization of triclosan nanoparticles for periodontal treatment, Int. J. Pharm. 294 (2005) 217−232.

[26] B. Moulari, H. Lboutounne, J.P. Chaumont, Y. Guillaume, J. Millet, Y. Pellequer, Potentiation of the bactericidal activity of *Harungana madagascariensis* Lam. ex Poir. (*Hypericaceae*) leaf extract against oral bacteria using poly(D,L-lactide-co-glycolide) nanoparticles: *in vitro* study, Acta Odontol. Scan. 64 (2006) 153–158.
[27] J. Bakó, M. Szepesi, I. Márton, J. Borbély, C. Hegedûs, Synthesis of nanoparticles for dental drug delivery systems, Forgorv. Sz. 100 (2007) 109–113.
[28] T.S.J. Kashi, S. Eskandarion, M. Esfandyari-Manesh, S.M.A. Marashi, N. Samadi, S.M. Fatemi, et al., Improved drug loading and antibacterial activity of minocycline-loaded PLGA nanoparticles prepared by solid/oil/water ion pairing method, Int. J. Nanomed. 7 (2012) 221–234.
[29] V. Klepac-Ceraj, N. Patel, X. Song, C. Holewa, C. Patel, R. Kent, et al., Photodynamic effects of methylene blue-loaded polymeric nanoparticles on dental plaque bacteria, Lasers Surg. Med. 43 (2011) 600–606.
[30] C. Xu, C. Lei, L. Meng, C. Wang, Y. Song, Chitosan as a barrier membrane material in periodontal tissue, J. Biomed. Mater. Res. B Appl. Biomater. 100 (2012) 1435–1443.
[31] I.M. Hamouda, Current perspectives of nanoparticles in medical and dental biomaterials, J. Biomed. Res. 26 (2012) 143–151.
[32] R. Kanaparthy, A. Kanaparthy, The changing face of dentistry: nanotechnology, Int. J. Nanomed. 6 (2011) 2799–2804.
[33] R. García-Contreras, L. Argueta-Figueroa, C. Mejía-Ruvalcava, R. Jiménez-Martínez, S. Cuevas-Guajardo, P.A. Sánchez-Reyna, et al., Perspectives for the use of silver nanoparticles in dental practice, Int. Dent. J. 61 (2011) 297–301.
[34] B.A. Sevinç, L. Hanley, Antibacterial activity of dental composites containing zinc oxide nanoparticles, J. Biomed. Mater. Res. Appl. Biomat. 948B (2010) 22–31.
[35] S.E. Elsaka, I.M. Hamouda, M.V. Swain, Titanium dioxide nanoparticles addition to a conventional glass-ionomer restorative: influence on physical and antibacterial properties, J. Dent. 39 (2011) 589–598.
[36] T.J. Boyd, G. Xu, D. Viscio, A. Gaffar, E.S. Arvanitidou, L. Fruge, Oral composition containing non-aggregated zinc nanoparticles, US0020201A1, 2007.
[37] A. Konzett, J. Pingitzer, B. Pregenzer, J. Wernisch, J. Wernisch, G.S. Lorenz, Bleaching agent and method and device for bleaching teeth using such a bleaching agent, WO036290A1, 2007.
[38] D.R. Monteiro, L.F. Gorup, A.S. Takamiya, E. Rodríguez de Camargo, A.C.R. Filho, D.B. Barbosa, Silver distribution and release from an antimicrobial denture base resin containing silver colloidal nanoparticles, J. Prosthodont. 21 (2012) 7–15.
[39] F. Zhang, Y. Cia, L. Xu, N. Gu, Surface modification and microstructure of single-walled carbon nanotubes for dental resin-based composites, J. Biomed. Mater. Res. Appl. Biomater. 86B (2008) 90–97.
[40] S. Klapdohr, N. Moszner, New inorganic components for dental filling composites, Monatsh. Chem. 136 (2005) 21–45.
[41] F. Nagano, D. Selimovic, M. Noda, T. Ikeda, T. Tanaka, Y. Miyamoto, et al., Improved bond performance of a dental adhesive system using nano-technology, Bio-Med. Mater. Eng. 19 (2009) 249–257.
[42] M. Du, Y. Zheng, Modification of silica nanoparticles and their application in UDMA dental polymeric composites, Polym. Compos. 28 (2007) 198–207.
[43] E.G.W. Müller, M. Wiens, Hydroxyapatite-binding nano- and microparticles for caries prophylaxis and reduction of dental hypersensitivity, WO010520A1, 2012
[44] A. Mihranyan, N. Ferraz, M. Strømme, Current status and future prospects of nanotechnology in cosmetics, Prog. Mater. Sci. 57 (2012) 875–910.
[45] W.H. Wang, Physicochemical characteristics of resin restorative material and its clinical application in repairing dental caries, J. Clin. Rehabil. Tissue Eng. Res. 14 (2010) 2983–2986.

[46] J. Cheng, G. Cheng, Nanosize selenium-containing teeth-whitening agent for sterilizing, removing smoking-induced dental stain and calculus, and whitening teeth, CN102090990A, 2011.
[47] Q. Ma, M. Shenglin, J. Kun, Y. Zhang, P.K. Chu, Immobilization of Ag nanoparticles/FGF-2 on a modified titanium implant surface and improved human gingival fibroblasts behavior, J. Biomed. Mater. Res. 98A (2011) 274–286.
[48] R.M. Gaikwad, I. Sokolov, Silica nanoparticles to polish tooth surfaces for caries prevention, J. Dent. Res. 87 (2008) 980–983.
[49] E.S. Kalivradzhiyan, V.M. Kashkarov, M.A. Kryuchkow, N.V. Chirkova, P.I. Manelyak, Z.V. Gavrillova, et al., Zinc-phosphate cement for fixation of undetachable dental prostheses with addition of silicon nanoparticles, RU2428165C1, 2011.
[50] D. Quintanar-Guerrero, E. Allémann, H. Fessi, E. Doelker, Preparation techniques and mechanisms of formation of biodegradable nanoparticles from preformed polymers, Drug. Dev. Ind. Pharm. 24 (1998) 1113–1128.
[51] E.K. Noriega-Pelaez, N. Mendoza-Muñoz, A. Ganem-Quintanar, D. Quintanar-Guerrero, Optimization of the emulsification and solvent displacement method for the preparation of solid lipid nanoparticles, Drug Dev. Ind. Pharm. 37 (2011) 160–166.
[52] C.E. Mora-Huertas, H. Fessi, A. Elaissari, Influence of process and formulation parameters on the formation of submicron particles by solvent displacement and emulsification-diffusion methods, critical comparison, Adv. Colloid. Interfac. 163 (2011) 90–122.
[53] A. Luzardo Álvarez, F. Otero Espinar, J. Blanco Méndez, The application of microencapsulation techniques in the treatment of endodontic and periodontal diseases, Pharmaceutics 3 (2009) 538–571.
[54] R.S. Leite, K.L. Kirkwood, Present and future non-surgical therapeutic strategies for the management of periodontal diseases, in: J. Manakil (Ed.), Periodontal Diseases—A clinician's Guide, InTech, 2012. Available from: <http://www.intechopen.com/books/periodontal-diseases-a-clinician-s-guide/present-and-future-non-surgical-therapeutic-strategies-for-the-management-of-periodontal-diseases/
[55] F.M. Chen, R.M. Shelton, Y. Jin, I.L.C. Chapple, Localized delivery of growth factors for periodontal tissue regeneration: role, strategies, and perspectives, Med. Res. Rev. 29 (2009) 472–513.
[56] M.L. Bruschi, H. Panzeri, O. de Freitas, E.H.G. Lara, M.P.D. Gremião, Sistemas de liberação de fármaco intrabolsa periodontal, Braz. J. Pharm. Sci. 42 (2006) 29–47.
[57] A. Leszczyńska, P. Buczko, W. Buczko, M. Pietruska, Periodontal pharmacotherapy—an updated review, Adv. Med. Sci. 56 (2011) 123–131.
[58] S.P. Vyas, V. Sihorkar, V. Mishra, Controlled and targeted drug delivery strategies towards intraperiodontal pocket diseases, J. Clin. Pharm. Ther. 25 (2000) 21–42.
[59] S. Pragati, S. Ashok, S. Kuldeep, Recent advances in periodontal drug delivery systems, Int. J. Drug Deliv. 1 (2009) 1–14.
[60] R.L. Dunn, A.J. Tipton, R.J. Harkrader, J.A. Rogers, Intragingival delivery systems for the treatment of periodontal disease, US005324520A, 1994.
[61] A. Bhardwaj, S.V. Bhardwaj, R. Pandey, Advances in periodontal drug delivery systems, Int. J. Novel Drug Deliv. Tech. 2 (2012) 271–275.
[62] Y. Izumi, A. Aoki, Y. Yamada, H. Kobayashi, T. Iwata, T. Akizuki, et al., Current and future periodontal tissue engineering, Periodontol 2000 (56) (2011) 166–187.
[63] F.M. Chen, Y. An, M. Zhang, New insights into and novel applications of release technology for periodontal reconstructive therapies, J. Control. Release 149 (2011) 92–110.
[64] L.M. Shaddox, C.B. Walker, Treating chronic periodontitis: current status, challenges, and future directions, Clin. Cosm. Invest. Dent. 2 (2010) 79–91.
[65] X.-M. Liu, R.A. Reinhardt, D. Wang, Drug delivery strategies for common orofacial diseases, J. Drug Target. 14 (2006) 583–597.

[66] S.K. Sahoo, S. Parveen, J.J. Panda, The present and future of nanotechnology in human health care, Nanomedicine 3 (2007) 20−31.
[67] A. Ganem-Quintanar, Étude de la perméabilité de la muqueuse orale: évaluation de différentes approaches pour augmenter le passage des principes actifs, Ph.D. thesis, Université de Genève/ Université Claude Bernard, Lyon, Genève, 1997.
[68] R.C. Mundargi, V.R. Babu, V. Rangaswamy, P. Patel, T.M. Aminabhavi, Nano/micro technologies for delivering macromolecular therapeutics using poly(D,L-lactide-co-glycolide) and its derivatives, J. Control. Release 125 (2008) 193−209.
[69] D. Quintanar-Guerrero, E, Allémann, R. Gurny, H. Fessi, E. Doelker, Method for producing aqueous colloidal dispersions of nanoparticles, WO0102087, 2001.
[70] N.S. Soukos, J.M. Goodson, Photodynamic therapy in the control of oral biofilms, Periodontol. 2000 55 (2011) 143−166.
[71] L.E. Chávez de Paz, A. Resin, K.A. Howard, D.S. Sutherland, P.L. Wejse, Appl. Environ. Microbiol. 77 (2011) 3892−3895.
[72] H. Liu, B. Chen, Z. Mao, C. Gao, Chitosan nanoparticles for loading of toothpaste actives and adhesion on tooth analogs, J. Appl. Polym. Sci. 106 (2007) 4248−4256.
[73] T.H. Dung, S.R. Lee, S.D. Han, S.J. Kim, Y.M. Ju, M.S. Kim, et al., Chitosan-TPP nanoparticle as a release system of antisense oligonucleotide in the oral environment, J. Nanosci. Nanotechnol. 11 (2007) 3695−3699.
[74] J.S. Son, K.-B. Lee, S.-G. Kim, T.-Y. Kwon, K.-H. Kim, Porous calcium phosphate granules containing drug-loaded polymeric nanoparticles for bone regeneration, Mater. Lett. 76 (2012) 243−246.
[75] H. Dixon, Q. Ni, J.A. McDonough, Nanoparticle-based targeted drug delivery for in vivo bone loss mitigation, US0070503A1, 2012.
[76] V. Klepac-Ceraj, N. Patel, X. Song, C. Holewa, C. Patel, R. Kent, et al., Photodynamic effects of methylene blue-loaded polymeric nanoparticles on dental plaque bacteria, Laser. Surg. Med. 43 (2011) 600−606.
[77] W. Neuberger, Microbe reduction in the oral cavity with photosensitizers, US0052798A1, 2004.
[78] W. Neuberger, Treatment of periodontal disease with photosensitizers, US0069781A1, 2008.
[79] T.C. Pagonis, J. Chen, C.R. Fontana, H. Devalapally, K. Ruggiero, X. Song, et al., Nanoparticle-based endodontic antimicrobial photodynamic therapy, J. Endod. 36 (2010) 322−328.
[80] R.D.S. Millan, M.E. Cortez, E.M.G. Raso, Controlled release system for chlorhexidine based on a resinous cement, BR004752, 2009.
[81] A. Kovtun, D. Kozlova, K. Ganesan, C. Biewald, N. Seipold, P. Gaengler, et al., Chlorhexidine-loaded calcium phosphate nanoparticles for dental maintenance treatment: combination of mineralizing and antibacterial effects, RSC Adv. 2 (2012) 870−875.
[82] H.S. Tiba, Antibacterial thermoplastic compound containing silver nanoparticles and the application of the same, BR2009004937A2, 2012.

CHAPTER

24 Orally Delivered Nanoparticle Drug Delivery Systems for Dental Applications and Their Toxicity on Systemic Organs

Yashwant Pathak[a] **and Charles Preuss**[b]

[a]*College of Pharmacy, University of South Florida, Tampa, Department of Pharmaceutical Sciences, FL, USA*
[b]*Department of Molecular Pharmacology and Physiology, Morsani College of Medicine, University of South Florida, Tampa, FL, USA*

CHAPTER OUTLINE

24.1 Introduction

The unprecedented growth of nanosciences [1–4] in every walk of life has created lots of optimism in nano applications for medicine and the field of dentistry is not lagging behind in the race.

Nanobiomaterials in Clinical Dentistry.

Several areas of dentistry are testing the fruits of nanotechnology with specific applications in oral diagnostics and dental biomaterials. Some of the areas in dentistry with reference to nanoparticulate drug delivery systems where nanotechnology is being explored include [5,6]

1. Nanoparticulate drug delivery systems for local anesthesia
2. Curing the hypersensitivity in oral treatments
3. Nanorobotic dentifrices
4. Dental durability and cosmetics applications in dentistry

Drug delivery and tissue engineering research areas have witnessed tremendous progress in recent years exploring and using the unlimited potential of these areas of research to improve human health. Recent development of nanotechnology provides opportunities to characterize, manipulate and organize matter systematically at the nanometer scale. The analytical techniques like SEM, TEM, and many developments in characterizing the materials and biomaterials with nanoscale architecture have been used as controlled release reservoirs for drug delivery and artificial matrices for tissue engineering. All these new developments have applications in dental research. Drug delivery systems can be synthesized and the drug release can be controlled with different composition, shape, size, and morphology. Their surface modifications using appropriate precursors and adjuvants can be manipulated to increase solubility, immune-compatibility, and cellular uptake. The limitations of current drug delivery systems include suboptimal bioavailability, limited effective targeting, and potential cytotoxicity. Promising and versatile nanoscale drug delivery systems include nanoparticles, nanocapsules, nanotubes, nanogels, and dendrimers. They can be used to deliver both small-molecule drugs and various classes of biomacromolecules, such as peptides, proteins, plasmid DNA, and synthetic oligodeoxynucleotides. Whereas traditional tissue engineering scaffolds were based on hydrolytically degradable macroporous materials, current approaches emphasize the control over cell behaviors and tissue formation by nanoscale topography that closely mimics the natural extracellular matrix (ECM). The understanding that the natural ECM is a multifunctional nanocomposite has motivated researchers to develop nanofibrous scaffolds through electro spinning or self-assembly. Nanocomposites containing nanocrystals have been shown to elicit active bone growth. Drug delivery and tissue engineering are closely related fields. In fact, tissue engineering can be viewed as a special case of drug delivery where the goal is to accomplish controlled delivery of mammalian cells. Controlled release of therapeutic factors in turn will enhance the efficacy of tissue engineering. From a materials point of view, both the drug delivery vehicles and tissue engineering scaffolds need to be biocompatible and biodegradable. The biological functions of encapsulated drugs and cells can be dramatically enhanced by designing biomaterials with controlled organizations at the nanometer scale.

Nanoscale drug delivery systems with nanoscale materials (10^{-9} to 10^{-7} m) can exhibit distinctive physical, electrical, mechanical, quantum, and optical properties [1]. Through rational design, nanoscale drug delivery systems can be manufactured to combine desirable modules, using both biological and synthetic polymeric materials, for various therapeutic applications, including implantable, inhalable, injectable, oral, and topical and transdermal drug delivery. Many properties of nanoscale drug delivery systems can be tailored for specific applications such as either improving the solubility or delaying the drug release by adjusting the hydrophobicity/hydrophilicity, attaching moieties to target the drug or its biodistribution, biocompatibility, biodegradability, modified drug release with appropriate drug encapsulation [1,2]

The review [5] provides an insight into various potential areas of dentistry that are being invaded by nanotechnology-based drugs and drug delivery systems. Current treatments for oral/dental diseases rely on the use of classical therapeutic agents which are applied or delivered, but in many cases their application and efficacy is limited by low level of absorption locally and lack of selectivity to target cells. The different treatments in dental areas of importance include caries control, restorations, tooth remineralization, management of dentinal hypersensitivity, dental caries vaccine, management of oral biofilm, root canal disinfection, local anesthesia, and periodontal infection [6–8]. Some areas are identified in dental applications demanding extensive research to emerge as a promising therapeutic strategy. The authors of the review have concluded by claiming that dentistry should follow the trend of probing matter at nanoscale to achieve a predictable treatment outcome.

24.2 Dental applications of nano drug delivery

24.2.1 Nanoparticulate drug delivery systems local anesthesia

Pain control is one of the top priorities in therapeutics in dental treatments and in spite of the recent advances in clinical investigation of new therapeutic agents, pain relief is still a significant challenge for dental physicians. The reasons include difficulties of correctly evaluating pain, underestimation of patient's pain, misconceptions about analgesic use and side effects, gaps in pain management process, and lack of acute pain service. Local anesthetics (LAs) are among the most widely used classes of pharmacological compounds, used to eliminate pain.

LAs are small molecules that could be easily eluted from the site of administration, thus limiting the analgesic property. Tan et al. [9] reported the nanogel systems for LAs such as bupivacaine–poly(DL-lactide-*co*-glycolide) nanospheres, procaine hydrochloride (PrHy) hydrogel delivery systems and showed that the drug release can be delayed over 7–15 h depending on the type of hydrogel combination used and also reported various factors affecting the drug release of LAs, which can be used in the dental scenario. The use of LA could be limited by the relatively short therapeutic action and systemic toxicity related to high drug plasma concentration as a result of fast systemic uptake. Improvement of regional administration of LAs could be achieved by incorporating them into drug delivery systems. Nanogels are probably one of the best candidates due to the lesser pain during injection and longer blood circulation time. However, designing a perfect candidate would require one to have a thorough knowledge of the interaction between the drug and the carrier and the effect of size and drug loading on drug release [9].

There are several reports relating the applications of nano drug delivery for LAs, Tan et al. [10] reported about PrHy from pH-responsive nanogels. Date and Nagarsenker [11] have reported the use of micro emulsions for LA delivery. Some of the drugs with LAs properties used in nanodelivery are clonixic acid [12], benzocaine-β-cyclodextrin inclusion complexes [13], bupivacaine-loaded poly (ε-caprolactone) microspheres [14], spray-dried bupivacaine-loaded microspheres [15], carrageenan microspheres containing allopurinol and LA agents [16], bupivacaine included in poly(acrylamide-*co*-monomethyl itaconate) hydrogels [17] and LA bupivacaine in biodegradable poly(DL-lactide-*co*-glycolide) nanospheres [18].

24.2.2 Curing the hypersensitivity in oral treatments

Dental hypersensitivity (DHS) is a major problem. The pain and discomfort from this problem negatively affect the patient's ability to practice proper oral hygiene. As a result, plaque builds up and the teeth and periodontal health become compromised [19]. One of the most important factors is diet. Giving patients a clear understanding of how diet affects DHS and how changing it can improve DHS is very important. Microscopic studies reported earlier show that when dentin is exposed for 5 min to fluids like red and white wine, citrus fruit juices, apple juice, and yogurt, they remove the smear layer and open up dentinal tubules [20]. The loss of the smear layer is known to enhance DHS [21]. One good tip is to tell patients not to brush right after ingesting acidic food or drink. A small sip of water after ingesting acidic food or drink will go a long way in helping DHS. Another important factor is brushing. Educating patients how to brush properly and recommending that they change their toothbrush every 3 months will also be helpful in reducing DHS [22]. Natural hypersensitive teeth have eight times higher surface density of dentinal tubules and diameter with twice as larger than nonsensitive teeth. Futuristic applications proposed involve the construction of reconstructive dental nanorobots, using native biological materials, could selectively and precisely occlude specific tubules within minutes, offering patients a quick and permanent cure [23].

24.2.3 Nanorobotic dentifrices

Frietas in his review article [23] described effective prevention which reduced caries in children and he suggested that a caries vaccine may be available in near future. A sub occlusal-dwelling nanorobotic dentifrice delivered by mouthwash or toothpaste could patrol all supragingival and subgingival surfaces at least once a day, metabolizing trapped organic matter into harmless and odorless vapors and performing continuous calculus debridement. These invisibly small ($1-10\ \mu m$) dentifrice robots, perhaps numbering $10^3 - 10^5$ nanodevices per oral cavity and crawling at $1-10\ \mu m/s$, might have the mobility of tooth amebas but would be purely inexpensive mechanical devices that would safely deactivate themselves if swallowed and would be programmed with strict occlusal avoidance protocols. Properly configured dentifrice robots could identify and destroy pathogenic bacteria residing in the plaque and elsewhere, while allowing the ~ 500 species of harmless oral microflora to flourish in a healthy ecosystem. Dentifrice robots would also provide a continuous barrier to halitosis, since bacterial putrefaction is the central metabolic process involved in oral malodor. With the tremendous developments in microelectromechanical systems and nanoelectromechanical systems and if these futuristic ideas become a reality and if this kind of daily dental care becomes available to everyone from an early age, conventional tooth decay, and gum disease will disappear into the annals of medical history. However the toxicity of such systems needs to be evaluated first before their clinical use.

Artificial phagocytes called microbivores could patrol the bloodstream, seeking out and digesting unwanted pathogens including bacteria, viruses, or fungi [24]. Microbivores would achieve complete clearance of even the most severe septicemic infections in hours or less. The nanorobots do not increase the risk of sepsis or septic shock because the pathogens are completely digested into harmless sugars, amino acids, and the like, which are the only effluents from the nanorobot [24].

24.2.4 Dental durability and cosmetics applications in dentistry

It has been proposed that tooth durability and appearance can be improved by replacing outer enamel layers with pure nanoscale sapphire and diamonds. These are more fracture resistant with high strength, possibly by embedding carbon nanotubes [25]. Durability and appearance of the tooth may be improved by replacing upper enamel layers with covalently bonded materials such as sapphire and diamonds. Nanotechnology has improved the properties of various kinds of fibers [26] which can be used in improving cosmetic appearance and also provide a possible alternative for delayed drug delivery at the site of action in the oral cavity [27]. Polymer nanofiber materials have been explored as drug delivery systems, scaffolds, and filters. Such scaffolds can also be used as drug delivery scaffolds to deliver osteoinductive and anti-inflammatory drugs. Carbon nanofibers with nanometer dimensions showed selective increase in osteoblast adhesion necessary for successful orthopedic/dental implant applications due to a high degree of surface roughness [27,28].

24.2.5 Nanophase alumina for dental applications

Alumina samples (with a nanophase grain size of 23 nm and a conventional grain size of 177 nm) were synthesized and evaluated for mechanical and cyto compatibility properties. Compared to the 177 nm grain size, the modulus of elasticity of the 23 nm alumina grain size decreased by 70%; ductility of alumina can, therefore, be controlled and improved through the use of nanophase formulations. Moreover compared to the 177 nm grain-size alumina, osteoblast (the bone-forming cells) adhesion on the 23 nm nanomaterial increased by 46%. The improved mechanical properties of nanomaterials, in addition to the biocompatibility of nanophase ceramics, constitute characteristics that promise improved orthopedic/dental implant efficacy. These nanophase alumina can also be explored for drug delivery locally in oral applications [8].

24.2.6 Nanoparticulate drug delivery in dental applications

Drug delivery scaffolds made of nanomaterials could aid in developing craniofacial tissue as well as for the delivery of therapeutic drugs following implantation, such as for periodontal disease treatment with antibiotics [29]. Controlled release of drugs or growth factors in vivo is highly desired to sustain their bioactivity [30] Hydrogels such as polyethylene glycol are often used as drug carriers because drugs can be easily incorporated into the hydrogel solution [31]. However, biodegradable polyesters such as poly(lactic-*co*-glycolic acid) (PLGA) can be made into nanospheres by a double-emulsion technique to achieve significantly longer controlled release compared with that of hydrogels.

PLGA nanospheres were used to deliver Bone Morphogenetic Protein-7 (BMP-7) to induce ectopic bone formation [32]. Nanospheres were immobilized on the nanofibers of a phase-separated nanofibrous scaffold without blocking interpore connections. Scaffolds with BMP-7 nanospheres without cells were implanted into rats and evaluated after 3 weeks. Scaffolds soaked with BMP-7 or with blank nanospheres contained only fibrous tissue, but scaffolds with BMP-7 nanospheres revealed initial bone formation [32]. A longer implantation time resulted in more significant bone formation in the nanofibrous scaffolds incorporated with BMP-7 nanospheres.

Similarly, platelet-derived growth factor releasing nanospheres immobilized on a phase-separated nanofibrous scaffold have been shown to promote angiogenesis [33]. The temporally and spatially controlled drug-delivering PLGA nanospheres on the nanofibrous scaffolds can be beneficially applied to dental and craniofacial tissue regeneration.

24.2.7 Treatment of oral cancer using nanoparticulate drug delivery system

Dendrimer nanoparticles will facilitate drug delivery in the treatment of oral cancer. A single dendrimer can carry an anticancer drug molecule that recognizes cancer cells, a therapeutic agent to kill those cells. Dendrimer nanoparticles have shown promise as drug delivery vehicles capable of targeting tumors with large doses of anticancer drugs. Nanoshells have a core of silica and a metallic outer layer. By manipulating the thickness of the layer, scientists can design beads to absorb near infrared light, creating an intense heat that is lethal to cancer cells. The physical selectivity to cancer lesion site occurs through a phenomenon called enhanced permeation retention [25]. Christoph et al. [34] have reported magnetic nanoparticles carrying mitoxantrone for the treatment of loco-regional cancer treatment in the oral cavity. Bhirde et al. [35] have shown the killing of the cancer cells in vivo and in vitro using epidermal growth factor (EGF) directed carbon nanotube-based drug delivery; they used anticancer agent cisplatin and EGF which were attached to single-walled carbon nanotubes (SWCNTs) to specifically target squamous cancer, and the nontargeted control was SWCNT−cisplatin without EGF. They have proposed the application of this approach in oral cancer.

24.3 Toxicity of nanoparticles

In general the toxicity of the nanoparticle drug delivery system can be caused by the drug itself, the nanoparticles or both. Other terms used for the toxicity of the drug itself are side effects or adverse drug reactions. The focus of this section is on the toxicity of nanoparticle drug delivery systems, i.e., the nanoparticles themselves. Four broad mechanisms for the toxicity of nanoparticles are [36]:

1. Cytotoxicity of one or more of the nanoparticle constituents which is an inherent property of the chemical compound
2. Cytotoxicity of one or more of the degradation products of the nanoparticle constituents
3. Endocytosed nanoparticle-mediated apoptosis (cell death)
4. Nanoparticle-mediated cell membrane lysis

The nanoparticles are toxic to the cells by mediating cell lysis and/or apoptosis. One important mechanism for cytotoxicity is oxidative stress mediated by the nanoparticles.

The largest literature for the toxicity of nanoparticles comes from the inhalation toxicity of particles with a mass of a mean diameter of 10 μm [37]. Therefore, there is a lot of literature on the nanoparticle-mediated pulmonary inflammation and tumors in animal models such as rats. Even though the focus of this chapter section is on the toxicity of nanoparticles from oral drug delivery

systems, inhalation nanoparticle toxicity can provide insights into the mechanism or mechanisms of nanoparticle drug delivery systems when used clinically for dentistry.

Three important characteristics that can affect the toxicity of nanoparticles are [36]:

1. Size
2. Shape
3. Charge

The size is the primary characteristic of a nanoparticle which is commonly defined as 100 nm, although drug delivery nanoparticles can be larger [36]. A murine macrophage cell line was exposed to 0.45 and 3.53 μm polystyrene nanobeads and it was found that cytotoxicity was mainly mediated by apoptosis and necrosis, respectively [38]. The size of the nanoparticle affects the physiochemical properties such as surface chemistry and charge [36].

The shape of the nanoparticle can affect the interaction of that particle with important macromolecules like potassium channels and blood cells like platelets. Carbon-based nanotubes (single-walled nanotubes) are rod shaped and carbon-based fullerenes are spherical shaped. The single-walled nanotubes were two- to threefold more potent in blocking different potassium channels than fullerenes [39]. The clinical relevance of this observation is that blocking potassium channels in the heart could cause cardiac arrhythmias. There was increased platelet aggregation in rats in vivo with single-walled nanotubes as compared with fullerenes [40].

The charge of the nanoparticle can affect its bioavailability and this is dependent on the nanoparticle's zeta potential which is a measure of the electrostatic potential at the surface of the particle [36]. Cationic nanoparticles such as gold and polystyrene can cause hemolysis and blood clotting, whereas anionic nanoparticles were found to be less toxic [37].

24.3.1 Toxicokinetics

Toxicokinetics is the study of the time course of absorption, distribution, metabolism, and elimination of a toxicant [41]. By understanding the toxicokinetics of nanoparticles, researchers, and clinicians can better assess the health risks of nanoparticles applied to dentistry. Absorption is the initial step in toxicokinetics and it can occur through many different routes including ingestion, inhalation, and dermal contact [42]. Parentally administered nanoparticles, e.g., intravenous and subcutaneous, can be important clinical routes of exposure for nanoparticles used in dental procedures. Once the nanoparticles are absorbed, they enter the systemic circulation where they are distributed throughout the body. There is evidence that nanoparticles whose diameter is smaller than 200 nm are able to distribute into the Central Nervous System (CNS) by crossing the blood−brain barrier [42]. Nanoparticles such as gold, silver, fullerenes, and carbon nanotubes are thought to be inert and do undergo biotransformation or metabolism [42]. However, quantum dots with attached protein structures can undergo proteolysis [42]. SWCNTs can undergo biotransformation by human neutrophils in vitro via the enzyme myeloperoxidase [43]. Two important routes of excretion for nanoparticles are urinary and biliary routes which are similarly observed with many clinically used drugs. For example, mice were intravenously given fluorescent dye-labeled silica nanoparticles which ranged in size from 50, 100, or 200 nm and the silica nanoparticles were found to be renally and biliary excreted [44] (Figure 24.1).

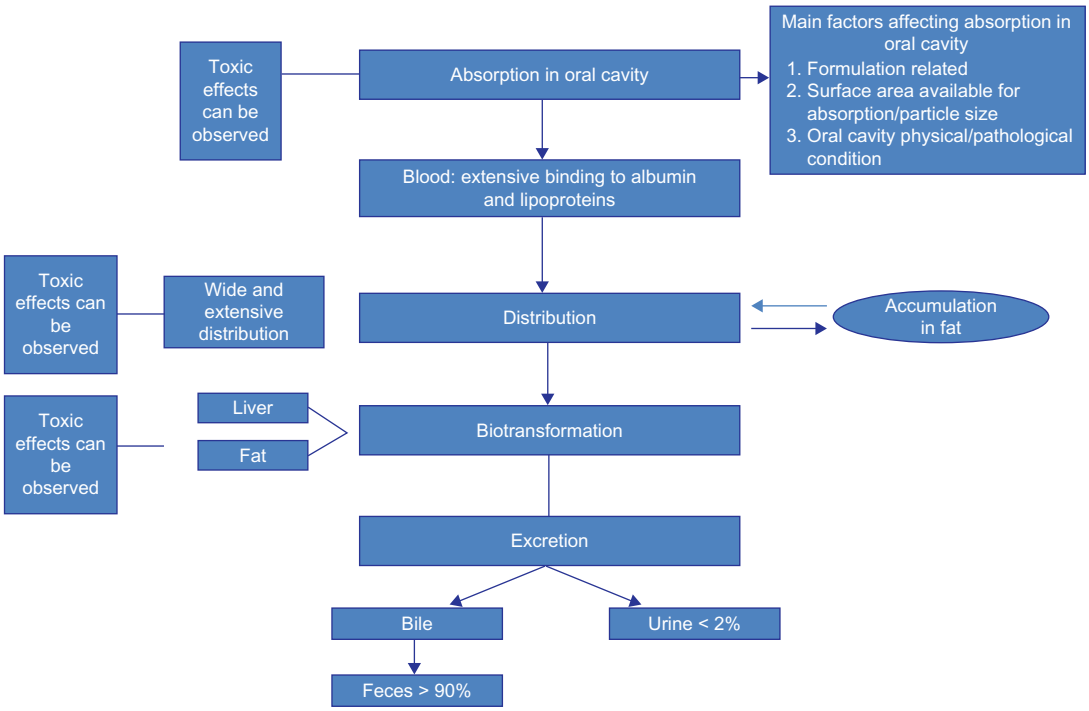

FIGURE 24.1

Schematic description of toxicokinetics for oral nanoparticulate drug delivery systems.

24.3.2 Acute and chronic toxicity

Nanoparticles because of their small size and increased surface area give them a different toxicity profile than their bulk chemical or larger particles of the same chemical composition [45]. An example of acute toxicity with nanoparticles is with nickel. A 38-year-old healthy man was exposed to nanoparticle-sized nickel while spraying them onto bushes for turbine bearings using a metal welding technique [46]. The patient died 13 days later. The inhaled nickel nanoparticle caused adult respiratory distress syndrome as well as acute tubular necrosis in the patient. Transmission electron microscope observation showed that nickel nanoparticles of <25 nm were present in lung macrophages of the patient. Nickel is a well-known toxicant and therefore, it is unlikely to be used as a dental nanoparticle drug delivery system. However, this occupational exposure provides clinically important insights into the acute toxicity of nanoparticles in humans. A small number of nude mice were intravenously given functionalized SWCNTs over a 4-month-period and the mice did not show signs of acute or chronic toxicity [47]. However, the functionalized SWCNTs persisted in liver and spleen macrophages of the mice over the 4 months which could be a concerning observation to be followed up in future larger animal studies.

24.3.3 Genotoxicity and carcinogenicity

Genotoxic chemicals cause mutations by damaging DNA and these mutations sometimes can cause cancer. Several toxicological tests which are used to assess the genotoxic potential of a chemical are listed below [42]:

1. Comet assay
2. Micronucleus test
3. Ames test
4. Mammalian cell gene mutation
5. Sister chromatid exchange
6. Chromosomal aberrations

The following list is of nanoparticles which demonstrated a positive genotoxic test [42]:

1. Chitosan and poly(methyl acrylic acid)
2. Silicon carbide
3. Poly-*N*-isopropylacrylamide
4. Quantum dots
5. SWCNT
6. Zinc oxide
7. Titanium oxide
8. Silver
9. Fullerene (C_{60})
10. Gold

Mice developed mesothelioma after intraperitoneal injections of multiwalled carbon nanotubes which is similar to side effects seen with intraperitoneal injections of asbestos [48]. Titanium dioxide and carbon black nanoparticles are carcinogenic in animal models when given via inhalation or intratracheal instillation [42].

24.3.4 Reproductive and developmental toxicity

The following nanoparticles were found to have reproductive and/or developmental toxicity in animal models [42]:

1. Titanium dioxide
2. Carbon black
3. SWCNTs
4. Multiwalled carbon nanotubes
5. Gold
6. Silver
7. Fullerene (C_{60})
8. Silica

Next are two examples of reproductive and developmental toxicity of nanoparticles in animal models. Titanium dioxide nanoparticles were injected subcutaneously to pregnant mice. The male

offspring were found to have changes to their genital and cranial nervous system as well as accumulation of titanium dioxide in their testes and brain in 6-week-old offspring [49]. This data suggests that titanium dioxide may harm the developing mouse embryo. Pregnant mice were injected intraperitoneally with fullerene (C_{60}) [50]. At a dose of 137 mg/kg of body weight, all the embryos died. At a dose of 50 mg/kg of body weight, 50% of the embryos were abnormal in shape especially in the head and tail areas. A clinical concern with these two examples is that nanoparticle drug delivery systems might have teratogenic effects in pregnant women who are exposed to them.

24.4 Conclusions

Even though there are wide arrays of promising applications, a concern with the use of orally delivered nanoparticle drug delivery systems in dentistry is that the nanoparticles might be inherently toxic. Many toxicology studies on nanoparticles are with the inhalation of particles with a size of 10 μm or less. Three important factors that can contribute to the toxicity of a nanoparticle are size, shape, and charge. Two common major mechanisms of toxicity are cell lysis and apoptosis. The absorption, distribution metabolism, and excretion, i.e., toxicokinetics can affect the toxicity of nanoparticles. A broad classification of toxic effects, i.e., toxicodynamics caused by nanoparticles are acute and chronic, genotoxic and carcinogenic, and reproductive and developmental. The majority of the toxicology literature is in animal models with few examples in humans. More rigorous studies need to be conducted on the safety of nanoparticle drug delivery systems when used in dentistry by clinicians and scientists of these important drug delivery systems in order to safeguard the patient's health.

References

[1] Y.V. Pathak, D. Thassu, Drug Delivery Nanoparticles: Formulation and Characterization, Informa Healthcare, New York, NY, 2009. p. 1–16.
[2] Y.V. Pathak, H. Tran, Advances in Nanotechnology and Applications, vol. 1, Centera, Louisville, KY, 2009. p. 18, 185.
[3] Y.V. Pathak, H. Tran, Advances in Nanotechnology and Applications, vol. 2, Centera, Louisville, KY, 2010. p., 4–5, 121–136.
[4] D. Thassu, M. Deleers, Y.V. Pathak, Nanoparticulate Drug Delivery Systems, 1–32, Informa Healthcare, New York, NY, 2009 185–212.
[5] A. Renugalakshmi, T.S. Vinothkumar, D. Kandaswamy, Nanodrug delivery systems in dentistry: a review on current status and future perspectives, Curr. Drug Deliv. 8 (5) (2011;) 586–594. Review. PubMed PMID: 21696348.
[6] S.R. Kumar, R. Vijaylakshmi, Nanotechnology in dentistry, Indian J. Dent. Res. 17 (2006) 62–69.
[7] M. Goldberg, R. Langer, X. Jia, Nanostructured materials for applications in drug delivery and tissue engineering, J. Bio. Mat. Sci Polym. Ed. 18 (2007) 241–268.
[8] T.J. Webster, R.W. Siegel, R. Bizios, Design and evaluation of nanophase alumina for orthopaedic/dental applications, Nanostruct. Mater. 12 (1999) 983–986.
[9] J.P.K. Tan, M.B.H. Tan, M.K.C. Tam, Application of nanogel systems in the administration of local anesthetics, Local Reg. Anesth. vol. 3 (August) (2010) 1–8.

[10] J.P.K. Tan, A.Q.F. Zeng, C.C. Chang, K.C. Tam, Release kinetics of procaine hydrochloride from pH-responsive nanogels: theory and experiments, Int. J. Pharm. 357 (2008) 305–313.
[11] A.A. Date, M.S. Nagarsenker, Parenteral microemulsions: an overview, Int. J. Pharm. 355 (2008) 19–30.
[12] J.M. Lee, K.M. Park, S.J. Lim, M.K. Lee, C.K. Kim, Microemulsion formulation of clonixic acid: solubility enhancement and pain reduction, J. Pharm. Pharmacol. 54 (2002) 43–49.
[13] L.M.A. Pinto, L.F. Fraceto, M.H.A. Santana, T.A. Pertinhez, S.O. Junior, E. de Paula, Physico-chemical characterization of benzocaine-β-cyclodextrin inclusion complexes, J. Pharm. Biomed. Anal. 39 (2005) 956–963.
[14] M.D. Blanco, M.V. Bernardo, R.L. Sastre, R. Olmo, E. Muniz, J.M. Teijón, Preparation of bupivacaine-loaded poly(ε-caprolactone) microspheres by spray drying: drug release studies and biocompatibility, Eur. J. Pharm. Biopharm. 55 (2003) 229–236.
[15] P.L. Corre, J.P. Estèbe, R. Clément, et al., Spray-dried bupivacaine-loaded microspheres: in vitro evaluation and biopharmaceutics of bupivacaine following brachial plexus administration in sheep, Int. J. Pharm. 238 (2002) 191–203.
[16] K. Tomoda, M. Asahiyama, E. Ohtsuki, T. Nakajima, H. Terada, M. Kanebako, et al., Preparation and properties of carrageenan microspheres containing allopurinol and local anesthetic agents for the treatment of oral mucositis, Colloids Surf. B 71 (2009) 27–35.
[17] M.V. Bernardo, M.D. Blanco, R. Olmo, J.M. Teijón, Delivery of bupivacaine included in poly(acrylamide-*co*-monomethyl itaconate) hydrogels as a function of the pH swelling medium, J. Appl. Polym. Sci. 86 (2002) 327–334.
[18] C.M. Moraes, R. de Lima, A.H. Rosa, E. de Paula, L.F. Fraceto, Encapsulation of local anesthetic bupivacaine in biodegradable poly(DL-lactide-*co*-glycolide) nanospheres: factorial design, characterization and cytotoxicity studies, Macromol. Symp. 281 (2009) 106–112.
[19] P.S. Madhu, S. Setty, S. Ravindra, Dentinal hypersensitivity?—Can this agent be the solution? Indian J. Dent. Res. 17 (2006) 178–184.
[20] M. Addy, E.G. Absi, D. Adams, Dentin hypersensitivity. The effects in vitro of acids and dietary substances on root-planed and burred dentin, J. Clin. Periodontol. 14 (1987) 274–279.
[21] M. Brännström, G. Johnson, Effects of various conditioners and cleaning agents on prepared dentin surfaces: a scanning electron microscopic investigation, J. Prosthet. Dent. 31 (1974) 422–430.
[22] R.H. Dababneh, A.T. Khouri, M. Addy, Dentin hypersensitivity—an enigma? A review of terminology, mechanisms, aetiology and management, Br. Dent. J. 187 (1999) 606–611.
[23] R.A. Freitas Jr, Nano-dentistry, J. Am. Dent. Assoc. 131 (2000) 1559–1566.
[24] R.A. Freitas Jr, Micro biovores artificial mechanical phagocytes using digest and discharge protocol, J. Evol. Technol. 14 (2005) 1–52.
[25] T.S.V. Satyanarayana, R. Rai, Nanotechnology: the future, J. Interdiscip. Dent. 1 (2) (2011) 93–100.
[26] A.V. Rybachuk, I.S. Chekman, T.Y. Nebesna, Nanotechnology and nanoparticles in dentistry, Pharmacol. Pharm. 1 (2009) 18–21.
[27] K. Jayaraman, M. Kotaki, Y. Zhang, et al., Recent advances in polymer fibers, J. Nanosci. Nanotechnol. 4 (2004) 65–67.
[28] R.L. Price, K. Ellison, K.M. haberstroh, et al., Nanometer surface roughness increase select osteoblasts adhesion on carbon nanofiber compacts, J. Biomed. Mater. 70 (2004) 38–40.
[29] M. Zamani, M. Morshed, J. Varshosaz, M. Jannesari, Controlled release of metronidazole benzoate from poly epsilon-caprolactone electrospun nanofibers for periodontal diseases, Eur. J. Pharm. Biopharm. 75 (2010) 179–185.
[30] R. Krishnamurthy, M. Manning, The stability factor: importance in formulation development, Curr. Pharm. Biotechnol. 3 (2002) 361–371.

[31] J. Elisseeff, W. McIntosh, K. Fu, T. Blunk, R. Langer, Controlled-release of IGF-I and TGF-β1 in a photopolymerizing hydrogel for cartilage tissue engineering, J. Orthop. Res. 19 (2001) 1098−1104.
[32] G. Wei, P.X. Ma, Macroporous and nanofibrous polymer scaffolds and polymer/bone-like apatite composite scaffolds generated by sugar spheres, J. Biomed. Mater. Res. A 78 (2006) 306−315.
[33] Q. Jin, G. Wei, Z. Lin, J. Sugai, S. Lynch, P.X. Ma, Nanofibrous scaffolds incorporating PDGF-BB microspheres induce chemokine expression and tissue neogenesis in vivo, PloS One 3 (2008) e1729.
[34] A. Christoph, J. Roland, J.S. Roswitha, B. Christian, H. Julia, E. Wolf, et al., Magnetic drug targeting—biodistribution of the magnetic carrier and the chemotherapeutic agent mitoxantrone after loco-regional cancer treatment, J. Drug Target. 11 (3) (2003) 139−149.
[35] A.A. Bhirde, V. Patel, J. Gavard, G. Zhang, A.A. Sousa, et al., Targeted killing of cancer cells in vivo and in vitro with EGF-directed carbon nanotube-based drug delivery, ACS Nano 3 (2009) 307−316.
[36] S. Costigan, The toxicology of nanoparticles used in healthcare products. <http://www.mhra.gov.uk/Safetyinformation/Generalsafetyinformationandadvice/Technicalinformation/Nanotechnology/index.htm/>, 2006 (accessed 05.09.12).
[37] W. DeJong, P. Borm, Drug delivery and nanoparticles: applications and hazards, Int. J. Nanomed. 3 (2008) 133−149.
[38] V. Olivier, J.L. Duval, M. Hindie, P. Pouletaut, M.D. Nagel, Comparative particle-induced cytotoxicity toward macrophages and fibroblasts, Cell Biol. Toxicol. 19 (3) (2003) 145−159.
[39] K.H. Park, M. Chhowalla, Z. Iqbal, F. Sesti, Single-walled carbon nanotubes are a new class of ion channel blockers, J. Biol. Chem. 278 (50) (2003) 50212−50216.
[40] A. Radomski, P. Jurasz, D. Alonso-Escolano, M. Drews, M. Morandi, T. Malinski, et al., Nanoparticle-induced platelet aggregation and vascular thrombosis, Br. J. Pharm. 146 (6) (2005) 882−893.
[41] D. Shen, Toxicokinetics, in: C. Klassen, J. Watkins, III (Eds.), Casarett and Doull's Essentials of Toxicology, second ed., McGraw-Hill, NewYork, NY, 2010 (online access).
[42] J. Zhou, V. Castranova, Toxicology of nanomaterials used in nanomedicine, J. Toxicol. Environ. Health Part B 14 (2011) 593−632.
[43] V.E. Kagan, N.V. Konduru, W. Feng, B.L. Allen, J. Conroy, Y. Volkov, et al., Carbon nanotubes degraded by neutrophil myeloperoxidase induce less pulmonary inflammation, Nat. Nanotechnol. 5 (2010) 354−359.
[44] M. Cho, W.S. Cho, M. Choi, S.J. Kim, B.S. Han, S.H. Kim, et al., The impact of size on tissue distribution and elimination by single intravenous injection of silica nanoparticles, Toxicol. Lett. 189 (2009) 177−183.
[45] G. Oberdorster, E. Oberdorster, J. Oberdorster, Nanotoxicology: an emerging discipline evolving from studies of ultrafine particles, Environ. Health Perspect. 113 (2005) 823−839.
[46] J.I. Phillips, F.Y. Green, J.C. Davies, J. Murray, Pulmonary and systemic toxicity following exposure to nickel nanoparticles, Am. J. Ind. Med. 53 (2010) 763−767.
[47] M.L. Schipper, N. Nakayama-Ratchford, C.R. Davis, N.W. Kam, P. Chu, Z. Liu, et al., A pilot toxicology study of single-walled carbon nanotubes in a small sample of mice, Nat. Nanotechnol. 3 (2008) 216−221.
[48] C. Poland, R. Duffin, I. Kinloch, A. Wallace, A. Seaton, V. Stone, et al., Carbon nanotubes introduced into the abdominal cavity of mice show asbestos-like pathogenicity in a pilot study, Nat. Nanotechnol. 3 (2008) 423−428.
[49] T. Ken, S. Ken-ichiro, I. Aki, K.-I. Miyoko, F. Rie, T. Masako, et al., Nanoparticles transferred from pregnant mice to their offspring can damage the genital and cranial nerve systems, J. Health Sci. 55 (2009) 95−102.
[50] T. Tsuchiya, I. Oguri, Y.N. Yamakoshi, N. Miyata, Novel harmful effects of fullerene on mouse embryos in vitro and in vivo, FEBS Lett. 393 (1996) 139−145.

Index

Note: Page number followed by "*b*", "*f*" and "*t*" refer to boxes, figures and tables, respectively.

C

D

E

F

G

N

O

P

Q

R

S